Issues 1-3 2019 | Volume 15

The Journal on Advanced Studies in Theoretical and Experimental Physics, including Related Themes from Mathematics

PROGRESS IN PHYSICS

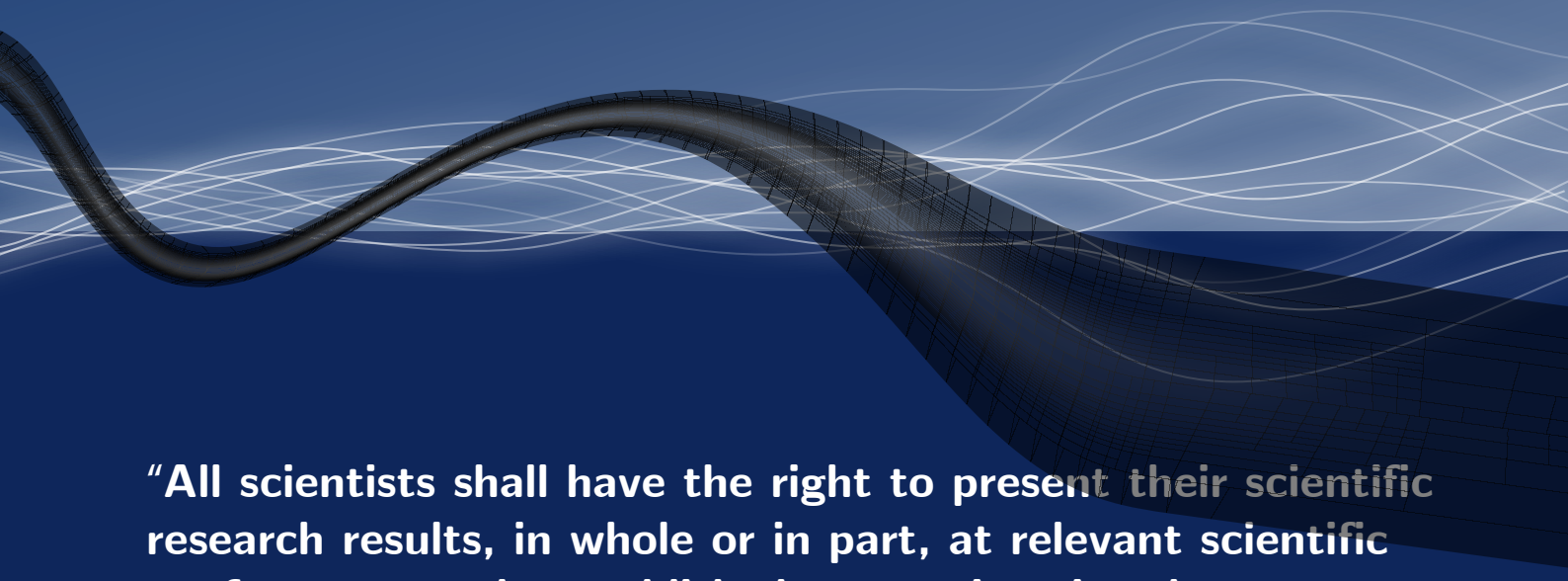

"All scientists shall have the right to present their scientific research results, in whole or in part, at relevant scientific conferences, and to publish the same in printed scientific journals, electronic archives, and any other media." — Declaration of Academic Freedom, Article 8

ISSN 1555-5534

The Journal on Advanced Studies in Theoretical and Experimental Physics, including Related Themes from Mathematics

PROGRESS IN PHYSICS

A quarterly issue scientific journal, registered with the Library of Congress (DC, USA). This journal is peer reviewed and included in the abstracting and indexing coverage of: Mathematical Reviews and MathSciNet (AMS, USA), DOAJ of Lund University (Sweden), Scientific Commons of the University of St. Gallen (Switzerland), Open-J-Gate (India), Referativnyi Zhurnal VINITI (Russia), etc.

Electronic version of this journal:
http://www.ptep-online.com

Postal Address

Department of Mathematics and Science,
University of New Mexico,
705 Gurley Ave., Gallup, NM 87301, USA

ISSN: 1555-5534 (print)
ISSN: 1555-5615 (online)

Standard Address Number: 297-5092
Printed in the United States of America

January 2019 **Vol. 15, Issue 1**

CONTENTS

Information for Authors

Progress in Physics has been created for rapid publications on advanced studies in theoretical and experimental physics, including related themes from mathematics and astronomy. All submitted papers should be professional, in good English, containing a brief review of a problem and obtained results.

All submissions should be designed in LaTeX format using *Progress in Physics* template. This template can be downloaded from *Progress in Physics* home page http://www.ptep-online.com

Preliminary, authors may submit papers in PDF format. If the paper is accepted, authors can manage LaTeXtyping. Do not send MS Word documents, please: we do not use this software, so unable to read this file format. Incorrectly formatted papers (i.e. not LaTeXwith the template) will not be accepted for publication. Those authors who are unable to prepare their submissions in LaTeXformat can apply to a third-party payable service for LaTeX typing. Our personnel work voluntarily. Authors must assist by conforming to this policy, to make the publication process as easy and fast as possible.

Abstract and the necessary information about author(s) should be included into the papers. To submit a paper, mail the file(s) to the Editor-in-Chief.

All submitted papers should be as brief as possible. Short articles are preferable. Large papers can also be considered. Letters related to the publications in the journal or to the events among the science community can be applied to the section *Letters to Progress in Physics*.

All that has been accepted for the online issue of *Progress in Physics* is printed in the paper version of the journal. To order printed issues, contact the Editors.

Authors retain their rights to use their papers published in *Progress in Physics* as a whole or any part of it in any other publications and in any way they see fit. This copyright agreement shall remain valid even if the authors transfer copyright of their published papers to another party.

Electronic copies of all papers published in *Progress in Physics* are available for free download, copying, and re-distribution, according to the copyright agreement printed on the titlepage of each issue of the journal. This copyright agreement follows the *Budapest Open Initiative* and the *Creative Commons Attribution-Noncommercial-No Derivative Works 2.5 License* declaring that electronic copies of such books and journals should always be accessed for reading, download, and copying for any person, and free of charge.

Consideration and review process does not require any payment from the side of the submitters. Nevertheless the authors of accepted papers are requested to pay the page charges. *Progress in Physics* is a non-profit/academic journal: money collected from the authors cover the cost of printing and distribution of the annual volumes of the journal along the major academic/university libraries of the world. (Look for the current author fee in the online version of *Progress in Physics*.)

Picometer Toroidal Structures Found in the Covalent Bond

Omar Yépez

Clariant Corporation, 2730 Technology Forest Blvd, The Woodlands, TX 77381. E-mail: omar.yepez@clariant.com

The same topology observed for the atom's nuclei is identified in the covalent chemical bond. A linear correlation is found between the normalized bond longitudinal cross section area and its correspondent bond energy. The normalization number is a whole number. This number is interpreted as the Lewis electron pair. A new electron distribution for different diatomic molecules follows. Same number of electrons present different bond energies, occupying different areas. Therefore, it is inferred that the chemical energy is a consequence of the mass defect or gain due to the mass fusion of valence electrons participating in the bond.

1 Introduction

The topological analysis of the electron density has provided useful information about the bonding in a molecule. However, not much progress has been made to reveal the fundamental features of chemical bonding postulated by Lewis, i.e. the electron pair. According to Lewis structures there are bonding electron pairs in the valence shell of an atom in a molecule, and there are also nonbonding pairs or lone pairs in the valence shell of many of the atoms in a molecule. So far, it has not been seen any evidence of electron pairing in the topological analysis of the electron density. An increased concentration of electron density is observed between the two bonded atoms, which could be interpreted as the electron density equivalent of a Lewis bonding pair [1]. Nevertheless, there is no way to be sure about it. The same occurs about the existence of lone pairs. This same reference arrives to the conclusion that electron pairs are not always present in molecules, and even when they are, they are not as localized as the approximate models may suggest [2].

Therefore, a method to measure the number of electrons that participate in the bond will definitely probe or not the existence of Lewis electron pairs.

In 1996 the shapes of the deuteron at the femtometer scale were reported. The deuteron presents three different shapes: a torus, a sphere inside another sphere and two separated spheres [3]. These are the same shapes observed in every single molecule's Laplacian of the electron density but at the picometer scale. It is inferred that those are the shapes of the electron while it is participating in the chemical bond. Lack of identifying these shapes with the electron misleads the molecule's topological analysis.

This paper uses this new shapes in the analysis of different diatomic molecules and CO_2. Thanks to this, the topology of the chemical bond is properly identified. The longitudinal cross section area of the bond is correlated with its bond energy. Only when this area is divided by a whole number, a linear correlation between this bond area and its energy occurs. This whole number is most of the time an even number and thus, it is interpreted as the electron pair. Consequently, an electron distribution in the molecule is possible. First time model independent evidence of the Lewis electron pair is found.

1.1 Electron pair topology

Covalent bonds or lone pairs will be detected by using the structures observed in Fig. 1, namely: the two separated spheres (***ts***), the torus (***t***) and the sphere in a sphere (***ss***). Valence electrons participating in the σ bond (two electrons involved) occur by adopting the two separated sphere structure, ***ts***. Double (four electrons involved) and quadruple bonds (eight electrons involved) also use this structure. A lone pair occurs as a torus shape around quadruple bonds or as a ***ss*** structure around more electronegative atoms. As the electronegativity of the nucleus increases, non-bonding electrons tend to form a toroidal structure around its atom helium core. This occurs until the next noble gas structure is fulfilled.

2 Experimental

By cutting the silhouette of the two separated sphere structure, involving the bonded atoms, the bond longitudinal cross section areas (bond area) were determined from the contour map of the Laplacian of its charge density. An example of such silhouette (green lines) can be observed in Fig. 3 for the fluorine molecule. They were printed on paper, cut and weighted. The bond length was used to calibrate the longitudinal cross section area measured in each bond. Then, these areas were correlated with their respective bond energies.

The contour map of the Laplacian of the charge density for fluorine, F_2 and dicarbon, C_2 molecules were found in [4], oxygen O_2 was found coordinated to a molibdenum atom in [5]. Nitrogen, N_2 is from [7]. Carbon monoxide, CO from [8]. Cyanide CN^- from [11]. Nitrogen monoxide, NO from [9] and carbon dioxide CO_2 was found in [10].

3 Results

Fig. 2 shows a straightforward correlation between the bond area divided by a number n and the bond energy of each bond. This number n is a whole number and it is interpreted as the

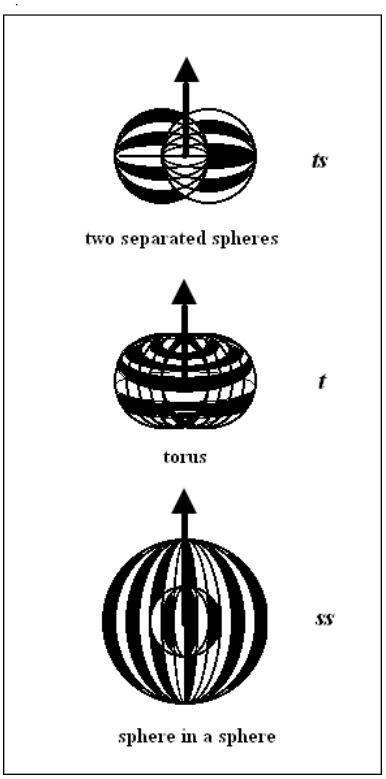

Fig. 1: Observables structures of the electron. This is after [3].

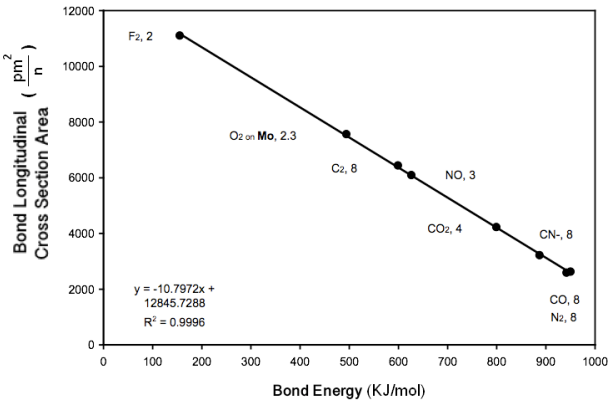

Fig. 2: Correlation between bond longitudinal cross section area and its energy for different diatomic molecules and CO_2.

number of electrons involved in the bond. It has to be stressed that the $y-$axis location for each experimental point is very sensitive to the number n. Fractions of this number makes the r^2 get lower than 0.999. It is clear that as the normalized bond area diminishes, the bond energy increases.

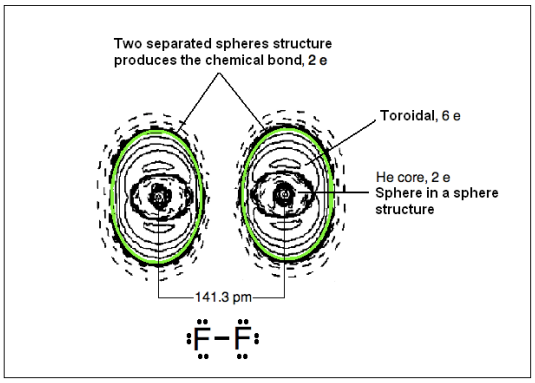

Fig. 3: Fluorine molecule. There is no discernible structures between the atoms. The different electron's structures are indicated. The green line shows where the bond was cut. The original figure is from [4]. Used under Creative Common License.

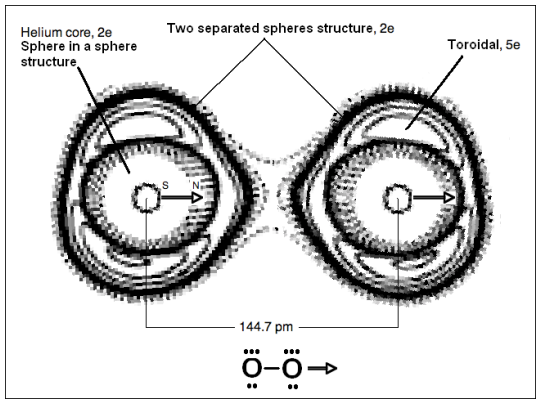

Fig. 4: Oxygen molecule coordinated by a Mo atom. The different electron's structures are indicated. The magnetic moments are shown with the arrow with North and South poles. The original figure is from [5]. Used with permission of the editors.

3.1 Homonuclear diatomic molecules

Fluorine, F_2. Fig. 3 shows the fluorine molecule. The sphere in a sphere structure is clearly observed at the center of each F atom. This is due to the helium core and account for two electrons. The next six electrons are in the toroidal structure around each helium core. As observed in Fig. 2, the F–F bond has two electrons. The two bonding electrons belong to both nuclei in a ***ts*** structure. Due to this bonding, there is no discernible structure between the F atoms. Therefore, one can still put a stroke between these two atoms, understanding that there is a bond through this structure. Hence F–F is all right. The dots around each F atom just denotes the pairing of each atom's 6 toroidal electrons. This is the usual Lewis structure.

Oxygen, O_2. Fig. 4 shows that the oxygen molecule highly resembles the fluorine one. The n number was not a whole

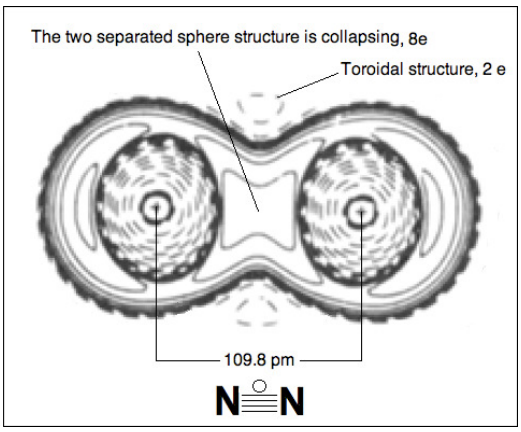

Fig. 5: Nitrogen molecule. The original figure is from [7]. Used with permission of the editors.

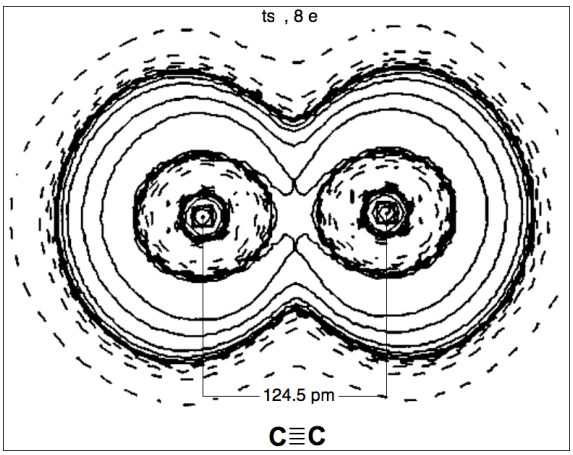

Fig. 6: Dicarbon molecule.The original figure is from [4]. Used under Creative Commons License.

number giving 2.3. The uncoupled electrons in each oxygen atom will produce a magnetic attraction in the line of the bonding. Probably, this may distort the molecule in a way to make it digress from the experimental trend observed. However, the resemblance to the fluorine molecule and the closeness of the n number to 2, strongly suggests that the number of electrons involve in the O–O bond is 2.

As a consequence, the toroidal structure on the oxygen's helium core, previously observed in F_2, necessarily have 5 electrons each. This odd number means two uncoupled magnetic momenta. One in each oxygen atom. They will align as indicated in the figure. This will create a net magnetic moment in the molecule, i.e. the oxygen molecule is paramagnetic.

The magnetic attraction is rendering a shorter bond area in this molecule. Probably, this is why this molecule is away from the general trend observed in Fig. 2. Dividing between a larger n number is just compensating this magnetic attraction. In other words, to have an $n = 2$ in this molecule, the energy of the O–O bond should be 410 kJ/mol and not the experimental 494 KJ/mol. f There have not been any consensus about how the oxygen's Lewis structure should be written. The molecule's paramagnetism does not help. This is because an uncoupled electron structure has to be written, somehow contradicting Lewis pairing hypothesis. O–O, O=O and O÷O has been proposed. From these structures, the more pertinent is O÷O because the dots are the two uncoupled electrons observed in Fig. 4. The Lewis structure printed in Fig. 4 indicates the existence of odd pairing, which is supported by the molecule paramagnetism.

Nitrogen, N_2. As it is noticeable from Fig. 5, the nitrogen atoms are not separated. This is probably due to the lower electronegativity in comparison with fluorine and oxygen molecules. The well defined ***ts*** structure previously observed for fluorine and oxygen disappears, giving way to the same structure but with its spheres more collapsed; this is covering both nitrogen atoms' helium cores.

According to the results from Fig. 2, four of the five nitrogen valence electrons are compromised in the N–N bond. Since this molecule is diamagnetic, it is believed that the two remaining electrons join forming a toroidal lone pair structure around the N–N bond. This ring will occur in the midpoint between the bonding nitrogens. Structures like this have been observed, for example in the acetylene molecule [12]. As a consequence of this electron distribution, all nitrogen's five valence electrons are joined and this is why this molecule presents the highest bond energy in the series F, O, N, C.

The usual Lewis structure is a triple bond between the nitrogens and two lone pairs, one at each nitrogen atom. However, this molecule has one of the highest bond energies and also the smaller bond area measured from the pool of molecules tested. Therefore, it should not surprise that a very high number of valence electrons join for this bond. Furthermore, there is no structures in Fig. 5 to justify the presence of lone pairs on either N atoms. As it was observed in F–F or in O÷O. Hence, the Lewis structure pictured in Fig. 5 with four strokes and the lone pair making a ring (torus) around the middle of the N–N bond is a new Lewis structure.

Dicarbon, C_2. Fig. 6 presents an even less collapsed ***ts*** structure in comparison with N_2. This is due to less number of valence electrons to bond and to the lower electronegativity that carbon has. The C–C bond in dicarbon involves all valence electrons from each carbon, i.e. 8, and they are around each atom's helium core. The diamagnetism of this molecule reveals that all its bonded electrons are magnetically coupled. Again, no lone pair structures are noticeable in this molecule. Hence, the Lewis structure depicted in Fig. 6 is new.

Upon comparing these four molecules, one can arrive to the conclusion that the chemical σ bond is mostly performed

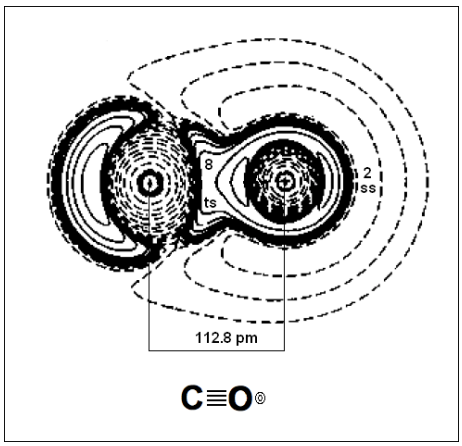

Fig. 7: Carbon monoxide. The two concentric semicircles in the Lewis structure represent an ***ss*** lone pair structure located on the oxygen atom. The original figure is from [8]. Used with permission of the editors.

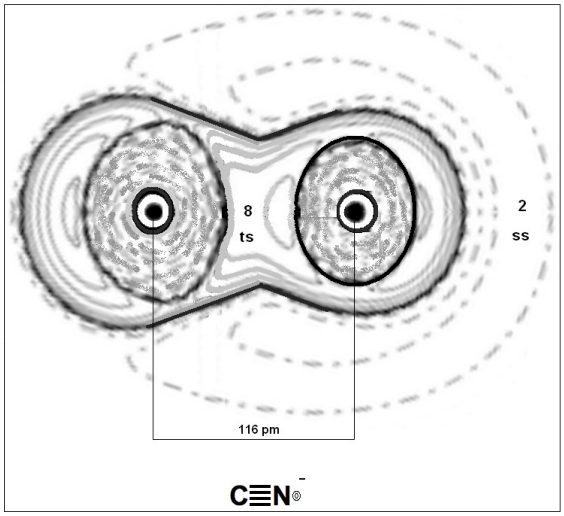

Fig. 8: Cyanide molecule.The two concentric semicircles in the Lewis structure represent an ***ss*** lone pair structure located on the nitrogen atom. The original figure is from [11]. Used with permission of the editors.

by this ***ts*** structure and the separation between the spheres depends on the atom's electronegativity. As the electronegativity of the bonded atoms diminishes, more electrons are involved in the bond.

3.2 Heteronuclear diatomic molecules

Carbon monoxide, CO. As observed in Fig. 2, the C–O bond involves 8 electrons. Accordingly, Fig. 7 presents the electron distribution in CO. From the 10 valence electrons to share: 4 from the carbon and 4 from the oxygen are joined around the helium core of each atom. The other 2 oxygen's valence electrons are in a lone pair. This is the ***ss*** structure over the oxygen's helium core.

This molecule is isoelectronic with N_2. However, the difference between the atoms' electronegativity makes the lone pair to form over the oxygen. In the case of N_2, there is no difference in electronegativity, and thus it is believed that its lone pair will be at the mid point between the N–N bond in a toroidal shape.

The current Lewis structure of CO is a triple bond between the carbon and the oxygen and one lone pair on each atom. Somehow trying to achieve the octet rule. The new Lewis structure is a quadruple bond for the C–O bond and one lone pair only on the oxygen in an ***ss*** structure. This last feature has been noted as two concentric circles in the new Lewis structure (see Fig. 7).

Finally, there is a controversy about the dissociation energy of CO. The values can be 881, 926, 949, 941 or 1070 KJ/mol coming from different kind of experiments [13]. In the case of Fig. 2, the value 926 KJ/mol from electron impact experiments or 949 KJ/mol from pre-dissociation data produced the best linear correlation with the other molecules of the group.

Cyanide, CN^-. As in the case of carbon monoxide, the C–N bond involves 8 electrons. Fig. 8 presents the electron distribution in the molecule: 4 valence electrons from carbon and 4 more from the nitrogen make this bond in an ***ts*** structure around the atoms' helium cores. The nitrogen however, remains with one uncoupled electron. Since this molecule is diamagnetic, an extra electron is needed to couple and cyanide finish with a negative charge. This charge is a ***ss*** lone pair, clearly observed on the nitrogen. This occurs on the nitrogen atom because it is more electronegative than carbon. The current Lewis structure is a triple bond between the carbon and the nitrogen and two lone pairs; one on each atom. This is to try to achieve the octet rule. Again, just like in the CO molecule, the new Lewis structure is a quadruple bond and the lone pair repeats on the more electronegative atom.

Nitrogen monoxide, NO. Fig. 9 presents the NO molecule. As observed in Fig. 2, the N–O bond involves three electrons. This will imply that one of those three electrons is not magnetically coupled with the other two and therefore, this molecule will be paramagnetic. In this join of three electrons, the nitrogen shares 1 and the oxygen shares 2. By this way, the nitrogen can couple the other 4 electrons as one toroidal structure around its helium core. The oxygen will arrange its other 4 electrons in the same manner. The current Lewis structure depicts an uncoupled electron on the nitrogen and a double bond between the nitrogen and the oxygen. The new Lewis structure leaves the odd electron in the N–O bond. Thus, this would be an example of a three electron bond and therefore, this bond is paramagnetic. Thus, the new Lewis structure draws a magnetic moment vector over the single N–

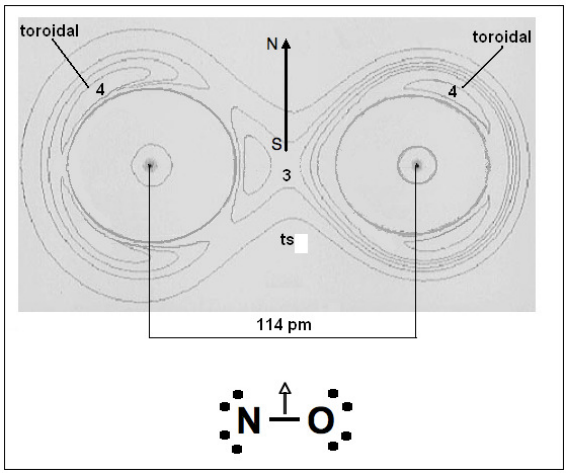

Fig. 9: Nitrogen monoxide molecule. It has a three electron σ bond. 4 electrons forms a toroidal structure around each atom's helium core. The original figure is from [9]. Used with permission of the editors.

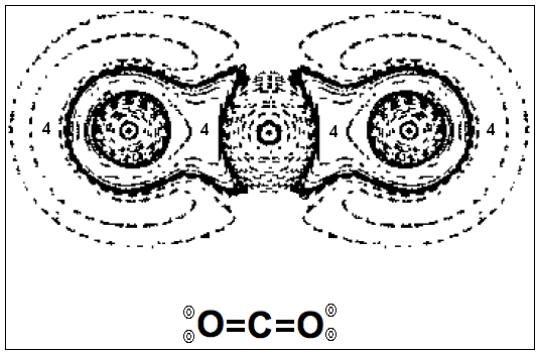

Fig. 10: Carbon dioxide, CO_2. The new Lewis structure specifies that the two lone pairs on the oxygen atoms are in an ***ss*** structure. The original figure is from [10]. Used with permission of the editors.

O bond. The two lone pair on each atom are also depicted.

Carbon dioxide CO_2. Fig. 10 shows that the 4 valence electrons of carbon are used at each side of the molecule to produce two C–O bonds with 4 electrons each. The remaining 4 electrons of the oxygen go to an ***ss*** lone pair over each oxygen atom. The current Lewis structure presents a double bond towards each oxygen atom and two lone pairs on each oxygen. The new Lewis structure just stresses that these lone pairs are in an ***ss*** structure.

4 Discussion

The three shapes observed in Fig. 1 are the "attractors" identified by Bader *et al* after the topological analysis of a large number of molecules [6]. Specifically, the core attractor can be identified as the ***ss*** shape; the bonding attractor as the ***ts*** shape and the non-bonding attractor as the toroidal shape. Given that the same shapes have been observed for the deuteron [3], it is inferred that these attractors are actually different shapes of the electron.

The results presented in Fig. 2 are paramount to understand the chemical bond. The bond area was found to be inverse proportional to the correspondent bond energy. Something similar has been observed before. It is common knowledge that as the number of bonds increases between two carbon atoms, the interatomic distance diminishes. By this way, a single bond is larger than a double bond and a double larger than a triple bond. Thus, it is not strange that another dimensional relationship does occur between the bond area and the bond energy. However, as observed in Fig. 2, the same number of bonding electrons, 8, produced the main chemical bond between the bonded atoms in: C_2, CN^- and CO, rendering different bond areas and bond energies. This means that those electrons are changing sizes in the bond and their longitudinal cross section area corresponds to different energies.

How all these electrons are together in a progressively smaller place? Electrostatic repulsion is non-existent in these arrangements. This is because, all these electron charges are neutralized by the counter charge from their atom nuclei. This will certainly help to have all of them in just one location. In a given molecule, most of the time an even number of electrons are found in the bond between two atoms. This is because the magnetic coupling between valence electrons magnetic momenta renders such even number and diamagnetism to the bond. Paramagnetism occurred in two cases O_2 and NO, to which, the electron distribution helped to locate where is the uncoupled electron producing it.

Another example of inverse proportion between the occupied longitudinal cross section area and the bond energy can be found in nuclear isotopes, where it is observed the general trend of reduction in the isotope radius as the number of neutrons increases in the isotope. Reference [14] presents such relationship for oxygen isotopes. This means more nuclear bonding energy to keep all those neutrons in the nucleus in a progressively smaller longitudinal cross section area. Just what was observed in Fig. 2 with electrons instead. Therefore, it is believed that no repulsive electric forces manifest in the chemical bond situation. More likely, the bonding electrons behavior is controlled by the properties of their masses, i.e. mass fusion.

Hence, before the bond can occur, valence electrons will naturally repel each other because of mass repulsion. Thus, an activation energy would be needed to overcome such repulsion. After that, the bond occurs as a consequence of valence electrons mass fusion. Consequently, this mass fusion defect or gain will translate to an energy release or increase respectively. This answers what in a molecule changes in mass to account for the chemical energy.

Received on October 6, 2018

References

1. Guillespie R. J. and Popelier P. L. A. Chemical Bonding and Molecular Geometry, from Lewis to Electron Densities. Oxford University Press, New York, 2001, Chapter 7.
2. Guillespie R. J. and Popelier P. L. A. Chemical Bonding and Molecular Geometry, from Lewis to Electron Densities. Oxford University Press, New York, 2001, p. 179.
3. Forest J. L., Pandharipande V. R., Pieper S. C., Wiringa R. B., Schiavilla R. and Arriaga A. *Phys. Rev. C*, 1996, v. 54, 646.
4. Chan W.-T. and HamiltonI. P. *J. Phys. Chem.*, 1998, v. 108, 2473.
5. Macchi P., Schultz A. J., Larsen F. K., and Iversen B. B. *J. Chem. Phys.*, 2001, v. 105, 9231.
6. Bader R. F. W. Atoms in Molecules, a Quantum Theory. Clarendon Press, Oxford, 1990, p. 294.
7. Bader R. F. W. *Chem. Rev.*, 1991, v. 91, 893.
8. Bader R. F. W., Johnson S., Tang T. H. and Popelier P. L. A. *J. Phys. Chem.*, 1996, v. 100, 15398.
9. Aray Y., Rodriguez J. and Lopez-Boada R. *J. Phys. Chem. A*, 1997, v. 101, 2178.
10. Bader R. F. W. and Keith T. A. *J. Chem. Phys.*, 1993, v. 99, 3683.
11. Daza M. C., Dobado J. A., Molina J. and Villaveces J. L. *Phys. Chem. Chem. Phys.*, 2000, v. 2, 4089.
12. Gadre S. R., Bhadane P. K. *Resonance*, 1999, v. 4, 14.
13. Pauling L. and Sheehan W. F. Jr. *Proc. N. A. S.*, 1949, v. 35, 359.
14. Lapoux V., Somà V., Barbieri C., Herbert H., Holt J. D. and Stroberg S. R. arXiv: nucl-ex/1605.07885v2.

Toward the Fields Origin

Jacques Consiglio

52, Chemin de Labarthe. 31600 Labastidette. France
E-mail: Jacques.Consiglio@gmail.com

Here I continue my analysis of particles mass and couplings, and show *why and how* the full SM particles spectrum exists and must exist; that it constitutes a mechanically coherent system of resonances, and *how* it is compatible with GR and cosmology.

1 Introduction

Here I show *why* the SM mass spectrum must exist, and *how* it comes to be what it is. This paper follows [1] where I use a mass equation to analyze the SM elementary particles mass spectrum, and [3] where I discuss cosmological density parameters and their history. It is structured as follows:

In Section 2, for the reader's convenience I first recall my main results related to particles mass; then I recall some of my results in cosmology.

In Section 3, I complement the analysis provided in [1] and show that the couplings and the resonances constitute a coherent system where each particle is a double sub-harmonic of the Planck mass.

Section 4 is the important one as it gives an origin to the SM particles; I show *why and how* the Planck mass imply the SM particles resonances, including also mass-less particles. It shows that this theory is about the very foundations of the physical world.

In Section 5, I show that the mass-resonance equation is compatible with cosmology and general relativity (GR). This is not trivial at all as it is based on the cube of a length, which seems in contradiction with the linear relation between wavelengths and energy. Doing so I show an effective symmetry of scale in GR and cosmology (which is already in [3]).

In Section 6, I discuss the fine structure constant; its interpretation in QED and its position in the field as depicted here.

When reading this paper, please keep in mind that each and every parameter of the standard theories which are analyzed here, when computed from the equations I give are well in the ranges given by CODATA (2014) and the Planck mission results [4], with no exception (the values needed to compute all quantities are provided).

2 Previous results, in very short

2.1 Particles resonances

In [1] and the references therein, I found a mass equation that comes in two slightly different instances; one for leptons and quarks:

$$m = \frac{X}{\left(\frac{1}{N\,P} + K\,D\right)^3} + \mu\,, \tag{1}$$

where N, P, K are integral numbers, X and μ are constant real parameters, and D is a real parameter which is particle group dependent; and one for massive bosons:

$$m = m_e \times \frac{\left(\frac{1}{N_e P_e} + K_e D_e\right)^3}{k\,\pi\left(\frac{1}{N_b P_b} + K_b D_b\right)^3}, \tag{2}$$

with index e for the electron and index b for a boson. The little k introduced at the denominator is computed using the following equation, which is deduced from their resonances geometry:

$$k^3\,\pi/144 = 266\,D_b\,(\pi/k)^{1/3}. \tag{3}$$

The numerical values for X and μ are of little interest here, but the relations between the different D is critical. At first, I evaluate D_e, X, and μ fitting the equation to the leptons masses.

$$X = 8.1451213299073\,\text{KeV}.$$

$$\mu = 241.676619539\,\text{eV}.$$

The fit is optimal in the sense that I take the smallest possible N, P, and K. Then for quarks I need to use the fine structure constant to modify the D:

$$D_q = D_e\,(1 + \alpha),$$

and finally, after modeling the field interactions related to the D and partly understanding the resonance substructure, I deduce for the Z and W bosons:

$$D_{WZ} = \frac{\alpha^2}{1\,+\,\alpha^2} + \frac{D_e}{2(1\,-\,\alpha^2)} - \frac{D_e^2}{6(1\,+\,\alpha^2)},$$

and for the H^0:

$$D_H = \frac{\alpha^2}{1\,+\,\alpha^2} + \frac{D_e}{2(1\,-\,\alpha^2)} - \frac{D_e^2}{1\,+\,\alpha^2}.$$

This set of parameters corresponds to the fundamental field because all particles masses are computed with X, μ, D_e, and α, which are constants. The form of the resonance is particle group dependent (leptons, quarks and massive bosons), and the coefficients of the resonances are particle dependent.

Empirical fit targeting minimal N and P gives the resonances in Tables 1, 2, and 3 where very simple patterns appear; stunningly for quarks and bosons only one resonance parameter is variable (N for quarks, and K for bosons).

Table 1: Electron, muon, tau in MeV/c^2.

-	P = N	K	Computed	Measured
e	2	2	0.510 998 9461	0.510 998 9461(31)
μ	5	3	105.658 3752	105.658 3745(24)
τ	9	5	1 776.84	1 776.82(16)

Table 2: Quarks resonances in MeV/c^2.

-	P	N	K	Computed	Estimate
u	3	2	−6	1.93	1.7 - 3.1
d	3	19/7	−6	5.00	4.1 - 5.7
s	3	7	−6	106.4	80 - 130
c	3	14	−6	1,255	1,180 - 1,340
b	3	19	−6	4,285	4,130 - 4,370
t	3	38	−6	172,380	172,040 ±190 ± 750

Please note that the up quark resonance is $2 = 38/19 = 14/7$, and that of the down is $19/7 = 38/14$; in both cases we have two resonances giving the same mass. This will be useful later and quite stunning. Note also that the single variable resonance parameter of quarks, which is N, depends on 2, 7, and 19. It is the same for bosons in Table 3, but with K.

Table 3: Bosons resonances in MeV/c^2.

-	P = N	K	Computed	Measured
$W^{\pm}$	12	−2	80, 384.9	80, 385 ± 15
Z^0	12	−7	91, 187.56	91, 187.6 ± 2.1
H^0	12	−19	125, 206	125.090 ± 240

Last, the three bosons widths are computed from resonance geometry and substructure in coherence with the Ds. They come as a difference in mass with a hypothetical particle where their K is shifted as follows:

$$K \to K + 1 + 1/24, \tag{4}$$

in the case of the W and Z, and for the H^0:

$$K \to K + 1/144/6\,. \tag{5}$$

The three Tables above correspond to the fundamental field, but there is also an adjacent field, where leptons also ring as shown in Table 4. It comes with the constraint P=K instead of P=N in Table 1. It uses different parameters (index α):

$$X_\alpha = 8.02160795579\,\mathrm{keV/c^2}, \tag{6}$$

$$\mu_\alpha = \mu\left(\frac{\pi}{2} + \frac{\pi}{137} + \left(\frac{2\pi}{137}\right)^2\right). \tag{7}$$

Table 4: Second view on electron, muon, tau in MeV/c^2.

-	P=K	N	Computed	Measured
e	2	2	0.510 998 9461	0.510 998 9461(31)
μ	3	8	105.658 3752	105.658 3745(24)
τ	4	16	1 776.84	1 776.82(16)

Expressions giving D_e, D_α, and α are given in the next subsection.

Now looking at the different resonances in the Tables 1, 2, 3, and 4, and keeping all distinct numbers except fractions we get two sums which will play a singular role; firstly with the Ns and Ps, we compute the sum of all integral resonances in the space domain:

$$\Sigma_{N,P} = 2+3+4+5+7+8+9+12+14+16+19+38 = 137\,. \tag{8}$$

Then the sum of all possible shifts in K, increasing or reducing the resonance lengths. The term $266 = 2{\times}7{\times}19$ is related to the bosons'little k and is the product of their Ks.

$$\Sigma_K = (2\times 7\times 19) + 2+3+4+5-6 = 274\,. \tag{9}$$

Finding 137 here is not only reminiscent of the fine structure constant; the sum can be exponentiated in order to separate the 12 terms into distinct independent oscillators. Then it also suggests that the SM mass spectrum is defined by N and P being sub-harmonic components of a high mass, logically the Planck mass and, conversely in K, that a second sub-harmonic system exist which is orthogonal. For simplicity I shall denote this "dual sub-harmonic".

2.2 Couplings

Based on the idea of sub-harmonics, I have deduced the reduced Planck mass resonance in [1], but the deduction is incomplete as I do not find an exact value for the lesser term of its specific coupling D_p. Now I use the following value:

$$D_p = \frac{1}{\sqrt{137^2 - 19\pi^2 + \dfrac{4\pi}{19}}}\,. \tag{10}$$

The first reason is that, if compared to the calculus of the fine structure constant in [2], the lesser term in (10) represents a spin 2 current - i.e. not a particle - and secondly the computed Planck mass is perfectly centered in error bars:

$$M_p = \sqrt{\frac{\hbar\, c}{8\pi\, G}} = \frac{X}{\left(D_p^4 + \dfrac{D_e}{266^2}\right)^3}\,. \tag{11}$$

Last, the expression (10) (together with (12) hereafter) will later be shown exact at least up to 15 decimal places. Other couplings have the same form as (10) which was generalized

after computing α firstly from the leptons resonance and then from the Bohr model in [1], and [2].

They are:

$$D_e = \frac{1}{\sqrt{(4\times(274+19))^2 + 7\pi^2 - \dfrac{19\pi}{19-1}}}\,, \tag{12}$$

$$D_\alpha = \frac{1}{\sqrt{(16\times(274+3))^2 + 2\times(274+19+1)\pi^2 - \dfrac{19}{4\pi}}}\,, \tag{13}$$

where $\frac{19}{4\pi}$ is best guess. And of course:

$$\alpha = \frac{1}{\sqrt{137^2 + \pi^2 - \dfrac{1}{137.5}\times\dfrac{1}{2}\times\left(1+\dfrac{1}{4}\right)}}\,, \tag{14}$$

where the lesser terms may be incomplete, but lead to a value in agreement with CODATA (2014).

2.3 Energy and cosmology

Based on the results in the previous subsection it becomes relevant to suppose that no freedom exist in the field parameters. It naturally raise the question of cosmological data; in particular the densities of matter, dark matter and the elusive dark energy. In [3], assuming that the universe has permanent critical density, like it has now, and that its observable radius R_U recesses at the speed of light, I have shown that the cosmological term Λ is not constant but:

$$\Lambda \approx \frac{2\pi}{3\,R_U^2}\,, \tag{15}$$

where $R_U = c\,T$, with T the universe age; and secondly that the dark and visible energies obey the following proportionality relation, at any epoch:

$$\rho_D = 2\pi^2\,\rho_V = \frac{2\pi^2}{2\pi^2+1}\,\rho_T = \frac{11}{8}\,\rho_{DE} = \frac{11}{3}\,\rho_{DM}\,, \tag{16}$$

where:

— ρ_V, is the "visible" energy density,

— ρ_{DE}, is the dark energy density,

— ρ_{DM}, is the (cold) dark matter density,

— ρ_T, is the total energy density, $\rho_T = \rho_{DM} + \rho_{DE} + \rho_V$ and

— $\rho_D = \rho_{DM} + \rho_{DE}$ is the total dark fields density.

Those two relation imply that all energy densities related to mass evolve like $1/R_U^2$; it will be used as argument in the following sections. Several other results come from the same hypothesis:

— MOND is GR weak field approximation in a universe where energy and space-time expand linearly together,

— The MOND parameter value is $a_0 = H\,c/2\pi$,

— Discrepancy between the Hubble parameter measured locally (SN1A) and measured from events close to the event horizon (CMB and BAO), by a factor $\approx 1 + 1/2\pi^2$.

— The discrepancy creates the illusion of accelerated expansion.

— The reduction of wavelengths also creates the illusion of an initial inflation, since when $t \to 0$ wavelengths become infinitely large.

Where all quantities are calculable, computed, epoch dependent, and agree with experimental data (except for the inflation factor which I could not compute).

3 Couplings and particles mass

In this section I first discuss correlations between coupling coefficients; then between couplings and particles resonances.

3.1 Melting resonances and gearings

The template for a coupling coefficient is:

$$D = \frac{1}{\sqrt{A^2 + B\,\pi^2 + C}}\,.$$

where each term on the right-hand side represent a length, and one of the coefficients B and C is negative. They are evaluated by simple division for D_e (12) and D_α (13) after their values are fit to experimental data (leptons masses). Note that α (14) is computed differently but the same method would hold, and D_p (10) is first logically deduced, and then verified by computing the Planck mass from (11).

Examination of the four coupling formulas shows identical and look-alike coefficients in distinct places; the same component appears sometimes as a straight line (in A), sometimes in the rotation (in B), and sometimes in C which, at least in α, is the inverse of a rotation length from which the term π^2 at the denominator is removed. Then each coupling represents a specific piece or view of a unique movement, where (part of) the movement has a numerically isolated effect; and this requires identification. Firstly:

— The term $275 = (137 + 1/2)\times 1/2$ in α (14) represents the same "physical object" as in 275 + 19 in D_α (13). I shall not give a definition of "physical object".

— This same term 275 + 19 in D_α represents the same "physical object" as 274 + 19 in D_e (12).

— The increment $274 \to 275$ is found to come from the round trip of the electron around the proton when computing α in [2].

Here the same object represented by 274 can be seen as a piece of rotation (when multiplied by π^2), a part of a simple length, and of an inverted length. Therefore it is irrelevant to believe in distinct "forces". The coupling system above is a single movement, a unique clockwork and each coupling is a length seen from a specific perspective.

Secondly, the same term 137 is in α (14) and D_p (10). It also represents a single "physical object".

— So 274 and 137 are the bottom line of the couplings - but we have 19 associated to 274 as a kind of excess.

— The excess may be understood as a mutual interaction between D_p and D_e; the former requiring 19 rotations of negative length (like a shortcut), meaning that the length 137 is reduced by the excess in 274 + 19 - and/or conversely.

Thirdly, by extension, all the terms 19, 19π, and $-19\pi^2$ also refer to a "single object".

Finally, the gearing components are three cube differences 1, 7, and 19 in α (14), D_e (12), and D_p (10) respectively, that is to say in the fundamental field; D_α is not fundamental and the exception to this rule.

This being said, the term $19 - 1$ at the denominator in D_e (12) is of high interest because like for the $1/275$ in α it must be understood as a rotation where the $1/\pi^2$ is removed, hence we should read $19\pi^2 - 1\pi^2$. Therefore, by the same identifications, it means that the term π^2 in α (14) is subtracted from $19\pi^2$ in D_p (10). Together with the terms 137 in the same formulas, this is more than a connection between the fundamental field and electromagnetism. It can be said that the coupling D_e has the role of "flushing" π^2, and then α out of the fundamental field - hence a single movement.

On the practical grounds of testability and technology, those two coefficients are very important outputs; because anything that we can do with electromagnetic forces has a corresponding effect in the fundamental field where, obviously, D_p is a very strong share of the unified super-force. We discuss the geometry of couplings that include a gearing, that is to say a simple clockwork which it is necessarily reversible. So I'll bet that the fundamental field, which is not gravity and actually much stronger than electromagnetism, can be manipulated... with electrons.

3.2 Resonances and couplings

The coherence between the coupling coefficients and the particles resonances is very impressive, to begin with the rotation terms in D_e and D_p, namely $-19\pi^2$ and $7\pi^2$:

— Quarks masses as computed in Table 2 depend on a single variable number N, which values are in {2, 19/7, 7, 14, 19, 38} and therefore only combine 2, 7, and 19.

— The ratio of the resonance term N is 2 between the charm and strange on the one hand, and the top and bottom on the other hand. It is interesting that it is also the ratios of their electric charge.

— Bosons resonances also depend only on 2, 7, and 19 for K but also for N = P = 12 = 19-7.

— A high term $266 = 2\times7\times19$ appears twice; to compute the bosons' little k and to compute the Planck mass. We logically assume that it is the simplest expression of the unified super-force.

— Finally, even though this is a little less direct, the leptons resonances in Table 1 can be written 5 = 7-2 for the muon, and 9 = 7+2 for the tau - thus combining a radial resonance 2 of the electron with the rotation term of D_e.

The second aspect is given in the equations (8) and (9) with the sums $\Sigma_{N,P} = 137$ and $\Sigma_K = 274$. It probably means that the SM field is complete and that there is no other particles to discover (except of course if more resonances exist with the same numbers). As mentioned before, my interpretation is that the SM massive particles spectrum is a set of dual sub-harmonics of the Planck mass. But interestingly, for two reasons, the Planck mass is not a particle:

— Firstly, $D_p^4 < D_e/266^2$, where the opposite relation (>) is verified by all particles, as required by the equation.

— Secondly, it combines two couplings instead of one and the resonances (N, P).

I may even give a third reason, which is that in quantum theory it should be the natural unit of mass where the gravitational coupling is 1, which has no reason to be a particle.

4 On the SM fields origin

At this point using the sums $\Sigma_{N,P} = 137$ and $\Sigma_K = 274$, I have deduced the equations (10) and (11) and computed the Planck mass under the assumption that it depends a minima on its sub-harmonics. But there should rather be a physical reason for the sub-harmonics to depend on the Planck mass, otherwise the construction seems absurd. Hence the next question: Can we find a *physical* origin to the SM particles spectrum in the Planck mass equations without knowing the dual sub-harmonic system and its components (i.e. the sums to 137 and 274)? To solve this question we shall assume the Planck mass equation (11) and the values of D_e and D_p with infinite precision.

Here the theoretical situation is unique and rather fantastic, because everything in the field now depend on two quantities: D_p and D_e. In effect, the adjacent field and α are flushed out of the fundamental field defined by those two quantities. In principle we have reached the bottom and the only way to create a resonance is by combining D_p and D_e; as said this unique and fantastic. But how do we get the SM spectrum? and why should we get it?

The Planck mass in (11) includes two ringing lengths D_p^4 and $D_e/266^2$. It is a resonant system from which we know very little but: a) a resonance implies perfectly balanced oscillating "forces" and b) since this is GR we can guess that either M_p defines the light cone or, at the opposite, that the light cone defines it. So assume that the ringing lengths are the effects of a single "force" that rests on the light cone; it splits in two components which are necessarily space (3D) and time (1D) and correspond to the coefficients D_p^4 and $D_e/266^2$ respectively. Those are orthogonal and simple projections, proportional to the sine and cosine of the "force" amplitude, so we have a physical angle ϕ:

$$\phi = \arctan\left(\frac{D_e}{266^2 \times D_p^4}\right) = 1.33509... \approx \frac{4}{3}\,. \qquad (17)$$

But now by construction of the equation we compare a simple 3-volume associated to D_p^4 to a length associated to $D_e/266^2$.

Since the Planck mass equation uses D_e and $K > 0$, it rings like a lepton of spin 1/2, and then a change in phase π of this resonance is associated to one unit of volume $4\pi/3$; and since this is the Planck mass, this change in phase also defines the units of time and length. Hence comparing the effect of the "force" (the change in phase) to the volume to which the "force" applies (the unit of volume) we get a ratio:

$$\psi = \frac{\left(\frac{4\pi}{3}\right)}{\pi} = \frac{4}{3} \tag{18}$$

which is *almost equal* to ϕ in (17) where the volume corresponds to D_p^4 and the change in phase to the length $D_e/266^2$. This ratio is expressed in unit of m^3/rad, and it links the phase of quantum theory to the volume of the mass equation. But *almost equal* means a difference where a perfect match is mandatory: now the difference $\phi - \psi$ is significant! We need a physical correction to (17) that gives exactly 4/3 and does not modify the Planck mass. And since we have reached the bottom, there is nothing else remaining but D_p and $D_e/266^2$ to implement the correction. Hence:

1) All we can do is add in (17) more currents of type D_p interfering with $D_e/266^2$, giving a suite of $h_i\, D_p^i\, D_e/266^2$, with h_i a harmonic coefficient.

2) The field is entirely defined by the particles resonances, including all charges, masses, etc, then each h_i should be a known term that we can recognize.

3) The suite of h_i should also include the mass-less field, and all resonances that we do not know of.

Then from the point 1) above, and in coherence with the two others, the correction has a very simple form:

$$4/3 = \arctan\left(\frac{D_e \sum_{i=0}^{\infty} h_i\, D_p^i}{266^2 \times D_p^4}\right), \tag{19}$$

with $h_0 = +1$ for the Planck mass.

Now we want to solve this equation, and for this we have a few criteria enabling to proceed by successive approximation on i growing ($i = 1$, then $i = 2$, etc...):

a) As a must, since $D_p \approx 1/137$, we expect a gain at order i of roughly two decimals compared to the order $i - 1$.

b) As a guideline, the result should be natural and then the effect of the correction at order i should be in the range of the optimum - but not equal. The optimum at order i being the value of h_i where the equality is verified with $h_j = 0$ for $j > i$.

c) As a result, each h_i should represent resonance(s). Here we can safely recognize what we know.

On this basis, the interesting part is for $0 < i < 8$:

— $h_1 = -1$,

— $h_2 = -7$,

— $h_3 = +25$,

— $h_4 = -81$,

— $h_5 = +(7 + 14 + 19 + 38 + \frac{38}{19} + \frac{14}{7} + \frac{38}{14} + \frac{19}{7}) \times 2\pi$,

— $h_6 = -556 = -(137 \times 4 + 8)$,

— $h_7 = -216 = -144 \times \frac{3}{2}$,

As we shall see this suite includes the entire SM particles spectrum.

The relative distance of each h_i to the optimum is given in Table 5 for each step.

Table 5: Optimum vs h_i value.

Order	Value	Δ vs optimum
h_1	1	$< 6\%$
h_2	7	$< 2.5\%$
h_3	25	$< 2.5\%$
h_4	81	$< 5\%$
h_5	≈ 549.33	$< 0.8\%$
h_6	556	$< 0.3\%$
h_7	216	$< 0.3\%$

The difference with 4/3 is now $\approx 3 \times 10^{-16}$, which is in the expected range for i=7, and each h_i is close to the optimum. The connection of this series to the particles resonances in Tables 1, 2, and 3 and to the SM spectrum is almost trivial:

a) At first we find the Muon and Tau products NP (25 and 81) from Table 1, for i = 3 and i = 4 respectively. One could wonder why we are not closer to the optimum; but recall the constraint N=P for these resonances (see [1]). In both cases, we have the closest square to the optimum.

b) Then at i=5 the sum of all quarks circular resonances multiplied by 2π (- meaning that each number here represents a resonance length or its inverse). It includes, and then confirms, the fractional resonance as guessed in [1] and recalled in section 2.1 following Table 2. Here the optimum is ≈ 554, but considering the factor 2π, the relevant part is less than 1 point away from its optimum.

c) For i=7 we find the product NP=144 of the bosons double circular resonances, but multiplied by 3 (for 3 bosons) and divided by 2 (possibly because it should be divided by 2π, but those masses are already divided by π in (2)).

d) It leads to understanding the other terms as it must include also the SM mass-less particles as resonances of coefficient 1 *, to which the mass equation does not apply:

— $h_1 = -1$, the photon,

— $h_2 = -7 = -(4 + 3)$, by similarity with h_3, h_4, and quarks'sum h_5, it splits into the electron NP=4 plus 3 mass-less neutrinos,

— $h_6 = -(137 \times 4 + 8)$, the expected UFO, 137 with 4 resonances, plus 8 mass-less gluons.

Finally, we have found all the resonances in N and P of the Tables 1, 2, and 3 (except for 3), but we also find $K \approx i$:

— $h_2 \rightarrow$ electron, $K = 2$ (Tables 1 and 4).

— $h_3 \rightarrow$ muon, $K = 3$ (Tables 1 and 4).

*Like a photon can be seen to ring 1 to 1 in E and B in Maxwell theory

— $h_4 \rightarrow$ tau, $K = 4$ (Table 4) and $K = 5$ (Table 1).

— $h_5 \rightarrow$ quarks, $K = -6$ (Table 2).

— $h_6 \rightarrow$ no known massive particles.

— $h_7 \rightarrow 2 \times 7 \times 19$, bosons' K in {-2, -7, -19} (Table 3), but also from $1/266^2$.

Here we have a perfect ordering and some interesting aspects emerge:

a) We notice that with h_4 the tau is exceptional; firstly it takes two K (one in the fundamental field and one in the adjacent field) and coincidentally, it is here that the D_p^i at the numerator of (19) cancels the D_p^4 at the denominator.

b) Identically, it is with the next coefficient, when $i > 4$, that the Ks become negative (quarks and bosons). So we have a clear border which is between h_4 and h_5.

c) This is also where the fine structure constant appears in the Ds for quarks and bosons.

d) The second exception is the bosons $266 = 2 \times 7 \times 19$ used in Σ_K; it is coherent with the term $1/266^2$.

So we see *why and how* the SM spectrum is there; it shows that this theory is not another parametric model. Here the Planck mass, space-time, and the SM spectrum are neither independent nor separable, but three aspects of the same unity. Incidentally, it also shows that the expressions giving D_p and D_e are exact at least up to the 15^{th} decimal.

But now, this leads to a few obvious deductions, some of which can be tested:

1) Three neutrino, no more,

2) Three charged lepton, no more,

3) Neutrinos ranks with the electron in h_2, which means something very odd in the field symmetry (or symmetries),

4) No quark of higher mass (than the top),

5) Quarks mixing disagree with the standard concept as we have 8 physical resonances but only 6 masses,

6) No additional boson (i.e. a single Higgs, no Z'),

7) One new resonance, 137, ranking with gluons in h_6.

The resonance 137 corresponds to $\Sigma_{N,P} = 137$ as the full massive matter field resonance; but locally, it could also be a kind of mass-less monopole à la Lochak [5] carrying the matter field signature. It comes in 4 instances, like this monopole, and it is consistent with the fourth power of D_p in (11).

5 Scale symmetry and compatibility with GR

The mass equation depends linearly on the inverse of a volume at the denominator (initially a volume at the numerator); then if we simply apply the metric variations in the gravitational field to this volume, the equation is obviously incompatible with Einstein's theory of general relativity. But GR assumes that particles *have* mass, which we know is wrong; and also, on the basis of the previous section, we can mean that this incompatibility is certainly due to the incompleteness of GR and even SR - think of the Planck mass relations to a) the light cone, b) the units of length/time and volume, and c) the SM particles spectrum. So let us come back to the origin of the equation as shown in [1] and find *how* it can be compatible with GR already.

I start in 1 dimension and consider 2 identical propagating waves crossing each other, giving:

$$m = X N^2 , \tag{20}$$

with N an integral number representing the number of oscillations crossing each other within a generic length "1", and X a constant of unit kg.m^{-1}. So the N^2 represents a length (or $1/N^2$ an inverted length). But for a resonance to exist we need a mirror which is not part of the resonance but has energy:

$$m = X N^2 + \mu , \tag{21}$$

Then I add the quantized length K D, repeated each time two oscillations cross:

$$m = \frac{X}{\frac{1}{N^2} + KD} + \mu , \tag{22}$$

with K an integral number and D a constant of unit m^{-1}. Finally, in 3 dimensions I take the cube and get the inverse of a volume at the denominator:

$$m = \frac{X}{\left(\frac{1}{NP} + KD\right)^3} + \mu , \tag{23}$$

where the unit of X changes to kg.m^{-3}, and $N^2 \rightarrow NP$, where N and P are two integral that may be different since we now also have a rotational degree of freedom. Hence this equation is incompatible with GR by construction. But now in [3], I found the equations (15) and (16) which imply that all relevant densities evolve like $\Lambda \sim 1/R_U^2$; *and then the density X follows the same law*, that is:

$$X = \frac{const.}{R_U^2} . \tag{24}$$

Here there is no absolute length and the only reference length to consider is R_U; the hypothetical length "1" introduced in (20) is then $\sim R_U$, the volume at the numerator of (1) and (2) is $\sim R_U^3$, and then mass is proportional to $R_U^3/R_U^2 = R_U$. Provided the universe does not create particles permanently, this is the hypothesis in [3]; so the equation is a fit with my results in cosmology.

In addition it is now evident *how* the mass equation is compatible with GR, because if we vary the position of a particle in the gravitational field, its wavelength also varies and it will "see" R_U in reverse proportions to this variation: the lesser (resp. the higher) a particle energy in the gravitational field, the longer (resp. the shorter) is wavelength for a given observer, the lesser (resp. the higher) the universe age ($R_U = c\,T$) it "see". Hence a beautiful symmetry of scale which applies only to massive particles and shows the universality of the result: at any place and any epoch, a particle rest mass is proportional to the universe age it locally sense with Λ or dark energy.

6 The fine structure constant

Firstly what is it? In QED, it is the probability for an electron to absorb or emit a virtual photon. But here it is computed in [3] as a relative length that depends on the electron resonance, its spin, and $\Sigma_{N,P} = 137$. As per (14) it includes:

- An amplitude 2/137, where 137 is the sum of all massive particles resonances except the up and down quark. Then the electron is 2/137 parts of the field.

- Spin 1/2 gives π^2, half a turn for one unit of 137, but also $275 = (137 + 1/2) \times 2$, where the spin appears as the factor 2 to get a full turn 2π; the term 1/2 is geometrical.

- An additional component 1/4 which corresponds firstly to the muon resonance 8 in Table 4 (giving $(137 + 1/2) \times 8$), but also I believe to the compositeness of the electron (in the form of 2 distinct currents).

So α is firstly how much the electron gears the field, how much it contributes to the field resonance; its share of the job; and not the opposite like in QED. This interaction is permanent, and not a probability. So, with respect to QED and its methods of calculus, what difference does it make? Absolutely none as long as symmetry remains. The field can even fluctuate, randomly or not.

Secondly, where is it? The answer is not obvious since we have only two harmonics of Table 4 in the expression (14) giving α, and nothing about it in Table 1. But we also have the sum $\Sigma_{N,P} = 137$ and the equation (7) linking μ and μ_α which is also based on π and 137. This link does not use X or X_α, so we can guess that α is in their difference. Since it is unit-less let us compute:

$$\frac{X + X_\alpha}{X - X_\alpha} \approx 131\,, \tag{25}$$

which we find in the expected range. Trying to invert the angle μ/μ_α in (7) to complement the clockwork, I eventually found an expression that holds at about $5\,10^{-9}$ with:

$$\frac{2\pi\,(X + X_\alpha)}{X\,(1-\alpha) - X_\alpha\,(1+\alpha)} = 137^2 - 137\,\pi + \frac{2}{137.5}\left(1 + \frac{1}{4}\right), \tag{26}$$

which is symmetrical in X, X_α, and α. From the reasoning in the previous sections and the form of this expression, it looks like this quantity represents the remainder of D_p^2 once α has been flushed out of the fundamental field.

7 Conclusion

I think I have shown that talking *free* parameters is blunt lie. I think I have also shown that piling up ad-hoc quantum fields to match anything is not such a great idea. Here the field is unique and its parameters are structurally coherent from α to Z^0 (necessarily including all other useful letters in between, even though I miss a few). It has the beauty of self definition, of self generation, and above all that of the necessarily unique: here there is only one, not even two. No two things of different nature; no particles "in" space. No vibrating thingy but only paths and dimensions - and then structures appear naturally by geometrical necessity; only structures from constraint, no freedom. How could it be less?

8 Addendum: what next?

Since the fit in section 4 is not perfect and despite the fact that the sets of {N, P} and {K} seem complete from the sums $\Sigma_{N,P}$ and Σ_K, we may try to continue the sequence of h_i and guess more resonances requiring more particles. I shall discuss two cases; I first assume that the SM is complete and as a second case I assume a graviton.

Assume the SM complete; then, following the suite of h_i in section 4 it was easy to fit down to a residual error of 3.88×10^{-43} (which is ridiculous) without introducing new quantities/resonances but only some mixes, inversions, widths, and a few numbers in π. I had to stop here because the h_i are decreasing rapidly down to $h_{17} \approx 0.00052$, which is much smaller than $D_p \approx 0.00734$.

Here is what I first found with possible correspondence:

— $h_8 = 156 = -(137 + 19) = -(144 + 12)$, no comment,

— $h_9 = -(38 + 19 - 1)$, t + b - 1 (Table 2),

— $h_{10} = -(\pi^2)$, geometry,

— $h_{11} = -(12 - 7/12)$, bosons N (Table 3) + 7/12 (new?),

— $h_{12} = -((7 + 1)/(14 + 1))$, (s + 1)/(c + 1) (Table 2),

— $h_{13} = -(3/4)$, inverse of 4/3,

— $h_{14} = -(1 + 1/24)$, W and Z bosons width (4),

— $h_{15} = -(1/7 + 4/(274 + 19 + 1))$, inverse of the rotation of D_e and that of D_α times 8,

— $h_{16} = -(1/(144 \times 6) + 1/((274 + 19) \times (16)))$, Higgs boson width (5) + inverse of D_e main coefficient times 4,

— $h_{17} = -(\pi^2/137^2)$, geometry, maybe from μ/μ_α (7).

It shows that I cannot predict any observable in this manner. But on the other hand, each expression above is so obviously related to a number used elsewhere that I wonder if the series may be right. The Table 6 gives the value or range of each harmonic coefficient and its distance to the optimum at each step. Now not only each harmonic stays close to the optimum, but the h_i seems to quickly converge to zero.

Table 6: Optimum vs h_i value.

Order	Value	Δ vs optimum (%)
h_8	156	< 0.5%
h_9	56	< 0.2%
h_{10}	≈ 9.87	< 0.9%
h_{11}	≈ 11.4	< 0.04%
h_{12}	≈ 0.533	< 1.1%
h_{13}	≈ 0.750	< 1.1%
h_{14}	≈ 1.042	< 0.12%
h_{15}	≈ 0.156	< 0.01%
h_{16}	≈ 0.00137	< 0.3%
h_{17}	≈ 0.000526	< 0.7%

Now assume a graviton; it requires to add a resonance "1", and the first place that makes sense is to add a massless boson in h_7 with: $h_7 = -217 = -(144 \times \frac{3}{2} + 1)$, and it can represent either the graviton or the photon (if misplaced in h_1); the residual error at order 7 is $< 4\,10^{-17}$ (instead of $3\,10^{-16}$) and its distance to the optimum is $< 0.06\%$. Then $h_8 \approx -(2\pi^2 + \frac{1}{\pi})$, with a residual error $< 7.5\,10^{-20}$ and a distance $< 0.2\%$ to the optimum. The terms in h_8 address 4-geometry with $2\pi^2$ the surface of a 4-sphere of radius unity, and the inverse of a change in phase π.

Submitted October 11, 2018

References

1. Consiglio J., On Quantization and the Resonance Paths. *Progress in Physics*, 2016, v. 12(3), 259–275.
2. Consiglio J., Take Fifteen Minutes to Compute the Fine Structure Constant. *Progress in Physics*, 2016, v. 12(4), 305–306.
3. Consiglio J., Are Energy and Space-time Expanding Together? *Progress in Physics*, 2017, v. 13(3), 156–160.
4. The Plank Collaboration. Planck 2015 results. I. Overview of products and scientific results. arXiv: 1502.01582.
5. Georges Lochak. The symmetry between Electricity and Magnetism and the equation of a leptonic Monopole. 2007, http://arxiv.org/abs/0801.2752

On the Cosmological Significance of Euler's Number

Hartmut Müller

E-mail: hm@interscalar.com

The paper derives and exemplifies the stabilizing significance of Euler's number in particle physics, biophysics, geophysics, astrophysics and cosmology.

Introduction

Natural systems are highly complex and at the same time they impress us with their lasting stability. For instance, the solar system hosts at least 800 thousand orbiting each other bodies. If numerous bodies are gravitationally bound to one another, classic models predict long-term highly unstable states [1, 2]. Indeed, considering the destructive potential of resonance, how this huge system can be stable?

In the following we will see that the difference between rational, irrational algebraic and transcendental numbers is not only a mathematical task. It is also an essential aspect of stability in complex systems.

Actually, if the ratio of any two orbital periods would be a rational number, periodic gravity interaction would progressively rock the orbital movements and ultimately cause a resonance disaster that could destabilize the solar system. Therefore, lasting stability in complex dynamic systems is possible only if whole number frequency ratios can be avoided.

Obviously, irrational numbers cannot be represented as a ratio of whole numbers and consequently, they should not cause destabilizing resonance interaction [3, 4].

Though, algebraic irrational numbers like $\sqrt{2}$ do not compellingly prevent resonance, because they can be transformed into rational numbers by multiplication. In the case of $\sqrt{2}$ as a frequency ratio, every even harmonic is integer, because $\sqrt{2} \cdot \sqrt{2} = 2$.

However, there is a type of irrational numbers called transcendental which are not roots of whole or rational numbers. They cannot be transformed into rational or whole numbers by multiplication and consequently, they do not provide resonance interaction.

Actually, frequencies of real periodical processes are not constant. Their temporal change is described by accelerations, the derivatives of the frequencies. Naturally, accelerations are not constant either.

Surprisingly, there is only one transcendental number that inhibits resonance also regarding accelerations and any other derivatives: it is Euler's number $e = 2.71828\ldots$, because it is the basis of the natural exponential function e^x, the only function that is the derivative of itself.

In this way, the number continuum provides the solution for lasting stability in systems of any degree of complexity. The solution is given a priori: frequency ratios equal to Euler's number, its integer powers or roots are always transcendental [5] and inhibit destructive resonance interaction regarding all derivatives of the interconnected periodic processes. Therefore, we expect that periodic processes in stable systems show frequency ratios close to integer powers of Euler's number or its roots. Consequently, the logarithms of the frequency ratios should be close to integer 0, 1, 2, 3, 4, ... or rational values $\frac{1}{2}, \frac{1}{3}, \frac{1}{4}, \ldots$

In the following we will exemplify our hypothesis in particle physics, biophysics, geophysics, astrophysics and cosmology. We start with the solar system.

Euler's number stabilizes the solar system

Let us analyze the ratios of the orbital periods of some planets. Saturn's sidereal orbital period [6] equals 10759.22 days, that of Uranus is 30688.5 days. The natural logarithm of the ratio of their orbital periods is close to 1:

$$\ln\left(\frac{30688.5}{10759.22}\right) = 1.05.$$

Jupiter's sidereal orbital period equals 4332.59 days, that of the planetoid Ceres is 1681.63 days. The natural logarithm of the ratio of their orbital periods is also close to 1:

$$\ln\left(\frac{4332.59}{1681.63}\right) = 0.95.$$

Not only neighboring orbits show Euler ratios, but far apart from each other orbits do this as well. Pluto's sidereal orbital period is 90560 days, that of Venus is 224.701 days. The natural logarithm of the ratio of their orbital periods equals 6:

$$\ln\left(\frac{90560}{224.701}\right) = 6.00.$$

In [7] we have analyzed the orbital periods of the largest bodies in the solar system including the moon systems of Jupiter, Saturn, Uranus and Neptune, as well as the exoplanetary systems Trappist 1 and Kepler 20. In the result we can assume that the stability of all these orbital systems is given by the transcendence of Euler's number and its roots.

Euler's number stabilizes biological rhythms

Biological processes are of highest complexity and their lasting stability is of vital importance. Therefore, we expect that established periodical biological processes show Euler frequency ratios. In fact, at resting state, the majority of adults

prefer to breath [8] with an average frequency of 15 inhale-exhale sequences per minute, while their heart rate [9] is close to 67 beats per minute. The natural logarithm of the ratio of these frequencies equals $1+\frac{1}{2}$:

$$\ln\left(\frac{67}{15}\right) = 1.50.$$

Mammals including human show electrical brain activity [10] of the Theta type in the frequency range between 3 and 7 Hz, of Alpha type between 8 and 13 Hz and Beta type between 14 and 34 Hz. Below 3 Hz the brain activity is of the Delta type, and above 34 Hz the brain activity changes to Gamma.

The frequencies 3 Hz, 8 Hz, 13 Hz and 34 Hz define the boundaries. The logarithms of their ratios are close to integer and half values:

$$\ln\left(\frac{8}{3}\right) = 0.98, \qquad \ln\left(\frac{13}{8}\right) = 0.49, \qquad \ln\left(\frac{34}{13}\right) = 0.96.$$

In [11] we have analyzed various biological frequency ranges and assume that their stability is given by the transcendence of Euler's number and its roots.

Euler's number stabilizes the atom

The most stable systems we know are of atomic scale. Proton and electron form stable atoms, the structural elements of matter. The lifespans of the proton and electron surpass everything that is measurable, exceeding 10^{30} years. No scientist ever witnessed the decay of a proton or an electron. What is the secret of their eternal stability?

In standard particle physics, the electron is stable because it is the least massive particle with non-zero electric charge. Its decay would violate charge conservation. Indeed, this answer only readdresses the question. Why then is the elementary electric charge so stable?

In theoretical physics, the proton is stable, because it is the lightest baryon and the baryon number is conserved. Indeed, also this answer only readdresses the question. Why then is the proton the lightest baryon? To answer this question, the standard model introduces quarks which violate the integer quantization of the elementary electric charge.

Now let us proof our hypothesis of Euler's number as universal stabilizer and analyze the proton-to-electron ratio 1836.152674 that is considered as fundamental physical constant [12]. It has the same value for the natural frequencies, oscillation periods, wavelengths, rest energies and rest masses of the proton and electron. In fact, the natural logarithm is close to seven and a half:

$$\ln(1836.152674) = 7.51.$$

This result suggests the assumption that the stability of the proton and electron comes from the number continuum, more specifically, from the transcendence of Euler's number, its integer powers and roots. In [13] we have analyzed the mass distribution of hadrons, mesons, leptons, the W/Z and Higgs bosons and proposed fractal scaling by Euler's number and its roots as model of particle mass generation [14]. In this model, the W-boson mass 80385 MeV/c^2 and the Z-boson mass 91188 MeV/c^2 appear as the 12 times scaled up electron rest mass 0.511 MeV/c^2:

$$\ln\left(\frac{80385}{0.511}\right) = 11.97, \qquad \ln\left(\frac{91188}{0.511}\right) = 12.09.$$

In [15] Andreas Ries did apply fractal scaling by Euler's number to the analysis of particle masses and in [16] he demonstrated that this method allows for the prediction of the most abundant isotopes.

Global scaling based on Euler's number

Our hypothesis about Euler's number as universal stabilizer allows us to calculate Pluto's orbital period from that of Venus multiplying 6 times by Euler's number:

$$\textit{Venus orbital period} \cdot e^6 = \textit{Pluto orbital period}.$$

Each time we multiply by Euler's number, we get an orbital period of a planet in the following sequence: Mars, Ceres, Jupiter, Saturn, Uranus and Pluto. Dividing by Euler's number, we get close to the orbital period of Mercury. Earth's orbital period we get multiplying by the square root of Euler's number. The same is valid for Neptune relative to Uranus.

Euler's number and its roots are universal scaling factors that inhibit resonance and in this way, stabilize periodical processes bound in a chain system. Pluto's orbital period can be seen as the 6 times scaled up by Euler's number orbital period of Venus or as the 3 times scaled up by Euler's number orbital period of Jupiter.

In the same way, the oscillation period of the electron can be seen as the $7 + \frac{1}{2}$ times scaled up oscillation period of the proton. Here it is important to understand that only scaling by Euler's number and its roots inhibits resonance interaction and provides lasting stability of the interconnected processes.

Now we could ask the question: Starting with the electron oscillation period, if we continue to scale up always multiplying by Euler's number, will we meet the orbital period, for instance, of Jupiter?

Actually, it is true. If we multiply the electron natural oscillation period 66 times by Euler's number, we meet exactly the orbital period of Jupiter:

$$\textit{electron oscillation period} \cdot e^{66} = \textit{Jupiter orbital period}.$$

The oscillation period of the electron has a duration of $2\pi \cdot 1.288089 \cdot 10^{-21} s = 8.0933 \cdot 10^{-21}$ s. Jupiter' orbital period takes 4332.59 days = $3.7331 \cdot 10^8$ s. In fact, the natural logarithm of the ratio of Jupiter' orbital period to the electron oscillation period equals 66:

$$\ln\left(\frac{3.7331 \cdot 10^8\ \text{s}}{8.0933 \cdot 10^{-21}\ \text{s}}\right) = 66.00.$$

PROPERTY	ELECTRON	PROTON
rest energy E	0.5109989461(31) MeV	938.2720813(58) MeV
rest mass $m = E/c^2$	$9.10938356(11) \cdot 10^{-31}$ kg	$1.672621898(21) \cdot 10^{-27}$ kg
blackbody temperature $T = E/k$	$5.9298446 \cdot 10^{9}$ K	$1.08881 \cdot 10^{13}$ K
angular frequency $\omega = E/\hbar$	$7.763441 \cdot 10^{20}$ Hz	$1.425486 \cdot 10^{24}$ Hz
angular oscillation period $\tau = 1/\omega$	$1.288089 \cdot 10^{-21}$ s	$7.01515 \cdot 10^{-25}$ s
angular wavelength $\lambda = c/\omega$	$3.8615926764(18) \cdot 10^{-13}$ m	$2.103089 \cdot 10^{-16}$ m

Table 1: The basic set of physical properties of the electron and proton (c is the speed of light in a vacuum, $\hbar$ is the reduced Planck constant, k is the Boltzmann constant). Data taken from Particle Data Group [12]. Frequencies, oscillation periods, temperatures and the proton wavelength are calculated.

Forming atoms and molecules, proton and electron are substantial components of biological organisms as well. Through scaling, Euler's number stabilizes biological processes down to the subatomic scales of the electron and proton. Dividing the angular frequency of the electron 48 times by Euler's number, we get the average adult human heart rate:

$$electron\ angular\ frequency\ /\ e^{48} = adult\ human\ heart\ rate.$$

In fact, the natural logarithm of the ratio of the average adult human heart rate 67/min to the electron angular frequency (tab. 1) equals -48:

$$\ln\left(\frac{67/60}{7.763441 \cdot 10^{20}}\right) = -48.00.$$

In a similar way, dividing the angular frequency of the proton 57 times by Euler's number, we get the average adult human respiratory rate:

$$proton\ angular\ frequency\ /\ e^{57} = adult\ respiratory\ rate.$$

In fact, the natural logarithm of the ratio of the average adult human resting respiratory rate 15/min to the proton angular frequency (tab. 1) equals -57:

$$\ln\left(\frac{15/60}{1.425486 \cdot 10^{24}}\right) = -57.00.$$

Through scaling by Euler's number, systemically important processes of very different scales avoid resonance. In [17] we have shown how the metric characteristics of biological systems are embedded in the solar system and prevented from destructive proton and electron resonance through scaling by Euler's number.

The exceptional stability of the electron and proton predestinates them as the forming elements of baryonic matter and makes them omnipresent in the universe. Therefore, the prevention of complex systems from electron or proton resonance is an essential condition of their lasting stability.

This uniqueness of the electron and proton predispose their physical characteristics (tab. 1) to be treated as natural metrology, completely compatible with Planck units. Originally proposed in 1899 by Max Planck, they are also known as natural units, because they origin only from properties of nature and not from any human construct. Natural units are based only on the properties of space-time.

Max Planck wrote [18] that these units, "regardless of any particular bodies or substances, retain their importance for all times and for all cultures, including alien and non-human, and can therefore be called natural units of measurement".

If now we express Jupiter's body mass in electron masses, we can see how Euler's number prevents Jupiter from destructive electron resonance. In fact, the logarithm of the Jupiter-to-electron mass ratio is close to the integer 132:

$$\ln\left(\frac{1.8986 \cdot 10^{27}\,\mathrm{kg}}{9.10938 \cdot 10^{-31}\,\mathrm{kg}}\right) = 131.98.$$

As we have seen already, the natural logarithm of the ratio of Jupiter's orbital period to the electron oscillation period equals 66 that is 132/2.

The same is valid for Venus. The natural logarithm of the ratio of Venus' orbital period 224.701 days = $1.9361 \cdot 10^7$ s to the electron oscillation period is close to the integer 63:

$$\ln\left(\frac{1.9361 \cdot 10^{7}\,\mathrm{s}}{8.0933 \cdot 10^{-21}\,\mathrm{s}}\right) = 63.04.$$

At the same time, the logarithm of the Venus-to-electron mass ratio is close to the integer 126 that is $2 \cdot 63$:

$$\ln\left(\frac{4.8675 \cdot 10^{24}\,\mathrm{kg}}{9.10938 \cdot 10^{-31}\,\mathrm{kg}}\right) = 126.01.$$

For Jupiter and Venus, now we can write down an equation that connects the body mass M with the orbital period T:

$$\left(\frac{T}{\tau_{\,electron}}\right)^2 = \frac{M}{m_{\,electron}}.$$

In [19, 20] we have shown that mass-orbital scaling arises as a consequence of macroscopic quantization in chain systems of harmonic quantum oscillators and can be understood as fractal equivalent of the Hooke's law. Saturn's moon system demonstrates square root mass-orbital scaling for one and the same body, like in the case of Jupiter and Venus. The moon systems of Jupiter and Uranus show, that mass-orbital scaling can be valid also for couples of different bodies. This may mean that the orbital period of a given body is not always a function of its own mass, but depends on the mass distribution in the whole system.

In [21] we have shown how global scaling by Euler's number determines the masses, sizes, orbital and rotation periods, orbital velocities and surface gravity accelerations of the largest bodies in the solar system.

Not only the bodies of Jupiter and Venus are prevented from destructive electron resonance, but the Sun as well. In fact, the logarithm of the Sun-to-electron mass ratio is close to the integer 139:

$$\ln\left(\frac{1.9884 \cdot 10^{30}\,\mathrm{kg}}{9.10938 \cdot 10^{-31}\,\mathrm{kg}}\right) = 138.94.$$

In this way, the body mass of Jupiter is the 7 times scaled down by Euler's number body mass of the Sun. The body masses of Neptune and Uranus appear as the 3 times scaled down by Euler's number body mass of Jupiter.

Scaling down by Euler's number another 3 times, we get the body mass of Venus. Again scaling down by Euler's number 2 times, we get the body mass of Mars. Scaling down by Euler's number 4 times, we get the body mass of Pluto, then dividing always by Euler's number we get the body masses of Haumea and Charon.

In [22] we did show that global scaling by Euler's number can be seen as stabilizing mechanism of planetary atmospheres that determines their stratification. In [23,24] we have applied scaling by Euler's number in engineering and developed methods of resonance inhibition and stabilization in ballistics, aerodynamics and mechanics.

Euler's number stabilizes the universe

Having analysed the solar system, now we venture into more distant regions of the Milky Way. However, we have to consider that distance measurement by parallax triangulation is precise enough only up to 500 light years. With the increase of the distances, indirect methods are applied blurring the difference between facts and model claims.

Currently there is no precise measurement of the distance to the Galactic Center, but 26,000 light years = $2.46 \cdot 10^{20}$ m seems an accepted estimation [25]. The natural logarithm of this distance divided by the proton wavelength (tab. 1) is close to the integer 83:

$$\ln\left(\frac{R_{\mathrm{GC-Sun}}}{\lambda_{\mathrm{proton}}}\right) = \ln\left(\frac{2.46 \cdot 10^{20}\,\mathrm{m}}{2.103089 \cdot 10^{-16}\,\mathrm{m}}\right) = 83.05.$$

If the current measurement is correct, it would mean that the solar system orbits the Galactic Center at a distance that avoids resonance interaction with it. Good for us.

The Andromeda galaxy M31 seems to be at a distance of 2.5 million ly = $2.365 \cdot 10^{22}$ m [26] away from the Milky Way (MW). The natural logarithm of this distance divided by the electron wavelength (tab. 1) is close to the integer 80:

$$\ln\left(\frac{R_{\mathrm{MW-M31}}}{\lambda_{\mathrm{electron}}}\right) = \ln\left(\frac{2.365 \cdot 10^{22}\,\mathrm{m}}{3.861593 \cdot 10^{-13}\,\mathrm{m}}\right) = 80.10.$$

For reaching the island of stability that corresponds with the integer logarithm 80, the M31-to-MW distance has to decrease by 240,000 ly down to 2.26 million light years:

$$\lambda_{\mathrm{electron}} \cdot e^{80} = 2.26 \cdot 10^{6}\ \mathrm{ly}.$$

They seem to do exactly this. M31 is approaching (more precisely, 2.5 million years ago was approaching) the Milky Way at about 100 kilometers per second, as indicated by blueshift measurements [27]. If this velocity is constant, the current distance to M31 should be already 1,000 light years shorter than the 2.5 million years old distance we can measure today.

Standard model calculations expect that both galaxies will collide in a few billion years [27]. Considering the stabilizing function of Euler's number, we expect that after reaching the integer logarithm 80, the approach will be finished and the distance between both galaxies will be stabilized at 2.26 million light years. In this way, the consideration of Euler's number as resonance inhibitor and universal stabilizer can modify predictions completely.

The cosmic microwave background radiation (CMBR) is traditionally interpreted as a remnant from an early stage of the observable universe when stars and planets didn't exist yet, and the universe was denser and much hotter. Admittedly, there are alternative models [28] in development proposing explanations for the CMBR which do not implicate standard cosmological scenarios. However, traditionally CMBR data is considered as critical to cosmology since any proposed model of the universe must explain this radiation.

If this cosmic background process is stable, its average temperature 2.725 Kelvin [29] should correspond with an integer power of Euler's number. In fact, the CMBR-to-proton blackbody temperature ratio is close to the logarithm -29:

$$\ln\left(\frac{\mathrm{T}_{\mathrm{CMBR}}}{\mathrm{T}_{\mathrm{proton}}}\right) = \ln\left(\frac{2.725\ \mathrm{K}}{1.08881 \cdot 10^{13}\ \mathrm{K}}\right) = -29.01.$$

In this way, the cosmic background seems to be stable, and the current temperature of the CMBR is not accidental.

We assume that global scaling by Euler's number stabilizes the whole universe [30], from the atoms up to the galaxies and the intergalactic space. In this case, any linear (non-logarithmic) observation of very large-scale structures will

discover a scaling-up-effect that appears as exponential expansion of the universe. At the same time, any linear observation of very small-scale structures will discover a scaling-down-effect that appears as exponential compression down to an apparent spacetime singularity.

Conclusion

The consideration of Euler's number as resonance inhibitor and universal stabilizer adds a new aspect to our comprehension of the evolution of the universe, explaining not only the stability of the solar orbital system, but also the stability of its trajectory through the galaxy.

On the example of the M31-MW approach we demonstrated how the consideration of Euler's number as stabilizer can modify predictions completely. Applying global scaling by Euler's number to planetary systems, we can identify stabilized astrophysical processes and predict the evolution of systems that are still in formation.

We have shown that the current cosmic background temperature is not accidental and manifests the cosmological significance of Euler's number as well.

Stabilizing the proton-to-electron ratio, Euler's number provides the formation of atoms. Euler's number stabilizes biological frequency ranges down to the subatomic scale and embeds them in the dynamics of the solar system.

Finally, the apparent expansion of the universe could turn out to be a compelling consequence of the stabilizing role of Euler's number and its integer powers.

Acknowledgements

The author is grateful to Viktor Panchelyuga, Dmitri Rabounski, Yuri Vladimirov, Dmitri Pavlov, Oleg Kalinin, Alexey Petrukhin and Leili Khosravi for valuable discussions.

Submitted on November 29, 2018

References

1. Heggie D. C. The Classical Gravitational N-Body Problem. arXiv: astro-ph/0503600v2, 11 Aug 2005.
2. Hayes B. The 100-Billion-Body Problem. American Scientist, v. 103, no. 2, 2015.
3. Dombrowski K. Rational Numbers Distribution and Resonance. *Progress in Physics*, 2005, v. 1, no. 1, 65–67.
4. Panchelyuga V.A., Panchelyuga M. S. Resonance and Fractals on the Real Numbers Set. *Progress in Physics*, 2012, v. 8, no. 4, 48–53.
5. Hilbert D. Über die Transcendenz der Zahlen e und π. *Mathematische Annalen*, 1983, v. 43, 216–219.
6. Astrodynamic Constants. JPL Solar System Dynamics. ssd.jpl.nasa.gov (2018).
7. Müller H. Global Scaling of Planetary Systems. *Progress in Physics*, 2018, v. 14, 99–105.
8. Ganong's Review of Medical Physiology (23rd ed.), p. 600.
9. Spodick D. H. Survey of selected cardiologists for an operational definition of normal sinus heart rate. *The American J. of Cardiology*, 1993, vol. 72 (5), 487–488.
10. Tesche C. D., Karhu J. Theta oscillations index human hippocampal activation during a working memory task. *PNAS*, vol. 97, no. 2, 2000.
11. Müller H. Chain Systems of Harmonic Quantum Oscillators as a Fractal Model of Matter and Global Scaling in Biophysics. *Progress in Physics*, 2017, v. 13, 231–233.
12. M. Tanabashi et al. (Particle Data Group), Phys. Rev. D 98, 030001 (2018), www.pdg.lbl.gov
13. Müller H. Fractal Scaling Models of Natural Oscillations in Chain Systems and the Mass Distribution of Particles. *Progress in Physics*, 2010, v. 6, 61–66.
14. Müller H. Emergence of Particle Masses in Fractal Scaling Models of Matter. *Progress in Physics*, 2012, v. 8, 44–47.
15. Ries A. Qualitative Prediction of Isotope Abundances with the Bipolar Model of Oscillations in a Chain System. *Progress in Physics*, 2015, v. 11, 183–186.
16. Ries A. Bipolar Model of Oscillations in a Chain System for Elementary Particle Masses. *Progress in Physics*, 2012, vol. 4, 20–28.
17. Müller H. Astrobiological Aspects of Global Scaling. *Progress in Physics*, 2018, v. 14, 3–6.
18. Max Planck. Über Irreversible Strahlungsvorgänge. *Sitzungsbericht der Königlich Preußischen Akademie der Wissenschaften*, 1899, vol. 1, 479–480.
19. Müller H. Scaling of Moon Masses and Orbital Periods in the systems of Saturn, Jupiter and Uranus. *Progress in Physics*, 2015, v. 11, 165–166.
20. Müller H. Scaling of body masses and orbital periods in the Solar system as consequence of gravity interaction elasticity. // Abstracts of the XII. International Conference on Gravitation, Astrophysics and Cosmology, dedicated to the centenary of Einstein's General Relativity theory. Moscow, PFUR, 2015.
21. Müller H. Scale-Invariant Models of Natural Oscillations in Chain Systems and their Cosmological Significance. *Progress in Physics*, 2017, v. 13, 187–197.
22. Müller H. Global Scaling of Planetary Atmospheres. *Progress in Physics*, 2018, v. 14, 66–70.
23. Müller H. The general theory of stability and objective evolutionary trends of technology. Applications of developmental and construction laws of technology in CAD. Volgograd, VPI, (1987).
24. Müller H. Superstability as a developmental law of technology. Technology laws and their Applications. Volgograd-Sofia, (1989).
25. Groom D. E. et al. Astrophysical constants. *European Physical Journal C*, vol. 15, 1, 2000, www.pdg.lbl.gov
26. Ribas I. et al. First Determination of the Distance and Fundamental Properties of an Eclipsing Binary in The Andromeda Galaxy. arXiv:astro-ph/0511045v1, 2005.
27. Cowen R. Andromeda on collision course with the Milky Way. *Nature.com*, 31 May 2012.
28. Lopez-Corredoira M. Non-standard models and the sociology of cosmology. Science Direct, *Studies in History and Philosophy of Modern Physics*, vol. 46, Part A, May 2014, pp. 86–96.
29. Fixsen D. J. The Temperature of the Cosmic Microwave Background. *The Astrophysical Journal*, vol. 707 (2), 916–920. arXiv:0911.1955, 2009.
30. Müller H. Global Scaling. The Fundamentals of Interscalar Cosmology. *New Heritage Publishers*, Brooklyn, New York, USA, (2018).

Retraction of "Outline of a Kinematic Light Experiment"

Christian M. Wackler

While re-examining the experimental proposal outlined in *Progress in Physics*, 2018, vol. 14, issue 3, pages 152–158, I became aware of a fatal flaw in its theory. A uniformly rotating disk and a light source pulsing at a constant rate cannot serve to determine whether the speed of light depends on the motion of the radiation source. Therefore, I retract the paper. Apologies are expressed to all readers. However, as the preliminary considerations developed in the article remain valid, it is much to be hoped that physicists will tackle the all-important light speed question experimentally.

Editor's comment:

In response to Wackler's retraction, his original article was removed from the journal's online archives. However, the print version of Progress in Physics still contains the original article, since the author solicited retraction after printing.

Submitted on December 15, 2018

Optical Absorption in GaAs/AlGaAs Quantum Well due to Intersubband Transitions

Suleiman B. Adamu[1], Inuwa A. Faragai[2], and Usman Ibrahim[3]

[1,3] Department of Physics, Sule Lamido University Kafin Hausa, P.M.B 048, Jigawa State, Nigeria.
E-mail: Sulbash@gmail.com

[2]Department of Physics, Kano State University of Science and Technology, Wudil, Kano.
E-mail: Ialiyufaragai@yahoo.co.uk

Intersubband transition in quantum wells have strong potential for device application and are challenging field of fundamental studies. In this paper, intersubband optical absorption in GaAs/AlGaAs quantum well is investigated. Using a simple numerical approach and mathematical modeling applied to the first two conduction subbands, simplified expression for the optical absorption is obtained. The results obtained shows that the dephasing and other scattering mechanism have impact on absorption peaks and can only be tolerated to certain limits.

1 Introduction

Since the early years of quantum well studies, intersubband transitions in quantum well (QW) structures have attracted much attention. Both theoretical and experimental investigation were carried out by different researchers [1].

Rybalko et al. [2] proposed new approach to study light absorption in tunnel-coupled GaAs/AlGaAs quantum wells for electro-optic. In addition, Refs. [3] report the investigation of the effect of intersubband optical transitions of the magnetic field and tilt angle. Many physical effects of a semiconductor in quantum well structures have been exploited, such as infrared photodetectors [4, 5]. Furthermore, intersubband transitions in a multiple quantum well (MQW) structures were reported in Refs. [6–8]. Numerical investigation for absorption spectra induced by an ultrafast infrared pulse on the double quantum well structure were studied by Wu [9].

In this paper, we will derive the equation of optical absorption in GaAs/AlGaAs quantum well, by the modified version of Lorentzian approximation that is well proven itself in describing of electronics properties of these semiconductors. The equation obtained will be numerically solved and discussed.

2 Model Equation

We consider an intersubband transition in a P-conduction band $n_{12} = 1, 2$, interacting with photon energy governed by

$$E_n = \frac{n\hbar^2}{2m_e^*}\left(\frac{\pi}{L}\right)^2, \tag{1}$$

where m_e^* is the electron effective mass in the conduction band, L is the length of the quantum well, $\hbar$ is the reduced Planks constant and the transition energy ΔE between the two subbands is obtained from $E_{12} = E_2 - E_1$.
After projection of the photon energy along the dipole moment, the optical absorption coefficient as in Ref. [10] can be written as

$$\alpha(\hbar\omega) = \frac{2\pi\omega}{n_r V c\epsilon_0}\sum_{\vec{k_t}} \mathrm{g}\left(E_b - E_a - \hbar\omega\right)\left|\hat{e}\,\vec{\mu}_{ba}\right|^2 (f_b - f_a), \tag{2}$$

where ω is the frequency of the photon energy, n_r is the refractive index, c is the velocity of light, $\mathrm{g}\left(E_b - E_a - \hbar\omega\right)$ is the line shape function, e the electronic charge, μ_{ba} is the intersubband dipole moment, V is the volume of the entire material, ϵ_0 is the permittivity of the material, f_b and f_a are the carrier densities populating subbands a and b, respectively. We consider numerically calculated transition adjusted to a simple Lorentzian approximation given by

$$\mathrm{g}\left(\Delta E\right) = \frac{1}{\pi}\frac{(\Gamma/2)}{\Delta E^2 + (\Gamma/2)^2}, \tag{3}$$

where Γ is the linewidth. Therefore the modified Lorentzian approximation in terms of photon energy can be written as

$$\mathrm{g}(\Delta E - \hbar\omega) = \frac{1}{\pi}\sum_{1\neq 2}\frac{(\Gamma/2)}{(\Delta E - \hbar\omega)^2 + (\Gamma/2)^2}, \tag{4}$$

where ΔE and $\hbar\omega$ are the transition photons energy between subband $(1, 2)$ and the adjusted frequency, respectively.
However, transition $(2, 1)$ occurs at the top conduction subband corresponds to the highest subband, after photon emission with electrons being annihilated from subband $a = 1$ to $b = 2$. Therefore, setting $(\Delta E - \hbar\omega) = 0$, in (4) one gets

$$\mathrm{g} = \frac{1}{\pi}\frac{1}{(\Gamma/2)}, \tag{5}$$

where Γ is the resulting Lorentzian broadening term, which we refer as dephasing energy in the subbands. Furthermore, the dipole moment is obtained by normalization of the enveloped wavefunction along the quantum well growth direction z, which is due to the electron excitation by the light

beam this can be expressed in the form

$$\mu_{21} = e \int_0^{L_z} \psi_2(z)\, z\, \psi_1(z) dz, \tag{6}$$

where

$$\psi_1(z) = \sqrt{\frac{2}{L_z}} sin\left(\frac{\pi}{L_z} z\right) \tag{7}$$

and

$$\psi_2(z) = \sqrt{\frac{2}{L_z}} sin\left(\frac{2\pi}{L_z} z\right). \tag{8}$$

However, to solve for the intersubband dipole moment we substituted (7) and (8) into (6), we get

$$\mu_{21} = \frac{2e}{L_z} \int_0^{L_z} sin\left(\frac{2\pi}{L_z} z\right) z\, sin\left(\frac{\pi}{L_z} z\right) dz. \tag{9}$$

Integrating eq. (9) simplifies to

$$\mu_{21} = -\frac{16}{9\pi^2} e L_z. \tag{10}$$

Equation (10) is the resulting dipole moment of the quantum well. We will now analyze the absorption coefficient due to intersubband transition in quantum well of GaAs/AlGaAs. Equation (10) lead to the absorption related to absorption coefficient of the intersubband governed by

$$\alpha(\hbar\omega) = \frac{\pi\omega}{n_r\, c\, \epsilon_0} \mathrm{g}\left(\Delta E - \hbar\omega\right) |\mu_{21}|^2 \left(N_2 - N_1\right), \tag{11}$$

where N_1 and N_2 are the population densities of the 1st and 2nd subbands, respectively.

However, when $N_2 = 0$, in which $E_1 < E_F < E_2$ in subband 1, then one finds

$$\alpha(\hbar\omega) = \frac{\pi\omega}{n_r\, c\, \epsilon_0} \mathrm{g}\left(\Delta E - \hbar\omega\right) |\mu_{21}|^2 N_1, \tag{12}$$

which is proportional to doping concentration. Furthermore, with $E_2 < E_F$ in subband 2, then

$$N_1 = \frac{m_e^* k_B T}{\pi\hbar^2 L_z} \ln\left[1 + e^{\left(\frac{E_F - E_1}{k_B T}\right)}\right], \tag{13}$$

where k_B is Boltzmann's constant, T is the temperature and E_F is the Fermi energy. Equation (13), can be simplified to

$$N_1 \approx \frac{m_e^*}{\pi\hbar^2 L_z} \left(E_F - E_1\right), \tag{14}$$

and subsequently,

$$N_2 \approx \frac{m_e^*}{\pi\hbar^2 L_z} \left(E_F - E_2\right). \tag{15}$$

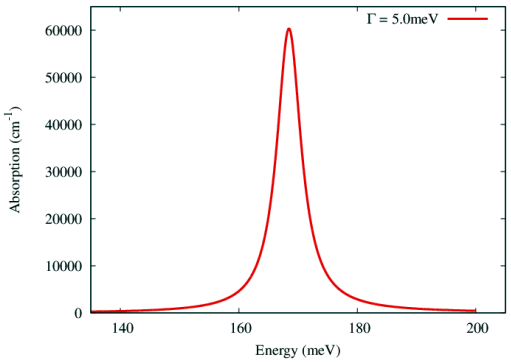

Fig. 1: Absorption spectra as a function of the incident photon energy in GaAs/AlGaAs dephasing energy $\Gamma = 5.0meV$.

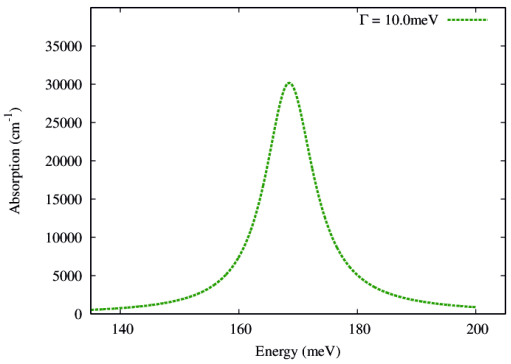

Fig. 2: Absorption coefficient against photon energy with dephasing energy $\Gamma = 10.0$ meV.

Finally, the optical absorption coefficient can be written as

$$\alpha(\hbar\omega) = \frac{\pi\omega}{n_r c \epsilon_0} \mathrm{g}\left(\Delta E - \hbar\omega\right) \left(\frac{16}{9\pi^2} e L_z\right)^2 \tag{16}$$

which is independent of doping concentration. The peak absorption is obtain where $\Delta E = \hbar\omega$ and can be expressed as

$$\alpha_{max}\left(\hbar\omega\right) = \frac{\omega}{n_r c \epsilon_0} \frac{1}{(\Gamma/2)} \left(\frac{16}{9\pi^2} e L_z\right)^2 N. \tag{17}$$

3 Results and Discussion

The result obtained for the absorption coefficient in the quantum well structure is computed and plotted using Equation (16) for 10 Å quantum well width and different dephasing energy. In figure 1, we plotted the optical absorption spectra as a function of photons energy with dephasing energy $\Gamma = 5.0$ meV. Figure 2 - 4 show absorption spectra with dephasing energies $\Gamma = 10.0$, 15.0 and 20.0 meV, respectively. In our result, one could clearly see that the absorption peaks decreases as the different dephasing energies are increase as shown in figure 5.

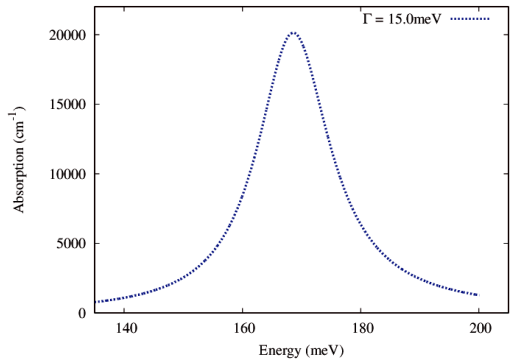

Fig. 3: Absorption coefficient against photon energy with dephasing energy $\Gamma = 15.0$ meV.

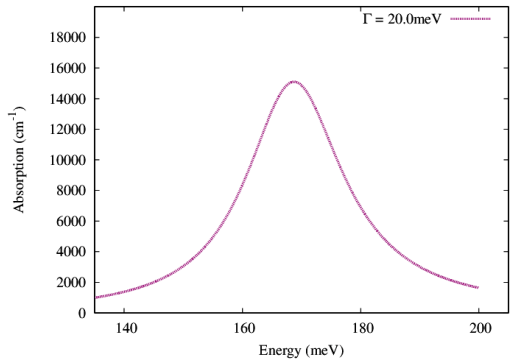

Fig. 4: Absorption coefficient as a function of the photon energy with dephasing energy $\Gamma = 20.0$ meV.

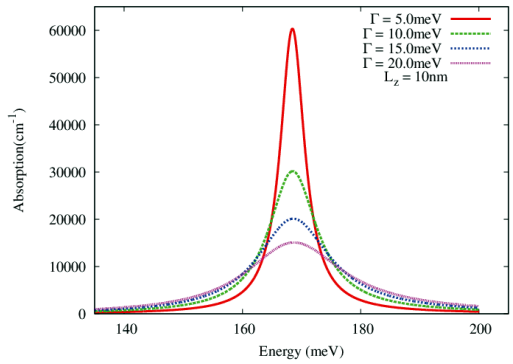

Fig. 5: Absorption coefficient as a function of the photon energy with various dephasing energy $\Gamma = 5.0, 10.0, 15.0$ and 20.0 meV and $L_z = 10$ nm.

4 Conclusion

On conclusion, we have showed the impacts of dephasing mechanism in the study of intersubbands optical absorption in GaAs/AlGaAs quantum well. Simulation results for transitions between the first two conductions subbands clearly revealed that, the optical absorption decreases with increasing the dephasing as indicated in figure 5. This effects can be controlled by adjusting the carries densities populating the lower subband or controlling the quantum well width, which will be presented in our next publications.

Acknowledgements

We are indebted to Abdullahi Mikailu for his time and assistance.

Submitted on December 23, 2018

References

1. Liu H. C., Levine B. F., Andersson J. Y. Quantum Well intersubband Transition Physics and Devices. Kluwer Academic Publishers, 1994.
2. Rybalko D. A., Ya Vinnichenko M., Vorobjev L. E., Firsov D. A., Balagula R. M., Yu Panevin V., Kulagina M. M., Vasil'iev A. P. Intersubband light absorption in tunnel-coupled GaAs/AlGaAs quantum wells for electro-optic studies, *Journal of Physics: Conference Series*, 2014, v. 541, 012081.
3. Kasapoglu E., Sari H., Sökmen I. Intersubband optical absorption in a quantum well under a tilted magnetic field. *Superlattices and Microstructures*, 2001, v. 29(1), 25–37.
4. F.D.P. Alves, G. Karunasiri, N. Hanson, M. Byloos, H.C. Liu, A. Bezinger, M. Buchanan, NIR, MWIR and LWIR quantum well infrared photodetector using interband and intersubband transitions, *Infrared Phys. Technol.*, 2007, v. 50, 182–186.
5. B.F. Levine, Quantum-well infrared photodetectors, *J. Appl. Phys.*, 1993, v. 74 (R1).
6. Gevorgyan A. H., Mamikonyan N. E., Kostanyan A. A., Kazaryan E. M. Intersubband optical absorption in GaAs parabolic quantum well due to scattering by ionized impurity centers, acoustical and optical phonons *Physica E: Low-dimensional Systems and Nanostructures*, 2018, v. 103, 246–251.
7. Shumilov A. A., Ya Vinnichenko M., Balagula R. M., Makhov I. S., Firsov D. A., Vorobjev L. E. Intersubband light absorption in double GaAs/AlGaAs quantum wells under lateral electric field, *Journal of Physics: Conference Series*, 2016, v. 690, 012017.
8. Vorobjev L. E., Danilov S. N., Titkov I. E., Firsov D. A., Shalygin V. A., Zhukov A. E., Kovsh A. R., Ustinov V. M., Ya Aleshkin V., Andreev B. A., Andronov A. A., Demidov E. V. Optical absorption and birefringence in GaAs/AlAs MQW structures due to intersubband electron transitions, *Nanotechnology*, 2000, v. 11, 218–220.
9. WU Bin-He. Transient Intersubband Optical Absorption in Double Quantum Well Structure. *Commun. Theor. Phys. (Beijing, China)*, 2005, v. 43(4), 759–764.
10. Ming, C Wu. EE 232 Lightwave Devices Lecture 9: Intersubband Absorption in Quantum Wells. University of California, Berkeley, Electrical Engineering and Computer Sciences Dept., 2008, 9–12.

The Cosmological Significance of Superluminality

Hartmut Müller

E-mail: hm@interscalar.com

The paper derives the constancy and the value of the speed of light from stability conditions in chain systems of harmonic quantum oscillators. It is also shown that these stability conditions lead to scale-invariant superluminal velocity quantization. The cosmological significance of superluminality is discussed.

Introduction

I remember well that day in 1997 when my teenage son was asking me: "Why is the speed of light so slow?"

In fact, 299792458 m/s is a very finite velocity, and it is not too high regarding even the solar system. In interstellar and intergalactic scales, it becomes obvious how disappointingly slow it really is.

One year later, reading on the pioneering research of Günter Nimtz [1], my heart started to beat faster. Already in 1992, Enders and Nimtz demonstrated that photonic tunneling proceeds at superluminal signal velocities. The signal velocity is the velocity of the transmitted cause, i.e. of the information. As they reported, no signal reshaping took place during tunneling and all frequency components were equally transmitted. Later superluminal amplitude modulated (AM) and frequency modulated (FM) microwave experiments were carried out using different photonic barriers. Mozart's 40th symphony was FM tunneled at a speed of $4.7c$ without any significant distortion [2].

Superluminal propagation of infrared pulses through periodic fiber Bragg gratings was experimentally demonstrated [3]. Velocities of nearly $3c$ were observed [4] in the propagation of electric pulses along coaxial lines having spatially periodic impedances.

Nevertheless, superluminal tunneling is still under discussion. However, while Nimtz argues with facts (measurements) for superluminal signal transmission, his opponents counter with purely theoretical approaches. One of the main counterarguments is the alleged violation of causality [5, 6].

Causality requires the existence of a maximum speed of physical interaction, but could it be that 299792458 m/s is already high enough? This is very unlikely, if we consider the unity of the universe up to scales of billions light years.

By the way, in astronomic calculations, gravitation is traditionally considered as being instantaneous. First Laplace [7] demonstrated that gravitation does not propagate with the speed of light c. Modern estimations [8] confirm a lower limit of $2 \cdot 10^{10}\, c$. Exceeding 299792458 m/s has nothing to do with time travel, grandfather paradox or any other violation of causality. This would be relevant in the case of an infinitely high velocity, but 299792458 m/s is finite.

Furthermore, the value 299792458 m/s does not follow from any established theory, and consequently, none of those theories had to be changed if the speed of light would be even 55 times higher than 299792458 m/s.

What exactly makes possible to exceed 299792458 m/s? The point is that the tunneling time does not depend on the barrier length. This was theoretically described by Thomas E. Hartman [9] in 1962. Thirty years later, the Hartman effect was demonstrated experimentally with evanescent microwaves by Enders and Nimtz [10]. Numerous studies [11] have shown that the tunneling time equals approximately the reciprocal frequency of the carrier wave, independently of the length and the type of barrier (periodic lattice structures, double prisms, undersized wave guides).

Probably, not only photons and phonons can tunnel, but also electrons [12, 13], protons [14] and atoms [15] can do it.

Is superluminality just a laboratory artefact? It is very unlikely that laboratory experiments can exceed the complexity of astrophysical phenomena. Indeed, there are superluminal processes observed in deep space.

Already in December 1901, Jacobus Kapteyn [16] reported on apparent superluminal motion in the ejecta of the nova GK Persei [17], which was discovered in February 1901 by Thomas Anderson. Superluminal motion is observed in radio galaxies, BL Lac objects, quasars, blazars and recently also in some galactic sources called microquasars [18–21]. Superluminal motion has been observed [22] in the jet of M87. Many of the jets are evidently not close to our line-of-sight. Therefore, their superluminal behavior cannot be dismissed easily as an illusion.

Within the special relativity theory, the speed of light is postulated (not derived) to be constant. Up to now, there have not been sufficiently convincing explanations why the speed of light should be constant and why it should have the value which it has.

As proposed Albrecht and Magueijo [23], the speed of light might vary with the age of the universe and it might not have been constant in early stages. They suggest that a variable speed of light might solve the horizon, flatness and cosmological constant problems. Christoph Köhn [24] proposed a 5D space parametrized with two time coordinates to explain the constancy of the speed of light in the observable universe. For very small length scales of the present universe, or for the very early universe, the model speed of light is not constant, but depends on space-time. This is consistent with

current conclusions from loop quantum gravity models [25] and the string theory [26].

In the following we will show that the constancy and the value of the speed of light can be derived from stability conditions in fractal chain systems of harmonic quantum oscillators. Furthermore, we will demonstrate that the same stability conditions lead to scale-invariant superluminal velocity quantization.

Methods

The most stable systems we know are of atomic scale. Proton and electron form stable atoms, the structural elements of matter. The lifespans of the proton and electron surpass everything that is measurable, exceeding 10^{30} years. No scientist ever witnessed the decay of a proton or an electron. Therefore, the proton-to-electron ratio 1836.152674 is considered as fundamental physical constant [27]. Well, but what is the secret of this eternal stability?

Up to now, there have not been sufficiently convincing explanations why the electron and the proton should be stable and why the proton-to-electron ratio should have exactly the value which it has. In standard particle physics, the electron is stable because it is the least massive particle with nonzero electric charge. Its decay would violate charge conservation [28]. Indeed, this answer only readdresses the question. Why then is the elementary electric charge so stable?

In a similar explanation, the proton is stable, because it is the lightest baryon and the baryon number is conserved [29]. Indeed, also this answer only readdresses the question. Why then is the proton the lightest baryon? To answer this question, the standard model introduces quarks which violate the integer quantization of the elementary electric charge that is needed to explain the stability of the electron.

In [30] we introduced fractal chain systems of harmonic quantum oscillators as model of matter and did show that frequency ratios equal to Euler's number $e = 2.718\ldots$, its integer powers and roots inhibit destructive internal resonance interaction and in this way, provide lasting stability [31].

Already Dombrowski [32] did show that irrational numbers inhibit destabilizing resonance interaction, because they cannot be represented as ratios of whole numbers. Though, algebraic irrational numbers like $\sqrt{2}$ do not compellingly prevent resonance, because they can be transformed into rational numbers by multiplication.

Surprisingly, only Euler's number inhibits resonance also regarding all derivatives of the bound periodic processes, because it is the basis of the real exponential function e^x, the only function that is the derivative of itself. Furthermore, Euler's number, its integer powers and roots are always transcendental [33] and therefore, they provide the solution for lasting stability in chain systems of any degree of complexity.

Many physical characteristics of harmonic quantum oscillators are connected with their frequency by the fundamental constants – the speed of light and the Planck constant. Therefore, within our model, Euler's number, its integer powers and roots define also the ratios of wavelengths, velocities, impulses, accelerations and energies which inhibit resonance interaction, and in this way, support lasting stability of the chain system.

This is why we expect that stable quantum systems show ratios of their physical quantities close to integer powers of Euler's number and its roots. Consequently, the natural logarithms of the ratios should be close to integer 0, 1, 2, 3, 4, ... or rational values $\frac{1}{2}, \frac{1}{3}, \frac{1}{4}, \ldots$ In fact, the natural logarithm of the proton-to-electron ratio is close to seven and a half:

$$\ln(1836.152674) = 7.515427\ldots \simeq 6 + \frac{3}{2}.$$

Already in the eighties the scaling exponent 3/2 was found in the distribution of particle masses by Valery Kolombet [34]. Applying hyperscaling [30] by Euler's number (tetration), we get the next approximation of the logarithm of the proton-to-electron ratio:

$$6 + \frac{e^e}{10} = 7.515426\ldots$$

This result supports our assumption that the stability of the proton and electron comes from the transcendence of Euler's number, its integer powers and roots. In this way, the proton mass appears as scaled up by Euler's number and its roots electron mass.

In [35] we have analyzed the mass distribution of hadrons, mesons, leptons, the W/Z and Higgs bosons and proposed fractal scaling by Euler's number and its roots as model of particle mass generation [36]. In this model, the W-boson mass 80385 MeV/c^2 and the Z-boson mass 91188 MeV/c^2 appear as the 12 times scaled up by Euler's number electron rest mass 0.511 MeV/c^2:

$$\ln\left(\frac{80385}{0.511}\right) = 11.97, \qquad \ln\left(\frac{91188}{0.511}\right) = 12.09.$$

Andreas Ries [37] did apply fractal scaling by Euler's number to the analysis of atomic masses and demonstrated that this method allows for the prediction of the most abundant isotopes.

In comparison to dimensionless constants like the proton-to-electron ratio, conversion constants define dimensional ratios. For instance, the Planck constant defines the energy one must invest to generate a harmonic quantum oscillation of a given frequency, and the speed of light defines the propagation space of such an oscillation.

Like one can measure distances in units of time, for example in light years, energy can be measured in units of frequency. Only the dimensions are different.

In this way, we can interpret the speed of light as fundamental space – time converter, the square of the speed of light as fundamental mass – energy converter and the Planck

DIMENSIONS	CONVERSION CONST.	VALUE
space – time	$\lambda / \tau = c$	299792458 m/s
energy – mass	$E / m = c^2$	$8.9875518 \cdot 10^{16}$ m^2/s^2
energy – time	$E \cdot \tau = \hbar$	$1.0545718 \cdot 10^{-34}$ Js
energy – space	$E \cdot s = \hbar \cdot c$	$3.1615267 \cdot 10^{-26}$ Jm
mass – space	$m \cdot s = \hbar / c$	$3.5176729 \cdot 10^{-43}$ kgm
mass – time	$m \cdot \tau = \hbar / c^2$	$1.1733694 \cdot 10^{-51}$ kgs

Table 1: Some fundamental conversion constants (c is the speed of light in a vacuum, $\hbar$ is the Planck constant). Data taken from Particle Data Group [27].

constant as fundamental time – energy converter. Some fundamental conversion constants are shown in table 1.

Table 1 is completely compatible with Planck units. Originally proposed in 1899 by Max Planck, they are also known as natural units, because they origin only from properties of nature and not from any human construct. Natural units are based only on the properties of space-time. Max Planck wrote [38] that these units, "regardless of any particular bodies or substances, retain their importance for all times and for all cultures, including alien and non-human, and can therefore be called natural units of measurement".

In [39] was demonstrated that the natural logarithm of the Planck-to-proton mass ratio equals 44. Consequently, one can define a dimensionless fundamental constant that equals to an integer power of Euler's number and contains the speed of light c, the Planck constant $\hbar$, the gravitational constant G and the proton rest mass m_p:

$$\frac{\hbar \cdot c}{G \cdot m_p^2} = e^{88}.$$

For the speed of light, now we can write:

$$c = c_0 \cdot e^{88},$$

where $c_0 = Gm_p^2/\hbar \simeq 1.8 \cdot 10^{-30}$ m/s can be interpreted as the velocity of free falling on each other proton masses at Planck length and Planck time. Assumed that the stability of any fundamental constant origins from Euler's number and its roots, we can generalize:

$$c_{n,m} = c \cdot e^{n/m},$$

where n, m are integer numbers. In general, the rational exponent is represented by finite continued fractions [30, 40]. The exponents n/m define a fractal set of stable velocities $c_{n,m}$ which are superluminal for $n > 0$.

In the following, we will verify the fractal set $c_{n,m}$ of stable subluminal and superluminal velocities on experimental and astrophysical data.

Results

Let us start with experimental data elaborated by Nimtz [1] in 1998, the barrier traversal time of a microwave packet through a multilayer structure inside a waveguide was measured. The center frequency has been 8.7 GHz. The tunneled signal traversed a 114.2 mm long barrier in 81 ps, whereas the signal spent 380 ps to cross the same air distance. Consequently, the group velocity of the tunneled signal was c (380/81) = $4.7c$ that is close to $c_{3,2} = c \cdot e^{3/2} = 4.5c$.

Already in 1995 a similar experiment was carried out by Aichmann et al. [41]. They modulated Mozart's 40th symphony on a microwave carrier. The modulation of the signal and thus the music traveled at the same superluminal velocity.

In another setup [42], amplitude modulated 9.15 GHz microwaves were generated by a synthesized sweeper, and a parabolic antenna transmitted parallel beams. The propagation time of the signal was measured across the air distance between transmitter and receiver and across the same distance but partially filled with a 28 cm long barrier of quarter wavelength slabs made of acrylic perspex. Each slab was 0.5 cm thick and the distance between two slabs was 0.85 cm. Two such structures were separated by an air distance of 18.9 cm forming a resonant tunneling structure. The signal tunneled the 28 cm long barrier in 125 ps that corresponds to a signal velocity of $7.5c$ that is close to $c_{2,1} = c \cdot e^2 = 7.3c$.

Mojahedi et al. [43] describe an experiment with single microwave pulses centered at 9.68 GHz. The signals tunneled through a one-dimensional photonic crystal with up to $2.5c$ that is close to $c_{1,1} = c \cdot e = 2.7c$. Hache et al. [4] studied the propagation of brief electric 10 MHz pulses along a coaxial line having a spatially periodic impedance. As well, signal velocities approximating $c_{1,1} = 2.7c$ were measured.

Remarkably, the same superluminal velocities were measured also by Hubble telescope observation. Superluminal motion at velocities close to $c_{1,1} = 2.7c$ was found [22] in two small features within the jet knot D about 200 pc from the nucleus of M87, the giant elliptical galaxy near the center of the Virgo Cluster. As well, the jet features DE and DW show velocities close to $c_{1,1} = 2.7c$, while the features DM, DE-W, HST-1α, HST-1γ, HST-1δ, HST-1ϵ and HST-2 show velocities close to $c_{3,2} = 4.5c$.

Other active galactic nuclei (AGN) show the same velocities of superluminal motion. Lister et al. [21] describe the parsec-scale kinematics of 200 different AGN jets based on 15 GHz VLBA data. Various components of the sources 0003+380, 0003-060, 0010+405 show velocities that approximate $c_{1,1} = 2.7c$ or $c_{3,2} = 4.5c$ or $c_{2,1} = 7.3c$.

Jorstad et al. [20] monitored the radio emissions in 42 gamma-ray bright blazars (31 quasars and 11 BL Lac objects) with the Very Long Baseline Array (VLBA) at 43, 22, 15 and 8.4 GHz and found superluminal motions with velocities approximating $c_{1,1} = 2.7c$ or $c_{3,2} = 4.5c$ or $c_{2,1} = 7.3c$ or $c_{5,2} = 12c$ or $c_{3,1} = 20c$ or $c_{7,2} = 33c$ respectively.

Now let us continue with astrophysical data of stable subluminal processes. In [30] we have analyzed the orbital velocities of large bodies in the solar system. For instance, the orbital velocity of Mercury oscillates between two points of Euler stability $c_{-17,2}$ = 61 km/s (perihelion) and $c_{-9,1}$ = 37 km/s (aphelion). The orbital verlocity of Venus is close to $c_{-9,1}$ = 37 km/s. Earth's orbital verlocity is close to $c_{-37,4}$ = 29 km/s. The orbital verlocity of Mars is between 21.97 and 26.50 km/s, approximating $c_{-19,2}$ = 22.4 km/s. Jupiter's orbital velocity is between 12.44 and 13.72 km/s, approximating $c_{-10,1}$ = 13.6 km/s. Saturn's orbital verlocity is between 9.09 and 10.18 km/s, approximating $c_{-31,3}$ = 9.8 km/s. The orbital verlocity of Uranus is between 6.49 and 7.11 km/s, approximating $c_{-32,3}$ = 7 km/s. Neptune's orbital verlocity is close to $c_{-11,1}$ = 5 km/s. Pluto's orbital verlocity oscillates between 6.10 and 3.71 km/s, approximating the same $c_{-11,1}$ = 5 km/s. By the way, the same velocities are typical for underground propagation of seismic P-waves [44].

Within our model, the quantized orbital velocities in the solar system are velocities of free fall, scaled up by Euler's number and its roots from the velocity of free falling on each other proton masses at Planck length and Planck time. The stability [45] of the orbital system origins from the transcendence of Euler's number, its integer powers and roots. In this way, Euler's number, its integer powers and roots define fractal sets of quantized subluminal and superluminal velocities established by stable periodical processes.

Conclusion

The worldwide-reproduced tunneling experiments show convincingly that the conditions required for superluminal signal transmission are not exotic. Therefore, it is possible to imagine that those conditions can emerge also in nature. For the same reason, the probability is quite high that conditions for superluminality can emerge in deep space, and this is already suggested by astrophysical observations.

Our model [30] of matter as fractal chain system of harmonic quantum oscillators suggests that stable processes establish subluminal or superluminal velocities corresponding to the speed of light scaled by integer powers of Euler's number and its roots. This circumstance could affect estimations of intergalactic distances and the meaning of the cosmic light horizon. Superluminal propagation of light and matter suggests the existence of cosmic superluminal horizons with a scale-invariant exponential distribution that follows the sequence of multiples of Euler's number.

In [31] we have discussed the cosmological significance of global scaling [46] and the stabilizing function of Euler's number regarding the apparent distances between the stars and galaxies.

The concept of process stability based on the avoidance of destructive resonance interaction provided by the transcendence of Euler's number and its roots, allowed us to derive the constancy and the value of the speed of light. Deriving the speed of light from the velocity of free falling on each other proton masses at Planck length and Planck time, perhaps we can reach a better understanding of gravitation and its sheer infinite velocity.

Acknowledgements

The author is grateful to Viktor Panchelyuga, Oleg Kalinin, Alexey Petrukhin and Leili Khosravi for valuable discussions.

Submitted on January 11, 2019

References

1. Nimtz G. Superluminal Signal Velocity. arXiv: physics/9812053v1 [physics.class-ph], (1998).
2. Nimtz G. *Prog. Quantum Electron.*, 2003, v. 27, 417.
3. Longhi S. et al. Measurement of superluminal optical tunneling times in double-barrier photonic band gaps. *Phys. Rev. E*, 2002, v. 65(4), 046610 // arXiv:physics/0201013.
4. Hache A., Poirier L. Long-range superluminal pulse propagation in a coaxial photonic crystal. *Applied Physics Letters*, 2002, v. 80(3), 518.
5. Nimtz G., Haibel A. Basics of Superluminal Signals. *Ann. Phys.* (Leipzig), 2002, v. 9(1), 1–5, arXiv: physics/0104063v1 [physics.class-ph] (2001).
6. Nimtz G. Superluminal Signal Velocity and Causality. *Foundations of Physics*, 2004, v. 34(12), 1889–1903.
7. Laplace P. Mechanique Celeste. 1825, pp. 642–645.
8. Van Flandern T. The Speed of Gravity – What the Experiments Say. *Physics Letters A*, 1998, v. 250, 1–11.
9. Hartman T. E. Tunneling of a wave packet. *Journal of Applied Physics*, 1962, v. 33(12), 3427.
10. Enders A., Nimtz G. Evanescent-mode propagation and quantum tunneling. *Physical Review E*, 1993, v. 48(1), 632–634.
11. Nimtz G. Tunneling Violates Special Relativity. arXiv: 1003.3944v1 [quant-ph], (2010).
12. Sekatskii S.K., Letokhov V. S. Electron tunneling time measurement by field-emission microscopy. *Phys. Rev. B*, 2001, v. 64, 233311.
13. Eckle P. et al. Attosecond Ionization and Tunneling Delay Time Measurements in Helium 2008. *Science*, 2008, v. 322, 1525.
14. Tuckerman M. E., Marx D. Heavy-Atom Skeleton Quantization and Proton Tunneling in Intermediate-Barrier Hydrogen Bonds. *Phys. Rev. Lett.*, 2001, v. 86(21), 4946–4949.
15. Lauhon L.J., Ho W. Direct Observation of the Quantum Tunneling of Single Hydrogen Atoms with a Scanning Tunneling Microscope. *Phys. Rev. Lett.*, 2000, v. 85, 4566.
16. Kapteyn J.C. Über die Bewegung der Nebel in der Umgebung von Nova Persei. *Astronomische Nachrichten*, 1901, v. 157(12), 201.
17. Shara M.M. et al. GK Per (Nova Persei 1901): HST Imagery and Spectroscopy of the Ejecta, and First Spectrum of the Jet-Like Feature. arXiv: 1204.3078v1 [astro-ph.SR] (2012).
18. Levinson A., Blandford R. On the Jets associated with galactic superluminal sources. arXiv: astro-ph/9506137v1, (1995).
19. Brunthaler A. et al. III Zw 2, the first superluminal jet in a Seyfert galaxy. arXiv: astro-ph/0004256v1, (2000).
20. Jorstad S.G. et al. Multiepoch Very Long Baseline Array Observations of Egret-Detected Quasars and BL Lacertae Objects: Superluminal Motion of Gamma-Ray Bright Blazars. *The Astrophysical Journal Supplement Series*, 2001, v. 134, 181–240.

21. Lister M.L. et al. MOJAVE X. Parsec-Scale Jet Orientation Variations and Superluminal Motion in AGN. arXiv: 1308.2713v1 [astro-ph.CO], (2013).
22. Biretta J.A., Sparks W.B., Macchetto F. Hubble Space Telescope Obesrvations of Superluminal Motion in the M87 Jet. *The Astrophysical Journal*, 1999, v. 520, 621–626.
23. Albrecht A., Magueijo J. A Time Varying Speed of Light as a Solution to Cosmological Puzzles. *Physical Review D*, 1999, v. 59(4), 043516.
24. Köhn C. The Planck length and the constancy of the speed of light in five dimensional space parametrized with two time coordinates. arXiv: 1612.01832v2 [physics.gen-ph], (2017).
25. Kiritsis E. Supergravity, D-brane Probes and thermal super Yang-Mills: a comparison. *Journal of High Energy Physics*, 1999, v. 9910(10).
26. Alexander S. On the varying speed of light in a brane-induced FRW Universe. *Journal of High Energy Physics*, 2000, v. 0011(17).
27. M. Tanabashi et al. (Particle Data Group), *Phys. Rev. D*, 2018, v. 98, 030001. www.pdg.lbl.gov
28. Steinberg R. I. et al. Experimental test of charge conservation and the stability of the electron. *Physical Review D*, 1999, v. 61(2), 2582–2586.
29. Nishino H. et al. Search for Proton Decay in a Large Water Cherenkov Detector. *Physical Review Letters*, 2009, v. 102(14), 141801, arXiv: 0903.0676.
30. Müller H. Scale-Invariant Models of Natural Oscillations in Chain Systems and their Cosmological Significance. *Progress in Physics*, 2017, v. 13, 187–197.
31. Müller H. On the Cosmological Significance of Euler's Number. *Progress in Physics*, 2019, v. 15, 17–21.
32. Dombrowski K. Rational Numbers Distribution and Resonance. *Progress in Physics*, 2005, v. 1, no. 1, 65–67.
33. Hilbert D. Über die Transcendenz der Zahlen e und π. *Mathematische Annalen*, 1983, v. 43, 216–219.
34. Kolombet V. Macroscopic fluctuations, masses of particles and discrete space-time, *Biofizika*, 1992, v. 36, 492–499.
35. Müller H. Fractal Scaling Models of Natural Oscillations in Chain Systems and the Mass Distribution of Particles. *Progress in Physics*, 2010, v. 6, 61–66.
36. Müller H. Emergence of Particle Masses in Fractal Scaling Models of Matter. *Progress in Physics*, 2012, v. 8, 44–47.
37. Ries A. Qualitative Prediction of Isotope Abundances with the Bipolar Model of Oscillations in a Chain System. *Progress in Physics*, 2015, v. 11, 183–186.
38. Max Planck. Über Irreversible Strahlungsvorgänge. *Sitzungsbericht der Königlich Preußischen Akademie der Wissenschaften*, 1899, vol. 1, 479–480.
39. Müller H. Gravity as Attractor Effect of Stability Nodes in Chain Systems of Harmonic Quantum Oscillators. *Progress in Physics*, 2018, v. 14(1), 19–23.
40. Panchelyuga V.A., Panchelyuga M.S. Resonance and Fractals on the Real Numbers Set. *Progress in Physics*, 2012, v. 8, no. 4, 48–53.
41. Aichmann H., Nimtz G., Spieker H. Verhandlungen der Deutschen Physikalischen Gesellschaft. v. 7, 1258, (1995).
42. Nimtz G. Superluminal Tunneling Devices. arXiv: physics/0204043v1 [physics.gen-ph], (2002).
43. Mojahedi M. et al. Time-domain detection of superluminal group velocity for single microwave pulses. *Phys. Rev. E*, 2000, v. 62(4), 5758–5766 .
44. Müller H. Quantum Gravity Aspects of Global Scaling and the Seismic Profile of the Earth. *Progress in Physics*, 2018, v. 14, 41–45.
45. Müller H. Global Scaling of Planetary Systems. *Progress in Physics*, 2018, v. 14, 99–105.
46. Müller H. Global Scaling. The Fundamentals of Interscalar Cosmology. *New Heritage Publishers*, Brooklyn, New York, USA, (2018).

Fermi Scale and Neutral Pion Decay

Paulo Roberto Silva

Departmento de Física (Retired Associate Professor), ICEx, Universidade Federal de Minas Gerais, Belo Horizonte, MG, Brazil.
E-mail: prsilvafis@gmail.com

A modified Fermi coupling of the weak interactions is proposed and in analogy with the Planck units, a Fermi scale is defined. We define a second Fermi length, a Fermi mass (related to the threshold energy for unitarity), and a Fermi time. The holographic principle (HP) is then applied to some two-dimensional objects, where the unit cell size is given by the second Fermi length. With the aid of non-linear Dirac equation, a formula is obtained relating the Fermi, the nucleon, and the electron masses. Another relationship is found, linking the second Fermi length to cosmological constant and Planck scales. Finally HP in 2-d is employed in a stationary condition for the free energy, as a means to evaluate the neutral pion decay time.

1 Introduction

Once fixed the separation of them, the gravitational interaction between two particles of equal masses goes with the product of the Newton's gravitational constant G times the mass squared. Analogously, the electrostatic interaction of two equal charges is given by the product of the K_e-constant, let us call it the Coulomb constant, times the electric charge squared.

In quantum mechanics (QM) or in quantum field theory (QFT), by considering for instance only the absolute value of the proton-electron attraction in the hydrogen atom, it is convenient to write

$$K_e e^2 = \alpha \hbar c. \tag{1}$$

In (1) we have: e the quantum of elementary electric charge, $\hbar$ the reduced Planck constant, c the speed of light in vacuum, and α is the electromagnetic coupling strength. Relation (1) can be translated to the gravitational interaction case and takes the form

$$GM^2 = \alpha_g \hbar c. \tag{2}$$

According to the QFT the couplings are running with the energy [1], and we may define an energy (mass) scale such that we have $\alpha_g = 1$ [2]. We call this mass the Planck mass, and using the value $\alpha_g = 1$ in (2), we obtain

$$M_{Pl} = \sqrt{\frac{\hbar c}{G}}\,. \tag{3}$$

The Compton length of a particle with the Planck mass gives the Planck length, and the Planck time can be also defined by using c. We have

$$L_{Pl} = \frac{\hbar}{M_{Pl}\, c} = \sqrt{\frac{\hbar G}{c^3}}\,, \tag{4}$$

$$t_{Pl} = \frac{L_{Pl}}{c} = \sqrt{\frac{\hbar G}{c^5}}\,. \tag{5}$$

An alternative way to obtain the Planck scale (units) is to compare the Compton length of a particle with its Schwarzschild radius [3]. As is posted in Wikipedia [4]:

"Originally proposed by the German physicist Max Planck, these units are also known as natural units because the origin of their definition comes only from properties of fundamental physics theories and not from interchangeable experimental parameters."

The idea of the Planck length as being the minimal length (related to a discreteness of the space-time?), was first proposed by C.A. Mead [5,6]. The difficulty to publish his results is commented by Mead [8] and also highlighted by Sabine Hossenfeld [9], in a more recent essay.

In reference [10], the Fermi coupling constant G_F was used as a means to estimate the muon decay time. The way of using G_F in those calculations resembles the employment of Newton gravitational constant G in the Newtonian mechanics. This has inspired the present author to look at the possibility of defining a Fermi scale (units) in an analogous way as the Planck's case (relations (3) to (5) of this work). Indeed in a recent paper [11], Roberto Onofrio conjectured that weak interactions could be a manifestation of gravity when investigated through high energy probes (short distances).

In section 2, we use estimates of G_F quoted in the literature, in order to evaluate numerically the principal Fermi units, namely the second Fermi length, the Fermi mass (the second Fermi energy), and the Fermi time. The second Fermi length is named this way, to avoid confusion with the usual Fermi length related to the electrical conductivity of metals, for instance.

In section 3, we use the Holographic Principle (HP) in two dimensions (2-d) plus a simple Dirac- like equation, besides a relation connecting the wave function to the entropy, as a means to obtain a closed relation encompassing the Fermi, the electron and the nucleon masses.

In section 4, the HP in 2-d is used again, relating the second Fermi length to a length related to the cosmological constant [12], the Planck length and the electromagnetic coupling α.

Section 5 provides an estimate of the neutral pion radius.

In section 6, the HP in 2-d is used to evaluate the neutral pion decay time.

Finally section 7 is reserved for the concluding remarks.

2 The Fermi scale (units)

In reference [10], the muon decay time was estimated starting from the relation

$$m_\mu c^2 = \frac{1}{R_W}\frac{G_F\, c^2}{h^2} m_\mu^2. \tag{6}$$

In (6) m_μ is the muon mass, G_F is the Fermi constant of the weak interactions and R_W is the weak radius of the muon. We observe from an inspection of (6) that it is possible to define a modified Fermi constant G_F^*, namely

$$G_F^* = \frac{G_F\, c^2}{h^2}. \tag{7}$$

It is convenient to write the "inverse transform" of (7) as

$$G_F = G_F^* \frac{h^2}{c^2}. \tag{8}$$

We will call (8): all-classic to quantum relativistic transmutation. The reason to do so is: G_F^* could in principle to exist in the realm of the classical mechanics, while G_F only makes sense in a quantum relativistic treatment. Observe that given a finite G_F^*, G_F vanishes if $h \to 0$, or if $c \to \infty$, and naturally when both things happen. As can be verified in (6) and (7) G_F^* behaves for the weak interactions as G works in the case of the Newton's gravitational theory. As weak interactions are non- linear interactions, it is possible to write a set of equations similar to Einstein equations, putting in those equations G_F^* in the place of G.

The Schwarzschild-like metric for these equations gives the Weak-Schwarzschild radius R_{WS}. Here we apply this recipe to a particle with the muon mass. We have

$$R_{WS} = \frac{2\, G_F^*\, m_\mu}{c^2} = 2\, R_W. \tag{9}$$

Substituting (7) into (9), we get

$$R_{WS} = \frac{2\, G_F\, m_\mu}{h^2}. \tag{10}$$

The establishment of a modified Fermi coupling, namely G_F^* (please see (7)) permit us immediately to define the Fermi scale (units) in analogous way we have proceed in the Planck scale case. Therefore taking in account relations (3) to (5) we can write

$$M_F = \sqrt{\frac{\hbar\, c}{G_F^*}}, \tag{11}$$

$$L_{SF} = \frac{\hbar}{M_F\, c} = \sqrt{\frac{\hbar\, G_F^*}{c^3}}, \tag{12}$$

$$t_F = \frac{L_{SF}}{c} = \sqrt{\frac{\hbar\, G_F^*}{c^5}}. \tag{13}$$

With respect to (11) we notice that as is discussed on page 526 of the book by Rohlf [13], in a modern description of the weak interactions, the weak coupling constant is running with the energy of the probe used to measure it. According to Rohlf [13], "The weak interaction rate cannot increase forever with increasing energy. At some very large energy, this would violate conservation of probability or unitarity. Unitarity is violated at the energy where the weak coupling becomes unity." In the present treatment this happens just at the energy scale given by the Fermi mass (M_F).

In order to estimate the quantities (11) to (13), related to the Fermi scale of length, let us take the value of G_F as quoted in the book by Rohlf (formula 18.33, page 509).

$$G_F = 8.96 \times 10^{-8}\ \text{GeV fm}^3. \tag{14}$$

By using (7), we have

$$G_F^* = 2.94 \times 10^{21}\ \text{Nm}^2/\text{kg}^2. \tag{15}$$

Substituting G_F^* given by (15) into relations (11) to (13), we find

$$M_F \cong 1.84\ \text{TeV/c}^2. \tag{16}$$

$$L_{SF} \cong 1.07 \times 10^{-19}\ \text{m}, \tag{17}$$

$$t_F \cong 3.57 \times 10^{-28}\ \text{s}. \tag{18}$$

3 Deducing the Fermi mass

In this section it is proposed that the Fermi mass can be deduced by considering the holographic principle (HP) in 2-d, plus a non-linear Dirac-like equation (NLDE). A formula relating an entropy estimate via HP in 2-d and the wave function evaluated in the NLDE is considered. We are inspired in the neutron weak decay given a proton, an electron and a neutrino.

Inspired in McMahon [14], the holographic principle in 2-d can be stated as

- The total information content of a 2-d universe, in this case a spherical surface of radius R_x, can be registered in the perimeter of one of its maximum circles.
- The boundary of this spherical surface, here the perimeter of its maximum circle, contains at most a single degree of freedom per unit cell length.

Making the requirement that the radius R_x coincides with the Compton wavelength of the nucleon λ_n and choosing the unit cell size as L_{SF}, we can write

$$S_1 = \frac{\pi\, \lambda_n}{L_{SF}}. \tag{19}$$

Meanwhile, let us consider the non-linear Dirac-like equation

$$\frac{\delta\phi}{\delta x} - \frac{1}{c}\frac{\delta\phi}{\delta t} = \frac{1}{\lambda_e}\phi - \frac{1}{\lambda_n}\phi^3. \tag{20}$$

In (20) λ_e stands for the Compton wavelength of the electron and the equation (20) is conceived within the structure of an abelian field theory. However in a paper dealing with the proton-electron mass ratio [15], a π-factor has appeared in an equation in order to take in account the curvature of the space due to the non-abelian character of the QCD. Therefore let us define

$$\phi = \pi\,\Psi. \tag{21}$$

Inserting (21) into (20), we look for the zero of the equation and we find

$$\Psi^2 = \frac{\lambda_n}{\pi^2\,\lambda_e}. \tag{22}$$

Now we combine the results of (19) and (22), but considering the possibility of an implicit spin-1 boson being at work. We write

$$3\,S_1\,\Psi^2 = 1. \tag{23}$$

The insertion of (19) and (22) into (23) gives

$$\lambda_n^2 = \frac{\pi}{3} L_{SF}\,\lambda_e. \tag{24}$$

Remembering that ($\hbar$ = c = 1)

$$\lambda_n = \frac{1}{m_n}, \quad \lambda_e = \frac{1}{m_e}, \quad L_{SF} = \frac{1}{M_F},$$

we finally obtain

$$3\,M_F\,m_e = \pi m_n^2. \tag{25}$$

Putting numbers in (25), we get

$$M_F \cong 1.8\ \mathrm{TeV/c^2}. \tag{26}$$

As we can see, the value here deduced for the Fermi mass, is very close to that obtained through of the use of the measured value of G_F displayed in (16).

4 Deducing the second Fermi length – II

In a previous section a modified Fermi coupling, G_F^*, was defined and we found that a Fermi scale could be constructed in analogy with the well-established Planck scale. Here we pursue another path towards the deducing o f the second Fermi length. The role played by relic neutrinos in cosmology and its possible connection with the cosmological constant problem [16,17], stimuli us to seek for a relationship between L_{SF} and R_Λ. Indeed according Cohen, Kaplan and Nelson [18], R_Λ may be thought as a geometric average between the ultraviolet (L_{Pl}) and the infrared (R_U) cut-offs of the gravitational interaction.

Meanwhile, although matter is globally electrically neutral, may be some connection to exist between charges fluctuations and the weak coupling. In this section we also intend to tie the Fermi scale L_{SF} to a new scale R_α, related to the electromagnetic coupling. Next we define R_α. We write

$$G\,M_\alpha^2 = \alpha^2\,\hbar\,c. \tag{27}$$

By taking $\hbar = c = 1$, we get from (27)

$$M_\alpha = \frac{\alpha}{\sqrt{G}}. \tag{28}$$

Based on (28) we take R_α as

$$R_\alpha = \frac{1}{M_\alpha} = \frac{L_{Pl}}{\alpha}. \tag{29}$$

Now let us consider a spherical surface universe of radius L_{SF}. We apply The HP in 2-d to it, which unit cell size of its maximum circle's perimeter is given by R_α, and we get the entropy S_2

$$S_2 = \frac{2\,\pi\,L_{SF}}{R_\alpha} = \frac{2\,\pi\,\alpha\,L_{SF}}{L_{Pl}}. \tag{30}$$

Turning to the relationship connecting the L_{SF} and the R_α scales, we may write the non-linear Dirac equation

$$\frac{\delta\Psi}{\delta x} - \frac{1}{c}\frac{\delta\Psi}{\delta t} = \frac{1}{R_\Lambda}\Psi - \frac{1}{L_{SF}}\Psi^3. \tag{31}$$

Looking at the zero of (31), we get

$$\Psi^2 = \frac{L_{SF}}{R_\Lambda}. \tag{32}$$

Now we make the requirement that

$$S_2\,\Psi^2 = 1 \tag{33}$$

and we find

$$L_{SF}^2 = \frac{R_\Lambda\,L_{Pl}}{2\,\pi\,\alpha}. \tag{34}$$

To numerically evaluate (34), we consider $R_\Lambda = \sqrt{L_{Pl}\,R_U}$ with $L_{Pl} = 1.6162 \times 10^{-35}$ m and $R_U = 0.8 \times 10^{26}$ m [19], which yields

$$L_{SF} \cong 1.12 \times 10^{-19}\ \mathrm{m}. \tag{35}$$

As can be verified, this value is close to that experimentally determined (please see equation (17)).

5 The pion radius

In a paper dealing with the quark confinement related to the metric fluctuations [20], we have estimated a string constant K given by

$$K = \frac{m_q^2\,c^3}{\alpha_s\,\hbar} = \frac{m_q^2}{\alpha_s}, \quad (\hbar = c = 1). \tag{36}$$

In (36) the symbols m_q and α_s, stand for the quark constituent mass and the strong coupling, respectively. Now let us take

$$K\,2\,R_\pi = m_\pi, \quad m_q = \frac{1}{2}m_\pi. \tag{37}$$

Combining the results of (36) and (37) and taking $\alpha_s \cong 1/3$ (please see ref. [21]), we obtain for the pion radius (being m_π the neutral pion mass)

$$R_\pi = \frac{2\,\alpha_s}{m_\pi} \cong \frac{2}{3\,m_\pi}. \tag{38}$$

Putting numbers in (38), we get

$$R_\pi \cong 0.98 \times 10^{-15} \text{ m} = 0.98 \text{ fm}. \tag{39}$$

6 Neutral pion lifetime from the holographic principle in 2-d

Let us consider the neutral pion decay, represented by the reaction

$$\pi^0 \to 2\,\gamma. \tag{40}$$

Taking in account the stationary condition for the free energy ($\Delta F = 0$), we get

$$\Delta U = T\,\Delta S. \tag{41}$$

Next we consider a 2-d universe, represented by a spherical surface of radius R_π and the entropy variation represented by the information contained on its maximum-circle perimeter, having a unit cell size equal to $2\,L_{SF}$. We can write

$$\Delta U = \frac{\alpha\,\hbar\,c}{R_\pi}, \quad \Delta S = \frac{\pi\,R_\pi}{L_{SF}}. \tag{42}$$

Besides this we consider

$$h\,\nu = \frac{h}{\tau} = T, \quad (k_B = 1). \tag{43}$$

Inserting the results of (42) and (43) into (41) and solving for τ, we obtain the neutral pion decay time given by

$$\tau = \frac{2\,\pi^2\,R_\pi^2}{\alpha\,c\,L_{SF}}. \tag{44}$$

Putting numbers in (44) we get

$$\tau_{estimated} = 0.81 \times 10^{-16} \text{ s}. \tag{45}$$

This value may be compared with [22]

$$\tau_{measured} = 0.84 \times 10^{-16} \text{ s}. \tag{46}$$

7 Concluding remarks

The estimate of the neutral pion decay time is usually obtained through the employment of the current algebra calculations. Partial conservation of the axial current (PCAC) prediction gives

$$\frac{h}{\tau} = \Gamma(\pi^0 \to 2\gamma) = \frac{\alpha^2\,m_\pi^3}{64\,\pi^3\,f_\pi^2}. \tag{47}$$

In the present paper, by using the concepts of the second Fermi length and the Hp in 2-d, we found a novel way to look at the neutral pion decay.

Meanwhile, Roberto Onofrio [11] conjectured that weak interactions should be considered as empirical evidences of quantum gravity at the Fermi scale. The "second" Fermi length estimated by Onofrio ($\sim 10^{-18}$ m) [11], is approximately one order of magnitude greater than that obtained in section 2 of this work. This comes from the fact that Onofrio used the expectation value of the Higgs field to fix the Fermi scale of energy, instead the unitary scale threshold we have used in the present work.

Submitted January 6, 2019

References

1. Kane G.L. Modern Elementary particle Physics, Addison-Wesley, (1994).
2. Silva P.R. arXiv: 0910.5747v1, (2009).
3. Roos M. Introduction to Cosmology, pp. 50, Wiley, 1995.
4. Wikipedia contributors, "Planck units", Wikipedia, The Free Encyclopedia, 18 Sep. 2015.
5. Mead C.A. *Phys. Rev. B*, 1964, v. 135, 849.
6. Mead C.A. *Phys. Rev.*, 1966, v. 143, 990.
7. Peres A., Rosen N. *Phys. Rev.*, 1960, v. 118, 335.
8. Mead C.A. *Physics Today*, 2001, v. 54(11), 15.
9. Hossenfeld S. `backreaction.blog.spot.com.br/2012/01/Planck_length_as_minimal_length.html`
10. Silva P.R. Weak Interactions Made Simple. viXra:1210.0014, (2012).
11. Onofrio R. On weak interactions as short-distance manifestations of gravity. arXiv:1412.4513v1[hep-ph], (Dec. 2014).
12. Silva P.R. arXiv: 0812.4007v1 [gr-qc], (Dec. 2008).
13. Rohlf J.W. Modern Physics from α to Z^0. Wiley, (1994).
14. McMahon D. String Theory Demystified. McGraw-Hill, (2009).
15. Silva P.R. Proton-electron mass ratio: a geometric inference. viXra:1312.0060, (2013).
16. Silva P.R. Weak Interaction and Cosmology. arXiv:0804.2683v1 [physics.gen-ph], (2008).
17. Silva P.R. *Braz. J. Phys.* 2008, v. 38, 587.
18. Cohen A., Kaplan D., Nelson A., *Phys. Rev. Lett.* 1989, v. 82, 4971.
19. Silva P.R. The Viscous Universe and the Viscous Electron, viXra:1507.0177, (2015).
20. Silva P.R. arXiv:0908.3282v1 [physics.gen-ph], (2009).
21. Silva P.R. *Int. J. Mod. Phys. A* 1997, v. 12, 1373.
22. Particle Data Group, *Phys. Lett.* 1988, v. 204B, 1.
23. Adler S.L. *Phys. Rev.* 1969, v. 177, 2426.
24. Bell J.S., Jackiw R. *Il Nuovo Cimento* 1969, v. 51, 47.

On the Incompatibility of the Dirac-like Field Operator with the Majorana Anzatz

Valeriy V. Dvoeglazov

UAF, Universidad Autónoma de Zacatecas Apartado Postal 636, Suc. 3, C. P. 98061, Zacatecas, Zac., México. E-mail: valeri@fisica.uaz.edu.mx

We investigate some subtle points of the Majorana(-like) theories. We show explicitly the incompatibility of the Majorana Anzatz with the Dirac-like field operator in the original Majorana theory in various spin bases.

1 Introduction.

Majorana proposed his theory of neutral particles [1], in fact, on the basis of the Dirac equation [2]. However, the quantum field theory has not yet been completed in 1937. The Dirac equation [2–4] is well known to describe the charged particles of the spin 1/2.

Usually, everybody uses the following definition of the field operator [5]:

$$\Psi(x) = \frac{1}{(2\pi)^3}\sum_h \int \frac{d^3\mathbf{p}}{2E_p}\Big[u_h(\mathbf{p})a_h(\mathbf{p})e^{-ip\cdot x} + v_h(\mathbf{p})b_h^\dagger(\mathbf{p})e^{+ip\cdot x}\Big], \tag{1}$$

as given *ab initio*. After actions of the Dirac operator at $\exp(\mp ip_\mu x^\mu)$ the 4-spinors ($u-$ and $v-$) satisfy the momentum-space equations: $(\hat{p} - m)u_h(p) = 0$ and $(\hat{p} + m)v_h(p) = 0$, respectively; the h is the polarization index; $\hat{p} = p^\alpha\gamma_\alpha$. It is easy to prove from the characteristic equations $Det(\hat{p} \mp m) = (p_0^2 - \mathbf{p}^2 - m^2)^2 = 0$ that the solutions should satisfy the energy-momentum relation $p_0 = \pm E_p = \pm\sqrt{\mathbf{p}^2 + m^2}$ with both signs of p_0.

However, the general method of construction of the field operator has been given in the Bogoliubov and Shirkov book [6]. In the case of the $(1/2, 0) \oplus (0, 1/2)$ representation we have:

$$\Psi(x) = \frac{1}{(2\pi)^3}\int d^4p\,\delta(p^2 - m^2)e^{-ip\cdot x}\Psi(p) = \frac{\sqrt{m}}{(2\pi)^3}\sum_{h=\pm 1/2}\int \frac{d^3\mathbf{p}}{2E_p}\theta(p_0)\Big[u_h(p)a_h(p)|_{p_0=E_p}e^{-i(E_pt-\mathbf{p}\cdot\mathbf{x})} + u_h(-p)a_h(-p)|_{p_0=E_p}e^{+i(E_pt-\mathbf{p}\cdot\mathbf{x})}\Big]. \tag{2}$$

$\theta(p_0)$ is the Heaviside function(al). During these calculations we did not yet assume, which equation did this field operator (namely, the $u-$ spinor) satisfy (apart from the Klein-Gordon equation), with negative- or positive- mass. The explicit introduction of the factor $\sqrt{m}$ is caused by the following consideration. The 4-spinor normalization is known [4] to be able being chosen to the unit:

$$\bar{u}_{(\mu)}(p)u_{(\lambda)}(p) = +\delta_{\mu\lambda}\,, \tag{3}$$
$$\bar{u}_{(\mu)}(p)u_{(\lambda)}(-p) = 0\,, \tag{4}$$
$$\bar{v}_{(\mu)}(p)v_{(\lambda)}(p) = -\delta_{\mu\lambda}\,, \tag{5}$$
$$\bar{v}_{(\mu)}(p)u_{(\lambda)}(p) = 0\,, \tag{6}$$

where μ and λ are the polarization indices. The action should be dimensionless in $c = \hbar = 1$. Thus, the Lagrangian density has the dimension $[energy]^4$, and the 4-spinor field, the dimension $[energy]^{3/2}$. From (3-6) we see that the momentum-space 4-spinors should be dimensionless in this formulation. The creation/ahhihilation operators should have the dimension $[energy]^{-1}$ if we want to keep the standard (anti) commutation relations (20-24). Therefore, a factor with the dimension $[energy]^{1/2}$ can be introduced explicitly in (2) for the sake of conveniency instead of that in the normalizations or in the anticommutation relations [5].

The creation/annihilation quantum-field operators are defined by their actions on the quantum-field states in the representation of the occupation numbers:

$$\begin{aligned} a_h^\dagger(E_p, \mathbf{p})|n>& = |n+1; \mathbf{p}, h>,\\ a_h(E_p, \mathbf{p})|n>& = |n-1; \mathbf{p}, h>,\end{aligned} \tag{7}$$

$$a_h(E_p, \mathbf{p})|0> = 0\,. \tag{8}$$

Their explicit forms and excellent discussion can be found in [7]. However, the action of $a_h(-p) \equiv a_h(-E_p, -\mathbf{p})$ on the quantum-field vacuum is different (according, in fact, to the consideration below). Namely, the QFT vacuum contains all negative-energy states according to the Dirac interpretation. So when acting $a_h(-E_p, -\mathbf{p})$ on the vacuum this operator changes it (destroys a "hole"). The result is *not* zero, as opposed to the action of $a_h(+E_p, \mathbf{p})$ on vacuum.*

In general we should transform $u_h(-p)$ to the $v(p)$ in order to follow the original Dirac idea, where antiparticles were treated as particles with negative energy. The procedure is the following one [8, 9]. In the Dirac case we should assume the

*The similar situation is encountered in quantum mechanics of harmonic oscillator, where the creation operator can be obtained after application of reflection operators to the annihilation operator, and vice versa. This is not surprising because quantum field theory has the oscillator representation too.

following relation in the field operator:

$$\sum_h v_h(p)b_h^\dagger(p) = \sum_h u_h(-p)a_h(-p)\,. \tag{9}$$

We need $\Lambda_{\mu\lambda}(\mathbf{p}) = \bar{v}_\mu(E_p,\mathbf{p})u_\lambda(-E_p,-\mathbf{p})$. By direct calculations, we find

$$-b_\mu^\dagger(p) = \sum_\lambda \Lambda_{\mu\lambda}(p)a_\lambda(-p)\,. \tag{10}$$

where $\Lambda_{\mu\lambda} = -i(\boldsymbol{\sigma}\cdot\mathbf{n})_{\mu\lambda}$, $\mathbf{n} \equiv \widehat{\mathbf{p}} = \mathbf{p}/|\mathbf{p}|$, and

$$b_\mu^\dagger(p) = +i\sum_\lambda (\boldsymbol{\sigma}\cdot\mathbf{n})_{\mu\lambda}a_\lambda(-p)\,. \tag{11}$$

Multiplying (9) by $\bar{u}_\mu(-E_p,-\mathbf{p})$ we obtain

$$a_\mu(-p) = -i\sum_\lambda (\boldsymbol{\sigma}\cdot\mathbf{n})_{\mu\lambda}b_\lambda^\dagger(p)\,. \tag{12}$$

The equations are self-consistent.

Next, we can introduce the helicity operator of the $(1/2,0)\oplus(0,1/2)$ representation:

$$\widehat{h} = \begin{pmatrix} \hat{h} & 0_{2\times2} \\ 0_{2\times2} & \hat{h} \end{pmatrix}. \tag{13}$$

where

$$\hat{h} = \frac{1}{2}\boldsymbol{\sigma}\cdot\widehat{\mathbf{p}} = \frac{1}{2}\begin{pmatrix} \cos\theta & \sin\theta e^{-i\phi} \\ \sin\theta e^{+i\phi} & -\cos\theta \end{pmatrix}, \tag{14}$$

which commutes with the Dirac Hamiltonian, thus developing the theory in the helicity basis. We can start from the Klein-Gordon equation, generalized for describing the spin-1/2 particles (i. e., two degrees of freedom), Ref. [3]; again $c = \hbar = 1$. If the 2-spinors are defined as in [10, 11] then we can construct the corresponding $u-$ and $v-$ 4-spinors in the helicity basis.

$$u_\uparrow = N_\uparrow^+\begin{pmatrix}\phi_\uparrow \\ \frac{E-p}{m}\phi_\uparrow\end{pmatrix} = \frac{1}{\sqrt{2}}\begin{pmatrix}\sqrt{\frac{E+p}{m}}\phi_\uparrow \\ \sqrt{\frac{m}{E+p}}\phi_\uparrow\end{pmatrix}, \tag{15}$$

$$u_\downarrow = N_\downarrow^+\begin{pmatrix}\phi_\downarrow \\ \frac{E+p}{m}\phi_\downarrow\end{pmatrix} = \frac{1}{\sqrt{2}}\begin{pmatrix}\sqrt{\frac{m}{E+p}}\phi_\downarrow \\ \sqrt{\frac{E+p}{m}}\phi_\downarrow\end{pmatrix}, \tag{16}$$

$$v_\uparrow = N_\uparrow^-\begin{pmatrix}\phi_\uparrow \\ -\frac{E-p}{m}\phi_\uparrow\end{pmatrix} = \frac{1}{\sqrt{2}}\begin{pmatrix}\sqrt{\frac{E+p}{m}}\phi_\uparrow \\ -\sqrt{\frac{m}{E+p}}\phi_\uparrow\end{pmatrix}, \tag{17}$$

$$v_\downarrow = N_\downarrow^-\begin{pmatrix}\phi_\downarrow \\ -\frac{E+p}{m}\phi_\downarrow\end{pmatrix} = \frac{1}{\sqrt{2}}\begin{pmatrix}\sqrt{\frac{m}{E+p}}\phi_\downarrow \\ -\sqrt{\frac{E+p}{m}}\phi_\downarrow\end{pmatrix}, \tag{18}$$

where the normalization to the unit was again used. Please note that as in Ref. [14] the $\gamma-$ matrices are the same as in the spinorial basis:

$$\gamma^0 = \begin{pmatrix}0_{2\times2} & 1_{2\times2} \\ 1_{2\times2} & 0_{2\times2}\end{pmatrix}, \quad \boldsymbol{\gamma}^j = \begin{pmatrix}0_{2\times2} & -\boldsymbol{\sigma}^i \\ \boldsymbol{\sigma}^i & 0_{2\times2}\end{pmatrix}. \tag{19}$$

Thus, in the helicity basis we also have $v_h(p) = \gamma_5 u_h(p)$ as usual. Next, both $u-$ and $v-$ spinors above are the eigenspinors of the helicity operator [14] because the 2-spinors ϕ_h are the eigenspinors of $\hat{h}$.*

We again define the field operator as in (2) except for the polarization index h, which now answers for the helicity (not for the third projection of the spin, see [14]). The commutation relations are assumed to be the standard ones [5,6,12,13], except for adjusting the dimensional factor(see the discussion above):

$$\left[a_\mu(\mathbf{p}), a_\lambda^\dagger(\mathbf{k})\right]_+ = 2E_p\delta^{(3)}(\mathbf{p}-\mathbf{k})\delta_{\mu\lambda}\,, \tag{20}$$

$$\left[a_\mu(\mathbf{p}), a_\lambda(\mathbf{k})\right]_+ = 0 = \left[a_\mu^\dagger(\mathbf{p}), a_\lambda^\dagger(\mathbf{k})\right]_+\,, \tag{21}$$

$$\left[a_\mu(\mathbf{p}), b_\lambda^\dagger(\mathbf{k})\right]_+ = 0 = \left[b_\mu(\mathbf{p}), a_\lambda^\dagger(\mathbf{k})\right]_+\,, \tag{22}$$

$$\left[b_\mu(\mathbf{p}), b_\lambda^\dagger(\mathbf{k})\right]_+ = 2E_p\delta^{(3)}(\mathbf{p}-\mathbf{k})\delta_{\mu\lambda}\,, \tag{23}$$

$$\left[b_\mu(\mathbf{p}), b_\lambda(\mathbf{k})\right]_+ = 0 = \left[b_\mu^\dagger(\mathbf{p}), b_\lambda^\dagger(\mathbf{k})\right]_+\,. \tag{24}$$

However, the attempt is now failed to obtain the previous result (11) for $\Lambda_{\mu\lambda}(p)$. In this helicity case

$$\bar{v}_\mu(p)u_\lambda(-p) = i\sigma^y_{\mu\lambda}\,. \tag{25}$$

Please remember that the changes of the spin bases are performed by the rotation in the spin-parity space.

2 Analysis of the Majorana Anzatz

It is well known that "*particle=antiparticle*" in the Majorana theory. So, in the language of the quantum field theory we should have

$$b_\mu(E_p,\mathbf{p}) = e^{i\varphi}a_\mu(E_p,\mathbf{p})\,. \tag{26}$$

Usually, different authors use $\varphi = 0, \pm\pi/2$ depending on the metrics and on the forms of the 4-spinors and commutation relations. It is related to the Kayser phase factor.

So, on using (11) and the above-mentioned postulate we come to:

$$a_\mu^\dagger(p) = +ie^{i\varphi}(\boldsymbol{\sigma}\cdot\mathbf{n})_{\mu\lambda}a_\lambda(-p)\,. \tag{27}$$

On the other hand, on using (12) we make the substitutions $E_p \to -E_p$, $\mathbf{p}\to-\mathbf{p}$ to obtain

$$a_\mu(p) = +i(\boldsymbol{\sigma}\cdot\mathbf{n})_{\mu\lambda}b_\lambda^\dagger(-p)\,. \tag{28}$$

The totally reflected (26) is $b_\mu(-E_p,-\mathbf{p}) = e^{i\varphi}a_\mu(-E_p,-\mathbf{p})$. Thus,

$$b_\mu^\dagger(-p) = e^{-i\varphi}a_\mu^\dagger(-p)\,. \tag{29}$$

Combining with (28), we come to

$$a_\mu(p) = +ie^{-i\varphi}(\boldsymbol{\sigma}\cdot\mathbf{n})_{\mu\lambda}a_\lambda^\dagger(-p)\,, \tag{30}$$

*However, when discussing the spin properties of $u(-p)$ and $v(-p)$ in the helicity basis one should clarify the notational issues. Due to $\phi_{\uparrow\downarrow}(-\mathbf{p}) = -i\phi_{\downarrow\uparrow}(\mathbf{p})$, $u_{\uparrow\downarrow}(-E_p,-\mathbf{p}) = \pm v_{\downarrow\uparrow}(E_p,\mathbf{p})$ we have $\widehat{h}u_{\uparrow\downarrow}(-E_p,-\mathbf{p}) = -\frac{1}{2}v_{\downarrow\uparrow}(E_p,\mathbf{p})$, and similarly for $v(-p)$ 4-spinors. However, the equation (25) below is valid within the used notation.

and

$$a^{\dagger}_{\mu}(p) = -ie^{i\varphi}(\boldsymbol{\sigma}^{*}\cdot\mathbf{n})_{\mu\lambda}a_{\lambda}(-p)\,. \qquad (31)$$

This contradicts with the equation (27) unless we have the preferred axis in every inertial system.

Next, we can use another Majorana anzatz $\Psi = \pm e^{i\alpha}\Psi^{c}$ with usual definitions

$$C = \begin{pmatrix} 0 & i\Theta \\ -i\Theta & 0 \end{pmatrix}\mathcal{K}\,, \quad \Theta = \begin{pmatrix} 0 & -1 \\ 1 & 0 \end{pmatrix} = -i\sigma^{y}\,. \qquad (32)$$

Thus, on using $Cu^{*}_{\uparrow}(\mathbf{p}) = iv_{\downarrow}(\mathbf{p})$, $Cu^{*}_{\downarrow}(\mathbf{p}) = -iv_{\uparrow}(\mathbf{p})$ we come to other relations between creation/annihilation operators

$$a^{\dagger}_{\uparrow}(\mathbf{p}) = \mp ie^{-i\alpha}b^{\dagger}_{\downarrow}(\mathbf{p})\,, \qquad (33)$$

$$a^{\dagger}_{\downarrow}(\mathbf{p}) = \pm ie^{-i\alpha}b^{\dagger}_{\uparrow}(\mathbf{p})\,, \qquad (34)$$

which may be used instead of (26). Due to the possible signs $\pm$ the number of the corresponding states is the same as in the Dirac case that permits us to have the complete system of the Fock states over the $(1/2,0)\oplus(0,1/2)$ representation space in the mathematical sense.* However, in this case we deal with the self/anti-self charge conjugate quantum field operator instead of the self/anti-self charge conjugate quantum states. Please remember that it is the latter that answers for neutral particles; the quantum field operator contains the information about more than one state, which may be either electrically neutral or charged.

As a discussion we observe that the origins and the consequences of the contradiction between (27) and (31) may be the following. In general, the QFT space reflection are performed by the unitary transformations in the Fock space. The time reflection is performed by the anti-unitary transformation. However, after writing the present paper I learnt from [15] about arguments of unitary time reversal on the first quantization level. What would be the influence of this proposition on the second quantization scheme and on the Majorana Anzatz should be the subject of future publications.

3 Conclusions

We conclude that something is missed in the foundations of the original Majorana theory and/or the Dirac "hole" theory. At the moment the above consideration points to the rotational symmetry breaking after application of the Majorana Anzatz in the $(1/2,0)\oplus(0,1/2)$ representation, for higher spins as well [16].

Acknowledgements

I acknowledge discussions with colleagues at recent conferences. I am grateful to the Zacatecas University for professorship.

Submitted on December 1, 2018

*Please note that the phase factors may have physical significance in quantum field theories as opposed to the textbook nonrelativistic quantum mechanics, as was discussed recently by several authors.

References

1. Majorana E. *Nuovo Cim.*, 1937, v. 14, 171.
2. Dirac P.A.M. *Proc. Roy. Soc. Lond. A*, 1928, v. 117, 610.
3. Sakurai J.J. Advanced Quantum Mechanics, Addison-Wesley, (1967).
4. Ryder L.H. Quantum Field Theory, Cambridge University Press, Cambridge, (1985).
5. Itzykson C. and Zuber J.-B. Quantum Field Theory, McGraw-Hill Book Co., (1980).
6. Bogoliubov N.N. and Shirkov D.V. Introduction to the Theory of Quantized Fields, 2nd Edition, Nauka, Moscow, (1973).
7. Schweber S.S. Introduction to Relativistic Quantum Field Theory, Harper & Row Publishers, New York, (1961).
8. Dvoeglazov V.V. *Hadronic J. Suppl.*, 2003, v. 18, 239.
9. Dvoeglazov V.V., *Int. J. Mod. Phys. B*, 2006, v. 20, 1317.
10. Varshalovich D.A., Moskalev A.N. and Khersonskiĭ V.K. Quantum Theory of Angular Momentum, World Scientific, Singapore, (1988), §6.2.5.
11. Dvoeglazov V.V., *Fizika B*, 1997, v. 6, 111.
12. Weinberg S. The Quantum Theory of Fields. Vol. I. Foundations, Cambridge University Press, Cambridge, (1995).
13. Greiner W. Field Quantization, Springer, (1996), Chapter 10.
14. Dvoeglazov V.V. *Int. J. Theor. Phys.*, 2004, v. 43, 1287.
15. Debergh N. *et al. J. Phys. Comm.*, 2018, v. 2, 115012.
16. Dvoeglazov V.V. *Int. J. Theor. Phys.*, 2019, v. 58, accepted manuscript.

Physical and Mathematical Consistency of the Janus Cosmological Model (JCM)

Jean-Pierre Petit[1], Gilles D'Agostini[2], and Nathalie Debergh[3]

Manaty Research Group

[1]jean-pierre.petit@manaty.net [2]gilles.dagostini@manaty.net [3]nathalie.debergh@manaty.net

The Janus Cosmological Model is based on a system of two coupled field equations. It explains the nature of dark matter and dark energy with negative mass and without the runaway paradox that arises in general relativity. We first recall how this system was built, from a simple Newtonian toy model to a relativistic bimetric theory, that is now improved in order to fulfill mathematical constraints and set up on a Lagrangian derivation.

1 The long genesis of the Janus Cosmological Model

Roots of the Janus Cosmological Model are like assembling different pieces of a puzzle. There are indeed several starting points for this bimetric approach. The first is the missing primordial antimatter, a problem solved in 1967 by Andrei Sakharov in [1] with the representation of the universe not as a single entity born from the beginning of time, but two spacetimes with opposite arrows of time communicating only through their common initial singularity, forming a "twin universe" in complete CPT symmetry, as represented in the didactic Figure 1.

Then, the first step is to consider that these two entities can interact gravitationally, which is equivalent to folding the object of Figure 1 on itself as in Figure 2.

In 1977, a first modeling using non relativistic theoretical tools is attempted in [2] and [3] with two Boltzmann equations coupled with Poisson's equation. We then realize Sakharov's seminal idea of a complete CPT symmetry between these two entities, an idea also independently used by other authors recently [4]. Such work suggests that a profound paradigm shift involving geometrical grounds should be performed.

Early 1990's, we explore, through computer simulations, what could emerge from interaction laws associated with a mix of positive and negative point masses, according to the following assumption. Interactions laws:

- Like masses attract, according to Newton's law.

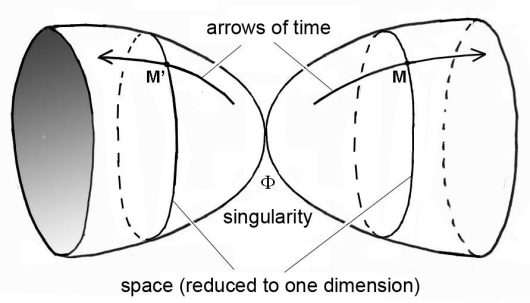

Fig. 1: 2D representation of Sakharov's twin universe model.

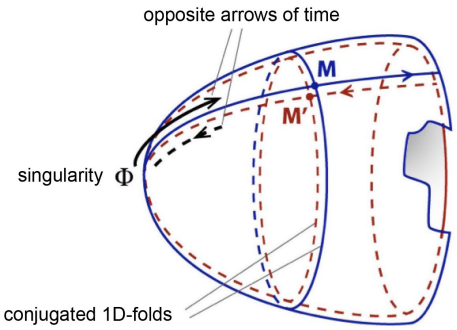

Fig. 2: Sakharov's model with "conjugate folds".

- Unlike masses repel, according to "anti-Newton".

At this stage, it is only a toy model. In 1992, first 2D simulations of two populations with opposite mass and same absolute value of density show a separation of the two entities, as shown in [5], a result reproduced below in Figure 3.

The purpose was to account for the large-scale structure of the universe, which admittedly wasn't a tight fit with these early experiments. But if we now introduce asymmetry in the two mass densities, taking a greater density for the negative mass species, then this population has a shorter Jeans time, hence it is the first to coalesce into conglomerates, by gravitational instability.

$$\text{if } |\rho^{(-)}| \gg \rho^{(+)} \quad \Rightarrow \quad t_{j^{(-)}} = \frac{1}{\sqrt{4\pi G\,|\rho^{(-)}|}} \ll t_{j^{(+)}} = \frac{1}{\sqrt{4\pi G\,\rho^{(+)}}} \tag{1}$$

Following simulations confirm this second hypothesis as they produce an evolution of the positive mass distribution into a large-scale structure with big negative mass conglomerates (optically invisible) repelling the positive mass matter in the remnant space around them as shown in [6], a decisive result reproduced below in Figure 4, this time in very good agreement with the observation of the lacunar, foam-

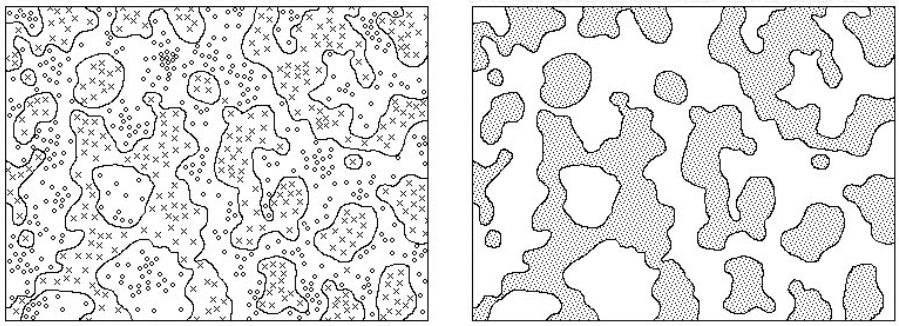

Fig. 3: Flocculation and percolation phenomena between two populations of opposite mass and same overall density. Right: Showing the optically-visible positive mass matter only.

like structure of the universe, where galaxies, clusters and superclusters are organized as a web of filaments, walls and nodes distributed around giant repulsive cosmic voids.

Same approach but different boundary conditions in [7], reproduced in Figure 5.

Such a scenario also produces, in 3D, a mechanism helping galaxy formation along. Indeed, after recombination, if large volumes of gas can coalesce into giant conglomerates, then a problem arises: how to dissipate such enormous gravitational energy transformed into heat? Considering an object of radius R, the amount of energy collected varies according to R^3 while the surface of the heatsink varies as R^2. Therefore, larger masses have a more important cooling time. But the constitution of the large-scale structure suggested by these simulations leads to a compression of the positive mass which distributes according to walls (as observed) that are actually sandwiched between two repulsive conglomerates of negative mass. A strong compression of the positive mass occurs in such planar structures, which are optimal for a quick radiative dissipation of energy, as explained in [6].

Besides 2D simulations, an effective confinement of galaxies despite their high peripheral velocity is analytically demonstrated using an exact solution of two Vlasov equations coupled with Poisson's equation, using the methodology exposed in [5]. The flat rotation curve obtained from such a solution, made possible by the repulsive effect of the surrounding negative mass, has been shown for the first time in [6], a curve reproduced in Figure 6. It is worth noting that such a typical rotation curve has been similarly obtained more recently using the same repulsive action of a negative mass distribution around galaxies, but from 3D computer simulations made by an independent researcher [8].

Using the exact solution of the analytical set of two Vlasov equations coupled with Poisson's equation (image of a 2D galaxy confined by a repulsive negative mass environment), we show in numerical simulations that the rotational motion of the galaxy generates a good-looking barred spiral structure in a few turns (1992 DESY results, published in [6] and [7]).

In order to progress beyond a simple toy model that opens up interesting prospects thanks to the various above-mentioned positive results, it was still necessary at that time to derive interaction laws from a coherent mathematical formalism. The introduction of negative mass in cosmology had been considered as soon as the 1950s, using general relativity, defined by the well-known Einstein field equations which may be written, with a zero cosmological constant:

$$R_{\mu\nu} - \frac{1}{2} R\, g_{\mu\nu} = +\chi T_{\mu\nu}. \qquad (2)$$

Let's notice that Einstein's equation describes the motion of point masses embedded in a given mass-energy field $T_{\mu\nu}$ along geodesics that derive from a single metric $g_{\mu\nu}$. Then, one gets Bondi's result from [9]. Interaction laws with a single metric:

- Positive masses attract everything.
- Negative masses repel everything.

Which inevitably produce the preposterous "runaway motion" paradox (see Figure 8), a term coined by Bonnor in [10].

Nonetheless, a few authors (Farnes [8], Chardin [11]) still consider that it is possible to introduce negative mass in cosmology keeping the general relativity framework, hence putting up with such phenomenon; despite the fact that the runaway motion has been associated with the possibility of perpetual motion machines since the 1950s, as discussed by Gold with Bondi, Bergmann and Pirani in [12].

On the contrary, from 1995 in [13] we propose a bimetric description of the universe with two coupled metrics and which produce trajectories along their own geodesics, for positive and negative mass particles, respectively. Then, the classical Schwarzschild solution allows, by simply reversing the integration constant, to get trajectories suggesting a gravitational repulsion of positive masses by a negative mass, and vice versa:

$$ds^2 = \left(1 - \frac{2GM}{rc^2}\right) c^2 dt^2 - \frac{dr^2}{1 - \dfrac{2GM}{rc^2}} - r^2 d\theta^2 - \sin^2\theta d\varphi^2, \quad (3)$$

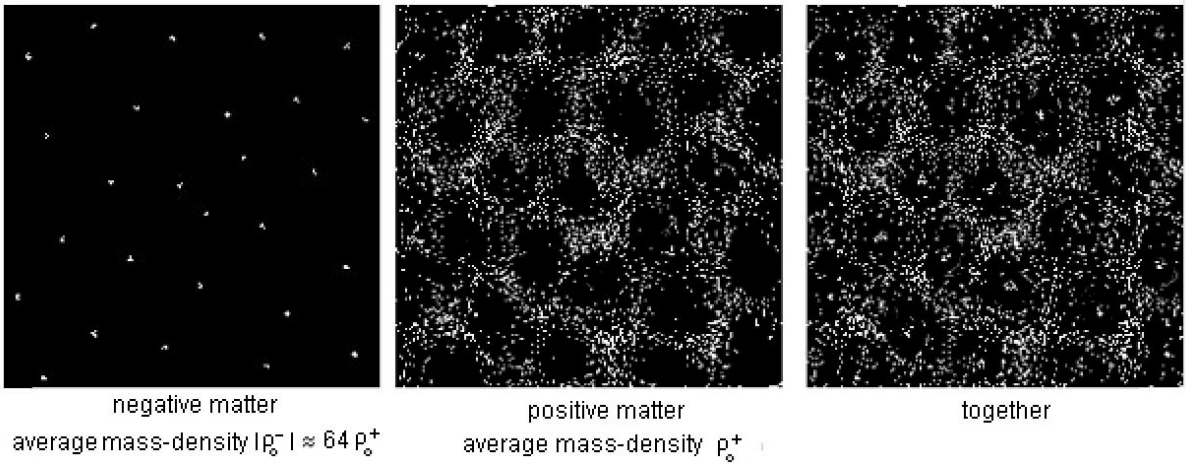

Fig. 4: Result of a 2D large-scale structure simulation [6].

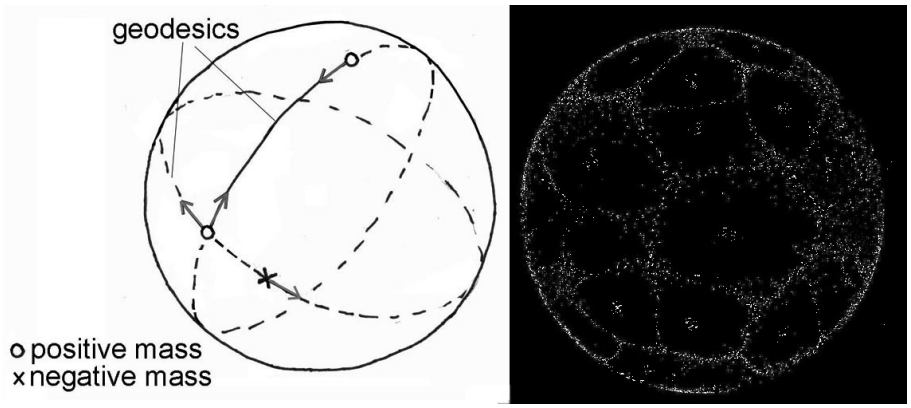

Fig. 5: Result of a 2D large-scale structure simulation on a 2-sphere [7].

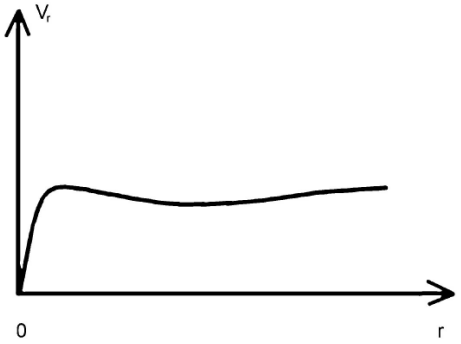

Fig. 6: Flat rotation curve of a galaxy surrounded by a negative mass distribution [6].

$$ds^2 = \left(1+\frac{2GM}{rc^2}\right)c^2dt^2 - \frac{dr^2}{1+\frac{2GM}{rc^2}} - r^2d\theta^2 - \sin^2\theta d\varphi^2. \quad (4)$$

Exploiting this idea, we introduce the concept of negative (diverging) gravitational lensing in the same paper [13]. Considering that a gap within a negative mass distribution is equivalent to a positive mass concentration, we suggest to attribute the strong gravitational lensing effects, observed in the vicinity of galaxies and galaxy clusters, not to a dark matter halo made of positive mass, but instead to their negative mass environment.

From 1994, we also suggest in [5] that such a bimetric description could result from the combination of two Lagrangian densities, due to two Ricci scalars $R^{(+)}$ and $R^{(-)}$. In 2001 [6], we proposed for the first time a system of two coupled field equations, which can be written as:

$$R^{(+)}_{\mu\nu} - \frac{1}{2}R^{(+)}g^{(+)}_{\mu\nu} = +\chi\left[T^{(+)}_{\mu\nu} + T^{(-)}_{\mu\nu}\right], \quad (5)$$

$$R^{(-)}_{\mu\nu} - \frac{1}{2}R^{(-)}g^{(-)}_{\mu\nu} = -\chi\left[T^{(+)}_{\mu\nu} + T^{(-)}_{\mu\nu}\right], \quad (6)$$

whose purpose was to account for the postulated interaction laws. Indeed, we make such laws emerge from a dual Newto-

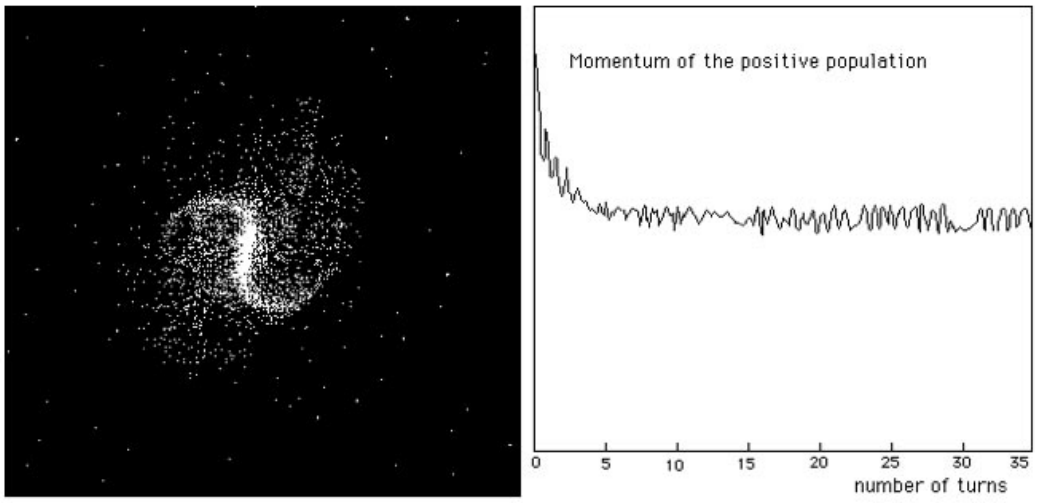

Fig. 7: 2D barred spiral structure [6, 7].

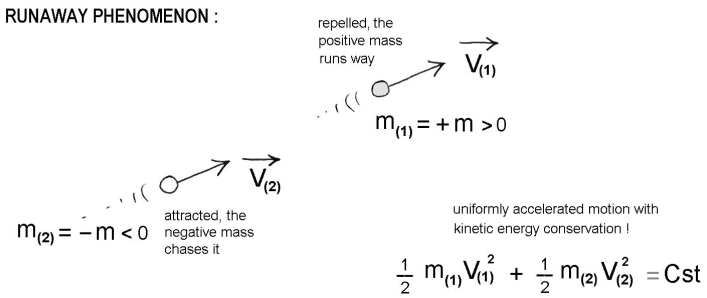

Fig. 8: Runaway motion in general relativity.

nian approximation of this system of two coupled equations. Depending locally on the type of dominant species in a given region of space, equations with no RHS produce solutions of type 36 or 37.

Aforementioned results of simulations showed that an asymmetry in the mass densities of the positive vs negative mass species is required to account for observations of the large-scale structure of the universe. Such density asymmetry can be caused, not because of a larger quantity of negative mass, but if the two space gauge factors $a^{(+)}$ and $a^{(-)}$ are different. Alas, at this level it is impossible to produce a time-dependent solution with $a^{(+)} \neq a^{(-)}$. Inconsistency becomes inevitable when FRLW metrics are introduced in the two field equations: similarly to Friedmann solutions, they produce a couple of differential equations in $a^{(+)}$, $a'^{(+)}$, $a''^{(+)}$ on one hand, and in $a^{(-)}$, $a'^{(-)}$, $a''^{(-)}$ on the other. In the calculation based on Einstein's equations, compatibility betweeen two equations leads to the relation $\rho a^3 = cst$ in the matter-dominated era, which expresses mass-energy conservation. In the bimetric framework of the Janus model based on the two coupled equations 5 and 6, such compatibility reduces the time-dependent solution to $a^{(+)} = a^{(-)}$.

Still in the same 2001 paper [6], we establish the connection between Sakharov's seminal work about two universes with opposite arrows of time, and negative gravity, using dynamical group theory from [14], which shows that time reversal goes with energy inversion, hence mass inversion as $-m = -E/c^2$. We then introduce the "Janus group" to handle the electric charge in a five-dimensional spacetime:

$$\begin{pmatrix} \lambda\mu & 0 & 0 \\ 0 & \lambda\,, L_0 & 0 \\ 0 & 0 & 1 \end{pmatrix} \qquad \text{with } \lambda = \pm 1 \quad \text{and } \mu = \pm 1, \quad (7)$$

where L_0 is the component of the orthochronous (forward in time) subset of the Lorentz group. It is the extension of the Poincaré group to five dimensions, which describes the existence of two different kinds of antimatter: one being C-symmetric with respect to normal matter, it has a positive mass; while the other antichronous (backward in time) antimatter is PT-symmetric and has a negative mass. Therefore,

the CPT theorem has to be reconsidered, since the exclusion of negative energy states follows on from an a priori axiom in quantum field theory, which postulates that the operator T has to be antiunitary and antilinear, a hypothesis not necessarily true as shown in [15].

Sakharov's conditions in [1] states that the baryon creation rate from an excess of quarks has been faster than the antibaryon creation rate from fewer antiquarks at $t > 0$, but such CP violation is opposite for $t < 0$ (the "initial singularity" triggering complete CPT reflections) thereby preserving the global symmetry of the whole universe. This allows to define the true nature of the invisible antichronous components of the universe: these are copies of antiparticles that are usually made in a lab, but with negative energy and mass, due to T-symmetry.

The invisibility of such objects is deduced from the idea that PT-symmetric antiparticles emit negative energy photons that follow null-geodesics of their own metric $g_{\mu\nu}^{(-)}$ hence escape detection by optical instruments that are made of positive mass matter.

In 2002, Damour and Kogan in [16] situate the issue with massive bigravity theories, where bimetry covers a different approach. In such models, two branes interact using various massive gravitons (hence the name) with a mass spectrum. The authors propose a Lagrangian derivation, based on an action, which leads to a system of two coupled field equations. But such a model, although mathematically consistent, does not stand up to scrutiny as it does not provide any solution able to be confronted with observations. As it has not been further pursued, it cannot answer this question.

On the other hand, in 2008 and 2009, Hossenfelder in [17] and [18] builds her own bimetric model involving negative mass, from a Lagrangian derivation where she produces a system of two coupled field equations. This time, LHS are identical to the system (5;6) which follows on from the presence of terms $R^{(+)}\sqrt{g^{(+)}}$ and $R^{(-)}\sqrt{g^{(-)}}$ in the Lagrangian densities considered. Exploiting her Lagrangian derivation, she reveals the determinant ratios of the two metrics $\sqrt{g^{(+)}/g^{(-)}}$ and $\sqrt{g^{(-)}/g^{(+)}}$ that had already been pointed out in previous work [19] and [20]. She finally tackles two Friedmann solutions, without confronting them to observational data. Actually, although sharing many similarities, having the same kind of coupled field equations regarding negative mass, a fundamental difference remains between Hossenfelder's bimetric theory and the Janus Cosmological Model.

Indeed, Hossenfelder doubts that the second entity can have an important effect on the distribution of standard matter, qualifying the gravitational coupling between the two species as "extremely weak". This is because "for symmetry reason" she considers that the absolute values of the mass density of the two populations should be of the same order of magnitude. Such hypothesis leads to a global zero field configuration, which does not fit with observations, as she notices. Then, examination of possible fluctuations seems to be her main concern. Not perceiving that a *profound dissymmetry* is on the contrary the key to the interpretation of many phenomena, including the acceleration of the cosmic expansion, she will not develop her model further during the following decade, focusing instead on other research topics.

Nonetheless, Hossenfelder points out a "smoking gun signal" that could highlight the existence of invisible negative mass in the universe, through the detection of diffracted light rays caused by diverging lensing, an effect previously predicted in [13]. We indeed showed from 1995 that photons emitted by high redshift galaxies ($z > 7$) are diffracted by the presence of invisible conglomerates of negative mass on their path. This reduces the apparent magnitude of such galaxies, making them appear as *dwarf*, which is consistent with observations.

In 2014 in [21] we take again the system (5;6) and attempt to modify it according to:

$$R_{\mu\nu}^{(+)} - \frac{1}{2} R^{(+)} g_{\mu\nu}^{(+)} = +\chi \left[T_{\mu\nu}^{(+)} + \varphi T_{\mu\nu}^{(-)} \right], \tag{8}$$

$$R_{\mu\nu}^{(-)} - \frac{1}{2} R^{(-)} g_{\mu\nu}^{(-)} = -\chi \left[\phi T_{\mu\nu}^{(+)} + T_{\mu\nu}^{(-)} \right]. \tag{9}$$

Introducing two functions $\varphi()$ and $\phi()$ that allow a time-dependent homogeneous and isotropic solution, so that $a^{(+)} \neq a^{(-)}$. This is possible by switching to the system:

$$R_{\mu\nu}^{(+)} - \frac{1}{2} R^{(+)} g_{\mu\nu}^{(+)} = +\chi \left[T_{\mu\nu}^{(+)} + \left(\frac{a^{(-)}}{a^{(+)}} \right)^3 T_{\mu\nu}^{(-)} \right], \tag{10}$$

$$R_{\mu\nu}^{(-)} - \frac{1}{2} R^{(-)} g_{\mu\nu}^{(-)} = -\chi \left[\left(\frac{a^{(+)}}{a^{(-)}} \right)^3 T_{\mu\nu}^{(+)} + T_{\mu\nu}^{(-)} \right]. \tag{11}$$

We obtained such a result by assuring energy conservation, not by deriving these equations from the system proposed in [18]. From (10;11) we then build an exact solution involving a large asymmetry, so that $|\rho^{(-)}| \gg \rho^{(+)}$, accounting fot the acceleration of the expansion of the universe. D'Agostini thereafter showed in 2018 in [22] that this exact solution is in very good agreement with latest observational data. In parallel we published in 2014 in [23] a Lagrangian derivation based on the functional relation:

$$\delta g^{(-)\mu\nu} = -\delta g^{(+)\mu\nu}, \tag{12}$$

giving the following system of two coupled field equations:

$$R_{\mu\nu}^{(+)} - \frac{1}{2} R^{(+)} g_{\mu\nu}^{(+)} = +\chi \left(T_{\mu\nu}^{(+)} + \sqrt{\frac{-\mathbf{g}^{(-)}}{-\mathbf{g}^{(+)}}}\, T_{\mu\nu}^{(-)} \right), \tag{13}$$

$$R_{\mu\nu}^{(-)} - \frac{1}{2} R^{(-)} g_{\mu\nu}^{(-)} = -\chi \left(T_{\mu\nu}^{(-)} + \sqrt{\frac{\mathbf{g}^{(+)}}{\mathbf{g}^{(-)}}}\, T_{\mu\nu}^{(+)} \right), \tag{14}$$

which is similar to Hossenfelder's system in her previous Lagrangian derivation [18], although both constructions are completely different. In our derivation, the square root in the determinant ratio of the metrics directly follows on from hypothesis (14). Let's recall that such a ratio always appears as soon as a bimetric approach is attempted, see for example [19] and [20]. Admittedly however, we cannot rule out that the system (15);(16), as well as the newer one exposed hereinbelow, can be considered as a particular case of Hossenfelder's own model.

In 2014 in [23] we extend the Janus framework to a class of solutions where the two speeds of light and, in the positive and negative sectors, are different. In 2018 in [25] we propose to evaluate the magnitude of their ratio, based on a study of the fluctuations in the CMB, which leads to the following conclusion:

$$\frac{a^{(-)}}{a^{(+)}} \simeq \frac{1}{100}, \qquad \frac{c^{(-)}}{c^{(+)}} \simeq \frac{1}{10}. \tag{15}$$

The combination of such different space scale factors and speeds of light would allow a gain factor of 1000 in travel time, regarding a hypothetical technology making apparent FTL interstellar travel by mass inversion possible, as evoked in [23] and [26].

The paper [23] then summarizes many observational data in good agreement with features of the Janus Cosmological Model.

2 The 2014 JCM and the Bianchi identities

From 2014, the Janus system of two coupled field equations (13; 14) satisfies the Bianchi identities, either trivially when the RHS are zero, or when one considers time-dependent homogeneous and isotropic solutions. However, inconsistency appears when one tries to describe with this system a time-independent situation with a spherical symmetry, modeling a star of constant density surrounded by a vacuum. Thus, a new modification of the equation system must be considered, as explained below.

Let's consider a portion of the universe where one of the two species is absent, e.g. the negative energy species, repelled away by a local concentration of positive mass. Let's limit our analysis to the search of a time-independent solution for a spherically symmetric system, and Newtonian approximation. The corresponding system is:

$$R^{(+)}_{\mu\nu} - \frac{1}{2} R^{(+)} g^{(+)}_{\mu\nu} = +\chi T^{(+)}_{\mu\nu}, \tag{16}$$

$$R^{(-)}_{\mu\nu} - \frac{1}{2} R^{(-)} g^{(-)}_{\mu\nu} = -\chi T^{(+)}_{\mu\nu}. \tag{17}$$

Then the two metrics have the form:

$$ds^{(+)2} = e^{\nu^{(+)}} c^2 dt^2 - e^{\lambda^{(+)}} dr^2 - r^2 d\theta^2 - r^2 \sin^2\theta\, d\phi^2, \tag{18}$$

$$ds^{(-)2} = e^{\nu^{(-)}} c^2 dt^2 - e^{\lambda^{(-)}} dr^2 - r^2 d\theta^2 - r^2 \sin^2\theta\, d\phi^2. \tag{19}$$

We consider a sphere whose radius r_s is filled by matter of constant density $\rho^{(+)}$ surrounded by vacuum. Outside of the sphere, the two metrics are:

$$ds^{(+)2} = \left(1-\frac{2m}{r}\right) c^2 dt^2 - \frac{dr^2}{1-\dfrac{2m}{r}} - r^2 d\theta^2 - r^2 \sin^2\theta\, d\phi^2, \tag{20}$$

$$ds^{(-)2} = \left(1+\frac{2m}{r}\right) c^2 dt^2 - \frac{dr^2}{1+\dfrac{2m}{r}} - r^2 d\theta^2 - r^2 \sin^2\theta\, d\phi^2, \tag{21}$$

with:

$$m = \frac{G}{c^2}\frac{4\pi r_s^3}{3}\rho^{(+)}. \tag{22}$$

We can write the stress-energy tensor as:

$$T^{(+)\nu}_{\ \ \mu} = \begin{pmatrix} \rho^{(+)} & 0 & 0 & 0 \\ 0 & -\frac{p^{(+)}}{c^2} & 0 & 0 \\ 0 & 0 & -\frac{p^{(+)}}{c^2} & 0 \\ 0 & 0 & 0 & -\frac{p^{(+)}}{c^2} \end{pmatrix}, \tag{23}$$

where $p^{(+)}$ is the pressure insides the star of radius r_s filled with constant density $\rho^{(+)}$. Equations (16) and (17) give the following differential equations:

$$p^{(+)\prime} = -\left(\rho^{(+)}c^2 + p^{(+)}\right)\frac{m(r) + 4\pi G p^{(+)} r^3/c^4}{r\,(r-2m(r))}, \tag{24}$$

$$p^{(+)\prime} = +\left(\rho^{(+)}c^2 + p^{(+)}\right)\frac{m(r) + 4\pi G p^{(+)} r^3/c^4}{r\,(r+2m(r))}, \tag{25}$$

where:

$$m(r) = \frac{G}{c^2}\frac{4\pi r^3}{3}\rho^{(+)}. \tag{26}$$

After Newtonian approximation:

$$p^{(+)} \ll \rho^{(+)}c^2 \quad , \quad r \gg 2m, \tag{27}$$

which gives:

$$p^{(+)\prime} = -\frac{\rho^{(+)}c^2 m(r)}{r^2}, \tag{28}$$

$$p^{(+)\prime} = +\frac{\rho^{(+)}c^2 m(r)}{r^2}. \tag{29}$$

So that we get a physical and mathematical contradiction, that must be cured.

3 Lagrangian derivation of a new JCM, as of 2019

Consider the two diagonal constant matrices:

$$I = \begin{pmatrix} 1 & 0 & 0 & 0 \\ 0 & 1 & 0 & 0 \\ 0 & 0 & 1 & 0 \\ 0 & 0 & 0 & 1 \end{pmatrix}, \quad \varphi = \begin{pmatrix} 1 & 0 & 0 & 0 \\ 0 & -1 & 0 & 0 \\ 0 & 0 & -1 & 0 \\ 0 & 0 & 0 & -1 \end{pmatrix}. \tag{30}$$

$$S = \int_{D4}\left[IR^{(+)}\sqrt{-g^{(+)}} + \varphi R^{(-)}\sqrt{-g^{(-)}} - \chi\,(I+\varphi)\,L^{(+)}\sqrt{-g^{(+)}} + \chi\,(I+\varphi)\,L^{(-)}\sqrt{-g^{(-)}}\right]\mathrm{d}^4x \tag{31}$$

$$\delta\int_{D4} R^{(+)}\sqrt{-g^{(+)}}\;\mathrm{d}^4x = \int_{D4}\left(R^{(+)}_{\mu\nu} - \frac{1}{2}R^{(+)}g^{(+)}_{\mu\nu}\right)\sqrt{-g^{(+)}}\;\delta g^{(+)\mu\nu}\;\mathrm{d}^4x \tag{32}$$

$$\delta\int_{D4} R^{(-)}\sqrt{-g^{(-)}}\;\mathrm{d}^4x = \int_{D4}\left(R^{(-)}_{\mu\nu} - \frac{1}{2}R^{(-)}g^{(-)}_{\mu\nu}\right)\sqrt{-g^{(-)}}\;\delta g^{(-)\mu\nu}\;\mathrm{d}^4x \tag{33}$$

$$\delta\int_{D4} L^{(+)}\sqrt{-g^{(+)}}\;\mathrm{d}^4x = \int_{D4} T^{(+)}_{\mu\nu}\sqrt{-g^{(+)}}\;\delta g^{(+)\mu\nu}\;\mathrm{d}^4x \tag{34}$$

$$\delta\int_{D4} L^{(-)}\sqrt{-g^{(-)}}\;\mathrm{d}^4x = \int_{D4} T^{(-)}_{\mu\nu}\sqrt{-g^{(-)}}\;\delta g^{(-)\mu\nu}\;\mathrm{d}^4x \tag{35}$$

$$ds^{(+)2} = \left(1 - \frac{8\pi G\,r_s^3\,\rho^{(+)}}{c^2}r\right)c^2dt^2 - \left(1 + \frac{8\pi G\,r_s^3\,\rho^{(+)}}{c^2}r\right)dr^2 - r^2d\theta^2 - \sin^2\theta d\varphi^2 \tag{36}$$

$$ds^{(-)2} = \left(1 + \frac{8\pi G\,r_s^3\,\rho^{(+)}}{c^2}r\right)c^2dt^2 - \left(1 - \frac{8\pi G\,r_s^3\,\rho^{(+)}}{c^2}r\right)dr^2 - r^2d\theta^2 - \sin^2\theta d\varphi^2 \tag{37}$$

$$\delta g^{(+)}_{00} = -\frac{8\pi G\,r_s^3\,\rho^{(+)}}{c^2}\,r\,\delta\rho^{(+)} = -\delta g^{(-)}_{00} \qquad \delta g^{(+)}_{11} = -\frac{8\pi G\,r_s^3\,\rho^{(+)}}{c^2}\,r\,\delta\rho^{(+)} = -\delta g^{(-)}_{11} \tag{38}$$

Introducing the action (eq. 31) and performing the following bivariation, taking account of $I\varphi = \varphi$ and $\varphi\varphi = I$, results in equations 32–35.

From a previous Lagrangian derivation [7] :

$$\delta g^{(-)\mu\nu} = -\delta g^{(+)\mu\nu} \tag{39}$$

Our goal: to set up a system of two coupled field equations providing joint solutions corresponding to Newtonian approximation. In such conditions the external metrics are given in equations (36) and (37).

We may consider that such metrics belong to subsets of Riemannian metrics with signature $(+---)$ which obey relationship (39) (see eqs. (38)). If we consider that (39) defines joint metrics, they obey:

$$R^{(+)}_{\mu\nu} - \frac{1}{2}R^{(+)}\,g^{(+)}_{\mu\nu} = +\chi\left(T^{(+)}_{\mu\nu} + \sqrt{\frac{-\mathbf{g}^{(-)}}{-\mathbf{g}^{(+)}}}\,\varphi\,T^{(-)}_{\mu\nu}\right), \tag{40}$$

$$R^{(-)}_{\mu\nu} - \frac{1}{2}R^{(-)}\,g^{(-)}_{\mu\nu} = -\chi\left(T^{(-)}_{\mu\nu} + \sqrt{\frac{\mathbf{g}^{(+)}}{\mathbf{g}^{(-)}}}\,\varphi\,T^{(+)}_{\mu\nu}\right). \tag{41}$$

4 Back to the star model

Starting from the new joint system (40);(41) we obtain the analogous of the system (16);(17) where, in the second equation, we would replace the tensor $T^{(+)}\,g^{(+)}_{\mu\nu}$ by $\hat{T}^{(+)}_{\mu\nu}$, so that:

$$\hat{T}^{(+)}_{00} = T^{(+)}_{00} = \rho^{(+)}, \tag{42}$$

$$\hat{T}^{(+)}_{ii} = -T^{(+)}_{ii} \qquad \text{with} \qquad \mathrm{j} = \{1,2,3\}, \tag{43}$$

$$R^{(-)}_{\mu\nu} - \frac{1}{2}\,R^{(-)}\,g^{(-)}_{\mu\nu} = -\chi\hat{T}^{(+)}_{\mu\nu}. \tag{44}$$

With the joint metrics (18) and (19), inside the star, plus compatibility conditions satisfying (20) and (21) at its border $r = r_s$ we get the following result:

$$p^{(+)\prime} = -\left(\rho^{(+)}c^2 + p^{(+)}\right)\frac{m(r) + 4\pi G p^{(+)}r^3/c^4}{r\,(r - 2m(r))}, \tag{45}$$

$$p^{(+)\prime} = -\left(\rho^{(+)}c^2 - p^{(+)}\right)\frac{m(r) - 4\pi G p^{(+)}r^3/c^4}{r\,(r + 2m(r))}, \tag{46}$$

with $m(r)$ given by (26).

Equation (45) is nothing but the famous Tolman-Oppenheimer-Volkoff equation.

Applying the Newtonian approximation, any inconsistency vanishes. Such equations mean that inside the star, the pressure counterbalances the gravitational pull. The geodesics are given by equations (48) and (49), with:

$$\hat{R}^2 = \frac{3c^2}{8\pi G\rho^{(+)}}. \tag{47}$$

Linearizing leads to equations (50) and (51). Notice that equation (52) fits (39).

$$ds^{(+)2} = \left[\frac{3}{2}\sqrt{1-\frac{r_s^2}{\hat{R}^2}} - \frac{1}{2}\sqrt{1-\frac{r^2}{\hat{R}^2}}\right]^2 c^2\mathrm{d}t^2 - \frac{\mathrm{d}r^2}{1-\dfrac{r^2}{\hat{R}^2}} - r^2\mathrm{d}\theta^2 - r^2\sin^2\theta\mathrm{d}\phi^2 \tag{48}$$

$$ds^{(-)2} = \left[\frac{3}{2}\sqrt{1+\frac{r_s^2}{\hat{R}^2}} - \frac{1}{2}\sqrt{1+\frac{r^2}{\hat{R}^2}}\right]^2 c^2\mathrm{d}t^2 - \frac{\mathrm{d}r^2}{1+\dfrac{r^2}{\hat{R}^2}} - r^2\mathrm{d}\theta^2 - r^2\sin^2\theta\mathrm{d}\phi^2 \tag{49}$$

$$ds^{(+)2} = \left(1 - \frac{3}{2}\frac{r_s^2}{\hat{R}^2} + \frac{1}{2}\frac{r^2}{\hat{R}^2}\right)c^2\mathrm{d}t^2 - \left(1 + \frac{3}{2}\frac{r_s^2}{\hat{R}^2} - \frac{1}{2}\frac{r^2}{\hat{R}^2}\right)\mathrm{d}r^2 - r^2\mathrm{d}\theta^2 - r^2\sin^2\theta\mathrm{d}\varphi^2 \tag{50}$$

$$ds^{(-)2} = \left(1 + \frac{3}{2}\frac{r_s^2}{\hat{R}^2} - \frac{1}{2}\frac{r^2}{\hat{R}^2}\right)c^2\mathrm{d}t^2 - \left(1 - \frac{3}{2}\frac{r_s^2}{\hat{R}^2} + \frac{1}{2}\frac{r^2}{\hat{R}^2}\right)\mathrm{d}r^2 - r^2\mathrm{d}\theta^2 - r^2\sin^2\theta\mathrm{d}\varphi^2 \tag{51}$$

$$\delta g_{00}^{(+)} = -\frac{4\pi G\left(3r_s^3 - r^2\right)}{3c^2}\,\delta\rho^{(+)} = -\delta g_{00}^{(-)} \qquad \delta g_{11}^{(+)} = -\frac{4\pi G\left(3r_s^3 - r^2\right)}{3c^2}\,r\,\delta\rho^{(+)} = -\delta g_{11}^{(-)} \tag{52}$$

5 Back to our basic assumption: $\delta g^{(-)\mu\nu} = -\delta g^{(+)\mu\nu}$

The time-dependent joint solutions presented in [21] correspond to the following FRLW metrics:

$$\mathrm{d}s^{(+)2} = \left(dx^0\right)^2 - a^{(+)^2}\frac{\mathrm{d}u^2 + u^2\,\mathrm{d}\theta^2 + u^2\,\sin^2\theta\,\mathrm{d}\varphi^2}{\left(1 + \dfrac{k^{(+)}\,u^2}{4}\right)^2}, \tag{53}$$

$$\mathrm{d}s^{(-)2} = \left(dx^0\right)^2 - a^{(-)^2}\frac{\mathrm{d}u^2 + u^2\,\mathrm{d}\theta^2 + u^2\,\sin^2\theta\,\mathrm{d}\varphi^2}{\left(1 + \dfrac{k^{(-)}\,u^2}{4}\right)^2}, \tag{54}$$

which give, with the single solution $k^{(+)} = k^{(-)} = -1$:

$$a^{(+)2}\frac{\mathrm{d}^2a^{(+)}}{(\mathrm{d}x^0)^2}, -\frac{8\pi G\rho_0}{3c_0^2} = 0 \tag{55}$$

$$a^{(-)2}\frac{\mathrm{d}^2a^{(-)}}{(\mathrm{d}x^0)^2}. + \frac{8\pi G\rho_0}{3c_0^2} = 0 \tag{56}$$

Whose exact parametric solutions are, for (55):

$$x^0 = \frac{4\pi G\rho_0}{3c_0^2}\left(1 + \frac{sh(2v)}{2} + v\right), \tag{57}$$

$$a^{(+)} = \frac{4\pi G\rho_0}{3c_0^2}ch^2(v), \tag{58}$$

and for (56):

$$x^0 = \frac{4\pi G\rho_0}{3c_0^2}\left(sh(2w) - 2\,w\right), \tag{59}$$

$$a^{(-)} = \frac{4\pi G\rho_0}{3c_0^2}\left(ch^2(w) - 1\right). \tag{60}$$

Let's compute the variations $\delta g_{\mu\nu}^{(+)}$ and $\delta g_{\mu\nu}^{(-)}$ under a variation $\delta\rho_0$ of their single parameter, the dominant matter density ρ_0. The variations $\delta g_{00}^{(+)}$, $\delta g_{00}^{(-)}$, $\delta g_{11}^{(+)}$, $\delta g_{11}^{(-)}$ depend on the factors $a^{(+)}\delta a^{(+)}$ and $a^{(-)}\delta a^{(-)}$. But we have:

$$\begin{aligned}&\frac{\mathrm{d}a^{(+)}}{\mathrm{d}x^0} = th(v),\\ &\frac{\mathrm{d}^2a^{(+)}}{(\mathrm{d}x^0)^2} = \frac{1}{\mathrm{d}x^0}\left(\frac{\mathrm{d}a^{(+)}}{\mathrm{d}x^0}\right) = \frac{3c_0^2}{4\pi G\rho_0}\frac{1}{2\,ch^4(v)},\end{aligned} \tag{61}$$

and similar equations for the second metric solution, so that $\delta a^{(+)}/\delta\rho_0 = \delta a^{(-)}/\delta\rho_0 = 0$ which fits our fundamental relationship (39).

6 Conclusion

A model is never definitively fixed in time. The set of two coupled field equations first established in [9] corresponded to a first step. The present paper proposes an updated system that has been mathematically enriched to give a precise description of the matter-dominated era. In its Newtonian approximation, it provides a new insight on astrophysics, especially in galactic dynamics which no longer depends on a set of a single Vlasov equation plus Poisson but on two Vlasov equations coupled with Poisson's equation. New results in that field will be published soon.

At the present time, JCM provides:

- joint solutions $\left(g_{\mu\nu}^{(+)}, g_{\mu\nu}^{(-)}\right)$ corresponding to the functional space of Riemannian metrics of signature $(+\,-\,-\,-)$, fitting fundamental relationship $g_{\mu\nu}^{(+)} = -g_{\mu\nu}^{(-)}$.
- with stationary and spherically symmetric conditions in the vacuum.
- time dependent homogeneous and isotropic solutions.

Which cover everything that can currently be confronted with observations.

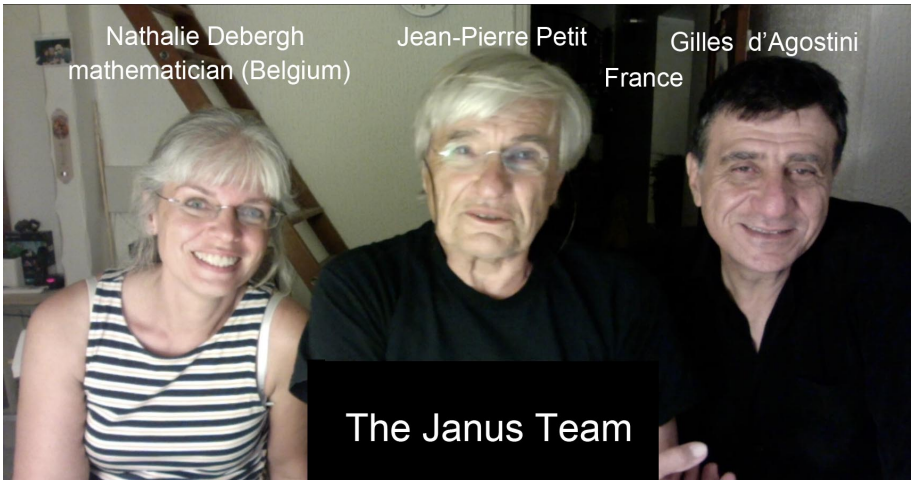

To a model already compliant with many observational data [22], a physically and mathematically coherent representation of joint geometries for positive energy and mass species, in the solar system and its neighborhood, has been added. Therefore, the Janus cosmological model agrees with classical verifications of general relativity.

By reversing this situation, considering instead a portion of space where negative mass largely dominates locally, i.e. where positive mass has been repelled away so its mass density can be taken equal to zero, we obtain the first coherent theoretical description of the *Great Repeller*, which has been exposed in [26].

When photons emitted by high redshift galaxies (z>7) cross negative mass conglomerates in the center of big cosmic voids, in the large-scale structure of the universe, negative gravitational lensing reduces their apparent magnitude, making them appear as dwarf galaxies, which is consistent with observations.

One may argue that the Janus theory exhibiting tow coupled metrics as a "natural" hypothesis with the confidence that subsequent results would eventually corroborate the postulate. However this bimetric model is formally sustained by a specific splitting of the Riemann Tensor which yields to 2nd rank tensor field equations, as shown in [27].

Submitted January 6, 2019

References

1. Sakharov A.D. Violation of CP invariance, C asymmetry, and baryon asymmetry of the universe. *JETP Letters*, 1967, v. 5(1), 24–26.
2. Petit J.-P. Univers jumeaux, énantiomorphes, à temps propre opposées. [Enantiomorphic twin universes with opposite proper times]. *Comptes Rendus de l'Académie des Sciences*, 1977, v. 263, 1315–1318.
3. Petit J.-P. Univers en interaction avec leurs images dans le miroir du temps. [Universes interacting with their opposite time-arrow fold]. *Comptes Rendus de l'Académie des Sciences*, 1977, v. 284, 1413–1416.
4. Boyle L., Finn K., Neil Turok N. CPT-Symmetric Universe. *Physical Review Letters*, 2018, v. 121, 251301. arXiv:1803.08928.
5. Petit J.-P. The missing-mass problem. *Il Nuovo Cimento B*, 1994, v. 109(7), 697–709.
6. Petit J.-P., Midy P., Landsheat F. Twin matter against dark matter. Marseille Cosmology Conference Where's the Matter? Tracing Dark and Bright Matter with the New Generation of Large Scale Surveys, Marseille, France, (2001).
7. Petit J.-P., d'Agostini G. Lagrangian derivation of the two coupled field equations in the Janus cosmological model. *Astrophysics and Space Science*, 2015, v. 357(67), 67.
8. Farnes J.S. A unifying theory of dark energy and dark matter: Negative masses and matter creation within a modified ΛCDM framework. *Astronomy & Astrophysics*, 2018, v. 620, A92. arXiv:1712.07962. doi:10.1051/0004–6361/201832898.
9. Bondi H. Negative Mass in General Relativity. *Reviews of Modern Physics*, 1957, v. 29(3), 423–428.
10. Bonnor W.B. Negative mass in general relativity. *General Relativity and Gravitation*, 1989, v. 21(11), 1143–1157.
11. Chardin G., Manfredi G. Gravity, antimatter and the Dirac-Milne universe. *General Relativity and Quantum Cosmology*, 2018, v. 239, 45. arXiv:1807.11198. doi:10.1007/s10751–018-1521–3.
12. Bondi H., Bergmann P., Gold T., Pirani F. Negative mass in general relativity in The Role of Gravitation in Physics: Report from the 1957 Chapel Hill Conference, Open Access Editions Epubli 2011. ISBN:978-3869319636.
13. Petit J.-P. Twin universes cosmology. *Astrophysics and Space Science*, 1995, v. 227(2), 273–307.
14. Souriau J.-M. "§14: A mechanistic description of elementary particles: Inversions of space and time" in Structure of Dynamical Systems. Progress in Mathematics. Boston: Birkhäuser, (1997). pp. 189–193. doi:10.1007/978–1–4612–0281–3_14. ISBN 978–1–4612–6692–1. Published originally in French in Structure des Systèmes Dynamiques, Dunod 1970.
15. Debergh N., Petit J.-P., d'Agostini G. On evidence for negative energies and masses in the Dirac equation through a unitary time-reversal operator. *Journal of Physics Communications*, 2018, v. 2(11), 115012. arXiv:1809.05046.
16. Damour T., Kogan I.I. Effective Lagrangians and universality classes of nonlinear bigravity. *Physical Review D*, 2002, v. 66, 104024. arXiv:hep-th/0206042.
17. Hossenfelder S. A Bi-Metric Theory with Exchange Symmetry. *Physical Review D*, 2008, v. 78(4), 044015. arXiv:0807.2838.
18. Hossenfelder S. Antigravitation. 17th International Conference on Supersymmetry and the Unification of Fundamental Interactions. Boston: American Institute of Physics, (2009). arXiv:0909.3456.

19. Lightman A.P., Lee D.L. New Two-Metric Theory of Gravity with Prior Geometry. *Physical Review D*, 1973, v. 8(10), 3293.

20. Rosen N. A bi-metric Theory of Gravitation. *General Relativity and Gravitation*, 1973, v. 4(6), 435–447.

21. Petit J.-P., d'Agostini G. Negative mass hypothesis in cosmology and the nature of dark energy. *Astrophysics and Space Science*, 2014, v. 354(2), 611.

22. D'Agostini G., Petit J.-P. Constraints on Janus Cosmological model from recent observations of supernovae type Ia. *Astrophysics and Space Science*, 2018, v. 363(7), 139.

23. Petit J.-P., d'Agostini G. Cosmological bimetric model with interacting positive and negative masses and two different speeds of light, in agreement with the observed acceleration of the Universe. *Modern Physics Letters A*, 2014, v. 29(34), 1450182.

24. Petit J.-P. Janus Cosmological Model and the Fluctuations of the CMB. *Progress in Physics*, 2018, v. 14(4), 226–229.

25. Petit J.-P., Debergh N., d'Agostini G. Negative energy states and interstellar travel. Advanced Propulsion Workshop. Estes Park, CO: Space Studies Institute, (September 2018).

26. Hoffman Y., Pomarède D., Tully R.B., Courtois H.M. The dipole repeller. *Nature Astronomy*, 2017, v. 1(2), 0036. arXiv:1702.02483.

27. Marquet P. On a 4th Tensor Gravitational Theory. *Progress in Physics*, 2017, v. 13(2), 106–110.

Non-commutativity: Unusual View

Valeriy V. Dvoeglazov

UAF, Universidad Autónoma de Zacatecas Apartado Postal 636, Suc. 3, C. P. 98061, Zacatecas, Zac., México. E-mail: valeri@fisica.uaz.edu.mx

Some ambiguities have recently been found in the definition of the partial derivative (in the case of presence of both explicit and implicit dependencies of the function subjected to differentiation). We investigate the possible influence of this subject on quantum mechanics and the classical/quantum field theory. Surprisingly, some commutators of operators of space-time 4-coordinates and those of 4-momenta are *not* equal to zero. We postulate the non-commutativity of 4-momenta and we derive mass splitting in the Dirac equation. Moreover, two iterated limits may not commute each other, in general. Thus, we present an example when the massless limit of the function of $E, \mathbf{p}, m$ does not exist in some calculations within quantum field theory.

1 Introduction

The assumption that the operators of coordinates do *not* commute $[\hat{x}_\mu, \hat{x}_\nu]_- \neq 0$ has been made by H. Snyder [1]. Therefore, the Lorentz symmetry may be broken. This idea [2, 3] received attention in the context of "brane theories". Moreover, the famous Feynman-Dyson proof of Maxwell equations [4] contains intrinsically the non-commutativity of velocities $[\dot{x}_i(t), \dot{x}_j(t)]_- \neq 0$ that also may be considered as a contradiction with the well-accepted theories (while there is no any contradiction therein).

On the other hand, it was recently discovered that the concept of partial derivative is *not* well defined in the case of both explicit and implicit dependence of the corresponding function, which the derivatives act upon [5]. The well-known example of such a situation is the field of an accelerated charge [6].* Škovrlj and Ivezić [7] call this partial derivative as '*complete* partial derivative'; Chubykalo and Vlayev, as '*total* derivative with respect to a given variable'. The terminology suggested by Brownstein [5] is 'the *whole*-partial derivative'.

2 Example 1

Let us study the case when we deal with explicite and implicite dependencies $f(\mathbf{p}, E(\mathbf{p}))$. It is well known that the energy in relativism is related to the 3-momentum as $E = \pm\sqrt{\mathbf{p}^2 + m^2}$; the unit system $c = \hbar = 1$ is used. In other words, we must choose the 3-dimensional mass hyperboloid in the Minkowski space, and the energy is *not* an independent quantity anymore. Let us calculate the commutator of the whole-partial derivatives $\hat{\partial}/\hat{\partial}E$ and $\hat{\partial}/\hat{\partial}p_i$. In order to make distinction between differentiating the explicit function and that which contains both explicit and implicit dependencies, the 'whole partial derivative' may be denoted as $\hat{\partial}$. In the general case one has

$$\frac{\hat{\partial} f(\mathbf{p}, E(\mathbf{p}))}{\hat{\partial} p_i} \equiv \frac{\partial f(\mathbf{p}, E(\mathbf{p}))}{\partial p_i} + \frac{\partial f(\mathbf{p}, E(\mathbf{p}))}{\partial E}\frac{\partial E}{\partial p_i}\,. \qquad (1)$$

Applying this rule, we find surprisingly

$$\begin{aligned}&\left[\frac{\hat{\partial}}{\hat{\partial} p_i}, \frac{\hat{\partial}}{\hat{\partial} E}\right]_- f(\mathbf{p}, E(\mathbf{p})) = \\ &\frac{\hat{\partial}}{\hat{\partial} p_i}\frac{\partial f}{\partial E} - \frac{\partial}{\partial E}\left(\frac{\partial f}{\partial p_i} + \frac{\partial f}{\partial E}\frac{\partial E}{\partial p_i}\right) = \\ &\frac{\partial^2 f}{\partial E \partial p_i} + \frac{\partial^2 f}{\partial E^2}\frac{\partial E}{\partial p_i} - \frac{\partial^2 f}{\partial p_i \partial E} - \frac{\partial^2 f}{\partial E^2}\frac{\partial E}{\partial p_i} - \frac{\partial f}{\partial E}\frac{\partial}{\partial E}\left(\frac{\partial E}{\partial p_i}\right).\end{aligned} \qquad (2)$$

So, if $E = \pm\sqrt{m^2 + \mathbf{p}^2}$ and one uses the generally-accepted representation form of $\partial E/\partial p_i = p_i/E$, one has that the expression (2) appears to be equal to $(p_i/E^2)\frac{\partial f(\mathbf{p}, E(\mathbf{p}))}{\partial E}$. Within the choice of the normalization the coefficient may be related to the longitudinal electric field in the helicity basis.† Next, the commutator is

$$\left[\frac{\hat{\partial}}{\hat{\partial} p_i}, \frac{\hat{\partial}}{\hat{\partial} p_j}\right]_- f(\mathbf{p}, E(\mathbf{p})) = \frac{1}{|E|^3}\frac{\partial f(\mathbf{p}, E(\mathbf{p}))}{\partial E}[p_i, p_j]_-\,. \qquad (3)$$

This should also not be zero according to Feynman and Dyson [4]. They postulated that the velocity (or, of course, the 3-momentum) commutator is equal to $[p_i, p_j] \sim i\hbar\epsilon_{ijk}B^k$, i.e., to the magnetic field. In fact, if we put in the coresponsdence to the momenta their quantum-mechanical operators (of course, with the appropriate clarification $\partial \to \hat{\partial}$), we obtain again that, in general, the derivatives do *not* commute $\left[\frac{\hat{\partial}}{\hat{\partial} x_\mu}, \frac{\hat{\partial}}{\hat{\partial} x_\nu}\right]_- \neq 0$.

Furthermore, since the energy derivative corresponds to the operator of time and the i-component momentum deriva-

*Firstly, Landau and Lifshitz wrote that the functions depended on t', and only through $t' + R(t')/c = t$ they depended implicitly on x, y, z, t. However, later (in calculating the formula (63.7)) they used the explicit dependence of R on the space coordinates of the observation point too. Jackson [8] agrees with [6] that one should find "a contribution to the spatial partial derivative for fixed time t from explicit spatial coordinate dependence (of the observation point)."

†The electric/magnetic fields can be derived from the 4-potentials which have been presented in [9].

tive, to $\hat{x}_i$, we put forward the following anzatz in the momentum representation:

$$[\hat{x}^\mu, \hat{x}^\nu]_- = \omega(\mathbf{p}, E(\mathbf{p}))\, F_\parallel^{\mu\nu}(\mathbf{p}) \frac{\partial}{\partial E}\,, \tag{4}$$

with some weight function ω being different for different choices of the antisymmetric tensor spin basis. The physical dimension of x^μ is $[energy]^{-1}$ in this unit system; $F_\parallel^{\mu\nu}(\mathbf{p})$ has the dimension $[energy]^0$, if we assume the mass shell condition in the definition of the field operators $\delta(p^2 - m^2)$, see [10]. Therefore, the weight function should have the dimension $[energy]^{-1}$. The commutator $[\hat{x}^\mu, \hat{p}^\nu]$ has the same form as in the textbook nonrelativistic quantum mechanics within the presented model.

In the modern literature, the idea of the broken Lorentz invariance by this method concurs with the idea of the *fundamental length*, first introduced by V. G. Kadyshevsky [11] on the basis of old papers by M. Markov. Both ideas and corresponding theories are extensively discussed. In my opinion, the main question is: what is the space scale, when the relativity theory becomes incorrect.

3 Example 2

In the previous Section (see also the paper [12]) we found some intrinsic contradictions related to the mathematical foundations of modern physics. It is well known that the partial derivatives commute in the Minkowski space (as well as in the 4-dimensional momentum space). However, if we consider that energy is an implicit function of the 3-momenta and mass (thus, approaching the mass hyperboloid formalism, $E^2 - \mathbf{p}^2c^2 = m^2c^4$) then we may be interested in the commutators of the whole-partial derivatives [5] instead. The whole-partial derivatives do not commute, as you see above. If they are associated with the corresponding physical operators, we would have the uncertainty relations in this case. This is an intrinsic contradiction of the SRT. While we start from the same postulates, on using two different ways of reasoning we arrive at the two different physical conclusions.

In this Section I would like to ask another question. Sometimes, when calculating dynamical invariants (and other physical quantities in quantum field theory), and when studying the corresponding massless limits we need to calculate iterated limits. We may encounter a rare situation when two iterated limits are not equal each other in physics. See, for example, Ref. [10]. We were puzzled calculating the iterated limits of the aggregate $\frac{E^2-\mathbf{p}^2}{m^2}$ (or the inverse one, $\frac{m^2}{E^2-\mathbf{p}^2}$, $c = \hbar = 1$):

$$\lim_{m\to 0} \lim_{E\to \pm\sqrt{\mathbf{p}^2+m^2}} \left(\frac{m^2}{E^2 - \mathbf{p}^2}\right) = 1\,, \tag{5}$$

$$\lim_{E\to \pm\sqrt{\mathbf{p}^2+m^2}} \lim_{m\to 0} \left(\frac{m^2}{E^2 - \mathbf{p}^2}\right) = 0\,. \tag{6}$$

Similar mathematical examples are presented in [13]. Physics should have well-defined dynamical invariants. Which iterated limit should be applied in the study of massless limits? The question of the iterated limits was studied in [14]. However, the answers leave room for misunderstandings and contradictions with the experiments. One can say: "The two limits are of very different sorts: the limit of $E \to \pm\sqrt{\mathbf{p}^2 + m^2}$ is a limit that subsumes the statement under the theory of Special Relativity. Such limits should be done first." However, cases exist when the limit $E \to \pm\sqrt{\mathbf{p}^2 + m^2}$ cannot be applied (or its application leads to the loss of the information). For example, we have for the causal Green's function used in the scalar field theory and in the $m \to 0$ quantum electrodynamics (QED), Ref. [15]:

$$D^c(x) = \frac{1}{(2\pi)^4}\int d^4p \frac{e^{-ip\cdot x}}{m^2 - p^2 - i\epsilon} \tag{7}$$
$$= \frac{1}{4\pi}\delta(\lambda) - \frac{m}{8\pi\sqrt{\lambda}}\theta(\lambda)\left[J_1(m\sqrt{\lambda}) - iN_1(m\sqrt{\lambda})\right] + \frac{im}{4\pi^2\sqrt{-\lambda}}\theta(-\lambda)K_1(m\sqrt{-\lambda}),$$

$\lambda = (x^0)^2 - \mathbf{x}^2$; J_1, N_1, K_1 are the Bessel functions of the first order. The application of $E \to \pm\sqrt{\mathbf{p}^2 + m^2} - i\delta$ results in non-existence of the integral. Meanwhile, the massless limit is made in the integrand in the Feynman gauge with no problems. Please remember that integrals are also the limits of the Riemann integral sums. The $m \to 0$ limits are made first sometimes.

Next, the application of the mass shell condition in the Weinberg-Tucker-Hammer $2(2S + 1)$-formalism leads to the fact that we would not be able to write the dynamical equation in the covariant form $[\gamma^{\mu\nu}\partial_\mu\partial_\nu - m^2]\Psi_{(6)}(x) = 0$. Apart, the information about the propagation of longitudinal modes would be lost (cf. formulas (19,20,27,28) of the first paper [10]). Moreover, the Weinberg equation and the mapping of the Tucker-Hammer equation to the antisymmetric tensor formalism have different physical contents on the interaction level [16, 17].*

Next, if we would always apply the mass shell condition first then we come to the derivative paradox of the previous Section. Finally, the condition $E^2 - \mathbf{p}^2 = m^2$ does not always imply the generally-accepted special relativity only. For instance, see the Kapuscik work, Ref. [18], who showed that similar expressions for energy and momentum exist for particles with $V > c$ and $m_\infty \in \mathfrak{R}e$.

Meanwhile, the case $m = 0$ appears to be equivalent to the light cone condition $r = ct$, which can be taken even without

*I take this opportunity to note that problems (frequently forgotten) may also exist with the direct application of $m \to 0$ in relativistic quantum equations. The case is: when the solutions are constructed on using the relativistic boosts in the momentum space the mass may appear in the denominator, $\sim 1/m^n$, which cancels the mass terms of the equation giving the non-zero corresponding result.

the mass shell condition to study the theories extending the special relativity. Not everybody realizes that it can be used to deduce the Lorentz transformations between two different reference frames. Just take squares and use the lineality: $r_1^2 - c^2t_1^2 = 0 = r_2^2 - c^2t_2^2$. Hence, in $d = 1 + 1$ we have $x_2 = \gamma(x_1 - vt_1)\,, \quad t_2 = \alpha(t_1 - \frac{\beta}{c}x_1)$ with $\alpha = \gamma = 1/\sqrt{1 - \frac{v^2}{c^2}}$, the Lorentz factor; $\beta = v/c$.

4 Example 3

The problem of explaining mass splitting of leptons (e, μ, τ) and quarks has a long history. See, for instance, a method suggested in Refs. [19], and some new insights in [20]. Non-commutativity [1] also exhibits interesting peculiarities in the Dirac case. Recently, we analyzed the Sakurai-van der Waerden method of deriving the Dirac (and higher-spin) equation [21]. We can start from

$$(EI^{(2)} - \boldsymbol{\sigma}\cdot\mathbf{p})(EI^{(2)} + \boldsymbol{\sigma}\cdot\mathbf{p})\Psi_{(2)} = m^2\Psi_{(2)}\,, \tag{8}$$

or

$$(EI^{(4)} + \boldsymbol{\alpha}\cdot\mathbf{p} + m\beta)(EI^{(4)} - \boldsymbol{\alpha}\cdot\mathbf{p} - m\beta)\Psi_{(4)} = 0\,. \tag{9}$$

E and $\mathbf{p}$ form the Lorentz 4-momentum. Obviously, the inverse operators of the Dirac operators exist in the non- commutative case. As in the original Dirac work, we have $\beta^2 = 1$, $\alpha^i\beta + \beta\alpha^i = 0$, $\alpha^i\alpha^j + \alpha^j\alpha^i = 2\delta^{ij}$.

We also postulate non-commutativity relations for the components of 4-momenta:

$$[E, \mathbf{p}^i]_- = \Theta^{0i} = \theta^i\,, \tag{10}$$

as usual. Therefore the equation (9) will *not* lead to the well-known equation $E^2 - \mathbf{p}^2 = m^2$. Instead, we have

$$\{E^2 - E(\boldsymbol{\alpha}\cdot\mathbf{p}) + (\boldsymbol{\alpha}\cdot\mathbf{p})E - \mathbf{p}^2 - m^2 \\ -i(\boldsymbol{\sigma}\otimes I_{(2)})[\mathbf{p}\times\mathbf{p}]\}\Psi_{(4)} = 0\,.$$

For the sake of simplicity, we may assume the last term to be zero. Thus, we arrive at

$$\left\{E^2 - \mathbf{p}^2 - m^2 - (\boldsymbol{\alpha}\cdot\boldsymbol{\theta})\right\}\Psi_{(4)} = 0\,. \tag{11}$$

We can apply the unitary transformation. It is known [22, 23] that one can* $U_1(\boldsymbol{\sigma}\cdot\mathbf{a})U_1^{-1} = \sigma_3|\mathbf{a}|$. For $\boldsymbol{\alpha}$ matrices we rewrite as

$$\mathcal{U}_1(\boldsymbol{\alpha}\cdot\boldsymbol{\theta})\mathcal{U}_1^{-1} = |\boldsymbol{\theta}|\begin{pmatrix}1&0&0&0\\0&-1&0&0\\0&0&-1&0\\0&0&0&1\end{pmatrix} = \alpha_3|\boldsymbol{\theta}|\,. \tag{12}$$

The explicit form of the U_1 matrix is ($a_{r,l} = a_1 \pm ia_2$):

$$U_1 = \frac{1}{\sqrt{2a(a+a_3)}}\begin{pmatrix}a+a_3 & a_l\\ -a_r & a+a_3\end{pmatrix} = \tag{13}$$
$$= \frac{1}{\sqrt{2a(a+a_3)}}[a + a_3 + i\sigma_2 a_1 - i\sigma_1 a_2]\,,$$
$$\mathcal{U}_1 = \begin{pmatrix}U_1 & 0\\ 0 & U_1\end{pmatrix}. \tag{14}$$

We now apply the second unitary transformation:

$$\mathcal{U}_2\alpha_3\mathcal{U}_2^\dagger = \begin{pmatrix}1&0&0&0\\0&0&0&1\\0&0&1&0\\0&1&0&0\end{pmatrix}\alpha_3\begin{pmatrix}1&0&0&0\\0&0&0&1\\0&0&1&0\\0&1&0&0\end{pmatrix} = \\ = \begin{pmatrix}1&0&0&0\\0&1&0&0\\0&0&-1&0\\0&0&0&-1\end{pmatrix}. \tag{15}$$

The final equation is then

$$\left[E^2 - \mathbf{p}^2 - m^2 - \gamma^5_{chiral}|\boldsymbol{\theta}|\right]\Psi'_{(4)} = 0\,. \tag{16}$$

In physical terms this implies mass splitting for a Dirac particle over the non-commutative space, $m_{1,2} = \pm\sqrt{m^2 \pm \theta}$. This procedure may be attractive as explanation of mass creation and mass splitting in fermions.

5 Conclusions

We found that the commutator of two derivatives may be *not* equal to zero. As a consequence, for instance, the question arises, if the derivative $\hat\partial^2 f/\hat\partial p^\nu\hat\partial p^\mu$ is equal to the derivative $\hat\partial^2 f/\hat\partial p^\mu\hat\partial p^\nu$ in all cases?† The presented consideration permits us to provide some bases for non-commutative field theories and induces us to look for further development of the classical analysis in order to provide a rigorous mathematical basis for operations with functions which have both explicit and implicit dependencies. Several other examples are presented. Thus, while for physicists everything is obvious in the solutions of the paradoxes, this is not so for mathematicians.

Acknowledgements

I am grateful to participants of conferences where this idea has been discussed.

Submitted on February 18, 2019

*Some relations for the components $\mathbf{a}$ must be assumed. Moreover, in our case $\boldsymbol{\theta}$ must not depend on E and $\mathbf{p}$. Otherwise, we must take the non-commutativity $[E, \mathbf{p}^i]_-$ into account again.

†The same question can be put forward when we have differentiation with respect to the coordinates too, that may have impact on the correct calculations of the problem of accelerated charge in classical electrodynamics.

References

1. Snyder H. *Phys. Rev.*, 1947, v. 71, 38; ibid., v. 72, 68.
2. Seiberg N. and Witten E. *JHEP*, 1999, v. 9909, 032, hep-th/9908142
3. Kruglov S.I. *Ann. Fond. Broglie*, 2002, v. 27, 343, hep-th/0110059; Sidharth, B.G. *Ann. Fond. Broglie*, 2002, v. 27, 333, physics/0110040.
4. Dyson F. *Am. J. Phys.*, 1990, v. 58, 209; Tanimura S. *Ann. Phys.*, 1992, v. 220, 229; Land M., Shnerb N. and Horwitz L. hep-th/9308003.
5. Brownstein K.R., *Am. J. Phys.*, 1999, v. 67, 639.
6. Landau L.D. and Lifshitz E.M. The Classical Theory of Fields. 4th revised English ed. [Translated from the 6th Russian edition], Pergamon Press, (1979). 402p., §63.
7. Škovrlj L. and Ivezić T. hep-ph/0203116.
8. Jackson J.D. hep-ph/0203076.
9. Jacob M. and Wick G.C. *Ann. Phys.*, 1959, v. 7, 404; Ruck H.M. and Greiner W. *J. Phys. G: Nucl. Phys.*, 1977, v. 3, 657.
10. Dvoeglazov V.V. *Int. J. Theor. Phys.* 1998, v. 37, 1915; idem., *Czech. J. Phys.*, 2000, v. 50, 225.
11. Kadyshevsky V.G. *Nucl. Phys.* v. B141, 477 (1978); Kadyshevsky V.G., Mateev M.D., Mir-Kasimov R.M. and Volobuev I.P. *Theor. Math. Phys.*, 1979, v. 40, 800 [*Teor. Mat. Fiz.*, 1979, v. 40, 363]; Kadyshevsky V.G. and Mateev M.D. *Phys. Lett.*, 1981, v. B106, 139; Kadyshevsky V.G. and Mateev M.D. *Nuovo Cim.*, 1985, v. A87, 324.
12. Dvoeglazov V.V. *Phys. Essays*, 2018, v. 31, 340.
13. https://en.wikipedia.org/wiki/Iterated Limit .
14. Ilyin V.A, Sadovnichii V.A. and Sendov B.Kh. Mathematical Analysis. Continuation, MSU, Moscow, (1987), in Russian; Ilyin V.A. and Poznyak E.G., Fundamentals of Mathematical Analysis. Vol. 1. Ch. 14. Functions of Several Variables, Fizmatlit, Moscow, (2002), in Russian.
15. Bogoliubov N.N. and Shirkov D.V. Introduction to the Theory of Quantized Fields. 2nd Edition, Nauka, Moscow, (1973), in Russian.
16. Weinberg S. *Phys. Rev.*, 1964, v. B133, 1318.
17. Tucker R.H. and Hammer C.L. *Phys. Rev.*, 1971, v. D3, 2448.
18. Kapuścik E. In: Relativity, Gravitation, Cosmology: Beyond Foundations. Ed. by Dvoeglazov V.V., Nova Science Pubs., Hauppauge, NY, USA, (2018).
19. Barut A.O. *Phys. Lett.*, 1978, v. B73, 310; idem., *Phys. Rev. Lett.*, 1979, v. 42, 1251; Wilson R., *Nucl. Phys.*, 1974, v. B68, 157.
20. Dvoeglazov V.V. *Int. J. Theor. Phys.*, 1998, v. 37, 1909; idem., *Adv. Appl. Cliff. Alg.*, 2008, v. 18, 579.
21. Dvoeglazov V.V. *Rev. Mex. Fis. Supl.* , 2003, v. 49, 99. (*Proceedings of the DGFM-SMF School, Huatulco, 2000*).
22. Berg R.A. *Nuovo Cimento*, 1966, v. 42A, 148.
23. Dvoeglazov V.V. *Nuovo Cimento*, 1995, v. A108, 1467.

The Journal on Advanced Studies in Theoretical and Experimental Physics, including Related Themes from Mathematics

PROGRESS IN PHYSICS

A quarterly issue scientific journal, registered with the Library of Congress (DC, USA). This journal is peer reviewed and included in the abstracting and indexing coverage of: Mathematical Reviews and MathSciNet (AMS, USA), DOAJ of Lund University (Sweden), Scientific Commons of the University of St. Gallen (Switzerland), Open-J-Gate (India), Referativnyi Zhurnal VINITI (Russia), etc.

Electronic version of this journal:
http://www.ptep-online.com

Postal Address

Department of Mathematics and Science,
University of New Mexico,
705 Gurley Ave., Gallup, NM 87301, USA

ISSN: 1555-5534 (print)
ISSN: 1555-5615 (online)

Standard Address Number: 297-5092
Printed in the United States of America

July 2019 **Vol. 15, Issue 2**

CONTENTS

Information for Authors

Progress in Physics has been created for rapid publications on advanced studies in theoretical and experimental physics, including related themes from mathematics and astronomy. All submitted papers should be professional, in good English, containing a brief review of a problem and obtained results.

All submissions should be designed in LaTeX format using *Progress in Physics* template. This template can be downloaded from *Progress in Physics* home page http://www.ptep-online.com

Preliminary, authors may submit papers in PDF format. If the paper is accepted, authors can manage LaTeXtyping. Do not send MS Word documents, please: we do not use this software, so unable to read this file format. Incorrectly formatted papers (i.e. not LaTeXwith the template) will not be accepted for publication. Those authors who are unable to prepare their submissions in LaTeXformat can apply to a third-party payable service for LaTeX typing. Our personnel work voluntarily. Authors must assist by conforming to this policy, to make the publication process as easy and fast as possible.

Abstract and the necessary information about author(s) should be included into the papers. To submit a paper, mail the file(s) to the Editor-in-Chief.

All submitted papers should be as brief as possible. Short articles are preferable. Large papers can also be considered. Letters related to the publications in the journal or to the events among the science community can be applied to the section *Letters to Progress in Physics*.

All that has been accepted for the online issue of *Progress in Physics* is printed in the paper version of the journal. To order printed issues, contact the Editors.

Authors retain their rights to use their papers published in *Progress in Physics* as a whole or any part of it in any other publications and in any way they see fit. This copyright agreement shall remain valid even if the authors transfer copyright of their published papers to another party.

Electronic copies of all papers published in *Progress in Physics* are available for free download, copying, and re-distribution, according to the copyright agreement printed on the titlepage of each issue of the journal. This copyright agreement follows the *Budapest Open Initiative* and the *Creative Commons Attribution-Noncommercial-No Derivative Works 2.5 License* declaring that electronic copies of such books and journals should always be accessed for reading, download, and copying for any person, and free of charge.

Consideration and review process does not require any payment from the side of the submitters. Nevertheless the authors of accepted papers are requested to pay the page charges. *Progress in Physics* is a non-profit/academic journal: money collected from the authors cover the cost of printing and distribution of the annual volumes of the journal along the major academic/university libraries of the world. (Look for the current author fee in the online version of *Progress in Physics*.)

The Dirac Equation and Its Relationship to the Fine Structure Constant According to the Planck Vacuum Theory

William C. Daywitt

National Institute for Standards and Technology (retired), Boulder, Colorado. E-mail: wcdaywitt@me.com

The Dirac equation and the fine structure constant are complementary and cannot be understood separately. The manifestly covariant Dirac equation in the Planck vacuum (PV) theory (8) is a coupling-charge equation, where e_*^2 is the squared coupling charge that couples the equation to the PV state. The laboratory-measured electron or proton mass is denoted by m. The corresponding fine structure constant is $\alpha \equiv e^2/e_*^2$ where e^2 is the squared charge of the electron or proton as measured in the laboratory. Both the Dirac particle spin and the fine structure constant have their origin in the electron or proton coupling to the PV state. The electron g-factor, with radiative corrections, is calculated from the fine structure constant; and the proton g-factor is roughly estimated from the electron g-factor and the proton structure constant. The radiative corrections in the QED theory are the result of photon interactions taking place within the *pervaded* PV state. The apparent ability of the electron to emit and absorb photons is due to the ability of the PV state to emit and absorb photons to and from free space.

1 Introduction

The theoretical foundation [1] [2] [3] of the PV theory rests upon the unification of the Einstein, Newton, and Coulomb superforces:

$$\frac{c^4}{G}\left(=\frac{m_*c^2}{r_*}\right)=\frac{m_*^2G}{r_*^2}=\frac{e_*^2}{r_*^2} \tag{1}$$

where the ratio c^4/G is the curvature superforce that appears in the Einstein field equations. G is Newton's gravitational constant, c is the speed of light, m_* and r_* are the Planck mass and length respectively [4, p.1234], and e_* is the coupling charge.

The two particle/PV coupling forces

$$F_e(r)=\frac{e_*^2}{r^2}-\frac{m_ec^2}{r} \quad \text{and} \quad F_p(r)=\frac{e_*^2}{r^2}-\frac{m_pc^2}{r} \tag{2}$$

the electron core $(-e_*, m_e)$ and proton core $(+e_*, m_p)$ exert on the invisible PV state; along with their coupling constants

$$F_e(r_e)=0 \quad \text{and} \quad F_p(r_p)=0 \tag{3}$$

and the resulting Compton radii

$$r_e=\frac{e_*^2}{m_ec^2} \quad \text{and} \quad r_p=\frac{e_*^2}{m_pc^2} \tag{4}$$

lead to the important string of Compton relations

$$r_em_ec^2=r_pm_pc^2=e_*^2=r_*m_*c^2 \quad (=c\hbar) \tag{5}$$

for the electron and proton cores, where $\hbar$ is the reduced Planck constant. The Planck particle Compton radius is $r_*=e_*^2/m_*c^2$, which is derived by equating the Einstein and Coulomb superforces from (1). To reiterate, the equations in (2) represent the forces the free electron or proton cores exert on the invisible PV space, a space that is itself pervaded by a degenerate collection of Planck-particle cores $(\pm e_*, m_*)$ [5]. The positron and antiproton cores are $(+e_*, m_e)$ and $(-e_*, m_p)$ respectively.

Finally, the Lorentz invariance of the coupling constants in (3) lead to the energy

$$i\hbar\frac{\partial}{\partial t}=ie_*^2\frac{\partial}{\partial ct} \tag{6}$$

and momentum

$$-i\hbar\nabla=-i\frac{e_*^2}{c}\nabla \tag{7}$$

operators of the quantum theory [5]. It should be noted that the two operators are proportional to the squared coupling charge e_*^2.

Section 2 expresses the Dirac equation in terms of PV parameters. Section 3 discusses the fine structure constant. Section 4 discusses the gyromagnetic g-factor. Section 5 discusses the electron g-factor and Section 6, the proton g-factor. Sections 5 and 6 are a work in progress that seek to relate the QED radiative corrections to the PV coupling model. Section 7 presents some comments and conclusions.

2 Dirac equation

Using (5), the manifestly covariant form [6, p.90] [Appendix A] of the Dirac equation for the Dirac particle cores (electron, positron, proton, antiproton) can be expressed as:

$$\left(ic\hbar\gamma^\mu\frac{\partial}{\partial x^\mu}-mc^2\right)\psi=\left(ie_*^2\gamma^\mu\frac{\partial}{\partial x^\mu}-mc^2\right)\psi= \tag{8}$$

$$\left[ie_*^2\gamma^0\frac{\partial}{\partial x^0}+i\begin{pmatrix}0 & cS_j\\ -cS_j & 0\end{pmatrix}\frac{\partial}{\partial x^j}-mc^2\right]\psi=0 \tag{9}$$

where the second term in (9) is summed over $j = 1, 2, 3$ and

$$\begin{pmatrix} 0 & cS_j \\ -cS_j & 0 \end{pmatrix} = \begin{pmatrix} 0 & e_*^2\sigma_j \\ -e_*^2\sigma_j & 0 \end{pmatrix} \tag{10}$$

where one of the charges in e_*^2 belongs to the free particle and the other to any one of the Planck-particle cores within the degenerate PV state. The $e_*^2\sigma_j/c$ from the 4x4 matrix in (10) are the 2x2 spin components of the S-vector

$$\vec{S} = \frac{e_*^2}{c}\vec{\sigma} \quad \left(= \hbar\vec{\sigma}\right) \tag{11}$$

that applies to all the Dirac particles. $\vec{\sigma} = (\sigma_1, \sigma_2, \sigma_3)$ is the Pauli spin vector, where the σ_js are 2x2 matrices.

3 Fine structure constant

Using the expressions in (5), the fine structure constant can be expressed as

$$\alpha = \frac{e^2}{e_*^2} = \frac{e^2}{r_* m_* c^2} = \frac{e^2}{r_p m_p c^2} = \frac{e^2}{r_e m_e c^2} \tag{12}$$

where e is the magnitude of the laboratory-observed electron/proton charge. If $e = e_*$, then the Compton relations in (5) yield $\alpha = 1$ for the Dirac equation. Thus it is clear that the fine structure constant provides the "bridge" over which the Dirac equation connects to the charge e.

4 Gyromagnetic ratio g

For (8) and (9), the g-factor is exactly $g = 2$ [7, p.667]. This gyromagnetic ratio represents the magnetic to mechanical moment-ratio (13) for the Dirac equation without radiative corrections.

In general (radiative corrections or not), the intrinsic magnetic moment $\vec{\mu}$ is related to the spin vector $\vec{s} = \vec{S}/2$ through the equations [6, p.81]

$$\vec{\mu} = g\mu_B\vec{s} \quad \rightarrow \quad g\mu_B = \frac{\mu}{s} \tag{13}$$

where g is the g-factor and μ_B is the Bohr magneton

$$\mu_B = \frac{e\hbar}{2m_e c} = \frac{ec\hbar}{2m_e c^2} = \frac{ee_*^2}{2m_e c^2} = \frac{er_e}{2} \tag{14}$$

where r_e is the electron Compton radius. Although the g-factor in (13) is exactly 2 for the Dirac equation, there is an anomalous-moment increase to this value due to radiative corrections [6, p.298].

Note that for the Dirac particles where $g = 2$, (13) yields

$$\vec{\mu} = er_e\vec{s} \quad \rightarrow \quad \frac{\mu}{s} = er_e\,. \tag{15}$$

However, this is an unacceptable result for the Dirac proton; so (13) is replaced here by

$$\vec{\mu} = g\mu_c\vec{s} \quad \rightarrow \quad \frac{\mu}{s} = g\mu_c \tag{16}$$

where $\mu_c = er_e/2$ for the electron and $\mu_c = er_p/2$ for the proton. Thus the correct baseline moments, normalized by their common spin, for the Dirac particles are given by (16) with $g = 2$, where

$$\frac{\mu_e}{s} = er_e \quad \text{and} \quad \frac{\mu_p}{s} = er_p \tag{17}$$

are the electron and proton magnetic dipole moments.

5 Electron g-factor

When radiative corrections are included with (8) and (9), photon exchanges taking place within the vacuum state lead to a small increase in the electron g-factor and a large increase in the proton g-factor. Using $\alpha^{-1} = 137.0$ [7, p.722] for the inverse fine structure constant in the Schwinger calculation [8] [6, p.298], the relative change in the electron magnetic moment is

$$\frac{\delta\mu}{\mu} = \frac{g}{2} - 1 = \frac{e^2}{2\pi c\hbar} = \frac{1}{2\pi}\frac{e^2}{e_*^2}$$

$$= \frac{\alpha}{2\pi} = 0.001162 \tag{18}$$

where one of the e_*s in the squared coupling charge e_*^2 belongs to the electron and the other to any one of the Planck-particle cores within the degenerate PV state.

In the QED theory, the result in (18) is considered to be a first order (in $\alpha/2\pi$) [6, p.82] radiative correction. Like this first order correction, the higher-order corrections are difficult to calculate, but produce increasingly accurate results based on the QED methodology.

Using (18) to second order in $\alpha/2\pi$ leads to

$$\frac{g}{2} - 1 = \frac{\alpha}{2\pi} - \left(\frac{\alpha}{2\pi}\right)^2 = 0.001160 \tag{19}$$

where the experimental g-factor is [6, p.298]

$$\left(\frac{g}{2} - 1\right)_{exp} = 0.0011596 \approx 0.001160\,. \tag{20}$$

The fortuitous agreement between (19) and (20) depends upon the choice of α in the first paragraph.

6 Proton g-factor

The electron is thought to be a true point particle [6, p.82] because it contains no internal structure, as does the proton [9]. In the present context, however, it is appropriate to associate the "size" of the electron and proton with their Compton radii, where the corresponding proton structure constant is defined here by

$$m_p = \frac{r_e}{r_p}m_e \quad \rightarrow \quad \left(\frac{r_e}{r_p}\right) = \frac{m_p}{m_e} \approx 1836\,. \tag{21}$$

This suggests that the proton g-factor change be estimated from the electron change,

$$\frac{g}{2} - 1 = \left[\frac{\alpha}{2\pi} - \left(\frac{\alpha}{2\pi}\right)^2\right]\frac{r_e}{r_p} = 0.001160\,\frac{r_e}{r_p} = 2.13 \qquad (22)$$

where the experimental g-factor is [6, p.82]

$$\left(\frac{g}{2} - 1\right)_{exp} = 1.79\,. \qquad (23)$$

The agreement between (22) and (23) is remarkable, considering the large magnitude of r_e/r_p. It remains to be seen, however, whether or not (22) leads to something more substantial.

7 Summary and comments

It probably comes as a surprise that the charge associated with the Dirac equation and the Dirac particles is the coupling charge e_*, rather than the well known electron/proton charge e. That bewilderment is due to the collection of Planck particle cores that pervade the PV state. If there were no such pervasion, there would be no photon scattering taking place within the vacuum state and no resulting need for the coupling charge and the radiative corrections from the QED theory.

Sections 5 and 6 present calculations that suggest the PV theory may provide an aid to, or an alternative for, the difficult QED calculations that have been so spectacularly successful. That, of course, remains to be seen. But another hint that the PV theory may be a help is the Schwinger result in Section 5:

$$\frac{\alpha}{2\pi} = \frac{e^2/2\pi r_*}{m_* c^2} = \frac{e^2/2\pi r_p}{m_p c^2} = \frac{e^2/2\pi r_e}{m_e c^2} \qquad (24)$$

where, if r_* is the "radius" of the Planck-particle cores in the PV pervaded space, then $2\pi r_*$ is the "circumference" of the corresponding "spheres" surrounding those cores. Further work will be focused on developing a complete PV approach to the radiative correction phenomenon.

Feynman [10, p.129] notes that: "There is a most profound and beautiful question associated with the coupling constant, e—the amplitude for a real electron to emit or absorb a real photon. It is a simple number that has been experimentally determined to be close to -0.8542455. (My physicist friends won't recognize this number, because thy like to remember it as the inverse of its square: about 137.03597 with an uncertainty of about 2 in the last decimal place. It [the fine structure constant] has been a mystery ever since it was first discovered more than fifty years ago, and all good theoretical physicists put this number up on their wall and worry about it.)" The mystery of the fine structure constant α resides in the photon scattering that takes place within the pervaded PV state. It is also noted that the apparent electron emission/absorption of photons has its source in the pervaded nature of that state.

Appendix A: The γ and β matrices

The 4x4 γ, β, and α_i matrices used in the Dirac theory are defined here: where [6, p.91]

$$\gamma^0 \equiv \beta = \begin{pmatrix} I & 0 \\ 0 & -I \end{pmatrix} \qquad (A1)$$

and ($j = 1, 2, 3$)

$$\gamma^j \equiv \beta\alpha_j = \begin{pmatrix} 0 & \sigma_j \\ -\sigma_j & 0 \end{pmatrix} \qquad (A2)$$

and where I is the 2x2 unit matrix and

$$\alpha_j = \begin{pmatrix} 0 & \sigma_j \\ \sigma_j & 0 \end{pmatrix} \qquad (A3)$$

where the σ_j are the 2x2 Pauli spin matrices

$$\sigma_1 = \begin{pmatrix} 0 & 1 \\ 1 & 0 \end{pmatrix},\ \sigma_2 = \begin{pmatrix} 0 & -i \\ i & 0 \end{pmatrix},\ \sigma_3 = \begin{pmatrix} 1 & 0 \\ 0 & -1 \end{pmatrix} \qquad (A4)$$

and $\boldsymbol{\alpha} = (\alpha_1, \alpha_2, \alpha_3)$. The zeros in (A1)–(A3) and (A5) are 2x2 null matrices.

The mc in (8) and (9) represents the 4x4 matrix

$$mc\begin{pmatrix} I & 0 \\ 0 & I \end{pmatrix} \qquad (A5)$$

and ψ is the 4x1 spinor matrix.

The zero on the right side of (9) represents the 4x4 null matrix and the zeros in (10) represent 2x2 null matrices. The S_j and σ_j in (10) are 2x2 matrices; so their parentheses represent 4x4 matrices.

The coordinates x^μ are

$$x^\mu = (x^0, x^1, x^2, x^3), \quad x^0 \equiv ct. \qquad (A6)$$

Received on February 28, 2019.

References

1. Davies P. Superforce: the Search for a Grand Unified Theory of Nature. Simon and Schuster, New York, 1984.
2. Daywitt W. C. A Model for Davies' Universal Superforce. *Galilean Electrodynamics*, 2006, v. 5, 83. See also www.planckvacuumDOTcom.
3. Daywitt W. C. The Trouble with the Equations of Modern Fundamental Physics. *American Journal of Modern Physics, Special Issue: Physics without Higgs and without Supersymmetry*, 2016, v. 5 (1-10, 22.
4. Carroll B. W., Ostlie D. A. An Introduction to Modern Astrophysics. Addison-Wesley, San Francisco, 2007.
5. Daywitt W. C. The Planck vacuum. Progress in Physics, 2009, v. 5, 20.
6. Gingrich D. M. Practical Quantum Electrodynamics. CRC, The Taylor & Francis Group, Boca Raton, 2006.
7. Leighton R. B. Principles of Modern Physics. McGraw-Hill, New York, 1959.
8. Schwinger J. On Quantum-Electrodynamics and the Magnetic Moment of the Electron. *Physical Review*, 1948, v. 73, 416.
9. Daywitt W. C. The Structured Proton and the Structureless Electron as Viewed in the Planck Vacuum Theory. *Progress in Physics*, 2015, v. 11 (2), 117.
10. Feynman R. P. QED: the Strange Theory of Light and Matter. Princeton University Press, Princeton, 1985.

A Derivation of Space and Time

Paul Bernard White

ORCID: 0000-0002-2681-3670. E-mail: pbwx@att.net

Four simple postulates are presented, from which we derive a (3+1)-dimensional structure, interpreted as ordinary space and time. We then derive further properties of space: isotropy and homogeneity; a rapid expansion within the first instant of time (*i.e.* inflation); and a continual and uniform expansionary pressure, due to a continual influx of (*non*-zero-point) energy that is uniformly distributed (*i.e.* dark energy). In addition, the time dimension is shown to have an "arrow". These results suggest that the four postulates may be fundamental to the construction of the physical universe.

1 Introduction

Systems that are based on information typically contain a basic information *element* and a basic information *structure*. In biological systems, for example, the basic information element is the nucleotide molecule, and the basic information structure is a *sequence* of nucleotides (*e.g.* a codon, or a gene). Likewise, for computer systems the basic information element is the bit, and the basic information structure is a sequence of bits (*e.g.* an 8-bit byte). And in natural language the basic information element is the letter or phoneme, and the basic information structure is a sequence of letters or phonemes (*e.g.* a word or a sentence).

Such systems must also have a way of translating or computing the information elements and structures into meaningful output. In biology this is accomplished by the operations of ribosomes, enzymes, *etc.*, acting on the nucleotide strings. For computers, the operations of logic gates on the bit strings typically perform this function. And in natural language the operations of lexical analysis, parsing, and context translate a string of letters/phonemes into meaning.

Similarly, if the *physical universe* is based on information (as many have speculated, *e.g.* [1–3]), then the following questions arise: (a) What is the basic information element for this system?; (b) what is the basic information structure for the system?; and (c) how are these elements and structures translated (or computed) into the meaningful output that we call the physical universe?

In answer to questions (a) and (b) above, I propose the following two postulates:

1. For creation of the physical universe, the basic information element is a type of *projection* – more specifically, *a projection from a prior level*.
2. The basic information structure is a *sequence* of such projections.

With respect to the first postulate, we may refer to both projections and levels as "elements" (or *basic* elements) of the system, but will reserve the term "basic *information* element" for the projections alone.

We now add two more postulates:

3. Each such projection is a *one*-dimensional *vector*, constituting a *different*, but related, one-dimensional space. (The basic relations between these projections/vectors are stated in the next postulate.)
4. Prior things (*e.g.* projections, levels, and constructions from them) are *independent* of subsequent things; and, conversely, subsequent things are *dependent* on prior things. (The terms prior, subsequent, dependent, and independent denote here *logical/ontological* relations. See *e.g.* [4].)

In [5], I use these four postulates (and two additional ones) to develop a model for the basic construction of the physical universe – including the construction of ordinary space and time themselves, the fundamental particles and interactions, *etc.* In the present paper, however, we will (for the sake of brevity) focus simply on constructing ordinary space and time, and their basic properties. That is, using the four postulates above, we will:

- derive a (3+1)-dimensional structure, interpreted as ordinary space and time
- show that the derived 3-dimensional space is isotropic and homogeneous, and that the time dimension has an "arrow"
- show that space undergoes a rapid expansion within the first instant of time (*i.e.* inflation)
- show that space undergoes a continual and uniform expansionary pressure, due to a continual influx of (*non*-zero-point) energy that is uniformly distributed (*i.e.* dark energy).

With respect to question (c) above, it will be shown that a method for translating sequences of projections into physical meaning is by taking into account the *relations* between projections – specifically, their dependence and independence relations (*i.e.* postulate 4). Once obtained, the above (bulleted) results can then be said to support the proposition that *the four stated postulates are fundamental to the construction of the physical universe*.

From now on, we will often refer to the model for constructing the ***p***hysical universe, developed herein, as system P.

2 Levels, projections, and relations: the structure and basic properties of system P

To construct our model for the physical universe (*i.e.* system P), we must begin with a *state* at which the things of the universe do not exist (otherwise our construction would be circular), *i.e.* a state that is absent the energy, elementary particles, and even space and time, as we know them. We will call this state *level 0 of system P*, or just *level 0*. We do not, however, presume that level 0 is a state of nothingness, or that nothing exists at level 0. We merely claim that nothing that comes into being with the construction of the physical universe exists at level 0; for level 0 is by definition a state that is immediately *prior* to the construction of the physical universe.

Recalling our first three postulates, we say that a projection from level 0, to be denoted as $\mathbf{p}_0$, generates a *new* state, which we call *level 1*. Likewise, a projection from level 1, denoted as $\mathbf{p}_1$, generates another new state, which we call *level 2*. And a projection from level 2, denoted as $\mathbf{p}_2$, yields *level 3*; and so on. So, in general, the projection $\mathbf{p}_k$ represents a sort of *displacement* from level k that generates level $k+1$ (for $k = 0, 1, 2, \ldots$); thus, relative to each other, level k is *prior*, and level $k+1$ is *subsequent*; also, relative to each other, $\mathbf{p}_k$ is prior, and $\mathbf{p}_{k+1}$ is subsequent. (Again, the terms "prior" and "subsequent" refer to logical/ontological priority and subsequence.)

In Fig. 1, where levels are represented by horizontal lines, and projections are represented by vertical arrows from a prior level to the next subsequent level, we illustrate the construction of levels 1 through 3 via the projections $\mathbf{p}_0$, $\mathbf{p}_1$, and $\mathbf{p}_2$. To the right of each level in Fig. 1 is shown the sequence of projections that is required to construct that level (the round brackets indicate a sequence, as is common in mathematics). Thus, the sequences of projections that are required to create levels 0, 1, 2, and 3 are ( ), $(\mathbf{p}_0)$, $(\mathbf{p}_0, \mathbf{p}_1)$, and $(\mathbf{p}_0, \mathbf{p}_1, \mathbf{p}_2)$, respectively; moreover, the latter sequence constructs *all* of the levels (above level 0) in Fig. 1.

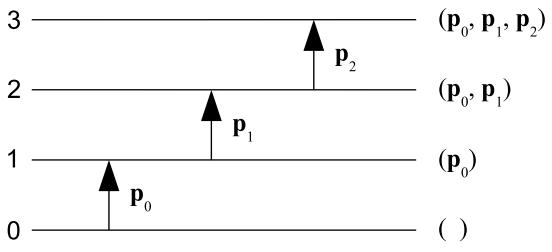

Fig. 1: Construction of levels 1 through 3 of system P via the projection sequence $(\mathbf{p}_0, \mathbf{p}_1, \mathbf{p}_2)$. The projection sequence that is required to construct a given level is shown to the right of that level.

As just described, the *order* of construction in system P starts with level 0 at the bottom of Fig. 1 and proceeds in the upward direction. Thus, level 0 is *prior* to all other elements (levels or projections) in system P, and *subsequent* to none; $\mathbf{p}_0$ is subsequent to level 0, but prior to level 1, $\mathbf{p}_1$, level 2, *etc.*; and so on. So, in general, a given element x in system P is subsequent to everything below it in Fig. 1, but prior to everything above it. By postulate 4, this means that element x is *dependent* on everything below it in Fig. 1, but *independent* of everything above it. Thus, for example, level 0 is independent of all other elements in system P, and dependent on none.

Since level 0 is our *starting point* (or starting *state*) for constructing system P, then we must say that it is a *nonconstructed* element of that system, whereas the subsequent projections and levels ($\mathbf{p}_0$, level 1, $\mathbf{p}_1$, level 2, *etc.*) are *constructed* elements of system P. So anything subsequent to level 0 is a *constructed* entity of the system.

2.1 Some properties of system P

Let x be a thing of system P (*e.g.* x is a level, a set of one or more projections, or something constructed from them). By postulate 4, things that are subsequent to x are (logically/ontologically) *dependent* on x. Such dependence implies that x is **in effect**, effective, operative, or **operant** at those subsequent things; or, alternatively, we say that those subsequent/dependent things are *within the* **scope** *of* x. Conversely, since things that are *prior* to x are *independent* of it, we say that x is *not* in effect or operant at those prior things; or, alternatively, we say that those prior/independent things are *not* within the scope of x. All of this is summarized in what will be called the **scope rule** for system P, stated as follows:

> A given thing in system P is in effect/operant at (*i.e.* contains within its scope) those things which are *subsequent*, and is not in effect at (does not contain within its scope) those things which are *prior*.

From this we may deduce the following corollary to the scope rule:

> A given *element* in system P (*i.e.* a projection or level) is in effect/operant at (contains within its scope) those elements that are *above* it in Fig. 1, and is not in effect at (does not contain within its scope) those elements that are *below* it in Fig. 1.

Thus, for example, since all of the *constructed* elements of system P (*i.e.* $\mathbf{p}_0$, level 1, $\mathbf{p}_1$, level 2, *etc.*) are subsequent to level 0 (or, conversely, level 0 is prior to them), then level 0 is in effect/operant at all of those things; or, all of those things are within the scope of level 0. Likewise, $\mathbf{p}_1$, level 2, $\mathbf{p}_2$, and level 3 are within the scope of level 1; but level 0 is *not* within the scope of level 1. And so on.

Since $\mathbf{p}_k$ is *not* in effect at level k, but *is* in effect at level $k+1$, then level $k+1$ represents the *state* at which the projection $\mathbf{p}_k$ first comes into effect; by the scope rule, $\mathbf{p}_k$ then *stays* in effect for all subsequent levels. Thus, the projection $\mathbf{p}_0$ first comes into effect at level 1, and stays in effect for levels 2 and 3; likewise, $\mathbf{p}_1$ first comes into effect at level 2, and stays in

effect for level 3. Let us say that the level at which a projection first comes into effect is its *native level*. Thus, level 1 is the native level for $\mathbf{p}_0$; level 2 is the native level for $\mathbf{p}_1$; and so on. That is, the native level for $\mathbf{p}_k$ is level $k+1$. Moreover, the concept of native level can be extended to things that are *constructed from* projections; thus, for example, something that is constructed using $\mathbf{p}_0$ and $\mathbf{p}_1$ (and no other projections) is native to level 2, since those two projections are first *jointly* in effect at that level. We note also that the projections that are in effect/operant at a given level are the *same* as the ones that are required to *construct* that level (as described earlier, and as listed in the sequences to the right of each level in Fig. 1).

In constructing the sequence of projections $(\mathbf{p}_0, \mathbf{p}_1, \mathbf{p}_2)$, since any projections that are in effect at level k are also in effect at the subsequent level $k+1$, then we can think of the latter level as *inheriting* all of the projections that are in effect at the former level. And since this is true of projections, then it is also true of anything that is associated with or constructed from them. This aspect of system P – whereby that which is in effect at one level (or, if you will, *generation*) is passed on to the next subsequent level (and thus, by extension, to *all* subsequent levels) – will be called the **inheritance rule**.

3 Constructing space and time in system P

Following postulate 3, let us model each projection as a one-dimensional *vector*; *i.e.* we model each $\mathbf{p}_k$ $(k = 0, 1, 2)$ as a one-dimensional vector going from level k to level $k+1$. Thus, $\mathbf{p}_0$ is a one-dimensional vector from level 0 to level 1; $\mathbf{p}_1$ is a one-dimensional vector from level 1 to level 2; and so on. These vectors are represented graphically by the vertical arrows in Fig. 1.

Moreover, each $\mathbf{p}_k$ constitutes a *different* one-dimensional space. Though they are different in this respect, the $\mathbf{p}_k$ are nevertheless *related* by the dependence and independence relations that have been postulated and discussed.

3.1 Constructing a (3+1)-dimensional structure at level 2 (and above)

Since $\mathbf{p}_0$ is the only projection in effect at level 1, and since (by postulate 3) it is *one* dimensional, then it is fair to say that system P is *one dimensional* at level 1.

Since both $\mathbf{p}_0$ and $\mathbf{p}_1$ are in effect at level 2, and since (by postulate 3) each of these constitutes a different one-dimensional space, then it might seem – at first glance – that system P should be *two* dimensional at level 2. But this would be wrong.

To get the correct dimensionality at level 2, we must take into account the *relations* between $\mathbf{p}_0$ and $\mathbf{p}_1$, as per postulate 4 – *i.e.* the fact that $\mathbf{p}_0$ is *independent* of $\mathbf{p}_1$, and that this relation is *asymmetric* ($\mathbf{p}_1$ is *dependent* on $\mathbf{p}_0$). Since $\mathbf{p}_0$ and $\mathbf{p}_1$ are *vectors*, we interpret that these relations imply a kind of (asymmetric) *linear* independence, with the following property: from the perspective of $\mathbf{p}_1$, the vector $\mathbf{p}_0$ may be collinear with $\mathbf{p}_1$, but is also free to be *noncollinear* with $\mathbf{p}_1$. With these considerations in mind, we ask the question: What is the *direction* of $\mathbf{p}_0$ with respect to $\mathbf{p}_1$? Or, in other words, how does $\mathbf{p}_0$ "look" relative to $\mathbf{p}_1$?

Since $\mathbf{p}_0$ may be both collinear and noncollinear with $\mathbf{p}_1$ (from the latter's perspective), then $\mathbf{p}_0$ may have a component parallel to $\mathbf{p}_1$, and may also have a component *perpendicular/orthogonal* (*i.e.* at 90 degrees) to $\mathbf{p}_1$. But, by symmetry, the perpendicular component can be anywhere in a two-dimensional *plane* orthogonal to $\mathbf{p}_1$. The two dimensions of this orthogonal plane, plus the one dimension parallel to $\mathbf{p}_1$, makes three dimensions. Thus, from the viewpoint of $\mathbf{p}_1$ (and from the perspective of level 2), $\mathbf{p}_0$ has *three* dimensions; *i.e.* $\mathbf{p}_0$ constitutes a *three*-dimensional space (whereas, recall that $\mathbf{p}_0$ has only one dimension at level 1). We might say, therefore, that the view of $\mathbf{p}_0$ from the perspective of $\mathbf{p}_1$ "bootstraps" the former from a one-dimensional vector into a three-dimensional space.

In summary, to construct its interpretation of $\mathbf{p}_0$, we can think of $\mathbf{p}_1$ as applying postulates 3 and 4 in succession: first, by postulate 3, $\mathbf{p}_0$ is a one-dimensional vector; second, by postulate 4, $\mathbf{p}_0$ is independent of $\mathbf{p}_1$ – which allows the former to have a component that is orthogonal to $\mathbf{p}_1$, with the result that $\mathbf{p}_1$ sees $\mathbf{p}_0$ as three dimensional.

Conversely, we can ask, how does $\mathbf{p}_1$ "look" relative to $\mathbf{p}_0$? Since $\mathbf{p}_1$ is *dependent* on $\mathbf{p}_0$, then the former is *not* free to have a component that is orthogonal to the latter, and so $\mathbf{p}_0$ sees $\mathbf{p}_1$ as being collinear; or, more simply, $\mathbf{p}_0$ sees $\mathbf{p}_1$ strictly as per postulate 3: as a *one*-dimensional vector.

So, at level 2 we have the three dimensions of $\mathbf{p}_0$, plus the one dimension of $\mathbf{p}_1$, for a total of *four* dimensions. Since system P is a model for constructing the physical universe, we interpret that the three dimensions of $\mathbf{p}_0$ are just the three dimensions of *ordinary space*, and the one dimension of $\mathbf{p}_1$ is the dimension of *time*; thereby yielding at level 2 the signature 3+1 space and time dimensions of our experience. The dimension of time, therefore, being a consequence of $\mathbf{p}_1$ (and $\mathbf{p}_0$), does not exist at levels 0 and 1, but only comes into existence at level 2; likewise, since ordinary, three-dimensional space is a consequence of $\mathbf{p}_0$ and $\mathbf{p}_1$, it also does not exist at levels 0 and 1, but only comes into existence at level 2.

Note that, although $\mathbf{p}_0$ itself is independent of $\mathbf{p}_1$, the triple dimensionality of $\mathbf{p}_0$ at level 2 is *not* independent of $\mathbf{p}_1$. That is, in the process described above, $\mathbf{p}_0$ only manifests as *three* dimensional when it is related to, or juxtaposed with, $\mathbf{p}_1$. Thus, the triple dimensionality of $\mathbf{p}_0$ at level 2 (*i.e.* the triple dimensionality of ordinary space) is in fact *dependent* on $\mathbf{p}_1$. Conversely, both $\mathbf{p}_0$ and $\mathbf{p}_1$ are *prior* to, and thus independent of, ordinary space.

We have shown, among other things, that $\mathbf{p}_0$ manifests differently at levels 1 and 2. At level 1 it is *one* dimensional. But when juxtaposed with $\mathbf{p}_1$ at level 2 it manifests as a *three*-dimensional space. Note that $\mathbf{p}_0$ itself does not change from level to level: it represents a projection from level 0 to level 1

wherever it appears (*i.e.* wherever it is in effect). This is analogous to *e.g.* the G nucleotide in biology, which is always the same molecule wherever it appears, but yields a different output (*i.e.* amino acid) depending on what other nucleotides/letters it is juxtaposed with in a sequence. In other words, like the letter G in a DNA sequence, the *meaning* of $\mathbf{p}_0$ is context dependent; which is just what we might expect for an element of a *language*, thus supporting our earlier notion that the basis of the physical universe is, to some degree at least, informational in nature.

We might say that level 2 has *two* dimensions as *input* (one dimension for $\mathbf{p}_0$, plus one for $\mathbf{p}_1$), but has *four* dimensions as *output* – three for $\mathbf{p}_0$, and one for $\mathbf{p}_1$. Which brings us back to question (c) in the introduction: How are the basic information elements of the model (which at level 2 are the inputs $\mathbf{p}_0$ and $\mathbf{p}_1$) translated (or, if you will, computed) into the meaningful output that we call the physical universe? We now see that at least a partial answer is that the *relations* between prior and subsequent elements are what translate them into meaningful output. In the present case, the independence relation between $\mathbf{p}_0$ and $\mathbf{p}_1$ at level 2 translates/transforms the manifestation of the former from a one-dimensional entity into a three-dimensional space.

We can thus say that the construction of each space at level 2 requires the participation of an *observer*, in the sense that $\mathbf{p}_1$ "observing" $\mathbf{p}_0$ constructs ordinary, three-dimensional space, and $\mathbf{p}_0$ "observing" $\mathbf{p}_1$ constructs one-dimensional time. With ordinary space *itself* constructed by an observation of sorts, it becomes more plausible that *e.g.* the *position* of an object *within* ordinary space might also be constructed by some type of observation, as seems to be the case in quantum mechanics (more about that in [5]).

The projections $\mathbf{p}_0$ and $\mathbf{p}_1$ are also operant at *level 3* (as per the scope rule), and the relations between them are the same as at level 2 (*i.e.* $\mathbf{p}_0$ is independent of $\mathbf{p}_1$, but not the converse). Thus, at level 3 – as at level 2 – $\mathbf{p}_0$ will appear to $\mathbf{p}_1$ as a three-dimensional space (*i.e.* ordinary space), and $\mathbf{p}_1$ will appear to $\mathbf{p}_0$ as a one-dimensional space (*i.e.* time). In other words, the spaces that exist at level 2 also exist at level 3. Indeed, as per the inheritance rule, we might say that level 3 *inherits* these spaces from level 2; or, more precisely, level 3 inherits $\mathbf{p}_0$, $\mathbf{p}_1$, and the relations between them from level 2, and uses them to *construct* ordinary space and time.

3.2 Isotropy and homogeneity of space

Recall that ordinary, three-dimensional space is created when $\mathbf{p}_0$ is viewed from the perspective of $\mathbf{p}_1$. So it follows that (a) the creation/construction of ordinary space is *dependent* on $\mathbf{p}_0$ and $\mathbf{p}_1$; and (b) $\mathbf{p}_0$ and $\mathbf{p}_1$ are *prior to*, and thus (by postulate 4) *independent of*, ordinary space.

Suppose now that an outcome of constructing ordinary space is that $\mathbf{p}_0$ (or $\mathbf{p}_1$) manifests with a particular orientation or direction within that space. Since this would make $\mathbf{p}_0$ (or $\mathbf{p}_1$) functionally dependent on ordinary space, and thus contradict (b) above, we conclude that the construction of ordinary space cannot result in $\mathbf{p}_0$ (or $\mathbf{p}_1$) having a particular direction/orientation within that space. Presumably, then, there is no way for the process that constructs ordinary space to establish a distinctive (*i.e.* special or preferred) direction within that space. We thus conclude that, as constructed above, ordinary space is perfectly *isotropic*.

Now suppose that an outcome of constructing ordinary space is that $\mathbf{p}_0$ (or $\mathbf{p}_1$) manifests with a particular *position* within that space. This, again, would make $\mathbf{p}_0$ (or $\mathbf{p}_1$) functionally dependent on ordinary space and thereby contradict (b) above; and so we conclude that the construction of ordinary space cannot result in $\mathbf{p}_0$ (or $\mathbf{p}_1$) having a particular position within that space. Presumably, then, the process that constructs ordinary space cannot establish a distinctive (*i.e.* special or preferred) position within that space. We thus conclude that, as constructed above, ordinary space is perfectly *homogeneous*.

In addition, the construction of ordinary space cannot result in either $\mathbf{p}_0$ or $\mathbf{p}_1$ manifesting as *vectors*, or *vector fields*, within that space; for if they did, then these projections/vectors would be functionally dependent on ordinary space, which would again contradict (b). Given that *vector* fields have been ruled out, it seems we have little choice but to assume that $\mathbf{p}_0$ and $\mathbf{p}_1$ manifest within ordinary space as uniform *scalar* fields – *uniform*, because any *non*uniformity would make the manifestations of $\mathbf{p}_0$ or $\mathbf{p}_1$ functionally dependent on ordinary space, which would, again, violate/contradict their independence from that space. Presumably, the uniform scalar field for $\mathbf{p}_0$ is just (raw, unstructured) ordinary space itself, and the uniform (one-dimensional) scalar field for $\mathbf{p}_1$ is just proper time.

Lastly, let us recall that $\mathbf{p}_0$ sees $\mathbf{p}_1$ as a one-dimensional *vector*. This, presumably, would impart some *directionality* to $\mathbf{p}_1$ – which, as we have concluded, could not manifest as a direction within ordinary space. Since $\mathbf{p}_1$ has been associated with *time*, we interpret that this directionality of $\mathbf{p}_1$ (with respect to $\mathbf{p}_0$) is just the "arrow" of time.

3.3 Rapid expansion of space within the first instant of time

Recall that $\mathbf{p}_0$ at level 1 is *one* dimensional – having, let us say, a length of p_0. The time dimension, being a result of $\mathbf{p}_1$, does not exist at this level/stage. Given that a one-dimensional object has *zero* volume, then the physical universe at this stage of development has a volume of zero.

Since the time dimension comes into existence with the projection $\mathbf{p}_1$, then the *advent* of $\mathbf{p}_1$ defines the time point $t = 0$, at which point p_0 has the value $p_0(t = 0)$, which may be denoted as $p_{0,0}$. So, at exactly $t = 0$, or within the first instant after it, the existence/perspective of $\mathbf{p}_1$ causes $\mathbf{p}_0$ to manifest as *three*-dimensional ordinary space, with a volume on the

order of $p_{0,0}^3$. Thus the volume of ordinary space goes from zero to around $p_{0,0}^3$ within a time interval of zero, or near-zero, length – which constitutes a potentially very large, perhaps infinite, rate of spatial expansion. I propose, therefore, that this rapid spatial expansion, triggered by the advent of $\mathbf{p}_1$ at $t = 0$, is the process known as *inflation* [6].

Note that, under the above mechanism, inflation has a natural beginning: the advent of $\mathbf{p}_1$ at $t = 0$. And it also has a natural *ending*: it ends when the volume of ordinary space is around $p_{0,0}^3$. So inflation only lasts for the time (if any) that it takes (from the perspective of $\mathbf{p}_1$) for the *one*-dimensional space of length $p_{0,0}$ to become the *three*-dimensional space of approximate volume $p_{0,0}^3$.

3.4 A continual influx of energy associated with $\mathbf{p}_0$, yielding a continual and uniform expansionary pressure on space

In constructing the sequence $(\mathbf{p}_0, \mathbf{p}_1, \mathbf{p}_2)$ for system P, let us assume that *energy* is needed to create each of the projections $\mathbf{p}_k$ (for $k = 0, 1, 2$). We can think of this energy as being stored along the length of $\mathbf{p}_k$, and/or as being stored in the *level* that is created by $\mathbf{p}_k$. So we can speak of "$\mathbf{p}_k$ energy", and/or we can speak of the energy, E_{k+1}, that $\mathbf{p}_k$ inputs into level $k + 1$. Thus, $\mathbf{p}_0$ is a *process* through which energy E_1 is input into level 1 of system P. Likewise, $\mathbf{p}_1$ is a process that inputs energy E_2 into level 2; and $\mathbf{p}_2$ is a process that inputs energy E_3 into level 3. The total energy, E_t, that is input into system P is therefore $E_t = E_1 + E_2 + E_3$. We assume that all of these energies are nonzero and positive, so the energy of system P at level 1 and above, due to contributions from the sources mentioned, is positive.

Now recall that the dimension of time is associated with $\mathbf{p}_1$. Since $\mathbf{p}_1$ does not exist at levels 0 and 1, then time also does not exist there; *i.e.* all time intervals are zero at those levels. Indeed, we can say that levels 0 and 1 are *independent of time*. But $\mathbf{p}_1$ *does* exist at level 2 and above; so time exists there, and *all* time intervals at those levels are *nonzero* (and presumably positive).

Thus, at level 1, energy is nonzero, but time is zero. At level 2 (and above), however, both energy and time (intervals) are *nonzero*. Consequently, at level 2 and above, the *product* of energy and time – the quantity known as *action* – is nonzero, and thus has a positive lower bound; *i.e.* at level 2 (and above) the action is *quantized*. We thus have the derivation of an action *quantum*, which we interpret to be the basis for the empirically-known "quantum of action", commonly referred to as *Planck's constant*, and denoted as h.

In the present model, therefore, the quantum of action, h, depends on both $\mathbf{p}_0$ and $\mathbf{p}_1$, and so does not exist at levels 0 and 1, but only comes into being at level 2. Thus, quantum mechanics, which is based on h, also comes into being at level 2 of system P. And therefore, due to the scope rule, both h and quantum mechanics are operant at level 2 and above; *i.e.* they are *native* to level 2.

The presence of h at levels 2 and 3 can, and we assume *does*, partition the energies E_2 and E_3 into a multiplicity of smaller chunks, yielding *many* objects/particles at those levels. The *absence* of h at level 1, however, means that the energy E_1 *cannot* be broken into chunks; and so the energy E_1 at level 1 constitutes a *single*, continuous entity. In addition, given that time exists at levels 2 and 3, we assume (as per special relativity) that the particles at those levels possess *mass*; and, given that time does *not* exist at level 1, we assume that the single entity at level 1 is *massless*. Furthermore, in [5] it is shown that the objects at level 3 have *internal* structure, whereas the objects at level 2 are *structureless*. These results lead us to identify the level-3 objects as *baryons*, and the level-2 objects as *leptons*. Moreover, since time exists at levels 2 and 3, then the input of energies (E_2 and E_3) into those levels can be, and we assume *is*, time limited – yielding a *finite* number of baryons at level 3, and a finite number of leptons at level 2.

Recall now that $\mathbf{p}_0$ is native to level 1, but *time* is native to *level 2*. Thus, $\mathbf{p}_0$ is *prior* to time. By postulate 4, this means that the $\mathbf{p}_0$ process, which pumps energy E_1 into level 1, is *independent of time*, and is therefore a *continual* process – *i.e.* it never stops, and so it must be happening right now. Consequently, the quantity E_1 is *always* increasing. Moreover, since E_1 is the energy of $\mathbf{p}_0$ at level 1, and since $\mathbf{p}_0$ (as seen by $\mathbf{p}_1$) *is* ordinary space, then it is clear that E_1 is just the energy of space itself. Hence, an always-increasing E_1 should yield a continual *expansionary* pressure on space. Indeed, an increase in E_1 may produce an increase in the *length* of $\mathbf{p}_0$, and thus an increase in p_0^3 (the size/volume of the physical universe).

Suppose now that the $\mathbf{p}_0$ process distributes its energy E_1 *nonuniformly* within space. This would make that process (and thus $\mathbf{p}_0$ itself) functionally *dependent* on space, and thereby contradict statement (b) in section 3.2. Consequently, the energy E_1 must be distributed *uniformly* throughout space. Since this process is also independent of time, then it is *constant in time*. So the continual influx of E_1 energy into the system via the $\mathbf{p}_0$ process yields an input of energy per unit volume of space that is uniform throughout space, and constant in time; in other words, E_1 yields a *cosmological constant*.

Taken all together, the above results suggest that we interpret E_1 to be the phenomenon known as *dark energy* [7]; *i.e.*

$$\text{dark energy} = E_1.$$

Moreover, since the $\mathbf{p}_0$ process and E_1 are *level-1* phenomena, but h only becomes operant at *level 2*, then dark energy/E_1 is prior to – and thus independent of – h and quantum mechanics, and so is *not* a zero-point energy.

4 Conclusion

A truly fundamental model of the universe must *derive* space and time – not just take them as given. Firstly, such a model

should derive the (3+1)-dimensionality of space and time, and the isotropy and homogeneity of space. Secondly, since inflation and dark energy are likely to be important factors in the construction of space, then the model should also derive them. As shown above, the present model meets these basic criteria, which indicates that the four stated postulates may be fundamental to the construction of the physical universe.

Acknowledgments

I would like to acknowledge the following people for enabling the research for this paper to take place: My late mother and late father, Margean A. White and Phillip B. White; my brother, Jeffrey C. White; John P. A. Higgins; and the late Louise L. Hay (The Hay Foundation).

Received on March 6, 2019

References

1. Wheeler J. A. It From Bit. In his: At Home in the Universe. AIP Press, 1994.
2. Wheeler J. A. The Computer and the Universe. *Int. J. Theor. Phys.*, 1982, v. 21, 6–7.
3. Davies P., Gregersen N. H., eds. Information and the Nature of Reality. Cambridge University Press, Cambridge, 2010.
4. Van Cleve J. Dependence. In: Audi R., ed. The Cambridge Dictionary of Philosophy. Cambridge University Press, Cambridge, 1995, p. 191.
5. White P. B. A Model for Creation: Part I. 2019, https:www.academia.edu/38496134.
6. Guth A. The Inflationary Universe. Perseus Books, Reading, MA, 1997.
7. Carroll S. M. Dark Energy and the Preposterous Universe. arXiv:astro-ph/0107571v2.

Twin Universes: a New Approach

Patrick Marquet
E-mail: patrick.marquet6@wanadoo.fr

In this article, we derive a differential form of Einstein's field equations using Cartan's free coordinates calculus. Under this form, we see that it is possible to infer another set of field equations dual to the original one and which displays a negative sign. We may then relate this system to the equations sustaining the twin Universe of the Janus Cosmological Model developed by the astrophysicist J.-P. Petit.

Introduction

As early as 2014, the astrophysicist J.-P. Petit put forward a model of Universe which harbors two fields equations with two sources: it is referred to as *The Janus Cosmological Model* (JCM) [1] which is inspired by the twin Universes theory first proposed by A. Sakharov [2].

Such a bi-metric is shown to account for the Dark Energy description and other unsolved observational data [3], provided one distinguishes our Universe as filled with positives masses and energies, from another wherein negative masses and negative energies are assigned to.

From the quantum physics perspective, negative energies have always played an unsavory role.

However, following a recent publication, it appears that both negative energies and masses are physically compatible if the time reversal operator is kept unitary within the Dirac formalism [4].

This considerable mathematical progress lends support to the Janus Model which relies on this symmetry.

So far, the few theories exhibiting two opposite metrics have been arbitrarily assumed as a "natural" hypothesis with the confidence that subsequent results would eventually corroborate this postulate. In this paper, we tackle the problem at the very early stage: With the aid of the Cartan calculus and using the Hodge star operation, we rewrite the Einstein's field equations under a differential form.

With this preparation, we naturally infer another set of field equations which displays a negative sign. This differential procedure thus provides a straightforward basis wherefrom the *Janus Model* can be substantiated.

Notations

Space-time: Greek indices α, β run from 0, 1, 2, 3. Space-time signature: -2. In the present text, $\varkappa$ is the Einstein's constant: $8\pi G/c^4$ where G is Newton's gravitational constant, although we adopt here $c = 1$.

1 Differential form of Einstein's field equations

1.1 The Cartan procedure

Let us consider a 4-pseudo-Riemannian manifold referred to a general basis e_α. The dual basis θ^β of one-forms are related to the local (Roman) coordinates $\{a\}$ by:

$$\theta^\beta \;=\; a^\beta_a \,\mathrm{d}x^a. \tag{1.1}$$

The (a^β_a) are called *vierbein* or *tetrad fields* [5].

We next define the *Cartan procedure*, a powerful coordinates free calculus which is extensively used in the foregoing.

Let us define the *connection forms* by:

$$\Gamma^\alpha_\beta \;=\; \left\{ {\alpha \atop \gamma\,\beta} \right\} \theta^\gamma. \tag{1.2}$$

The first Cartan structure equation is related to the torsion by [6, p.40]:

$$\Omega^\alpha \;=\; \frac{1}{2}\, T^\alpha_{\ \gamma\,\delta}\, \theta^\gamma \wedge \theta^\delta \;=\; \mathrm{d}\theta^\alpha \;+\; \Gamma^\alpha_\gamma \wedge \theta^\gamma, \tag{1.3}$$

where $T^\alpha_{\ \gamma\,\delta} \;=\; \frac{1}{2}\big[\Gamma^\alpha_{\ [\gamma\,\delta]} - \Gamma^\alpha_{\ [\delta\,\gamma]}\big]$ is the torsion tensor.

In the Riemannian framework alone, it reduces obviously to:

$$\mathrm{d}\theta^\alpha \;=\; -\Gamma^\alpha_\gamma \wedge \theta^\gamma. \tag{1.4}$$

The *second Cartan structure equation* is defined as [6, p.42]:

$$\Omega^\alpha_\beta = \frac{1}{2}\, R^\alpha_{\beta\gamma\delta}\, \theta^\gamma \wedge \theta^\delta = \mathrm{d}\Gamma^\alpha_\beta + \Gamma^\alpha_\gamma \wedge \Gamma^\gamma_\beta, \tag{1.5}$$

$R^\alpha_{\beta\gamma\delta}$ are here the curvature tensor components.

Defining the absolute exterior differential D of a tensor valued p-form of type (r, s)

$$(D\phi)_{j_1\ldots j_s}{}^{i_1\ldots i_r} = \mathrm{d}\phi_{j_1\ldots j_s}{}^{i_1\ldots i_r} + \Gamma^{i_1}_k \wedge \phi_{j_1\ldots j_s}{}^{k\,i_2\ldots i_r} + \ldots - \Gamma^{\ k}_{j_1} \wedge \phi_{k\,j_2\ldots j_s}{}^{i_1\ldots i_r} - \ldots$$

we can write for example the *Bianchi identities* in a very simple way as:

$$D\Omega^\alpha \;= \Omega^\alpha_\beta \wedge \theta^\beta, \tag{1.6}$$

$$D\Omega^\alpha_\beta \;= 0. \tag{1.7}$$

1.2 The Einstein equations

1.2.1 The Einstein action

We first recall the *Hodge star* operator definition for an oriented n-dimensional *pseudo-Riemannian manifold* $(\mathrm{M}, \mathbf{g})$ whose volume element determined by $\mathbf{g}$ is:

$$\boldsymbol{\eta} \;=\; \sqrt{-\mathbf{g}}\; \theta^0 \wedge \theta^1 \wedge \theta^2 \wedge \theta^3.$$

Let $\Lambda_k(E)$ be the subspace of completely *antisymmetric multilinear forms* on the real vector space E.

The *Hodge star operator* * is a *linear isomorphism* *: $\Lambda_k(E) \to \Lambda_{n-k}(M)$ $(k \leqslant n)$. If $\theta^0, \theta^1, \theta^2, \theta^3$ is an oriented basis of 1-forms, this operator is defined by:

$$^*(\theta^{i_1} \wedge \theta^{i_2} \wedge \ldots \wedge \theta^{i_k}) = \\ = \frac{\sqrt{-g}}{(n-k)!} \left[\epsilon_{j_1 \ldots j_n} \, g^{j_1 i_1} \ldots g^{j_k i_k} \, \theta^{j_{k+1}} \wedge \ldots \wedge \theta^{j_n} \right]. \quad (1.8)$$

With this preparation, the Einstein action simply reads:

$$^*R \;=\; R\,\boldsymbol{\eta}\,. \quad (1.9)$$

We shall need this action expressed in terms of tetrads.

Proof: With $\sigma^{\mu\nu} = {}^*(\theta^\mu \wedge \theta^\nu)$ and taking into account (1.8) we have

$$\sigma_{\beta\gamma} \wedge \Omega^{\beta\gamma} \;=\; \frac{1}{2}\,\sigma_{\beta\gamma}\, R^{\beta\gamma}{}_{\mu\nu}\, \theta^\mu \wedge \theta^\nu$$

and

$$^*(\theta^\mu \wedge \theta^\nu) \;=\; \frac{1}{2}\,\boldsymbol{\eta}_{\beta\alpha\sigma\rho}\, g^{\beta\mu}\, g^{\alpha\nu}\, \theta^\sigma \wedge \theta^\rho$$

i.e.

$$\sigma_{\beta\gamma} \;=\; \frac{1}{2}\,\boldsymbol{\eta}_{\beta\gamma\sigma\rho}\, \theta^\sigma \wedge \theta^\rho. \quad (1.10)$$

Thus,

$$\sigma_{\beta\gamma} \wedge \theta^\mu \wedge \theta^\nu \;=\; \frac{1}{2}\,\boldsymbol{\eta}_{\beta\gamma\sigma\rho}\, \theta^\sigma \wedge \theta^\rho \wedge \theta^\mu \wedge \theta^\nu \;=\; (\delta^\mu_\beta\, \delta^\nu_\gamma \,-\, \delta^\mu_\gamma\, \delta^\nu_\beta)\boldsymbol{\eta}$$

and:

$$\sigma_{\beta\gamma} \wedge \Omega^{\beta\gamma} \;=\; \frac{1}{2}\,(\delta^\mu_\beta\, \delta^\nu_\gamma \,-\, \delta^\mu_\gamma\, \delta^\nu_\beta)\, R^{\beta\gamma}_{\mu\nu}\boldsymbol{\eta} \;=\; R\,\boldsymbol{\eta} \;=\; {}^*R.$$

Taking into account (1.10) let us now compute the absolute exterior differential:

$$D\sigma_{\beta\gamma} \;=\; \frac{1}{2}\,D\,(\boldsymbol{\eta}_{\beta\gamma\sigma\rho}\, \theta^\sigma \wedge \theta^\rho).$$

In an orthonormal system $\boldsymbol{\eta}_{\beta\gamma\sigma\rho}$ is constant and: $D\,\boldsymbol{\eta}_{\beta\gamma\sigma\rho} \;=\; 0$.

This reflects the fact that in the *Riemannian framework* (metric connection), orthonormality is preserved under parallel transport as well as the transported vector magnitude. Therefore:

$$D\sigma_{\beta\gamma} \;=\; \boldsymbol{\eta}_{\beta\gamma\sigma\rho} D\theta^\sigma \wedge \theta^\rho.$$

Now, bearing in mind that the basis θ^σ is a *tensor valued 1-form of type (1,0)*, the first structure equation reads [7]:

$$D\theta^\sigma \;=\; \Omega^\sigma$$

and

$$D\sigma_{\beta\gamma} \;=\; \boldsymbol{\eta}_{\beta\gamma\sigma\rho}\, \Omega^\sigma \wedge \theta^\rho = \Omega^\sigma \wedge \sigma_{\beta\gamma\sigma}\,.$$

The latter is zero for the torsion free Riemann connection: $D\sigma_{\beta\gamma} \;=\; 0$.

In the same way, we can show that

$$D\sigma^{\beta\gamma}{}_\alpha = \mathrm{d}\sigma^{\beta\gamma}{}_\alpha + \Gamma^\beta_{\ \delta} \wedge \sigma^{\delta\gamma}{}_\alpha + \Gamma^\gamma_{\ \delta} \wedge \sigma^{\beta\delta}{}_\alpha - \Gamma^\delta_{\ \alpha} \wedge \sigma^{\beta\gamma}{}_\delta \quad (1.11)$$

with

$$\sigma^{\beta\gamma}{}_\alpha \;=\; {}^*(\theta^\beta \wedge \theta^\gamma \wedge \theta_\delta),$$

(where all indices are raised or lowered with $g_{\alpha\beta}$ from $\boldsymbol{g} \;=\; g_{\alpha\beta}\,\theta^\alpha \otimes \theta^\beta$).

1.2.2 The Einstein field equations

From (1.10), we infer:

$$\sigma_{\beta\gamma\delta} \;=\; \boldsymbol{\eta}_{\beta\gamma\delta\lambda}\, \theta^\lambda. \quad (1.12)$$

Under the variation of $\delta\theta^\beta$ of the orthonormal tetrad fields, we have

$$\delta(\sigma_{\beta\gamma} \wedge \Omega^{\beta\gamma}) = \delta\sigma_{\beta\gamma} \wedge \Omega^{\beta\gamma} + \sigma_{\beta\gamma} \wedge \delta\Omega^{\beta\gamma}\,.$$

Now, using (1.10) and (1.12) yields:

$$\delta\sigma_{\beta\gamma} \;=\; \frac{1}{2}\,\delta(\boldsymbol{\eta}_{\beta\gamma\delta\lambda}\, \theta^\delta \wedge \theta^\lambda) \;=\; \delta\theta^\delta \wedge \sigma_{\beta\gamma\delta}\,.$$

Then, applying the varied second structure equation

$$\delta\Omega^{\beta\gamma} = \mathrm{d}\delta\Gamma^{\beta\gamma} + \delta\Gamma^\beta_{\ \eta} \wedge \Gamma^{\eta\gamma} + \Gamma^\beta_{\ \eta} \wedge \delta\Gamma^{\eta\gamma}$$

we obtain

$$\delta(\sigma_{\beta\gamma} \wedge \Omega^{\beta\gamma}) = \delta\theta^\gamma \wedge (\sigma_{\beta\gamma\delta} \wedge \Omega^{\beta\gamma}) + \mathrm{d}(\sigma_{\beta\gamma} \wedge \delta\Gamma^{\beta\gamma}) - \\ - \mathrm{d}\sigma_{\beta\gamma} \wedge \delta\Gamma^{\beta\gamma} + \sigma_{\beta\gamma} \wedge (\delta\Gamma^\beta_{\ \eta} \wedge \Gamma^{\eta\gamma} + \Gamma^\beta_{\ \eta} \wedge \delta\Gamma^{\eta\gamma}) \quad (1.13)$$

from the second line, we extract:

$$\mathrm{d}\sigma_{\beta\gamma} + \sigma_{\beta\gamma} \wedge (\Gamma^\eta{}_\gamma + \Gamma_{\beta\eta})$$

which is just: $D\sigma_{\beta\gamma}$. However, we know that: $D\sigma_{\beta\gamma} \;=\; 0$, and finally, the Einstein action variation is:

$$\delta(\sigma_{\beta\gamma} \wedge \Omega^{\beta\gamma}) \;=\; \delta\theta^\beta \wedge (\sigma_{\beta\gamma\delta} \wedge \Omega^{\gamma\delta}) \;+\; \mathrm{d}(\sigma_{\beta\gamma} \wedge \delta\Gamma^{\beta\gamma}) \quad (1.14)$$

(exact differential). The global Lagrangian density with matter is written:

$$\boldsymbol{L} \;=\; -\left(\frac{1}{2}\,\varkappa\right)^*\boldsymbol{R} \;+\; \boldsymbol{L}_{mat}\,.$$

Setting ${}^*T_\beta$ as the energy-momentum 3-form for *bare* matter we have the varied matter lagrangian density:

$$\boldsymbol{L}_{mat} \;=\; -\delta\theta^\beta \wedge {}^*T_\beta\,.$$

and taking into account (1.14) the global variation is:

$$\delta(\boldsymbol{L}) \;=\; -\delta\theta^\beta \wedge \left[\frac{1}{2}\,\varkappa\,\sigma_{\beta\gamma\delta} \wedge \Omega^{\gamma\delta} + {}^*T_\beta\right] \;+\; (\text{exact differential}).$$

We eventually arrive at the field equations under the differential form:

$$-\frac{1}{2}\sigma_{\beta\gamma\delta}\wedge\Omega^{\gamma\delta} \;=\; \varkappa\,{}^{*}T_{\beta}\,, \tag{1.15}$$

where T_α is related to the energy-momentum tensor $T_{\alpha\beta}$ by $T_\alpha = T_{\alpha\beta}\,\theta^\beta$.

In the same manner, one has: $G_\alpha = G_{\alpha\beta}\,\theta^\beta$ so that these identifications lead to the field equations with a source in the classical form:

$$G_{\alpha\beta} \;=\; R_{\alpha\beta} - \frac{1}{2}\,g_{\alpha\beta}\,R \;=\; \varkappa\,T_{\alpha\beta}\,, \tag{1.16}$$

$G_{\alpha\beta}$ is conserved but not $T_{\alpha\beta}$, therefore we should look for the appropriate r.h.s. tensor.

To this effect we start by reformulating (1.15) as

$$-\frac{1}{2}\,\Omega_{\beta\gamma}\wedge\sigma^{\beta\gamma}{}_{\alpha} \;=\; \varkappa\,{}^{*}T_{\alpha} \tag{1.17}$$

and we use the second structure equation under the following form

$$\Omega_{\beta\gamma} \;=\; \mathrm{d}\Gamma_{\beta\gamma} \;-\; \Gamma_{\mu\beta}\wedge\Gamma^{\mu}{}_{\gamma} \tag{1.18}$$

so as to obtain:

$$\mathrm{d}\Gamma_{\beta\gamma}\wedge\sigma^{\beta\gamma}{}_{\alpha} = \mathrm{d}\left(\Gamma_{\beta\gamma}\wedge\sigma^{\beta\gamma}{}_{\alpha}\right) + \Gamma_{\beta\gamma}\wedge d\sigma^{\beta\gamma}{}_{\alpha}\,. \tag{18bis}$$

Then using (1.11) in (1.18bis), we infer:

$$\begin{aligned}\mathrm{d}\Gamma_{\beta\gamma}\wedge\sigma^{\beta\gamma}{}_{\alpha} &= \mathrm{d}\left(\Gamma_{\beta\gamma}\wedge\sigma^{\beta\gamma}{}_{\alpha}\right) + \\ &+ \Gamma_{\beta\gamma}\wedge\left(\Gamma^{\beta}{}_{\delta}\wedge\sigma^{\delta\gamma}{}_{\alpha} - \Gamma^{\gamma}{}_{\delta}\wedge\sigma^{\beta\delta}{}_{\alpha} - \Gamma^{\delta}{}_{\alpha}\wedge\sigma^{\beta\gamma}{}_{\delta}\right).\end{aligned} \tag{1.19}$$

Adding the second contribution ($\Gamma^\alpha\ \gamma\wedge\Gamma^\gamma\ \beta$) of (1.18) to (1.19), we obtain the Einstein field equations in a new form:

$$-\frac{1}{2}\,\mathrm{d}(\Gamma_{\beta\gamma}\wedge\sigma^{\beta\gamma}{}_{\alpha}) \;=\; \varkappa\,({}^{*}T_{\alpha} \;+\; {}^{*}t_{\alpha}), \tag{1.20}$$

where

$${}^{*}t_{\alpha} \;=\; \left(-\frac{1}{2}\,\varkappa\right)\Gamma_{\beta\gamma}\wedge(\Gamma_{\delta\alpha}\wedge\sigma^{\beta\gamma\delta} - \Gamma^{\gamma}{}_{\delta}\wedge\sigma^{\beta\delta}{}_{\alpha}), \tag{1.21}$$

where ${}^{*}t_\alpha$ should be here interpreted as *energy* and *momentum 3-form of the gravitational field* generated by this matter.

Equation (1.20) readily implies the conservation law:

$$\mathrm{d}({}^{*}T_{\alpha} \;+\; {}^{*}t_{\alpha}) \;=\; 0\,. \tag{1.22}$$

Within the *Riemannian framework*, we know that the gravitational field cannot be localized, which is reflected by the fact that ${}^{*}t_\alpha$ does not transform as a tensor with respect to gauge transformations.

Indeed, as $\Gamma_{\beta\gamma}$ can be made zero at any given point of the Riemannian manifold, this 3-form vanishes.

To the 3-form ${}^{*}t_\alpha$ is thus associated the antisymmetric Einstein-Dirac pseudo-tensor $(\Theta^a_b)_{ED}$ [8].

In order to explicitly write down (1.20) with a *true* 3-form on the r.h.s., one should add the *3-form of the energy-momentum for the vacuum* denoted by $({}^{*}t_\alpha)_{vac}$.

Equation (1.22) eventually satisfies the conservation law:

$$\mathrm{d}[{}^{*}T_{\alpha} \;+\; ({}^{*}t_{\alpha})_{gravity}] \;=\; 0 \tag{1.23}$$

with:

$$({}^{*}t_{\alpha})_{gravity} \;=\; {}^{*}t_{\alpha} \;+\; ({}^{*}t_{\alpha})_{vac}\,. \tag{1.24}$$

To the 3-form $({}^{*}t_\alpha)_{vac}$ corresponds the tensor

$$(t_{\alpha\beta})_{vac} \;=\; \left(-\frac{1}{2}\,\varkappa\right)\Xi\,g_{\alpha\beta}\,, \tag{1.25}$$

where Ξ is the variable cosmological term which replaces the cosmological constant Λ as [9]:

$$G_{\alpha\beta} = R_{\alpha\beta} - \frac{1}{2}\,g_{\alpha\beta}\,R = \varkappa\left[T_{\alpha\beta} + (t_{\alpha\beta})_{ED}\right] + \Xi\,g_{\alpha\beta}\,. \tag{1.26}$$

2 Two opposite field equations

Since we deal with a Lorentzian manifold $n = 4$, repeated application of the duality operation *, gives:

$${}^{*}({}^{*}G_{\beta}) \;=\; -\,{}^{*}G_{\beta}\,, \tag{2.1}$$

$${}^{*}(\varkappa\,{}^{*}T_{\beta}) \;=\; -\,(\varkappa\,{}^{*}T_{\beta})\,. \tag{2.2}$$

The Cartan formalism thus allows for two "opposite" field equations to appear.

Can we find its physical meaning? A straightforward justification can be provided by the *Janus model* of J.P. Petit whose universes exhibit opposite energy/masses.

This model is characterized by two types of distinct metric tensors ${}^{(+)}g_{\mu\nu}$ and ${}^{(-)}g_{\mu\nu}$, which imply two distinct field equations:

$${}^{(+)}G_{\beta\mu} = {}^{(+)}R_{\beta\mu} - \frac{1}{2}\,{}^{(+)}g_{\beta\mu}{}^{(+)}R = \varkappa\left[{}^{(+)}T_{\beta\mu} + \varpi^{(-)}T_{\beta\mu}\right], \tag{2.3}$$

$${}^{(-)}G_{\beta\mu} = {}^{(-)}R_{\beta\mu} - \frac{1}{2}\,{}^{(-)}g_{\beta\mu}{}^{(-)}R = \varkappa\left[{}^{(-)}T_{\beta\mu} + \omega^{(+)}T_{\beta\mu}\right], \tag{2.4}$$

where ${}^{(+)}g_{\mu\nu}$ refers to positive mass/energy particles while ${}^{(-)}g_{\mu\nu}$ refers to negative mass/energy particles with the corresponding Ricci tensors ${}^{(+)}R_{\mu\nu}$ and ${}^{(-)}R_{\mu\nu}$.

Here ${}^{\pm}T_{\mu\nu}$ is the massive tensor which implicitly contains the gravitational field tensor defined from (1.24).

With our definition, we then have the obvious correspondences:

$${}^{*}G_{\beta} \;\to\; {}^{(+)}G_{\beta\mu}\,, \qquad {}^{*}T_{\beta} \;\to\; {}^{(+)}T_{\beta\mu} + \varpi^{(-)}T_{\beta\mu}\,,$$

$${}^{*}({}^{*}G_{\beta}) \;\to\; {}^{(-)}G_{\beta\mu}\,, \quad {}^{*}({}^{*}T_{\beta}) \;\to\; -\left({}^{(-)}T_{\beta\mu} + \omega^{(+)}T_{\beta\mu}\right).$$

Each solution of (2.3) and (2.4) is a *Friedmann-Lemaitre-Roberston-Walker metric*

$$ {}^{(\pm)}\mathrm{d}s^2 = \mathrm{d}t^2 - {}^{(\pm)}a(t)^2 \, \frac{\mathrm{d}u^2 + u^2\left(\mathrm{d}\theta^2 + \sin^2\theta\,\mathrm{d}\varphi^2\right)}{\left(1 + \dfrac{k\,u^2}{4}\right)^2}, \qquad (2.5) $$

where k is referred to as the *curvature index*: $\{-1, 0, 1\}$.

Ultimately, inspection shows that:

$$ \varpi = \frac{{}^{(-)}a^3}{{}^{(+)}a^3} \quad \text{and} \quad \omega = \frac{{}^{(+)}a^3}{{}^{(-)}a^3}, \quad \omega = \varpi^{-1}. \qquad (2.6) $$

3 Conclusions and outlook

According to the Cosmological Janus Model, mass and charge inversions simultaneously result from time reversal which grant the theory a particularly simple and exhaustive symmetry.

As a final point, let us emphasize that the *JCM* bi-metric scheme is far from being an arbitrary postulate as it proves consistent with the newest developments in astrophysics.

It is also formally sustained by a specific splitting of the *Riemann tensor* in two 2nd rank tensor field equations as shown in [10]. This 4th rank tensor theory eventually leads to the space-time of constant curvature (i.e. in vacuum). It thereby copes with the recent view suggesting that the laws of physics are invariant under the symmetry group of *De Sitter* space (maximally symmetric space), rather than the *Poincaré* group of Special Relativity [11–14].

Submitted on March 24, 2019

References

1. Petit J.-P., D'Agostini G. Negative mass hypothesis in cosmology and the nature of the dark energy. *Astrophysics and Space Sciences*, 2014, v. 354, 611–615.
2. Sakharov A.D. Cosmological models of the Universe with reversal a time arrow. *Soviet Physics JETP*, 1980, v. 52, issue 3, 689–693 (translated from: *ZhETF*, 1980, v. 52, 349–351).
3. Petit J.-P., D'Agostini G. Constraints on Janus Cosmological model from recent observations of supernovae type Ia. *Astrophys. Space Sci.*, 2018, v. 363, 139.
4. Debergh N., Petit J.-P., D'Agostini G. On evidence for negative energies and masses in the Dirac equation through a unitary time-reversal operator. *J. Phys. Comm.*, 2018, issue 2, 115012.
5. Marquet P. Lichnerowicz's Theory of Spinors in General Relativity: the Zelmanov Approach. *The Abraham Zelmanov Journal*, 2012, v. 5, 117–133.
6. Kramer D., Stephani H., Hertl E., Mac Callum M. Exact Solutions of Einstein's Field Equations. Cambridge University Press, 1979.
7. Straumann N. General Relativity and Relativistic Astrophysics. Springer-Verlag, Berlin, 1984.
8. Dirac P.A.M. General Theory of Relativity. Princeton University Press, 2nd edition, Cambridge University Press, 1975, p. 61.
9. Marquet P. Vacuum background field in General Relativity. *Progress in Physics*, 2016, v. 12, issue 4, 314–316.
10. Marquet P. On a 4th rank tensor gravitational field theory. *Progress in Physics*, 2017, v. 13, issue 2, 106–110.
11. Aldrovani R., Beltran Almeida J.P., Pereira J.G. Some implications of the cosmological constant to fundamental physics. arXiv: gr-gc/0702065.
12. Lev F.M. De Sitter symmetry and quantum theory. arXiv: 1110.0240.
13. Aldrovani R., Beltran Almeida J.P., Pereira J.G. De Sitter Special Relativity. 2007.
14. Inönü E., Wigner E.P. *Proc. Natl. Acad. Scien.*, 1953, v. 39, 510.

Evidence of Residual Strong Interaction at Nuclear-Atomic Level via Isotopic Shift in LiH-LiD Crystals

V. G. Plekhanov[1] and J. Buitrago[2]
[1] Informatika ja Arvutustehnika Instituut, Tallinn, Estonia
E-mail: vgplekhanov@gmail.com
[2] Department of Astrophysics of the University of La Laguna, Faculty of Physics, 38205, La Laguna, Tenerife (Spain)
E-mail: jbuitrag@ull.es

Artificial activation of the strong interaction by adding one neutron to the nucleus causes the global reconstruction of the macroscopic characteristics of solids. The experimental evidence of macroscopic manifestation of the strong interaction in the optical spectra of solids which differ by one neutron from each other (using LiD crystals instead LiH ones) is presented for the first time. As far as the electromagnetic and weak interactions are the same in both kind of crystals, it only changes the strong interaction, therefore the renormalization of the energy of electromagnetic excitations (electrons, excitons, phonons) is carried out by the strong nuclear interaction. The necessity to take into account some new residual inter-relations between strong and electromagnetic interactions are underlined. An interpretation of the isotopic shift caused by the addition of one neutron is also discussed. From the experimental value of the isotopic shift we obtain a residual strong coupling constant equal to 2.4680.

1 Introduction

To the present we have a clear picture about the different kind of interactions and their main scenarios: electromagnetic ones for the realm of atomic physics and strong interactions for nuclear physics [1, 2]. However, in this articles we would like to report about some new experimental evidence, together with a tentative theoretical interpretation, pointing towards some relationship between both kind of interactions, which seems to lead to a new understanding in which nuclear forces can reach outside the nucleon boundaries and manifest themselves at the atomic level, at least in the magnetic manifestation. In what follows we shall try to explain how residual strong like interactions can affect, via electronic excitations (electrons, excitons, phonons) through isotopic effects, the binding energy of the dielectrics LiH and LiD crystals [3].

Nowadays in text books and elsewhere the separation of electromagnetic and strong interactions is tacitly assumed. Our results shine a new light on some residual interaction (ultimately based in the character of magnetic forces, of electromagnetic or color origin, which by their very nature, are difficult to conceal within the elusive nucleon physical boundary) between both kind of forces which is experimentally manifested trough isotopic shift. We hope that the results that we report in this paper will give a new insight about the manifestation of nuclear forces, by isotopic shift, beyond the nuclear domain.

2 Experimental results

In this part we shall describe the results of the optical spectroscopy of isotope-mixed solids (see, also [3]). The apparatus used in our experiments has been described in several previous publications [4, 5]. For clarity, we should mentioned here that immersion home-made helium cryostat and two identical double-prism monochromators were used. One monochromator was used for the excitation and the other, which was placed at right-angle to the first, for analyzing the luminescence and scattering of light. In our experiments we investigated two kinds of crystals (LiH and LiD) which only differ by the addition of one neutron. In view of the high hygroscopy of the investigated samples, the crystals were cleaved directly in liquid (superfluid) helium in the cryostat bath [4]. This makes possible to prepare samples with a clean surface. We found no changes in the free-exciton luminescence or resonance Raman scattering (RRS) [5] spectra when a sample with such a surface was studied for periods lasting 15 hours. The crystals were synthesized from 7Li metal and hydrogen 99.7 per cent purity and deuterium of 99.5 per cent purity (see, e.g. [3, 5] and references therein). We should remind very briefly about the electronic excitations in solids. According to modern concept, the excitons can be considered [6] as the excitation of the N-particles system: An electron from the valence band of insulators (see Fig. 1) is excited into the conduction band.

The attractive Coulomb potential between the missing electron in the valence band, which can be regarded as a positively charged hole, and the electron in the conduction band gives a hydrogen-like spectrum with an infinitive number of bound state and ionization continuum. In this article we call the bound states of electron-hole (e-h) pairs exciton states (exc), while we refer to ionized e-h pairs as free carriers. However, the expression free carriers does not imply that the effect of the strong Coulomb forces between electronic excitation could be neglected. Thus, an exciton state can be built by appropriate superposition of e-h pairs, which in a simple two-band model for cubic crystal symmetry is

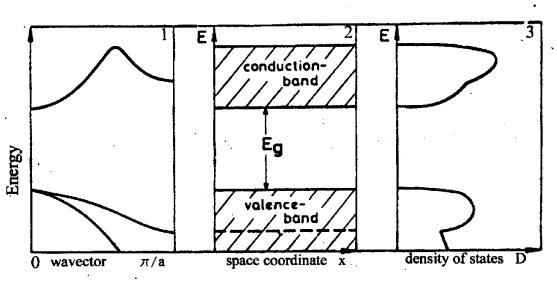

Fig. 1: Various possibilities to present the band-structure of homogeneous, undoped insulator (semiconductor). 1 - the dispersion relation, i.e. the energy E as a function of the wave vector, 2 - the energy regions of allowed and forbidden states as function of a space coordinate x and, 3 - the density of states (all curves are schematic ones).

given (for more details see [6]). As demonstrated some time ago [4] most low - energy electron excitation in LiH crystals are the large-radius excitons [6]. Exciton luminescence is observed when LiH (LiD) crystals are excited in the midst of the fundamental absorption. The spectrum of exciton photoluminescence of LiH crystals cleaved in liquid (superfluid) helium consists of a narrow (in the best crystals, its half-width is E $\leq$ 10 meV) phononless emission line and its broader phonon repetitions, which arise due to radiative annihilation of excitons with the production of one to five longitudinal optical (LO) phonons (see Fig. 2).

The phononless emission line coincides in an almost resonant way with the reflection line of the exciton ground state which is indication of the direct electron transition X_1 - X_4 of the first Brillouin zone [4].The lines of phonon replicas form an equidistant series biased toward lower energies from the resonance emission line of excitons. The energy difference between these lines in LiH crystals is about 140 meV, which is very close to the calculated energy of the LO phonon in the middle of the Brillouin zone and which was measured in (see, e.g. [3] and references therein). As we can see from Fig. 2 the photoluminescence spectrum of LiD crystals is largely similar to the spectrum of intrinsic luminescence of LiH crystals. The isotopic shift of the zero phonon emission line of LiH crystals equals 103 meV. There are, however, some related distinctions. Firstly the zero-phonon emission line of free excitons in LiD crystals shifts to the short-wavelength side on 103 meV. The second difference concludes in less value of the LO phonon energy, which is equal to 104 meV. Comparison of the experimental results on the luminescence and light scattering [3] in the crystals which differ by only one neutron is allowed to the main conclusion motivating this work: The addition of one neutron (using LiD crystals instead LiH ones) produce an unexpected increase of 103 meV in the exciton energy which seems rather difficult to explain within the conventional solid state physics scenario.

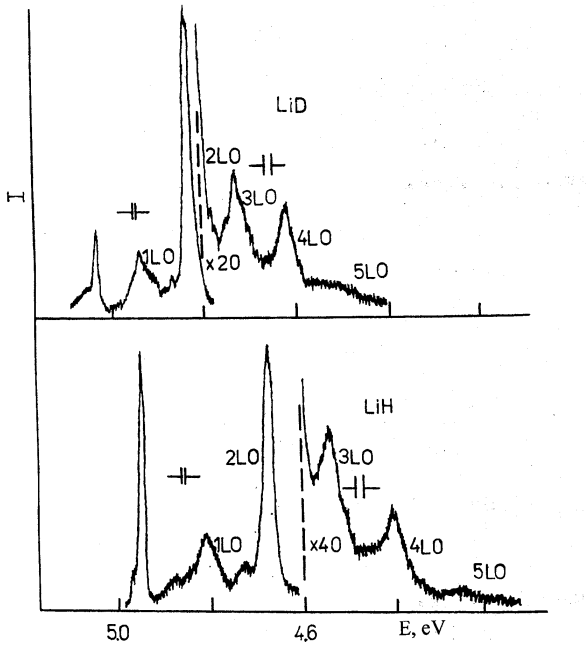

Fig. 2: Photoluminescence spectra of free excitons at 2 K in LiH and LiD crystals cleaved in superfluid helium.

3 Interpretation of the Isotopic Shift

We are used to find characteristic energies, mostly due to electrical interactions, of the order of one eV in the atomic and molecular scenarious. The reported experimental result of 0.103 eV emerging from magnetic-like interaction (magnetic forces are a factor v/c weaker than electric ones) is a surprising result pointing towards something that has not been observed before. The following comments, although tentative, pretend to give a plausible physical picture of new dynamical effects extending beyond the undefined borders of nucleons. From many experiments in QCD we know that direct forces between quarks are strong color analogues of electrostatic forces. However, in QCD, like in all gauge theories formulated within the context of special relativity, magnetic effects are unavoidable. In its more simple-minded description, electrostatic-like interactions between quarks have an origin and sink in the individual quarks confined in a nucleon. However, since quarks are not at rest, magnetic-like effects have to arise. The question we now ask is whether these effects should be limited to the inside-nucleon region or, perhaps, propagate outwards. In the absent of magnetic monopoles, magnetic force lines are closed. Moreover, magnetic fields are related to the SO(3) rotation group and its SU(2) covering group and it is not evident, at least in principle, if they couple only to ordinarily charged particles (remember that the SU(2) group is also contained in SU(3)). Consequently, in what follows, we shall consider, as an Ansatz, that magnetic color like

forces also couple to charged leptons. From the experimental results described before which arise by adding a single neutron to the LiH crystal:

$$LiH + n \longrightarrow LiD.$$

It seems that the 0.103 eV value should be regarded as an isotopic shift attributed to the magnetic moment of the charge-neutral neutron.

We are already familiar with the dipole-dipole magnetic interaction arising from the hyperfine splitting in the Hydrogen atom (for an adequate, to our purpose, study see [7]). The ground state wave function for the electron in the Hydrogen atom, including the spin part, is

$$\psi_0 = (\pi {a_0}^3)^{-1/2} e^{-r/a_0} |s>, \tag{1}$$

a_0 being the Bohr radius. We also need the energy of a magnetic dipole $\vec{m}_1$ in a magnetic field $\vec{B}$ produced by another dipole ($\vec{m}_2$) given by

$$H = -\vec{m}\,\vec{B}.$$

$$H = -\frac{1}{4\pi}\frac{1}{r^3}\left[3(\vec{m}_1\hat{r})(\vec{m}_2\hat{r}) - \vec{m}_1\,\vec{m}_2\right] - \frac{2}{3}(\vec{m}_1\,\vec{m}_2)\delta^3(\vec{r}). \tag{2}$$

As is well known, for s states with spherical symmetry the first term vanishes and only the second term involving a delta function contributes. This is essential as the wave function (1) has a finite value for $r = 0$ so that the energy comes out from a contact-interaction (see [7]). The magnetic dipole-dipole interaction can thus be treated as a perturbation. In first order perturbation theory:

$$E' = \int {\psi_0}^* H \psi_0 dV. \tag{3}$$

As mentioned, only the second term contributes giving:

$$E' = -\frac{2}{3} < \vec{m}_1\,\vec{m}_2 > |\psi_0(0)|^2 = -\frac{2}{3}\frac{1}{\pi {a_0}^3} < \vec{m}_1\,\vec{m}_2 > . \tag{4}$$

For the electron-proton we have two configurations according to the spin of both particles:

$$\vec{m}_1 = \gamma_p \vec{S}_p, \qquad \vec{m}_2 = -\gamma_e \vec{S}_e.$$

(γ: gyromagnetic ratio; $\gamma = (e/2m)g$, the g-factor being 2.0023 for the electron and 5.5857 for the proton.)

According to equation (4), we obtain for the triple and singlet states in Hydrogen, the energies

$$E'_t = \frac{1}{3}\frac{e^2}{a_0^3 m_e M_p} g_p = 1.4685 \times 10^{-6}\ \text{eV}$$

and

$$E'_s = -\frac{e^2}{a_0^3 m_e M_p} g_p = -4.4054 \times 10^{-6}\ \text{eV},$$

with a gap $\Delta E' = 5.874 \times 10^{-6}$, coincident with the hydrogen hyperfine splitting experimental result.

Similar calculations can be easily carried out for Deuterium (spin 1 and gyromagnetic ratio $g_d = 1.71$) with the results:

$$E'_{3/2} = 4.4980 \times 10^{-7}\ \text{eV},$$

$$E'_{1/2} = -8.9960 \times 10^{-7}\ \text{eV},$$

$$\Delta E'_d = E'_{3/2} - E'_{1/2} = 1.3494 \times 10^{-6}\ \text{eV}.$$

Turning now to the *Isotopic shift* issue, from the above values, we have four alternatives depending on the relative spins, however, as the lowest energy for both LiH and LiD is the corresponding to singlet states, we shall choose:

$$\Delta E = (E'_s)_H - (E'_{1/2})_D = -3.5058 \times 10^{-6}\text{eV}, \tag{5}$$

far from the experimental 0.103 eV. Next we shall assume that the experimental isotopic shift of 0.103 eV is the result of the onset of a residual strong interaction when the neutron is added, accordingly we do not modify $(E'_s)_H$ but modify $(E'_{1/2})_D$ in the following way: In Hydrogen the absolute value of the charge is the same so that in electric or magnetic interactions the coupling constant is $\alpha = e^2$. However, as the neutron do not have electric charge, in the dipole magnetic interaction the effective coupling constant can be defined through the transformation

$$\alpha = e^2 \longrightarrow (\alpha_s)_{\text{eff}} = e\, e_s. \tag{6}$$

The Bohr radius is thus modified:

$$a'_s = \frac{1}{e\, e_s}\frac{1}{m_e}.$$

From (4), it is easy to obtain

$$(E'_{1/2})_D = -\frac{4}{3} g_d \frac{(\alpha'_s)^4 m_e^2}{M_d}. \tag{7}$$

Inserting in (5) the 0.103 experimental value for ΔE and solving for α'_s, we obtain:

$$\alpha'_s = 0.1342,$$

and a *strong charge*

$$e_s = \frac{0.1342}{0.08542} = 1.5710,$$

leading to a strong coupling constant $e_s^2 = \alpha_s = 2.4680$. Quite large in comparison with the normal fine structure constant.

4 Conclusions

The experimental evidence of the macroscopic manifestation of strong nuclear interaction in optical spectra of solids which are differing by one neutron from each other has been presented for the first time. This evidence is based on two independent experimental results, which is directly seen from luminescence and reflection spectra. Our interpretation is based in the neutral charge of the neutron which in turn is responsible for the observed isotopic shift. We should be aware of the delicate interplay between solid state physics translated for a theoretical interpretation to the nuclear and subnuclear background which we have tried to accomplish in a way that could be regarded as somewhat tentative but unavoidable given the uncertainties laying in the strong magnetic-like interaction between nucleons and electrons.

Submitted on April 22, 2019

References

1. Henley E.M., Garcia A. Subatomic Physics. World Scientific Publishing Co., Singapore, 2007.
2. Griffiths G. Introduction to Elementary Particles. Wiley - VCH, Weinheim, 2008.
3. Plekhanov V.G. Isotopes in Condensed Matter. Springer, Heidelberg, 2013.
4. Plekhanov V.G. Experimental manifestation of the effect of disorder on exciton binding energy in mixed crystals. *Phys. Rev. B*, 1996, v. 53, 9558–9593.
5. Plekhanov V.G. Macroscopic manifestation of the strong nuclear interaction in the optical spectra of solids. In: *Proceedings of XXV International Seminar on Interactions of Neutrons with Nuclei*, ISINN - 25, Dubna, Russia, 2018, pp. 49–56.
6. Knox R.S. Theory of Excitons. Academic Press, New York - London, 1963.
7. Griffiths D. Hyperfine splitting of the ground state of hydrogen. *American Journal of Physics*, 1982, v. 50, no. 8, 698–703.

Can We Hide Gravitational Sources behind Rindler Horizons?

Michael Edward McCulloch

SoBMS, Plymouth University, Plymouth, UK. E-mail: mike.mcculloch@plymouth.ac.uk

When an object accelerates in one direction, a Rindler horizon forms in the opposite direction and information from behind it cannot reach the object. Here it is shown that it is possible to test for this effect since it predicts that if an object, say a disc, is rotationally accelerated by over $\sim 10^{10}\,\mathrm{m/s^2}$ then the Rindler horizon it sees should come close enough to hide part of the Earth and therefore it should not feel all the Earth's gravity. This effect could be detected by measuring the disc's weight.

1 Introduction

Hawking [1] showed that the strong gravity at the edge of a black hole produces an event horizon that can separate paired virtual particles leading to Hawking radiation and black hole evaporation. Fulling [2], Davies [3] and Unruh [4] showed that a similar effect occurs for accelerating objects in that a Rindler horizon [5] forms at a distance of c^2/a from the side they are accelerating away from (where c is the speed of light and a is the acceleration of the object). This horizon similarly produces radiation so that an accelerated object will perceive a warm background full of blackbody radiation whereas an unaccelerated body will see a cold background with no radiation. This is called Unruh radiation [4] and for typical accelerations it has too long a wavelength to be detectable, but it may have been observed coming from plasmons propagating at high acceleration around the surface of a gold nanotip [6].

McCulloch [7, 8] proposed a new model for inertia (called quantised inertia, or QI) that assumes that the inertia of an object is due to the Unruh radiation it sees when it accelerates. The Rindler horizon that appears in the opposite direction to its acceleration damps the Unruh radiation on that side of the object producing a radiation pressure differential that looks like inertial mass [8]. Also, when accelerations are extremely low the Unruh waves become very long and are also damped, this time in all directions, by the Hubble horizon (Hubble-scale Casimir effect). This leads to a new loss of inertia as accelerations become tiny. QI modifies the standard inertial mass (m) to a modified one (m_i) as follows:

$$m_i = m\left(1 - \frac{2c^2}{|a|\,\Theta}\right), \tag{1}$$

where c is the speed of light, Θ is twice the Hubble distance, $|a|$ is the magnitude of the relative acceleration of the object relative to surrounding matter. Eq. 1 predicts that for terrestrial accelerations (eg: $9.8\,\mathrm{m/s^2}$) the second term in the bracket is tiny and standard inertia is recovered, but in low acceleration environments, for example at the edges of galaxies (when a is tiny), the second term in the bracket becomes larger and the inertial mass decreases in a new way so that QI can predict galaxy rotation without the need for dark matter [9].

Putting Eq. 1 into Newton's second and gravity laws gives

$$F = ma = m\left(1 - \frac{2c^2}{|a|\,\Theta}\right) = \frac{GMm}{r^2} \tag{2}$$

and finally

$$a = \frac{GM}{r^2} + \frac{2c^2}{\Theta}\,. \tag{3}$$

This predicts cosmic acceleration (the new second term) without the need for dark energy [7]. In this paper this same result is derived a different way, simply using Ernst Mach's attitude that "what cannot be observed does not exist". It is argued that, since Rindler horizons are boundaries for information, then sources of gravity behind them disappear from the point of view of the accelerated object. It is shown here that this effect predicts cosmic acceleration, given the known baryonic mass of the cosmos, and may allow us to hide gravitational sources behind horizons producing new kinds of thrust.

2 Method

If we consider a photon travelling at the speed of light in the centre of its own Hubble sphere (see Fig. 1). Due to the impossibility of any light from the left hand side of the cosmos catching up to the photon, we can say that, as far as the photon knows, there is no mass there at all. All the mass is hidden by the Rindler horizon. Therefore, there is a gravitational imbalance as the photon can be aware of a lot of matter in front of it in the direction of its acceleration, but nothing behind. We can calculate this gravitational acceleration as follows

$$a = \frac{GM}{r^2}\,. \tag{4}$$

We can assume from standard geometry that the centre of mass of the semi-sphere in front of the photon is 3/8ths of the radius away, and the radius and baryonic mass of the cosmos are estimated to be 4.4×10^{-10} m and $10^{52\pm1}$ kg, so

$$a = \frac{6.67 \times 10^{-11} \times 10^{52\pm1}}{(3/8 \times 4.4 \times 10^{26})^2} = 2.45 \times 10^{-11\pm1}\mathrm{m/s^2}. \tag{5}$$

The predicted acceleration (given the error bars) agrees with the observed cosmic acceleration and with the critical acceleration below which galactic dynamics deviate from Newton: $2 \times 10^{-10}\mathrm{m/s^2}$.

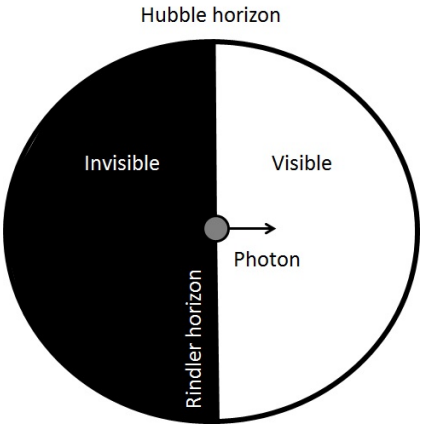

Fig. 1: A schematic showing the Hubble horizon (as a black circle). A photon (the central grey circle) moves rightwards at the speed of light, so it has a Rindler horizon passing through it, and no information from the black-shaded volume can get to it. This means that, following Mach, the gravitational mass from that black region is irrelevent and the gravitational pull from the right hand half of the cosmos now dominates, causing an acceleration which predicts the cosmic acceleration.

3 A test

If we consider a spinning disc, then every particle within it is accelerating towards the spin axis, and each particle perceives a Rindler horizon that is outside the disc. As the rotational acceleration is increased the horizon moves closer to the spin axis. What would happen if the horizon was closer than the Sun or the Earth? Would this hide their gravitational effect from the point of view of the accelerated object? (see an earlier brief discussion of this in [10]).

To calculate the spin rate required to pull the Rindler horizon in closer than a distance d_R we assume a disc of any material of radius r, spinning at R rpm (rotations per minute). The centripetal acceleration (a) at different radii (r) of the disc is given by

$$a = \frac{v^2}{r} = \frac{(2\pi rR/60)^2}{r} = \frac{4\pi^2 rR^2}{3600}\,, \tag{6}$$

where the 60 comes from the number of seconds in a minute. The Rindler horizon forms in the direction opposite to the acceleration at a distance given by

$$d_R = \frac{c^2}{a}\,. \tag{7}$$

We can now substitute Eq. 6 in Eq. 7

$$d_R = \frac{3600\,c^2}{4\pi^2 rR^2} = \frac{900\,c^2}{\pi^2 rR^2}\,. \tag{8}$$

Eq. 8 shows the distance of the Rindler horizon (d_R) for a particle within a disc spinning at R rpm and at a radius r from the spin centre. It shows that the faster the disc spins (R increases) the distance to the Rindler horizon decreases very rapidly and the Rindler horizon is closer for particles at the disc's edge (when r is large).

4 Results & discussion

Eq. 8 can be rearranged to calculate the rotation rate R (in rpm) needed to bring the Rindler horizon closer than a body a distance d_R away

$$R = \sqrt{\frac{900\,c^2}{\pi^2 r d_R}}\,. \tag{9}$$

The following table shows the object to be hidden by the Rindler horizon in the first column. The second column shows its distance (d) away from a lab on the Earth's surface. The third column shows the acceleration needed, in a linear sense, to hide the object. The fourth column shows the rpm required for a spinning disc to achieve that acceleration, at a radius of 0.1 m. The fifth column shows the gravitational acceleration ($a_g = GM/d^2$) produced by that object that will disappear and affect the dynamics of the disc (but only those parts of it above the critical acceleration).

Object	Distance	a	rpm	a_g
		Eq. 7	Eq. 9	
		(m/s^2)		(m/s^2)
Sun	1 AU	600,000	23 k	0.006
Earth	6371 km	1.43×10^{10}	3589 k	9.8

Table 1: The Table shows for two objects (column 1), the distances from a lab on the Earth's surface to the object (column 2), the accelerations needed to hide the object behind Rindler horizons (column 3), the rpm needed for that acceleration for a disc at a radius of 0.1 m (column 4) and the acceleration exerted by the object on the disc (column 5).

The rotation required to hide the Sun should be achievable since gyroscopes often have rotation rates of 30,000 rpm and medical centrifuges can spin at 100,000 rpm. The rotation rate required would be lower for a larger disc. Of course, only the part of the disc that has an acceleration vector pointing away from the Sun (the Sunward side) would feel the disappearence of the Sun's effect, including its gravitational force. The gravitational acceleration due to the Sun is $GM_\odot/r^2 = 0.006\,m/s^2$ (this is 0.06% of g). The Sun's width in the sky is about half a degree so only an area of about 1/(360*2) of the disc would be affected and then also only the area of the disc outside the radius of 0.1m. So if the disc was 0.2m in radius the affected area would be the total area times (1/720)×(3/4). Therefore, the average acceleration for the whole disc would be $0.006 \times (1/720) \times (3/4) = 6.25 \times 10^{-6} m/s^2$.

From a practical point of view it would be far more useful to hide the Earth's gravity since then launching objects would become easier. The acceleration required to do so: 1.43×10^{10} (see Table 1), has just been achieved for the first time by [11] who spun a microscopic sphere of radius $r = 4\times10^{-6}$ m using circularily polarised light to suspend and rotate it in vacuo at $R = 6 \times 10^8$ rpm. This is an acceleration, using Eq. 6 of $1.58 \times 10^{10}\mathrm{m/s^2}$ which agrees with the acceleration needed to pull the Rindler horizon close enough to hide the Earth's gravity (Table 1, column 3).

5 Conclusion

It is proposed here that Rindler horizons have physical consequences beyond their effects on light: they are able to hide gravitational sources.

It is shown that assuming that gravitational sources can be hidden in this way, predicts the cosmic acceleration.

The effect could be tested using discs with extreme spins, which should break free from distant gravitational sources.

Acknowledgements

Many thanks to J. Lucio for proof-reading this manuscript, and to DARPA for funding grant HR001118C0125.

Submitted on May 5, 2019

References

1. Hawking S. Black hole explosions. *Nature*, 1974, v.248, 30.
2. Fulling S.A. Nonuniqueness of Canonical Field Quantization in Riemannian Space-Time. *Phys. Rev. D.*, 1973, v.7, 2850.
3. Davies P.C.W. Scalar production in Schwarzschild and Rindler metrics *J. Phys. A.*, 1975, v.8, 609.
4. Unruh W.G. Notes on black hole evaporation. *Phys. Rev. D.*, 1976, v.14, 870.
5. Rindler W. Relativity, special, general and cosmological. Oxford University Press, 2001.
6. Smolyaninov I.I. Photoluminescence from a gold nanotip in an accelerated reference frame *Physics Letters A*, 2008, v.372, 7043–7045.
7. McCulloch M.E. Modelling the Pioneer anomaly as modified inertia. *MNRAS*, 2007, v.376, 338.
8. McCulloch M.E. Inertia from an asymmetric Casimir effect. *EPL*, 2013, v.101, 59001.
9. McCulloch M.E. Galaxy rotations from quantised inertia and visible matter only. *Astrophys. & Space Sci.*, 2017, v.362, 149.
10. McCulloch M.E. Physics from the edge: a new cosmological model for inertia. World Scientific, 2014.
11. Arita Y., Mazilu M. and Dholakia K. Laser-induced rotation and cooling of a trapped microgyroscope in vacuum. *Nature Communications*, 2013.

A Mathematical Definition of "Simplify"

Craig Alan Feinstein

2712 Willow Glen Drive, Baltimore, Maryland 21209. E-mail: cafeinst@msn.com

Even though every mathematician knows intuitively what it means to "simplify" a mathematical expression, there is still no universally accepted rigorous mathematical definition of "simplify". In this paper, we shall give a simple and plausible definition of "simplify" in terms of the computational complexity of integer functions. We shall also use this definition to show that there is no deterministic and exact algorithm which can compute the permanent of an $n \times n$ matrix in $o(2^n)$ time.

1 Introduction

In 2013, the author asked the following quesiton titled "Is there a 'mathematical' definition of 'simplify'?" on the popular mathematics website MathOverflow.net [1]:

> "Every mathematician knows what 'simplify' means, at least intuitively. Otherwise, he or she wouldn't have made it through high school algebra, where one learns to 'simplify' expressions like $x(y + x) + x^2(y + 1 + x) + 3(x + 3)$. But is there an accepted rigorous 'mathematical' definition of 'simplify' not just for algebraic expressions but for general expressions, which could involve anything, like transcendental functions or recursive functions? If not, then why? I would think that computer algebra uses this idea."

The answers there indicated that even though every mathematician knows intuitively what "simplify" means, there is still no universally accepted definition of "simplify". In fact, one of the answers (by Henry Cohn) indicated that "In full generality, there provably isn't any method for complete simplification". (He was referring to elementary functions of a real variable.) In this paper, we shall give a simple and plausible definition of "simplify" in terms of the computational complexity of integer functions. We shall also use this definition to show that there is no deterministic and exact algorithm which can compute the permanent of an $n \times n$ matrix in $o(2^n)$ time.

2 A definition of "simplify"

Consider the following definition of "simplify":

Definition: An algebraic expression (recursive or non-recursive) for a function $f : \mathbb{Z} \to \mathbb{Z}$ *cannot be simplified* if there is no other algebraic expression for f which can be computed faster.

For example, the expression $xw+yz+xz+yw$ can be simplified to $(x + y)(w + z)$, since computing $(x + y)(w + z)$ takes only one multiplication and two additions, while computing $xw + yz + xz + yw$ takes four multiplications and three additions. And we can also see clearly that the expression $(x + y)(w + z)$ cannot be simplified.

As another example, let $f : \mathbb{Z} \to \mathbb{Z}$ be the function which satisfies the recursive formula, $f(n) = f(n-1) + 1$ and $f(0) = 0$. This recursive formula can be simplified to $f(n) = n$, since computing the recursive formula for f takes $\Theta(n)$ time, while computing the formula $f(n) = n$ is trivial. And the formula $f(n) = n$ clearly cannot be simplified.

And let $f : \mathbb{N} \to \mathbb{N}$ be the function which satisfies the recursive formula, $f(n) = f(n-1) + f(n-2)$ and $f(1) = f(2) = 1$, the Fibonacci sequence. This recursive formula can be simplified, since it is possible to prove that $f(n)$ equals $\phi^n/\sqrt{5}$ rounded to the nearest integer, where $\phi = (1 + \sqrt{5})/2$, which can be computed exponentially faster than the recursive formula can be computed [4].

3 Computing the permanent of a matrix

Let $A = (a_{ij})$ be a matrix of integers. The permanent of A is defined as:

$$\mathrm{perm}(A) = \sum_{\sigma \in S_n} \prod_{i=1}^{n} a_{i\sigma(i)},$$

where S_n is the symmetric group [5]. The fastest known deterministic and exact algorithm which computes the permanent of a matrix was first published in 1963 and has a running-time of $\Theta^*(2^n)$ [3]. It is still considered an open problem by the mathematics and computer science community whether this time can be beaten. Now consider the following theorem and proof, which we shall discuss afterwards:

Theorem: There is no deterministic and exact algorithm which can compute the permanent of an $n \times n$ matrix in $o(2^n)$ time.

Proof: For any row i, the permanent of matrix A satisfies the recursive formula

$$\mathrm{perm}(A) = \sum_{j=1}^{n} a_{ij} \cdot \mathrm{perm}(A_{ij}^{\#})$$

and $\text{perm}([a_{11}]) = a_{11}$, where $A^{\#}_{ij}$ is the $(n-1)\times(n-1)$ matrix that results from removing the i-th row and the j-th column from A. This formula cannot be simplified, so the fastest algorithm for computing the permanent of a matrix is to apply this recursive formula to matrix A. Since this involves recursively evaluating the permanent of $\Theta(2^n)$ submatrices of A, each corresponding to a subset of the n columns of A, we obtain a lower bound of $\Theta(2^n)$ for the worst-case running-time of any deterministic and exact algorithm that computes the permanent of a matrix. □

At first, this proof makes sense intuitively, but if one thinks about it a little more, one might become skeptical, since one could argue the same for the determinant of a matrix, that there is no deterministic and exact algorithm which can compute the determinant of an $n \times n$ matrix in $o(2^n)$ time (which is known to be false) - for any row i, the determinant satisfies the recursive formula

$$\det(A) = \sum_{j=1}^{n} (-1)^{i+j} a_{ij} \cdot \det(A^{\#}_{ij})$$

and $\det([a_{11}]) = a_{11}$, which is almost the same as the recursive formula for the permanent of a matrix.

However, there is a big difference between the two recursive formulas: There are negative signs in the formula for the determinant, so it is not inconceivable that one might be able to cancel most of its terms out, if one is clever. And in fact this is the reason why it is possible to compute the determinant of a matrix in polynomial-time: If one performs elementary row operations on matrix A with pivot $a_{11} \neq 0$, converting it to a matrix B with zeroes in the last $n-1$ entries of column 1, then the determinant of A will equal the determinant of B and we will also obtain a simpler formula for the determinant:

$$\det(A) = a_{11} \cdot \det(B^{\#}_{11}).$$

This trick ultimately leads to a polynomial-time algorithm for computing the determinant of a matrix, if one applies it recursively to the matrix $B^{\#}_{11}$, exchanging rows when necessary.

However, in the case of the permanent of a matrix, no trick like this is possible, since there are only positive signs in its formula. To gain some insight as to why this is so, consider the following analogy: Suppose we want to subtract two large positive numbers with a tiny difference, say $a = 12,345,678,907$ and $b = 12,345,678,903$. One could compute a minus b by applying the normal subtraction procedure that one learns in elementary school to each digit of these two numbers, but one does not have to do this; if we let $c = 12,345,678,900$, then we will obtain the same answer by computing $(a - c)$ minus $(b - c)$, which amounts to subtracting only the last digits of each number, 7 minus 3. But there are no short-cuts like this for adding a and b, since none of their digits can be cancelled out. And for this same reason, it is possible to cancel out lots of terms in the formula for the determinant but not in the formula for the permanent, as the elementary row operations which are performed on matrix A when computing its determinant via the algorithm described above are analogous to subtracting c from both a and b.

But then one might ask, "The proof above said 'This formula cannot be simplified'. But how can I be sure of this?" The answer to this question is that we know that the above recursive formula for the permanent cannot be simplified, because we have tried every possible way to simplify it and saw that each way fails: To be specific, we tried to multiply the factors, a_{ij} and $\text{perm}(A^{\#}_{ij})$, of the summands together, but we failed since the two factors are completely independent from one another. And we tried adding the summands together, but we also failed since the factors a_{ij} found in each summand are completely independent from one another and are also completely independent from each $\text{perm}(A^{\#}_{ij})$; furthermore, we found that since $\text{perm}(A^{\#}_{ij})$ is different in each term, it is impossible to use the distributive law to decrease the computational complexity of the recursive expression. And finally, we noticed that the row choice of i is irrelevant in the recursive formula for the permanent, so no choice of i is better than any other choice. What other things are there to try that could possibly make the expression simpler? Nothing, since we have already considered every mathematical operation in the recursive formula for the permanent. Therefore, the recursive formula for the permanent cannot be simplified, i.e., it has the best computational complexity of any algebraic expression for the permanent of a matrix.

This type of reasoning is not new or foreign; it is essentially the same type of reasoning that a high school math student uses to simplify algebraic expressions. Also note that only if one is careful in one's analysis and considers every possible way to simplify an algebraic expression can one prove that an algebraic expression indeed cannot be simplified; merely claiming that an algebraic expression cannot be simplified does not make it so. But sometimes it is so obvious that an algebraic expression cannot be simplified that writing down a full explanation of this is unnecessary. Also, it turns out that one can use similar reasoning to prove that there is no deterministic and exact algorithm which solves the Traveling Salesman Problem in polynomial-time [2].

4 Conclusion

While everyone in the mathematics community understands intuitively what "simplify" in mathematics means, there is still no universal definition of "simplify". In this paper, we have defined "simplify" in terms of the computational complexity of an integer function and have shown that this definition can be used to prove that there is no deterministic and exact algorithm which can compute the permanent of an $n \times n$ matrix in $o(2^n)$ time.

Submitted on May 11, 2019

References

1. Feinstein C.A. Is there a 'mathematical' definition of 'simplify'? https://mathoverflow.net/q/126519/7089
2. Feinstein C.A. The Computational Complexity of the Traveling Salesman Problem. *Global Journal of Computer Science and Technology*, 2011, v. 11, Issue 23, 1–2. https://arxiv.org/abs/cs/0611082
3. Ryser H.J. Combinatorial Mathematics. Carus Math. Monograph No. 14, 1963.
4. Fibonacci Number. *MathWorld — A Wolfram Web Resource.* http://mathworld.wolfram.com/FibonacciNumber.html
5. Permanent. *MathWorld — A Wolfram Web Resource.* http://mathworld.wolfram.com/Permanent.html

Science's Dilemma – a Review on Science with Applications

Linfan Mao

Chinese Academy of Mathematics and System Science, Beijing 100190, P.R. China
Academy of Mathematical Combinatorics & Applications(AMCA), Colorado, USA
E-mail: maolinfan@163.com

Actually, different views result in different models on things in the universe. We usually view a microcosmic object to be a geometrical point and get into the macrocosmic for finding the truth locally which results in a topological skeleton or a complex network. Thus, all the known is local by ourselves but we always apply a local knowledge on the global. *Whether a local knowledge can applies to things without boundary*? The answer is negative because we can not get the global conclusion only by a local knowledge in logic. Such a fact also implies that our knowledge on a thing maybe only true locally. *Could we hold on the reality of all things in the universe globally*? The answer is uncertain for the limitation or local understanding of humans on things in the universe, which naturally causes the science's dilemma: it gives the knowledge on things in the universe but locally or partially. Then, *how can we globally hold on the reality of things in the universe? And what is the right way for applying scientific conclusions, i.e., technology*? Clearly, different answers on these questions lead to different sciences with applications, maybe improper to the universe. However, if we all conform to a criterion, i.e., the coexistence of human beings with that of the nature, we will consciously review science with that of applications and get a right orientation on science's development.

1 Introduction

As is known to all that being is nature. Science discovers rulers on things existed in the universe with observable physical evidence. It is a systematic knowledge on the universe in the view of human beings. However, it enables human beings coexistence with the universe thousand million years. Today, it is the time to review science's function on reality of things in the universe with speculation on questions for science. For example, *does the science hold with the universe globally, or only partially*? And *what is the right application of science*? All the answers will push forward science, and establish a right view on its applications.

2 Nature's laws

Science is established on an assumption that "*the universe is operating in order*" which implies the existence of natural laws, i.e., the inherent law on the existence and motion of things in the universe but independent on humans. This assumption is general accepted by scientific community or human beings without questions. Now, a more basic but philosophical question in front of humans is that *could we really holds on natural laws without artificial conditions*? And furthermore, *is human's ability with or without boundaries*? Although there exist certain differences in the eastern and western cultures but the answer is the same, i.e., we can only stand in awe of and never destroy the nature, such as the *Platonism* in Plato's Dialogues: "*the universals exist independently of particulars*", and the *Tao* and *Name* in Tao Te Ching: "*the Tao experienced is not the eternal Tao, the Name named is not the eternal Name; the unnamable is the eternally real and naming is the origin of all particular things*". All of these views conclude that the known natural laws are understood by human beings ourself. They are only laws in our eyes, maybe not the really natural laws.

How do we understand the reality or establish the knowledge on a thing T in the universe? We assume there is an abstract T defined by a conception, i.e., *name* distinguished from other things and usually identified T with known characters, gradually little by little and from time to time. For example, let $\mu_1, \mu_2, \cdots, \mu_n$ be the known on T and $\nu_i, i \geq 1$ unknown characters at a time t. Then, T is understood by [1]

$$T = \left(\bigcup_{i=1}^{n}\{\mu_i\}\right)\bigcup\left(\bigcup_{k\geq 1}\{\nu_k\}\right), \tag{1}$$

a *Smarandache multispace* [2] or *parallel universe* [3] in logic at the time t on its connotation and extension, which also reveals the diversity or complexity on the reality of things T. Then, *what is thing T and what is its reality*? Philosophically, the reality of a thing T is nothing else but the state characters (1) of existed, existing or will existing things whether they can be or not observable or comprehensible by human beings at time t. Thus, we can only hold on T by its an asymptotic $T^\circ = \bigcup_{i=1}^{n}\{\mu_i\}$ at time t, and deeply convince that $T^\circ \to T$ if the time $t \to \infty$. This is the essential notion that natural laws can be understood, i.e., establishing science of humans.

3 Science's limitation

As humans enter the 21st century, science has made great achievements both in theory and its applications. It greatly improved the ability to respond of natural disasters, brings more and more conveniences to human life. In fact, science

is the systematic knowledge with continuously improvement on asymptotically natural laws dependent on observation and speculation of ourself, maybe with the aid of instruments. Certainly, different standings for the observer will result in different observations, i.e., the macrocosmic or the microcosmic which result in different speculating models.

3.1 Macrocosmic object

A macrocosmic object is large enough to be visible by the naked eyes of humans. For knowing the behavior of macrocosmic objects, the observer only needs to stand out of the observing object, holds on the overall situation, i.e., its outside behavior, particularly, planetary motion which establishes classical mechanics. It should be noted that the thinking pattern of classical mechanics is essentially

$$\begin{array}{lll} \text{Macrocosmic Object} & \overset{Abstract}{\longrightarrow} & \text{Particle} \\ & \overset{Abstract}{\longrightarrow} & \text{Geometrical Point} \end{array}$$

with 2 assumptions, i.e., ① there exists an abstract geometrical space $\mathbb{R}^3\times\mathbb{R}$ in the universe, and ②, all physical quantities can be accurately measured by humans.

As is known to all, the classical mechanics is applying only to those of objects A moving at low speeds, characterizing an object of quality m by a pair $\{\mathbf{x}, \mathbf{v}\}$, where $\mathbf{x}$ is the coordinates of A with a directed velocity $\mathbf{v}$ at points $\mathbf{x}$. For example, if A moves in a conservative field with potential energy $U(\mathbf{x})$, then the force acting on A is $\mathbf{F} = -\frac{\partial U}{\partial \mathbf{x}} = m\ddot{\mathbf{x}}$ by the second law of Newton, and generally, the Euler-Lagrange equations [4]

$$\frac{\partial L}{\partial x_i} - \frac{d}{dt}\frac{\partial L}{\partial \dot{x}_i} = 0, \quad 1 \le i \le n \tag{2}$$

in $\mathbb{R}^n$ for the Lagrangian $L = T - U$ of A, where $T(\mathbf{x})$ is the moving energy of A.

Although it is on macrocosmic objects, the classical mechanics found the intrinsic essence of motion, i.e., force. For example, Newton realized the gravity by an apple fell on his head from a tree and proposed the law of universal gravity $F = G\frac{M_1M_2}{R^2}$ between 2 bodies with masses M_1 and M_2 respectively, where R is the distance of the 2 bodies and G the constant of universal gravity. Although Newton's law is an approximation of gravity, it is useful in aerospace engineering. By this law, we have known the cosmic speeds surround the earth, escaped from the earth or the solar system are respectively 7.9 km/s, 11.2 km/s and 16.7 km/s which enables launching satellites for space exploration and communication of humans.

By the general relativity, i.e. *all the laws of physics take the same form in any coordinate system* and the equivalence principle, i.e., *there are no difference for physical effects of the inertial force and the gravitation in a field small enough*, Einstein presented the gravitational equations

$$R_{\mu\nu} - \frac{1}{2}\,g_{\mu\nu}R = \kappa T_{\mu\nu}, \tag{3}$$

where, $T_{\mu\nu}$ is the energy-momentum tensor, $R_{\mu\nu} = R^{\alpha}_{\mu\alpha\nu} = g^{\alpha\beta}R_{\alpha\mu\beta\nu}$, $R = g^{\mu\nu}R_{\mu\nu}$ are respectively the *Ricci tensor*, *Ricci scalar curvature* and $\kappa = \frac{8\pi G}{c^4} = 2.08\times10^{-48}\ \mathrm{cm^{-1}\ g^{-1}\ s^2}$.

Clearly, an immediate application of Einstein's gravitational equations is on the spacetime structure of the universe. For example, if it is in vacuum, i.e., $T_{\mu\nu} = 0$, the Einstein gravitational equations were solved due to the assumption of spherically symmetric distribution of matters and get the Schwarzschild metric $d^2s = g_{\mu\nu}dx^{\mu\nu}$ by

$$ds^2 = -c^2dt^2 + a^2(t)\left[\frac{dr^2}{1-Kr^2} + r^2\left(d\theta^2 + \sin^2\theta d\varphi^2\right)\right] \tag{4}$$

with $g_{tt} = 1$, $g_{rr} = -\frac{R^2(t)}{1-Kr^2}$, $g_{\phi\phi} = -r^2R^2(t)\sin^2\theta$, which also predicts the existence of black hole in the universe. Combining the cosmological hypothesis, i.e., *there are no difference at different points and different orientations at a point of the universe on the metric* 10^4 *l.y.*, Friedmann presented the *Standard Model on Universe* which resulted in the *Big Bang theory* in thirties of the 20th century and the scenario of the universe, i.e., it has a beginning.

Certainly, classical mechanics successfully explains a few astronomical phenomena, particularly, the planetary motion laws in front of humans thousands years. However, it is only an interpreting on the extrinsic behaviors but difficult on the internal cause, the basis for the change of objects. Today, we have known there is an additional assumption on a moving object in classical mechanics, i.e., all parts of the object are moving in coherence or synchronization. It is this assumption that can not enables humans globally understanding the nature of objects because the non-coherence, i.e., contradiction is the general but the coherence is the special, and all of us know that it is the contradiction or non-coherence pushes forward the change of things. Thus, holding on the nature of an object enables human's observation entering the microcosmic world with the aid of instruments and exploring microcosmic behavior of objects, i.e., microcosmic particles.

3.2 Microcosmic particle

A matter can be always divided into submatters, then subsubmatters and so on. A natural question on this subdividing is *whether or not it has a terminal point*? The answers are the same both for the Easterners and Westerners. For example, the ancient Chinese had a notion that *everything is composed by five elements, i.e., metal, wood, water, fire and soil* and also, the notion that *everything is composed entirely of various imperishable, indivisible elements*, i.e., there exist atoms in Atomism of Leucippus and Democritus, which finally results in the structure theory on matters. Today, it is already

a public knowledge that all matters are made up of atoms, i.e., microcosmic particles composed of nucleus with electrons. There are 118 atoms known by humans which consist of known matters on the earth. Generally, we understand a matter by the composite of elementary particles with a thinking pattern following

$$\text{Matter} \xrightarrow{Decompose} \text{Microcosmic Particles} \xrightarrow{Abstract} \text{Complex Network}$$

where the complex network is an inherit structure of the matter on microcosmic particles and different subjects discuss microcosmic behaviors of particles.

3.2.1 Physics

Clearly, the subdividing on a matter can be done infinite times just like the claim that "*it will be never exhausted if you cut half on a stick each day*" on World Chapter of Zhuang Zi in the ancient China. However, this process can not be applied to hold on matters because the life time of a human is not infinite. The motivation of particle physics is to determine the nature of irreducibly smallest detectable particles [5], called *elementary particles* such as those of *fundamental fermions* including quarks, antiquarks, leptons, antileptons and *fundamental bosons* including gauge bosons, Higgs boson and the *fundamental interactions* for explaining their behavior and then, the origin of the universe. Certainly, there are also unmatters between a matter and its antimatter which is partially consisted of matter but others antimatter [6]. However, the behavior of a microcosmic particle maybe indefinite. It is this character that results in humans characterizing microcosmic particles by wave function, a complex-valued probability amplitude.

In the non-relativistic quantum mechanics, we know that the wave function $\psi(t, x)$ of a particle of mass m obeys the Schrödinger equation

$$i\hbar\frac{\partial\psi}{\partial t} = -\frac{\hbar^2}{2m}\nabla^2\psi + U \tag{5}$$

with the Planck constant $\hbar = 6.582 \times 10^{-22}$ MeVs and the potential energy U of field which characterizes the behavior of microcosmic particles.

Certainly, physics has promoted the progress of human society with the deeply understanding of matters from the macrocosmic to the microcosmic such as those of the applications of steam engine, the electricity with radio communication, nuclear energy, laser, electronic computer technology and so on. We seriously conclude that if there were no the development of physics, there would be no other sciences and no modern life of humans.

3.2.2 Chemistry

According to the notion that chemical compounds are not a random but rather definite one of atoms, the chemistry determines the composition, structures and properties of matters, particularly on atomic and molecular systems for the pattern and multiplicity of bonding between atoms in a molecule for explaining chemical reactions of matters. Although physics and chemistry are both on the structure of matters, the chemistry discusses the coarse-graining particles, i.e., atoms and molecules with chemical dynamics on rates of chemical reactions, but not on the fermions, bosons and their interactions.

Chemistry is beneficial for humans with a core topic, i.e., *how to create new matters to meet the needs of our daily life* in its developing. If there were no chemistry there would be no modern life of humans. For example, the chemical fertilizer increases the production of crops for maintaining the survival of population, the chemical pesticides kill insects harmful to crop growth, the medicines heals the sick with life extended, the plastics and synthetic fibers are used both in industrial and consumer products such as those of keyboard, mouse, plastic cup, slippers in our daily life, machinery, electronic appliances, automobile products, and furthermore, the dynamite, bombs and missile in military. None of them is not the application of chemistry.

3.2.3 Biology

Historically, biology is the oldest subject with the development of science in natural philosophy because humans ourself is also one specie of livings on the earth. Observation enables humans held on the elementary rotate regulation of plants on seasons, i.e., *spring germination with harvest or leaves fallen in autumn* and the reproduction regulation of humans and other animals such as "*pregnancy* 10 *months with childbirth in a day*" of humans, enables humans living together with the nature in about 5 million years. Certainly, the birth and the death are the two sides but all of us wish to hold on the laws of livings with production, the central issues of biology.

According to the notion that the basic unit of life is cell, the basic unit of heredity is genes and all life on the earth changes and develops through evolution, biology is such a science that on the life and living organisms respectively at molecular, cell, genes and heredity with variation levels and the process of grow and developing. Certainly, all major issues in the developing of humans society such as those of population growth, food safety, health, environmental pollution and resource depletion have a closely relationship with the life sciences. The project on human genome puts into effect with development will enables humans understanding the mechanism of growth, development, physiological activities and pathogenesis of diseases, which provides methods of prevention and control strategies on diseases of human bod-

ies, particularly, the gene and cell engineering. For examples, the transgentic technology can improves the crops resistance to insects for solving the pesticide residue problem and improving the quality of agricultural products; the antigen gene can applicable to the production of edible crop vaccine; the animal organs can be transplanted into a human body to play the role of such human organs, the cloning technology can detectable the fetal genetic defects, treats the injury of nervous system, achieves the asexual reproduction and saves the endangered species; the gene editing can correctable the defective gene for the treatment; the gene engineering can applicable to the environmental governance for recycling the pesticides and industrial wastes, and the large-scale animal cell culture can produces vaccines, breeds good varieties, detects the difference between virus strains and identifies the bacterial species for disease treatment, . . . , etc.

3.3 Science's limitation

However, all scientific conclusions of humans hold on conditions. *Is there such a scientific conclusion constraint without conditions*? The answer is negative both in theoretical and experimental sciences because of the boundary of humans. For example, all theorems are true with an obvious or implication that "*if p then q*" in mathematics. Even if the elementary conclusions $1 + 1 = 2, 1 \times 2 = 2$ known by pupils is such one only because they are implicit, i.e., "*if* $1, 2 \in (\mathbb{Z}; +, \times)$ *then* $1 + 1 = 2$ *and* $1 \times 2 = 2$", where $(\mathbb{Z}; +, \times)$ is the integer ring.

Similarly, we have known that sciences such as those of physics, chemistry, biology on a matter T by the macrocosmic are on its external behaviors with an additional assumption that all of its microcosmic particles are synchronous because it is abstracted to be a point with relatively external motion in space. We conclude that force is the internal factor of motion, creates new matters by chemistry and apply bionics to enrich human's living by simulating other creatures to conform the nature.

All of us known that the external causes operates through internal factor but a scientific conclusion on a matter T by the microcosmic is only partial or local nature because T is a complex system or a complex network in the thinking pattern. Until today, we lack of effective methods, even lack of such a mathematics on complex network or complex system which can not enables us hold on the whole matter T in theory unless all its microcosmic particle are in synchronization. So, we have only an incomplete or non-comprehensive science for things in the universe which is the limitation of human's science, an immediately conclusion of formula (1), i.e., the boundary of humans. In this case, we can hardly conclude that a scientific conclusion is true in the whole universe because it is understanding only by humans ourself, an intelligent creature happily born on the earth and it is a conclusion on known or unknown conditions.

4 Science's dilemma

4.1 Reality

Science's function is to understand the reality of things T, i.e., their state of existed, exists or will exist in the universe, whether or not they are observable or comprehensible by humans. However, this is difficult from the limitation of science because all scientific conclusions of humans are true constraint with conditions. They are locally or partially true, not freely with conditions or on the whole universe because we hold it little by little with an asymptotic T° of T, not T itself at a time t by formula (1). Usually, the physical laws are characterized by differential equations. Even for physical reality with differential equations, there are also 3 simple but basic questions should be answered.

Question I *Could a special solutions be applied to the whole universe*?

The answer of Question I is obviously negative unless the equations have a unique solution but there are not this case in most cases. For example, Schwarzschild spacetime (4) is a special solution of the Einstein's gravitational equations (3) in an assumption that all matters are spherically symmetric distributed in the universe with $T_{\mu\nu} = 0$ or vacuum. It is this kind of spacetimes that the standard model, the Big Bang hypothesis and black holes born on the universe. We are applying a special solution for characterizing the universe and believe it without a shadow of doubt in any place of the universe. However, there are infinite many solutions of Einstein's gravitational equations [7, 8]. But why the Schwarzschild spacetime was selected only for the universe because we are all fond of the symmetry and the uniformity on space, and we are firmly believing the spacetime structure of the universe should be so by observed datum of humans, at least in the nearby airspace of the earth.

Question II *Are the reality of things T really one of solutions of its equations*?

Science is established on an assumption that the reality or all behavior of a thing T can be characterized by mathematics, particularly, the second order differential equations in physics. However, the observation shows that a microcosmic particle is in two or more possible states of being, i.e., superposition such as the asking question of Schrödinger for the alive or dead of the cat in a box with poison switch. We can not even say which solution of Schrödinger equation (5) is the behavior of the particle because each solution is only one determined state in the eyes of humans.

Certainly, a reasonable or the multiverse interpretation on superposition of particles was presented by H. Everett in 1957. He explained the superposition of particles with an assumption that the wave function of an observer would be interacted with a superposed object [9] and concluded that different worlds in different quantum system obey equation (5) with an interpretation that the superposition of a particle

develops like a 2-branching universe. Thus, the answer of Question II is uncertain even if T is a microcosmic particle.

Today, it is just the Everett's multiverse interpretation on Schrödinger's cat enlightens humans known that the alive or dead of the cat is entangled and we can not say the cat is alive or dead separately. Philosophically, the Everett's multiverse notion on the superposition of particles is alluded in a famous fable, i.e., *the blind men with an elephant* or the formula (1). Today, this notion revolutionized changes an ambiguous interpretation that the reality of a thing T must be one but maybe all solutions of its differential equations and applies extensively to modern sciences. For example, it is the quark model that successfully classified all known elementary particles by mathematical symmetry but the quark model is indeed a multiverse and generally, all particles are nothing else but a multiverses [3] or complex networks in the microcosmic view.

Question III *Could the mathematics already characterizes the reality of things T?*

There is an exciting convincingness that mathematics can already characterizes the reality of all things, i.e., *Everything is Nothing Else but Mathematics* popularly in scientific community today, particularly, the *Mathematical Universe Hypothesis* in physics, a duplication of Pythagorean's assertion that "*Everything is a Number*". However, this notion is incorrect at least for today's mathematics because all mathematical systems should be homogenous without contradictions in logic. We can not conclude the equality

$$\text{Mathematical reality} \overset{\text{equal to}}{\longleftrightarrow} \text{Reality of things}$$

both in theory and practice. For instance, let H_1, H_2, H_3, H_4 and H_1', H_2', H_3', H_4' be two groups of horses constraint with running on respectively 4 straight lines

$$\textcircled{1}\begin{cases} x+y = 2 \\ x+y = -2 \\ x-y = -2 \\ x-y = 2 \end{cases} \quad \text{or} \quad \textcircled{2}\begin{cases} x = y \\ x+y = 4 \\ x = 2 \\ y = 2 \end{cases}$$

on the Euclidean plane $\mathbb{R}^2$. Clearly, the first system is non-solvable because $x+y=-2$ is contradictious to $x+y=2$, and so that for equations $x-y=-2$ and $x-y=2$ but the second system is solvable with $(x,y)=(2,2)$. *Could we conclude that the behavior of horses H_1', H_2', H_3', H_4' are a point $(2,2)$ and H_1, H_2, H_3, H_4 are nothing*? The answer is certainly not because all of the horses are running on the Euclidean plane $\mathbb{R}^2$ but we have known nothing by the solution of the two equation systems because the solvability of systems ① and ② only implies the orbits intersection in $\mathbb{R}^2$.

Why is this happening? It is because that while humans characterize a thing T in the universe by mathematics, it is usually complied with the compatible assumption of mathematics on T and often forgotten the original intention, i.e., hold on the reality of things T but have too much trust on the mathematical solution. Consequently, mathematics should be extended to include the non-mathematics for reality of things in the universe [1] because the contradictions exist everywhere in the eyes of humans. We can not conclude yet that mathematics can characterizes the reality of all things T in the universe until today.

4.2 Science's dilemma

Science's limitation naturally leads to a dilemma of science immediately. It gives the knowledge for humans but the knowledge is local or partial on things in the universe which always shows dual characters to humans, i.e., the beneficial or the harmful. However, it is easy to overstate the benefits but look without sees harms on a scientific achievement in a business community today. In this case, it is easy to breed the human's insatiable desires with immoderately abusing scientific achievements, and then brings a disaster finally to humans ourselves if it applies without constraints, particularly motivated only by the benefits of commercial interests. All of the harms come from the misunderstanding on science and incorrect applications of scientific achievements such as those cases following.

Physics has promoted the progress of humans but it also brought harmful things to human's living environment. For example, it pushes forward the aerospace industry which enables the exploration of humans on outer space. However, more and more satellites, space stations, probes, rocket debris and explosive fragments, working or abandoned are floating in space, disturbing the normally working of universe and also threatening the further exploration of humans because the aerocraft maybe collided with such an indefinable trashes in the space. Even in the daily life of humans we can also find the harms of applying physics. For example, the communicant equipments and facilities such as those of mobile phone, radio, TV station, microwave station bring convenience to humans but the radiate electromagnetic signals into space from time to time. However, it impacts on the health of humans, tested by the practice.

Chemistry has created new matters to meet the needs of humans but it caused complex problems simultaneously with its benefits to humans, for instance the environmental pollution, the resource depletion, the side effects of drugs, the pesticide residues and the lethal diseases such as cancer prevalence. Why these unpleasant things happen is because we have only a superficial understanding the fate, transport, toxicity on chemical products and without a comprehensive conclusion for their impacts on the environment and humans. For example, the plastics enables us protecting from wet but can not be degraded shortly by the nature, and we do not know the mechanism of accumulation of the pesticides in the food chain with impact on humans [10] until today.

Biology has brought benefits to humans but it presented

negative effects also to humans at the same time. For examples, the transgentic technology improved the resistance of crops but destroys those insects that feed on these pests which breaks the ecological chain, results in the structural change and deterioration of soil and the water pollution; the eating transgentic food maybe caused the modified gene invades human cells, produces pathogenic virus and harmful or lethal results including cancer and other negative effects; the cloning technology impacts on the nature and the social morality. Although the gene editing corrected or removed defect genes but will affects the normal functions of other cells at the same time, and while it reducing the genetic variation it maybe destroys a species just because of one disease, i.e., it increases the risk of infectious diseases and hypoimmunity or loss of other functions.

4.3 Out of dilemma

There are 2 sides for getting out of science's dilemma. One is the establishing of science in microcosmic level, i.e., *Microcosmic Science* for a complete understanding of things in the universe and two, is the self-awareness of human's ourself, the essence for out of the crisis.

4.3.1 Microcosmic science

As we know in the thinking pattern

$$\text{Matter} \overset{\overset{Decompose}{\longrightarrow}}{\underset{Abstract}{\longrightarrow}} \begin{matrix}\text{Microcosmic Particles}\\ \text{Complex Network}\end{matrix}$$

the reality of a thing T is the behavior with motivation of an abstracted complex network in the microcosmic level. Certainly, there are more microcosmic observing datum on the units, cells or microcosmic particles of matters by scientific instruments. Each of them appears in a space position at observing time and all of them are interrelated, for instance all cells in an animal. A microcosmic science is such a science established on the microcosmic datum of matters, including theory and experimental subjects. It must be established over 1-dimensional skeleton, i.e., topological graphs $\overrightarrow{G}$. However, we have no effective tools or methods, even no mathematics for such a work. Even though there is graph theory in mathematics but it is essentially discussing on binary relationship of elements without metrics, can not be immediately applied to understand the reality of matters, particularly, the microcosmic science.

Could we establish such a mathematics over topological graphs for microcosmic science? The answer is positive inspired by traditional Chinese medicine. Certainly, there are 12 meridians which completely reflects the physical condition of human body in traditional Chinese medicine [11], i.e., the lung meridian of hand-TaiYin (LU), the large intestine meridian of hand YangMing (LI), the stomach meridian of foot-YangMing (ST), the spleen meridian of foot-TaiYin (SP), the heart meridian of hand-ShaoYin (HT), the small intestine meridian of hand-TaiYang (SI), the urinary blandder meridian of foot-TaiYang (BL), the kidney meridian of foot-ShaoYin (KI), the pericardium meridian of hand-JueYin (PC), the sanjiao meridian of hand-ShaoYang (SJ), the gall bladder meridian of foot-ShaoYang (GB), the liver meridian of foot-JueYin (LR) in *Standard China National Standard* (GB 12346-90).

Notice that maintaining the balance of Yin (Y^-) with that of Yang (Y^+) is the foundation of Chinese culture, particularly on a healthy human body. According to the view of traditional Chinese medicine, if there exists an imbalanced acupoint on one of the 12 meridians this person must has illness and in turn, there must be imbalance acupoints on the 12 meridians for a patient. Thus, finding out which acupoint on which meridian is imbalance with Y^- more than Y^+ or Y^+ more than Y^- is the main duty of a Chinese doctor. Then, by the natural ruler, i.e., *reducing the excess with supply the insufficient* of the universe, the doctor regulates the meridian by acupuncture or drugs so that the patient recovers balance on the imbalance acupoint [11], which is the essential treatment of traditional Chinese medicine.

Although a matter can be infinitely subdivided into submatters, the success of traditional Chinese medicine implies that there exists an inherited a topological skeleton or graph G in things, particularly, human body in the universe. By view of biology, there are only 2 kinds of things, i.e., living or death body which suggest 2 mathematical elements holding with conservation laws for things in the universe in the microcosmic level following:

Element 1 (Non-Living Body). A *continuity flow* $\overrightarrow{G}^L$ is an oriented embedded graph $\overrightarrow{G}$ in a topological space $\mathcal{S}$ associated with a mapping $L : v \to L(v)$, $(v,u) \to L(v,u)$, 2 end-operators $A^+_{vu} : L(v,u) \to L^{A^+_{vu}}(v,u)$ and $A^+_{uv} : L(u,v) \to L^{A^+_{uv}}(u,v)$ on a Banach space $\mathfrak{B}$ over a field $\mathfrak{F}$ with $L(v,u) = -L(u,v)$, $A^+_{vu}(-L(v,u)) = -L^{A^+_{vu}}(v,u)$ for $\forall (v,u) \in E\left(\overrightarrow{G}\right)$ and holding with continuity equation

$$\sum_{u\in N_G(v)} L^{A^+_{vu}}(v,u) = L(v) \ \text{ for } \ \forall v \in V\left(\overrightarrow{G}\right).$$

Element 2 (Living Body). A *harmonic flow* $\overrightarrow{G}^L$ is an oriented embedded graph $\overrightarrow{G}$ in a topological space $\mathcal{S}$ associated with a mapping $L : v \to L(v) - iL(v)$ for $v \in E\left(\overrightarrow{G}\right)$ and $L : (v,u) \to L(v,u) - iL(v,u)$, 2 end-operators $A^+_{vu} : L(v,u) - iL(v,u) \to L^{A^+_{vu}}(v,u) - iL^{A^+_{vu}}(v,u)$ and $A^+_{uv} : L(v,u) - iL(v,u) \to L^{A^+_{uv}}(v,u) - iL^{A^+_{uv}}(v,u)$ on a Banach space $\mathfrak{B}$ over a field $\mathfrak{F}$, where $i^2 = -1$, $L(v,u) = -L(u,v)$ for $\forall (v,u) \in E\left(\overrightarrow{G}\right)$ and

holding with continuity equation

$$\sum_{u\in N_G(v)}\left(L^{A^+_{vu}}(v,u)-iL^{A^+_{vu}}(v,u)\right)=L(v)-iL(v)$$

for $\forall v\in V\left(\overrightarrow{G}\right)$.

Notice that if we let the Banach space to be $\mathfrak{B}\times\mathfrak{B}$ then the Element 2 is only a special Element 1 with complex vector. However, it reflects living bodies with respective real, imaginary parts $L(v,u)$, $-L(v,u)$ appearing in pair. If one lost then the counterpart is no longer exists, i.e., it is depth. This notion can be also used to explain the entangled state, i.e., the alive or dead of Schrödinger's cat in the box by a complex state $A-iA$ in such a way that alive for an $A\neq\mathbf{0}$ but dead if $A=\mathbf{0}$.

According to the structure of the 12 meridians on human body, we can classify them into 3 classes, i.e., *paths*: LU, LI, SP, HT, SI, KI, PC, LR; *trees*: GB, ST, SJ and a circuit attached with 2 pathes P_{m_1}, P_{m_2}: BL. Define an oriented graph

$$\begin{aligned}\overrightarrow{G} \;=\;& P_{11}(LU)\bigcup P_{20}(LI)\bigcup P_{21}(SP)\bigcup\\ & P_9(HT)\bigcup P_{19}(SI)\bigcup P_{27}(KI)\bigcup\\ & P_9(PC)\bigcup P_{14}(LR)\bigcup T_{44}(GB)\bigcup\\ & T_{45}(ST)\bigcup T_{23}(SJ)\bigcup G_{67}(BL)\bigcup\\ & P_{28}(DU)\bigcup P_{24}(RN)\end{aligned}$$

with orientations:

chest→hand→head→foot→chest

in human body and $L:\ v\in V(\overrightarrow{G})\to L(v)-iL(v)$ and $L:\ (v,u)\in E(\overrightarrow{G})\to L(v,u)-iL(v,u)$, where DU and RN are respectively the DU and REN meridians on human body, $P_n(X), T_n(X)$ and $G_n(X)$ denote the path, tree or graph of meridian of order n. Then, $\overrightarrow{G}^L$ is nothing else but a harmonic flow equivalent to human body by the view of traditional Chinese medicine, a kind of Element 2 of order 361.

As shown in references [7, 8, 12, 13], the Elements 1 and 2 can be applied to characterize the behavior of things T in the universe with $\overrightarrow{G}^L$ a globally mathematical elements in the sense that if $\mathfrak{G}$ is a closed family of graphs under union operation, $\mathfrak{B}$ is a Banach or Hilbert space, then all Elements 1 or 2, i.e., $\overrightarrow{G}^L$ with $\overrightarrow{G}\in\mathfrak{G}$ respectively form a Banach or Hilbert flow space and closed under the action of differential and integral operators with a few generalized theorems in functionals. Particularly, they can be used to characterize the dynamic behavior of things T, living or non-living bodies in the universe by Euler-Lagrange equations

$$\frac{\partial\overrightarrow{G}^L}{\partial x_i}-\frac{d}{dt}\frac{\partial\overrightarrow{G}^L}{\partial\dot{x}_i}=\mathbf{O},\quad 1\leq i\leq n$$

where, $\overrightarrow{G}^L$ is the harmonic or continuity flow inherited in T, $L(v,u)$ is the Lagrangian on edge (v,u) and $\mathbf{O}$ is the zero-flow $\overrightarrow{G}^{\mathbf{0}}$, i.e., a labeling $\mathbf{0}:(v,u)\to\mathbf{0}$ for $(v,u)\in E\left(\overrightarrow{G}\right)$.

5 Human self-awareness

The original intention of science is to understand things in the universe, promote the survival and development of humans ourself and then, construct a harmonious system of humans with the nature. Historically, human's experience verified times that the more intruding with higher damage of humans on the nature, the more serious nature's punishments on humans society are. The leader is nothing else but humans ourself in the couple of humans and the nature. As discussed in the previous. Science has itself limitation and all of its achievements is only the local or the partial, and what humans gotten maybe always a local conclusion on the reality of things in the universe. For example, humans have not really understood the internal and external mechanism of planets, only hold on their's laws by observations. In this case, discussing the capture of asteroids for energy or human alien migration is not realistic, and the result in harming to the universe is immeasurable.

Hence, science needs returning to a rational research on the respecting with protecting of the nature, and abandons the idea that humans are the center and wish to govern the universe by a limited understanding. Furthermore, we are need also to distinguish a scientific research is for human survival with development or only serves to human's enjoying because the later is causing the loss of human's natural instincts sometimes. Science should returns to the theme of harmonious development of humans with the nature. While researching a scientific problem, it should takes more times on the maybe harming to humans and to the universe with extents for its application. In this case, *is to discuss the destruction of the earth then migrates to other planets or develops with the earth*? In addition, *is to research the destruction of our universe and then migrates to other universes*? The answer is obvious because we have only one earth and one universe on which we live. It can be only harmonious with but not destroying the earth or the universe if we would like to a sustainable developing. Even if it were necessary to exploit the resources of the earth or the universe, we should also be minimized the natural intrusion and maximized the use of natural resources constraint with a model of circular development.

We have faced survival problems such as those of population growth, food safety, health, environmental pollution and resource depletion today. However, the greatest crisis facing humans is not the poverty or unfair allocation of natural resources but the greed with ignorance, and hopefully to govern the universe by our own understanding or a realization dependent on local or partial perception of the nature, particularly, the abusing of scientific achievements such as those of the overdevelop or overuse of resources, vehicles, internet,

farm chemicals and biological products. The main step for out of the crisis needs the human self-awareness, i.e., abandoning their arrogance and developing harmoniously with the nature because we have only a local or partial understanding for reality of things in the universe. Even though we have established science on things T, it is only an understanding of humans ourself on the earth, maybe not the reality of things in the whole universe. Thus, the only viable way for human's continually generations is to develop with the nature.

Submitted on May 7, 2019

References

1. Mao L. Mathematics on non-mathematics - A combinatorial contribution. *International J. Math. Combin.*, 2014, v. 3, 1–34.
2. Smarandache F. *Paradoxist Geometry*, State Archives from Valcea, Rm. Valcea, Romania, 1969, and in *Paradoxist Mathematics*, Collected Papers (Vol. II), Kishinev University Press, Kishinev, 5–28, 1997.
3. Tegmark M. Parallel universes, in *Science and Ultimate Reality: From Quantum to Cosmos*, ed. by J.D. Barrow, P.C.W. Davies and C.L. Harper, Cambridge University Press, 2003.
4. Mao L. Combinatorial Geometry with Applications to Field Theory. The Education Publisher Inc., USA, 2011.
5. Nambu Y. Quarks: Frontiers in Elementary Particle Physics. World Scientific Publishing Co. Pte. Ltd, 1985.
6. Smarandache F. and Rabounski D. Unmatter entities inside nuclei, predicted by the Brightsen nucleon cluster model. *Progress in Physics*, 2006, no. 1, 14–18.
7. Mao L. Extended Banach $\overrightarrow{G}$-flow spaces on differential equations with applications, *Electronic J. Mathematical Analysis and Applications*, 2015, v. 3, no. 2, 59–91.
8. Mao L. A review on natural reality with physical equation. *Progress in Physics*, 2015, v. 11, 276–282.
9. Everett H. Relative state formulation of quantum mechanics. *Rev. Mod. Phys.*, 1957, v. 29, 454–462.
10. Committee on Mathematical Sciences Research for DOE's Computational Biology and National Research Council of the National Academies, *Mathematics and 21st Century Biology*, National Academy Press, USA, 2005.
11. Zhang Z. Comments on the Inner Canon of Emperor (Qing Dynasty, in Chinese), Northern Literature and Art Publishing House, 2007.
12. Mao L. Complex system with flows and synchronization. *Bull. Cal. Math. Soc.*, 2017, v. 109, no. 6, 461–484.
13. Mao L. Harmonic flow's dynamics on animals in microscopic level with balance recovery. *International J. Math. Combin.*, 2019, v. 1, 1–44.

The Origin of Inertial Mass in the Spacetime Continuum

Pierre A. Millette

E-mail: PierreAMillette@alumni.uottawa.ca, Ottawa, Canada

In this paper, we revisit the nature of inertial mass as provided by the Elastodynamics of the Spacetime Continuum (*STCED*). We note that, in addition to providing a physical explanation for inertial mass and for wave-particle duality, it answers unresolved questions pertaining to mass: It provides a direct physical definition of mass independent of the operational definition of mass currently used. It shows that, in general, a singular "point" particle is not physically valid and that particles need to be given a finite volume to avoid invalid results and give physically realistic ones. It confirms theoretically the equivalence of inertial and gravitational mass. It demonstrates that Mach's principle (or conjecture) is incorrect in that inertia originates from the massive dilatation associated with a spacetime deformation, not from interaction with the average mass of the universe. It shows that the electromagnetic field is transverse and massless, and that it contributes to the particle's total energy, but not to its inertial mass.

It must also be said that the origin of inertia is and remains ***the*** *most obscure subject in the theory of particles and fields. A. Pais, 1982 [1, p. 288]*

... the notion of mass, although fundamental to physics, is still shrouded in mystery. M. Jammer, 2000 [2, p. ix]

1 Introduction

In this paper, we revisit the nature of inertial mass as provided by the Elastodynamics of the Spacetime Continuum (*STCED*) [3, 4]. *STCED* is a natural extension of Einstein's General Theory of Relativity which blends continuum mechanical and general relativistic descriptions of the spacetime continuum. The introduction of strains in the spacetime continuum as a result of the energy-momentum stress tensor allows us to use, by analogy, results from continuum mechanics, in particular the stress-strain relation, to provide a better understanding of the general relativistic spacetime.

2 Elastodynamics of the Spacetime Continuum

The stress-strain relation for an isotropic and homogeneous spacetime continuum is given by [3, 4]

$$2\bar{\mu}_0\,\varepsilon^{\mu\nu} + \bar{\lambda}_0\,g^{\mu\nu}\varepsilon = T^{\mu\nu} \tag{1}$$

where $\bar{\lambda}_0$ and $\bar{\mu}_0$ are the Lamé elastic constants of the spacetime continuum: $\bar{\mu}_0$ is the shear modulus (the resistance of the spacetime continuum to *distortions*) and $\bar{\lambda}_0$ is expressed in terms of $\bar{\kappa}_0$, the bulk modulus (the resistance of the spacetime continuum to *dilatations*):

$$\bar{\lambda}_0 = \bar{\kappa}_0 - \bar{\mu}_0/2 \tag{2}$$

in a four-dimensional continuum. $T^{\mu\nu}$ is the general relativistic energy-momentum stress tensor, $\varepsilon^{\mu\nu}$ the spacetime continuum strain tensor resulting from the stresses, and

$$\varepsilon = \varepsilon^{\alpha}{}_{\alpha}\,, \tag{3}$$

the trace of the strain tensor obtained by contraction, is the volume dilatation ε defined as the change in volume per original volume [9, see pp. 149–152] and is an invariant of the strain tensor. It should be noted that the structure of (1) is similar to that of the field equations of general relativity,

$$R^{\mu\nu} - \tfrac{1}{2}\,g^{\mu\nu}R = -\varkappa\,T^{\mu\nu} \tag{4}$$

where $R^{\mu\nu}$ is the Ricci curvature tensor, R is its trace, $\varkappa = 8\pi G/c^4$ and G is the gravitational constant (see [3, Ch. 2] for more details).

3 Inertial mass in *STCED*

In *STCED*, as shown in [3,4], energy propagates in the spacetime continuum (*STC*) as wave-like deformations which can be decomposed into *dilatations* and *distortions*. *Dilatations* involve an invariant change in volume of the spacetime continuum which is the source of the associated rest-mass energy density of the deformation. On the other hand, *distortions* correspond to a change of shape (shearing) of the spacetime continuum without a change in volume and are thus massless.

Thus deformations propagate in the spacetime continuum by longitudinal (*dilatation*) and transverse (*distortion*) wave displacements. This provides a natural explanation for wave-particle duality, with the massless transverse mode corresponding to the wave aspects of the deformations and the massive longitudinal mode corresponding to the particle aspects of the deformations.

The rest-mass energy density of the longitudinal mode is given by [4, see Eq. (32)]

$$\rho c^2 = 4\bar{\kappa}_0\varepsilon \tag{5}$$

where ρ is the rest-mass density, c is the speed of light, $\bar{\kappa}_0$ is the bulk modulus of the *STC*, and ε is the volume dilatation given by (3). Integrating over the 3-D space volume,

$$\int_{V_3} \rho c^2\,\mathrm{d}V_3 = 4\bar{\kappa}_0 \int_{V_3} \varepsilon\,\mathrm{d}V_3\,, \tag{6}$$

and using

$$m = \int_{V_3} \rho \, \mathrm{d}V_3 \tag{7}$$

in (6), where m is the rest mass (often denoted as m_0) of the deformation, we obtain

$$mc^2 = 4\bar{\kappa}_0 \, V_{\varepsilon s} \tag{8}$$

where

$$V_{\varepsilon s} = \int_{V_3} \varepsilon \, \mathrm{d}V_3 \tag{9}$$

is the space volume dilatation corresponding to rest-mass m, and spacetime continuum volume dilatation ε is the solution of the 4-D dilatational (longitudinal) wave equation [3, see Eq. (3.35)]

$$(2\bar{\mu}_0 + \bar{\lambda}_0) \, \nabla^2 \varepsilon = -\partial_\nu X^\nu \tag{10}$$

where ∇ and ∂ are the 4-D operators and X^ν is the spacetime continuum volume force.

This demonstrates that mass is not independent of the spacetime continuum, but rather mass is part of the spacetime continuum fabric itself. Hence mass results from the dilatation of the spacetime continuum in the longitudinal propagation of energy-momentum in the spacetime continuum. Matter does not warp spacetime, but rather, matter *is* warped spacetime (*i.e.* dilated spacetime). The universe consists of the spacetime continuum and energy-momentum that propagates in it by deformation of its structure.

It is interesting to note that Pais, in his scientific biography of Einstein *'Subtle is the Lord...'*, mentions [1, p. 253]

> The trace of the energy momentum tensor does vanish for electromagnetic fields but not for matter.

which is correct, as shown in [5, 6], where the zero trace of the electromagnetic field energy-momentum stress tensor is reflected in the zero mass of the photon. The missing link in general relativity is the understanding that the trace of the energy-momentum stress tensor is related to the trace of the spacetime continuum strain tensor and is proportional to the mass of matter as given by (5) and (8).

There are basic questions of physics that can be resolved given this understanding of the origin of inertial mass. The following sections deal with many of these unresolved questions.

3.1 Definition of mass

An important consequence of relations (5) and (8) is that they provide a definition of mass. The definition of mass is still one of the open questions in physics, with most authors adopting an indirect definition of mass based on the ratio of force to acceleration [15, see Ch. 8]. However, mass is one of the fundamental dimensions of modern systems of units, and as such, should be defined directly, not indirectly. This is a reflection of the current incomplete understanding of the nature of mass in physics. *STCED* provides a direct physical definition of mass: *mass is the invariant change in volume of spacetime in the longitudinal propagation of energy-momentum in the spacetime continuum*.

Note that the operational definition of mass ($m = F/a$) is still needed to measure the mass of objects and compare them. Jammer covers the various operational and philosophical definitions of mass that have been proposed [2, Ch. 1].

3.2 Point particles

The fact that the mass of a particle corresponds to a finite spacetime volume dilatation $V_{\varepsilon s}$ shows that a singular "point" particle is not physically valid. All particles occupy a finite volume, even if that volume can be very small. Problems arising from point particles are thus seen to result from the abstraction of representing some particles as point objects. Instead, particles need to be given a finite volume to give physically realistic results and avoid invalid results.

3.3 Equivalence of inertial and gravitational mass

Einstein's general relativistic principle of equivalence of inertial and gravitational mass can be given added confirmation in *STCED*. As shown in [5, 7], the Ricci tensor can also be decomposed into dilatation and distortion components. The dilatation component can be shown to result in Poisson's equation for a newtonian gravitational potential [3, see Eq. (2.44)] where the gravitational mass density is identical to the rest-mass density identified in *STCED*. This confirms theoretically the equivalence of inertial mass and gravitational mass, as demonstrated experimentally within the accuracy currently achievable [10].

3.4 Mach's principle

Mach's principle, a terminology first used by Einstein [1, p. 287], was not explicitly stated by Mach, and hence various takes on its statement exist. One of the better formulation holds that one can determine rotation and hence define inertial frames with respect to the fixed stars [11, see pp. 86–88]. By extension, inertia would then be due to an interaction with the average mass of the universe [11, see p. 17].

This principle played an important role in the initial development of general relativity by Einstein which is well documented by Pais [1, pp. 283–287]. It also had an impact on the initial work performed in cosmology by Einstein who was searching for a cosmological model that would be in accord with Mach's principle. Einstein's evolving perspective on Mach's work is best summarized by Pais [1, p. 287]:

> So strongly did Einstein believe at that time in the relativity of inertia that in 1918 he stated as being on equal footing three principles on which a satisfactory theory of gravitation should rest [Mach's principle was the third] ... In later years, Einstein's enthusiasm for Mach's principle waned and finally vanished.

Modifications of Einstein's Theory of General Relativity have been proposed in an attempt to incorporate Mach's principle into general relativity (see for example [12, 13]).

The book *Gravitation and Inertia* by Ciufolini and Wheeler [14], with its emphasis on geometrodynamics and its well-known sayings "spacetime tells mass how to move and mass tells spacetime how to curve" and "inertia here arises from mass there", explores these ideas in detail. However, it is important to realize that this perspective is an interpretation of Einstein's field equations of general relativity (4). These equations are simply a relation between the geometry of the spacetime continuum and the energy-momentum present in its structure. *STCED* shows that mass is not outside of the spacetime continuum telling it how to curve (so to speak), but rather mass is part of the spacetime continuum fabric itself participating in the curvature of the spacetime continuum. The geometry of the spacetime continuum is generated by the combination of all spacetime continuum deformations which are composed of longitudinal massive dilatations and transverse massless distortions.

As shown in [3, §2.5], the geometry of spacetime used in (4) can thus be considered to be a linear composition (represented by a sum) of *STC* deformations, starting with the total energy-momentum generating the geometry of general relativity, $T^{\mu\nu}_{GR}$, being a composition of the energy-momentum of the individual deformations of *STCED*, $T^{\mu\nu}_{STCED}$:

$$T^{\mu\nu}_{GR} = \sum T^{\mu\nu}_{STCED} \,. \tag{11}$$

Substituting into (11) from (1) and (4), we obtain

$$-\frac{1}{\varkappa}\left[R^{\mu\nu} - \tfrac{1}{2}\, g^{\mu\nu} R\right] = \sum \left[2\bar{\mu}_0\, \varepsilon^{\mu\nu} + \bar{\lambda}_0\, g^{\mu\nu}\varepsilon\right] . \tag{12}$$

Contraction of (12) yields the relation

$$\frac{1}{\varkappa}\, R = \sum 2(\bar{\mu}_0 + 2\bar{\lambda}_0)\, \varepsilon \tag{13}$$

which, using (2) and (5), simplifies to

$$\frac{1}{\varkappa}\, R = \sum 4\, \bar{\kappa}_0\, \varepsilon = \sum \rho\, c^2 \tag{14}$$

i.e. the curvature of the spacetime continuum arises from the composition of the effect of individual deformations and is proportional to the rest-mass energy density present in the spacetime continuum. Substituting for $R/\varkappa$ from (14) into (12), and rearranging terms, we obtain

$$\frac{1}{\varkappa}\, R^{\mu\nu} = \sum \left[(\bar{\lambda}_0 + \bar{\mu}_0) g^{\mu\nu}\varepsilon - 2\bar{\mu}_0\, \varepsilon^{\mu\nu}\right] . \tag{15}$$

Eqs. (14) and (15) give the relation between the microscopic description of the strains (*i.e.* deformations of the spacetime continuum) and the macroscopic description of the gravitational field in terms of the curvature of the spacetime continuum resulting from the combination of the many microscopic displacements of the spacetime continuum from equilibrium. The source of the inertia is thus in the massive dilatation associated with each deformation, and Mach's principle (or conjecture as it is also known) is seen to be incorrect.

3.5 Electromagnetic mass

The advent of Maxwell's theory of electromagnetism in the second half of the nineteenth century led to the possibility of inertia resulting from electromagnetism, first proposed in 1881 by J. J. Thomson [15, see Chapter 11]. The application of the concept of electromagnetic mass to the electron discovered by J. J. Thomson in 1897, by modelling it as a small charged sphere, led to promising results [16, see Chapter 28]. One can then calculate the energy in the electron's electric field and divide the result by c^2. Alternatively, the electromagnetic momentum of a moving electron can be calculated from Poynting's vector and the electromagnetic mass set equal to the factor multiplying the electron's velocity vector. Different methods give different results.

Using the classical electron radius

$$r_0 = \frac{e^2}{m_e c^2} \tag{16}$$

where e is the electronic charge and m_e the mass of the electron, then the electromagnetic mass of the electron can be written as

$$m_{em} = k_e\, \frac{e^2}{r_0 c^2} \tag{17}$$

where the factor k_e depends on the assumed charge distribution in the sphere and the method of calculation used. For a surface charge distribution, $k_e = 2/3$, while for a uniform volume distribution, $k_e = 4/5$. Numerous modifications were attempted to get $m_{em} = m_e$ [15, 16] with Poincaré introducing non-electrical forces known as "Poincaré stresses" to get the desired result. This is a classical treatment that does not take relativistic or quantum effects into consideration.

It should be noted that the simpler classical treatment of the electromagnetic mass of the electron based purely on the electric charge density of the electron is a calculation of the static mass of the electron. In *STCED*, the charge density ϱ can be calculated from the current density four-vector j^ν (see [3, §4.3])

$$j^\nu = \frac{\varphi_0}{\mu_0}\, \frac{2\bar{\mu}_0 + \bar{\lambda}_0}{2\bar{\mu}_0}\, \varepsilon^{;\nu} \tag{18}$$

where φ_0 is the *STC electromagnetic shearing potential constant*, which has units of $[\mathrm{V}\cdot\mathrm{s}\cdot\mathrm{m}^{-2}]$ or equivalently [T], μ_0 is the electromagnetic permeability of free space, and $\varepsilon^{;\nu}$ can be written as the dilatation current $\xi^\nu = \varepsilon^{;\nu}$. Substituting for j^ν from (18) in the relation [23, see p. 94]

$$j^\nu j_\nu = \varrho^2 c^2, \tag{19}$$

we obtain the expression for the charge density

$$\varrho = \frac{1}{2}\,\frac{\varphi_0}{\mu_0 c}\,\frac{2\bar{\mu}_0 + \bar{\lambda}_0}{2\bar{\mu}_0}\,\sqrt{\varepsilon^{;\nu}\varepsilon_{;\nu}}\,. \tag{20}$$

Note the difference between the electromagnetic permeability of free space μ_0 and the Lamé elastic constant $\bar{\mu}_0$ used to denote the spacetime continuum shear modulus.

We see that the charge density derives from the norm of the gradient of the volume dilatation ε, *i.e.*

$$\begin{aligned}\|\varepsilon^{;\nu}\| &= \sqrt{\varepsilon^{;\nu}\varepsilon_{;\nu}} \\ &= \sqrt{\left(\frac{\partial\varepsilon}{\partial x}\right)^2 + \left(\frac{\partial\varepsilon}{\partial y}\right)^2 + \left(\frac{\partial\varepsilon}{\partial z}\right)^2 + \frac{1}{c^2}\left(\frac{\partial\varepsilon}{\partial t}\right)^2}\end{aligned} \tag{21}$$

in cartesian coordinates, and from the above, (20) becomes

$$\varrho = \frac{1}{2}\,\frac{\varphi_0}{\mu_0 c}\,\frac{2\bar{\mu}_0 + \bar{\lambda}_0}{2\bar{\mu}_0}\,\|\varepsilon^{;\nu}\|\,. \tag{22}$$

The charge density is a manifestation of the spacetime fabric itself, however it does not depend on the volume dilatation ε, only on its gradient, and it does not contribute to inertial mass as given by (5). The electromagnetic mass calculation is based on the energy in the electron's electric field and we now consider electromagnetic field energy in *STCED* to clarify its contribution, if any, to inertial mass. This also covers the calculation of electromagnetic mass from the Poynting vector.

3.6 Electromagnetic field energy in the spacetime continuum

As shown in [8], the correct special relativistic relation for momentum p is given by

$$p = m_0\, u\,, \tag{23}$$

where m_0 is the proper or rest mass, u is the velocity with respect to the proper time τ, given by $u = \gamma v$, where

$$\gamma = \frac{1}{(1-\beta^2)^{1/2}}\,, \tag{24}$$

$\beta = v/c$, and v is the velocity with respect to the local time t. When dealing with dynamic equations in the local time t instead of the invariant proper time τ, momentum p is given by

$$p = m^* v\,, \tag{25}$$

where the relativistic mass m^* is given by

$$m^* = \gamma m_0\,. \tag{26}$$

Eq. (25), compared to (23), shows that relativistic mass m^* is an effective mass which results from dealing with dynamic equations in the local time t instead of the invariant proper time τ. The relativistic mass energy m^*c^2 corresponds to the total energy of an object (invariant proper mass plus kinetic energy) measured with respect to a given frame of reference [8]. As noted by Jammer [2, p. 41],

> Since [velocity v] depends on the choice of [reference frame] S relative to which it is being measured, [relativistic mass m^*] also depends on S and is consequently a relativistic quantity and not an intrinsic property of the particle.

Using the effective mass, we can write the energy E as the sum of the proper mass and the kinetic energy K of the body, which is typically written as

$$E = m^* c^2 = m_0\, c^2 + K\,. \tag{27}$$

If the particles are subjected to forces, these stresses must be included in the energy-momentum stress tensor, and hence added to K. Thus we see that the inertial mass corresponds to the proper or rest mass of a body, while relativistic mass does not represent an actual increase in the inertial mass of a body, just its total energy (see Taylor and Wheeler [17], Okun [18–20], Oas [21, 22]).

Considering the energy-momentum stress tensor of the electromagnetic field, we can show that $T^{\alpha}{}_{\alpha} = 0$ as expected for massless photons, while

$$T^{00} = \frac{\epsilon_0}{2}\,(E^2 + c^2 B^2) = U_{em} \tag{28}$$

is the total energy density, where U_{em} is the electromagnetic field energy density, ϵ_0 is the electromagnetic permittivity of free space, and E and B have their usual significance for the electric and magnetic fields (see [3, §5.3]). As $m_0 = 0$ for the electromagnetic field, the electromagnetic field energy then needs to be included in the K term in (27).

In general, the energy relation in special relativity is quadratic, given by

$$E^2 = m_0^2\, c^4 + p^2 c^2\,, \tag{29}$$

where p is the momentum. Making use of the effective mass (26) allows us to obtain (25) from (29) [6], starting from

$$m^{*2} c^4 = \gamma^2 m_0^2\, c^4 = m_0^2\, c^4 + p^2 c^2\,. \tag{30}$$

This section provides a description of the electromagnetic field energy using a quadratic energy relation which corresponds to the more complete classical treatment of the electromagnetic mass of the electron based on the Poynting vector of the electron in motion.

In *STCED*, energy is stored in the spacetime continuum as strain energy [6]. As seen in [4, see Section 8.1], the strain energy density of the spacetime continuum is separated into two terms: the first one expresses the dilatation energy density (the mass longitudinal term) while the second one expresses the distortion energy density (the massless transverse term):

$$\mathcal{E} = \mathcal{E}_{\parallel} + \mathcal{E}_{\perp} \tag{31}$$

where

$$\mathcal{E}_{\parallel} = \frac{1}{2}\,\bar{\kappa}_0 \varepsilon^2 \equiv \frac{1}{32\bar{\kappa}_0}\,\rho^2 c^4\,, \tag{32}$$

ρ is the rest-mass density of the deformation, and

$$\mathcal{E}_\perp = \bar{\mu}_0\, e^{\alpha\beta} e_{\alpha\beta} = \frac{1}{4\bar{\mu}_0}\, t^{\alpha\beta} t_{\alpha\beta}\,, \tag{33}$$

with the strain distortion

$$e^{\alpha\beta} = \varepsilon^{\alpha\beta} - e_s\, g^{\alpha\beta} \tag{34}$$

and the strain dilatation $e_s = \frac{1}{4}\,\varepsilon^{\alpha}{}_{\alpha}$. Similarly for the stress distortion $t^{\alpha\beta}$ and the stress dilatation t_s. Then the dilatation (massive) strain energy density of the deformation is given by the longitudinal strain energy density (32) and the distortion (massless) strain energy density of the deformation is given by the transverse strain energy density (33).

As shown in [3, §5.3.1] for the electromagnetic field, the longitudinal term is given by

$$\mathcal{E}_\parallel = 0 \tag{35}$$

as expected [24, see pp. 64–66]. This result thus shows that the rest-mass energy density of the electromagnetic field, and hence of the photon is zero, *i.e.* the photon is massless. The transverse term is given by [3, §5.3.2]

$$\mathcal{E}_\perp = \frac{1}{4\bar{\mu}_0}\left[\epsilon_0^2\left(E^2 + c^2B^2\right)^2 - \frac{4}{c^2}\,S^2\right] \tag{36}$$

or

$$\mathcal{E}_\perp = \frac{1}{\bar{\mu}_0}\left[{U_{em}}^2 - \frac{1}{c^2}\,S^2\right] \tag{37}$$

where $U_{em} = \frac{1}{2}\,\epsilon_0(E^2 + c^2B^2)$ is the electromagnetic field energy density as before and S is the magnitude of the Poynting vector. The Poynting four-vector is defined as [3, §5.4]

$$S^\nu = (cU_{em}, \boldsymbol{S})\,, \tag{38}$$

where U_{em} is the electromagnetic field energy density, and $\boldsymbol{S}$ is the Poynting vector. Furthermore, S^ν satisfies

$$\partial_\nu S^\nu = 0\,. \tag{39}$$

Using definition (38) in (37), we obtain the transverse massless energy density of the electromagnetic field

$$\mathcal{E}_\perp = \frac{1}{\bar{\mu}_0 c^2}\, S_\nu S^\nu\,. \tag{40}$$

The indefiniteness of the location of the field energy referred to by Feynman [16, see p. 27-6] is thus resolved: the electromagnetic field energy resides in the distortions (transverse displacements) of the spacetime continuum.

Hence the electromagnetic field is transverse and massless, and has no massive longitudinal component. The electromagnetic field has energy, but no rest mass, and hence no inertia. From *STCED*, we see that electromagnetism as the source of inertia is not valid.

Electromagnetic mass is thus seen to be an unsuccessful attempt to account for the inertial mass of a particle from its electromagnetic field energy. The electromagnetic field contributes to the particle's total energy, but not to its inertial mass which *STCED* shows originates in the particle's dilatation energy density (the mass longitudinal term) which is zero for the electromagnetic field.

4 Discussion and conclusion

In this paper, we have revisited the nature of inertial mass as provided by the Elastodynamics of the Spacetime Continuum (*STCED*) which provides a better understanding of general relativistic spacetime. Mass is shown to be the invariant change in volume of spacetime in the longitudinal propagation of energy-momentum in the spacetime continuum. Hence mass is not independent of the spacetime continuum, but rather mass is part of the spacetime continuum fabric itself.

STCED provides a direct physical definition of mass. In addition, it answers many of the unresolved questions that pertain to the nature of mass:

- The mass of a particle corresponds to a finite spacetime volume dilatation $V_{\varepsilon s}$ and particles need to be given a finite volume (as opposed to "point particles") to give physically realistic results and avoid invalid results.
- It confirms theoretically the equivalence of inertial and gravitational mass.
- The source of inertia is in the massive dilatation associated with each deformation, and Mach's principle (or conjecture), which holds that inertia results from interaction with the average mass of the universe, is seen to be incorrect.
- The electromagnetic field is transverse and massless, and has no massive longitudinal component. It has energy, but no rest mass, and hence no inertia. The electromagnetic field contributes to the particle's total energy, but not to its inertial mass.

STCED thus provides a physical model of the nature of inertial mass, which also includes an explanation for wave-particle duality. This model leads to the clarification and resolution of unresolved and contentious questions pertaining to inertial mass and its nature.

Received on May 27, 2019

References

1. Pais A. 'Subtle is the Lord...': The Science and the Life of Albert Einstein. Oxford University Press, Oxford, 1982.
2. Jammer M. Concepts of Mass in Contemporary Physics and Philosophy. Princeton University Press, Princeton, 2000.
3. Millette P. A. Elastodynamics of the Spacetime Continuum: A Spacetime Physics Theory of Gravitation, Electromagnetism and Quantum Physics. American Research Press, Rehoboth, NM, 2017.

4. Millette P. A. Elastodynamics of the Spacetime Continuum. *The Abraham Zelmanov Journal*, 2012, vol. 5, 221–277.
5. Millette P. A. On the Decomposition of the Spacetime Metric Tensor and of Tensor Fields in Strained Spacetime. *Progress in Physics*, 2012, vol. 8 (4), 5–8.
6. Millette P. A. Strain Energy Density in the Elastodynamics of the Spacetime Continuum and the Electromagnetic Field. *Progress in Physics*, 2013, vol. 9 (2), 82–86.
7. Millette P. A. Dilatation–Distortion Decomposition of the Ricci Tensor. *Progress in Physics*, 2013, vol. 9 (4), 32–33.
8. Millette P. A. On Time Dilation, Space Contraction, and the Question of Relativistic Mass. *Progress in Physics*, 2017, vol. 13 (4), 202–255.
9. Segel L. A. Mathematics Applied to Continuum Mechanics. Dover Publications, New York, 1987.
10. Roll P. G., Krotkov R., and Dicke R. H. The Equivalence of Inertial and Passive Gravitational Mass. *Annals of Physics*, 1964, vol. 26, 442–517.
11. Weinberg S. Gravitation and Cosmology: Principles and Applications of the General Theory of Relativity. John Wiley & Sons, New York, 1972.
12. Brans C. and Dicke R. H. Mach's Principle and a Relativistic Theory of Gravitation. *Physical Review*, 1961, vol. 124 (3), 925–935.
13. Goenner H. F. M. Mach's Principle and Theories of Gravitation. In Barbour J. B., Pfister, H., Eds. Mach's Principle: From Newton's Bucket to Quantum Gravity. Birkhäuser, Boston, 1995, pp. 442–457.
14. Ciufolini I. and Wheeler J. A. Gravitation and Inertia. Princeton University Press, Princeton, NJ, 1995.
15. Jammer M. Concepts of Mass in Classical and Modern Physics. Dover Publications, New York, (1961) 1997.
16. Feynman R. P., Leighton R. B., Sands M. Lectures on Physics, Volume II: Mainly Electromagnetism and Matter. Addison-Wesley Publishing Company, Reading, Massachusetts, 1964.
17. Taylor E. F., Wheeler J. A. Spacetime Physics: Introduction to Special Relativity, 2nd ed. Freeman, New York, 1992, pp. 250–251.
18. Okun L. B. The Concept of Mass. *Physics Today*, 1989, v. 42 (6), 31–36.
19. Okun L. B. The Einstein Formula: $E_0 = mc^2$. "Isn't the Lord Laughing?". *Physics–Uspekhi*, 2008, v. 51 (5), 513–527. arXiv: physics.hist-ph/0808.0437.
20. Okun L. B. Energy and Mass in Relativity Theory. World Scientific, New Jersey, 2009.
21. Oas G. On the Abuse and Use of Relativistic Mass. arXiv: physics.ed-ph/0504110v2.
22. Oas G. On the Use of Relativistic Mass in Various Published Works. arXiv: physics.ed-ph/0504111.
23. Barut A. O. Electrodynamics and Classical Theory of Fields and Particles. Dover Publications, New York, 1980.
24. Charap J. M. Covariant Electrodynamics: A Concise Guide. The John Hopkins University Press, Baltimore, 2011.

A Space Charging Model for the Origin of Planets' Magnetic Fields

Tianxi Zhang

Department of Physics, Alabama A & M University, Normal, Alabama
E-mail: tianxi.zhang@aamu.edu

Both theoretical models and experimental results have indicated that a body surrounded by plasma is negatively charged to a potential around 2-3 times greater than the thermal potential of the ambient plasma. This potential difference shows that the body holds some extra electric charge. In this paper, we formulate an expression to compute the extra electric charge from the ambient plasma. It is shown that the total electric charge on a body basically depends on its size and the characteristics of the ambient plasma. When the body size is big or the ambient plasma is dense, the extra electric charge is large. Since all solar planets are imbedded within the solar wind plasma, they may also be charged due to the same physics. Analyzing the charging behavior of planets, we find that the solar planets are significantly charged. The circular electric currents or charge flows caused by planets's spinning produce magnetic fields. The magnetic fields predicted by the present space charge model basically agree with the measurements on the global magnetic fields of planets (including the Moon). Also, the polarity biases and reversals of planet magnetic fields are discussed. Therefore, a possible explanation for the origin of the magnetic fields of planets is proposed.

1 Introduction

The origin of the geomagnetic field has been puzzling physicists for hundreds of years. In 1600, Willian Gilbert believed that the Earth is permanently magnetized, like a giant magnet. Albert Einstein considered the origin of the geomagnetic field to be one of the five most important unsolved problems in physics. So far, tons of data on the geomagnetism have been accumulated [1]. In general, the geomagnetic field resembles the field generated by a dipole magnet located at the center of the Earth. The locations of the north and south geomagnetic poles are randomly varied and reverse each other at irregular periods [2-4]. The intensity of the geomagnetic field is transiently changed and in average about 0.5 G, which is slowly decayed. It is generally believed that the geomagnetic field is affected by various external events, such as the tides, aurora, solar flares, sunspots, and so on.

In order to explain the geomagnetic phenomena, various models have been proposed, which are conveniently classified into dynamo and non-dynamo models. As a non-dynamo model, the permanent magnetization of the Earth could not explain the polarity reversals of the geomagnetic field. The charge separation arising from the thermoelectric effect is, however, relatively small in comparison with the geomagnetic field [5]. In addition, some other effects were suggested - such as the gyromagnetic effect, the hall effect, the galvanomagnetic effect, the differential rotation effect, the electromagnetic induction by magnetic storms, and the Nernst-Ettinghauser effect, etc. [6-11].

Larmor [12-13] was the first to suggest that large astronomical bodies might have magnetic fields that arise from a self-exciting dynamo process. However, Cowling [14] showed that this disc dynamo was damped and cannot maintain such a field very long. Later, other dynamo theories were developed, such as magnetohydrodynamic dynamo, kinematic dynamo, turbulent hydromagnetic dynamo, and so on [15-22]. Although it is generally accepted today that the geomagnetic field arises from dynamo action in the Earth's liquid outer core, there is no viable hydrodynamic geodynamo model as described by McFadden and Merrill [23] because there are so many unclear parameters being included in the governing equations.

The study of the magnetic fields of planets offers the key to an understanding of the origin of the geomagnetic field. Until recently, information about the magnetic fields of planets came mostly from indirect measurements or from flyby missions. The measurements are generally sparse in both spatial and temporal distribution and only provide us a first-order picture of the magnetic fields of planets.

The solar planets can be conveniently classified into two types (type-I and type-II) according to their magnetic fields being local or global. A type-I planet has a weak global magnetic field, such as Venus, Mars, or Pluto (also the Moon). These planets are almost naked to the solar wind plasmas because of lack of (or very weak) magnetospheres [24]. Their atmospheres are usually not strong enough to sheath out the solar wind and partially ionized especially at the upstream. However, the type-II planets (including Mercury, Earth, Jupiter, Saturn, Uranus, and Neptune) have strong global magnetic fields. The solar wind plasmas are separated from these planets by their powerful magnetospheres except at their poles. The solar wind electric currents can still interact with the Earth through partially ionizing the neutral atoms in the atmosphere at the poles. The early measurements did

show that electric currents were observed in both the air and the Earth during aurora taking place [25-27].

Dynamo theorists suggested that the global magnetic fields of the type-II planets were excited due to their interior dynamo actions, which are critically dependent of the size and spin of the planets. The main reason Venus lacks a dynamo is because it spins slower than the Earth does. The reason Mars lacks a dynamo is because it is smaller than the Earth. However, Mercury probably has a dynamo action even though it is smaller and its spinning period is longer than Mars. A dynamo model may not easily answer why Mercury has a dynamo but Mars does not.

In this paper, a theoretical space charge model for the origin of the global magnetic fields of planets is proposed. The purpose of this paper is not to be against dynamo theories instead of to suggest another possibility. According to the space charge physics, a body floating in the space plasma will be charged. This phenomenon has been actually observed during space experiments. The electric charge on a large conducting spherical body is further derived. If the body is spinning, the electric charge will generate a circular electric current, which induces a magnetic field. It is shown that the induced magnetic field depends not only on the size and spin period of the body, but also on the characteristics of the ambient plasma. For very large bodies, such as planets, the induced magnetic fields could be as big as the measurements. Analyzing the magnetic fields and electric charging processes of the two types of planets results in a consistent explanation for the magnetic fields of all planets, including the Moon. The polarity biases and reversals of the planet magnetic fields are also discussed with this model. In addition, it should be noted that this model has not included the effects of atmosphere, body motion, and plasma instabilities on current collection. The relative motion between the body and the environmental plasma was shown to increase current collection along the magnetic field lines [28]. The field aligned current-driven instabilities was shown to greatly heat charged particles [29-30] and hence can also increase the current collected by the body.

2 Space Charging

Experimentally and theoretically, it has been shown that a satellite moving (or floating) in space plasmas itself becomes usually negatively charged, since the number of electrons incident on its surface is greater than the number of ions [31] (see Figure 1a). The absorption of electrons and ions essentially depends on the size of the body, the surface potential, the material properties of the body, and the state of the ambient plasma. In some special cases, a body may be positively charged.

The amount of electric charges and the absolute value of potential increase as long as the number of electrons and the number of ions being absorbed on its surface are not identical. Since the increasing potential slows down the electric

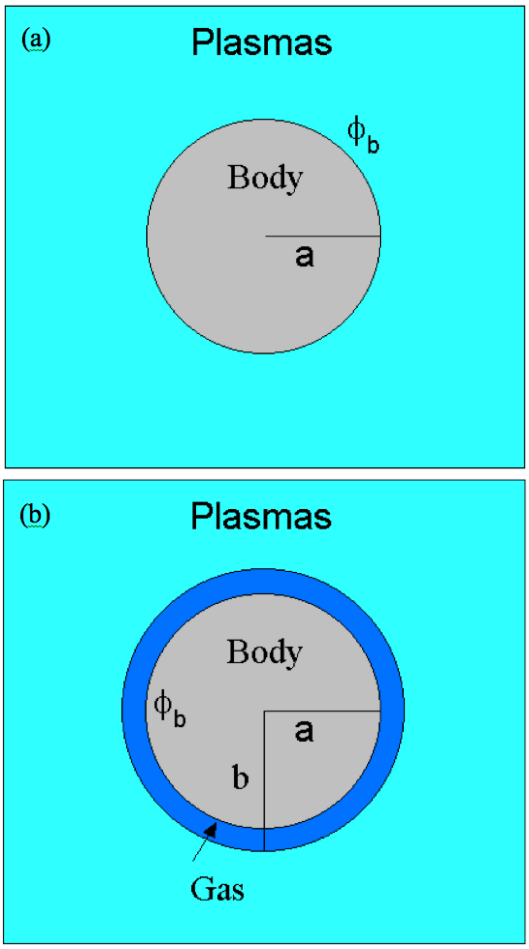

Fig. 1: Schematic diagrams for space charge model. (a) Without a neutral gas layer; (b) with a neutral gas layer.

accumulating processes, an "equilibrium" state for charge accumulating (i.e. a state in which the total electric current incident on the body is equal to zero) is finally attained if the ambient plasma is vast. In this situation, the electric potential at the surface of the body, is determined by

$$\phi_0 \simeq -\frac{k_B T_e}{e} \ln \sqrt{\frac{2k_B T_e}{\pi m_e V_0^2}} = -\alpha \phi_{th}. \qquad (1)$$

Here the potential at infinite distance (or outside the plasma sheath) has been chosen to be zero; k_B is the Boltzmann constant; e is the proton electric charge; the subscript e refers to the electron species; T_e is the electron temperature; m_e is the electron mass; V_0 is the velocity of the body relative to the ambient plasma - which is generally much larger than the ion thermal velocity and less than the electron thermal velocity; ϕ_{th} is the thermal potential which is defined by $k_B T_e/e$; and α is the factor which is given by the nature logarithm in Eq. (1). For example, we consider that a spherical body is

moving in the ionosphere plasma. The thermal potential is $\phi_{th} \sim 0.11$ V if $T_e \sim 0.1$ eV is chosen for the plasma. The factor α is $\alpha \sim 2.58$ if $V_0 = 8$ km/s is chosen for the body. Then the electric potential at the body surface is estimated as $\phi_0 \sim -0.3$ V, which is in agreement with space measurements. For a motionless or slowly moving body (i.e., $V_0 = 0$ or much smaller than the ion thermal velocity), the result is $\phi_0 \sim 2.57$ V [32].

If the body is separated from the plasma by a thin layer of neutral gas (see Figure 1b), the region of neutral gas will get extra electrons since the electrons incident into the neutral gas region are more than the ions. For a quasi-neutral plasma the number of electrons entering the neutral gas in a unit time through a unit area is determined as the electron flux ($n_0\bar{v}_e/4$), which is much greater than that of ion ($n_0\bar{v}_i/4$). Here n_0 is the number density of electron (or ion) of the quasi-neutral plasma; $\bar{v}_e$ and $\bar{v}_i$ are the mean velocity of electrons and ions, respectively. These extra electrons will diffuse toward the body because both the electron density and the electric potential have gradients. That is to say, the body will be charged. The total amount of electric charge distributed on the body and within the neutral gas should be generally greater than that without the gas layer. In present study, we limit our analyses in cases of very thin layer and hence ignore the effects of neutral gas on the charge of the body.

If the electric potential distribution is given, the electric charge on the body can be obtained. For a spherical body within a medium (including free space, dielectric medium, plasma, etc.), the density of electric charge distributed on the body surface is given by

$$\sigma_b = -\epsilon \left.\frac{d\phi}{dr}\right|_{r=a}, \tag{2}$$

where a is the radius of the body; ϕ is the electric potential distribution; r is the radial coordinate; and ϵ is the dielectric permittivity. For a static (or slowly moving) electrically conducting body, the density of electric charge on the surface is constant. Hence, the total electric charge of the body is

$$Q_b = -4\pi\epsilon a^2 \left.\frac{d\phi}{dr}\right|_{r=a}, \tag{3}$$

In the free space, a spherical body with $a = 1$ m and $\phi_0 = -0.2$ V will be charged to $Q_b = 4\pi\epsilon_0 a\phi_0 \sim -2 \times 10^{-11}$ Coulomb.

If the medium is plasma, however, the relationship between the total electric charge and the electric potential of the body will be complex. The total electric charge or the numbers of electrons and ions being absorbed by a body essentially depends not only on the potential and size of the body, but also on the state of plasma. In this case, the electric potential distribution must be generally determined through solving the Poisson equation,

$$\nabla^2\phi = -\frac{1}{\epsilon}\sum_{j=i}^{j=e} n_j q_j. \tag{4}$$

For a body with size much greater than the Debye length, however, the potential near the body can be approximately obtained only by solving the one-dimensional Poisson equation,

$$\frac{d^2\phi}{dr^2} = -\frac{n_{e0}e}{\epsilon}\left(e^{-\phi/\phi_{th}} + e^{\phi/\phi_{th}}\right). \tag{5}$$

Here the Boltzmann number density distributions have been applied for both electrons and ions. Integrating Eq. (5) one times with respect to r, we obtain

$$\frac{d\phi}{dr} = \sqrt{\frac{2n_{e0}e\phi_{th}}{\epsilon}\left(e^{-\phi/\phi_{th}} + e^{\phi/\phi_{th}} - 2\right)}. \tag{6}$$

At the surface of the body (i.e. at $r = a$), it becomes

$$\left.\frac{d\phi}{dr}\right|_{r=a} = \sqrt{\frac{2k_B T_e n_{e0}}{\epsilon}\left(e^{-\alpha} + e^{\alpha} - 2\right)}. \tag{7}$$

By substituting Eq. (7) into Eq. (3), we obtain a formula to estimate the electric charge of a large conducting body floating in space plasmas

$$Q_b = -4\pi a^2\sqrt{2\epsilon_0 k_B T_e n_{e0}\left(e^{-\alpha} + e^{\alpha} - 2\right)}, \tag{8}$$

where the dielectric permittivity has been replaced to that of free space, since we do not consider a very dense plasma. Therefore, the body is in general to be negatively charged. The amount of charge on the body depends not only on the size and potential of the body but also on the temperature and density of the ambient plasma.

Now we consider the case in which a body is moving relative to the ambient plasma. When the velocity of the body is in the range of, $v_{Te} \gg V_0 \gg v_{Ti}$, the number density of ions near the body is no longer the Boltzmann distribution, where v_{Te} and v_{Ti} are the thermal velocities of electrons and ions. In the upstream, the number density of ions is not interfered by the body if the body surface does not reflect particles. In the downstream, however, the number density of ions is almost zero since the ions slowly respond to the motion of the body. In this case, the total electric charge on the body surface (or Eq. 3) is similarly derived as

$$Q_b = -2\pi\epsilon_0 a^2\left(\left.\frac{d\phi^F}{dr}\right|_{r=a} + \left.\frac{d\phi^R}{dr}\right|_{r=a}\right), \tag{9}$$

where ϕ^F and ϕ^R are the electric potential distributions in the upstream and downstream, respectively. The electric potential distributions can be determined by

$$\frac{d^2\phi^F}{dr^2} = -\frac{n_{e0}e}{\epsilon_0}\left[1 - \exp\left(\frac{\phi^F}{\phi_{th}}\right)\right], \tag{10}$$

$$\frac{d^2\phi^R}{dr^2} = \frac{n_{e0}e}{\epsilon_0}\exp\left(\frac{\phi^R}{\phi_{th}}\right). \quad (11)$$

By integrating both Eq. (10) and Eq. (11) with respect to r once, we obtain the electric fields at the surface as

$$\left.\frac{d\phi^F}{dr}\right|_{r=a} = \sqrt{\frac{2k_BT_en_{e0}}{\epsilon_0}(e^\alpha - \alpha)}, \quad (12)$$

$$\left.\frac{d\phi^R}{dr}\right|_{r=a} = \sqrt{\frac{2k_BT_en_{e0}}{\epsilon_0}(e^\alpha - 1)}. \quad (13)$$

By substituting Eq. (12) and Eq. (13) into Eq. (9), we obtain the total electric charge of the body as

$$Q_b = -2\pi a^2\sqrt{2\epsilon_0k_BT_en_{e0}}\left(\sqrt{e^\alpha - \alpha} + \sqrt{e^\alpha - 1}\right). \quad (14)$$

This expression gives a value much greater than that from Eq. (8) if $\alpha \ll 1$. When α is not small, however, the result from Eq. (14) approaches that from Eq. (8).

If the body is spinning, the electric charge on the body surface will generate an electric circular current. This current then induces a magnetic field with poles on the spinning axis. The maximum value of the magnetic field is derived as

$$B = -\frac{\pi}{4}\mu_0\frac{Q_b}{\tau}, \quad (15)$$

where μ_0 is the permeability of free space, $\mu_0 = 4\pi \times 10^{-7}$ H/m; τ is the spin period of the body; and Q_b is given by either Eq. (8) or Eq. (14) according to the motion of the body.

Since the circular current is induced by the self-rotation of a charged body other than by the electric charges moving on the body, the magnetic field induced by the circular current (Eq. 15) is independent of the conductivity of the body surface. If the body surface is made of insulate (i.e., infinite conductivity) material, the density of electric charge will not be constant. In this case, we need to integrate Eq. 2 on the entire body surface to obtain the total charge. It is generally believed that all solar planets are not made of insulate materials. Therefore, this magnetic field formula (Eq. 15) can be generally employed to predict the induced magnetic field of a self-rotated large conducting body, such as an orbit satellite, the Moon, and the solar planets. The required parameters are the radius of the body, the spinning period of the body, the velocity of the body relative to plasma flow, the electron temperature of the ambient plasma, and the non-perturbed density of the ambient plasma. The induced magnetic field will be great when the body is large, the spin is fast, and the plasma is dense. According to the presented model the Mercury magnetic field could be greater than the Mars magnetic field because the solar wind plasma around Mercury is much denser than that around Mars.

For an orbit satellite with a conducting spherical surface, the typical required parameters are, $a = 1$ m, $T_e = 1500$ K, $n_{e0} = 10^6$ cm^3, and $V_0 = 8$ km/s. Substituting T_e and V_0 into Eq. (1) we show that the conducting satellite is charged to a potential equal to $\sim -2.6\phi_{th}$; that is, $\alpha \sim 2.6$. Substituting a, T_e, n_{e0}, and the value of α into Eq. (8) (or Eq. 14) we obtain the electric charge of the satellite, $Q_s \simeq 2 \times 10^{-8}$ Coulomb, which is much larger than that in the free space. Furthermore, if the satellite is self-rotated with a spin period, $\tau_s = 1$ seconds, the induced magnetic field, from Eq. (9), will be $B_s = 2 \times 10^{-11}$ Gausses, which is quite small. It should be noted that the rotation of the satellite does not significantly affect the ambient plasma because the linear speed at the surface due to body rotation is much smaller than the thermal velocities of ions and electrons. The presented model does not include the magnetic field effect on the body charging (or current collection) process. If the magnetic field or the body electric potential is not high, such effect is negligible [33].

3 The magnetic fields of the Moon and planets

Now, employing the space charging model proposed above, we study the magnetic fields of the Moon and planets. The predictions on the magnetic fields are compared with the measurements.

According to the space charge model, the magnetic field of a body is determined by giving the five parameters: the size and spin period of the body, the density and temperature of the plasma, and the velocity of the plasma flow. Table 1 shows the interplanetary conditions for the Moon and planets [34-35]. The solar wind velocity, density, and temperature are shown in the third to fifth column. The magnetic field of the solar wind near each planet and the distance between the Sun and each planet are also shown in this table (see the sixth and second columns). The radii and spin periods of the Moon and planets are shown in the second and third columns in Tables 2 and 3.

As mentioned in the Introduction, the Moon and type-I planets (e.g. Venus, Mars, and Pluto) are almost naked to the

Table 1: Interplanetary properties: Distance to the Sun $L_{\rm Sun}$ (AU), Solar Wind Velocity $V_{\rm SW}$ (km/s), Density $n_{\rm SW}$ (cm^{-3}), Temperature (10^4 K), and Magnetic Field (nT).

Planet	$L_{\rm Sun}$	$V_{\rm SW}$	n_{SW}	T_{SW}	B_{SW}
Mercury	0.4	430	50	20	35
Venus	0.7	430	14	17	10
Earth (or Moon)	1	430	7	15	6
Mars	1.5	430	3	13	3
Jupiter	5.2	430	1/4	9	1
Saturn	9.6	430	1/16	7	1/2
Uranus	19	430	1/50	6	1/4
Neptune	30	430	1/160	5	1/7
Saturn	39	430	1/200	4	1/10

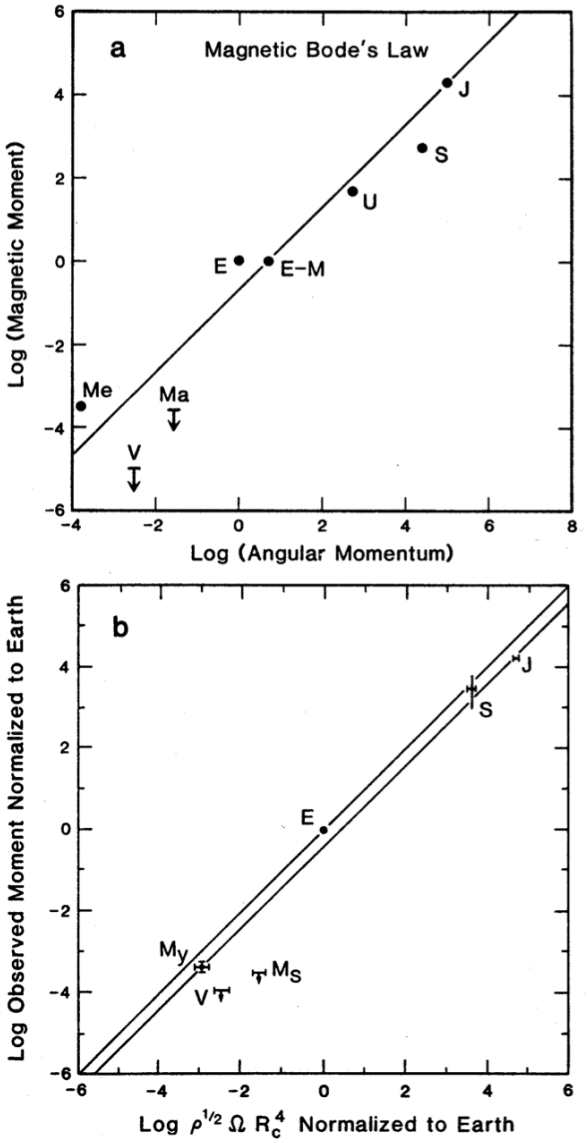

Fig. 2: (a) Relationship between planetary magnetic moment and angular momentum by the original magnetic Bode's law (Russell 1987). (b) Relationship between planetary magnetic moment and the core radius by the dynamo theory-based scaling law (Busse 1976.

solar wind plasmas (actually, they have very thin and weak gas (or atmosphere) layers). The condition, $v_{Te} \gg V_0 \gg v_{Ti}$, which is used for the deduction of Eq. 14, is generally satisfied for the Moon and the type-I planets. In this case, the ambient plasma is the solar wind, which has speed $\sim$ 400 km/s and temperature $T_e \sim T_i \sim 10^5$ K. It is not difficult to show that the solar wind speed is much smaller than the electron thermal speed but much greater than the ion thermal speed. Therefore, the space charging model proposed in the previous section (i.e. Eq. 14) can be directly employed to quantitatively predict their present magnetic fields. For the Moon, the required five parameters are, $a = 1.738\times10^6$ m, $T_e \sim 1.5\times10^5$ K, $n_{e0} \sim 7$ cm^{-3}, $V_0 = 430$ km/s, and $\tau_M = 2.36 \times 10^5$ seconds. At first, using T_e and V_0, we show, from Eq. 1, that the Moon is charged to a potential equal to $\sim -\phi_{th}$ (that is, $\alpha \sim 1$, with this value of α, the Eq. 14 predicts a result without a significant difference from Eq. 8). Then, substituting a, T_e, n_{e0}, and the value of α into Eq. 8 (or Eq. 14), we can obtain the electric charge of the Moon, $Q_M \sim -640$ Coulomb. Finally from Eq. 9, the induce lunar magnetic field (B_M) predicted by the present model is about $B_M \sim 3$ nT. The measurements actually indicate that the intensity of the global magnetic field of the Moon does not exceed 2 to 3 nT (Table 2; [36]).

For Venus, the prediction on the magnetic field by the present model is about 6 nT, which agrees with the measurements. Space experiments indicated that the intrinsic value of the magnetic field at the surface of Venus could not be greater than 5 nT [37].

For Mars, the prediction on the magnetic field by the present model is about 200 nT. In the 1970s, the soviet Mars 3 and 5 probes measured a field about 30 - 60 nT near the equator, at periapisis (at an altitude of 1500 km) [38-40]. Since the magnetic field of Mars on its surface is several times greater (for the Earth, the factor is $\sim 2-4$) than that measured at an altitude of 1500 km, the Mars' magnetic field could be as big as 150 nT, which also agrees with the present model prediction.

We also predict the magnetic field for Pluto although we have not had any measurement available so far. Based on the present model, the Pluto's magnetic field is estimated to be about 0.1 nT, which is ordinarily the same as the magnetic field of the solar wind there. Therefore, the predictions by the space charge model on the magnetic fields of the Moon and the type-I planets basically agree with the measurements (see Table 2, [36-40].

For the type-II planets (such as the Earth), however, we cannot directly obtain the present magnetic fields from Eqs. 1, 8, and 9 because the solar wind plasmas are separated from these planets by their strong magnetospheres. But, we can apply the present model to estimate the ancient magnetic fields of planets if the characteristics of the initial solar wind are known. The following gives some analyses for the type-II

Table 2: Model predictions on B for the type-I planets including Moon and Pluto in comparison with data B_0.

Planet	R (km)	τ (10^5 s)	B_0 (nT)	B (nT)
Venus	6055	210	≤ 5	6
Moon	1738	23.6	≤ 3	3
Mars	3398	0.886	~ 150	200
Pluto	1150	5.519	$\sim$	0.1

planet magnetic fields based on the evolutionary characteristics of solar system. In the next section, the type-II planet magnetic fields are further discussed through considering the polar aurora plasmas as their charging sources. If so, the present model can still be used and predicts results closer to the measurements.

It is widely believed that the Sun went through FU Orionis and T-Tauri phases of evolution [1, 41]. A T-Tauri (in the pre-main sequence) star is partially characterized by violent outbursts of material, very strong magnetic field, and an increased luminosity of about six magnitudes. Observations actually indicated very massive winds from these early-type stars [42]. Preliminary results from the studies of meteorites and lunar rocks also indicated that the average solar wind speed might have been considerably greater some $3-4\times10^9$ years ago [42,43].

Thus, it is reasonable to assume that the Sun initially emitted a strong solar wind. During that time period, all our planets were greatly charged from such massive solar wind plasmas and induced magnetic fields with different intensities due to their different sizes and rotation speeds. If the initial solar wind is $\sim 10^3 - 10^6$ times denser than the present solar wind, the ancient (or initial) magnetic fields are some tens to thousands times greater than the present fields for the Moon and the type-I planets. For the type-II planets, the ratios of the ancient fields to the present fields are in the range of $\sim 1-100$. Thus, the planets with small size and slowly spinning (such as the Moon and type-I planets) also excited considerably great intrinsic magnetic fields, which probably had magnetosphere-like structures during early periods. However, their magnetic fields are easily decayed as the solar wind becomes weak due to their weak abilities to maintain such fields. Large, fast spinning planets (such as the type-II planets) developed very strong magnetic fields and formed powerful magnetospheres - which are also decayed, but relatively more stable than the type-I planets, because they last a longer time in the decaying process.

Observations show that the planet's magnetic field is stronger if its magnetosphere is bigger. According to the presented model, the denser the ambient plasma is, the more charge the body is charged, which is proportional to the induced magnetic field. For the type-II planets (e.g. the Earth), the nearest ambient plasma is the plasmasphere (ionopshere) or the aurora plasma in the pole regions. For these plasmas (see [44]), the electron or ion density is $\sim 10^5$ to 10^6 cm^{-3} which is much denser than the solar wind plasma. The electron or ion temperature is $\sim 10^3$ to 10^4 K. In these regions, most of ions are O^+, which has a thermal velocity around 1 km/s, which is much less than the minimum speed ($\sim$ 8 km/s) for a particle to escape out by overcoming the Earth gravitation. Therefore, the Earth's (as well as other type II planets') gravity may maintain its magnetic field (or magnetosphere) through trapping the particles of plasmasphere or plasma in the aurora regions. The magnetic field itself also helps the planet to trap the particles of magnetosphere. The electrons can be trapped by the ions although the electron thermal velocity may be greater than the minimum escaping speed. Within a relative stable solar wind, the value of the magnetic field or the size of the formed magnetosphere actually depends on the planet gravity. The bigger the gravity is, the stronger the magnetic field is or the bigger the magnetosphere forms if the other parameters are the same.

The results predicted by the present model are very high in absolute values under the assumption that the ancient solar wind density varied in the range of 10^3-10^6 times denser than the present value. During such a long time interval, the planets' magnetic fields were greatly decreased when the solar wind density was greatly decreased. For the type-II planets, we have compared (in the following several paragraphs) the relative results predicted by the present model on the ancient magnetic fields of planets with the measurements and found a good agreement between them.

The fourth column of Table 3 shows the measurements of the magnetic fields for the type-II planets, which are normalized by dividing the geomagnetic field. A 300 nT magnetic field was measured for Mercury [45]; a 15 Gausses magnetic field at the north pole was measured for Jupiter [46]; and orderly $\sim$ 1 Gausses' magnetic fields were measured for Saturn, Uranus, and Neptune [47]. The fifth column of Table 3 shows the predictions of the ancient magnetic fields for the type-II planets, which are normalized by the ancient geomagnetic field. Comparing the fourth column with the fifth column of Table 3, we found that the normalized ancient magnetic fields of planets predicted by the space charging model basically agree with the present field measurements [45-48]. The Saturn's magnetic field (or magnetosphere) could be decayed more than the Jupiter's probably due to the lower gravity (or density) of Saturn.

The decays of planet magnetic fields were probably affected by their gravitation. It is reasonable to assume that a planet with large gravity has more power to maintain its magnetosphere through trapping its particles. To consider such gravity effect, we propose a formula for the present magnetic field of a type-II planet by introducing an arbitrary coefficient,

Table 3: Model predictions on B/B_e for ancient magnetic field for the type-II planets in comparison with data B_0/B_e for present magnetic field.

Planet	R (km)	τ (10^5 s)	B_0/B_e	B/B_e
Mercury	2439	51	$\sim 1/100$	1/130
Earth	6371	0.864	≤ 1	1
Jupiter	71600	0.354	~ 30	45
Saturn	60000	0.368	~ 2	13
Uranus	25600	0.621	~ 1	1
Neptune	24765	0.567	$\sim 1/2$	1/2

$f(g)$, to the Eq. 15 as

$$B = -\frac{\pi}{4}\mu_0 f(g)\frac{Q_b}{\tau}, \tag{16}$$

where g is the gravity at the planet surface and Q_b is the body charge of the planet, which is given by either Eq. 8 or Eq. 14. Then, the magnetic moment of the planet can be derived as

$$M = -\frac{2\pi}{3}a^2 f(g)\frac{Q_b}{\tau}. \tag{17}$$

It can be seen that the magnetic moment of the planet is proportional to a^4 because of $Q_b \propto a^2$. It is also proportional to the square root of the solar wind pressure and inversely proportional to the planet spin period. On the other hand, the magnetic Bode's law also called the Shuster or the Blackett hypothesis established that the magnetic moments of the planets were proportional to their angular moments (see Figure 2a and [49-50]). The scaling law predicted that the planet magnetic moments were proportional to the rotation rate times the fourth power of the core radius (see Figure 2b and [51]).

In order to compare the results predicted by the present space charging model with the predictions by either the magnetic Bode's law or by the scaling law, we plot our model predictions on the magnetic moments of the type-II planets versus the observations in Figure 3. The magnetic moments from both the model predictions and the observations are normalized to the Earth and are shown in log scales. Figure 3a has not included the gravitation effect and Figure 3b gives the results with the gravitation effect by assuming that the coefficient is linearly proportional to the gravity ($f(g) \propto g$). The observation data are from [1].

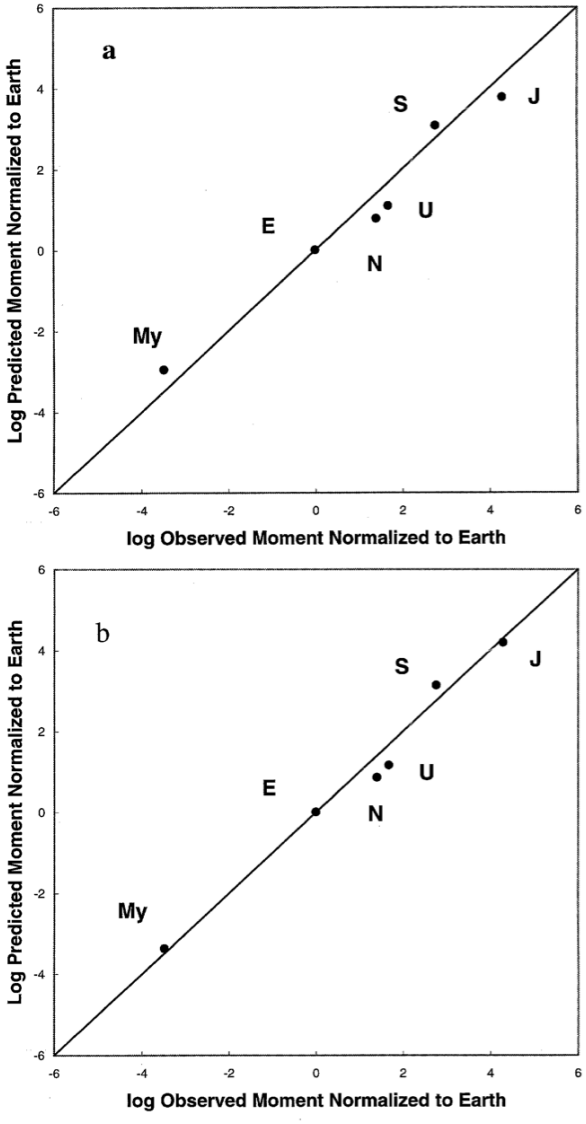

Fig. 3: Planetary magnetic moments normalized to the Earth predicted by the space charge model versus those from measurements. (a) Without the gravity effect; (b) with the gravity effect.

4 Discussions and Conclusions

In this section, we briefly discuss the following items: 1) current collection of planets with magnetospheres and 2) the polarity biases and reversals of the magnetic fields of planets. Then, we give our conclusions of this study.

Although the Earth and other type-II planets are not completely naked to the solar wind plasmas, their poles are widely opened to the outer space due to the double funnel magnetic structures. The solar and interstellar winds as well as the energetic particles can easily, through the magnetic field lines (or double funnels), come down into the polar regions of the planets to excite and to ionize the gases near the surfaces. This is the phenomena of aurora. The aurora plasmas are much denser than the solar wind plasma. The density of a typical aurora plasma could be as high as $\sim 10^5$ to 10^6 cm^{-3} which is much denser than the solar wind plasma with density less than ~ 100 cm^{-3} [44]. Therefore, these planets are probably charged at their poles especially during aurora taking place. The early experimental measurements showed that electric currents were actually observed in the air and in the Earth while the aurora was taking place [25-27]. The correlation between the Earth current and the geomagnetic activity was also found. It is interesting that if we consider the aurora plasma as the source plasma to charge the Earth, the present model predicts a result very closer to the measurement.

For the Earth, observation records show that the aurora events asymmetrically occur at the two (i.e. North and South) poles [52]. The Northern aurora events are generally more frequent and intense than the Southern aurora events. The reason is probably due to that the spinning geomagnetic field lines drift the entering (or coming down) electrons apart from the axis of spinning at the North but towards the axis of spin-

ning at the South. That is to say, the charging process at the North is faster than that at the South. This difference leads to an electric current from pole to pole. If the conductivity is different from place to place (or non-uniform) on the Earth's surface, the electric current from pole to pole will not be uniformly distributed on the Earth's surface. This polar current and the circular current will generate a total magnetic field, which biases from its rotation axis. Both the biases and the value of the induced magnetic field are transiently changed because the space charging process is transient.

The observations indicated that the geomagnetic field varies in two (long and short) time scales. In the long time (usually greater than about 100 years) scale, the field strength is decreased and the biased angle (or the orientation) of the field also changes in a certain regulation (see [1] and reference therein). On the other hand, the geomagnetic field changes transiently or in a short time scale [53]. The presented model do predict a magnetic field with such kinds of variations because the solar wind plasma transiently (short time) changes and slowly (long time) decays its plasma density. That is, according to the presented model, the planet magnetic fields should have the two time scale variation behaviors. For the type-I planets (including the Moon), the transient changes of the fields are significant because they are directly charged from solar wind plasmas (or they get extra electrons directly from the solar wind plasmas). For the type-II planets, however, the transient changes of the fields may not be significantly affected by the variation of the solar wind parameters because they do not get extra electrons directly from the solar wind plasmas. The global field does not significantly change because it is impossible for the huge magnetosphere to follow the changes of the solar wind even with the daily and season effects.

According to the present model, the original magnetosphere is arisen due to the proposed mechanism for the unmagnetized body. The unmagnetized body collected extra electric charges from the initial solar wind and formed a strong magnetosphere. If there were no solar wind later, the originally formed magnetosphere would have not existed for such a long time because of the charge being quickly released. In fact, the solar wind only slowly becomes weak. It resists (slows) the releasing of the body charge through refilling some electric charge to the body. This refilling process is actually the current collection process of a magnetized body, which can collect extra electric current (or charge) along its field lines (or at its pole regions). Therefore the energy source of the magnetosphere (or the planet magnetic field) is the solar wind. The gravity of the body also helps to maintain the magnetosphere through trapping its particles as we have discussed above.

The present model predicts that all the solar planets (including the Earth and the Moon) are negatively charged. This conclusion is in agreement with measurements if we analyze the orientation of the magnetic field and the spin direction for each planet. On the other hand, space experiments have indicated that a spacecraft could be positively charged when it has a special environment (e.g. when it goes to a great distance) [54]. Thus if the Earth becomes positively charged due to some special solar wind conditions, the orientation of its magnetic field will be reversed. But how and in what special conditions the Earth becomes positively charged is open for further study.

By the way, it should be noted that there are really a lot of current systems in the planet's magnetosphere, such as currents on the magnetospheric boundary, magnetotail currents, the ring currents, the field-aligned currents and so on. Since any plasma current will locally form a return current in the plasma, it will not have a significant contribution to the planet's global magnetic field.

In summary, we have developed a theoretical model for the origin of the magnetic fields of planets. According to the space charging physics, we have shown that a body spinning within plasma is charged and generates a dipole magnetic field. The field intensity depends on the size, the spinning speed of the body, and the state of the ambient plasma. For a large and fast spinning body in dense and hot plasma, the generated magnetic field is big. The model predictions on the present magnetic fields of the Moon, Venus, Mars and Pluto agree with the measurements; and the relative magnetic fields of Mercury, Earth, Jupiter, Saturn, Uranus, and Neptune predicted by the present model also agree with the measured data. Furthermore, this model offers an understanding of the polarity biases and reversals of the planets' magnetic fields, and hence may provide a new possible explanation for the origin of the magnetic fields of planets.

Acknowledgement

This work was supported by the NASA research and education program (NNG04GD59G), NASA EPSCoR program (NNX07AL52A), NSF CISM program, Alabama A & M University Title III program, National Natural Science Foundation of China (G40890161), and NSF REU program (PHY-1263253 & PHY-1559870).

Submitted on June 3, 2019

References

1. Merrill R.T., McElhinny M.W., McFadden P.L. The magnetic field of the Earth (Academic Press, Inc.), 1996.
2. McFadden P.L. *et al*. Reversals of the earth's magnetic field and temporal variations of the dynamo families. *Journal of Geophysics Research*, 1991, v. 96, 3923–3933.
3. Mary C., Courtillot V.A. Three-Dimensional Representation of Geomagnetic Reversal records. *Journal of Geophysics Research*, 1993, v. 98, 22461–22475.
4. Cortini M., Barton C.C. Chaos in geomagnetic reversal records: A comparison between Earth's magnetic field data and model disk dynamo data. *Journal of Geophysics Research*, 1994, v. 99, 18021–18033.
5. Merrill R.T., McElhinny, M.W., Stevenson D.J. Evidence for long-term ,asymmetries in the Earth's magnetic field and possible implictions for

dynamo theories. *Physics of the Earth and Planetary Interiors*, 1979, v. 20, 75–82.

6. Barnett S.J. Gyromagnetic effects, theory and experiments. *Physica*, 1933, v. 13, 24–58.
7. Vestine E.H. The earth's core. *Transactions of the American Geophysics Union*, 1954, v. 35, 63–72.
8. Inglis D. R. Theories of the Earth's Magnetism. *Reviews of Modern Physics*, 1955, v. 27, 212–248.
9. Chatterjee J.S. The Crust as the Possible Seat of Earth's Magnetism. *Journal of Atmosphere and Terrestrial Physics*, 1956, v. 8, 233–239.
10. Stevenson D. Planetary magnetism. *Icarus*, 1974, v. 22, 403–415.
11. Hibberd F.H. The origin of the Earth's magnetic field. *Proceedings of Royal Society of London - Mathematical and Physical Sciences*, 1979, v. A369, 31–45.
12. Larmor J. Possible Rotational Origin of Magnetic Fields of Sun and Earth. *Electrical Review*, 1919, v. 85, 412.
13. Larmor J. How Could a Rotating Body such as the Sun become a Magnet. *Reports of British Association*, 1919, v. 87, 159–160.
14. Cowling T.G. The magnetic field of sunspots. *Monthly Notices Royal Astronomical Society*, 1933, v. 94, 39–48.
15. Elsasser W.M. Induction effects in terrestrial magnetism part I. Theory. *Physical Review*, 1946, v. 69, 106–116.
16. Bullard E.C. The magnetic field within the Earth. *Proceedings of the Royal Society of London*, 1949, v. A197, 433–453.
17. Bullard E.C., Gellman D. Homogeneous Dynamos and Terrestrial Magnetism. *Philosophical Transactions of the Royal Society of London*, 1954, v. A247, 213–278.
18. Roberts G.O. Spatially periodic dynamos, *Philosophical Transactions for the Royal Society of London*, 1970, v. A266, 535–558.
19. Roberts G.O. Dynamo action of fluid motions with two-dimensional periodicity. *Philosophical Transactions for the Royal Society of London*, 1972, v. A271, 411–454.
20. Gubbins D. Theories of the geomagnetic and solar dynamics. *Reviews of Geophysics and Space Physics*, 1974, v. 12, 137–154.
21. Bullard E.C., Gubbins D. Generation of magnetic fields by fluid motions of global scale. *Geophysical and Astrophysical Fluid Dynamics*, 1977, v. 8, 43–56.
22. Moffatt H.K. Magnetic field generation in electrically conducting fluids (Cambridge University Press, New York), 1978.
23. McFadden P.L., Merrill R.T. Inhibition and geomagnetic field reversals. *Journal of Geophysics Research*, 1993, v. 98, 6189–6199.
24. Bagenal F. in Solar System Magnetic Fields (E. R. Priest, Ed., D. Reidel Publishing Company, Holland), 1986, pp. 224–254.
25. Hessler V.P., Wescott, E.M. Correlation between Earth-current and geomagnetic disturbance. *Nature*, 1959, v. 184, 627.
26. Fleming J.A. Terrestrial Magnetism and Electricity (J. A. Fleming, Ed., Dover Publications, Inc., New York), 1949, pp. 49–58
27. Helsley C.E. Magnetic properties of lunar dust and rock samples. *Science*, 1970, v. 167, 693–695.
28. Zhang T.X. *et al.* Current collection by tethered satellite TSS-1R. Seminar Presentation at Center for Space Plasma and Aeronomic Research, 1999.
29. Zhang T.X. Solar 3He-rich events and ion acceleration in two stages. *Astrophysical Journal*, 1995, v. 449, 916–929.
30. Zhang T.X. Solar 3He-rich events and electron acceleration in two stages. *Astrophysical Journal*, 1999, v. 518, 954–964.
31. Al'pert Y.L., Gurevich A.V., Pitaevskii L.P. Space physics with artificial satellites (Consultants Bureau, Now York), 1965, 63–105.
32. Herr J. L., K. S. Hwang, and S. T. Wu, *Proceedings of the 26th AIAA Plasmadynamics and Lasers Conference* (San Diego), 1995.
33. Parker L.W., Murphy B.L. Potential buildup on an electron-emitting ionospheric satellite. *Journal of Geophysics Research*, 1967, v. 72, 1631–1636.
34. Slavin J.A., Holzer R.E. Solar wind flow about the terrestrial planets. I - Modeling bow shock position and shape. *Journal of Geophysics Research*,1981, v. 86, 11401–11418.
35. Russell C.T., Baker D.N., Slavin J.A. The magnetosphere of Mercury, in Mercury (F. Vilas, C. R. Chapman, and M. S. Matthews, Eds.,The University of Arizona Press, Tucson), 1988, pp. 514–561.
36. Colburn D.S., in The Moon (S. K. Runcorn and H. C. Urey, Eds., D. Reidel Publishing Company, Dordrecht, Holland), 1971, pp. 355–371.
37. Burgess E., Venus, an Errant Twin (Columbia University Press, New York), 1985, pp. 47–48.
38. Mutch T.A. *et al.* The Geology of Mars (Princeton University Press, New Jersey), 1978, pp. 39–40.
39. Russell C.T. The magnetic field of Mars - Mars 3 evidence re-examined, *Geophysical Research Letters*, 1978, v. 5, 81–84.
40. Russell C.T. The magnetic field of Mars - Mars 5 evidence re-examined, *Geophysical Research Letters*, 1978, v. 5, 85–88.
41. Taylor S.R. Solar system evolution: A new perspective (Cambridge Univ. Press, Cambridge U.K.), 1992, pp. 58–59.
42. Holzer T. E., in the Solar system plasma physics, V.I, (C. F. Kennel, L. J. Lanzerotti, and E. N. Parker, Eds., North-Holland Publishing Company, Amsterdam-New York-Oxford), 1979, pp. 101–176.
43. Heymann D., in The solar output and its variation (O. R. White et al. Eds., Colorado Associated University Press, Boulder), 1978, pp. 405–427.
44. Al'pert Y.L. Space plasma (Cambridge University Press, Now York), 1983.
45. Connerney J. E. P. and N. F. Ness, in Mercury (F. Vilas, C. R. Chapman, and M. S. Matthews, Eds., The University of Arizona Press, Tucson), 1988, pp. 494–513.
46. Encrenaz T., Bibring T.P., Blanc M. The solar system (Spring-Verlag Berlin Heidelberg), 1990, pp. 211–214.
47. Burgess E. Uranus and Neptune (Columbia University Press, New York), 1988, pp. 82–83.
48. Bergstralh J.T., Miner, E.D. in Uranus (J. T. Bergstralh, E. D. Miner, and M. S. Matthews Eds., The University of Arizona Press, Tucson), 1991, pp. 3–25.
49. Luhmann J.G., Russell C.T., Brace L. H., Vaisberg O.L. The Intrinsic Magnetic Field and Solar-Wind Interaction of Mars, *in Mars* (The University of Arizona Press, Tucson & London), 1992, pp. 1090–1134.
50. Russel C.T. Planetary magnetism. In *Geomagnetism*, (J. A. Jacobs ed., Orlando Academic Press), 1987, v. 2, 458–523.
51. Busse F. H. Generation planetary magnetism by convection. *Physics of the Earth and Planetary,* 1976, v. 12, 350–358.
52. Laundal K.M. Ostgaad N. Asymmetric auroral intensities in the Earth's Northern and Southern hemispheres. *Nature*, 2009, v. 460, 491–493.
53. Matsushita S., Campbell, W.H. Physics of geomagnetic phenomena (Academic Press INC., New York), 1967.
54. Whipple E.C. Potentials of surfaces in space. *Reports on Progress in Physics*, 1981, v. 44, 1197–1250.
55. Chapman S. Solar plasma geomagnetism and aurora. Gordon and Breach, Science Publishers, Inc., New York, 1964.

On the Fluid Model of the Spherically Symmetric Gravitational Field

Alexander Kritov
E-mail: alex@kritov.ru

The radial flow within the frame of analogue hydrodynamic approach to gravitational field with spherical symmetry is reviewed. Such alternative models of gravity, for example the river model of black holes and the analogue gravity, do not satisfy the continuity equation for the radial fluid flow. The presented model considers a case of incompressible fluid with non-zero source-sink field that can reconcile the continuity equation with the analogue gravity. Based on modelling of a fluid parcel's evolution with time, three cases are reviewed resulting in the Schwarzschild, the Schwarzschild-de Sitter (SdS) and the Schwarzschild-Anti de Sitter(AdS) metrics. The parameters of the model are exactly determined. The model can support a view on the de Sitter cosmology and can serve as its alternative interpretation via such hydrodynamic approach.

1 Introduction

General Relativity (GR) is a widely accepted theory of gravitation. However, in spite of its mathematical beauty and concordance with experiments, as it is well known, it also has a few difficulties: first of all, it is still problematic to merge GR with quantum mechanics; secondly, GR is not fully sufficient in explaining few observable effects in the cosmology (such as rotation curves of the galaxies); and lastly it is not a singularity-free theory. In this article an alternative approach to gravitation based on the fluid/aether model is reviewed.

Such interpretations (not dismissing GR) always existed in parallel, starting from Lenz and Sommerfeld who reported his ideas in Lectures on Theoretical Physics [12] in 1944. In the 1960s, a number of authors discussed this topic following Lenz's idea, see [10, 11]. The approach uses Special Relativity (SR) only to derive the same results as GR [3–5,7,9]. Even if this model still captures the interest of the researchers, it is not widely accepted, and usually is considered through the prism of a "heuristic" approach as it was reviewed in [13].

Such four-vector model of gravity describes a spherically symmetric gravitational field via the Lorenz invariant four-potential which are the same as the components of four-vector "aether" velocity

$$v^\alpha = \left(\frac{\phi}{c}, v^r, v^\varphi, v^\theta\right) \tag{1}$$

where ϕ is the scalar gravitational potential *, and

$$v = \sqrt{\frac{2Gm}{r}} \tag{2}$$

is the radial velocity as measured by co-moving observer given for the case of a static, non-rotating mass m without charge and $v^\varphi = v^\theta = 0$. The velocity in case of the Kerr-Newman metric is obtained in [6], and in case of the de Sitter metric is reviewed in [3]. According to such approach the curvature of spacetime is the consequence of movement of some medium (or even space itself [2]). The concept implies that *something moves and therefore space curves*, [4–6]. Due to this motion the special relativistic length contraction leads to spatial curvature in gravity and the special relativistic time dilation causes time dilation in gravitational field respectively.

The Schwarzschild metric written in the $(-+++)$ sign convention generated by radial flow is given by

$$ds^2 = -c^2\left(1 - \frac{v^2}{c^2}\right)dt^2 + \left(1 - \frac{v^2}{c^2}\right)^{-1} dr^2 + r^2\, d\Omega^2 \tag{3}$$

where $d\Omega^2 = \sin^2\theta\, d\phi^2 + d\theta^2$ and the coordinate velocity is given by (2). Even if such model fully suffices to describe all effects of GR, it has two drawbacks: first, it is based on the abstract concept of moving space and does not hypothesize about the nature of what moves. It should be *something* that moves instead of nothing. Secondly, it is applicable to spherically symmetrical fields only. The second point is not as solid as the first one, because most of the objects in the universe demonstrate spherical symmetry, especially in the physics of elementary particles where the phenomena of gravitation originates.

2 The analogue gravity and its problem with the hydrodynamic continuity equation

Though, even if the ideas for a fluid theory of the gravitation were reported before [16], recently, as a continuation and generalization of such approach, the analogue gravity model was proposed [1, 14, 15]. It is based explicitly on *fluid hydrodynamics*, and it uses the acoustic metric for a moving fluid in general form (not only for spherically symmetric case) as

$$g^{\mu\nu} = \frac{\rho}{c}\begin{bmatrix} -\left(c^2 - v^2\right) & \vdots & -v^j \\ \cdots\cdots & . & \cdots\cdots \\ -v^i & \vdots & \delta^{ij} \end{bmatrix}. \tag{4}$$

*For example, the reader may check that such effective potential given by $(v_0 c)$ (its second term of the Taylor series) leads to the correction of Newtonian potential and to the same result for the anomalous perihelion precession of Mercury as GR.

In spherically symmetric case it suggests that density of the fluid should change as $r^{-3/2}$ and therefore the conformal factor appears as in the acoustic metric as

$$ds^2 \propto r^{-3/2}\left[-c^2\left(1-\frac{v^2}{c^2}\right)dt^2+ \right. \\ \left. +\left(1-\frac{v^2}{c^2}\right)^{-1}dr^2+r^2d\Omega^2\right]. \tag{5}$$

Then it creates an issue for the metric itself. The suggested workaround [1] is to represent the fluid density as perturbation $\rho=\rho_0+\rho'$ i.e. as linearized fluctuations around the background value. This is good to model the metric in approximation but again the first term does not satisfy the continuity equation.

It should be noted that such value for the velocity (2) in the frame of the fluid analogue model of gravity is not derived from any hydrodynamic equation. Moreover the inflow through the sphere of radius r as $4\pi r^2 b = r^{3/2}$ is clearly incompatible with the continuity equation. The presented approach suggests to resolve the conformal factor problem in the analogue gravity by conjecturing the fluid's *constant density* and sink-source term in the continuity equation which represents an evolution of fluid parcel's volume with time in the Lagrangian frame .

3 The continuity equation for the model

Let's consider an ideal inviscid isentropic fluid. In Lagrangian co-moving frame of reference the use of relativistic equation of the continuity is not *required* and also because, as discussed in [4], the metric in the co-moving frame is flat. In case of presence of sink-source term the equation of continuity in Lagrangian frame is

$$\frac{\partial\rho}{\partial t}+\rho\nabla\cdot(\vec{v})=\sigma \tag{6}$$

where σ is the sink-source term. In case of constant density ρ_0 it reduces to

$$\nabla\cdot(\vec{v})=\frac{\sigma}{\rho_0}=\frac{\partial\dot{V}}{\partial V} \tag{7}$$

where the rate of volume production per time within a control volume was denoted as $\dot{V}$. Let's now consider the spherically symmetric case and take some volume with radius r. Using the Gauss-Ostrogradsky theorem then

$$4\pi r^2 v(r)=\dot{V}(r)=\frac{1}{\rho_0}\int_0^r\sigma(r)4\pi r^2 dr \tag{8}$$

where $\dot{V}$ represents the total volume integral of sink-sources σ within a sphere of radius r. So the radial velocity can be obtained from (8) as

$$v(r)=\frac{\dot{V}}{4\pi r^2}. \tag{9}$$

In (9) the rate of volume production is a function of time in Lagrangian frame $\dot{V}(t)$, or in Eulerian frame is a function of only radial distance $\dot{V}(r)$ respectively, and the flow is stationary.

It is important to make note on a sign of the velocity (2). The approach is valid for both – for positive and negative values of the velocity (2) because it comes to the metric (3) as squared value. Many authors treat the river model of gravity with radial flow going in inward direction to the center of gravity. However, in the present model it is considered opposite – the outward flow of the fluid and the positive sign for velocity (placing coordinate center at the point mass) which means that the flow is decelerated going from the point mass center and has also negative acceleration.

4 The linear model, the Schwarzschild metric

Let's now consider the point mass m and the spherical coordinate center is placed in m. The point mass m emits the volume parcels V_n of the fluid at some constant rate ω_m with initial position $r=0$ and time $t=0$. The parameter ω_m is denoted in such way because of an assumption that it depends on the property of point mass itself or even may be linearly proportional to the value of point mass m. So every time interval

$$\Delta t = 1/\omega_m, \tag{10}$$

one n^{th} parcel of the fluid V_n appears near the point m and no initial velocity is considered. Following the above, let's assume that every parcel V_n further grows linearly with time in its respective Lagrangian frame as *

$$V_n=\omega V_0 t \tag{11}$$

where $V_0=m_0\rho_0$ and ω are some external constants which do not depend on the property of point mass, and ω is in the same way linearly proportional to a parameter m_0. Then the total number of produced parcels during time t is

$$n=\omega_m t. \tag{12}$$

So, the volume of n^{th} parcel in row is given by

$$V_n=\frac{\omega}{\omega_m}V_0 n. \tag{13}$$

Importantly, time in Lagrangian frame (local co-moving frame of every fluid's parcel) is synchronized with time of the observer resting at infinity (see [5] for more details on this). So, the time interval given by (10) is the same in the co-moving frame of parcel as well as in the reference frame of point mass.

In order to find $\dot{V}$ within a sphere of some fixed radius r, first a total volume produced by sum of all such parcels has

*For simplicity one can imagine the emitted volume parcels V_n as growing spherical bubbles, though fluid parcels have no actual form.

to be defined. Summation of (13) yields

$$V(t) = \sum_{1}^{n} V_n = \frac{\omega}{\omega_m} V_0 \frac{n^2}{2} = \frac{1}{2}\,\omega_m \omega V_0 t^2 \qquad (14)$$

where an approximation that $n \approx n+1$ for a relatively big number of parcels was used. Taking time derivative and substituting into (9) leads to

$$v = \frac{dr}{dt} = \frac{\omega_m \omega V_0 t}{4\pi r^2}\,. \qquad (15)$$

Solving this differential equation for $r(t)$ one can find the equation of motion for the fluid as

$$r(t) = \left(\frac{3\omega_m \omega V_0 t^2}{8\pi} + c_1\right)^{1/3} \qquad (16)$$

where c_1 is an arbitrary constant and represents initial position of parcel at time $t = 0$ which has to be zero, so c_1 is zeroed. Expressing $t(r)$ from (16) and substituting this into the original equation (15) results in the fluid velocity $v(r)$ in Lagrangian frame as

$$v = \frac{dr}{dt} = \left(\frac{1}{6\pi}\frac{\omega_m \omega V_0}{r}\right)^{1/2}\,. \qquad (17)$$

So as a result, the radial velocity is inversely proportional to the square root of the radial distance as (2), which reproduces the Schwarzschild metric. But still, the unknown parameters in the expression are to be determined.

The fluid acceleration is

$$\frac{dv}{dt} = \frac{\partial v}{\partial t} + (v\nabla)\,v\,. \qquad (18)$$

For a stationary radial flow the acceleration is given only by the convective term, therefore

$$a = \nabla\left(\frac{v^2}{2}\right) = -\frac{1}{12\pi}\frac{\omega_m \omega V_0}{r^2}\,. \qquad (19)$$

This acceleration is negative for the positive value of the velocity (17), and as the coordinate center was placed in the center of mass m, it means that the flow is decelerated in outward direction. However, as it was noted above, the corresponding metric (3) remains the same regardless of the velocity sign.

5 The volume conversion relation and the uncertainty principle

Let's introduce the volume V_m such as

$$V_m = \frac{m}{\rho_0} \qquad (20)$$

where m is the mass of the point source. And let's assume that ω_m represents de Broglie wave frequency of the mass m, and m_0 is given by the uncertainty principle with rigorous factor of two (where it originates because of the non-commutativity of the quantum operators [8]) as

$$m_0 c^2 = \rho_0 V_0 = \frac{1}{2}\,\hbar\omega\,. \qquad (21)$$

This means that the fluid parcel's mass m_0 is not observable during the time ω^{-1}. Then

$$V_m \omega = 2\omega_m V_0\,. \qquad (22)$$

Further this expression will be referred as the volume conversion relation with the exact factor of two. Therefore (17) becomes

$$v = \left(\frac{\omega^2}{12\pi\rho_0}\frac{m}{r}\right)^{1/2}\,. \qquad (23)$$

Regarding the mass-energy conservation, the point mass m does not act as actual source studied in classical fluid dynamics, because at time $t = 0$ an outgoing parcel has zero volume $V_n = 0$ and zero mass accordingly, therefore there is no actual mass flow from the point mass m. The linear mass growth of a parcel is also governed by the uncertainty principle and it is not observable during the time ω^{-1}.

6 The hyperbolic model, the SdS metric

Presumably the linear dependency of $V_n(t)$ in the model above can be just an approximation of some unknown odd function and the linear function of t in (11) represents just a first term of its Taylor series. Choosing to test the hyperbolic sine one may assume that V_n changes with time in its respective Lagrangian frame as

$$V_n = V_0 \sinh(\omega t)\,. \qquad (24)$$

Considering that time in co-moving frame of parcel now is not synchronized with time running at the clock of the observer at rest at infinity, but the time coordinate transform is given by

$$t' = \frac{1}{\omega}\sinh(\omega t) \qquad (25)$$

where t' is proper time in co-moving parcel's frame.

Following the same procedure, as in the previous model, the total number of produced fluid parcels during time t is given by (12). And the volume of n^{th} parcel in row is given by

$$V_n = V_0 \sinh\left(\frac{\omega}{\omega_m} n\right)\,. \qquad (26)$$

The sum of all such parcels provides the total volume produced by time t as

$$V(t) = \sum_{1}^{n} V_n = V_0 \frac{\sinh^2\left(\frac{n}{2}\frac{\omega}{\omega_m}\right)}{\sinh\left(\frac{1}{2}\frac{\omega}{\omega_m}\right)} \qquad (27)$$

where $n \approx n+1$ for a relatively big number of parcels. The value of $\sinh\left(\frac{1}{2}\frac{\omega}{\omega_m}\right)$ is very small and can be easily approximated without a loss of precision as $\frac{1}{2}\frac{\omega}{\omega_m}$ *. Then, using trigonometric identity and t instead of n let's rewrite (27) in simpler form as

$$V(t) = \frac{\omega_m V_0}{\omega}\left(\cosh(\omega t) + 1\right) \tag{28}$$

where factor $1/2$ disappears because of the trigonometric conversion. Taking time derivative and using the volume conversion relation (22) it becomes

$$\dot{V} = \frac{1}{2}\,\omega V_m \sinh(\omega t)\,. \tag{29}$$

With the use of (9) the differential equation is

$$v = \frac{dr(t)}{dt} = \frac{\omega V_m \sinh(\omega t)}{8\pi r(t)^2}\,. \tag{30}$$

Solution for $r(t)$ provides the equation of motion as

$$r(t) = \left({r_0}^3 + \frac{3V_m \cosh(\omega t)}{8\pi}\right)^{1/3}\,. \tag{31}$$

Applying boundary condition as $r = 0$ when $t = 0$ the equation of motion becomes simply

$$r(t) = \left(\frac{3V_m}{8\pi}\right)^{1/3}\left(\cosh(\omega t) - 1\right)^{1/3}\,. \tag{32}$$

Expressing the hyperbolic sine from this and then substituting it into (30) leads to

$$v(r) = \left(\frac{V_m\omega^2}{12\pi r} + \frac{\omega^2 r^2}{9}\right)^{1/2} \tag{33}$$

or with use of the definition of V_m (20) the resulting radial velocity is

$$v(r) = \left(\frac{\omega^2}{12\pi\rho_0}\frac{m}{r} + \frac{\omega^2 r^2}{9}\right)^{1/2}\,. \tag{34}$$

So the hyperbolic model leads to the same radial velocity as in the previous model (23), but with the additional term. Using (18) the fluid acceleration is

$$a = -\frac{\omega^2}{24\pi\rho_0}\frac{m}{r^2} + \frac{\omega^2 r}{9}\,. \tag{35}$$

7 Determination of the model parameters

The association of the first term in (35) with Newtonian gravitational acceleration allows expressing the value for fluid density via ω as

$$\rho_0 = \frac{\omega^2}{24\pi G}\,. \tag{36}$$

*For example for the proton mass such approximation would give an error of order less than 10^{-40}.

Then substituting ω from this into the second term of (35) gives the repulsive acceleration as

$$a_{rep} = \frac{8\pi}{3}\rho_0 G r\,. \tag{37}$$

This term can be also treated as the Newtonian gravitational force from uniformly distributed mass that has the equation of state $p = -\rho c^2$ and satisfies stress-energy equivalent

$$\rho_0 + \sum_i \frac{p_i}{c^2} = -2\rho_0 \tag{38}$$

as given in [13, see the expressions (45–46)]. Assuming the constant density ρ_0 (36) is equal to the critical density, the value for ω can be defined via the Hubble constant as

$$\omega = 3H\,. \tag{39}$$

And the repulsive acceleration as given by (35) is

$$a_{rep} = H^2 r = \frac{c^2\Lambda}{3}r\,. \tag{40}$$

The radial velocity of the fluid (34) based on (3) and using (39) leads to

$$\begin{aligned} ds^2 = &-\left(1 - \frac{2Gm}{c^2 r} - \frac{H^2 r^2}{c^2}\right)c^2 dt^2 + \\ &+ \left(1 - \frac{2Gm}{c^2 r} - \frac{H^2 r^2}{c^2}\right)^{-1} dr^2 + r^2 d\Omega^2 \end{aligned} \tag{41}$$

that corresponds to the Schwarzschild-de Sitter metric for the hyperbolic model.

8 The harmonic model, the Schwarzschild-AdS metric

Using the sine function in (25) which could be treated as a simple harmonic oscillation of a fluid parcel volume $V_n(t)$. Following the same procedure (substituting sinh() with sin() instead) it is easy to see that the result would be the same as it was in previous model (34) but with a difference in sign of the second term

$$v(r) = \left(\frac{\omega^2}{12\pi\rho_0}\frac{m}{r} - \frac{\omega^2 r^2}{9}\right)^{1/2} \tag{42}$$

which with the use of (39) and (3) obviously leads to the Schwarzschild-Anti de Sitter metric.

9 Conclusions

The model results in full accordance with known metrics with exact accuracy by the coefficients based on assumptions of the volume conversion equation (22) and of the equality of the fluid density to the critical density value. The forces, the Newtonian gravitational and the repulsive cosmological, both

appear natively in the hyperbolic model. Therefore the model may support a view on applicability of the static de Sitter metric for cosmology. In presented approach the de Sitter Universe is also empty in the sense that the mass of the matter is attributed to the medium with constant density ρ_0. While the matter objects may reside statically at the fixed coordinates of the metrics (41), the space-time curvature (resulting in both attractive gravitation and repulsion) originates in a motion of the medium. The equation of state and the stress-energy of such fluid were suggested (38). However, one should be cautious to apply GR for further analysis of the solutions, because only Special Relativity is considered in the frame of the present approach.

The fluid parcels can be treated as virtual particles emitted by an elementary particle with the constant rate given by the de Broglie frequency, and on the other hand they can be considered as "growing bubbles of space". An individual parcel is not observable during the cosmological time, and its mass and volume are constrained by the uncertainty principle as shown.

The evolution of parcel's volume with time was modelled by odd functions. The odd functions have property of being asymmetric under time-reversal transformation. The requirement for such time asymmetry to generate velocities applicable to describe different metrics for gravitational field could be a topic for future study. Further analysis is required on finite boundary conditions (when a fluid parcel originates at time $t = 0$ at finite radius) and on corresponding event horizons. The temporal coordinate transform (25) as a base of the hyperbolic model, a possible correspondence of the cosmological scale factor to the proposed volume increase require further analysis.

Received on May 17, 2019

References

1. Barcelo C., Liberati S., Visser M. Analogue Gravity. arXiv: gr-qc/0505065.
2. Braeck S., Gron O. A river model of space. arXiv: gr-qc/1204.0419.
3. Cuzinatto Z. Z., Pimentel B. M., Pompeia P. J. Schwarzschild and de Sitter solution from the argument by Lenz and Sommerfeld. *American Journal of Physics*, 79:662, 2011. arXiv: gr-qc/1009.3249.
4. Czerniawski J. What is wrong with Schwarzschild's coordinates. arXiv: gr-qc/0201037.
5. Czerniawski J. The possibility of a simple derivation of the Schwarzschild metric. arXiv: gr-qc/0611104.
6. Hamilton A. J. S., Lisle J. P. The river model of black holes. *American Journal of Physics*, 2008, v. 76, 519–532. arXiv: gr-qc/0411060.
7. Kassner K. A physics-first approach to the Schwarzschild metric. *Advanced Studies in Theoretical Physics*, 2017, v. 11 (4), 179–212. arXiv: gr-qc/1602.08309.
8. Robertson H. P. The Uncertainty Principle. *Physical Review*, 1929, v. 32, 163–164.
9. Rowlands P. A simple approach to the experimental consequences of general relativity. *Physics Education*, 1999, v. 32 (1), 49.
10. Sacks W. M, Ball J. A. Simple Derivation of the Schwarzschild Metric. *American Journal of Physics*, 1968, v. 36, 240.
11. Shiff L. I. On Experimental Tests of the General Theory of Relativity. *American Journal of Physics*, 1960, v. 28, 340.
12. Sommerfeld A. Electrodynamics. Lectures on Theoretical Physics, Vol. III, Academic Press, New York, 1952.
13. Visser M. Heuristic Approach to the Schwarzschild Geometry. arXiv: gr-qc/0309072.
14. Visser M. Acoustic Propagation in Fluids: An Unexpected Example of Lorezian Geometry. arXiv: gr-qc/9311028.
15. Weinfurtner S. Emergent Spacetimes. arXiv: gr-qc/0711.4416v1.
16. Winterberg F. Vector Theory of Gravity with Substratum. *Zeitschrift für Naturforschung A*, 1988, v. 43 (4), 369–384.

GR = QM: Revealing the Common Origin for Gravitation and Quantum Mechanics via a Feedback Signal Approach to Fundamental Particle Behavior

Franklin Potter

8642 Marvale Drive, Huntington Beach, CA 92646 USA. E-mail: frank11hb@yahoo.com

By allowing the fundamental particles of the Standard Model to communicate via "feedback signals" within a vacuum lattice of mathematical nodes at the Planck scale, one learns that this approach toward understanding fundamental physics reveals the surprising common origin of quantum mechanics and of general relativity. This "feedback signal" approach is shown to be equivalent to the path integral approach but also the underlying reason for its success.

1 Introduction

The $GR = QM$ in the title refers to a recent suggestion [1] that perhaps the long-standing theoretical conflict between general relativity and quantum mechanics is not insurmountable. In fact, the conjecture has been that they may actually be closely related, or at least they could have the same fundamental origin.

Herein I establish the common fundamental origin for gravitation and quantum mechanics. A non-traditional approach to fundamental particle behavior is required, one that agrees with the successful effective Standard Model (SM) of leptons and quarks [2] but treats these particles as harmonic oscillators emitting and receiving scalar waves at their Compton frequencies [3]. A fundamental particle, such as an electron, communicates with the surrounding discrete vacuum lattice of mathematical nodes via these scalar "feedback signals". Therefore, a particle itself actively determines its subsequent behavior even in the absence of the SM local gauge fields.

The surprising result is that the common origin of quantum mechanics and of general relativity arises directly by simply analyzing particle behavior in sufficient geometrical detail.

2 A brief particle physics review

In this section I offer a brief review of some of the physics consequences if one considers both the internal symmetry space for defining the particle states of the SM and our (3+1)-D spacetime to be discrete spaces. Such possibilities may be necessary in order to justify (1) treating the internal symmetry space and spacetime as C^2 unitary space lattices of mathematical nodes and (2) proposing the leptons, hadrons, and electroweak (EW) bosons to be 3-D particles behaving as harmonic oscillators. If one chooses to accept these concepts outright, one can skip forward to Section 3 for the details of the feedback signal approach.

Recall that the SM describes the known local gauge interactions, color and electroweak, via its $SU(3)_C$ x $SU(2)_L$ x $U(1)_Y$ lagrangian, so I will ignore these gauge interactions in the discussion ahead. The leptons, the hadrons formed from quarks and gluons, and the EW interaction bosons $W^{\pm}$, Z^0, and γ, are the fundamental particles defined [2] in the internal symmetry space whose behavior in spacetime will be explained in terms of the feedback signal approach. That is, I am treating these three categories of fundamental particles as 3-D objects and not as point particles. The justification is provided below.

The proposed feedback signal approach can only be self-consistent if each fundamental fermion, i.e., lepton or quark, "gathers in" the immediate surrounding lattice nodes in its own unique way. That is, I assume that (3+1)-D spacetime is a discrete lattice of mathematical nodes, and a particle's collection of lattice nodes, perhaps at the Planck scale, must have a different discrete rotational symmetry for each different fundamental fermion family. These assumptions are in contrast to the same SU(2) point particle continuous symmetries for each family in the traditional interpretation of the SM.

Specifically, one finds that only discrete symmetry binary subgroups of the unit quaternion group Q, which is equivalent to SU(2), suffice, with each binary subgroup of Q having two EW isospin $\pm\frac{1}{2}$ states in each fermion family. Therefore, being binary subgroups of Q, and of SU(2) x U(1), all the mathematical machinery of the SM remains valid. Moreover, the important left-handed fermion state preference for the weak interaction is dictated by the mathematical properties of the quaternion multiplications for the weak interaction.

I have identified 3 discrete symmetry binary subgroups of Q that define the 3 physical lepton families [4–6]. They are these specific 3 binary subgroups acting in the R^3 subspace of C^2: the [332] binary subgroup for the electron family; the [432] binary subgroup for the muon family; and the [532] binary subgroup for the tau family. They are known also as the binary tetrahedral group 2T, the binary octahedral group 2O, and the binary icosahedral group 2I, respectively, and correspond to special discrete binary rotations of 3-D objects called regular polyhedrons in the 3-D real space R^3. No more lepton families are predicted because there are no more binary subgroups of Q that require a 3-D space.

The fact that Nature agrees with the 3 lepton families representing these 3 binary subgroups of Q is verified by the

first principles derivation [6, 7] of the neutrino PMNS mixing angles from their three quaternion generators by collectively mimicking the SU(2) generators, i.e., the three Pauli generators. The empirical values of the lepton mixing angles now agree within 1σ to each of these theoretical absolute values: $\theta_{12} = 34.281°$, $\theta_{23} = 42.859°$, $\theta_{13} = 8.578°$. Conceptually, this EW flavor state mixing to produce the mass states occurs because a valid renormalizable conformal field theory requires a continuous symmetry such as in the lagrangian of the SM. This lepton family mixing therefore guarantees that the 3 discrete symmetry binary subgroups defining the lepton families collectively behave as the SU(2) of the SM.

I have identified also 4 related discrete symmetry binary subgroups [4, 5, 8] that define four 4-D quark families in R^4: [333], [433], [343], and [533], corresponding to the only regular polytopes in R^4. The mathematical and physical consequences of these discrete symmetry groups for 4 quark families are discussed in Appendix A. The 4-D quarks and 4-D gluons combine according to QCD to form the 3-D hadrons, the baryons and mesons, or one can use intersection theory to establish the same results.

Note that the 3-D lepton states in R^3 and the 4-D quark states in R^4 both fit into the proposed 2-D unitary space C^2. Our (3+1)-D spacetime for discussing the particle bahavior also fits into C^2. I am assuming that the two spaces, the internal symmetry space for particle definition and spacetime for the physics behavior join together seamlessly. Therefore, this $C^2 = R^4$ space is proposed to be the one I need to consider to be discrete and composed of mathematical nodes. The nodes are equally spaced on average at the Planck scale when no fundamental particles are in existence.

Each fermion family with its own unique discrete symmetry binary subgroup has two Q or SU(2) orthogonal $\pm\frac{1}{2}$ states, but they will be mass-energy degenerate unless they form the two new physical orthogonal states of different energies as dictated by QM. Therefore, each lepton and each quark family has two weak isospin flavor states that have different mass values with a characteristic oscillation occurring between the two original mathematical states at the Compton frequency and Compton wavelength

$$\omega_C = \frac{mc^2}{\hbar}, \quad \lambda_C = \frac{h}{mc}. \tag{1}$$

For the electron, its Compton values are $\omega_C \approx 7.8 \text{ x } 10^{20}$ Hz and $\lambda_C \approx 2.4 \text{ x } 10^{-12}$ meters. Therefore, the Compton wavelength of each fundamental particle will be many orders of magnitude larger than the Planck distance of about 10^{-35} meters. Consequently, the proposed vacuum lattice structure of nodes appears to be a continuous space for the fundamental particles.

Although the effective SM lagrangian has the continuous symmetry local gauge group $SU(3)_C \text{ x } SU(2)_L \text{ x } U(1)_Y$, addons called horizontal discrete symmetry groups are now becoming acceptable alternatives for defining the lepton family states, particularly with the advent of neutrino mixing and non-zero neutrino mass states [2]. However, the discrete symmetry binary subgroups of the unit quaternion group Q that I have proposed for the leptons and quarks retain the successful predictions of the SM without the need to introduce any additional horizontal discrete symmetries to its lagrangian.

That is, all the successes of the SM have been retained by my specific discrete symmetry approach for the fermions while the geometrical sources of some of its physical properties have been elucidated. I cannot overemphasize this retention of the SM mathematical and physical properties, with perhaps the SM being a useful approximation even down to the Planck scale.

The above brief review of my discrete symmetry approach to the SM has been included in order to introduce some of the mathematical connections that propose some unconfirmed physics possibilities and also to justify using a discrete spacetime of mathematical nodes as both the origin of the fundamental fermions of the SM and as an active participant in their physical behavior. I will show how this approach leads directly to the special theory of relativity (STR), path integrals, quantum mechanics (QM), and the general theory of relativity (GTR), as explained in the discussion ahead.

3 The feedback signal approach

Spacetime itself at the Planck scale of about 10^{-35} meters could be a discrete space described by a uniform lattice of mathematical nodes. Therefore, I assume that our physical (3+1)-D spacetime agrees with a uniform lattice in the unitary space C^2 (or equivalently R^4) at or near the Planck scale and that each fundamental lepton family forms its particle states by "gathering in" lattice nodes to form its own unique discrete symmetry 3-D objects. This "gathering in" process distorts the lattice locally with the amount of lattice distortion extending outward in a decreasing manner with increasing distance, i.e., as inverse distance.

If I assume that the undistorted, uniformly spaced lattice has no net energy density, then the positive mass-energy of a fundamental particle is related to the amount of lattice distortion in some yet-to-be-determined way. I expect this mass-energy to be balanced by an equal negative energy value that retains the overall net zero energy total even for the distorted lattice. Perhaps the increased "stretch distance" between the nodes outside the particle definition volume provides negative energy that is the balancing factor for an assumed zero total energy for the Universe.

Recall that Clifford algebra and Bott periodicity [9] dictate a conjugate $R^4 = C^2$ space. In this conjugate space for anti-particles, the same mathematical properties of the uniformly spaced lattice would apply, again producing a positive mass-energy for the anti-particle states.

Each fundamental particle oscillating at its characteris-

tic frequency, its Compton frequency ω_C, is proposed to be emitting scalar waves, call them "feedback signals", into the surrounding vacuum lattice to eventually reach everywhere. The particle source could be undergoing "breathing mode" oscillations and emitting spherical waves isotropically into its environment. One must not identify these oscillations with electromagnetic waves because they are just propagating lattice distortions that allow lattice nodes to communicate with their nearest neighbors.

According to the special theory of relativity (STR), there exists a limiting speed for mass-energy transfer. I will take this maximum speed to be c, the speed of light in a vacuum, although there could be a higher speed limit if some day a photon is determined to possess a very tiny mass value.

Let a particle oscillate at its Compton frequency

$$\omega_C = \frac{mc^2}{\hbar}, \tag{2}$$

with m the particle's mass value, c the speed of light in a vacuum, and $\hbar$ being Planck's constant divided by 2π.

The feedback signals obey the standard scalar wave equation, a hyperbolic partial differential equation in three spatial variables x, y, z, and one time variable t. Its scalar function u(x,y,z,t) obeys

$$\nabla^2 u - \frac{\partial^2 u}{c^2 \partial t^2} = 0. \tag{3}$$

Solutions of this equation for spherical symmetry have no angular dependence, so the feedback signal amplitude u(r,t) depends only upon the radial distance according to

$$\left(\frac{\partial^2}{\partial r^2} + \frac{2}{r}\frac{\partial}{\partial r} - \frac{\partial^2}{c^2 \partial t^2} \right) u(r,t) = 0. \tag{4}$$

The solutions for a single frequency ω have the form

$$u(r,t) = \frac{A}{r} e^{i(\omega t \pm kr)} \tag{5}$$

where the wavenumber k = ω/c and the peak intensity I(r) = $|A|^2/r^2$, i.e., the inverse square dependence.

This feedback signal approach requires the fundamental particle to behave as a microscopic 'antenna' moving within and communicating with the lattice and with other particles via its feedback signals. For example, the electron oscillating at ω_C = 7.77 x 10^{20} Hz disturbs the surrounding lattice at the same frequency ω_C, and this oscillatory disturbance propagates radially outward in all directions at speed c. By treating the particle as an antenna, the particle not only emits its feedback signals but also can absorb its own feedback signals returning from scatterings in the lattice environment.

I can describe the electron's oscillation in more detail. Although I have its oscillations only at the Compton frequency ω_C, such ideal behavior cannot be maintained once signals return from the environment, even when the electron is at rest. There will exist a small spread in frequency values about its Compton frequency according to Fourier analysis. Therefore, a Q value can be assigned to represent the small spread in frequency values, just as for any other harmonic oscillator. The signal emissions have a small spread in frequencies also, but for simplicity I will ignore this property unless needed for clarification purposes. Therefore, I will continue to use a single characteristic Compton frequency ω_C even though we understand that the oscillator does not have an infinite Q value.

The lattice nodes act as a *transponder* to the feedback signals, absorbing and immediately emitting them equally in all directions for all frequencies, all amplitudes, and with no phase shift. That is, each small volume element in the lattice must absorb some of the incident feedback signals and then emit immediately the feedback signals at the original frequency into all directions isotropically. One can think of a single lattice node or of a specific collection of lattice nodes acting together as a transponder, but considering the same type of transponder everywhere for simplicity.

If one wishes to introduce a non-zero phase shift at each transponder, then a simple modification could be to have the phase shift value be the same for all the transponders and be independent of the feedback signal frequency. Either constraint can be eliminated for a more complicated vacuum lattice. I have chosen the simplest assumption of no phase shift and equal response for all frequencies and amplitudes.

I had initially allowed the feedback signals to have an arbitrary velocity v_0. However, I learned that if one lets the speed of the feedback signals $v_0 = c$, the speed of light in a vacuum, then this simple feedback signal approach permits the direct derivation of the phenomena and equations of special relativity, general relativity, and quantum mechanics, with all of them agreeing with the present theories. The biggest surprise occurred when I learned that general relativity and quantum mechanics would then have the same fundamental origin.

In the sections ahead I will use many parts of my original 1982 attempt toward establishing this feedback signal approach as a viable approach but with some added updates here and there to provide a 21st century perspective. The identification of the gravitational interaction is one recent addition.

4 Single particle behavior at uniform velocity

Let a lone fundamental particle, such as a single electron in the Universe, be a 3-D physical harmonic oscillator oscillating at its Compton frequency ω_C with its antenna-like behavior emitting its feedback signal oscillations into the surrounding discrete lattice of uniformly spaced mathematical nodes, perhaps separated by the Planck distance of about 10^{-35} meters. As far as the electron is concerned, with its Compton wavelength of about 2.4 x 10^{-12} meters, the lattice appears to be continuous. Likewise for all other particles composed of leptons and of quarks, i.e., the hadrons, as well as the interaction bosons of the SM.

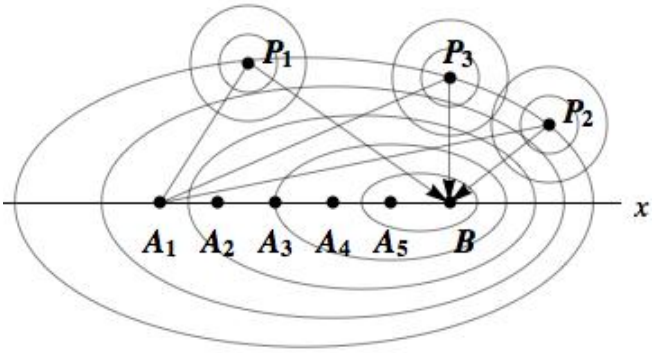

Fig. 1: Feedback signals are emitted by an electron at its previous successive equal-phase positions A_i. P_1 and P_2 are two of numerous transponders in the surrounding 3-D space on equal-phase ellipsoids for the signals from electron position A_1 only. This uniform velocity electron has moved forward at $0.866c$ to B where the returning feedback signals define its present location.

Either way, having a discrete space or a continuous space, the oscillations of the particle will appear as feedback signals traveling in the surrounding space R^3 (the subspace of R^4 and C^2) and progress through the space at the constant velocity c with decreasing amplitude as the radial distance from the particle increases. Why require a decreasing amplitude? Because we must consider the concept of energy conservation associated with these outgoing and incoming feedback signals.

For simplicity only, I ignore at first the "permanent" space distortion of the lattice caused by the formation and presence of each fundamental particle. Therefore, the feedback signals propagate through a lattice in which the average lattice node spacings remain the same separation distance everywhere. Later on I will remove this restriction in order to discuss gravitational effects between two fundamental particles.

Both a coordinate space and a momentum space description of this feedback signal approach is considered. Single particle behavior in coordinate space is shown in Fig. 1. If the electron had been at rest, then all the positions A_i and position B would coincide and the ellipses would be circles centered at B to exhibit the spherical symmetry. However, this electron has been moving at a uniform velocity in the +x direction and is now at location B receiving feedback signals from the transponders P_i everywhere in space. The surrounding ellipsoids are equal-phase locations for the outgoing feedback signals emitted by the electron at previous equally-spaced successive electron positions A_i for $i = 1,2,3,4,5$.

In this lab frame as the electron moves by, the diagram shows three feedback signal rays, from A_1 to P_1 to B, from A_1 to P_2 to B, and from A_1 to P_3 to B, of equal total length that have feedback signals arriving at B exactly in-phase with the particle oscillation when the particle arrives at B. These rays are a few examples of the feedback signals that have been emitted isotropically into 4π solid angle by the particle when at A_1.

Only a specific subset of all the equal-phase ellipsoids are shown in Fig. 1. Note also that each larger ellipsoid represents a lesser signal amplitude at the transponders along the ellipsoid, being a further distance away from the source, and that all feedback signals returning from the same 3-D ellipsoid have identical amplitudes and phases because their total path distances are equal. Because the transponders in space are everywhere, all emitted signals will eventually reach one of them. I will later explain how all the multiple scattering paths from the A_i to B are related to the path integral concept considered by R.P. Feynman in his approach to quantum mechanics and classical mechanics [10].

If the particle has just come into existence, then the signals will have not reached very far into the surrounding space. In almost all practical cases the particle has existed for a time long enough so that the signals will have permeated to tremendous distances and an approximate steady-state condition will have been established, with the outgoing and incoming signal amplitude totals approximately matching at the particle's new location B.

Recall that I have chosen no phase delay for the transponders. Incoming feedback signals to the transponder from any direction are immediately emitted into all directions. Their spherically symmetrical emission pattern, shown at each P_i, assumes that all space locations, and therefore all transponders, are identical, behave identically, and will "scatter" feedback signals. This ideal transponder behavior is the simplest possible for determining the subsequent behavior of the particle.

5 Frequency shifted feedback signals

The feedback signals sent forward and backward along the electron's velocity (momentum) vector in the x-direction experience frequency shifts. Signals sent in the forward direction with frequency ω_C return from those transponders at a higher frequency $\omega_C + \Delta\omega$ because the moving particle encounters the equally-spaced equal-phase maximum signal amplitudes at shorter time intervals than when the particle is at rest. That is, these returning signals at frequency $\omega_C + \Delta\omega$ are blue-shifted according to the relativistic Doppler expression

$$\omega' = \omega_C + \Delta\omega = \sqrt{\frac{1 + v/c}{1 - v/c}}\,\omega_C. \qquad (6)$$

And those feedback signals returning from transponders in the backward direction are red-shifted to the lower frequency by taking the opposite sign of the electron's velocity v.

One important consequence of this feedback signal approach is that a steady-state equilibrium can be maintained for the electron moving at a constant velocity. There is symmetric behavior in the two coordinate directions perpendicu-

lar to the velocity direction but a constant asymmetric reach in the x-direction of motion. For example, in Fig. 1 consider the outermost ellipsoid scattering the feedback signals emitted from position A_1. The backward sampling distance for a particular ellipsoid is shorter than the forward sampling distance in the environment.

In the steady-state condition for a single electron in the universe, the returning signals from all directions should not change the electron's constant velocity because there is no amplitude change in any of the returning signals, and their phases from all directions agree at the new electron position B. If there were no frequency shifts in the x-component of the feedback signal frequencies, then one might calculate the contributions by either of two methods: (1) adding up the returning signals from the rear and from the front by considering cones of equal solid angles on opposite sides of B and using elliptic functions of the second kind, or (2) adding up the returning signals along a line through B at any angle θ with respect to the velocity vector direction. Using the second method, one would add contributions along a line at angle θ to achieve

$$-\sqrt{\frac{1 + v\cos\theta_f/c}{1 - v\cos\theta_f/c}}\,\nu + \sqrt{\frac{1 - v\cos\theta_b/c}{1 + v\cos\theta_b/c}}\,\nu = 0, \qquad (7)$$

where the first term represents signals returning from the forward direction at angle θ_f and the second term returning signals from the back at angle θ_b. Because one can constrain $0 \leq |\theta| \leq \pi/2$ for the forward direction, then along the same line θ_b = -($\pi/2$ +θ_f) and the sum is always zero because the cosines have opposite signs in diagonally opposite quadrants.

However, that method does not apply for this situation. Why not? Because we must account for the frequency shifts by integrating over the surface area of each ellipsoid separately for the feedback signals returning from the forward direction and those returning from the backward direction in order to determine the net effect. In Fig. 1, one recognizes that the plane passing through points P_3 and B perpendicular to the x-axis separates the two surface parts for each ellipsoidal surface integral, thereby separating the backward returning feedback signals from the forward returning ones.

In terms of the semi-major axis b and the semi-minor axis a, the ellipsoid's eccentricity

$$\epsilon = \sqrt{(b^2 - a^2)/b^2}. \qquad (8)$$

The solid angle of the ellipsoidal cap on the right of B subtended from A_1 is

$$\Omega_{cap} = 2\pi\,(1 - \cos\theta) \qquad (9)$$

where θ is the angle between the ray from A_1 to P_3 and the x-axis. The solid angle subtended by the left side is

$$\Omega_{left} = 4\pi - \Omega_{cap} = 2\pi\,(1 + \cos\theta). \qquad (10)$$

Substituting the pertinent geometrical values, one obtains

$$\Omega_{cap} = 2\pi\left(1 - \frac{2\epsilon^3}{\sqrt{1 + 4\epsilon^6}}\right). \qquad (11)$$

These geometrical factors are multiplied by the frequencies returning from each point on the ellipsoidal surfaces. Along the x-axis one obtains:

$$\Omega_{cap}\,\omega' = 2\pi\left(1 - \frac{2\epsilon^3}{\sqrt{1 + 4\epsilon^6}}\right)\sqrt{\frac{1 + v/c}{1 - v/c}}\,\omega_C, \qquad (12)$$

and

$$\Omega_{left}\,\omega' = 2\pi\left(1 + \frac{2\epsilon^3}{\sqrt{1 + 4\epsilon^6}}\right)\sqrt{\frac{1 - v/c}{1 + v/c}}\,\omega_C. \qquad (13)$$

Substituting $\epsilon = \beta = v/c$, assuming $v << c$, and expanding the expressions in a Taylor series, their difference becomes

$$\text{Diff} \approx -4\pi\,\omega_C\,\beta\,(\beta^2 - 1) \approx 4\pi\,\omega_C\,\beta, \qquad (14)$$

i.e., proportional to the velocity v as expected, verifying that the uniform velocity will be maintained along the x-axis.

If one desires to check the result for relativistic velocities, the complete integration over the cap and the surface area remainder would be necessary. The frequency shifts can be large enough to put the returning feedback signals outside the high Q absorption curves. However, the integration verifies that the uniform velocity is maintained.

6 Inertia and Mach's principles

The idea of inertia considered in the early 1600s by Galileo and others proposed that a body maintains its state of uniform motion unless acted upon by an outside net force.

In the previous section, my feedback signal approach reveals the origin for this Law of Inertia. That is, the vacuum lattice itself plays an active and important role in maintaining the state of a particle's uniform motion. The feedback signals scatter from the transponders to arrive back in-phase to determine the particle's new location.

Information about the environment is brought back to determine the continuous behavior of the particle. Long-lived particles can establish a steady-state communication with the environment, but short-lived particles learn only transient information about their immediate environment. Fast particles near the speed of the feedback signals sample only an extremely small distance perpendicular to the trajectory direction.

The distant parts of the Universe play their role in determining the particle motion locally because feedback signals from way out there are added to the closer contributions to determine its new location. Mach's principle connecting local behavior to the influences from far reaches of the Universe therefore fits well in this feedback signal approach. The origin of the inertia concept is established.

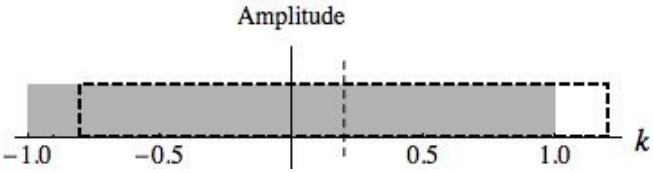

Fig. 2: The momentum-space x-component amplitude contribution at B of the returning feedback signals for the electron at rest [solid rectangle] versus the contributions of the feedback signals [dashed rectangle] in the x-direction for the electron at a uniform velocity.

7 The momentum-space description

What does the particle do with its own returning signals? And with other particle's signals, which may be at the same frequency or at other frequencies? The response to any feedback signals by the particle depends upon whether the feedback signals lie within the response range of frequencies for its inherent harmonic oscillator, meaning that feedback signals are absorbed if they lie within the absorption response curve defined by its Q value. That is, a particle is not a transponder and will be frequency selective. And, in contrast to the transponders, which maintain their initial properties forever, the future behavior of the particle can be affected.

The x-component momentum-space behavior of the electron's feedback signals is shown in Fig. 2. The gray rectangle represents the equal x-momentum contributions from all 4π solid angle for the electron at rest in the lab frame, being symmetrical about $k_x = 0$. Left to right, from $-k_x$ to 0 to $+k_x$, one has the momentum-space total amplitude contributions from the x-components of the returning feedback signals. The dashed rectangle represents the same electron moving at a constant velocity v, so this dashed rectangle is the original rectangle displaced by the x-momentum of the particle. Out-of-phase returning feedback signals will change the distribution.

8 Time asymmetry

In addition to continuous Lie symmetries, discrete symmetries are important in particle physics. Experiments in the 1950s and 1960s established both parity P and charge-parity CP violation for the weak interaction. Theoretically, one expects CPT invariance, which includes the time reversal operation T, and to this date all evidence points toward CPT conservation [2]. CP violation occurs for the weak interaction, so then T violation must occur for the weak interaction also in order to maintain CPT invariance. The mathematical source [6] of the weak interaction CP violation is simply the mathematics of products of unit quaternions in the group Q, the leptons, quarks, and weak bosons all being represented by quaternions.

This feedback signal approach to particle behavior possesses a fundamental time asymmetry, the expected T violation. Consider a free particle with its Compton frequency ω_C in uniform motion in the lab frame. To the moving particle, as we demonstrated earlier, its returning feedback signals from the forward direction are blue-shifted to a higher frequency and those returning from the backward direction are red-shifted to a lower frequency.

Now introduce time reversal via the operator T, i.e., have the electron move backwards at the same uniform velocity as if running a video backwards. The particle will be emitting bluish feedback signals in the new backward direction and their returning signals from the transponders would be red-shifted back to the original Compton frequency ω_C. The new forward emitted reddish signals will return as blue-shifted back to the original ω_C also. Therefore, the environment appears symmetrical in the forward and backward directions, so the particle should not be moving. There is a conflict with the hypothesis of time reversal symmetry. Therefore, time reversal symmetry is violated. Time reversal cannot occur in Nature.

Hence, a definite time direction is an inherent feature of the feedback signal approach. The moving particle "knows" its forward direction in the time coordinate. All particles would possess this time asymmetry property. For the anti-particles, which exist in the mathematically conjugate space to our normal space, they would also have one time direction only, forward for them but perhaps in the backward direction mathematically for us.

Consequently, time travel backwards in time would be impossible in our Universe of particles unless, perhaps, one changes all the material particles to their anti-particles that are conjectured to have the opposite time direction in the conjugate space. And time travel forward in time faster than normal would be impossible also because there would exist a conflict with the particle behavior we have established via the feedback signal approach.

9 Origin of Special Relativity

Does this feedback model of particle behavior, as developed so far, lead to the special theory of relativity (STR)? If one examines the successive series of ellipsoids shown in Fig. 1, these ellipsoids belong to a set of curves with eccentricity $\epsilon = \beta = v/c$, the ratio of the electron's velocity divided by the speed of light. Therefore, as $\beta = v/c \to 1$, then also $\epsilon \to 1$.

In order to derive the expected STR equations, two assumptions about the feedback signals must be accepted:

1. the speed of the feedback signals in all reference frames is the same constant c, and
2. the perpendicular distances are invariant.

In the laboratory frame the feedback signals from each A_i to an ellipsoidal shell and back to the electron now at B will arrive in-phase at B, the definition of the new location of the free electron. A specific path within an ellipsoidal shell

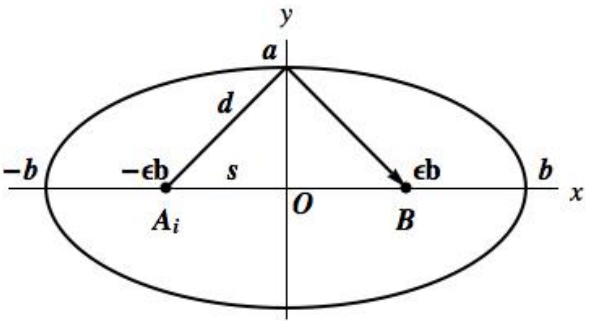

Fig. 3: Constant phase ellipsoid parameters for deriving special relativity relations in a vacuum with an eccentricity $\epsilon = \beta = v/c$.

is shown in Fig. 3. The feedback signal goes from A_i at one focus of the ellipsoid to B at the other focus in the same time that the electron goes from A_i to B via a straight trajectory through the origin O.

I can now do the standard derivation, with the feedback signals instead of with light rays. Let the lab frame be the primed frame. The perpendicular distance from O to a, the semi-minor axis distance, and back is

$$2\Delta y = 2ct, \tag{15}$$

and, using the geometrical properties of the ellipsoid,

$$2\Delta y' = 2s\left[\frac{c^2}{v^2} - 1\right]^{1/2}, \tag{16}$$

with $s = vt'$. Because the perpendicular distances in the two reference frames are equal, $\Delta y' = \Delta y$, the time intervals are related by

$$t' = \frac{t}{\sqrt{1 - v^2/c^2}} \tag{17}$$

and the distance intervals along the velocity vector in the x-diection are related by

$$\ell' = \ell\sqrt{1 - v^2/c^2}. \tag{18}$$

These relations are the fundamental equations of STR for the coordinate and time measurements. In Subsection 9.2 the relativistic energy and momentum expressions are derived. But first some geometrical properties of ellipsoids must be introduced.

9.1 Ellipsoidal geometry

In terms of the semi-major axis length b and the semi-minor axis length a, the ellipsoid's eccentricity is given by Eq. 8. If the perpendicular semi-minor axis length a is held fixed in both perpendicular directions to the x-direction as $\beta = \epsilon \to 1$, the semi-major axis value

$$b = \frac{a}{\sqrt{1 - \epsilon^2}} \to \infty. \tag{19}$$

At the same time the surface area of the ellipsoid as a prolate spheroid becomes

$$S.A. = 2\pi a^2 + 2\pi\frac{ab\,\sin^{-1}\epsilon}{\epsilon} \sim 2\pi a^2 + 2\pi ab \to \infty, \tag{20}$$

while the ellipsoid volume increases as

$$\text{Volume} = \frac{4}{3}\pi \text{ba}^2 \to \infty. \tag{21}$$

With the ellipsoids stretching out along the x-axis, the velocity direction, as a consequence of $\beta = \epsilon \to 1$, the number of in-phase ellipsoids that can "scatter" feedback signals from the A_i to B is rapidly decreasing. Or so it seems that way! As a check, consider the feedback signal that goes rearward from A_i to -b and then is scattered forward to B. If the electron's velocity $v \sim c$, then immediately after the feedback signal's emission directed toward -b comes the return feedback signal to arrive at B simultaneously and in-phase with the electron. Consequently, only a very small distance into the environment behind and sideward will be sampled to determine the electron's behavior.

The minimum sampling distance in the direction perpendicular to the x-axis might seem to be the semi-minor axis distance

$$a = \frac{ct'}{2}\sqrt{1 - \beta^2} \to 0. \tag{22}$$

However, the particle's Compton wavelength, or actually half the Compton wavelength, is the minimum sampling distance when $v \sim c$.

9.2 Energy and momentum

Using Fig. 3 again, one can determine several other important consequences in STR via the feedback signal approach. Relativistic energy and momentum can be related to the volume of the ellipsoid. If this statement is true, then the electron at rest has its mass-energy $E = mc^2$ determined by its "spherical volume" density when $\epsilon = 0$. Note that this fundamental particle volume will maintain a discrete rotational symmetry corresponding to the binary subgroup properties of each fundamental particle. So the "spherical volume" is an idealized spherical approximation in which the particle exists.

The ellipsoid volume when $\beta \ll 1$ is expressed as

$$V = \frac{4}{3}\pi ba^2 = \frac{4}{3}\pi\frac{a^3}{\sqrt{1 - \epsilon^2}} \simeq \frac{4}{3}\pi a^3\left(1 + \frac{1}{2}\beta^2 + \ldots\right) \tag{23}$$

or, when multiplied by c^2, is

$$Vc^2 = \left(\frac{4}{3}\pi a^3\right)c^2 + \frac{1}{2}\left(\frac{4}{3}\pi a^3\right)v^2 + \ldots, \tag{24}$$

which can be compared favorably to the familiar STR expansion of $m = m_0/\sqrt{1 - v^2/c^2}$ as

$$mc^2 = m_0c^2 + \frac{1}{2}m_0v^2 + \ldots \tag{25}$$

in which the second term on the right in Eqs. 24 & 25 expresses the increase of the mass-energy due to the particle's velocity, also known as the kinetic energy, and defines p = mv.

The simplest conclusion is that mass-energy is directly associated with the distorted volume of the space lattice occupied by the electron and depends upon the mass density

$$\rho(m_0) = \frac{6}{\pi}\,\frac{m_0^4 c^3}{h^3}, \tag{26}$$

which reminds us that each type of fundamental particle distorts the lattice space in its own way to pack in its unique amount of mass-energy.

But there is more to behold! The vacuum, i.e., the lattice of mathematical nodes, must contribute the energy per unit volume which can be assimilated into the moving particle to increase its total energy according to STR. Until now I have assumed that the uniformly-spaced lattice does not have energy per unit volume, which is probably correct, but now we learn that the *distorted* lattice created by the particle at rest (and when in motion) is the energy source. At this point in my earlier research in the 1970s and 1980s I realized that each fundamental particle in Nature should have a different symmetry in order to agree with my discovery of the mass-energy relation to the volume enclosed.

In 1984, by accident, I found the significant clue to the lepton family symmetries that indicated that they could be representing specific discrete symmetry binary subgroups of SU(2), i.e., the unit quaternion group Q. That is, the 3 lepton families could be representing the specific 3-D discrete symmetry binary subgroups of Q named [3,3,2], [4,3,2], and [5,3,2], and also exhibit properties and behavior that suggests that the SM is a good theory all the way down to the Planck scale with its possible discrete lattice of mathematical nodes.

10 Origin of Feynman path integrals

Physicist R.P. Feynman is credited with providing a relativistic path integral approach to quantum mechanics (QM) in the 1940s and applying this method to better understand the foundations of physics. Today, practically all areas of physics continue to use path integrals to investigate the behavior of Nature at all levels [11].

The fundamental idea behind the path integral calculation is that a particle, such as an electron, "sniffs out" all possible paths between its initial location A and its final location B. Each possible path contributes its QM amplitude and phase angle to the path integral. Most paths contribute very little to this limit of the sum because their path lengths from A to B are so long that not only are their QM amplitude values reduced significantly but also their phase values differ enough to cancel each other. Two path examples are shown in Fig. 4 that will have significantly different contributions to the amplitudes at B.

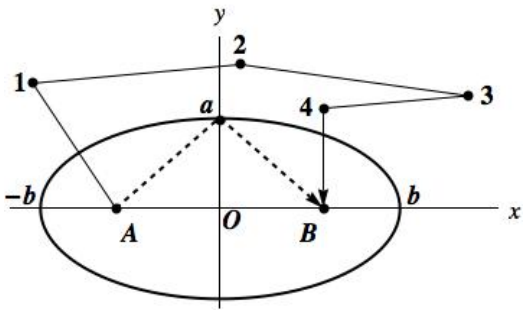

Fig. 4: Two vastly different paths from A to B: (1) Path A,1,2,3,4,B, and (2) Path A, a, B. Feedback signals travel both paths. Or, in the path integral approach, the electron "sniffs out" both paths.

The actual classical path taken will be among the paths that collectively make the biggest contribution to the path integral, because this classical path will be the one for which the nearby paths have almost the exact same contribution to the path integral. Note that this path integral approach is based upon the mathematical principle of least time, which dictates that the actual classical path will be the one for which many nearby paths have the least time difference for going from A to B. Fundamentally, the method agrees with the least action principle.

The path integral approach is a proven method that works for all of physics, quantum and classical, meaning that the path integral results agree with all the known fundamental laws of Nature. Therefore, if the feedback signal approach is the source of the path integral method, then one can explain why path integrals successfully describe all of physics! Or vice-versa!

Feedback signals are emitted by a fundamental particle into all directions and undergo multiple transponder scatterings between the initial position A of the electron and its next position B, such as the simple 5-component path in Fig. 4. All the possible paths taken by these feedback signals going from A to B can be considered collectively identical to the "sniffing" out all possible paths from A to B in the path integral approach. Each feedback signal path is then a contributor to the path integral with its specific amplitude and phase angle.

Therefore, the underlying mathematical reason why the path integral approach works so impeccably well is that fundamental particles are using feedback signals to sample their environment in order to determine their subsequent behavior. Thus, one could use path integrals as the preferred mathematical method to describe all the results of the particle feedback signal behavior.

There exist many mathematical ways to represent the path integral method. One interesting visual way [12] to represent this limit of the sum over all paths is to use equal length arrows for each path and point them in the correct phase direction in an Argand diagram shown in Fig. 5. That is, each path

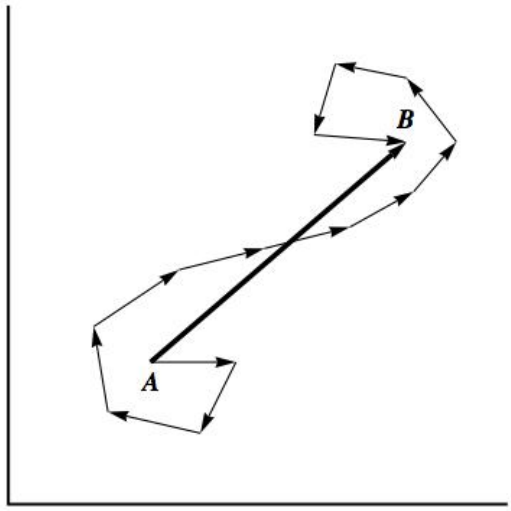

Fig. 5: Argand diagram of the phases for the different paths. Only 13 different paths are shown here, but the general idea of finding their total contribution to the amplitude is represented by the length of the arrow from A to B.

to the current position will have a different phase, therefore a different angle with respect to the horizontal real axis and the vertical imaginary axis in this complex 2-D space.

Nearby paths will have almost the same phase angle, will point in nearly the same direction, and will add a significant distance to the total vector sum in the diagram. Those arrows with opposite directions may cancel out completely. Each phase arrow is produced by a different path from the start to the current position B. The path integral amplitude is the length of the long straight arrow from beginning to end, A to B in the diagram, and the probability to be at the current position is the absolute value of its square.

In summary, each arrow also represents a feedback signal path and its phase contribution at location B, the current position of the electron. Again, one must add up all the feedback signal amplitudes arriving at B to find their total amplitude, which will depend upon the distance traveled and the phase at arrival at B. The electron position will be at the new maximum amplitude value. Therefore, we have conceptual and mathematical agreement with the path integral.

11 Origin of quantum mechanics

The rules of quantum mechanics (QM) can be derived from the path integral approach. But the path integral approach has its origin in the feedback signal approach as described above. At this point I could simply consider using path integrals to derive the 3 rules of QM. But deriving QM by the feedback signal approach provides a better "feeling" for how any particle behaves in the single slit and double slit experiments. There is no surprise because the feedback signal approach has been shown to be equivalent to the path integral approach.

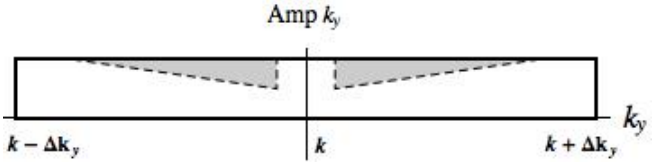

Fig. 6: While passing through the single slit the particle will experience diffraction spreading in the y direction because the feedback signals returning from the wall will produce phase shifts in the shaded regions (approximate idealized representation).

Here are those 3 rules of QM from which all its consequences can be derived [13]. But first I must recall the definition of an event in relativistic QM. A QM event is defined as a set of initial and final conditions, e.g., an electron leaves the source, arrives at the detector, and nothing else happens. The first principles of QM [i.e., the 3 rules] are:

1. Each event in an ideal expereiment is described by a complex number ψ that is called the probability amplitude, the event probability P being the square of the absolute value $|\psi|^2$.
2. When an event can occur in several alternative ways, the total probability amplitude Ψ for the event is the sum of the probability amplitudes for each way considered separately. There is an interference term $2\psi_1\psi_2$:
$$\Psi = \psi_1 + \psi_2$$
$$P = |\psi_1 + \psi_2|^2 .$$
3. If an experiment is performed that is capable of determining whether one or the other alternative is actually taken, the probability of the event is the sum of the probabilities for each alternative. The interference is lost:
$$P = P_1 + P_2.$$

Note that one does not need to actually do the measurement for this sum of probabilities to apply. Simply having the capability to do the measurement is enough to eliminate the interference terms.

11.1 Diffraction

Consider a fundamental particle moving along the x-axis approaching a narrow vertical slit extending upward along the z-axis in a solid material wall that extends to infinite distances perpendicular to the x-axis. The slit is symmetrical about the x-axis in both perpendicular directions. The particle approaches the slit from the left, goes through the slit, and recedes away from the slit to the right. One can put a "screen" of particle detectors behind the slit to measure the particle's arrival pattern.

As the particle approaches the slit the returning feedback signals define its new positions as before. Those signals re-

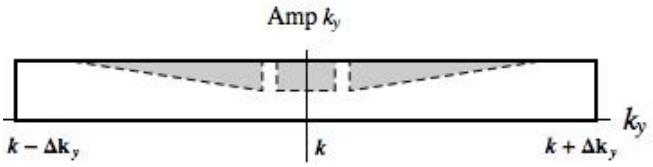

Fig. 7: After passing through the double slits the electron will experience diffraction and interference spreading in the y direction because the feedback signals returning from the wall will produce phase shifts in the shaded regions (approximate idealized representation).

turning directly from the open slit portion of the wall introduce no phase shift, and the returning signals from the volume of "empty" space on either side of the wall, front and back, also do not introduce a phase shift.

We now need to determine the phase shift effects of the wall on the behavior of the particle. Its matter content introduces phase shifts δ^a on the approach and δ^r on the recession, with the same phase shift values for each of the infinite series of feedback signal ellipsoids. The resulting amplitude values at the particle's position will depend also upon the total round trip distance.

Our concern is what happens in k-space on the back side of the slit both along the x-direction of the electron's travel and what happens in both perpendicular y and z directions. The angular distribution of the feedback signals from each ellipsoid will produce changes in the y-amplitude A(k_y) according to the actual distribution of matter around the slit. The new k_y amplitudes are shown in Fig. 6 for inside and immediately behind the slit. Within the free particle rectangular box are shaded regions for possible examples of the phase-shifted signals returning from the particles in the wall around the slit.

With left-right symmetry in the slit region itself in the y direction, there exist symmetrical amplitude decreases as shown in Fig. 6 but no net acceleration. Instead, the change in the distribution of the amplitude in k_y space leads to a symmetrical spreading of the particle according to Fourier analysis. If the wall effectively stretches to infinity, then the major contribution comes from the slit region around $k_y = 0$. One has a broadened diffraction pattern produced which has the amplitude

$$U'(y) = U(y) + 2\Delta k\, A'(k_0) \exp\left[i(\omega(k_{0y})t - k_{0y}y)\right] \times \frac{\sin\, \Delta k_y(y - v_{0y}t)}{\Delta k_y(y - v_{0y}t)}. \quad (27)$$

The term U(y) is the standard distribution in coordinate space for a free particle. The important result is the increased spread in the y-direction to produce the expected diffraction pattern, as represented by the 2nd term.

11.2 Interference

This feedback signal approach also reproduces the double slit interference pattern for the feedback signals because of the k_y momentum distribution shown in Fig. 7. In coordinate space the behavior of the feedback signals at each slit is wave-like but now one cannot determine in principle whether the particle goes through either slit because the feedback signals pass through both slits simultaneously. The amplitudes are added to produce interference before calculating the total probability.

Only when the experimental setup is such that one could determine the slit used by the particle do we get the addition of the probabilities. The mathematics tells us that whether one "looks" or not is irrelevant, but as long as one "could look", then the interference terms are absent in the probability expression.

I have explained how the particle's feedback signal behavior at a slit exactly dictates the behavior of a particle as described by QM, both for diffraction and interference. Hence, the 3 rules outlined at the beginning of this section for the first principles of QM follow directly from the diffraction and interference of the feedback signals, thereby revealing the origin of QM.

12 Origin of gravitation

Now consider the behavior of two different particles with different mass-energy values. The case of two identical particles exchanging feedback signals is discussed in Appendix B, where the connection between particle spin and quantum statistics agrees with Fermi-Dirac and Bose-Einstein behavior.

The analysis developed here first outlines the feedback signal source of the gravitational interaction. Then I discuss its agreement with the standard geometrical curvature approach to the general theory of relativity (GTR).

As an example, let's bring a muon into the environment of our electron with both particles at rest initially. I ignore their electromagnetic charge interaction, which is understood to be a local interaction described by the Standard Model, requiring the exchange of virtual photons.

Therefore, the muon has its Compton frequency about 207 times higher and a wavelength about 207 times shorter than for the electron. Thus, in Fig. 8, I cannot do justice to both particles at the same time by drawing their feedback signal ellipsoids to relative scale. Consequently, I only show different wavelength signals emitted by each, but they are not to scale.

Both particles emit their characteristic frequency feedback signals into the vacuum lattice. Each high Q particle has a nearly zero ability to absorb the signals from the other particle. Therefore, the biggest contribution to the amplitude and phase changes of the returning feedback signals comes from the lattice distortion surrounding each particle.

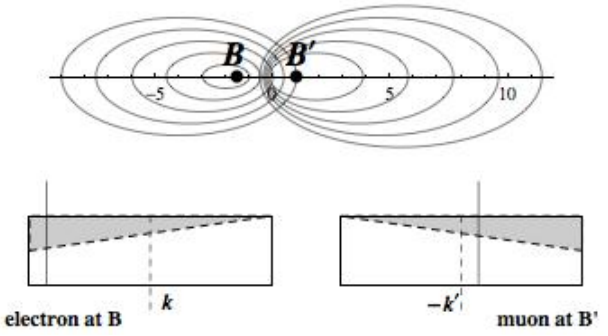

Fig. 8: As two "assumed neutral" particles approach each other, the transponders in the vacuum lattice handle both sets of feedback signals simultaneously. The signals returning from these transponders are a different phase than for the free particle. The instantaneous effects in k-space are shown in momentum space with the new k values at the dashed lines (*approximate idealized representation exagerated*).

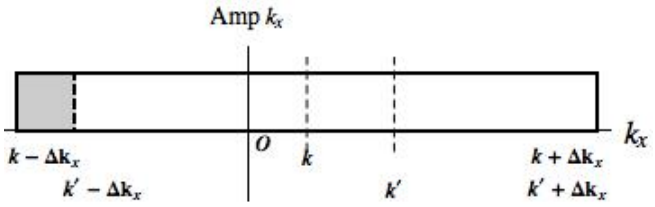

Fig. 9: Whenever a "chunk" of k-space is absent (the gray area) near k-Δ k_x, there will be an acceleration in the +x direction. Usually the feedback signals returning from the forward direction are out-of-phase, the source being the transponders around other particles in the environment ahead.

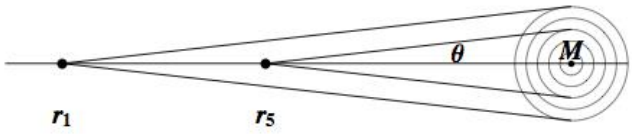

Fig. 10: As a neutral particle of mass m approaches from the left toward another neutral particle of mass M, the transponders in the vacuum lattice handle both sets of feedback signals simultaneously. Shown are paths from positions r_1 and r_5 subtending the same angle θ to the distorted space around M as "seen" from the approaching particle. The feedback signals returning from these two rings of transponders around M return with a different phase than for the free particle without the presence of M. (approximate representation exagerated).

Meanwhile, the transponders in space continue to behave as before, except that their separations have changed because they no longer have identical average spacings between the nodes. Whereas the node spacings are expected to be closer where the particle is defined by its discrete symmetry, their spacings are further apart outside this immediate region. As conjectured earlier, perhaps this node spacing difference in the two regions keeps the lattice total energy value at zero. One now has a lattice with non-uniform node spacings everywhere compared to the original uniform lattice that has no fundamental particles.

Transponders around the electron will continue to scatter the muon's higher frequency feedback signals isotropically into all directions. The lattice distortion will cause these feedback signals to return to the muon out-of-phase with returning feedback signals from other directions, thereby reducing the total amplitude from the forward direction toward the electron, as shown in the Fig. 8 momentum space diagram.

Therefore, the original spherical symmetry of the returning feedback signals around the muon is gone and the muon must either move toward or away from the electron. One can appreciate that the out-of-phase returning signals reduce the total feedback signal amplitude from the electron's direction, which means that the muon will begin to move toward the electron. Why? As shown in Fig. 8, the center-of-momentum for the muon's feedback signal distribution has moved toward the electron. So there is an attraction toward the other particle.

What does the less massive electron do? The same, but in the opposite direction toward the muon of greater mass M. The feedback signals going to the muon region are returned to the electron out-of-phase. Again, the out-of-phase returning feedback signals reduce the total amplitude arriving from the muon's direction, resulting in electron movement toward the muon. That is, the electron's center-of-momentum distribution has moved toward the muon. There is a mutual attraction between the two particles.

The acceleration of each particle occurs when there is a change in phase of the feedback signals arriving from any direction. For example, suppose the particle "senses" that a "chunk" of k-space is absent near k_0-Δk, as shown in Fig. 9. This situation occurs when returning feedback signals from the forward direction are out-of-phase with the oscillation phase of the particle itself. The center of the momentum rectangle will move from k to k' corresponding to a faster moving electron with k' > k, meaning that the particle has moved ahead of the expected uniform velocity location in the corresponding coordinate diagram.

The acceleration is caused by feedback signal amplitude changes as a result of phase changes in the feedback signals as the particle approaches a mass M, an effect directly related to the distortions in the lattice geometry around M. This distortion produces the spacetime curvature associated with GTR gravitation, as explained in the next Section.

In Fig. 10 are shown our two "neutral" particles of masses *m* and M, with *m* approaching the distortion volume around M. One sees immediately for the same angle θ subtended by the feedback signal ray toward M as *m* approaches M, there will be a shorter distance of roundtrip travel for the feedback

signals as they approach one another. And the feedback signals from m will sample regions of greater and greater lattice distortions upon moving closer to the center of M.

In Fig. 11 is an approximation to the result of both effects on the momentum-space amplitude distribution for the two positions shown in Fig. 10, i.e., r_1 and r_5. As more and more amplitude is missing, the change in momentum will increase, i.e., the acceleration toward M will increase upon nearing M as the momentum value increases toward $+k_x$. This type of behavior is expected for the gravitational interaction, because the lattice distortion amount depends upon the mass-energy of M.

The feedback signals are scalar waves given by Eq. 4 in the form $(A/r)\exp[i(\omega(k)t - kx)]$ that are emitted, scattered, and returned, so we can go from the momentum space to coordinate space behavior using the Fourier Transform to obtain the total amplitude at the new, accelerated position for the wave packet

$$U(x) = \int_{k_0-\Delta k_x}^{k_0+\Delta k_x} A(k_0)\ \exp\ [i\,(\omega(k)t - k_x x)]\ dk_x. \qquad (28)$$

And if we assume

$$\omega(k) = \omega(k_0)\ +\ (k - k_0)\left(\frac{d\omega}{dk}\right), \qquad (29)$$

then the composite feedback signal at the electron, i.e., the total amplitude at its new accelerated position is

$$U(x) = \quad 2\Delta k_x\, A(k_0) \exp\,[i\,(\omega(k_0)t - k_0 x)] \quad \frac{\sin \Delta k_x(x - v_0 t)}{\Delta k_x(x - v_0 t)}. \qquad (30)$$

This modulated monochromatic wave does not spread in time, an important property of this feedback signal approach for the behavior of particles.

As $v \to c$, the ellipsoids become more prolate, the Δk_x increases with each equal time interval, and the wave packet of the electron adjusts smoothly. In the limit, the sideward sampling of the environment does not extend beyond the Compton wavelength λ_c and the feedback signals are sampling less of the surrounding space, thus reducing any further acceleration. This behavior agrees with the special theory of relativity (STR).

By considering the acceleration in more detail, one would discover that the smaller range in wave numbers in momentum space spreads the particle wave packet in the x-direction. When a new constant velocity is achieved, the particle wave packet reverts to its normal size. In the perpendicular y- and z-directions in which $v_y = v_z = 0$ as before, a symmetrical hole appears in k_y-space and k_z-space during the acceleration but returns to normal when the acceleration is done. Hence, some temporary lateral spreading of the wave packet occurs also in these directions perpendicular to the accelerated motion along the x-direction.

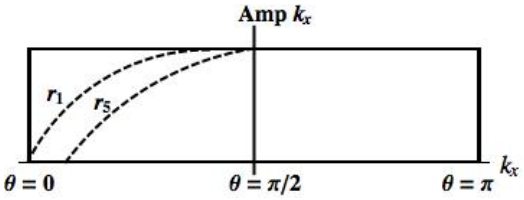

Fig. 11: As the particle approaches M, the feedback signals returning from the two transponder rings have a different phase than for the free particle. The possible reduction of the amplitudes in k-space are shown for positions r_1 and r_5 in Fig. 10, with contributions to the k-space distribution removed above the dashed lines for a range of angles. (approximate representation exagerated).

One could consider further properties of the electron in terms of its de Broglie wavelength = h/p for non-relativistic momentum values in order to discuss the wave packet behavior for the electron. However, the feedback signal approach is all that's needed to understand the electron's behavior in response to another particle that also distorts the lattice.

I have described particle motion in terms of its dependence upon the integral of all the feedback signals returning from the environment back to the source-receiver location. Equal weighting for all k values has been used. In the idealized acceleration example, a rectangularized "chunk" of k-space was missing. Actually, one should consider that some of the feedback signals are returning from all directions with a different phase with respect to the k-space signals returning in a uniformly spaced euclidean lattice. The phase differences would produce a "hole" in k_x-space that can have positive and negative values. All the possibilities could be examined via computer simulations.

13 Gravitation from the Radius Excess

A lattice distortion occurs not only at the particle's origin but also throughout the surrounding space and spacetime. No longer does the lattice have uniformly spaced nodes. As we move further and further away from the origin of each particle, this lattice distortion becomes less and less.

The physics consequences can be understood by first separating the analysis into two parts: the 3-D space part, and then the time part for the (3+1)-D spacetime of our physical world. The two parts are put together to assemble the spacetime of Einstein's GTR.

13.1 The 3-D space part

In the uniformly spaced 3-D sublattice part of C^2 with nodes but with no particles yet, consider an imaginary thin spherical shell with a radius R >> d, the lattice node spacing. Then euclidean geometry dictates a radius value from its surface

area A

$$R = \sqrt{\frac{A}{4\pi}}. \tag{31}$$

Now in this 3-D sublattice consider the electron to have been in existence at the origin so that its characteristic distortion exists everywhere with the amount of distortion decreasing inversely with distance. At the one Compton wavelength distance from the center of the particle, that is, greater than about 10^{-12} meters from the electron's distortion center, one is far enough away to consider an imaginary spherical surface surrounding the electron as a good approximation at all further radial distances.

We measure the distance in a discrete space by counting the nodes along a radial path. Therefore, the measured radius r_{meas} from the electron's center to any outside distance will be greater than for the undistorted lattice because nodes will have been pulled inward. In fact, the radial difference between the distorted lattice and their euclidean lattice is called the *radius excess* expressed by [14]

$$\text{Radius excess} = r_{meas} - \sqrt{\frac{A}{4\pi}}. \tag{32}$$

Note that in the limit when the enclosed mass-energy inside R is reduced to zero, then the radius excess will reduce to the previous zero value. Therefore, let the radius excess be directly proportional to the enclosed mass-energy amount m, in this case the mass of the electron. Then do a dimensional analysis to predict

$$\text{Radius excess} = r_{meas} - \sqrt{\frac{A}{4\pi}} = \frac{G}{3c^2}m. \tag{33}$$

The factor 1/3 comes from the geometry of a 3-D sphere and is the numerical factor for the second term in the Taylor expansion of the sine function.

This radius excess is the important quantity which, according to Einstein's GTR, is indeed proportional to the mass of the particle enclosed by the imaginary sphere at radius R. That is, for a fixed R value, the distance measured by counting the nodes will be greater for the more massive particle enclosed. Note that the radius excess defined here is a measure of the 3-D geometrical curvature produced by the mass-energy m, and that this radius excess expression actually defines the average curvature just above the chosen surface area.

The quantity $G/3c^2 \sim 2.5 \times 10^{-28}$ meters/kilogram, a very small number. Therefore, in order to get a "feeling" for the radius excess magnitude, insert the pertinent values to learn that the radius excess for the electron is extremely small:

$$\text{Electron}: \quad \text{radius excess} = 2.3 \times 10^{-60} \text{ meters!} \tag{34}$$

Also, for Earth: 1.5 millimeters; for the Sun: 0.5 kilometers.

13.2 The time part of (3+1)-D spacetime

Now for the time coordinate contribution. The principle of equivalence states that one cannot distinguish between a gravitational field and an accelerated reference frame for a locally uniform gravitational field. Applying this equivalence principle, Einstein found that time varies from place to place.

The time coordinate will be modified near the mass m. Let v be the relative velocity between a source and a receiver, with the received frequency ω' being related to the emitted frequency ω by Eq. 6 for STR. For $v^2/c^2 << 1$, the approximation is

$$\omega' = \omega\,(1 + v/c). \tag{35}$$

If the receiver is accelerating, then the receiver will have an additional velocity gt, where g is the acceleration value and t is the time interval it takes light to travel the distance H from source to receiver.

Using the equivalence principle, the g is now the gravitational acceleration and H becomes the radial height difference in the gravitational field. For the clock at the radial height h_2 above the clock at height h_1, with $H = h_2 - h_1$,

$$\omega_2 - \omega_1 = \frac{gH}{c^2}, \tag{36}$$

so that the excess rate is

$$\omega_1 \frac{gH}{c^2}. \tag{37}$$

From STR, there is the correction factor of the opposite sign for the speed in case of the moving clocks

$$\omega_2 = \omega_1 \sqrt{1 - v^2/c^2}, \tag{38}$$

which for low speeds $v << c$, becomes

$$\omega_2 = \omega_1(1 - v^2/2c^2), \tag{39}$$

predicting the defect in the rate of the moving clock to be

$$-\omega_1 v^2/2c^2. \tag{40}$$

Combining the two effects produces

$$\Delta\omega = \omega_1 \left(\frac{gH}{c^2} - \frac{v^2}{2c^2}\right). \tag{41}$$

This frequency shift of the moving clock means that if one measures a time interval dt on a fixed clock, the moving clock registers the time interval

$$dt\left[1 + \left(\frac{gH}{c^2} - \frac{v^2}{2c^2}\right)\right]. \tag{42}$$

Therefore, the total time excess over the whole trajectory is the integral

$$\frac{1}{c^2}\int \left(\frac{gH}{c^2} - \frac{v^2}{2c^2}\right) dt, \tag{43}$$

which is to be a maximum, thereby obeying the principle of least action. I.e., the particles always take the longest proper time. Note that this law does not rely upon any of the coordinates.

One can see this result better in the alternative formulation by multiplying Eq. 43 by -mc^2, where m is the mass of the particle, so that the integral is over the kinetic energy minus the gravitational potential energy which, by the principle of least action, must be a minimum.

13.3 The two main laws of GTR

Therefore, the two main laws of GTR have been established by starting from the idea that each fundamental particle distorts the lattice into its own discrete symmetry. The distortion continues to all distances, and phase changes in the returning feedback signals are produced by the distorted lattice.

Equivalently, the distorted lattice around each particle is the source of the radius excess proportional to the enclosed mass producing the distortion, and this radius excess leads to the two main laws of gravitation.

These laws are:

1. The curvature expressed in terms of the excess radius is proportional to the mass inside a sphere, by Eq. 33.
2. Objects move so that their proper time between two end conditions is a maximum.

The first law, Einstein's field equation, reveals exactly how the geometry of spacetime changes in the presence of matter. The second law, Einstein's equation of motion, reveals how objects move when there are only gravitational forces. So the entire spacetime is distorted in the presence of matter.

Can we understand the factor of about 10^{40} for the relative strength of the electric force to the gravitational force between the two electrically charged particles, two electrons, for example. There is a significant physical and conceptual difference between the two forces. The electric force relies upon the local gauge interaction of the SM by the exchange of virtual photons, whereas the gravitational force as determined by the feedback signal approach does not have the exchange of a virtual particle for a local gauge interaction. The gravitational acceleration results from particle responses to their returning feedback signals from the environment. Whether the factor of about 10^{40} can be derived by exploiting this difference is expected but has not been achieved at present.

14 Review of steps taken

Here are the sequence of steps taken to establish that QM and GTR have a common origin determined by the feedback signal approach, based upon the fact that QM, the SM, STR, and GTR are all successful theories that agree with Nature:

1. The lepton and quark particle states respect the electroweak symmetry SU(2) x U(1) of the SM, but the actual two orthogonal fundamental particle states per fermion family are dictated by the discrete symmetry binary subgroups of the unit quaternion group Q, or equivalently, SU(2).
2. The two physical orthogonal EW flavor states in each lepton and quark family are formed by the linear superposition of the two mathematical states, and they oscillate at the Compton frequency ω_C as 3-D entities in R^3. Hadrons combine their 4-D quarks and gluons to make 3-D particles also, obeying QCD.
3. One assumes that (3+1)-D spacetime corresponds to a 2-D complex lattice $C^2 = R^4$ filled with uniformly spaced mathematical nodes acting as ideal transponders.
4. The fundamental fermion "gathers in" the mathematical nodes to form its correct discrete symmetry binary subgroup with its lattice distortion extending outward into the lattice.
5. The "breathing mode" flavor state oscillations of the particle emit scalar waves into the lattice. I have called these "feedback signals".
6. The transponders in the lattice "scatter" these feedback signals into all directions isotropically with no phase shift and with the same response for all frequencies and amplitudes.
7. STR, the principle of inertia, Mach's principle, the path integral approach, QM, and the one direction of time, are all derived by analyzing the details of the feedback signal behavior.
8. The lattice distortion around each fundamental particle is the source of phase changes in the returning feedback signals at the original particle, resulting in an acceleration toward the other particle.
9. Gravitational curvature is shown to agree with the lattice distortion associated with each particle, so the acceleration produced by the feedback signal approach is the gravitational acceleration of GTR.
10. Therefore, QM and GTR have the common origin as established by the behavior of particles in response to the feedback signals.

15 Summary

This feedback signal approach toward understanding particle behavior successfully explains the origin of QM, the path integral method that allows one to calculate quantum mechanical and classical physics behavior, and gravitational acceleration. The approach involves fundamental particles behaving as "antennas" emitting and absorbing scalar waves at their Compton frequencies, scalar waves that I have called feedback signals. These feedback signals are scattered isotropically by a discrete lattice of nodes representing spacetime.

Gravitation has been shown to be the consequence of the lattice distortion around particles by changing the amplitude and phase of the feedback signals that are returning from regions surrounding mass-energy concentrations, in agreement with the radius excess derivation of GTR.

Therefore, I have revealed the common origin for gravitation and quantum mechanics.

The remaining question is whether fundamental particles, such as the electron, do indeed emit and receive these feedback signals as described in this approach. If so, then not only must fundamental particles be using these feedback signals but also all composite entities such as a proton and very massive objects must rely upon them for determining their physical behavior.

Acknowledgements

The author thanks Sciencegems.com for continuing support for fundamental theoretical investigations into problems of importance toward understanding the behavior of Nature.

Submitted on June 27, 2019

References

1. Susskind L. Dear Qubitzers, GR = QM. arXiv: 1708.03040v1 [hep-ph].
2. Tanabashi et al. (Particle Data Group). The Review of Particle Physics, 2018. *Phys. Rev. D98, 030001*.
3. Potter F. A Naive Feedback Model of Particle Motion. *Department of Physics and Astronomy research paper files, University of California, Irvine* , 1982.
4. Potter, F. Discrete internal symmetry groups for leptons and quarks. The Fourth Family of Quarks and Leptons, 2nd International Symposium, proceedings, D.B. Cline & Amarjit, eds. 1989.
5. Potter, F. Geometrical basis for the Standard Model, *Int. J. Theor. Phys.*, 1994, v. 33 279–305.
6. Potter, F. Geometrical Derivation of the Lepton PMNS Matrix Values. *Progress in Physics*, 2013, v. 9(3), 29. Online: www.ptep-online.com/2013/PP-34-09.PDF.
7. Potter F. Exact Neutrino Mixing Angles from Three Subgroups of SU(2) and the Physics Consequences. Workshop in Neutrinos (WIN) 2017 UC Irvine, June 19-24, 2017 Online: indico.fnal.gov/event/9942/session/4/contribution/23/material/slides/0.pdf
8. Potter, F. CKM and PMNS mixing matrices from discrete subgroups of SU(2). *J. Phys.: Conf. Ser.*, 2015, v. 631, 012024. Online: iopscience.iop.org/article/10.1088/1742-6596/631/1/012024/pdf.
9. Baez, J. This Week's Finds in Mathematical Physics (Week 105). Online: math.ucr.edu/home/baez/week105.html, 1995. (accessed 6/6/2019).
10. Feynman, R.P. & Hibbs, A.R. Quantum Mechanics and Path Integrals. Dover Publications, Mineola, NY, 2010.
11. MacKenzie, R. Path Integral Methods and Applications. arXiv: quant-ph/0004090.
12. Feynman, R.P. QED: The Strange Theory of Light and Matter. Princeton University Press, Princeton, NJ, 2014.
13. Feynman, R.P., Leighton, R.B., Sands, M. The Feynman Lectures in Physics: Quantum Mechanics. Addison-Wesley Publishing, Reading, MA, 1965.
14. Feynman, F. Chapter 42: Curved Space. Online: www.feynmanlectures.caltech.edu/11_42.html.
15. Arhrib, A. and Hou, W.-S. CP Violation in Fourth Generation Quark Decays. arXiv: 0908.0901v1 [hep-ph].
16. Hou, George W.-S. Source of CP Violation for the Baryon Asymmetry of the Universe. arXiv: 0810.3396v2 [hep-ph].
17. Wilczek, F. QCD made simple. *Physics Today*, 2000, v. 53(8), 22–28.
18. Pich, A. Quantum Chromodynamics. arXiv: hep-ph/9505231v1.
19. Sheffer, A. Kuratowski's Theorem. Online: www.math.caltech.edu/~2014-15/2term/ma006b/10%20Planar3.pdf (accessed 6/7/2019).
20. Conway, J.H. and Sloane, N.J.A. Sphere Packings, Lattices and Groups, 3^{rd} ed. Springer-Verlag, New York, 1998.
21. Fitzpatrick, R. Two-Electron System. Online: farside.ph.utexas.edu/teaching/389/lectures/node96.html (accessed 6/6/2019).

Appendix A: Quark states

I have proposed [4, 5, 8] that the 4 discrete symmetry binary subgroups that define four 4-D quark families in R^4 are: [333], [433], [343], and [533], corresponding to the only regular polytopes in R^4. The predicted quark mixing angles produce values that generally agree with their empirical values in the standard 3x3 CKM submatrix of its 4x4 quark mixing matrix CKM4. This quark family mixing therefore guarantees that the 4 discrete symmetry binary subgroups defining the quark families collectively behave as the SU(2) of the SM.

Having 4 quark families creates two different conflicts: (1) no 4th quark family has been discovered yet, and (2) there needs to be triangle anomaly cancellation, usually assumed to mean 3 lepton families paired against 3 quark families but with no verification of which lepton family pairs with which quark family. With regard to the first conflict, the mass values of the 4th family quarks could be quite large, so that either they cannot be produced at the LHC [15] or they decay too quickly. The triangle anomaly gets resolved directly because the collective lepton family mimicking SU(2) exactly cancels the collective quark family mimicking SU(2), one-to-one.

The influence of the 4th quark family may yet appear in rare decays of the other quarks and might resolve several extant problems, including being the source of the baryon asymmetry of the Universe (BAU) by providing a needed factor of at least a 10^{13} increase [16] in the Jarlskog constant and by also explaining the muon g-2 discrepancy.

Therefore, the 4-D quark states are clearly distinguished from the 3-D lepton states, the leptons not being capable of having a color charge, which is now a 4-D property. The origin of the three color charge states comes directly from 4-D rotations, which require two simultaneous rotations in orthogonal planes, and there are only three different pairs of orthogonal planes in R^4. The three different color charges, r,g,b, defined by simultaneous rotations in the three pairs of orthogonal planes, can be shown equivalent to the three color charges of SU(3)-color. Even more important, having quark states and gluon states defined in R^4 means they cannot ex-

ist in R^3, so quark confinement becomes geometrically explained also.

Finally, the 4-D quark and gluon states must combine according to quantum chromodynamics (QCD) to make the mesons and baryons, i.e., the 3-D hadrons. Intersection theory in mathematics can handle this geometrical concept of intersecting 4-D objects to make 3-D objects.

However, QCD theory predicts [17, 18] a self-contained world for the quarks and gluons, with only color changes allowed and no possibility of quark decay. So why does Nature need the leptons? The mathematical answer follows from Kuratowski's theorem [19] in graph theory: all graphs will reduce to the K_5 or $K_{3,3}$ graphs, the only graphs that retain their integrity. Fortunately, at least for quarks, the [333] discrete symmetry binary subgroup of the up/down quark family represents the K_5 graph, so all other quarks will decay eventually to this first family. The stability of the electron may also be a consequence because [332] is related to [333].

Also recall that only 4N-dimensional normal spaces have a conjugate space of the same dimension according to Clifford algebra and Bott periodicity [9]. So, there will be the simultaneous existence of the 4-D anti-particle real internal symmetry space as required by the SM. The next larger space with a conjugate space, R^8, is equivalent to a 10-D spacetime. For discrete spaces, icosians related to the binary icosaheral group [532] provide a direct connection [20] from our discrete R^4 to the discrete space R^8, which obeys the discrete symmetry operations of Weyl E_8.

The particles exist in our discrete SO(3,1) spacetime, so the icosians produce a second discrete symmetry Weyl E_8 for spacetime. Combining discrete spacetime with the discretee internal symmetry group therefore makes the discrete product group Weyl E_8 x Weyl E_8, equivalent to the discrete symmetry group I call "discrete" SO(9,1). Hence, there exists a *unique* connection from the SM gauge group to "discrete" SO(9,1) in a 10-D spacetime.

Appendix B: Identical particles and quantum statistics

Consider two identical particles. What behavior will the feedback signal approach predict?

Two neutral identical particles are to be considered, so that we can ignore any local gauge interactions of the SM, both particles beginning at rest with respect to each other. In the general case, feedback signals emitted at the same Compton frequency ω_1 by each particle are absorbed, phase shifted, and emitted by the other identical particle back into the surrounding space.

Their existence in each other's environment means that the identical particles can become phase-locked, either with in-phase or with out-of-phase normal modes, as is the case for two identical-frequency quantum harmonic oscillators communicating to each other, with their final locked-in phase relationship becoming 0 or π.

The two possible normal mode frequencies for any two harmonic oscillators communicating via an exchange of energy represented by Γ are

$$\Omega = \frac{1}{2}(\omega_1 + \omega_2) \pm \Gamma, \tag{44}$$

but the two identical high Q fundamental particles will have $\omega_2 = \omega_1$, so

$$\Omega = \omega_1 \pm \Gamma. \tag{45}$$

Which physical property of a particle actually determines the difference between the two phase-locked states? Because the single free particle does not have phase-shifted returning feedback signals, the phase shifts introduced by the other identical particle can be a function of differences only:

$$\text{phase shift} = f(\omega_i - \omega_j, A_i - A_j, P_i - P_j), \tag{46}$$

where ω is the Compton frequency, A is the signal amplitude, and the P could be some other factor such as the intrinsic spin.

As we know, the physical factor P called particle intrinsic spin S is the key. Different particle angular momentum spin states need to be considered, such as a scalar S = 0, a spinor S = 1/2, and a vector S = 1, in order to determine the general result.

Consider the scalar particles first, the ones with intrinsic spin S = 0. At first the feedback signals returning from the direction of the other identical scalar particle might not be in-phase, so the two particles are accelerated toward each another because the returning feedback signals from the vacuum transponders in the direction opposite the other particle are in-phase. Eventually, the scalar particles can become locked in-phase with each other's oscillations and can occupy the same point in space. So these two S = 0 identical particles behave as bosons obeying Bose-Einstein statistics.

Now consider a system of two spin S = 1/2 electrons. QM requires [21] that their overall asymmetric wavefunction be the product of position eigenvalues and the total spin quantum numbers. There are three triplet spinor states having S = 1 symmetric with respect to the exchange of the electrons, with the spatial part being asymmetric so that the probability of the two electrons being at the same point in space is zero. But for the singlet S = 0 spinor state, the spin part is asymmetric and the spatial part is symmetric, thereby enhancing the probability to be at the same point in space, i.e., there is an attraction to one another.

Applying geometry by rotating the two S = 1/2 identical particles together in the triplet S = 1 state by 360°, one determines that the feedback signals will return with a phase that produces an increased amplitude pushing each particle away from the direction of the other identical particle. Therefore, a repulsion occurs to produce an increased separation. Called Pauli repulsion, this response is the source of Fermi-Dirac statistics.

In the total S = 0 case for two spin S = 1/2 particles, i.e., with spins opposite, the feedback signal amplitudes at each particle decrease by adding in the returning signals from the direction of the other identical particle. There is attraction, so this total S = 0 spin state is allowed for two electrons at the same point in space. That is, the spatial wavefunction is even but the spin wavefunction for this total S = 0 state is anti-symmetric.

Finally, when both particles each have S = 1, the total spin states are S = 2 and S = 0. The geometrical factors will produce a result identical to the total S = 0 Bose-Einstein behavior for two scalar particles, i.e., there is a feedback signal amplitude decrease that results in an attraction.

Back to Cosmos

F. M. Sanchez[1], V. A. Kotov[2], M. Grosmann[3], D. Weigel[4], R. Veysseyre[5], C. Bizouard[6], N. Flawisky[7], D. Gayral[8], L. Gueroult[9]

[1]Professor (retired), Université Paris 11, Orsay, France. E-mail: hol137@yahoo.com.
[2]Astronomer, CrAO*, Nauchny, Crimea, Russian Federation. E-mail: vkotov43@mail.ru.
[3]Professor (retired), Université Louis Pasteur, Strasbourg, France. E-mail: michelgrosmann@me.com.
[4]Professor (retired), Université de Dijon et Paris 6, France. E-mail: dominiqueweigel118@gmail.com.
[5]Professor (retired), École Centrale, Paris, France. E-mail: renee.veysseyre@gmail.com.
[6]Astronomer, OBSPM, Paris, France. E-mail: christian.bizouard@obspm.fr.
[7]Architect/Math Instructor, ENSA† Paris Malaquais, France. E-mail: flawisky@free.fr.
[8]Computer Science Engineer. E-mail: denis.gayral@epita.fr.
[9]Lecturer (retired), ENSA Paris Malaquais, France. E-mail: lgueroult@hotmail.com.

The antique concept of a permanent Cosmos is reintroduced as a perfect deterministic computer, inverting the Anthropic Principle and interpreting the dimensionless parameters as optimal calculation bases. The later are unified in the Topological Axis, which exhibits the string theory dimension series $d = 4k + 2$, with the emphasis on the values 26 (visible universe) and 10 (the hydrogen-pion couple). The 1-D extension of the Holographic Principle defines the Grandcosmos and a 10^{61} trans-plankian quantified time. This confirms the matter-antimatter oscillatory bounce and resolves at last the vacuum energy dilemma. The intervention of the sporadic groups implies the mathematics-physics fusion which is confirmed by 10^{-9} precise relations, showing four force connection with the Eddington constant 137 and the Atiyah one. The Holic Principle, the generalized Holographic Principle and Eddington's theory must unlock particle physics, with composite d quark and massive string, gluon, photon and graviton. The standard evolutionary cosmology will soon be excluded by the observation of mature galaxies in the very far-field.

Contents

1 The hierarchy and computation principles

There is presently an intense debate in the physics community. While a minority believes in an Ultimate Theory, a large majority have abandoned such hope and believes seriously in the extreme consequence of the "Anthropic Principle", the Multiverse conundrum [1]. The present article settles the debate in favor of a *single steady-state flickering* cosmos (Section 4), a kind of synthesis between the two historic main cosmologies, since it can be viewed as a *Permanent Big Bang*.

Only a minority thinks physics and mathematics are really unified, while a large majority separate the two domains (so separating also biology). The criteria for the uniqueness of the Cosmos is the mathematical character of the measured dimensionless parameters. Indeed, we show in Section 2 that *the latter obeys the Topological Axis, Fig. 1, and, for the first time, they are connected with a series of ppb relations involving e, π and γ* (Section 9.4). This article shows also that the discovery of the sporadic groups, with, in particular, the monstruous moonshine correlation [2], is a crucial discovery for

*Crimean Astrophysical Observatory
†École Nationale Supérieure d'Architecture

physics (Section 8.5).

In this debate unicity-multiplicity, pure mathematicians believe that progress can be obtained only when the Ultimate Theory has been discovered. However, the history of physics shows that one can progress without knowing the ultimate laws. This no-said principle can be called the *"Hierarchy Principle"*. So, when Proust and Dalton found whole numbers in chemical reactions, they were prefiguring atomic physics. The same for Balmer, spectral lines and wave mechanics. Idem for Mandeleev, atomic masses and nuclear physics. Also, when Mandel found whole numbers in biology, he anticipated genetics. In the same manner, *this article prefigures the fundamental theory, but precising its arithmetical foundation: the Holic Principle*, recalled in Section 6. We interpret this central role of whole numbers by assuming that the Cosmos is a perfect computer. This is the very foundation of quantum physics. The Section 3 shows the overall holographic quantification, breaking the Planck wall by a factor 10^{61}, solving at last the vacuum quantum energy dilemma and *justifying why the Cosmos is so large*. This *"Optimal Computation Principle"* enlightens the First Principle of Thermodynamics, the energy conservation. This is a more direct and logical explanation than the standard "time uniformity".

This reinstates the Laplace determinism, involving non-local hidden variables, which are identified with the Cosmos, so rejecting the standard Copenhagen statistical interpretation of quantum mechanics. It seems that the pre-scientific role of chance is a common point between three misleading views in present mainstream thinking. Firstly, in biology, the assimilation of Darwin's rough argumentation with a scientific theory (see Discussion). Secondly, in quantum physics, the so-called "uncertainty principles", which are only manifestations of the general wave propagation (field and *flickering* matter), through Fourier transform properties. Thirdly, in cosmology, the above recurse to the Multiverse conundrum.

While it was already shown that main dimensionless parameters are present both in musical scales and in DNA characteristics [3], this article goes further, by showing they are *calculation bases*.

The abnormal efficiency of elementary 3-fold dimensional analysis is justified in Section 5, confirming the reality of the Grandcosmos, essential in Coherent Cosmology [3]. The c-free analysis gives simply and directly the supercycle period in an all-deterministic Cosmos, with dimension $d = 30$, given by the Holic Principle. An elementary calculation gives also a good approximation of the *invariant* Hubble radius, in a formula which was present for a century in astrophysics textbooks: the limit of a star radius when the number of atoms reduces to unity. We recall that in Coherent Cosmology, the Hubble radius R is defined by the relative redshift law

$$\Delta f/f = l/R$$

of l-distant galaxy groups, in the *exponential* recession.

Finally, there is the central problem of infinity. While it is welcome in mathematics, it is condemned in physics. The domination of mathematics blocked for years the quantum mechanics, annonced by the above discoverers, from Proust to Mandel. Indeed, Planck believed in the *mathematical continuum*, and was reluctant of his own *physical discovery*, until 1912, when Poincaré demonstrated that the quantification of matter-light interaction was mandatory [4]. The continuum has the advantage that it simplifies formulas, by the virtue of the computation properties of e and π. Thus, the vastness of the Cosmos is a compromise, but at the expense of *a necessary rationalization of e and* π, as shown in this article.

Thus, there must exist multi-base algorithms able to explain the compatibility between these two principles, Hierarchy and Computation, which seems at first sight somewhat contradictory. The key is the analysis of the dimensionless parameters (about 30 in the standard model), which are tightly contrived by a mysterious "fine-tuning". Happily, the Hierarchy Principle applies: only three dimensionless parameters: a, p, and a_G are sufficient to explain the main structures of the world [1]. Two of them are precisely measured: the electric constant $a \approx 137.035999139(31)$, known with 0.23 ppb precision, and the proton-electron mass ratio $p \approx 1836.15267245$ (75), known with 0.4 ppb precision. The gravitational coupling constant a_G was the square of the ratio Planck/proton mass, subjected to a relatively large imprecision 10^{-4} due to the imprecision on G measurement. In fact, we consider rather the inverse of α and α_G, we note a and a_G.

One reads [1]:

> For example, the size of a planet is the geometric mean of the size of the Universe and the size of an atom; the mass of man is the geometric mean of the mass of a planet and the mass of a proton. Such relationships, as well as the basic dependencies on α and α_G from which they derive, might be regarded as coincidences if one does not appreciate that they can be deduced from known physical theory, with the exception of the Universe, which cannot be explained directly from known physics... This line of arguments, which is discussed later, appeals to the 'anthropic principle'.

This is misleading since, as soon as the fine-tuning involves the observable Universe radius, it signals the existence of a fundamental theory that must take into account the *antique Cosmos concept, which, as Eddington claimed [5], must be permanent*. Extending this to the standard spatial homogeneity, this leads to the Perfect Cosmological Principle, the very foundation of the steady-state cosmology and the starting point of Coherent Cosmology [3].

2 The cosmic fine-tuning and the topological axis

We look here for a systematic organization of dimensionless physical quantities stemming from cosmology, astrophysics, particle physics, theoretical physics and mathematics. The most famous fine tuning implies cosmic quantities, awkward-

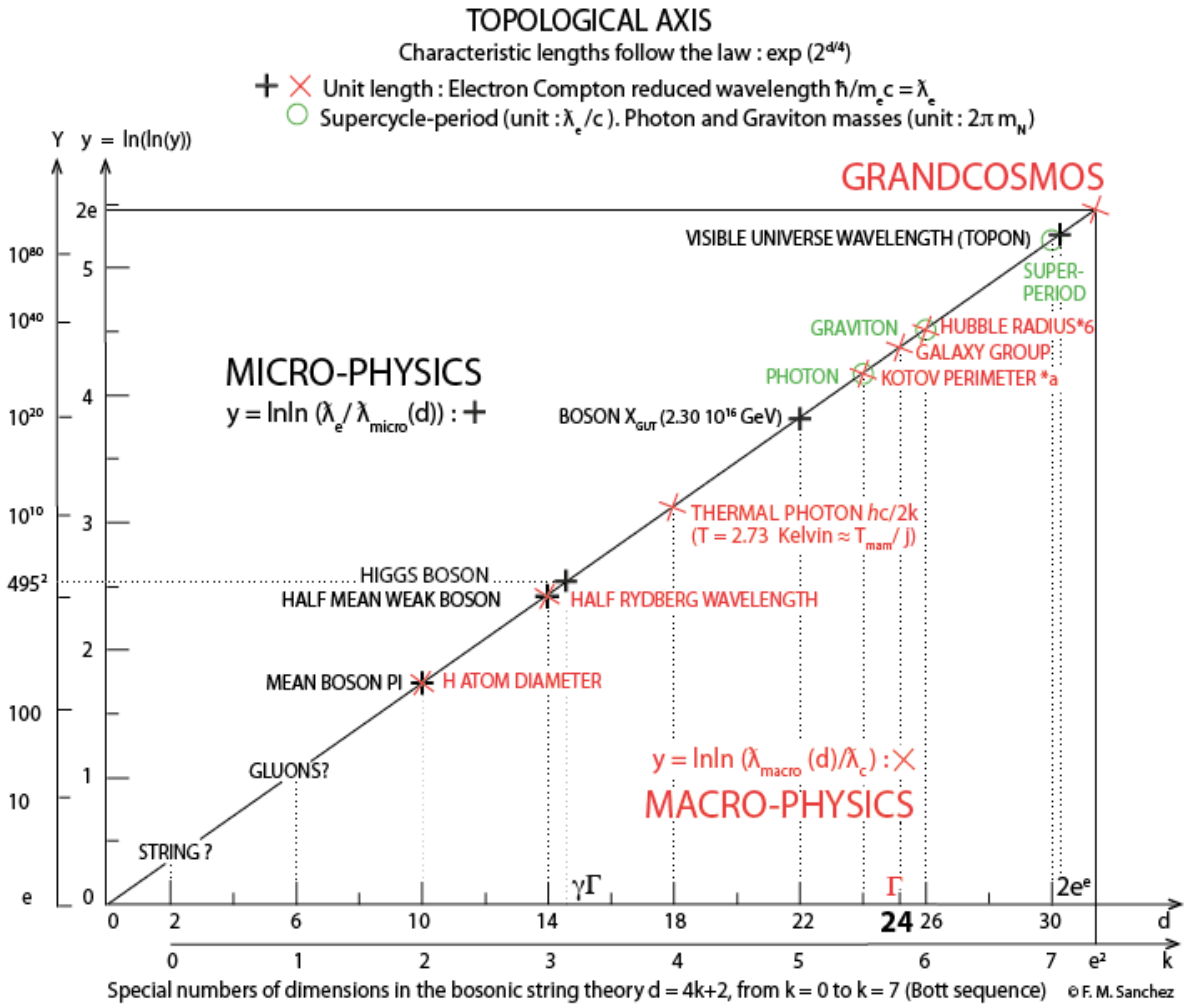

Fig. 1: The Topological Axis (data in Table 1). The double natural logarithms $y = \ln(\ln(Y))$ of the main dimensionless physical quantities Y corresponds to the special string dimension series $d = 4k + 2$, from $k = 0$ to $k = 7$, characteristics of the Bott sequence [27]. This is the reunion of height 2D-1D holographic relations, hence the name "Topological Axis". Two relations come from the double large number correlation [5], one comes from the Carr and Rees weak boson-gravitation relation (2), and one comes from the Davies analysis [11], involving the Cosmological Microwave Background (CMB) wavelength. *On the macrophysics side, with length unit $\lambda\!\!\!^{-}_e$, the electron Compton reduced wavelength*, 6 × Hubble radius 13.812 billion light-years, (3), is tied to the bosonic critical dimension 26, while Bott reduction $\Delta d = 8$ leads firstly to $d = 18$: it is the *thermal photon* (CMB). This temperature $T \approx 2.725820805$ Kelvin, (38), is identified to the common temperature of the couple Universe-Grandcosmos. It is tied to the the mammal wavelength through the Sternheimer scale factor j (Section 8.3); another Bott reduction leads to $d = 10$ (superstring dimension): it is the *hydrogen atom*, and finally to $d = 2$: the *massive string*, about 2.1 GeV. For the number 24 of transverse dimensions, it is the *Kotov length* (Section 4.3), multiplied by a factor about $2\pi a$, with $a \approx 137.036$. For $d \approx \Gamma$, the Atiyah constant (Section 8.2), it is the *galaxy group* radius, a characteristic cosmic length (10^6 light-years, Section 2.1). For $k \approx e^2$, $y \approx 2e$, it is the *Grandcosmos* radius (Section 3). The Space-Time-Matter Holic dimension $d = 30$ (Section 6) is tied to c times the cosmic *supercycle period* (Section 5). *On the microphysics side, with the same length unit $\lambda\!\!\!^{-}_e$*, Bott reductions from $d = 30$ lead to the *gauge bosons*: $d = 22$ for the Grand Unification Theory (GUT) one, (2.30×10^{16} GeV), $d = 14$ for the weak one and $d = 6$ for the (*massive*) gluons, about 8.6 MeV. For the intermediary superstring value $d = 10$, there is the mean *pion*. For $d \approx \gamma \times \Gamma$, $Y \approx 495^2$ the square of the diminished Green-Schwarz string dimension (496 − 1), it is the *Brout-Englert-Higgs boson* (125.175 GeV). For $k \approx 2e^e$, it is the *topon*, the visible Universe wavelength, the space quantum, which identifies with the monoradial unit length of the Bekenstein-Hawking Universe entropy (Section 3). *With unit 2π times the Nambu mass $m_N = am_e$* [15], $d = 24$ and 26 corresponds to the *photon and graviton masses*, defined by the two-step holographic interaction [3], Section 7.1. This is the extrapolation towards smaller numbers of the Double Larger Number correlation. The central dimension is $d = 16$, for a total of 2^7 string dimensions in the Bott sequence. This suggests a liaison with the Eddigton's matrix 16 × 16 [5].

Table 1: Topological Axis $f(d) = \exp(2^{d/4})$. Data with $R = 2a_G\lambda\!\!\!^{-}_e = 2\hbar^2/Gm_em_pm_H \approx 13.812$ Glyr, $R_{GC} = 2r_e^6/l_P^5 \approx 9.0758 \times 10^{86}$ m

$\lambda\!\!\!^{-}_M = 2l_P^2/R \approx 3.9989 \times 10^{-96}$ m, $T = \hbar^4/\rho_c^{3/2}G_F^{5/2} \approx 5.4829 \times 10^{57}$ s, $l_K = \lambda\!\!\!^{-}_e(a_Ga_w)^{1/2}$, $m_{ph} = a_wm_{gr} \approx 1.222 \times 10^{-55}$ kg

Physical element	k	$d = 4k + 2$	$\ln(\ln(f(d)))$	$\ln(\ln($Measured ratio$))$ [17]	Predictions ($\lambda\!\!\!^{-}_e = ar_e = ct_e$)
string	0	2	0.347		$m_{string} \approx 2.1$ MeV ?
gluon	1	6	1.040		$m_{gluon} \approx 8.6$ MeV ?
mean pion	2	10	1.733	$\ln(\ln(268.60)) \approx 1.722$	
H atom diameter	2	10	1.733	$\ln(\ln(274.22)) \approx 1.725$	
half mean weak boson	3	14	2.426	$\ln(\ln(8.378 \times 10^4)) \approx 2.428$	
Higgs boson	-	$\gamma\Gamma \approx 14.533$	2.518	$\ln(\ln(2.449 \times 10^5)) \approx 2.518$	$m_{Higgs} \approx 125.175\ GeV$?
thermal photon	4	18	3.119	$\ln(\ln(hc/2k\theta_{CMB}\lambda\!\!\!^{-}_e)) \approx 3.035$	
boson GUT	5	22	3.812		$m_{GUT} \approx 2.30 \times 10^{16}$ GeV ?
photon	5.5	24	4.159		$\ln(\ln(m_N/m_{ph})) \approx 4.130$
Kotov perimeter	5.5	24	4.159	$\ln(\ln(2\pi l_K/r_e)) \approx 4.159$	
Hubble radius R*6	6	26	4.5054	4.506(3) [6]	$\ln(\ln(6R/\lambda\!\!\!^{-}_e)) \approx 4.5054$
graviton	6	26	4.505		$\ln(\ln(m_N/m_{gr})) \approx 4.485$
supercycle period	7	30	5.199		$\ln(\ln(T/t_e)) \approx 5.199$
topon	-	$2e^e$	5.253		$\ln(\ln(\lambda\!\!\!^{-}_e/\lambda\!\!\!^{-}_M)) \approx 5.523$
Grandcosmos	e^2	-	5.432		$\ln(\ln(R_{GC}/\lambda\!\!\!^{-}_e)) \approx 5.433$

ly called the "Double Large Number Problem". If it is a "problem" for standard evolutionary cosmology, it is a precious clue in the steady-state cosmology based on the above *Perfect* Cosmological Principle (spatial *and* temporal homogeneity). This cosmological fine-tuning leads directly to a *gravitational hydrogen molecule model of the visible universe* [3].

This defines the Universe Hubble radius $R = 2a_G\lambda\!\!\!^{-}_e$, where the factor 2 comes from the bi-atomic structure, and where $\lambda\!\!\!^{-}_e = \hbar/cm_e$ is the electron Compton reduced wavelength, while the gravitational coupling constant is $a_G = \hbar c/Gm_pm_H$, where m_p and m_H are the proton and hydrogen atom masses. So, *the speed c is eliminated*, in accordance with the Coherent Cosmology which needs signal celerity far exceeding c. This gives $R \approx 13,812$ Gly, corresponding to a Hubble constant 70.790 (km/s)/Megaparsec, compatible with the most recent measurements [6]: 72(3) (km/s)/Megaparsec. The latter confirms the value measured by the 1a type novae, while the standard optimization of 6 parameters results in a lower value, by 9%. This is a significant refutation of the standard cosmology, but the fact that the so-called Universe age is about 13.8 Gyr cannot be due to chance. This means that the standard approach has something right [10], but the standard interpretation is false: in fact the Big Bang is permanent.

Consider the wavelength of the visible Universe with critical mass $M = Rc^2/2G$:

$$\lambda\!\!\!^{-}_M = \hbar/Mc \approx 4.00 \times 10^{-96}\,\mathrm{m}\,. \tag{1}$$

This "topon" corresponds to the value $n \approx 2e^e$, close to the touchstone $n = 30$ of the Topological Axis, see Fig. 1. This scheme illustrates the function $f(n + 4) = f^2(n)$ and stems from the imbrication of relations of the form $\lambda\!\!\!^{-}_e/l_{micro} \sim (l_{macro}/\lambda\!\!\!^{-}_e)^2$, followed by $l_{macro}/\lambda\!\!\!^{-}_e \sim (\lambda\!\!\!^{-}_e/l'_{micro})^2$, leading to:

$$\lambda\!\!\!^{-}_e/\lambda\!\!\!^{-}_M \sim (R/\lambda\!\!\!^{-}_e)^2 \sim (\lambda\!\!\!^{-}_e/\lambda\!\!\!^{-}_X)^4$$
$$\sim (\lambda_{CMB}/\lambda\!\!\!^{-}_e)^8 \sim (\lambda\!\!\!^{-}_e/\lambda\!\!\!^{-}_W)^{16} \sim (2r_H/\lambda\!\!\!^{-}_e)^{32}$$
$$\sim (\lambda\!\!\!^{-}_e/l_{Gl})^{64} \sim (\lambda\!\!\!^{-}_{str}/\lambda\!\!\!^{-}_e)^{128} \sim 2^{2^8}\,.$$

This series include the Cosmic Microwave Background wavelength λ_{CMB} and a string wavelength $\lambda\!\!\!^{-}_{str}$, with mass about 2 MeV. Hence, the correlation is eight-fold. They include implicitly the above double fine-tuning and three more relations that have been independently reported [3]. Thus, only three relations are really new. The overall large number 2^{256} has an obvious computational character, confirmed below by the dramatic appearance of the Eddington Large Number.

In particular, as Davies quoted [11] *"The fact that* $R/\lambda_{CMB} \sim a_G^{3/4}$ *seems to indicate yet another large-number coincidence"*. By this order of magnitude, we infer rather precise relations. With the hydrogen radius r_H, we observe $R/r_H \approx (4\pi\lambda_{CMB}/r_H)^4$, precise to 0.6%. Considering the standard cosmological neutrino background (CNB), which wavelength is defined by $(\lambda_{CNB}/\lambda_{CMB})^3 = 11/4$, we note that $R/\lambda\!\!\!^{-}_e \approx (\lambda^2_{CNB}/\lambda_{CMB}\lambda\!\!\!^{-}_e)^4$ to 1.7%. The appearance of the neutrino field is conform with the synthesis of the two main cosmologies, where the single Bang is replaced by a matter-antimatter Oscillatory Bounce [10].

It was noted in [1] that a_G is of order W^8, where W is the W boson-electron mass ratio. With the above R value, one observes the following more symmetrical relation involving the other (neutral) weak boson Z, in the 0.01% indetermination of W and Z:

$$R/(\lambda\!\!\!^{-}_p\lambda\!\!\!^{-}_H)^{1/2} \approx (WZ)^4 \tag{2}$$

where $\lambda\!\!\!^{-}_p$ and $\lambda\!\!\!^{-}_H$ are the proton and hydrogen reduced wavelengths. The precision of this formula will be pulled to the ppb range in Section 9.4, by intervention of canonical mathematical constants.

The gravitational hydrogen molecule model [3] implies the following double correlation, which is the simplest case of Eddington's statistical theory [5]: the position of a "reference particle" is supposed to be determined with an uncertainty of $R/2$. For N particles of mass m components of the visible Universe, the deviance is statistically divided by $\sqrt{N}$, where $N = M/m$. If m is the principal value of the effective mass of the electron in the hydrogen atom, $m = m'_e = m_e m_p/m_H$, and if, moreover, one equates the deviance $R/(2\sqrt{(M/m'_e)})$ to the hydrogen reduced wavelength $\lambda\!\!\!^{-}_H = \hbar/cm_H$, one gets:

$$R/2\lambda\!\!\!^{-}_H = (M/m'_e)^{1/2} = \hbar c/Gm_e m_p\,. \tag{3}$$

This is the definitive interpretation of the Double Large Number fine-tuning. So, while the two pillars of physics, relativity and quantum theory are unable to conciliate gravitation and particle physics, the third pillar, statistical physics, directly makes this connection in cosmology [5].

Recall that, contrary to what is often stated, quantum physics does not limit to microphysics. Indeed, the exclusion principle applies in both solid state physics and in stellar physics. In particular, for a star containing N_s atoms, in which the pressure has reached the quantum degeneracy value (case of white dwarfs), exclusion principle applies for electrons, and the star radius is about $R/N_s^{1/3}$ [3]. So the formula giving the Hubble radius R, a very difficult measurement which puzzled a whole century, was implicitly contained in astrophysics textbooks. Eddington was aware of this Cosmologic Exclusion Principle, but he could not conclude since, at his epoch, the Hubble measurement for R was false by an order of magnitude.

The reason for this discrepancy is that *Lemaître and Hubble considered galaxies of the Local Group, which do not participate in the so-called space expansion*. In fact, it is sufficient to introduce a repulsive force proportional to separation distance, for explaining the steady-state exponential recession. *The repulsive force is equivalent to reintroduce the Einstein cosmological constant in the General Relativity equations, but with invariant value* $1/R^2$.

The distance for which this force exceeds attractive gravitation between galaxies is about 10^6 light years [3], a typical galaxy group radius, which corresponds, in the Topological Axis, to the Atiyah constant Γ, (Section 8.3), see Fig. 1.

In the steady-state cosmology of Bondi, Gold [7] and Hoyle [8], such a repulsive force between galaxy groups is necessary, in order to avoid a big chill due to the thermodynamics second principle. But, inside a galaxy group, another evacuation mechanism must occur: *it would be the role of the massive black holes*.

3 The toponic holographic quantification

In the above steady-state cosmological model, the Perfect Cosmological Principle implies the invariance of the Universe mean mass density ρ, defined at large. This predicts also the exponential recession of galaxy groups, with time constant R/c being compensated by the appearance of m_n massive neutrons at rate c^3/Gm_n, corresponding to about one neutron by century in a cathedral volume. The invariant visible Universe radius R is then defined by the Schwarzschild relation, so that each topon, with wavelength $\lambda\!\!\!^{-}_M = \hbar/Mc = 2l_P^2/R$ is the center of an equivalent R-radius black hole, of critical mass $M = Rc^2/2G$. The Bekenstein-Hawking entropy of this black hole Universe shows a 1-D extension [3] of the standard Holographic Principle, until now devoted to 3-D application only [12]:

$$S_{BH} = A/4 = \pi(R/l_P)^2 = 2\pi R/\lambda\!\!\!^{-}_M \tag{4}$$

where A is the horizon sphere area and $l_P = (G\hbar/c^3)^{1/2}$ is the Planck length. Note that, while the standard evolutionary cosmology uses differential equations, which are not adapted to a single Universe, as Poincaré stated [9], the Permanent Cosmology must favor such integral relations. Here it is the *Archimedes testimony tying the disk area to its perimeter*.

The topon breaks the so-called "Planck wall" by a factor $l_P/\lambda\!\!\!^{-}_M \approx 10^{61}$. This explains why this holographic relation was long time unnoticed. Indeed, it was admitted that l_P was the quantum of space: in fact *the Planck length is an intermediate holographic length only*.

The gravitational potential energy of a critical homogeneous sphere is $-(3/5)GM^2/R = -(3/10)Mc^2$, while the *non-relativistic* kinetic energy of galaxies is $(3/10)Mc^2$ [3]. Their sum is therefore zero: the density of the so-called "dark energy" is compatible with 7/10, so that dark energy was a trivial false problem. The relativity theory is a local theory that does not apply in cosmology at large: galaxies actually reach speed c, and, crossing the horizon, enter a Grandcosmos of radius R_{GC}, given, as a first approximation, by the symmetrical monochrome holographic relation:

$$S_{BH} = \pi(R/l_P)^2 = 2\pi R^{(0)}_{GC}/l_P \tag{5}$$

with $R^{(0)}_{GC}/R = l_P/\lambda\!\!\!^{-}_M \sim 10^{61}$. The conservation of the time constant $t = R/c = R^{(0)}_{GC}/C$ introduces a canonical velocity $C \sim 10^{61}c$, lifting the veil on an energy larger than that of the visible Universe by a factor of 10^{122}, which can be identified with the l_P-normalized quantum energy of vacuum, checked by the Casimir effect [13]. *The central problem of quantum cosmic physics is thus solved*. Moreover, the objections against the Hawking approach using transplankian frequencies are wiped out [14].

In a better approximation, justified below, R is replaced in the above relation by $R' = 2\hbar^2/Gm_N^3 \approx 18.105$ Gly, where $m_N = am_e$ is the Nambu mass [15], of central importance in

particle physics. Indeed, the half radius $R'/2$ has a simpler definition than $R/2$: it corresponds to the elimination of c between the classical electron radius and the Planck length [3]. In this way, the sphere of radius R' appears as the spherical hologram representation of the outer Grandcosmos:

$$S'_{BH} = \pi(R'/l_P)^2 = 2\pi R_{GC}/l_P \,. \tag{6}$$

This value will be confirmed in Section 5 (Fig. 6).

The toponic quantification hypothesis assumes that the mass of a particle is an exact sub-multiple of the critical mass M of the visible Universe: $m = M/N_m$. Thus its wavelength is $N_m \lambda\!\!\!^{-}_M$, allowing the following holographic extension of the above monoradial holographic conservation:

$$S_{BH} = \pi(R/l_P)^2 = 2\pi R/\lambda\!\!\!^{-}_M = 2\pi N_m R/\lambda\!\!\!^{-}_m \,. \tag{7}$$

This series of diametrical circles generate, by scanning, the approximation of a sphere: thus it goes from the disk to the sphere with area $4\pi(R/l_P)^2$. Note that *this justifies the factor* $\frac{1}{4}$ *in the BH entropy*. But, for the approximation to be sufficient, *the numbers* N_m *must be very large*. In this way, the Cosmos computer can use the computational properties of the mathematical constants of the continuous analysis, such as e and π, (Sections 8 and 9).

The immensity of the Cosmos thus receives a computational holographic explanation, which is much simpler than that of standard cosmology, where initial conditions, during Planck time, would be adjusted with extreme precision, even with inflation.

With $N_{Ed} = 136 \times 2^{256}$ the Eddington large number, one observes that N_{Ed} times the neutron mass, corrected by the classical ratio H/p, gives the effective mass $3M/10$ to 41 ppm, so that:

$$Mm_p = m_P^4/m_e m_H \approx (10N_{Ed}/3)m_H m_n \tag{8}$$

This directly involves the Planck mass m_P, which presently has no known interpretation, except that it is close to the mass of the human ovocyte [3]. In this way, the local inertia is related to the distant masses, in accordance with the Mach principle, which the relativity theory does not explain. Another shortcoming of this theory is that it does not define any inertial frame. However, the Doppler asymmetry of the cosmic background indicates that the speed of our local group of galaxies is about 630 km/s. The cosmic background is, therefore, tied to the Newton absolute frame, the Grandcosmos.

The mathematical continuity is excluded by the above Computation Principle, so the time associated to the above "topon":

$$t_M = \lambda\!\!\!^{-}_M/c = \hbar/Mc^2 \approx 1.33 \times 10^{-104} s \tag{9}$$

is the new candidate for the "chronon", the "quantum of time", so the oscillatory bounce has a frequency about 10^{104} Hz [10]. The CPT symmetry (Charge conjugation-Parity inversion-Time reversal) connects this matter-antimatter oscillation with the parity violation in particle physics and biology.

4 The tachyonic flickering space-time-matter

The tachyonic hypothesis is consistent with the non-local character of quantum mechanics.

4.1 The single electron cosmology

The single-electron cosmology [3] uses the electron indeterminacy, which is the real basis of the Exclusion Principle, giving a horizon value R_1 only dependent of the principal value of the hydrogen radius $a' = aH/p$, by respect to $\lambda\!\!\!^{-}_e$. It is the value for which the mean cosmic value is also the atomic one:

$$\frac{\sum(1/n)}{\sum(1/n^2)} = a' \tag{10}$$

with the sum running from 2 to $R_1/\lambda\!\!\!^{-}_e$. This implies:

$$R_1 = \lambda\!\!\!^{-}_e \exp((\pi^2/6 - 1)a' + 1 - \gamma) \approx 15.77465\,\text{Gly}$$

very close (0.4 ppm) to $R_1 = (p_G/p_0)(\beta R R')^{1/2}$, where $p_G = P/2^{127/2}$, with $P = \lambda\!\!\!^{-}_e/l_P$, $\beta = (H - p)^{-1}$ the Rydbergh correction factor and $p_0 = 6\pi^5$ the Lenz-Wyler value p (Section 9.2). Moreover, there is a direct connection with the Grandcosmos radius and the topon, to 0.90 %:

$$\lambda\!\!\!^{-}_M = 2l_p^2/R \approx R_1^3/R_{GC}^2 \,. \tag{11}$$

This *synthesis relation* confirms the coherence of the whole procedure. It will be of central importance in the following.

4.2 The Cosmic Coherent Oscillation (CCO)

The Kotov non-doppler cosmic oscillation [16] is not considered seriously, since it seems to violate the most basic prerequisite of physics, the generality of Doppler phenomena. Interpreting this as a tachyonic phenomenon, we identified the Kotov period $t_K \simeq 9600.06(2)$ s, taking the electron characteristic time $t_e = \lambda\!\!\!^{-}_e/c$ as unit, to the simplest relation eliminating c between a_G and $a_w = \hbar^3/G_F m_e^2 c$, the well measured (3×10^{-7}) dimensionless electroweak coupling constant a_w :

$$t_K/t_e = (a_G a_w)^{1/2} \,. \tag{12}$$

This weak coupling constant [1] $a_w = (E_F/m_e c^2)^2$ is defined from the Fermi energy [17]: $E_F \approx 292.806161(6)\,\text{GeV} \approx 573007.33(25)\, m_e c^2$, itself tied to the weak force constant $G_F \equiv (\hbar c)^3/E_F^2 \approx 1.4358509(7) \times 10^{-62}\text{Joule} \times \text{m}^3$. This introduces the product of two area speeds, confirming the flickering hypothesis:

$$(\lambda\!\!\!^{-2}_e/t_K)(\hbar/(m_p m_H)^{1/2} = (GG_F)^{1/2} \tag{13}$$

so the best measured cosmic quantity, the Kotov period, implies a symmetry between gravitation and weak nuclear force.

This specifies the G value to 10^{-6} precision (ppm). It is compatible with the well-elaborate (10^{-5}) BIPM measurement [18], at several sigmas from the Codata value [17], but the later is the mean between discordant measurements. Computer analysis shows that this value of G is compatible with the following well-defined value, with $d_e \approx 1.001159652$ the relative electron magnetic moment [17] :

$$(2^{127}/a_G)^{1/2} \approx d_e(H/p)^3$$
$$\Leftrightarrow$$
$$G \approx 6.6754552 \times 10^{-11}\,\mathrm{kg^{-1}m^3s^{-2}}.$$

A value ppb confirmed in Section 9. One notes:

$$\sqrt{(R_1/a_w l_K)} \approx 4\pi p/p_0 \leftrightarrow t_K \approx 9600.591445\,\mathrm{s}$$

a relation independent from G. This Kotov period t_K value will be confirmed, in the ppb range, in Section 9.4. It is associated [3] with the photon mass $m_{ph} = \hbar/c^2 t_K \approx 1.222\times10^{-55}$ kg. The connection with the graviton mass is proposed in Section 7.1.

The following relation (0.1%), will be very useful in the Section 5:

$$M/m_{ph} \approx (3/e)O_M^2 \qquad (14)$$

with O_M the cardinal order of the Monster group [19]. The Monster Group, the largest of 26 sporadic groups, is suspected by some researchers to play a central role in physics: indeed string theory allows a bridge between apparently unconnected mathematical theories [2].

4.3 The omnipresence of CCO in astrophysics

With $t = R/c$, the relation $(t\,t_K^2)^{1/3} \approx 10.8$ years, compatible with the famous 11-year sun period was noted. It was proposed that this unexplained phenomenon, responsible for moderate periodic climate variation, was also of flickering cosmic origin [20]. This hypothesis has been recently confirmed by the straight temporal profile of the phenomena, showing it is tied to a quantum process [21].

Remarkable enough, a "mysterious" period $\approx 1/9$ days of the Sun's pulsations has been predicted long before its actual discovery in 1974. Namely, 73 years ago, French amateur astronomer Sevin (1946) claimed that "la période propre de vibration du Soleil, c'est-a-dire la période de son infra-son (1/9 de jour), a joué un role essentiel dans la distribution des planètes supérieures". Presumably, the Sevin "vibration period" of the Sun was merely an issue of his reflections about resonances and distances inside the solar system. Nevertheless, solar pulsations with exactly that period were discovered, after decades – and independently of Sevin's paper – by a few groups of astrophysicists. Soon the presence of the same period, or timescale, was found in other objects of the Cosmos too [16].

Opponents emphasize often that t_K is very close to the 9$^{\text{th}}$ harmonic of the mean terrestrial day: the corresponding ratio – of the length of a day to the t_K period – is equal to 8.99943(1) – and claim thus the t_K oscillation of the Sun should be regarded as an artifact (see, *e.g.* Grec and Fossat, 1979; Fossat *et al.*, 2017). As a matter of fact, however, the t_K period occurs to be the best commensurate timescale for the spin rates of all the most massive and fast-rotating bodies of the solar system, in general.

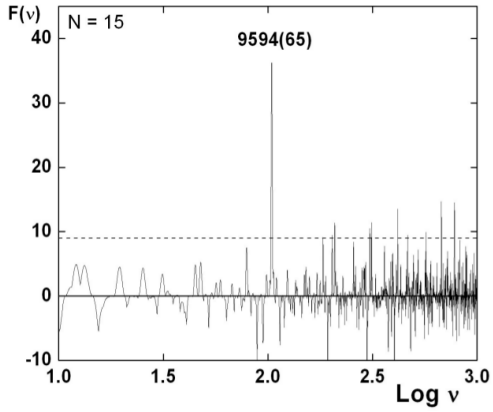

Fig. 2: Resonance-spectrum $F(\nu)$ computed for 15 motions of the largest, fast-spinning bodies of the solar system. On horizontal axis is logarithm of frequency ν in μHz, the dashed horizontal line shows a 3θ C.L., and the primary peak yields to the best – commensurable period 9594(65) s.

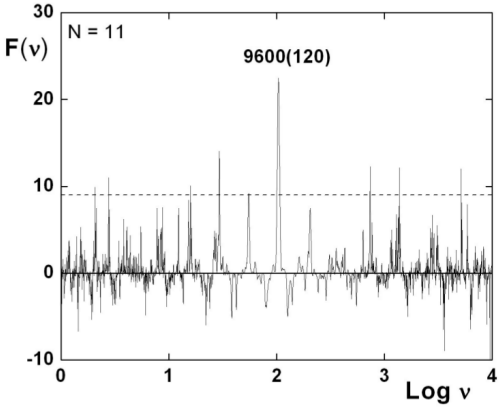

Fig. 3: Same as Fig. 2, for $N = 11$ sizes "diameters" of the solar system (with $c = 1$ and the π factor for inner orbits). The highest peak corresponds to the spatial scale 9600(120) light-sec.

This is obvious from Fig. 2, which shows the resonance spectrum $F(\nu)$, calculated for 15 motions of 12 largest, fast spinning, objects of the system (with the mean diameters $\geq$ 500 km and periods inferior to 2 days: six planets, three asteroids and three satellites, leaving apart trans-neptunian objects; see Kotov, 2018). The peak of the best commensurability corresponds to a period of 9594(65) s, which coincides well, within the error limits, with t_K at about 5.3θ C.L., *i.e.*

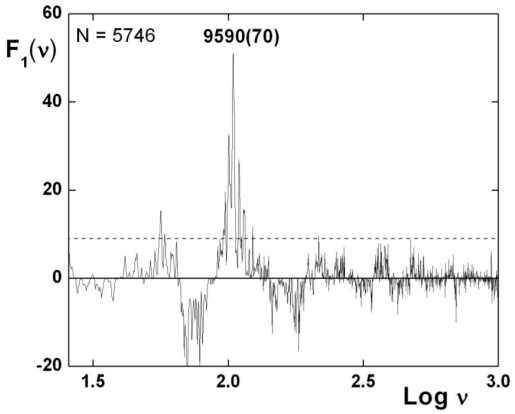

Fig. 4: Resonance-spectrum $F_1(\nu)$, computed for $N = 5746$ binaries with periods inferior to 5 days. Horizontal axis gives logarithm of the trial frequency ν in μHz, the dashed line indicates a 3θ C.L., and the major peak corresponds to a timescale of 9590(70) s.

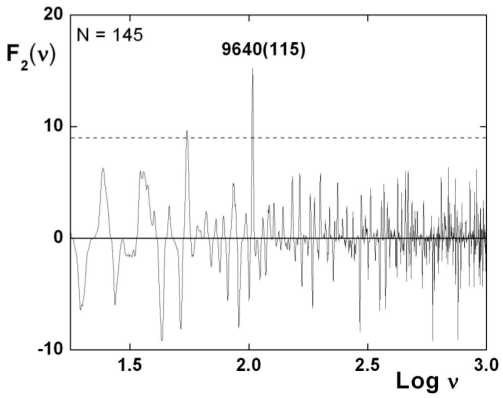

Fig. 5: Same as Fig. 4, for the $F_2(\nu)$ spectrum, computed for $N = 145$ exoplanets with P inferior to 1.5 days. The strongest peak of the composite commensurability corresponds to a period of 9640(115) s, at nearly 3.9θ significance (after Kotov, 2018).

with a chance probability 10^{-7}.

It seems very puzzling also that the spatial scale $l_K \approx 19.24$ A.U. occurs to be the best commensurate with orbital sizes of the main planetary orbits of the solar system, – see Fig. 3, where the resonance spectrum $F(\nu)$ is plotted for 11 orbits, including those of asteroid belt, Pluto and Eris (orbital "diameters" were approximated by the major axes, and for the inner orbits they were multiplied by π). The primary peak – of the best commensurability – corresponds to the spatial scale 9600(120) light-sec., or 19.24(3) A.U., at 4.7θ C.L. (Kotov, 2013).

Close binaries are characterized by the t_K resonance too, with the π number as a factor of ideal incommensurability of motions, or frequencies (Kotov, 2018). Fig. 4 shows the resonance spectrum, or metrics of motion, $F_1(\nu) \equiv F(\pi \times \nu/2)$, computed for 5746 close binaries, including cataclysmic variables and related objects. The major peak, with C.L. of about 7θ, corresponds to the timescale 9590(70) s, coinciding within the error limits with t_K (the stellar data were taken from all available binary stars catalogues and original papers).

To compute the $F_1(\nu)$ spectrum, the program finds – for each test frequency ν – deviations of ratios $(2\nu_i/\pi\nu)k \geq 1$ from the nearest integers, and determines then the least-squares minimum of such deviations. Here, ν is the test frequency, ν_i minus the frequency of a given object, $i = 1, 2, ...N$ – the ordinal number, with N, the total number of observed periods in a sample of objects, and the power $k = 1$ or -1. The factor of two in Eq. (2) takes into account that second half of the orbit repeats the first one, and the transcendental number π appears as a factor of orbital stability, or "idea" incommensurability, of motions, or frequencies (the π number, in fact, characterizes geometry of space; for details see Kotov, 2018).

Recently it was shown, that the t_K timescale characterizes, statistically, the motion of superfast exoplanets too, see Fig. 5.

It was shown in fact, that a number of superfast exoplanets, with periods inferior to 2 days, revolve around parent stars with periods, near-commensurate with timescales t_1 and /or $2t_1/\pi$, where $t_1 = 9603(85)$ s agrees fairly well with the period $t_K \approx 9600$ s of the so-called "cosmic oscillation" found firstly in the Sun, then – in other variable objects of the Universe (the probability that the two timescales would coincide by chance is near 3×10^{-4}).

4.4 The Tifft, Arp and Pioneer effects

Another unexplained effect is the 75(5) km/s periodicity in the galactic redshift [22]. Now, this speed $v_1 \approx ca/F$ corresponds to the following quantum resonance, with the electron classical radius $r_e = \lambda\!\!\!^{-}_e/a$ and where $m_F = m_e\sqrt{a_w}$ is the Fermi mass:

$$v_n/n = v_1 = \hbar/r_e m_F \,. \tag{15}$$

The Halton Arp observations of chains of galaxies with different redshifts [23] was also rejected. But it could be the sign of the galactic regeneration constantly maintaining the visible Universe mass: this is sustained by the following section proving the invariance of the mean mass density ρ_c.

Much controversial is the Pioneer deceleration [24] $g_{Pi} \approx 8.7 \times 10^{-10}\,\mathrm{ms}^{-2}$. It corresponds to the Pioneer time $t_{Pi} = c/g_{Pi} \approx 3.4 \times 10^{17}$ s close to $t = R/c \approx 4.3587 \times 10^{17}$ s. The following section will show a connection between the Kotov, Tifft and Pioneer effects.

5 The logic of prospective dimensional analysis

Physics uses principally *physical quantities* of the type $Q = M^x L^y T^t$, where M, L and T are Mass, Length and Time measurements, and where the exponents are rational numbers. However, the addition of measures of different categories has no significance. This seems at first sight illogical since, fundamentally, a product is a sum of additions. So, *there must*

be a hidden common nature for the three categories, mass, length and time. This sustains the above single electron cosmic model [3].

This suggests a 3-D geometrical model. Indeed, consider $t = R/c$, and $M' = R'c^2/2G$ the critical mass in the above holographic sphere representing the Grandcosmos. Summing the square of $\ln(M'/m_e)$, and two times the square of $\ln(R/\lambda\!\!\!^{-}_e) = \ln(t/t_e)$, one gets, to 40 ppm:

$$\ln^2(M'/m_e) + \ln^2(R/\lambda\!\!\!^{-}_e) + \ln^2(t/t_e) \approx \ln^2(R_{GC}/\lambda\!\!\!^{-}_e) \qquad (16)$$

showing the Grandcosmos ratio. This traduces, in function of $P = m_P/m_e$, $p = m_p/m_e$, $H = m_H/m_e$ by:

$$\ln^2(P^4/a^3) + 2\ln^2(P^2/pH) \approx \ln^2(2P^5/a^6)\,. \qquad (17)$$

Moreover, to 10^{-7}, corresponding to 7×10^{-6} precision on the above G value:

$$\ln^2(P^4/a^3) + 2\ln^2(P^2/pH) \approx \exp(4e{-}1/a)\,. \qquad (18)$$

This is a dramatic geometrical confirmation (Fig. 6) of the visible Universe-Grandcosmos holographic couple.

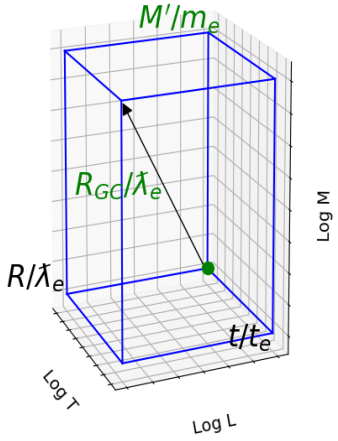

Fig. 6: *Geodimensional Universe-Grandcosmos couple*, with unit length the electron Compton reduced wavelength. In a 3-D superspace, logarithms of physical ratios are considered vectors. The Grandcosmos radius appears as the norm of the vector using for length and time projections the same value $R/\lambda\!\!\!^{-}_e = t/t_e$. For the mass projection it is M'/m_e where M' is the critical mass in the Grandcosmos reduced spherical hologram. This is a dramatic geometrical confirmation (not dependant of the base for logarithms) of the Extended (2D-1D) Holographic Principle applied to the Bekenstein-Hawking Universe entropy (6). The Grandcosmos existence cannot be denied since the relation involving *natural* logarithms with e and a reach precision 10^{-7}.

Another crucial point in physics is the existence of invariant fundamental constants. Thus, association of three of them must give characteristic values of M, L, T. So, approaching a domain in physics necessitates to calculate characteristic values (M, L, T) from the three universal constants which are the most pertinent in the considered domain. This prospective dimensional analysis is largely used in fluid mechanics, where the equations are intractable. However, it is largely ignored in other domains because there is not really mathematical foundation, apart the above essential remarks. The triplet $c, G, \hbar$ which define the above Planck units is a notable exception.

Moreover, in virtue of the above Hierarchy Principle, the lack of theoretical justification is not a reason to neglect prospective dimensional analysis.

The elimination of c in the above R formula means that the simplest basic dimensional analysis starting from $\hbar$, G and m, the electron-proton-neutron mean mass, gives a good approximation for $R/2$. Indeed, in the hypothesis of a coherent Cosmos, it is logical to discard c which is far two small a speed. This has not been observed during one century since c is always believed to be the single mandatory foundation of space-time. The warning of Poincaré [25], the true discoverer of relativity: *"use 4-D space-time, but do not confound Space and Time"* has long been forgotten, and physicists have unwisely put $c = 1$ in their equations.

In his three first minutes of cosmology (Sept. 1997), the first author obtained the length:

$$l\{\hbar, G, m\} = \hbar^2/Gm^3 \approx R/2 \qquad (19)$$

but it took nine years to get this published [20], and it appeared later [3] that m must be considered more precisely as the cubic root of the product $m_e m_p m_H$. Moreover, the above critical condition links the time $t = R/c$ and the mean mass density by the c-free formula:

$$\rho_c = 3/8\pi G t^2 \approx 9.41198\times10^{-27}\,\mathrm{kg}\times\mathrm{m}^{-3}\,. \qquad (20)$$

Thus, the mainstream idea of a temporal variability of the mean density ρ_c cannot be to sustain, meaning that ρ_c must be considered a fundamental constant. This writes:

$$t\{\hbar, \rho_c, G\} = 1/\rho_c^{1/2}G^{1/2} = (R/c)(8\pi/3)^{1/2}\,. \qquad (21)$$

This idea of ρ_c being a fundamental constant permits to define the Hubble radius R without any ambiguity: this is the radius of the sphere containing a critical mass. This justifies the above application of the Bekenstein-Hawking entropy.

Opponents would say that the center of a black hole presents a singularity: that is indeed the case for the topon in the above flickering space- mass-time hypothesis. Others will argue that the flying galaxies cannot reach the celerity c at horizon, but, as recalled above, relativity is a local theory, so do not apply to cosmology at large. Indeed, even General Relativity in unable to define any Galilean frame, while the Foucault pendulum shows it directly, realizing the Cosmic Microwave Background frame, identified with the Grandcosmos frame, as seen above.

Introducing the Fermi constant G_F, the associated c-free length is very particular, to 1.7%:

$$l\{\hbar, \rho_c, G_F\} = \hbar/\rho_c^{1/2}G_F^{1/2} \approx 9.07154\times10^9 m \approx \lambda\!\!\!^{-2}_e/l_P\,.$$

Now, most dramatically, the following mandatory c-free times are close to each over (0.7%):

$$T\{\hbar, \rho_c, G_F\} = \hbar^4/\rho_c^{3/2} G_F^{5/2} \approx 5.4829 \times 10^{57}\,\mathrm{s} \qquad (22)$$

$$T'\{\hbar, G, m\} = \hbar^3/G^2 m^5 \approx 5.5224 \times 10^{57}\,\mathrm{s}\,. \qquad (23)$$

One would conceive it is the deterministic supercycle period, which matches the Topological Axis at $n = 30$, the holic dimension (see Section 6), to 4%. Comparing T with the Kotov non-doppler Cosmic Oscillation period $t_K \approx 9600.60(2)$ s, one observes, to 0.04 % and 0.2 %:

$$T/t_K \approx O_M/\sqrt{2} \approx e^a/\sqrt{a_w}$$

where O_M, the cardinal order of the Monster Group, have been detected in the Section 4.2, again in relation with the Kotov period. Eliminating the latter, this introduces the above t_M chronon :

$$T/t_M \approx (3/e\sqrt{2}) O_M^3 \qquad (24)$$

The simplest interpretation follows: *this is the number of quantum events in a supercycle of period T, in a perfectly deterministic Cosmos*.

Introducing the above Pioneer abnormal deceleration g_{Pn}, one gets the time: $t\{G, m_e, g_{Pn}\} = (Gm_e/g_{Pn}^3)^{1/4} = (t_{Pn}^3 t'_e)^{1/4}$, where $t_{Pn} = c/g_{Pn}$ and $t'_e = Gm_e/c^3$. This time is compatible with: $t\{G, m_e, g_{Pn}\} = t_K/(F/a)^2$, where the above Tifft factor F/a appears. The implication of the time $t'_e = Gm_e/c^3 = 2.2568 \times 10^{-66}$ s confirms the above Planck wall breakdown.

6 The arithmetical logic: Holic Principle

In the hypothesis of an arithmetical Cosmos, the ultimate equations must be diophantine. The simplest one is $T^2 = L^3$, where T is a time ratio and L a length one, resolved, since 2 and 3 are co-prime, by:

$$T^2 = L^3 = n^6 \qquad (25)$$

where n is a whole number, showing the classical 6-D phase-space of point mechanics. Considering the exponents, this particularizes the usual 3-D space, but attributes 2 dimensions for the time, in conformity with an independent study [26].

This is the degenerate arithmetic form of the 2D-3D holographic principle.

This is *also* Kepler's third law. It was the simplest one of his three laws, and the realization of his research of harmony. Indeed, its diophantine form says more: it gives $L = n^2$, *the orbit law in the hydrogen atom and in our gravitational molecule model*, where the visible Universe corresponds only to the first orbital. This suggests at once the existence of a Grandcosmos.

Before the superperiod was recognized, the first version of the Topological axis [3] showed an overall dissymmetry. This was another sign for the Grandcosmos existence. Now, this corresponds to $d = 30$, the natural extension of the above diophantine equation:

$$T^2 = L^3 = M^5 = n^{30} \qquad (26)$$

where M is a mass ratio. Recall that the lifetime of an unstable particle depends on the 5th power of its mass. This holic dimension 30 is the touchstone of the Topological axis, from which the gauge bosons are deduced by Bott reductions [27] (Fig. 1).

This is called the Holic Principle, but limited to *the apparent MLT world only*. The Complete Holic Principle [29] involves a field term F^7, and so introduces the dimension $30 \times 7 = 210$. This is confirmed by (to 0.56 %, -0.65 %, -0.59 %, -0.32 %):

$$R/\lambda\!\!\!^{-}_e \approx s_4^5 \approx f(26)/6 \approx \Gamma^{28}/5 \approx (2/\delta)^{210} \qquad (27)$$

where $s_4 = 2\pi^2 a^3$ is the area of the 4-sphere of radius a and Γ is the Atiyah constant (Section 8.3). Moreover (0.1 %, 0.03 % and 0.9 %):

$$2/\delta = 2R/R' \approx \ln p/\ln a \approx \ln a/\ln \Gamma \approx \ln \Gamma/\ln f \qquad (28)$$

where f is the inverse strong coupling constant (Section 8.3). This confirms the central computational role of $\delta = R'/R = pH/a^3$, which is to 1.6 ppm: $\delta \approx e^{2/e^2}$. This implies a geo-combinatorial relation between a and p:

$$p^{(p^2)} \sim (a^2)^{(a^3)} \qquad (29)$$

showing a symmetry between basic powers of a and p.

7 The special holographic relations

The holographic technique, based on the properties of a coherent wave, is by far the most efficient way to treat huge information, in particular in optics [28].

The students of the first author realized in 1987 a hologram by scanning a 1 mW security power laser beam upon a photosensitive area of 0.6 m^2. The emulsion depth 10 microns permitted false color to be obtained by varying illumination through a photomask, and use of a shrinkable emulsion chemical process. The information contained in this hologram reached 10^{15} bit, obtained in 12 minutes of scanning exposition. Then, the first author claimed *"such an efficient way of dealing information must be used by Nature"*. Turning to the impressive data of particle physics, after an intensive study, holographic relations were indeed found, and its arithmetical form, the Holic Principle was presented at ANPA 16 (Cambridge, 1994) [29].

In Sept. 1997, the Orsay University attributes a sabbatical year, giving time to reexamine the foundation of cosmology. *In the three first minutes, the half-radius of visible Universe was obtained*. After several weeks, the scanning holography of Section 3 was established. After rejection by the Orsay

University and the French Academy, this was put in March 1998 in a closed draft in the Académie des Sciences de Paris, under the title *"L'Univers conserve-t-il l'information ?"*. The next year, the initial form of the Topological Axis was rejected by the French Academy, when an anonymous referee argued that "le Big Bang est avéré".

Strangely enough, when the first author's publication was blocked (1993-1995), a Holographic Principle was coined by some theoreticians [12], which were not specialists in holography. The origin of this appellation is not clear. One may think that the name comes from the idea of dimension reduction, from 3-D to 2-D, similar to the visual impression in current visible holograms (in fact holography is only the 2-D restitution of a propagating wave). It this respect, it is strange that no one tried to extend this process to 1-D. The idea of temporal 1-D holography was proposed in the first author's thesis as soon as 1975 [30].

While the standard Holographic Principle is limited to using the Plank area, it is natural to suppose that there are other holographic units. In fact, *the Topological Axis is the reunion of eight 1D-2D holographic relations*. We present here four more confirmations.

7.1 The graviton and photon masses

The electromagnetic interaction is not really understood, especially the photon concept [31]. The main lesson of modern physics is that everything (light *and* matter) propagates by waves (quanta appearing only at the detection). This implies directly the non-local hidden variable (Cosmos), without involving the so-called EPR paradox [32]. Indeed, a coherent wave is represented by a unitary operator: we have shown that the quantum formalism is very similar to the holographic one, describing an interaction by a two-step holographic process. We recall that convergent and divergent waves lead to an oscillation [3]. This is known as the particle exchange of a massive boson associated with any interaction. Here, it is assumed that the boson has a tachyonic speed C_1. Now, the resonance condition is that the wavelengths are identical, by analogy with the Gabor condition [33]. So, for the electron wave and the weak wave:

$$\lambda\!\!\!^{-}_e = \hbar/m_e c = \hbar/m_{gr} C_{gr} \tag{30}$$

$$\lambda\!\!\!^{-}_w = \hbar/m_w c = \hbar/m_{ph} C_{ph}\,. \tag{31}$$

Equaling the tachyonic celerities to C_1, and m_{ph} with $\hbar/cl_K$ [34], taking account of the *ppb correlation* tying R_1 and l_K (Section 4.2), one gets:

$$C_1/c = m_e/m_{gr} = m_w/m_{ph} = l_K/\lambda\!\!\!^{-}_w \approx R_1/\lambda\!\!\!^{-}_e(4\pi p/p_0)^2\,. \tag{32}$$

This leads to $m_{ph} \approx 1.2222 \times 10^{-55}$ kg, and $m_{gr} \approx 3.7223 \times 10^{-67}$ kg, which fit canonical places in the Topological Axis (Fig. 1). This means (0.8 %):

$$a_w = m_{ph}/m_{gr} \approx f(26)/f(24) \tag{33}$$

calling for further study.

7.2 The conservation of information

The Grandcosmos holographic reduction radius R' shows in itself an holographic relation with the CMB Wien wavelength $l_{CMB} = hc/kTv$, with $v = 5(1 - e^{-v}) \approx 4.965114245$, and the proton radius, identified, as a first approximation, to $\lambda\!\!\!^{-}_e/\sqrt{D} \approx 8.7029 \times 10^{-16}$ m (0.1 %, -0.1 % and 87 ppm):

$$e^a \approx 4\pi(R'/l_{CMB})^2 \approx (2\pi/3)(r_p/l_P)^3 \approx \sqrt{3} M_B/m_P \tag{34}$$

where $M_B = 2M/\sqrt{n}$ is the baryonic mass of the Universe [3]. The factor $\sqrt{3}$ implies a new holographic relation (see the "neutron relation" in Section 8.3):

$$4\pi(R/e^a l_P)^2 \approx (4\pi/3)n \approx (4\pi/3)(v\pi^2/4)^3\,. \tag{35}$$

Since the holographic technique uses coherent radiation, this seems incompatible with the CMB thermal character. But *in a totally deterministic cosmos, there is no paradox*. This question is connected with the black hole information paradigm [35]. Independently of our approach, an argument in favor of a total conservation of information was tied to a non-evolution cosmology [36].

So, while General Relativity and quantum physics disagree about the nature of space-time, especially the non-locality phenomena, they agree for complete determinism, leading to *the definitive rejection of the Copenhagen statistical interpretation*.

The Wien wavelength enters (0.03 %):

$$l_{CMB}/\lambda\!\!\!^{-}_e \approx P/pHa^3 \tag{36}$$

confirming that the cosmic temperature is invariant. Note that the measured proton "charge radius" $8.775(5) \times 10^{-16}$ m is slightly distinct from the above value. There is presently a "proton radius puzzle" [37].

7.3 The cosmic temperature

In the gravitational hydrogen molecule model [3], the Hubble radius R shows the following 1D-2D special holographic relation, using the wavelengths of the electron, proton and hydrogen, while the background wavelength appears in the logical extension, the 3-D term involving the molecular hydrogen wavelength:

$$2\pi R/\lambda\!\!\!^{-}_e = 4\pi\lambda\!\!\!^{-}_p\lambda\!\!\!^{-}_H/l_P^2 \simeq (4\pi/3)(\lambda\!\!\!^{-}_{CMB}/\lambda\!\!\!^{-}_{H2})^3\,. \tag{37}$$

The above relation gives $T_{CMB} \approx 2.73K$. Moreover it is another dramatic example of c-free dimensional analysis [3]. With the measured temperature of the cosmic background, there is a small gap compatible with $(H/p_G)^2 p/6\pi^5$, where $p_G^2 = P^2/2^{127}$, with $P = \lambda\!\!\!^{-}_e/l_P$. This eliminates l_P, producing a relation independent of G, implying $T_{CMB} \approx 2.725820805$ Kelvin. Recall that $2^{127} - 1$ is the most famous prime number in the history of mathematics, being the last term of the

Combinatorial Hierarchy [3] of special imbricated Mersenne numbers 3, 7, 127, the sum of which is 137 (Section 8.2):

$$2^{2^{2^{2^2-1}-1}-1}-1 = 2\pi^2\lambda_{CMB}^3/\lambda\!\!\!^{-}_e\lambda\!\!\!^{-2}_H \tag{38}$$

which is the area of the 4-sphere of radius $\lambda_{CMB}/\lambda\!\!\!^{-}_m$, where $\lambda\!\!\!^{-}_m = (\lambda\!\!\!^{-}_e\lambda\!\!\!^{-2}_H)^{1/3}$. This proves the relevance of the Lenz-Wyler approximation for the proton/electron mass ratio $p_0 = 6\pi^5$, (Section 9.2).

7.4 The Holic Principle and CCO

The sphere of radius $R' = 2r_e^3/l_P^2$, where $r_e = \lambda\!\!\!^{-}_e/a$ is the electron classical radius is the Grandcosmos hologram (Section 3). Its HB entropy writes: $\pi(R'/l_P)^2 = (\pi/2)(R'/r_e)^3$, *i.e.* with a wrong geometric coefficient. However, the HB entropy of the visible Universe shows a nearly geometric term, with imprecision $4/3\delta \approx 1.017$:

$$\pi(R/l_P)^2 \approx (2\pi/3)(R/r_e)^3 \tag{39}$$

which is a holographic conservation in *the half-sphere of the visible universe*. By analogy with the above scanning process filling the whole sphere (Section 3), the above Kotov length l_k (Section 4.3) permits to introduce two holographic relations, involving the whole sphere (0.90 % and 2.6 %):

$$\pi(R/l_K)^2 \approx 2\pi l_K/r_e \tag{40}$$

$$(4\pi/3)(R/l_K)^3 \approx 4\pi(r_e/l_P)^2\,. \tag{41}$$

The deviation of the first relation is very close to that of (11): $R_1^3 \approx R_{GC}^2\lambda\!\!\!^{-}_M$. This induces, with precision 17 ppm, identified to 0.3 ppm with $np^2/H^2\sqrt{pH}$, and 0.08 %:

$$(R_{GC}l_P/Rr_e)^2 \approx (R_1l_K/Rr_e)^3 \approx 3^{1/3}\mu^{35} \tag{42}$$

showing a quasi-holic form implying μ, the muon/electron mass ratio. The complete holic form with dimension 210 is shown by the study of the BH entropy of the Grandcosmos: (12 ppm, 100 ppm, 42 ppm):

$$\begin{aligned}\mu^{210} &\approx \pi^{-3/2}(R_{GC}/l_P)^4 \approx 4\pi\tau^{137}(a/137)^2\\ &\approx O_M^9 \ln D(p/n)^2\,.\end{aligned} \tag{43}$$

Ths is a perfect illustration of the Hierarchy Principle. Thus the expected correlation [38] [39] of $\ln D$ with 4π is confirmed. The existence of a final theory based on the Holic Principle (Section 6) and the Grandcosmos cannot be denied. The interpretation is clear: *the 4-D space-time of Grandcosmos is associated with a 9-D space involving the Monster. This opens a path towards the Final Theory.*

The term $R_1l_K/R'r_e$ is close to (1%) $\sqrt{O_M} \approx 2a^2P$ (0.18 %). The study of deviations shows the intermediate bosons ratios W and Z, with values specified to the ppb range in Section 9.4, leading to (-4 and 3.5 ppm, 0.3%):

$$O_M(FR'/PR_1)^2 \approx W^4(137/a)^3 \tag{44}$$

$$(F^3R_1/2a^3R')^2 \approx Z^4(a/137)(p_0/p)^2\,. \tag{45}$$

This refines the relation $a_w/WZ \approx \sqrt{a}$ known (0.1 %) in particle theory (0.3 and -0.4 ppm)

$$137p_0W^2Z^2/pa_w^2 \approx \sqrt{O_M}/(2a^2P) \approx e^{1/-4a}\,. \tag{46}$$

Thus, in first approximation ($e^{-1/4a} \approx 0.036$ %), the square root of the Monster order is the ratio of the Rydberg wavelength $2a^2\lambda\!\!\!^{-}_e$ to the Planck length.

8 The role of intermediary mathematical constants

8.1 The electrical constant a

The electrical constant a characterizes the Coulomb force between two l-distant elementary charges at rest:

$$F_{qq} = \hbar c/al^2\,. \tag{47}$$

Since any electrical charge is a whole multiple of unitary charge q (a relativistic invariant), *any electrical force depends only on the above constants and whole numbers*. Hence, it is logical that a appears central in atomic physics and in many fine-tuning relations [1].

However, theorists focused on one property only, the appearance of its fifth power in the hydrogen hyperfine spectra, calling its inverse α, the "fine-structure constant".

Many researchers looked for the mathematical origin of a. In quantum electrodynamics, $\sqrt{a}$ is connected with the electron magnetic abnormal factor, which is very precisely measured [17]: $d_e \approx 1.00115965218076(27)$. It is readily seen that $\sqrt{a} \approx \exp(\pi/2)^2$. From $i = e^{(i\pi/2)}$, this writes $i^{-\ln i}$ and the study of deviation leads to, with $a_e = a/d_e$ (29 ppb):

$$i^{-\ln i}/\sqrt{d_e} \approx (\sqrt{a_e} + 1/\sqrt{a_e})^2\,. \tag{48}$$

The slight deviation is not a valid objection, since *Nature must use rational approximations for* π. Indeed, the fractional development for the corresponding π value is 3, 7, 15, 1, $(\tau/\mu)^2$, with μ and τ the normalised masses of the heavy leptons. It is a formal rationalisation, focussing on an acute problem of present standard model, which is unable to explain the three families of particles. Thus, the study of the muon and tau mass ratios is crucial. One observes (1 ppm, 56 ppm, 0.02 %):

$$\begin{aligned}2/\delta &\approx (1/2d_e)\ln(pH)/\ln a\\ &\approx (1/d_e^2)\ln\tau/\ln\mu \approx d_e^2\ln s/\ln\tau\end{aligned} \tag{49}$$

where s is the Higgs ratio (Section 9.4). The following Koide relation [40], *which has a mathematical justification in terms of circulant matrix* [46], correctly predicted τ at an epoch (around 2000) during which its measurement was false to 3 σ. It writes:

$$(1+\mu+\tau)/2 = (1+\sqrt{\mu}+\sqrt{\tau})^2/3 = p_K\,. \tag{50}$$

This Koide relation, quite discarded by the scientific community, is another sign of the serious incompleteness of the present particle physics standard. This Koide-Sanchez constant will be precised to ppb precision in Section 9.4.

8.2 The Eddington constant 137

The initial Eddington proposal for a was the whole number 136, being the number of independent parameters in the symmetric matrix 16×16. Note that *$n = 16$ is the central dimension of the Topological Axis*. Later, one unity was added, becoming 137 [5]. It shows a symmetry between the 11 dimensions of M theory (a synthesis of five string theories) and the 4 of space-time. Indeed: $137 = 11^2 + 4^2$, while, as seen above: $11/4 = (\theta_{CMB}/\theta_{CNB})^3$.

Since Riemann series are tied to the prime number distribution, it seems odd and incredible that mathematicians have not point out the primes appearing in the harmonic series since it is the single Riemann pole. It seems that the basic precept *all occurs in the pole* was forgotten in this case.

As ancient Egyptians used only fractions of type $1/n$, they were certainly aware of this particular harmonic series: $S_5 = 137/60$. Indeed it appears in the Ptolemaic approximation for π: $\pi_{Pt} = 377/120 = 2 + S_5/2$.

It is strange that Eddington's theory was rejected as soon as a appeared to deviate from 137. Indeed, the following shows that *137 plays a central role in ppb fine-tuning analysis*. Note that Nambu [15] showed that the mass $m_N = 137m_e$ is central in particle physics.

One may interpret $137+1$ as the sum of the numbers of dimensions in the Topological Axis [3], taking into account the double point (H atom-pion couple) for the superstring value $d = 10$, and the remarkable sum:

$$\sum_{k=7}^{k=0}(4k+2) = 2^7 \,. \tag{51}$$

So $137 = 2^7 - 1 + 3 + 7$, *i.e.* the Combinatorial Hierarchy form [41]. But this appears also as $137 = 135 + 2$, showing the string dimension 2. Indeed, one obtains the value $a \approx 137.035999119$ compatible with measurement value in:

$$\ln 137/\ln(a/137) \approx (2 + 135/d_e)^2 \tag{52}$$

meaning that *the ratio $a/137$ acts as a canonical ratio*.

Considering the product of the T.A. dimensions:

$$P_d = \Pi_{k=7}^{k=0}(4k+2) = 2^8 3^4 5^2 7^1 11^1 13^1 \tag{53}$$

which is a simple sub-multiple of the cardinal order of the Suzuki group, and a simple multiple of the three other sporadic groups M_{11}, M_{12} and J_2 [19]. With l_W the mean of the CMB and CNB Wien lengths (0.06 %):

$$P_d \approx l_W/\lambda_e \,. \tag{54}$$

The pertinence of the Topological Axis series is thus confirmed, calling for further study.

8.3 The Atiyah and Sternheimer constants

Sir Michael Atiyah was a precursor in the search for unity in mathematics and physics. In his last work [42], the Bernoulli function $x/(1 - e^{-x})$ plays a central role. *This is the kernel of the thermal Planck law*. Considering the above Wien reduced constant $v = hc/kT\lambda_{Wien}$, one notes that $a \approx e^v - 2\pi$, suggesting a to be a trigonometric line. Indeed $\cos a \approx 1/e$, and, to 65 ppb:

$$a \approx 44\pi - \arccos(1/e) \tag{55}$$

a formula diffused on the web, but without indication of its connection with the Planck law. Moreover, v appears in the normalised neutron mass $n \approx 1838.6836089(17)$ (13 ppb):

$$n^{1/3} \approx v\,(\pi/2)^2 \,. \tag{56}$$

The small deviation is attributed to a rationalisation of π involving again the heavy leaptons: 3, 7, 16, $-(1+\tau/\mu)^2$.

Another central constant in the Planck law is the irrational Apery constant $\xi(3) \approx 1.20205691$. The number of photons in a sphere of radius r is: $n_{ph}(r) = (4\pi/3)(r/l_{ph})^3$ with $l_{ph} = (hc/k_B\theta)(16\pi\xi(3))^{-1/3}$. The photon density is $l_{ph}^{-3} \approx 410.872$ photons/cm^3. The standard value is 410.7(4) cm^{-3} [17].

The critical photon/baryon ratio is $\eta_{cr} = n_{ph}(R)m_n/M$. While the number of photons exceeds the baryon number, it is the contrary for the energy densities, which is, for the CMB alone $u_{CMB} = (\pi^2/15)\hbar c/\lambda\!\!\!^{-4}_{CMB}$. However, the energy density of the sum CMB and CNB is the latter times $1 + 3 \times (7/8)(4/11)^{4/3} \approx 1.681321953$, to be compared to $u_{cr} = \rho_{cr}c^2$. One notes the dramatic relation between these two canonical ratios, with the 2 factor coming from photon polarisation (0.4 %):

$$\sqrt{2\eta_{cr}} \approx \frac{u_{cr}}{u_{CMB+CNB}} \,. \tag{57}$$

This is an Eddington-type relation, confirming that there are only three neutrinos, and ruining again the standard *evolutionary* cosmology. Moreover (0.08 %):

$$E = l_{ph}^{(CMB)}/\lambda\!\!\!^{-}_e \approx (\pi a^2)^2 \,. \tag{58}$$

This term is central in the unification number [29] (0.07 %):

$$U = \Phi^{137} \approx (1 - e^{-v})^{-1}\,(\pi a^2)^6 \,. \tag{59}$$

We recall that this quasi-whole number, based on the golden number Φ, shows a holic character [29] (0.03, 1, 0.07 %, 43 ppm, 0.4 %) :

$$U \approx (\pi P/Dp_K)^2 \approx E^3 \approx (pH/2a)^7 \approx (\tau^2/\mu^3)^{210}\,\sqrt{\delta} \tag{60}$$

with $D = 196883$ the Monster Moonshine dimension [43].

Atiyah introduced also the constant

$$\Gamma = \gamma a/\pi \tag{61}$$

as a simplification term. One observes:

$$2/\delta = 2a^3/pH \approx (1/2d_e)\ln(pH)/\ln a \approx \ln a/\ln\Gamma\,. \quad (62)$$

With $w = F/W$, this leads to (22 ppm): $a/\Gamma = \pi/\gamma \approx w^\delta$ while, with $z = F/Z$ (3 ppm): $137/\Gamma \approx z^{\sqrt{f}/2}$. Recall that $wz \approx \sqrt{a}$, while f is the Bizouard strong constant precising the inverse 8.44(5) of the standard "strong coupling constant" [17]:

$$f = a_w/2\pi(pH)^{3/2} \approx 8.43450\,. \quad (63)$$

In cosmology, Γ and the canonical e^π enter the following dramatic simplification of the above (Section 4.1) single-electron cosmic formula (0.3 ppm):

$$a' = ((\ln(R_1/\lambda\!\!\!^{-}_e)+\gamma-1)/(\pi^2/6-1)) \approx \ln(R/\lambda\!\!\!^{-}e)+\Gamma+e^\pi \quad (64)$$

so confirming the R value to 45 ppm.

Moreover, this confirms the role of $j = 8\pi^2/\ln 2$, the Sternheimer scale factor [3] (to 0.013 %, 0.013 %, 0.046 %):

$$j \approx \ln(R/\lambda\!\!\!^{-}e) + \Gamma \approx a - e^\pi \approx e^\pi \ln a\,. \quad (65)$$

The Titts group order $13 \times 2^{11}3^35^2$ [44] completes the biophysics relations involving central temperatures [3]:

$$j \approx T_{mam}/T_{CMB} \approx O_T/W \quad (66)$$

$$10^2 \approx T_{H_2O}/T_{CMB} \approx O_T/Z\,. \quad (67)$$

The pertinence of O_T is confirmed by the 2 ppb relation, where 71 is the biggest prime in the Monster order:

$$2 \times 137^2 + 21 = 23^2 \times 71 \approx 3 \times 137 d_e O_T/D\,. \quad (68)$$

The mammal wavelength enters (1%)

$$(Rl_P)^{1/2} \approx hc/kT_{mam}\,. \quad (69)$$

It is known that the reduced series $8k' + 2$ gives for $k' = 1$ and 3 the canonical values 10 and 26. Now the value $k' = 2$, $d = 18$ is at last interpreted: *the couple thermal photon-Life is at the upper center of the Topological Axis*, while the down center is the Higgs boson (Fig. 1). The real center, as seen above, is the dimension $d = 16$. Moreover, to 0.1%, the water triple point enters (0.1 and 1 %):

$$(R'l_P)^{1/2} \approx hc/k\theta_{H_2O} \quad (70)$$

$$\theta_{H_2} \times \theta_{O_2} \approx \theta_{H_2O} \times \theta_{CMB}\,. \quad (71)$$

This shows that chemistry is also involved [3].

The study of the 22 amino-acids [3] has shown that j is also a computation base. Indeed, to 2%: $j^{22} \approx 3P^2$ and, more precisely, to 0.01 % : $j^{22} \approx Pp_E^7$ where $p_E \approx 1847.599459$ is the Eddington mass ratio of the couple proton-electron, the roots ratio in the Eddington equation $10x^2 - 136x + 1 = 0$.

8.4 The ubiquity of a^a

Since 137 is a number of parameters, it must be interpreted as a dimension *i.e.* a privileged exponent. However, from the Computation Hypothesis, a must be an optimal base also. *So the term a^a must be central.*

Indeed, apart a π factor, a^a is the Grandcosmos volume with unit length the hydrogen radius, to 0.4 and 0.5 %:

$$(4\pi/3)(R_{GC}/r_H)^3 \approx a^a/\pi \approx 3(1/\ln 2)^{\sqrt{pH}}\,. \quad (72)$$

Note that the $\ln 2$ *factor involves information theory*. This relation is tied to the following property of the above unification factor (0.06 and 0.1 %):

$$U = \Phi^{137} \approx a^{p/a} \approx (1/\ln 2)^{pn/137^2}\,. \quad (73)$$

Moreover, the dramatic relation $a^a \approx e^{p/e}$ has been connected with the fifth optimal musical scale (306 notes) and to the operational definition of e [3]. Hence, we look here for its manifestations in classical mathematics.

The famous Lucas-Lehmer primality test uses the series of whole numbers $N_{n+1} = N_n^2 - 2$, starting from $N = 4 = u_3 + 1/u_3$, with $u_3 = \sqrt{3} + 2$. The latter is a special case of diophantine generators $u_n = \sqrt{n} + \sqrt{(n+1)}$, whose entire powers are close to whole numbers. One shows that $N_n \approx u_3^{(2^n)}$, and for n = 9:

$$u_3^{(2^9)} \approx (2(137^2 + 48))^{64} \approx a^a \quad (74)$$

defining a to 39 ppm and showing that the Rydberg term $2a^2$ plays a central role.

Also, with the Pell-Fermat generator $u_1 = 1 + \sqrt{2}$:

$$a^a \approx u_1^{3\times(2^8-1)} \quad (75)$$

which defines a to 0.3 ppm. So the number a establishes a connection between u_1 and u_3, two of the simplest arithmetic generators. This opens a *new research in pure mathematics*.

8.5 The intervention of sporadic groups

One observes, to 30 ppm, 0.5 % and 0.05 %:

$$O_M \approx (\ln\ln\ln O_M)^{2(136+d_e)} \approx (\pi/2)^{2a'd_e^2} \approx (F/af)^{20}\,. \quad (76)$$

Moreover (0.036 % and 0.038 %):

$$O_M^{1/10} \approx 495^2 \approx f(\gamma\Gamma) \quad (77)$$

where $495 = g_0/16$, implying the order g_0 of the smallest sporadic group (Mattieu) order M_{11}. Note that 495 is a unity less than the Green-Schwarz string dimension 496, the third perfect number, after 6 and 28. The precision 1.7 ppm of $f(\gamma\Gamma) \approx 495^2(a/137)$ suggests that the Higgs ratio is 495^2, corresponding to 125.175 GeV (Fig. 1 and Table 1).

The product of the 6 pariah group orders verifies (7 ppm):

$$\Pi_{pariah} \approx (F/a)^{20}/d_e^2 \tag{78}$$

thus, the above cosmic Tifft ratio F/a (Section 4.4) is directly tied to the six pariah groups. This establishes a connection between the six pariah groups and the Monster group (0.7 %):

$$\Pi_{pariah}/O_M \approx f^{20}\,. \tag{79}$$

These six pariah groups are not identified to form any family. By contrast, the 20 normal sporadic groups form the so-called *happy family* which is closely related to the Monster. The product of the 20 groups of the happy family shows, to 0.015%, 1% and 0.45 %:

$$\Pi_{happy} \approx \delta \times a^a \approx (j/495)^2\,\Gamma^{210} \tag{80}$$

where $j/495$ is close to the weak mixing angle 0.23116(12) [17], to 0.45 %. This confirms the above Complete Holic Principle, and the computation role of Γ. Moreover, to 2%: $a^a \approx \Gamma^{209}$. From the order of the Baby-Monster $O_B \approx \Gamma^{24}$, and $209 = 137 + 3 \times 24$ (1 and 2 %):

$$O_B \approx \Gamma^{24} \approx (a/\Gamma)^{a/3} \tag{81}$$

where $a/\Gamma = \pi/\gamma$ is the above canonical Atiyah ratio.

The total product of the 26 sporadic orders Π_{26} verifies (0.27 %):

$$\Pi_{26} \approx (9/2)(R_{GC}/\lambda\!\!\!^{-}_M)^2\,. \tag{82}$$

Now Π_{26} is close to the holic term $e^{4\times 210}$, whose a^{th} root is very remarkable (65ppm, 98 ppm, 5 ppb):

$$e^{4\times 210/a} \approx 2e^{2e} \approx H/4 \approx 26 \times (2 \times 26 + 1)/3\,. \tag{83}$$

Note that p/g_0 is close to the above weak mixing angle (0.3 %). This ratio appears as calculation base in the product of cardinal orders of the Monster and the baby-Monster groups, to 1%, 0.2 %, and 1 %:

$$O_M O_B \approx H^{2H/a} \approx (g_0/p)^a \approx (496/j)^{137} \tag{84}$$

confirming the central role of the weak mixing angle. The photon number in the visible universe is (0.1 % and 0.2 %):

$$n_{ph} \approx (3/\pi)\, e^{e^6/2} \approx \sqrt{\delta}\, O_M O_B\,. \tag{85}$$

With N_{ph} the photon number in the Grandcosmos, and $N_n = M_{GC}/m_n$ the equivalent neutron number in the Grandcosmos, one observes (3 %, 0.5 %):

$$\sqrt{N_{ph} N_n} \approx e^{n/3} \approx (O_M^3/U)^2 \tag{86}$$

confirming that the Grandcosmos is the external thermostat of the visible Universe. This is tied to (3 %, 0.08%, 2.5%,1%):

$$e^{137e} \approx U e^{n/6} \approx (e/3) e^{ea} \approx O_M^3 \approx 496^{60}\,. \tag{87}$$

With the tachyonic ratio $V = R_{GC}/R = C/c$, the orders of the two giant sporadic groups enter (0.2 %, 0.1 % and 79 ppm):

$$V \approx 44\pi N_S \approx (a/\pi) O_M D \approx (a/\pi) O_B P a^{3/2} \tag{88}$$

where $N_S = 2^{65} \times 3^{41} \times 5^{28}$ is the Systema number [45].

The corrected Eddington's number $N'_{Ed} = a \times 2^{256}$, where 136 is replaced by a, shows (4.5 ppm and 0.03 %):

$$N'_{Ed} \approx 6 \times 137 P O_M \approx (3/4) a p a_w (V/O_M)^9\,. \tag{89}$$

With the 4D area $s_4 = 2\pi^2 a^3$, the holic reduction

$$(R/\lambda\!\!\!^{-}_e)^7 \approx (3/2) O_M^5 \approx s_4^{35} \tag{90}$$

implies $O_M^{1/7} \approx s_4$. Indeed, the Monster appears to be close to the seventh power of the pariah group J_3 (0.2 ppm):

$$O_M \approx d_e J_3^7 \sqrt{p/p_0}\,. \tag{91}$$

The above relations proves that physics establish unexpected bridges between sporadic groups, including the Titts one.

9 The fine-tuning with basic mathematical constants

We look here for relations involving basic mathematical constants, noting firstly that, to 6.5 ppm: $p \approx \Gamma(\pi e)^2$.

9.1 The optimal calculation base e confirmed

The electron magnetic moment $2d_e$ appears in (0.7 ppm):

$$a/\Gamma = \pi/\gamma \approx 2d_e \times e\,(p_0/p)^2\,. \tag{92}$$

The Topological Axis shows clearly that the Grandcosmos is defined by the following conjunction (1%):

$$f(k = e^2) = \exp(2^{e^{2+1/2}}) \approx \exp(e^{2e} + e^2) \tag{93}$$

where the supplementary term $\exp(e^2)$ is close to $a^{3/2}$. Note the following properties of the "economic number" e^{e^e}, to 0.4 %, 6 ppm and 0.8 ppm:

$$e^{e^e} \approx (\ln p)^{\ln p} \approx 137(e^e)^3 \approx e^e a \sqrt{pH}(p/p_0)^2\,. \tag{94}$$

With $a_1 = a - 1$ (8 ppm, 0.2 ppm, and 0.05 %):

$$e^{e^e}/a_1^2 \approx 4 \ln P \approx a \ln(9/2) \approx 5^{2^7} \tag{95}$$

showing the role of musical bases 2, 3 and 5. Note that the Topological Axis terminal term e^2 is the limit of the following musical series:

$$(3/2)^5 \approx (4/3)^7 \approx (5/4)^9 \approx (6/5)^{11} \approx ... \approx (1 + 1/n)^{2n+1}$$

a series converging more rapidly than the classical $(1 + 1/n)^n$. The first two terms defines the occidental 12 tones scale. Note that, to 0.6 % and 0.03 %:

$$R/\lambda\!\!\!^{-}_e \approx 2^{2^7} \tag{96}$$

$$R'/\lambda\!\!\!^{-}_e \approx (3^3)^{(3^3)} . \quad (97)$$

The canonical ratio $R_{GC}/\lambda\!\!\!^{-}_M = 2P^9/a^6 pH$ confirms the Full Holographic Principle, to 0.04 %:

$$R_{GC}/\lambda\!\!\!^{-}_M \approx (137e/a)^{2\times 210} \quad (98)$$

exhibiting (0.3 ppm): $(a/137)^{420} \approx (137-3)/120$ with $137-3 = 7+127$ showing the Combinatorial Hierarchy terms [3].

9.2 The Lenz-Wyler formula

Wyler published a value approaching a to 0.6 ppm and confirmed the pertinence of the Lenz approximation which plays a central role above: $p_0 = 6\pi^5 \approx p$ to 18.824 ppm.

The Lenz-Wyler formula is the product of the area by the volume of a 3D cube with side π. If one considers a 3D cube with side 5, privileging again the identification dimension = exponent, this gives $6\times 5^5 = 137^2 - 19$. This is not a chance coincidence because this relation has long time been deduced from basic considerations on quarks [29]. Indeed with $u = 5$ and $d = 6$, the combination $uud = 150$, whose power 3/2 is close to H, while the combination $udd \approx (n/a)^2$ shows the neutron/electron mass ratio n. This leads to (0.012 %) $6\times 5^5 \approx (aH/n)^2$. Note that, with $q = 2^{12}$ to 0.03 %, 2.5 % and 41 ppm:

$$R_{GC}/\lambda\!\!\!^{-}_e \approx q\times 5^{137} \approx 6^{137}/q^2 \approx 6^{128}/(1+1/\sqrt{2}) .$$

Since $R/\lambda\!\!\!^{-}_e \approx 2^{128}$, *the factorisation of 6 leads to a natural Universe-Grandcosmos partition*, and to the following approximation for the tachyonic celerity ratio (0.01%)

$$U = C/c \approx 3^{128}(p_K/p_G\delta)^2$$

where p_K is the Koide-Sanchez constant (see Section 9.5). This confirms the role of the correspondence quark up = 5 and *quark d = 6 with a double structure*. This elimination of q leads to (2.6 %): $(R_{GC}/\lambda\!\!\!^{-}_e)^3 \approx (uud)^{137}$.

It is an example of *immergence*, *i.e.* deducing the small from the large, in a striking similitude between cosmology and nuclear physics. Another example was encountered in Section 2.4, where dimensional analysis gives the visible Universe radius, in an easier way than the equivalent one for the hydrogen atom radius, since for this case there is no evidence that c must be left out. Another example signals a general misconception: the coherence of the stimulated emission in a laser is a *global effect* in a homogeneous media (atomic coherence).

9.3 The Archimedes constant π as a calculation base

From (27), the value of the topological function for the main string dimension 26 renders, to 0.1%, the same Lenz-Wyler form $f(26) \approx 6(2\pi^2a^3)^5$, where $2\pi^2a^3$ is the area of a 4-sphere of radius a. Moreover, with n/p the mass ratio neutron/proton, to 0/3%, 0.02% and 1 ppm:

$$(p/n)(R/\lambda\!\!\!^{-}_e)^2 \approx (f(26)/6)^2 \approx (2\pi^2a^3)^{10} \approx \pi^{155} . \quad (99)$$

The corresponding approximation π_R of π shows the fractional series 3, 7, 16, $-u$, with $u \approx 2\times 137$, confirming again the rationalization hypothesis of Section 3. This leads to the rational value $\pi_R = (355u-22)/(113u-7)$. This corresponds to the above G value to 10 ppb accuracy. Since $(R/\lambda\!\!\!^{-}_e)^2 \approx 2^{256}$, this illustrates the following musical relation involving again 137: $2^{1/155} \approx \pi^{1/256} \approx (2\pi)^{1/3\times 137}$. The scale with 155 notes is not known, but 137 appears also in the classical musical scales [3]. Whole powers of π appear in the even order Riemann series, and in: $a \approx 4\pi^3 + \pi^2 + \pi$ (Reilly formula, 2 ppm), while $a \approx \pi^{9/2}2^{-1/3}$ (8 ppm). Moreover, with $P = \lambda\!\!\!^{-}_e/l_P$ (0.3 and 0.07 %):

$$P^3 \approx \pi^{a-2} \approx (2\pi R/\lambda\!\!\!^{-}_e)(2\pi l_K/r_e) \quad (100)$$

confirming the Planck volume and the Kotov length.

9.4 The four forces connection in ppb fine-tuning

The particle standard model achieved the unification between electromagnetism and weak nuclear force, with extension to strong nuclear force in the Grand Unification Theory (GUT), but without any synthesis with gravitational force. However, the Topological Axis shows clearly that GUT gauge boson with 2.3×10^{16} GeV seems confirmed. Very precisely, in Section 4.2, it is proven that the CCO oscillation reveals a symmetry between the electroweak and gravitational forces. So we look here for a precise relation involving the 4 force parameters, a (electric), a_w (weak nuclear), f (strong nuclear) and a_G (gravitation). The later force is equivalently represented by $p_G = P/2^{127/2}$, with $P = m_P/m_e$.

With the Atiyah constant $\Gamma = \gamma a/\pi$ (Section 8.2), inside the 0.5 ppm measurement precision: $a_w = F^2 = (137\times 2\Gamma)^3$. Now a_w is a cube: $a_w = (\lambda\!\!\!^{-}_e/l_{eF})^3$, with $l_{eF} = (G_F/m_ec^2)^{1/3}$:

$$\lambda\!\!\!^{-}_e/l_{eF} \approx 137\times 2\Gamma \quad (101)$$

$$F = a_w^{1/2} = E_F/m_ec^2 \approx 573007.3652 \quad (102)$$

$$aF/\sqrt{(pH)} = 2\pi a f pH/F \approx \pi(4n/\Gamma)^3/p_G \approx \mu^2 \quad (103)$$

where μ is the muon/electron mass ratio, *inside its 20 ppb undetermination*, so proposing the value:

$$\mu \approx 206.7682869 . \quad (104)$$

Note that $4n/\Gamma$ is close (3.4 ppm) to the monstrous 5th term 292.6345909 in the fractional development of π which is itself very close to $n/2\pi$ to 3.4 ppm. Since the fractional development of π is to this date an unsolved problem, *this confirms that current mathematics is incomplete and that Nature uses rational approximations of* π. From the Koide relation, the corresponding value is $\tau \approx 3477.441701$, tied to the economic number (0.6 ppm):

$$e^{e^e} \approx \tau(2a)^3/137^2 . \quad (105)$$

From $\tau \approx e^{3e}$ and $8a \approx e^7$, this illustrates the reduction $e^e \approx 7 + 3e$. The pertinence of the economic number is confirmed.

The corresponding Koide-Sanchez constant is

$$p_K \approx 1842.604994\,.$$

This leads to three ppb relations, where $\pi_a = (355u + 22)/(113u + 7)$, with $u = a\sqrt{2}/3$, and $H_e = 8e^{2e}$ is the economic 33 ppm approximation of H:

$$p_K^4/pH \approx (4\pi_a)^4 a \approx (p_G H_e/aH)^4 D^2/n(D+1) \qquad (106)$$

$$n\tau/2 \approx HH_e(D/(D+1))^3(p_K/p_G)^9 \qquad (107)$$

where D and $D + 1$ are the characteristic numbers of the Moonshine correlation [43]. This confirms the Eddington symmetry hydrogen-tau lepton [5].

The above relations show a dual form, the first one without any numerical factor:

$$ap_G/\pi\sqrt{(pH)} \approx (nF/137^2\Gamma^3)^3 \approx (4n/\Gamma)^3/F\,. \qquad (108)$$

Now, as was recalled above, the exponents represent the number of dimensions. So, this represents a dimensional reduction, eliminating 137, from 9-D and 6-D to 3-D, which could be associated with the superstring theory, where the equations are coherent only if space has 9 dimensions, and if the 6 supplementary dimensions unfold on very small distances [47].

The following weak boson ratios W and Z match (1): $R/\sqrt{(\lambda\!\!\!^{-}_p \lambda\!\!\!^{-}_H)} \approx (WZ)^4$ *in the ppb range*:

$$W \approx 137^2\Gamma/3d_e \qquad (109)$$

$$Z \approx ap^2\pi^4/137d_e n\,. \qquad (110)$$

The ultimate theory must explain these ppb relations.

10 Discussion

For many, cosmology is the hardest chapter of physics. This modern negative opinion is in fact in contrast with the ancient culture, for which *the cosmology is the first of all sciences, so must be the simplest*. In the original meaning of the word "revolution", this article is a return to the source of science, the "all is whole number" of Pythagoras. Even the degenerate form of topological or holographic relations, the simplest diophantine equations, the Holic Principle, shows direct pertinence. In particular, it emphasizes the 30 dimensions, which appear decisive in the Topological Axis, and are identified with the sum of 26 string dimensions and 4 of usual spacetime.

The distinction between length and time must be emphasized, as Poincaré, the father of 4-D relativity theory recommended [25]. Indeed their confusion, by writing $c = 1$, impeded the fact that the Hubble-Lemaître radius R is a trivial length, directly given by the prospective c-free dimensional analysis, which gives also the cosmic temperature (37) and the cosmic supercycle period (22).

This means also that the International System must go back to only three fundamental unities, Mass, Length and Time.

The Hierarchy and Computation principles presented in Section 1 are confirmed both by the Topological axis, the geodimensional Universe-Grandcosmos couple, and the monomial relations (*i.e.* merely products of parameters). These accurate monomial relations reunify mathematics and physics. The precision reaches the ppb domain: they cannot be due to chance. This shows how the so-called "free parameters" are misnamed: they are imposed by Nature proving the Cosmos unicity. As Atiyah wrote, rather misleadingly [42]:

> Nobody has ever wondered what the Universe would be if π were not equal to 3.14159.... Similarly no one should be worried what the Universe would be if a were not 137.035999...

In fact a must be rational, and the mathematical π is illusion. Nevertheless, this article is a *definite refutation* of the Multiverse hypothesis. In this respect, the high precision in the measurement of the electric and Fermi constants, proton, neutron and muon masses, Kotov cosmic period, and, with lesser precision, the background temperature, must be saluted as decisive achievements.

The pertinence of these simple monomial relations cannot be admitted by the standard community, arguing for instance that since the proton is composite, its mass cannot enter simple relations. The same argument is presented for the theoretical dependence of the electric constant a with other constants, or with the energy level. These are reductionist arguments, unable to explain the fine-tuning phenomena, and leading to the sterile concept of unexplained emergences. By contrast, the holistic approach implies the concept of *immergence*, resulting from the ancestral idea that Cosmos simplicity is the real origin of science. It is strange, revealing and troubling that this term *immergence* is a neologism.

The Cosmos concept has long been forgotten. This is the reason why quantum physics is not really understood. Indeed, the simple fact that the propagation of anything, light or matter, is wavy, while the reception is a quantum, was a central mystery along the last century. This simple fact induces non-locality, so the necessary intervention of cosmology. Moreover, the optimal utilisation of the wavy propagation is holography, whose formalism is similar to the quantum one. Thus it is logical to find holographic relations in cosmology. Moreover, the similitude between the formalisms of quantum physics and holography is so tight that the double-step holography is similar to the double step of any interaction: tachyonic propagation – non-local cosmic optimisation – local quantum reception.

Thus tachyonic-holography physics is necessary. Hence, it was an error to reject the bosonic string theory under the pretext it involves tachyons [49]. Quite the contrary, it is an essential advantage. This is confirmed by the central impor-

tance of the bosonic dimension $d = 26$ in the Topological Axis, which is nothing that the extension to smaller numbers of the Double Large Number coincidence, that only Eddington interpreted correctly, by rejecting the single Bang model. Many invoked the temporal variation of the parameters, which is a negation of the idea that physics have universal laws. Finally, the expedient of the Anthropic Principle was imposed to the community by some leaders: this is definitely refuted in this article.

Moreover, the standard Holographic Principle must be generalized to wavelengths other than the Planck length, in particular the topon, the visible Universe wavelength, in 1-D holography, which breaks by an enormous factor, about 10^{61} a taboo of current thinking: the Planck wall, resolving the vacuum energy dilemma factor 10^{122}, and sustaining the Oscillatory bounce model which unifies the two main cosmologies.

This leads back to the main hypothesis of this article: the Cosmos is a computer, and the dimensionless parameters are calculation bases. A common point with the brain is precisely this *multibase* character, experienced in musical sensation. It is no chance that the parameters are encountered in the musical scales and DNA chain. Thus, intelligent life receives a justification: to help the cosmological computation. This Inverted Anthropic Principle answers the first of all questions: *why one asks questions?*

Thus, *intelligent life must be universal*. The famous Fermi question "where are they?" is not a paradox, since any abnormal observation is *a priori* rejected by a dogmatic community. This destroys the Darwin "accidental life" approach, a generally admitted so-called "theory" with too much missing links [48].

The same rejection seems to apply now to the Sternheimer "scale wave" and Atiyah's last work. The present article shows that at least parts of these works are very pertinent. This follows the rejection (with the notable exception of Schrödinger) of Eddington [5] himself. Only Eddington interpreted rightly the Cosmic Large Number correlations, as recalled in this article. While he dared to apply the exclusion principle in cosmology, it is the basis of our single electron cosmologic model (Section 4.1) which rehabilitates once more his work. Also, fortunately, the large theoretical advance of Eddington is now recognized [51], but without mentioning a crucial point: *he predicted the tau fermion with a right order of mass*, 30 years before its surprising discovery, calling it heavy mesotron [5]. Moreover, it seems that no one realizes that the Eddington prediction for the baryon number in the visible Universe is so accurate. Note that many mocked the Eddington Large Number, not to speak of his number 137, completely rehabilitated by the monomial relations.

However, curiously, Eddington believed in the Copenhagen statistical interpretation. Thus, he did not reach the above conclusions. At his epoch the holography was not yet discovered: *it is a strange, and revealing, fact of science history that this essential property of wave propagation was so lately discovered* [33]. However, with his Large Number which fits so well the cosmic neutron population, Eddington anticipated the present physics-arithmetic fusion and its touchstone, the Holic Principle.

11 Conclusions: cosmic simplicity at work

The present article confirms the Topological Axis, which was obtained by the simplest visualizing method to represent in a single figure the characteristic lengths in macro and microphysics, taking the electron reduced Compton wavelength as unity. *The double logarithm representation was the simplest one, and it appeared later that this was the reunion of a series of height 1D-2D holographic relations, respecting the topologico-algebraic Bott sequence*.

The application of the old direct scientific method, looking for fine tuning between physical parameters leads to a return to the Perfect Cosmological Principle implying a steady-state Cosmos, confirmed by holographic relations. The standard cosmological principle was unduly limited to spatial homogeneity. The relativity theory, unable to define an inertial frame, is a local one and do not apply to cosmology at large: the absolute space is reestablished, realized by the Microwave Cosmic Background, which identifies with the Grandcosmos frame. Meanwhile, the Kotov period is an absolute clock, the *déphasage* of coherent oscillations between quasars being ruled by the tachyonic celerity.

The simplest model, the gravitational hydrogen molecule gives the Hubble radius R, explaining the 2 factor and justifying the elimination of c, as in the hydrogen atom Haas-Bohr model [3]. This corresponds to a Hubble constant 70.790 (km/s)/Megaparsec, consistent with the recent measurement [6]: 72(3) Megaparsec/(km/s), which confirms the direct novae measurement, but disagrees (3σ) with the standard value.

The simplest statistical theory of Eddington gave another justification to R. Also, particularly simple and elegant is the Large Eddington number, giving correctly the number of neutrons in the trivial fraction $3M/10$ of the observable universe, *probably the most dramatic prediction in scientific history*.

The simplest proof of the computation basis character of the electrical parameter a is provided by the multiple appearance of the terms e^a and a^a.

The profound significance of a number of dimensions is the number of independent variables, which is a fundamental invariant, whatever the theory [54]. So, it is logical to advance a hypothesis that 26 physical parameters are defined by the 26 sporadic cardinal orders. Since Sporadic Groups are associated with octonion algebra [55], this rejoins a prediction of Atiyah's last work, the essential role of octonion algebra in the final theory [42].

The problem of the stability of the solar system must be revisited, taking into account seriously a cosmic influence, characterized by the Kotov period and length. Also the Pi-

oneer, Tifft and Arp effects must be seriously considered, guided by the flickering time-length-mass concept.

This article answers several main problems:

- 1/ Unification gravitation-quantum physics, by rehabilitating the forgotten Eddington statistical theory.
- 2/ The real significance of quantum physics, by assuming physics is based on arithmetics.
- 3/ The overall unification by showing that cosmology is the basis of united science.
- 4/ The role of dimensionless parameters, by proving that they are optimal basis of computation tied with the Holographic Principle and its arithmetic form, the Holic Principle, which explains why normal space has 3 dimensions.
- 5/ The necessity of the Cosmos vasteness resulting from holographic scanning and the rationalization of e and π.
- 6/ The acceleration of expansion, which was predicted by the Eddington *invariant* cosmological constant $1/R^2$, is tied to a repulsive force proportional to distance, leading to *exponential* recession. There is no need of the so-called "dark energy".
- 7/ The very existence of dark matter is proven, from the number of neutrons in the trivial fraction 3/10 of the visible Universe critical mass, which identifies with the very symmetric Eddington number 136×2^{256}. *The nature of dark matter would be simply a matter-antimatter oscillation in phase quadrature with the ordinary one* [3].
- 8/ The introduction of the topon in the Holographic Principle justifies at last the 10^{122} gap between vacuum energy and that of the visible Universe.
- 9/ The Grandcosmos is huge, but not infinite, in conformity with the Cosmological Computational Principle.

In short, the rediscovered Cosmos unifies the two main modern cosmologies in a rapid matter- antimatter oscillatory bounce. The Cosmos appears as *simple, unique, permanent, computational, deterministic, transplanckian, cyclic, topological and inverse-anthropic*. It is now clear that present mathematics and particle physics are incomplete, and this Coherent Cosmology announces a reunification of *philosophy, mathematics, physics, chemistry, computational science and biology*. In particular, the pre-Socratic Parmenide philosophy of permanence must be reconsidered favorably.

12 Predictions

This article leads to many predictions, in particular:

- 1/ The very large infrared telescopes will show in the very far field old galaxies instead of expected young ones. Then no artifice, such as inflation, dark energy, multiverse, ..., will not save the standard evolutionary model, based on the imperfect cosmological principle.
- 2/ The CMB temperature and the baryon mean density will appear temporal invariant.
- 3/ The particle physics will integrate the Koide relation together with the Koide-Sanchez constant, and introduce composite quark down and massive photon, graviton, gluons and string. Also the supersymmetry will restablish the Eddington connection proton-tau.
- 4/ The computational software should be boosted by the principle of multibase computation.
- 5/ The DNA chain will reveal as a 1-D temporal hologram, see [52].
- 6/ The Lucas-Lehmer series, in connection with the canonical generators ($\sqrt{n} + \sqrt{(n+1)}$), especially the Planck-Fermat one ($1 + \sqrt{2}$) will define a.
- 7/ The 26 sporadic groups as well as the Titts one will reveal determinant in the Ultimate Theory.
- 8/ The Eddington Fundamental Theory will be revisited, especially the genesis of his Large Number, so clearly tied to the 16×16 symmetric matrix.
- 9/ The Combinatorial Hierarchy [41] and Moulin systemic approach [45] will be reconsidered.

Received on April 2, 2019

References

1. Carr B. J. and Rees M. J. The anthropic principle and the structure of the physical world. *Nature*, 1979, v. 278, 605–612.
2. Borcherds R. Monstruous Moonshine and Monstruous Lie Superalgebras. *Invent. Math.*, 1992, v. 109, 405–444.
3. Sanchez F. M. A Coherent Resonant Cosmology Approach and Its Implications in Microphysics and Biophysics. *Progress in Theoretical Chemistry and Physics*, 2017, v. 30, 375–407, DOI 10.1007/978-3-319-50255-7-23. Sanchez F. M. Coherent Cosmology. vixra: 1601.0011. Sanchez F. M., Kotov V. and Bizouard C. Towards Coherent Cosmology. *Galilean Electrodynamics*, 2013, special issue, 63–80.
4. Poincaré H. Sur la théorie des quanta. *J. de Physique*, 1912, v. 2, 5.
5. Eddington A. S. The Fundamental Theory. Cambridge, 1946.
6. Bonvin V. *et al*. H0LiCOW-V. New COSMOGRAIL time delays of HE0435-1223: H0 to 3.8% precision from strong lensing in a flat ΛCDM model. *Monthly Notices of the Royal Astronomical Society*, 2017, v. 465 (4), 4914–4930. arXiv: astro-ph/1607.01790v2.
7. Bondi H. and Gold T. The steady-state theory of the expanding universe. *Monthly Notices of the Royal Astronomical Society*, 1948, v. 108, 252.
8. Hoyle F. A new model for the expanding universe. *Monthly Notices of the Royal Astronomical Society*, 1948, v. 108, 272–382.
9. Poincaré H. Dernières pensées. Flammarion, 1913, pp 102–103.
10. Sanchez F. M., Kotov V. A. and Bizouard C. Towards a synthesis of two cosmologies: the steady-state flickering Universe. *J. Cosmology*, 2011, v. 17, 7225–7237.
11. Davie P. The Accidental Universe. *C.U.P.*, 1993, 92.
12. Bousso R.The Holographic Principle. *Reviews of Modern Physics*, 2002, v. 74, 834.

13. Duplantier B. Introduction a l'effet Casimir. *Séminaire Poincaré*, 2002, v. 1, 41–54.
14. Damour T. The Entropy of Black Hole. *Sem. Poincaré*, 2003, v. 2, 89–115.
15. Nambu H. An empirical Mass Spectrum of Elementary Particles. *Prog. Theor. Phys.*, 1952, v. 7 (5), 595–6.
16. Kotov V. A. and Lyuty V. M. The 160-min. periodicity in the optical and X-ray observations of extragalactic objects. *Compt. Rend. Acad. Sci. Paris*, 1990, v. 310, Ser. II, 743–748. Fossat E., Boumier P., Corbard T., et al. Asymptotic g modes: Evidence for a rapid rotation of the solar core. *Astron. Astrophys.*, 2017, v. 604, A40, 1–17. DOI: 10.1051/0004-6361/201730460. Grec G., Fossat E. Calculation of pseudo solar narrow band oscillations produced by atmospheric differential extinction. *Astron. Astrophys.*, 1979, v. 77, 351–353. Kotov V. A. Evolution of the Sun and the Earth: the (un)known period 1.035 years. *Izv. Krym. Astrofiz. Obs.*, 2013, v. 109 (1), 232–253. Kotov V. A. Fast spinning of planets. *Earth Moon Planets*, 2018, v. 122 (1), 43–52. DOI:10.1007/s11038-018-9520-6. Sevin É. Sur la structure du système solaire. *Compt. Rend. Acad. Sci. Paris*, 1946, v. 222, 220–221. Kotov V. A. Motion of the fast exoplanets. *Astrophys. Space Sci.*, 2018, v. 363 (3), 1–5. DOI: 10.1007/s10509-018-3278-1.
17. Tanabashi M. *et al*. (Particle Data Group). The review of particle physics. *Phys. Rev. D*, 2018, v. 98, 030001. http://pdg.lbl.gov.
18. Quinn T., Speake C., Parks H., Davis R. The BIPM measurements of the Newtonian constant of gravitation, G. *Phil.Trans. R. Soc. A*, 2014, v. 372, 20140032. http://dx.doi.org/10.1098/rsta.2014.0032
19. Aschbacher M. Sporadic Groups. Cambridge Univ. Press, 1994.
20. Sanchez F. M. Towards the grand unified Holic Theory. In Pecker J.-C. and Narlikar J., eds. Current Issues in Cosmology. Cambridge Univ. Press, 2006, p. 257–260.
21. Kotov V. A. and Sanchez F. M. Solar 22 years cycle. *Astrophys. Space Sci.*, 2017, v. 362 (6), 1–6. DOI: 10.1007/s10509-016-2985-8.
22. Tifft, W. G. Redshift periodicities, The Galaxy-Quasar Connection. *Astrophysics and Space Science*, 2006, v. 285 (2), 429.
23. Arp H. The origin of Companion Galaxies. *Astrophysical Journal*, 1998, v. 496, 661–669.
24. Nieto M. and Anderson J. Using Early Data to Illuminate the Pioneer Anomaly. *Class. Quant. Grav.*, 2005, v. 22, 5345–5354. arXiv: gr-qc/0507052.
25. Poincaré H. La mécanique nouvelle. Gauthiers-Villars, 1924. Jacques Gabay, 1989.
26. Bars I. Gauge Duality, Conformal Symmetry, and Space-Time with Two Times. *Phys. Rev. D*, 1998, v. 58. arXiv: hep-th/9803188.
27. Cartan H. Démonstration homologique des théorèmes de périodicité de Bott I. *Séminaire Henri Cartan*, 1959-1960, v. 12 (2), n° 16, 1–16.
28. Grosmann M. and Meyrueis P. Optics and Photonics Applied to Communication and Processing. *SPIE*, Jan. 1979.
29. Sanchez F M. Holic Principle: The Coherence of the Universe. Entelechies, 16th ANPA, Sept. 1995, p, 324–344.
30. Sanchez F. M. Cohérence Temporelle d'ordre supérieur d'un laser déclench multimode. Doctorate Thesis, Orsay, number 1478, 1975, p. 11.
31. Okun L. B. Photon: history, mass, charge. Int. Conf. on the Photon, Warsaw University, 2005. arXiv: hep-ph/0602036.
32. Einstein A., Podolski B. and Rosen N. Can Quantum-Mechanical Description of Physical Reality Be Considered Complete. *Phys. Rev.*, 1935, v. 47, 777.
33. Gabor D. A new microscopic principle. *Nature*, 1948, v. 161, 777–778.
34. Marchal C. Physics with photons of non-zero rest mass. Proceedings of 28th Intern. Workshop, Protvino, Russia, 2005, p. 152–166.
35. Preskill J. Do Black Holes Destroy Information? International Symposium on Black Holes, Membranes, Wormholes, and Superstrings. arXiv: hep-th/9209058.
36. Nikolic H. Resolving the black-hole information paradox by treating time on an equal footing with space. *Physics Letters B*, 2009, v. 678 (2), 218–221. arXiv: gr-qc/0905.0538.
37. Carlson C. E. The proton radius puzzle. *Progress in Particle and Nuclear Physics*, 2015, v. 82, 59–77.
38. Witten E. The Three-Dimensional Gravity Revisited. arXiv: hep-th/0706.3359.
39. Sanchez F. M. Electrical Moonshine. vixra: 1801.0067.
40. Koide Y. Fermion-Boson Two-Body Model of Quarks and Leptons and Cabibbo Mixing. *Lett. Nuovo Cimento*, 1982, v. 34, 201.
41. Bastin T. and Kilmister C. W Combinatorial Physics. World Scientific, 1995.
42. Atiyah M. The fine-structure constant, 4th Heidelberg Laureate Forum conference (2018). https://www.heidelberg-laureate-forum.org/blog/video/lecture-monday-september-24-2018-sir-michael-francis-atiyah/.
43. Conway J. H. and Norton S. P. Monstrous Moonshine. *Bull. London Math. Soc.*, 1979, v. 11 (3), 308–339.
44. Titts J. Algebraic and abstract simple groups. *Annals of Mathematics, second series*, 1964, v. 80, 313–329.
45. Moulin T. Utilisation en physique et biologie de référentiels spatio-structuro-temporels engendrés par des relateurs arithmétiques. 11eme Congrès International de Cybernétique, Symposium 4, Namur, (1986).
46. Brannen C. A. The Lepton Masses. http://brannenworks.com /MASSES2.pdf, 2006.
47. Polchinski J. String Theory, Vol 1. Cambridge University Press, 1998, p. 22.
48. Chauvin R. Le Darwinisme ou la fin d'un mythe. ed. du Rocher, 1997
49. Woit P. Not Even Wrong: The Failure of String Theory and the Search for Unity in Physical Law. Basic books, 2006
50. Larin S. A. Quantum Chromodynamics with massive gluons. arXiv: hep-ph/1304.8107.
51. Durham I. T. Sir Arthur Eddington and the Foundations of Modern Physics. 2006, p. 111. arXiv: quant-ph/0603146v1 .
52. Widom A., Swain J., Srivastava Y. N., S. Sivasubramanian S. Electromagnetic signals from bacterial DNA. arXiv: physics.gen-ph/1104.3113v2.
53. Salingaros N. Some remarks on the algebra of Eddington's E Numbers. *Foundations of Physics*, 1985, v. 15 (6), 683—691.
54. Weigel D., Veysseyre R. and Carel C. Sur les symboles du groupe d'espace d'une wüstite de tri- incommensurabilité cubique et sur les groupes de Bravais de sa famille cristalline dans l'espace euclidien à six dimensions. *C.R. Acad. Sci. Paris*, 1987, v. 305, ser. II, 349–352.
55. Atiyah M. private communication, December 2018.

The Journal on Advanced Studies in Theoretical and Experimental Physics, including Related Themes from Mathematics

PROGRESS IN PHYSICS

A quarterly issue scientific journal, registered with the Library of Congress (DC, USA). This journal is peer reviewed and included in the abstracting and indexing coverage of: Mathematical Reviews and MathSciNet (AMS, USA), DOAJ of Lund University (Sweden), Scientific Commons of the University of St. Gallen (Switzerland), Open-J-Gate (India), Referativnyi Zhurnal VINITI (Russia), etc.

Electronic version of this journal:
http://www.ptep-online.com

Postal Address

Department of Mathematics and Science,
University of New Mexico,
705 Gurley Ave., Gallup, NM 87301, USA

ISSN: 1555-5534 (print)
ISSN: 1555-5615 (online)

Standard Address Number: 297-5092
Printed in the United States of America

October 2019 **Vol. 15, Issue 3**

CONTENTS

Information for Authors

Progress in Physics has been created for rapid publications on advanced studies in theoretical and experimental physics, including related themes from mathematics and astronomy. All submitted papers should be professional, in good English, containing a brief review of a problem and obtained results.

All submissions should be designed in LaTeX format using *Progress in Physics* template. This template can be downloaded from *Progress in Physics* home page http://www.ptep-online.com

Preliminary, authors may submit papers in PDF format. If the paper is accepted, authors can manage LaTeXtyping. Do not send MS Word documents, please: we do not use this software, so unable to read this file format. Incorrectly formatted papers (i.e. not LaTeXwith the template) will not be accepted for publication. Those authors who are unable to prepare their submissions in LaTeXformat can apply to a third-party payable service for LaTeX typing. Our personnel work voluntarily. Authors must assist by conforming to this policy, to make the publication process as easy and fast as possible.

Abstract and the necessary information about author(s) should be included into the papers. To submit a paper, mail the file(s) to the Editor-in-Chief.

All submitted papers should be as brief as possible. Short articles are preferable. Large papers can also be considered. Letters related to the publications in the journal or to the events among the science community can be applied to the section *Letters to Progress in Physics*.

All that has been accepted for the online issue of *Progress in Physics* is printed in the paper version of the journal. To order printed issues, contact the Editors.

Authors retain their rights to use their papers published in *Progress in Physics* as a whole or any part of it in any other publications and in any way they see fit. This copyright agreement shall remain valid even if the authors transfer copyright of their published papers to another party.

Electronic copies of all papers published in *Progress in Physics* are available for free download, copying, and re-distribution, according to the copyright agreement printed on the titlepage of each issue of the journal. This copyright agreement follows the *Budapest Open Initiative* and the *Creative Commons Attribution-Noncommercial-No Derivative Works 2.5 License* declaring that electronic copies of such books and journals should always be accessed for reading, download, and copying for any person, and free of charge.

Consideration and review process does not require any payment from the side of the submitters. Nevertheless the authors of accepted papers are requested to pay the page charges. *Progress in Physics* is a non-profit/academic journal: money collected from the authors cover the cost of printing and distribution of the annual volumes of the journal along the major academic/university libraries of the world. (Look for the current author fee in the online version of *Progress in Physics*.)

From the Geometry of the FLRW to the Gravitational Dynamics

Alexander Kritov
E-mail: alex@kritov.ru

The approach when the scale factor that describes the expansion of space, being its pure geometrical property, is derived from the dynamical (the Friedman) equations is questioned. The opposite path when the geometry determines the dynamics is more consistent, but not vice versa. Starting from the FLRW, the equivalent form of the metric in static coordinates is proposed. Based of few models for $a(t)$ the corresponding static metrics are derived. Further dynamics and the analogue of the Friedman equations can be obtained as consequence. The embedding of the FLRW geometry into the higher-dimensional Minkowski space as the hypersurface can be considered as the base for the model. The deceleration parameter for the Schwarzschild-de Sitter (SdS) case is reviewed based on such approach.

1 Introduction

In recent author's work [5] the hydrodynamic model of spherically symmetric gravitational field was reviewed. As it was shown the gravitational metrics can be modelled by expanding parcels of the fluid based on the respective functions of the volume change with time in co-moving frame. As it has explicit similarity with the space expansion, the present attempt is to use the geometrical approach to describe spherically symmetric gravitational filed starting from the FLRW metric.

2 The FLRW metric

Let's consider the static pseudo-Minkowski coordinates with the observer M at rest in the center. The static spherical coordinates are to be denoted as t, r, θ, ϕ, where r is coordinate distance to the observer P who is at rest, but is attached to the point of expanding space. The co-moving coordinates are given as T, R, θ, ϕ, where R is co-moving distance (from M to P). Respectively, time T is measured by the observer P. If space expands, the point P, attached to it, moves in the static coordinate system, so as observed by M, the motion of P represents the function of coordinate distance $r(t)$. The correspondence between the static coordinate and the co-moving distance is given by

$$r = Ra \tag{1}$$

where $a(T)$ is the scale factor. Then the proper velocity measured by the observed P,*

$$v = \frac{dr}{dT} = \frac{dR}{dT}\, a + R\, \frac{da}{dT} \tag{2}$$

and point P is at rest in its reference frame, so the first term is identically zero therefore

$$v = R\dot{a}\,. \tag{3}$$

*This is not coordinate velocity. This velocity is ratio of coordinate distance change to time measured in co-moving observer's clock.

Using (1) then

$$v = \frac{dr}{dT} = r(T)\, \frac{\dot{a}}{a}\,. \tag{4}$$

This expression provides the velocity of the space motion due to its expansion or the velocity of the reference frame attached to point P in the static coordinate system where r is the coordinate distance.

The Friedmann–Lemaître–Robertson–Walker (FLRW) metric in the spatially flat case ($k = 0$) is given by

$$ds^2 = -c^2 dT^2 + a(T)^2 \left(dR^2 + R^2 d\Omega^2 \right) \tag{5}$$

where $d\Omega^2 = \sin^2\theta d\phi^2 + d\theta^2$ and $a(T)$ is the scale factor. The metric is written explicitly in comoving coordinates, attached to the point of expanding space. Using (1) we may write

$$dr = \dot{a}R dT + a dR$$

from which

$$dR = \frac{dr}{a} - v\, \frac{dT}{a}\,.$$

Substituting it into the FLRW metric (5) leads to

$$ds^2 = -c^2 \left(1 - \frac{v^2}{c^2} \right) dT^2 - 2v dT dr + dr^2 + r^2 d\Omega^2 \tag{6}$$

which is the Gullstrand-Painlevé form of the metric which is spatially flat and describes co-moving observer in its free float with velocity v. The transformation of time coordinate T from co-moving to fixed frame of reference t is given by

$$dT = dt - \frac{v}{c^2} \left(1 - \frac{v^2}{c^2} \right)^{-1} dr\,. \tag{7}$$

The substitution of this expression into (6) leads to the respective static metric

$$ds^2 = -c^2 \left(1 - \frac{v^2}{c^2} \right) dt^2 + \left(1 - \frac{v^2}{c^2} \right)^{-1} dr^2 + r^2 d\Omega^2 \tag{8}$$

where velocity v is to be determined from (4). The velocity v is called the river velocity in [2, 4] and the shift in ADM formalism. Importantly, the metric (8) is equivalent to the FLRW, but written in the static coordinate systems of the observer M. Such form of the metric is known, starting from Lenz and Sommerfeld [11] and used in the river model of black holes and similar analogous models [3,4] for the spherically symmetric gravitational field.

The proposed approach starts from a certain function for the scale factor $a(T)$, and then the solution of the equation (4) provides the velocity $v(r)$ resulting in the corresponding metric in static coordinate system based on (8).

As it was stressed in the author's previous work [5], the sign of the velocity v does not play a role, as it comes to the metric as squared value. In the present approach the value of the velocity as given in (4) is obviously positive ($\dot{a} > 0$) and as coordinate center is placed in the center point of M the velocity is radial and directed outwards.

3 The case of the de Sitter metric

The easiest case to demonstrate the proposed approach is the de Sitter metric. The starting point is $a(T) = e^{H_0 T}$, or equivalently, the constancy of the Hubble constant with time

$$H_0 = \frac{\dot{a}}{a}\,. \tag{9}$$

Then using (4) gives

$$v = rH_0\,. \tag{10}$$

And substitution into (8) leads to

$$ds^2 = -\left(1 - \frac{H_0^2 r^2}{c^2}\right)c^2dt^2 + \left(1 - \frac{H_0^2 r^2}{c^2}\right)^{-1} dr^2 + r^2 d\Omega^2 \tag{11}$$

which is the de Sitter metric as expected.

4 The case of the Schwarzschild metric

Let's now assume that

$$a(T) \propto T^{2/3}\,. \tag{12}$$

Then, using (4), it follows that

$$v(r) = \frac{c_1}{r^{1/2}} \tag{13}$$

where c_1 - is an integration constant. Then the substitution into (8) leads to the form the Schwarzschild metric with precision by constant c_1. In order to determine the meaning of the integration constant, it is required to normalize (12), for example in such way that $a(0) = 1$

$$a = (\omega T + 1)^{2/3} \tag{14}$$

where ω is some constant. Then it would imply

$$r = r_0\,(\omega T + 1)^{2/3} \tag{15}$$

where r_0 is the initial coordinate distance at time $T = 0$. Then the velocity

$$v = \frac{2}{3}\left(\frac{\omega^2 r_0^3}{r}\right)^{1/2}\,. \tag{16}$$

The equation shows that the integration constant in (13) should have correspondence to the initial volume and therefore to the central mass, if one introduces a density in the equation. Proposed boundary conditions allow to put the scale factor function in direct relation with the particle mass and to remove the initial singularity.

Interestingly from (13) and (1) the scale factor in terms of the coordinate distance is simply $r = r_0 a$. From that, using (1), the co-moving distance is $R = r_0$. As expected, the scale factor a changes with time instead of the co-moving distance R which remains constant and always equals to its initial value in the static coordinates.

5 The Schwarzschild-de Sitter (SdS) metric

As suggested in [10] the scale factor that describes current Universe expansion within the frame of standard model of the cosmology has following form

$$a(T) = \sinh\left(\frac{3}{2}H_0 T\right)^{2/3}\,. \tag{17}$$

This corresponds (differing by factor of 2) to proposed in the hyperbolic model [5]*

$$a\,(T) = (\cosh(3H_0 T) - 1)^{1/3}\,. \tag{18}$$

Then using (4)

$$v = \frac{dr}{dT} = r_0\,\frac{H_0 \sinh\,(3H_0 T)}{(\cosh(3H_0 T) - 1)^{2/3}} \tag{19}$$

from which

$$r(T) = r_0\,(\cosh\,(3H_0 T) - 1)^{1/3} \tag{20}$$

where r_0 is integration constant with dimension of length. Expressing hyperbolic sine from this and substitution into (19) leads to

$$v = \left(H_0^2 r^2 + \frac{2r_0^3 H_0^2}{r}\right)^{1/2}\,. \tag{21}$$

Exact determination of the constant r_0 for the volume can be found in [5]. It was suggested that such volume can be associated with the mass via the fluid density. The substitution into (8) leads to the SdS metric

$$\begin{aligned} ds^2 = &-\left(1 - \frac{2Gm}{c^2 r} - \frac{H_0^2 r^2}{c^2}\right)c^2dt^2 + \\ &+ \left(1 - \frac{2Gm}{c^2 r} - \frac{H_0^2 r^2}{c^2}\right)^{-1} dr^2 + r^2 d\Omega^2\,. \end{aligned} \tag{22}$$

*Obviously the presented approach has direct correspondence to the cited author's fluid model via $\dot{V} \propto a^2\dot{a}$ and $V(t) \propto a^3$.

6 The embedding the FLRW geometry

The embedding of the de Sitter geometry in the pseudo-Euclidian five-dimensional space is well known and was obtained by Robertson [7, 8]. This corresponds to embedding of the spatially flat FLRW metric with $a(t) = e^{H_0 t}$. However, as demonstrated in [9] and reviewed in [1] the generalization of the FLRW metric ($k = 0$) embedding is possible via reconstruction of the respective curve and the Minkowski five-dimensional metric is

$$t' = \frac{1}{2}\int \frac{\dot{a}^2 - 1}{\dot{a}}\, dT\,, \quad r' = \frac{1}{2}\int \frac{\dot{a}^2 + 1}{\dot{a}}\, dT\,, \quad \text{and } x' = x \quad y' = y \quad x' = z\,. \tag{23}$$

The embedding of the FLRW metric with the hyperbolic function as (17) was reviewed in [6], however it was concluded that the integral has no analytical expression.

7 On the deceleration parameter for the SdS metric

Presented approach provides a simple way to determine the deceleration parameter

$$q_0 = -\frac{\ddot{a}a}{\dot{a}^2}\,. \tag{24}$$

And as

$$\alpha = \ddot{a}R \quad v = \dot{a}R \quad r = Ra \tag{25}$$

then for the SdS metric using the deceleration parameter can be expressed via coordinate distance as

$$q_0 = \frac{Gm - H_0^2 r^3}{2Gm + H_0^2 r^3}\,. \tag{26}$$

In case of mass m is uniformly distributed within a sphere and if the density is expressed in terms of $\Omega_M = \rho/\rho_{crit}$ then the deceleration parameter is

$$q_0 = \frac{1}{2}\frac{\Omega_M - 2}{\Omega_M + 1}\,. \tag{27}$$

In case of $\Omega_M = 0.27$ it gives the deceleration parameter $q_0 = -0.68$ which is close to the observed value. As example the equation results in $q_0 = -1$ for empty the de Sitter Universe, and $q_0 = -0.4$ in case of $\Omega_M = 1$.

8 The Friedman equations

In the frame of present approach the dynamical Friedman equations appear as a result of the original scale factor function. In general case, as the resulting metric provides us with the values for acceleration $\alpha(r)$ and the velocity $v(r)$ and with use of (25) the Friedman equations are derived. In case of the SdS metric, the first Friedman equation can be directly obtained from the result (21)

$$\left(\frac{\dot{a}}{a}\right)^2 = H_0^2\left[1 + \frac{2}{a^3}\right]. \tag{28}$$

In the reverse way it obviously would reproduce (17). In case of uniformly distributed matter it has following form

$$\left(\frac{\dot{a}}{a}\right)^2 = H_0^2\,(1 + 2\Omega_M)\,. \tag{29}$$

The second Friedman equation is from (21)

$$\frac{\ddot{a}}{a} = H_0^2\left[1 - \frac{1}{a^3}\right] \tag{30}$$

or for uniformly distributed matter in terms of Ω_M

$$\frac{\ddot{a}}{a} = H_0^2\left[-\frac{1}{2}\Omega_M + 1\right]. \tag{31}$$

Another types of functions $a(t)$ can be proposed and in that way would originate different dynamical equations that could be analysed for its compliance with the cosmological observations.

9 Conclusions

The spatial expansion phenomena is considered as the space flow. The curvature of space-time in the static four-dimensional coordinate systems emerges as the consequence of such motion. Then the dynamics and the physical forces are derived from the resulting metric. The scale factor being the primary property of space should have the fundamental significance (instead of being secondary consequence of the dynamical equations). Because of the reviewed boundary conditions the scale factor may originate on the elementary particle level and can be a key for understanding the origin of gravity. The function for $a(t)$ that results in the SdS metric was reviewed, the deceleration parameter is determined (27) and the result is close to the observed value.

Received on July 1, 2019

References

1. Akbar M. M. Embedding FLRW Geometries in Pseudo-Euclidian abd Anti-de Sitter Spaces. arXiv: gr-qc/1702.00987v2.
2. Braeck S., Gron O. A river model of space. arXiv: gr-qc/1204.0419.
3. Czerniawski J. The possibility of a simple derivation of the Schwarzschild metric. arXiv: gr-qc/0611104.
4. Hamilton A. J. S., Lisle J. P. The river model of black holes. *American Journal of Physics*, 2008, v. 76, 519–532. arXiv: gr-qc/0411060.
5. Kritov A. On the Fluid Model of the Spherically Symmetric Gravitational Field. *Progress in Physics*, 2019, v. 15 (2), 101–105.
6. Lachiéze-Rey M. The Friedman-Lemaître models in perspective. *Astronomy ans Astrophysics*, 2000, v. 364, 894–900.
7. Robertson H. P. On Relativistic Cosmology. *Phylosophy Magazin*, 1928, v. 5, 835–848.
8. Robertson H. P. Relativistic Cosmology. *Review of Modern Physics*, 1933, v. 5, 62–90.
9. Rosen J. Embedding of Various Relativistic Riemannian Spaces in Pseudo-Euclidean Spaces. *Review of Modern Physics*, 1965, v. 37, 204–214.
10. Sazhin M. V., Sazhina O. S., Chadayammuri U. The Scale Factor in the Universe with Dark Energy. arXiv: astro-ph/1109.2258v1.
11. Sommerfeld A. Electrodynamics. Lectures on Theoretical Physics, Vol. III. Academic Press, New York, 1952.

The Physics of Transcendental Numbers

Hartmut Müller

E-mail: hm@interscalar.com

The difference between rational, irrational algebraic and transcendental numbers is not only a mathematical task, but appears to be a stability criterion in complex dynamic systems. This paper introduces an approach to study the physical consequences of arithmetic properties of real numbers being ratios of measured quantities. This approach allows reformulating and resolving some unsolved tasks in particle physics, astrophysics and cosmology.

Introduction

Natural systems are highly complex and at the same time they impress us with their lasting stability. For instance, the solar system hosts at least 800 thousand orbiting each other bodies. If numerous bodies are gravitationally bound to one another, classic models predict long-term highly unstable states [1, 2] that contradict the physical reality in the solar system. In the last century, advanced models [3–7] were developed, which explain basic features of the solar system formation. However, many metric characteristics of the solar system they do not predict. The problem is that Kepler's laws, the Newton law of gravitation and the Einstein field equations allow for an infinite diversity of orbits.

In reality, however, planets in the extrasolar systems Trappist 1, Kepler 20 and many others have nearly the same orbits as some moons of Jupiter, Saturn, Uranus and Neptune [8]. Why they prefer similar orbits if there are infinite possibilities? Up to now, there have not been sufficiently convincing explanations why the solar system has installed the orbital periods 87.97 days (Mercury), 224,70 days (Venus), 365.25 days (Earth), 686.97 days (Mars), 4.60 years (Ceres), 11.87 years (Jupiter), 29.46 years (Saturn), 84.02 years (Uranus), 164.80 years (Neptune) and 248.00 years (Pluto). In conventional models, they appear as to be accidental.

Furthermore, celestial mechanics does not know any law concerning the periods of planetary rotation. Though, if the periods of rotation are accidental, why then have the Moon and the Sun similar periods of rotation? Why have the Earth, Mars and the planetoid Eris similar periods of rotation? Why have Jupiter, Saturn and the planetoid Ceres similar periods of rotation?

Not only orbital and rotational periods, but also the Earth axial precession cycle (25,770 years), the obliquity variation cycle (41,000 years) as well as the apsidal precession cycle and the orbital eccentricity cycle (both 112,000 years) appear as to be accidental. And this isn't just a shortcoming of astrophysics only.

In particle physics, bosons are considered to have no rest mass, and there are no convincing explanations why the W/Z-bosons must be 90 times as massive as the proton. A rough shortcoming of the Higgs-mechanism of particle mass generation is that the origin of the Higgs-mass itself is not elaborated and this leads to a vicious circle.

Furthermore, there is no convincing explanation why the proton-to-electron mass ratio must be close to 1836 and why these fermions are stable.

Of course, in the standard model, the electron is stable because it is the least massive particle with non-zero electric charge. Its decay would violate charge conservation. Actually, this answer only readdresses the question: What causes then the stability of the elementary electric charge? In the same model, the proton is stable, because it is the lightest baryon and the baryon number is conserved. However, also this answer only readdresses the question: Why then is the proton the lightest baryon? To answer this question, the standard model introduces quarks which violate the conservation of the integer elementary electric charge.

Measurements of the cosmic microwave background radiation (CMBR) are critical to cosmology, since any proposed model of the universe must explain it. However, in Big Bang cosmology, its current average temperature of 2.725 K appears to be accidental, because CMBR is interpreted as a remnant from an early stage of the observable universe when stars and planets didn't exist yet, and the universe was denser and much hotter.

This paper introduces an approach that considers arithmetic properties of the measured ratios of physical quantities. This approach allows not only answering our questions above, but also reformulating and resolving some unsolved tasks in paticle physics, astrophysics and cosmology.

Methods

Measurement is the source of data that allow us developing and proofing theoretical models of the reality. The result of a measurement is the ratio of two physical quantities where one of them is the reference quantity called unit of measurement. In general, this ratio is a real value that can approximate a rational, irrational algebraic or transcendental number.

In [9] we have shown that the difference between rational, irrational algebraic and transcendental numbers is not only a mathematical task, but it is also an essential aspect of stability in complex systems. For instance, integer and rational

frequency ratios provide resonance interaction that can destabilize a system.

With reference to the solar system and its stability, we may therefore expect that the ratio of any two orbital periods should be not rational. However, it is not so simple to clarify the type of number a measured ratio approximates. In general, there is no possibility to know it for sure. For example, how can we find out if the Venus-to-Earth orbital period ratio approximates a rational, irrational algebraic or transcendental number?

From the first impression, the obtained value 0.615 seems to be a rational number, but higher resolution data [10] deliver more digits, for example 0.615198 years = 224.701 days = 224 days, 16 hours and 49 minutes. Indeed, also this value is an average. In reality, the sidereal orbital period of Venus is not constant, but varies between 224.695 days = 0.61518 years and 224.709 days = 0.61522 years. According to classic models, that is due to perturbations from other planets, mainly Jupiter and Earth. As well, the orbital period of the Earth is not constant, but shows cyclic variations in the duration up to 7 minutes [11]. However, several authors [12, 13] have suggested that the Venus-to-Earth orbital period ratio coincides with 8/13 approximating the golden section $\phi = (\sqrt{5}-1)/2 = 0.618\ldots$ that is an irrational algebraic number.

It is remarkable that approximation interconnects all types of real numbers – rational, irrational algebraic and transcendental. In 1950, the mathematician Khinchin [14] made an important discovery: He could demonstrate that continued fractions deliver biunique (one-to-one) representations of all real numbers, rational and irrational. Whereas infinite continued fractions represent irrational numbers, finite continued fractions represent always rational numbers. In this way, any irrational number can be approximated by finite continued fractions, which are the convergents and deliver always the nearest and quickest rational approximation.

It is notable that the nearest rational approximation of an irrational number by a finite continued fraction is not a task of computation, but only an act of termination of the fractal recursion. For example, the golden number $\phi = (\sqrt{5}+1)/2$ has a biunique representation as simple continued fraction:

$$\phi = 1 + \cfrac{1}{1 + \cfrac{1}{1 + \cfrac{1}{1 + \cdots}}}.$$

To save space, in the following we use square brackets to write down continued fractions, for example the golden number $\phi = [1; 1, 1, \ldots]$. So long as the sequence of denominators is considered as infinite, this continued fraction represents the irrational number ϕ. If we truncate the continued fraction, the sequence of denominators will be finite and we get a convergent that is always the nearest rational approximation of the irrational number ϕ.

Let's see how it works. Increasing always the length of the continued fraction, we obtain a sequence of rational approximations of ϕ, from the worst to always better and better ones (see Table 1).

Figure 1 demonstrates the process of step by step approximation. As we can see, the rational approximations oscillate around the eigenvalue ϕ of the continued fraction that is shown as dotted line. With every step the approximation comes closer and closer to ϕ, never reaching it and describing a damped asymptotic oscillation around ϕ.

In 1950 Gantmacher and Krein [15] have demonstrated that continued fractions are solutions of the Euler-Lagrange equation for low amplitude harmonic oscillations in simple chain systems. Terskich [16] generalized this method for the analysis of oscillations in branched chain systems. The continued fraction method can also be extended to the analysis of chain systems of harmonic quantum oscillators [17].

The rational approximations of the golden number ϕ are always ratios of neighboring Fibonacci numbers – the elements of the recursive sequence 1, 1, 2, 3, 5, 8, 13, 21, 34, 55, 89, ... where the sum of two neighbors always yields the following number [18].

As we can see, only the 10^{th} approximation gives the cor-

Table 1: Approximations of the irrational number ϕ.

$[1] = 1$
$[1; 1] = 2$
$[1; 1, 1] = 3/2 = 1.5$
$[1; 1, 1, 1] = 5/3 = 1.\overline{66}$
$[1; 1, 1, 1, 1] = 8/5 = 1.6$
$[1; 1, 1, 1, 1, 1] = 13/8 = 1.625$
$[1; 1, 1, 1, 1, 1, 1] = 21/13 = 1.\overline{615384}$
$[1; 1, 1, 1, 1, 1, 1, 1] = 34/21 = 1.\overline{619047}$
$[1; 1, 1, 1, 1, 1, 1, 1, 1] = 55/34 = 1.\overline{61764705882352941}$
$[1; 1, 1, 1, 1, 1, 1, 1, 1, 1] = 89/55 = 1.\overline{618}$

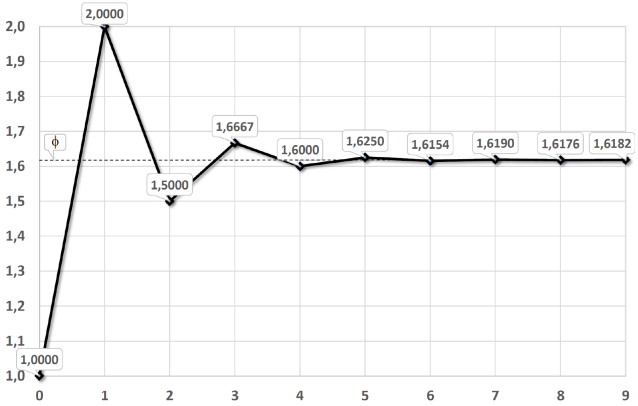

Fig. 1: The approximation steps 0 – 9 of the golden number $\phi = 1.618\ldots$ (dotted line) by continued fraction $[1; 1, 1, \ldots]$.

rect third decimal of ϕ. The approximation process is very slow because of the small denominators. In fact, the denominators in the continued fraction of ϕ are the smallest possible and consequently, the approximation speed is the lowest possible. The golden number ϕ is therefore treated as the "most irrational" number in the sense that a good approximation of ϕ by rational numbers cannot be given with small quotients.

On the contrary, transcendental numbers can be approximated exceptionally well by rational numbers, because their continued fractions contain large denominators and can be truncated with minimum loss of precision. For instance, the simple continued fraction of the number $\pi = 3.1415927\ldots = [3; 7, 15, 1, 292, \ldots]$ delivers the following sequence of rational approximations:

$[3] = 3$
$[3; 7] = 3.\overline{142857}$
$[3; 7, 15] = 3.\overline{14150943396226}$
$[3; 7, 15, 1] = 3.1415929\ldots$

We can see that the 2nd approximation delivers the first 2 decimals correctly, and the 4th approximation shows already 6 correct decimals.

Much like the continued fraction of the golden number ϕ contains only the number 1, a prominent continued fraction [19] of Euler's number contains all natural numbers as denominators and numerators, forming an infinite fractal sequence of harmonic intervals:

$$e = 2 + \cfrac{1}{1 + \cfrac{1}{2 + \cfrac{2}{3 + \cfrac{3}{4 + \cdots}}}}.$$

As Euler's number is transcendental, it can also be represented as a continued fraction with quickly increasing denominators:

$$e = 1 + \cfrac{2}{1 + \cfrac{1}{6 + \cfrac{1}{10 + \cfrac{1}{14 + \cdots}}}}.$$

In this way, already the 4th approximation delivers the first 3 decimals correctly and returns in fact the rounded Euler's number $e = 2.71828\ldots$ of 5 decimals' resolution:

1
3
$2.\overline{714285}$
$2.7183\ldots$

This special arithmetic property of continued fractions [20] of transcendental numbers has the consequence that transcendental numbers are distributed near by rational numbers of small quotients or close to integers, like $e^3 = 20.08\ldots$ or $e^{4.5} = 90.01\ldots$. This can create the impression that complex systems like the solar system provide ratios of physical quantities that approximate rational numbers. More likely, they approximate transcendental numbers, which are located close to rational numbers.

Namely, transcendental numbers define the preferred ratios of quantities which avoid destabilizing resonance interaction [9]. In this way, they sustain the lasting stability of periodic processes in complex dynamic systems. At the same time, a good rational approximation can be induced quickly, if the system temporarily requires local resonance interaction. Though, algebraic irrational numbers like $\sqrt{2}$ or the golden number ϕ do not compellingly prevent resonance, because they can be transformed into integer or rational numbers by multiplication.

Among all transcendental numbers, Euler's number $e = 2.71828\ldots$ is unique, because its real power function e^x coincides with its own derivatives. In the consequence, Euler's number allows inhibiting resonance interaction regarding any interacting periodic processes and their derivatives. Because of this unique property of Euler's number, complex dynamic systems tend to establish relations of quantities that coincide with values of the natural exponential function e^x for integer and rational exponents x.

Therefore, we expect that periodic processes in real systems prefer frequency ratios close to Euler's number and its rational powers. Consequently, the logarithms of the frequency ratios should be close to integer 1, 2, 3, 4, ... or rational values $\frac{1}{2}, \frac{1}{3}, \frac{1}{4}, \ldots$ In [21] we exemplified our hypothesis in particle physics, astrophysics, cosmology, geophysics, biophysics and engineering.

Thanks to Khinchin's [14] discovery, any real number has a biunique representation as a continued fraction. Now let's apply this to the real argument x of the natural exponential function e^x itself:

$$x = [n_0; n_1, n_2, \ldots, n_k]. \tag{1}$$

All denominators $n_1, n_2, \ldots, n_k$ of the continued fraction including the free link n_0 are integer numbers. All numerators equal 1. The length of the continued fraction is given by the number k of layers.

The canonical form (all numerators equal 1) does not limit our conclusions, because every continued fraction with partial numerators different from 1 can be transformed into a canonical continued fraction using the Euler equivalent transformation [22]. With the help of the Lagrange [23] transformation, every continued fraction with integer denominators can be represented as a continued fraction with natural denominators that is always convergent [24].

Now we are going to study the fractal distribution of the rational eigenvalues of the finite continued fractions (1). The

first layer is given by the truncated after n_1 continued fraction:

$$x = [n_0; n_1] = n_0 + \frac{1}{n_1}.$$

For the beginning we take $n_0 = 0$. The denominators n_1 follow the sequence of integer numbers ±1, ±2, ±3 etc. The second layer is given by the truncated after n_2 continued fraction:

$$x = [n_0; n_1, n_2] = n_0 + \cfrac{1}{n_1 + \cfrac{1}{n_2}}.$$

Figure 2 shows the first and the second layer in comparison. As we can see, reciprocal integers $\pm 1/2, \pm 1/3, \pm 1/4, \ldots$ are the attractor points of the distribution. In these points, the distribution density always reaches a local maximum. Whole numbers $0, \pm 1, \ldots$ are the main attractors of the distribution.

Now let's remember that we are observing the fractal distribution of rational values $x = [n_0; n_1, n_2, \ldots, n_k]$ of the real argument x of the natural exponential function e^x. What we see is the fractal distribution of transcendental numbers of the type $\exp([n_0; n_1, n_2, \ldots, n_k])$ on the natural logarithmic scale. Near integer exponents the distribution density of these transcendental numbers is maximum.

Consequently, for integer exponents x, the natural exponential function e^x defines attractor points of transcendental numbers and create islands of stability.

Figure 2 shows that these islands are not points, but ranges of stability. Integer exponents $0, \pm 1, \pm 2, \pm 3, \ldots$ are attractors which form the widest ranges of stability. Half exponents $\pm 1/2$ form smaller islands, one third exponents $\pm 1/3$ form the next smaller islands and one fourth exponents $\pm 1/4$ form even smaller islands of stability etc.
For rational exponents, the natural exponential function is always transcendental [25]. Increasing the length of the continued fraction (1), the density of the distribution of transcendental numbers of the type $\exp([n_0; n_1, n_2, \ldots, n_k])$ is increasing as well. Nevertheless, their distribution is not homogeneous, but fractal. Applying continued fractions and truncating them, we can represent the real exponents x of the natural exponential function e^x as rational numbers and make visible their fractal distribution.

Here I would like to underline that the application of continued fractions doesn't limit the universality of our conclusions, because continued fractions deliver biunique representations of all real numbers including transcendental. Therefore, the fractal distribution of transcendental eigenvalues of the natural exponential function e^x of the real argument x, represented as continued fraction, is an inherent characteristic of the number continuum. This characteristic we call the Fundamental Fractal [26].

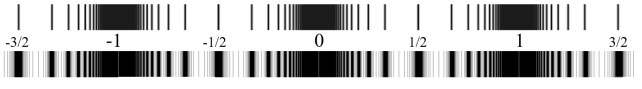

Fig. 2: The Fundamental Fractal – the fractal distribution of transcendental numbers of the type e^x with $x = [n_0; n_1, n_2, \ldots, n_k]$ on the natural logarithmic scale for $k = 1$ (first layer above) and for $k = 2$ (second layer below) in the range $-3/2 \leqslant x \leqslant 3/2$.

In physical applications, the natural exponential function e^x of the real argument x is the ratio of two physical quantities where one of them is the reference quantity called unit of measurement. Therefore, we can rewrite the equation (1):

$$\ln(\mathrm{X/Y}) = [n_0; n_1, n_2, \ldots, n_k], \tag{2}$$

where X is the measured physical quantity and Y the unit of measurement.

In this way, the natural exponential function e^x of the rational argument $x = [n_0; n_1, n_2, \ldots, n_k]$ generates the set of preferred ratios X/Y of quantities which avoid destabilizing resonance and in this way, provide the lasting stability of real systems regardless of their complexity. This is a very powerful conclusion, as we will see in the following.

Results

Now let's apply this result to our first example of the Venus-to-Earth orbital period ratio. In this case, X = 224.701 days and Y = 365.256363 days. Following (2) we calculate the natural logarithm ln (X/Y):

$$\ln\left(\frac{Venus\ orbital\ period}{Earth\ orbital\ period}\right) = \ln\left(\frac{224.701}{365.256363}\right) = -0.49.$$

We can see that this logarithm is close to $-1/2$. The deviation is only 0.01. In accordance with (2), $n_0 = 0$ and $n_1 = 2$. Consequently, the Venus-to-Earth orbital period ratio is close to an attractor point of the Fundamental Fractal, the center of a local island of stability.

In fact, the ratios of the orbital periods in the solar system approximate Euler's number and its rational powers [9]. Obviously, in this way, the solar system can ovoid destabilizing resonance of the orbital motions and reach lasting stability. For instance, Saturn's sidereal orbital period [27] equals 10759.22 days, that of Uranus is 30688.5 days. The natural logarithm of the ratio of their orbital periods is close to 1:

$$\ln\left(\frac{Uranus\ orbital\ period}{Saturn\ orbital\ period}\right) = \ln\left(\frac{30688.5}{10759.22}\right) = 1.05.$$

Jupiter's sidereal orbital period equals 4332.59 days, that of the planetoid Ceres is 1681.63 days. The natural logarithm of the ratio of their orbital periods is also close to 1:

$$\ln\left(\frac{Jupiter\ orbital\ period}{Ceres\ orbital\ period}\right) = \ln\left(\frac{4332.59}{1681.63}\right) = 0.95.$$

Not only neighboring orbits show Euler ratios, but far apart from each other orbits do this as well. Pluto's sidereal orbital

period is 90560 days, that of Venus is 224.701 days. The natural logarithm of the ratio of their orbital periods equals 6:

$$\ln\left(\frac{\textit{Pluto orbital period}}{\textit{Venus orbital period}}\right) = \ln\left(\frac{90560}{224.701}\right) = 6.00.$$

In [8] we have analyzed the orbital periods of the largest bodies in the solar system including the moon systems of Jupiter, Saturn, Uranus and Neptune, as well as the exoplanetary systems Trappist 1 and Kepler 20. In the result we can assume that the stability of all these orbital systems is given by the transcendence of Euler's number and its rational powers.

The most stable systems we know are of atomic scale. Because of their exceptional stability, proton and electron form stable atoms, the structural elements of matter. The lifespans of the proton and electron surpass everything that is measurable, exceeding 10^{30} years. The proton-to-electron ratio 1836.152674 is considered as fundamental physical constant [28] and it has the same value for their rest energies and rest masses, frequencies and wavelengths. The natural logarithm is close to seven and a half:

$$\ln(1836.152674) = 7.515427\ldots \simeq 6 + \frac{3}{2}.$$

This result suggests the assumption that the stability of the proton and electron comes from the number continuum, more specifically, from the transcendence of Euler's number and its rational powers. Already in the eighties the scaling exponent 3/2 was found in the distribution of particle masses by Valery Kolombet [29]. Applying hyperscaling [26] by Euler's number (tetration), we get the next approximation of the logarithm of the proton-to-electron ratio:

$$6 + \frac{e^e}{10} = 7.515426\ldots$$

We suppose that hyperscaling by Euler's number causes the exceptional stability of proton and electron.

In [17] we have analyzed the mass distribution of hadrons, mesons, leptons, the W/Z and Higgs bosons and proposed scaling by Euler's number and its roots as model of particle mass generation [30]. In this model, the $W^{\pm}$-boson mass 80385 MeV/c^2 and the Z^0-boson mass 91188 MeV/c^2 appear as the 12 times scaled up electron rest mass 0.511 MeV/c^2:

$$\ln\left(\frac{W^{\pm}}{electron}\right) = \ln\left(\frac{80385}{0.511}\right) = 11.97.$$

$$\ln\left(\frac{Z^0}{electron}\right) = \ln\left(\frac{91188}{0.511}\right) = 12.09.$$

Expected, the square root of Euler's number defines the next island of stability – in fact, the corresponding state of matter was discovered in 2012 and interpreted [31] as Higgs-boson H^0 with the rest mass 125.18 GeV/c^2:

$$\ln\left(\frac{H^0}{electron}\right) = \ln\left(\frac{125180}{0.511}\right) = 12.41.$$

Euler's number and its rational powers are universal scaling factors that inhibit resonance and in this way, stabilize periodic processes bound in a chain system. This approach we call Global Scaling [21]. The rest energy of the proton can be seen as the $6+\frac{3}{2}$ times scaled up rest energy of the electron. In the same way, Pluto's orbital period can be seen as the 6 times scaled up by Euler's number orbital period of Venus or as the 3 times scaled up by Euler's number orbital period of Jupiter. Here it is important to understand that only scaling by Euler's number and its rational powers inhibits resonance interaction and provides lasting stability of bound processes and allows for the formation of stable atoms or stable planetary systems, for instance.

Now we could ask the question: Starting with the electron oscillation period, if we continue to scale up always multiplying by Euler's number, will we meet the orbital period, for instance, of Jupiter?

Actually, it is so. If we multiply the electron oscillation period 66 times by Euler's number, we meet exactly the orbital period of Jupiter:

$$\ln\left(\frac{T_{Jupiter\ orb}}{\tau_{electron}}\right) = \ln\left(\frac{3.7434\cdot 10^8\ \mathrm{s}}{8.093\cdot 10^{-21}\ \mathrm{s}}\right) = 66.00.$$

Jupiter's orbital period $T_{Jupiter\ orb}$ = 4332.59 days = 3.7434×10^8 s. The oscillation period of the electron $\tau_{electron}$ derives from its rest energy $E_{electron}$ = 0.511 MeV:

$$\tau_{electron\ angular} = \hbar/E_{electron} = 1.288\times 10^{-21}\mathrm{s},$$

$$\tau_{electron} = 2\pi\cdot\tau_{electron\ angular} = 8.093\times 10^{-21}\mathrm{s}.$$

$\hbar$ is the reduced Planck constant. Data taken from [28]. Similarly, the oscillation period of the proton τ_{proton} derives from its rest energy E_{proton} = 938.272 MeV:

$$\tau_{proton\ angular} = \hbar/E_{proton} = 7.015\times 10^{-25}\mathrm{s},$$

$$\tau_{proton} = 2\pi\cdot\tau_{proton\ angular} = 4.408\times 10^{-24}\mathrm{s}.$$

Within our approach, electron and proton define two complementary classes of stability in the sense of the avoidance of destabilizing resonance. Here and in the following, we use the letter E for electron stability and the letter P for proton stability. In accordance with (2), we use rectangle brackets for continued fractions. For example, E[66] means the main attractor 66 of electron stability. In the solar system, this attractor stabilizes the orbital period of Jupiter.

The main attractor E[63] stabilizes the orbital period of Venus. The siderial orbital period of Venus $T_{Venus\ orb}$ equals 224.701 days = 1.9414×10^7 s:

$$\ln\left(\frac{T_{Venus\ orb}}{\tau_{electron}}\right) = \ln\left(\frac{1.9414\times 10^7\ \mathrm{s}}{8.093\times 10^{-21}\ \mathrm{s}}\right) = 63.04 = E[63].$$

Not only the orbits of planets and planetoids, but also the orbits of moons are stabilized by the Fundamental Fractal (2).

For example, the main attractor $E[61]$ stabilizes the orbital period $T_{Moon\ orb}$ = 27.321661 days = 2.36059×10^6 s of the Moon:

$$\ln\left(\frac{T_{Moon\ orb}}{\tau_{electron}}\right) = \ln\left(\frac{2.36059 \times 10^6\ \mathrm{s}}{8.093 \times 10^{-21}\ \mathrm{s}}\right) = 60.94 = E[61].$$

The attractor $E[62]$ stabilizes the orbital period of Saturn's moon Iapetus $T_{Iapetus\ orb}$ = 79.3215 days = 6.8534×10^6 s:

$$\ln\left(\frac{T_{Iapetus\ orb}}{\tau_{electron}}\right) = \ln\left(\frac{6.8534 \times 10^6\ \mathrm{s}}{8.093 \times 10^{-21}\ \mathrm{s}}\right) = 62.00 = E[62].$$

As well, it is not surprising that Ceres, the largest body of the main asteroid belt, orbits the Sun close to a main attractor. The orbital period of Ceres $T_{Ceres\ orb}$ equals 1681.63 days = 1.4529×10^8 s:

$$\ln\left(\frac{T_{Ceres\ orb}}{\tau_{electron}}\right) = \ln\left(\frac{1.4529 \times 10^8\ \mathrm{s}}{8.093 \times 10^{-21}\ \mathrm{s}}\right) = 65.05 = E[65].$$

Now let us analyze some rotational periods. Although the rotation of Venus is retrograde, its period $T_{Venus\ rot}$ = 5816.667 hours = 2.094×10^7 s is close to the main attractor $E[65]$:

$$\ln\left(\frac{T_{Venus\ rot}}{\tau_{electron\ angular}}\right) = \ln\left(\frac{2.094 \times 10^7\ \mathrm{s}}{1.288 \times 10^{-21}\ \mathrm{s}}\right) = 64.96 = E[65].$$

As well, the full rotational period of the Sun $T_{Sun\ rot}$ = 34.3 days = 2.9635×10^6 s fits with a main attractor:

$$\ln\left(\frac{T_{Sun\ rot}}{\tau_{electron\ angular}}\right) = \ln\left(\frac{2.9635 \times 10^6\ \mathrm{s}}{1.288 \times 10^{-21}\ \mathrm{s}}\right) = 63.00 = E[63].$$

As we have seen, the main attractor $E[63]$ stabilizes the rotational period of the Sun as well as the orbital period of Venus. From this, directly follows:

$$T_{Venus\ orb} = 2\pi \cdot T_{Sun\ rot}$$

Although π is transcendental, its real power function π^x does not coincide with its own derivatives. Therefore, π cannot inhibit resonance interaction regarding the derivatives of periodic processes, but it does not violate the transcendence [32] of Euler's number. Within our approach, 2π connects stable rotation with stable orbital motion.

In addition, the main attractor $E[65]$ stabilizes the orbital period of Ceres as well as the rotational period of Venus. From this, directly follows:

$$T_{Ceres\ orb} = 2\pi \cdot T_{Venus\ rot}$$

Obviously, preferred rotational periods are not accidental, but follow the Fundamental Fractal (2) and are connected by 2π with stable, avoiding resonance orbital periods.

Within our approach, the approximation level of an attractor of stability indicates evolutionary trends. For example, the orbital period of Venus must still decrease for reaching the center of $E[63]$. On the contrary, the orbital period of the Moon must still increase for reaching the center of $E[61]$. Actually, exactly this is observed [33].

While all the orbital and rotational periods we have analyzed are stabilized by main attractors of electron stability, the rotational period of Mars $T_{Mars\ rot}$ = 24.62278 hours = 88642 s approximates a main attractor of proton stability:

$$\ln\left(\frac{T_{Mars\ rot}}{\tau_{proton\ angular}}\right) = \ln\left(\frac{88642\ \mathrm{s}}{7.015 \times 10^{-25}\ \mathrm{s}}\right) = 67.01 = P[67].$$

The rotational period of the Earth $T_{Earth\ rot}$ = 23.934 hours = 86164 s approximates the same attractor $P[67]$:

$$\ln\left(\frac{T_{Earth\ rot}}{\tau_{proton\ angular}}\right) = \ln\left(\frac{86164\ \mathrm{s}}{7.015 \times 10^{-25}\ \mathrm{s}}\right) = 66.98 = P[67].$$

This means that the main attractor $P[67]$ stabilizes the rotational periods of Mars and Earth. Furthermore, the attractor $P[71]$ stabilizes the orbital period $T_{Earth\ orb}$ = 365.25636 days = 3.1558×10^7 s of the Earth:

$$\ln\left(\frac{T_{Earth\ orb}}{\tau_{proton}}\right) = \ln\left(\frac{3.1558 \times 10^7\ \mathrm{s}}{4.408 \times 10^{-24}\ \mathrm{s}}\right) = 71.05 = P[71].$$

Obviously, the Earth's orbital eccentricity variation cycle $T_{Earth\ orb\ ecc} \approx 112,600$ years = 3.5533×10^{12} s is stabilized by the main attractor $E[77]$:

$$\ln\left(\frac{T_{Earth\ orb\ ecc}}{\tau_{electron\ angular}}\right) = \ln\left(\frac{3.5533 \times 10^{12}\ \mathrm{s}}{1.288 \times 10^{-21}\ \mathrm{s}}\right) = 77.00 = E[77].$$

This attractor stabilizes also the Earth's apsidal precession cycle $\approx 112,000$ years. The Earth's orbital inclination variation cycle $T_{Earth\ orb\ inc} \approx 70,000$ years = $2.209 \cdot 10^{12}$ s is stabilized by the attractor $E[76;2]$:

$$\ln\left(\frac{T_{Earth\ orb\ inc}}{\tau_{electron\ angular}}\right) = \ln\left(\frac{2.209 \times 10^{12}\ \mathrm{s}}{1.288 \times 10^{-21}\ \mathrm{s}}\right) = 76.51 = E[76;2].$$

The obliquity variation cycle of the ecliptic $T_{Ecliptic\ obliquity} \approx 41,000$ years = 1.2938×10^{12} s is stabilized by the main attractor $E[76]$:

$$\ln\left(\frac{T_{Ecliptic\ obliquity}}{\tau_{electron\ angular}}\right) = \ln\left(\frac{1.2938 \times 10^{12}\ \mathrm{s}}{1.288 \times 10^{-21}\ \mathrm{s}}\right) = 75.99 = E[76].$$

The Earth's axial precession cycle $T_{Earth\ axial\ prec} \approx 25,770$ years = 8.1328×10^{11} s is stabilized by the attractor $E[75;2]$:

$$\ln\left(\frac{T_{Earth\ axial\ prec}}{\tau_{electron\ angular}}\right) = \ln\left(\frac{8.1328 \times 10^{11}\ \mathrm{s}}{1.288 \times 10^{-21}\ \mathrm{s}}\right) = 75.52 = E[75;2].$$

The Earth's axial nutation period $T_{Earth\ axial\ prec}$ = 18.6 years = 5.8696×10^8 s is stabilized by the main attractor $P[74]$:

$$\ln\left(\frac{T_{Earth\ axial\ prec}}{\tau_{proton}}\right) = \ln\left(\frac{5.8696 \times 10^8\ \mathrm{s}}{4.408 \times 10^{-24}\ \mathrm{s}}\right) = 73.97 = P[74].$$

The Chandler wobble of the Earth's axis $T_{Chandler\ wobble}$ = 433 days = 3.741×10^7 s is stabilized by the main attractor P[73]:

$$\ln\left(\frac{T_{Chandler\ wobble}}{\tau_{proton\ angular}}\right) = \ln\left(\frac{3.741 \times 10^7\ \mathrm{s}}{7.015 \times 10^{-25}\ \mathrm{s}}\right) = 73.05 = P[73].$$

As we have seen, within our approach, the current orbital and rotational periods in the solar system do not appear as to be accidental, but correspond with islands of stability defined by Euler's number and its rational powers that allow avoiding destabilizing resonance. This is valid not only for the solar system, but also for exoplanetary systems as we have shown in [8]. Furthermore, our approach explains the durations of the axial precession cycle including the nutation period and the Chandler wobble, the obliquity variation cycle, the orbital inclination variation cycle, the apsidal precession cycle and the orbital eccentricity cycle of the Earth.

In [21] we have shown that the divisibility of their integer logarithms interconnects all the main attractors of electron and proton stability and causes interscalar effects, which stabilize also biophysical periodical processes.

Concluding this overview, I would like to mention that, within our approach, the current average temperature $\mathrm{T}_{\mathrm{CMBR}}$ = 2.725 K [34] of the cosmic microwave background radiation (CMBR) does not appear to be accidental. On the contrary, obviously, this process is stable, because its average temperature is close to a main attractor of proton stability:

$$\ln\left(\frac{\mathrm{T}_{\mathrm{CMBR}}}{\mathrm{T}_{\mathrm{proton}}}\right) = \ln\left(\frac{2.725\ \mathrm{K}}{1.0888 \times 10^{13}\ \mathrm{K}}\right) = -29.01 = P[-29].$$

The proton blackbody temperature $\mathrm{T}_{\mathrm{proton}} = E_{proton}/k$ derives from the proton rest energy $E_{proton} = 938.272\,MeV$ and the Boltzmann [28] constant k.

Consequently, the current temperature of the CMBR is not accidental, and it is highly unlikely that this temperature will still decrease.

In [35] we have shown that integer powers of Euler's number define also the ratios of fundamental physical constants. In our approach, this means that the transcendence of Euler's number stabilizes energy-frequency and energy-mass conversions and makes possible the existence of fundamental physical constants. For instance, the 88^{th} power of Euler's number stabilizes the ratio of the speed of light c, the Planck constant $\hbar$, the proton rest mass m_p and the gravitational constant G:

$$\frac{\hbar \cdot c}{G \cdot m_p^2} = e^{88}. \tag{3}$$

Quantum mechanics only postulates, but does not derive the constancy of the Planck constant as well as general relativity postulates the constancy of the gravitational constant, but does not derive it. Also special relativity postulates, but does not derive the constancy of the speed of light. Up to now, there have not been sufficiently convincing explanations why the speed of light should be constant, why it should have the value 299792458 m/s and why it should be the maximum possible velocity in the universe.

Within our approach, we can derive the speed of light c from other fundamental physical constants stabilized by integer powers of Euler's number. Naturally, the proton is not the only stable particle. The electron is stable as well. Furthermore, the proton-to-electron ratio is stabilized by Euler's number and its rational powers. From this and (3), directly follows that 299792458 m/s is not the maximum speed. Indeed, rational powers of Euler's number define a logarithmically fractal set of stable velocities $c_{n,m}$ which are superluminal for $n > 0$:

$$c_{n,m} = c \cdot e^{\,n/m}$$

where n, m are integer numbers. In general, the rational exponents are finite continued fractions (1). In [35] we verified the fractal set $c_{n,m}$ of stable subluminal and superluminal velocities on experimental and astrophysical data.

Conclusion

In this paper, we discussed the physical significance of transcendental numbers approximated by ratios of physical quantities. In particular, the transcendence of Euler's number allows avoiding destabilizing resonance interaction in real systems and appears to be a universal criterion of stability.

For instance, Euler's number and its rational powers stabilize the orbital and rotational periods of planets, planetoids and moons in the solar system.

Our approach allows deriving the mass ratios of the fundamental elementary particles electron, proton, $W^{\pm}$, Z^0 and H^0-boson as well as the temperature 2.725 K of the cosmic microwave background from Euler's number and its rational powers. Integer powers of Euler's number stabilize also the ratios of the fundamental physical constants $\hbar$, c, G.

Acknowledgements

The author is grateful to Simon Shnoll, Viktor Panchelyuga, Valery Kolombet, Svetlana Zaichkina, Oleg Kalinin, Viktor Bart, Sergey Surin, Alexey Petrukhin, Erwin Müller, Michael Kauderer, Ulrike Granögger and Leili Khosravi for valuable discussions.

Submitted on August 16, 2019

References

1. Heggie D. C. The Classical Gravitational N-Body Problem. arXiv: astro-ph/0503600v2, 11 Aug 2005.
2. Hayes B. The 100-Billion-Body Problem. *American Scientist*, 2015, v. 103, no. 2.
3. Williams I. O., Cremin A.W. A survey of theories relating to the origin of the solar system. Qtly. Rev. RAS 9: 40-62, (1968), ads.abs.harvard.edu/abs.
4. Alfven H. Band Structure of the Solar System. // Dermot S. F. Origin of the Solar System. pp. 41-48. Wiley, (1978).

5. Woolfson M. M. The Solar System: Its Origin and Evolution. *Journal of the Royal Astronomical Society*, 1993, v. 34, 1–20.
6. Van Flandern T. Our Original Solar System-a 21st Century Perspective. MetaRes. Bull. 17: 2-26, (2008). D21, 475–491, 2000.
7. Woolfson M. M. Planet formation and the evolution of the Solar System. arXiv:1709.07294, (2017).
8. Müller H. Global Scaling of Planetary Systems. *Progress in Physics*, 2018, v. 14, 99–105.
9. Müller H. On the Cosmological Significance of Euler's Number. *Progress in Physics*, 2019, v. 15, 17–21.
10. Venus Fact Sheet. NASA Space Science Archive. www.nssdc.gsfc.nasa.gov.
11. Fedorov V. M. Interannual Variations in the Duration of the Tropical Year. Doklady Earth Sciences, 2013, Vol. 451, Part 1, pp. 750–753, (2013) // Doklady Akademii Nauk, 2013, Vol. 451, No. 1, pp. 95–97., (2013).
12. Pletser V. Orbital Period Ratios and Fibonacci Numbers in Solar Planetary and Satellite Systems and in Exoplanetary Systems. arXiv:1803.02828 (2018).
13. Butusov K. P. The Golden Ratio in the solar system. *Problems of Cosmological Research*, vol. 7, Moscow–Leningrad, 1978.
14. Khintchine A. Continued fractions. University of Chicago Press, Chicago, 1964.
15. Gantmacher F. R., Krein M. G. Oscillation matrixes, oscillation cores and low oscillations of mechanical systems. Leningrad, 1950.
16. Terskich V. P. The continued fraction method. Leningrad, 1955.
17. Müller H. Fractal Scaling Models of Natural Oscillations in Chain Systems and the Mass Distribution of Particles. *Progress in Physics*, 2010, v. 6, 61–66.
18. Devlin K. The Man of Numbers. Fibonacci's Arithmetic Revolution. Bloomsbury Publ., 2012.
19. Yiu P. The Elementary Mathematical Works of Leonhard Euler. Florida Atlantic University, 1999, pp. 77–78.
20. Perron O. Die Lehre von den Kettenbrüchen. 1950.
21. Müller H. Global Scaling. The Fundamentals of Interscalar Cosmology. *New Heritage Publishers*, Brooklyn, New York, USA, (2018).
22. Skorobogatko V. Ya. The Theory of Branched Continued Fractions and mathematical Applications. Moscow, Nauka, 1983.
23. Lagrange J. L. Additions aux elements d'algebre d'Euler. 1798.
24. Markov A. A. Selected work on the continued fraction theory and theory of functions which are minimum divergent from zero. Moscow–Leningrad, 1948.
25. Hilbert D. Über die Transcendenz der Zahlen e und π. *Mathematische Annalen*, Bd. 43, 216–219, 1893.
26. Müller H. Scale-Invariant Models of Natural Oscillations in Chain Systems and their Cosmological Significance. *Progress in Physics*, 2017, v. 13, 187–197.
27. Astrodynamic Constants. JPL Solar System Dynamics. ssd.jpl.nasa.gov (2018).
28. Tanabashi M. et al. (Particle Data Group), Phys. Rev. D 98, 030001 (2018), www.pdg.lbl.gov
29. Kolombet V. Macroscopic fluctuations, masses of particles and discrete space-time, *Biofizika*, 1992, v. 36, 492–499.
30. Müller H. Emergence of Particle Masses in Fractal Scaling Models of Matter. *Progress in Physics*, 2012, v. 8, 44–47.
31. Bezrukov F. et al. Higgs boson mass and new physics. arXiv:1205.2893v2 [hep-ph] 27 Sep 2012.
32. Bailey D. H. Numerical Results on the Transcendence of Constants Involving pi, e, and Euler's Constant. *Mathematics of Computation*, 1988, v. 50(181), 275–281.
33. Bills B. G., Ray R. D. Lunar Orbital Evolution: A Synthesis of Recent Results. *Geophysical Research Letters*, v. 26, Nr. 19, pp. 3045–3048, (1999)
34. Fixsen D. J. The Temperature of the Cosmic Microwave Background. *The Astrophysical Journal*, vol. 707 (2), 916–920. arXiv:0911.1955, 2009.
35. Müller H. The Cosmological Significance of Superluminality. *Progress in Physics*, 2019, v. 15, 26–30.

A New Understanding of the Matter-Antimatter Asymmetry

Linfan Mao

1. Chinese Academy of Mathematics and System Science, Beijing 100190, P.R. China
2. Academy of Mathematical Combinatorics & Applications(AMCA), Colorado, USA
E-mail: maolinfan@163.com

There are no theory on antimatter structure unless the mirror of its normal matter, with the same mass but opposite qualities such as electric charge, spin,$\cdots$, etc. to its matter counterparts holding with the Standard Model of Particle. In theory, a matter will be immediately annihilated if it meets with its antimatter, leaving nothing unless energy behind, and the amounts of matter with that of antimatter should be created equally in the Big Bang. So, none of us should exist in principle but we are indeed existing. A few physicists explain this puzzling thing by technical assuming there were extra matter particles for every billion matter-antimatter pairs, or asymmetry of matter and antimatter in the end. Certainly, this assumption comes into beings by a priori hypothesis that the matter and antimatter forming both complying with a same composition mechanism after the Big Bang, i.e., antimatter consists of antimolecules, antimolecule consists of antiatoms and antiatom consists of antielectrons, antiprotons and antineutrons without experimental evidences unless the antihydrogen, only one antimolecule. *Why only these antimatters are detected by experiments*? *Are there all antimatters in the universe*? In fact, if the behavior of gluon in antimatter, i.e., antigluon is not like the behavior but opposites to its matter counterparts or reverses gluon interaction $\mathcal{F}_{g^k}$ to $-\mathcal{F}_{g^k}$, $1 \leq k \leq 8$ complying with the Standard Model of Particle, then the residual strong interaction within hadrons is repulsion. We can establish a new mechanism of matter and antimatter without the asymmetry assumption but only by composition theory of matter, explain the asymmetry of matter-antimatter and why only these antimatters found, claim both the attractive and repulsive properties on gravitation. All of the conclusions are consistent with known experiments on matter and antimatter.

1 Introduction

Antimatter and dark energy are both physical reality in the universe. An antimatter is literally, a mirror image with the same mass but reversed electrical charges and spin as its correspondent normal matter such as those of positrons, antiprotons, antideuteron,$\cdots$ and antihydrogen. The most interesting phenomenon on antimatter $\overline{M}$ is that if it collides with its normal matter M will completely annihilate into energy E in global energy shortage today. For example,

$$e^- + e^+ \to \gamma + \gamma,$$

i.e., an electron e^- collides with a positron e^+ will completely transforms to 2 photons γ, an energy form.

Antimatter was first theoretically considered by Paul A.M.Dirac in 1928 for his equation $E = \pm mc^2$ which allowed for the negative energy existence, corespondent to anti-particles in the universe. And then, Carl Anderson discovered positron, the first evidence that antimatter existed in 1932. A few famous things signed the founding of antimatter $\overline{M}$ are listed following ([2],[3]):

(1) Positron by C. Anderson in 1932;

(2) Antiprotons by E. Segrè and O. Chamberlain et al at Bevatron of Berkeley in 1955;

(3) Antineutron by B. Cork et al at Bevatron of Berkeley in 1957;

(4) Antideuteron by Antonino Zichichi et al at CERN in 1965;

(5) Antihydrogen by W. Oelert et al at CERN in 1995.

In fact, modern physics convinces that there exists elementary antiparticle for every elementary particle ([4]), founded in its decay, scattering and radiation such as those known rulers following:

(1)(β-Decay) $n \to p + e^- + \overline{\nu}_e$, i.e., a neutron n can spontaneously decays to a proton p, a electron e^- and antineutrino $\overline{\nu}_e$;

(2)(Scattering) $\gamma + \gamma \to e^- + e^+$, i.e., a photon γ collides with another γ will scattering an electron e^- and a positron e^+;

(3)(Radiation) $e^- \to e^- + \gamma$, i.e., a high level electron e^- jumps to a low level e^- will radiating a proton γ.

For explaining the observation that the universe is expanding at an accelerating rate, the dark energy is suggested in the standard model of cosmology in 1998 ([15]). But, neither its detecting nor forming mechanism is hold by humans unless it contributes 68% energy to the total energy in the observable universe. *Where does*

it comes from and how is it formed? Certainly, the dark energy and antimatter are both related to Big Bang but we have no a theory for explaining their born and rulers in universe. The key point is holding on the forming of antimatter with action on matter.

Usually, antimatter is understood as the mirror of its normal matter with the same mass but opposite qualities such as electric charge, spin,$\cdots$, etc. to its matter counterparts, holds with the Standard Model of Particle, and a priori hypothesis that the matter and antimatter forming both comply with a same composition mechanism after the Big Bang by humans, i.e., a matter consists of molecules, a molecule consists of atoms, a atom consists of electrons, protons and neutrons,$\cdots$, and an antimatter also consists of antimolecules, an antimolecule also consists of antiatoms, an antiatom also consists of antielectrons, antiprotons and antineutrons, $\cdots$, respectively, a mirror composition theory on antimatter ([17]). However, there are no antimatter unless elementary antiparticles, and only one antimolecules, i.e., antihydrogen found by experimental evidence. Then, *why only these antimatters are detected and where are other antimatters hidden, or there are no other antimaters*? Furthermore, *could we claim the composition mechanism of antimatter is the same that of matter*? We can certainly not unless only by purely imagination. The central factor is the behavior of antigluon in antimatter. Clearly, gluon is an attraction in the composition of normal matter by the Standard Model of Particle. But, *is antigluon only an attraction, or its counterpart, a repulsion*? By its action property, antigluon should be a repulsion, not a mirror of a normal gluon complying with the Standard Model of Particle.

However, if the action of antigluon is a repulsion, we can easily explain why we exist, naturally abandoning the asymmetry assumption and understanding well the material constitution. We can therefore establish a new mechanism of matter and antimatter without the asymmetry assumption but only by composition theory of matter, explain the asymmetry of matter-antimatter and the scenery behind the Big Bang. We also discuss the property of gravitation between matters, antimatters, i.e., attraction and repulsion, the source of dark energy and clarify a few confused questions on applying antimatter in this paper.

2 Antimatter's Composition

2.1 Antimatter's Quark Structure

As is well known, atoms appear as a building block of all matters with a microcosmic structure, i.e., a nuclei consisting of electrons, protons and neutrons, $\cdots$, etc.. Notice that the action in QCD is an integral of Lagrangian density over space-time following

$$S_{QCD} = \frac{1}{4}\int d^4x F^k_{\mu\nu}F^{k\mu\nu} + \int d^4x\overline{q}\left(\gamma^\nu D_\nu + m_q\right)q$$

where, the first term is the gluon interaction described by the field strength tensor F^k_μ, where

$$\begin{aligned} F^k_{\mu\nu} &= \partial_\mu F^k_\nu - \partial_\nu F^k_\mu + g_s\lambda^k_{ij}F^i_\mu F^j_\nu, \\ D_\mu &= \partial_\mu + ig_sF^k_\mu\lambda_k \end{aligned}$$

and the second term is the quark action with quark mass m_q. In the Standard Model of Particle, baryons such as those of the proton and neutron are bound of 3 quarks q and antiquarks $\overline{q}$, and mesons including gluon, W and Z particles consist of a quark q and an antiquark $\overline{q}$, explains the strong and weak force well in an atom.

Notice that gluons are carrier of the strong interaction in the Standard Model of Particle, which is attraction of quarks in hadrons such as those shown in Fig.1

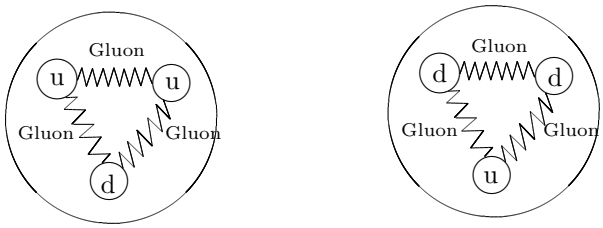

Fig. 1

and each quark or antiquark carries one of red r, green g, blue b or antired $\overline{r}$, antigreen $\overline{g}$, antiblue $\overline{b}$, i.e., color-charges resulting in 8 gluons listing following which characterizes strong interaction of quarks with exchanging gluons

$$\begin{aligned} &g^1 = r\overline{g},\ g^2 = r\overline{b}, \\ &g^3 = g\overline{b}, \\ &g^4 = \tfrac{1}{\sqrt{2}}\left(r\overline{r} - b\overline{b}\right), \\ &g^5 = g\overline{r},\ g^6 = b\overline{r},\ g^7 = b\overline{g}, \\ &g^8 = \sqrt{6}\left(r\overline{r} + b\overline{b} - 2g\overline{g}\right). \end{aligned} \tag{2.1}$$

Moreover, g^i is an attraction if $R_1 < r < R_2$, and a repulsion if $r < R_1$ for integers $1 \le i \le 8$ by experiments ([5]) such as those shown in Fig. 2

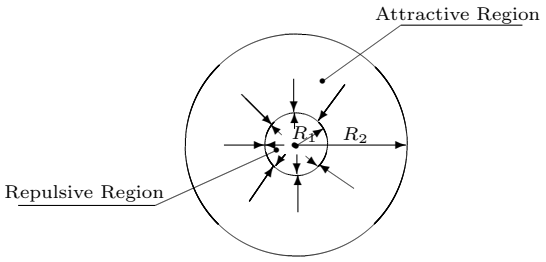

Fig. 2

where r is the distance of 2 quarks and $R_1 = 5\times10^{-14}$cm, $R_2 = 4\times10^{-12}$cm are respective the attractive, repulsive radius of quark.

Clearly, the composition theory of matter by quarks and gluons are essentially the new globally mathematical elements introduced in [14], i.e., continuity flows and discussed extensively on their mathematical characters in [9]-[13], or combinatorial geometry in [5]-[8].

Noticed that one Yin (Y^-) and one Yang (Y^+) constitute everything of universe in Chinese culture. We therefore know that there maybe 2 kind assumptions on the behavior of gluons hold with the Standard Model of Particle in the region $R_1 < R_2$ following:

Attraction Assumption. In this case, the composition of antimatters is the same as the ruler of matters, i.e., antimatter consists of antimolecules, antimolecule consists of antiatoms and antiatom consists of antielectrons, antiprotons and antineutrons. However, there are no such composition evidences unless one antimolecule, the antihydrogen $\overline{H}$, and all other composition matters are not found until today. In fact, such a composition mechanism only is a wishing thinking of humans with a priori hypothesis that all antigluons are attractive with the same color-charges (2.1) that of gluons, and the residual strong interaction within hadrons and antihadrons is attraction which forms the matter and antimatter. However, experimental evidences allude that the reality maybe not this case, resulting in the next assumption.

Repulsion Assumption. In this case, antigluons are all repulsive or interactions $\mathcal{F}_{\overline{g}^i}$ listed following

$$\begin{cases} \mathcal{F}_{\overline{g}^1} = -\mathcal{F}_{g^1} = -\mathcal{F}_{r\overline{g}}, \\ \mathcal{F}_{\overline{g}^5} = -\mathcal{F}_{g^5} = -\mathcal{F}_{g\overline{r}}, \\ \mathcal{F}_{\overline{g}^2} = -\mathcal{F}_{g^2} = -\mathcal{F}_{r\overline{b}}, \\ \mathcal{F}_{\overline{g}^6} = -\mathcal{F}_{g^6} = -\mathcal{F}_{b\overline{r}}, \\ \mathcal{F}_{\overline{g}^3} = -\mathcal{F}_{g^3} = -\mathcal{F}_{g\overline{b}}, \\ \mathcal{F}_{\overline{g}^7} = -\mathcal{F}_{g^7} = -\mathcal{F}_{b\overline{g}}, \\ \mathcal{F}_{\overline{g}^4} = -\mathcal{F}_{g^4} = -\mathcal{F}_{\frac{1}{\sqrt{2}}(r\overline{r}-b\overline{b})}, \\ \mathcal{F}_{\overline{g}^8} = -\mathcal{F}_{g^8} = -\mathcal{F}_{\sqrt{6}(r\overline{r}+b\overline{b}-2g\overline{g})}. \end{cases} \tag{2.2}$$

where $\mathcal{F}_{g^i}$ denotes interaction of gluon g^i for integers $1 \le i \le 8$. Notice that (2.2) will finally results in a repulsion of residual strong interaction within antiprotons and antineutrons such as those shown in Fig. 3.

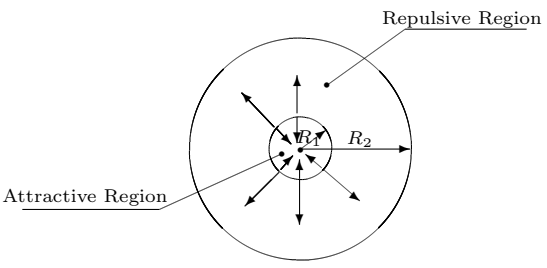

Fig. 3

Although we have also no experimental evidences on the repulsive behavior, likewise the attraction assumption on antigluons, we can explain the behavior of antimatters and the source of dark energy in the universe well by this assumption.

2.2 Antigluon's Repulsive Behavior

Let R_1, R_2 be the attractive, repulsive radius of a quark, respectively and let r be the distance to the center of a quark. We know the interaction behavior of gluons, antigluons $g^i, \overline{g}^i$, $1 \le i \le 8$ by Fig.2 and Fig.3 following.

Particle Name	$r < R_1$	$R_1 < r < R_2$	$r > R_2$
Gluon	Repulsion	Attraction	**0**
Antigluon	Attraction	Repulsion	**0**

Table 2.1

Whence, the residual strong interaction within an antiproton or an antineutron is repulsive, and an antiproton can not be bound with an antiproton, an antiproton can not be bound with an antineutron, and an antineutron can not also be bound with an antineutron in theory. We should discuss the residual strong interaction $\mathcal{F}$ combining with electromagnetism in detail. Let $D(p_1, p_2)$ be the minimum distance of 2 particles p_1, p_2. Then, by the ruler that like charges repel but unlike charges attract each other in nature, we easily know that

$$\begin{cases} D(\overline{p}_1, \overline{p}_2) > 0 & \text{if } p_1,\ p_2 \text{ both are antiproton;} \\ D(\overline{p}_1, \overline{p}_2) \ge 0 & \text{if one of } p_1,\ p_2 \text{ is antineutron,} \end{cases} \tag{2.3}$$

which implies that the minimum distance> 0 for 2 stable antiprotons, ≥ 0 for a stable antiproton with a stable antineutron or 2 stable antineutrons.

2.2.1 Antimatter's Combination Mechanism

Surely, the repulsive property of antigluons generates the antimatters following.

Antinucleon. We are easily know that there are no other stable antinucleon unless antiproton $\overline{P}$, antineutron $\overline{N}$ by the antigluon's behavior because the residual strong interaction of antiprotons, antineutron is repulsive, i.e., there are no stable antinucleon composed of more than 1 antiprotons or an antiproton with antineutrons.

Certainly, A.Zichichi et al at CERN of European and L.Redman et al at Brookhaven of USA artificially synthesized antideuterium $\overline{D}$ in 1965 which is consisted of an antiproton and an antineutron, and also followers such as those of antitritiu nucleon $\overline{T}$, antihelium nuclei $\overline{He}$, $\cdots$, etc. In fact, all of these antinucleons are made in laboratory with high energy but not stable, i.e., they

exist only a short time. *Why this happens*? It is subjectively explained by the notion that the antinucleon was finally annihilated with its nucleons counterpart. However, there are no experimental evidence for this explaining, and there are no such an annihilation observed but only the graspable feature of antinucleon disappeared from the eyes of humans.

This phenomenon can be explained naturally by the repulsive property of antigluons. Certainly, an antiproton can composed with antiprotons, antineutrons initially under the bombing of particle beam of high energy. However, as soon as an antinucleon forms, i.e., $D(p_1, p_2) < 0$ for antiparticles p_1, p_2 consisting of the antinucleon, the the residual strong interaction within the antinucleon acts on each antiparticle. It is repulsive. It will spontaneously separates antiparticles until $D(p_1, p_2) \geq 0$ for all of them, never needs the assumption that they are annihilated with their nucleon counterparts.

Antimolecule. A nucleon captures electrons to balance charges, and similarly, an antinucleon also captures positrons to make charge balance in theory, i.e. antimolecule. Thus, an antiproton $\overline{P}$, an antideuterium nucleus $\overline{D}$, an antitritiu nucleus $\overline{T}$ or generally, an antinucleon can be bound with one positron to produce antihydrogen $\overline{H}$, antideuterium $\overline{D}$, antitritiu $\overline{T}$, and generally, bound with positrons for balancing charges in the antinucleon to produce antimolecule $\overline{M}$ because the nuclear force between antinucleon and positrons is electromagnetism, an attractive force.

However, all of these antimolecules $\overline{M}$ are unstable unless the antihydrogen $\overline{H}$ because of the repulsive property of antigluons. Thus, even we can artificially synthesize antimolecules $\overline{M} \neq \overline{H}$ in high energy, $\overline{M}$ will spontaneously disintegrates to antihydrogen $\overline{H}$ or antineutrons one by one, such as those shown in Fig.4 for an antideuterium $\overline{D}$ in the universe.

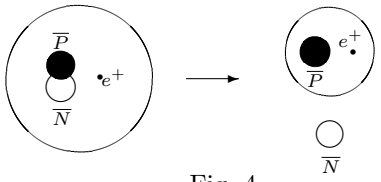

Fig. 4

Whence, an antimolecule $\overline{M}$ is unstable if $\overline{M} \neq \overline{H}$. It can only exists in high external pressure for resisting the repulsion of residual strong interaction. We summary the states of antimolecules Table 2.2.

$\overline{M}$	Existing	State	Synthesized
$\overline{M} \neq \overline{H}$	High energy	Unstable	No
$\overline{H}$	Usual condition	Stable	Yes

Table 2.2

Indeed, W.Oelert et al artificially synthesized a few antihydrogens at CERN in 1995 but these antihydrogens only exist in 4×10^{-8}s ([2]), seems likely to contradict the stable behavior of antihydrogen listed in Table 2.2. *How do we explain this case*? Notice that the experiment of W.Oelert et al verified that all antihydrogens are annihilated with hydrogens, not appearing of an unstable behavior, i.e.,

$$\overline{H} \ + \ H \rightarrow \text{ Engery}$$

because our earth is full of hydrogens, consistent with Table 2.2. Thus, we can classify known and unknown but maybe existing antimatters in Table 2.3.

$\overline{M}$	External Energy	State	Verified
e^+	Usual energy	Stable	Yes
$\overline{P}$	Usual energy	Stable	Yes
$\overline{N}$	Usual energy	Stable	Yes
$\overline{H}$	Usual energy	Stable	Yes
Antideuteron	High energy	Unstable	Yes
$\overline{M} \neq \overline{H}$	High energy	Unstable	No

Table 2.3

As is well-known, positron was found in constituents of cosmic rays, and we can imitate the Big Bang and get antimatters in high energy laboratory. However, they are unstable unless antiprotons, antineutrons and antihydrogens implied by Repulsion Assumption in Table 2.3. Then, *where are the hiding places of antimatters* $\overline{M} \neq \overline{H}$ *in the universe*? Theoretically, we are easily to get stable antimatters likewise to pick up a small stone on the earth but unstable antimatters can be only obtained in the situation of high energy, i.e., near or in fixed stars or high energy laboratory hold with

$$\mathcal{F}_{\text{epf}} \ > \ \mathcal{F}_{\text{rsa}}, \tag{2.4}$$

where $\mathcal{F}_{\text{epf}}$, $\mathcal{F}_{\text{rsa}}$ are respectively the external pressure force and the residual strong interaction within antiproton or antineutron of repulsion. Certainly, the equation (2.4) also explains the reason that why it is hard to get an antimatter $\overline{M} \neq \overline{H}$ in the laboratory of humans because it needs higher energy $\mathcal{F}_{\text{epf}}$ to bind antiprotons and antineutrons and we have no such a powerful laboratory until today. But, *why are we also hard to get antiprotons and antineutrons on the earth, both of them are stable*? It is because the earth is full of protons and neutrons, or matters, which results in the transiently existing of antiproton and antineutron after they come into beings in the laboratory.

Then, *where is the stable antimatter and why can we not find them outside laboratory unless the positron*? All

stable antimatters should be far away from galaxy. Otherwise, they will be annihilated with their counterparts matter. Thus, stable antimatters can be only existing in intergalactic spaces. There may be 2 existing forms of antimatters following:

C1. Free Antimatter. The free antimatter includes free positron, free antiproton, free antineutron and free antihydrogen. They are floating on space one by one, and if one of them collides with its matter counterpart it will annihilates into repulsive energy, which will further separates free antimatters to avoid collision again and finally, stable.

C2. Antimatter Star. The antimatter star includes antiproton star, antineutron star, antihydrogen star or their combination. As it is well-known, there are matters such as those of oxygen, nitrogen, argon, carbon dioxide, hydrogen and other matters in space but no proton stars, and an antimatter on the star may be collided with its matter star into annihilation. However, an antimatter star will be finally stable because if $D(\overline{p}_1, \overline{p}_2) \geq 0$, the residual strong interaction between antiparticles $\overline{p}_1$ and $\overline{p}_2$ is $\mathbf{0}$, i.e., stably existed. And *why can they not be annihilated with their counterparts matter completely*? Affirmatively, antimatters on surface of the star will be annihilated with their matter counterparts. But, as soon as the annihilation happens, a repulsion energy between the matter and antimatter star appears, which will finally pushes the matter and antimatter away until their distance $D(p, \overline{p}) > 0$ and forms a neutral space. A simple calculation enables us knowing respectively the upper density d_p, d_n and d_c of antiproton star, antineutron star and other antimatter stars as follows:

$$\begin{aligned} d_p &\leq \left(\frac{1}{16\times 10^{-16}}\right)^3 \times (1.6726231\times 10^{-27}) kg/m^3 \\ &= (2.44140625\times 10^{44}) \times (1.6726231\times 10^{-27}) kg/m^3 \\ &= 4.08355249\times 10^{17} kg/m^3, \\ d_n &\leq \left(\frac{1}{6.8\times 10^{-16}}\right)^3 \times 1.6749286\times 10^{-27} \\ &= (3.18033788\times 10^{45}) \times (1.6749286\times 10^{-27}) \\ &= 5.32683887\times 10^{18} kg/m^3, \\ d_c &< 5.32683887\times 10^{18} kg/m^3. \end{aligned}$$

3 Matter-Antimatter's Scenery Behind the Big Bang

Certainly, antimatter formed accompanying with matter after the Big Bang, i.e., the universe exploded into a seething fireball consisting of equal particles and antiparticles, and radiation. And then, the universe expanded rapidly, cooling in the process, and finally the matter and antimatter formed, which is in accordance with the sentence: *All things are known by their beings, and all beings come from non-beings* in Chapter 40 of TAO TEH KING, a well-known Chinese book written by Lao Zi, an ideologist in ancient China. We are able to build up a scenery of what happened, i.e., the forming of universe after the Big Bang ([16]) following.

STEP 1. Around 10^{-34} seconds, the universe burst its banks in a rush of expansion, growing at an exponential rate, i.e., inflation. During this period, energy, first repulsion and then, attraction were created to fill the expanding universe, which are the source of matter and antimatter in the universe.

STEP 2. Around 10^{-10} seconds, both of the strong repulsive and attractive force separated out. The pairs of quark and antiquark, the gluon and antigluon would have moved freely about in a very hot state called a quark-gluon or antiquark-gluon plasmas. By the hot pressure originated from the Big Bang, antimatter first come into being with a process that antiquark-gluon plasmas were composed to antiprotons, antineutrons and antiatoms as they captured positrons, and then antimolecules or antimatters one by one.

STEP 3. In about 10^{-7} seconds, the universe had cooled enough for the quark-gluon plasma to convert into the proton, neutron, and antimatter be spontaneously separated to antihydrogens, antiprotons, antineutrons under the residual strong interaction within an antiproton or an antineutron at the same time. All of them were freely floating.

STEP 4. Around 1 second, a few pair of matter and antimatter such as those of electron and positron, proton and antiproton, neutron and antineutron were annihilated into repulsive energy when they collided and then, pushed the matter and antimatter away until a neutral space appeared. Otherwise, the antimatter freely floated with its counterpart matter in the space.

STEP 5. Once the universe was a few seconds old, it became cool enough for the combination of protons and neutrons to form hydrogens, heliums, and antimatter were separated to antihydrogen, antiprotons, antineutrons, and positrons were thrown out from antimolecules. Certainly, it may be annihilated if the hydrogens, heliums collided with antihydrogen or antihelium existed in this time.

STEP 6. In about half an hour after the Big Bang, the amount of matter settled down but was constantly battered by the huge amount of light radiation, and in the meanwhile, antimatter stars were formed along with the cosmic inflation by their repulsion of interaction. Free antimatter also exists if they were not annihilated with its counterpart matter.

STEP 7. In about 3×10^5 years, the universe had become dilute and cool enough for light to go its own way unimpeded. More atoms and molecules started to form

by nuclei capturing electrons, and matter was born gradually, and antimatters were stable unless free positrons, which will annihilated if they collided with electrons.

STEP 8. In about 10^9 years, there began to form stars, fixed stars, planets, and appearing lives with existed stable antimatters in the universe. After 1.37×10^{10} years apart from the Big Bang, the universe evolves at its present visible and observable state, both including matters and stable antimatters.

Although antiproton or antineutron stars have not be determined by humans today, they are indeed existing and will be found in the universe someday.

4 Application's Preconditions

As we discussed, there are no antimatter likewise matters on the earth and there are no stable antimatter unless free antimatter such as those of positrons, free antiprotons, free antineutrons, free antihydrogens and antimatter stars, i.e., antiprotron star, antineutron star or their combination in universe. It is completely different from the normal matter's world. There are no possibility for the birth of living antibeings, no antipeoples, and it is only a symmetrical mirror of elementary particles but with a different mechanism on composing antimatters.

Certainly, the most interested character for humans today is that antimatter can be completely annihilated into clean energy if it collides with its counterpart matter, without any waste left over. However, where and how to extract it, and how to reserve it are 3 typical problems should be solved before its universal applied.

Problem 1. Antimatter Searching. By the repulsion assumption, one could find antimatter only in its 2 states following.

1. **High Energy.** In this case, there are 2 places maybe find antimatter, i.e., the place in or near fixed stars in universe and the high energy laboratory. As we known, all materials made by humans technology can not arrive at any fixed stars unless new high heat resistant material be created someday. Certainly, we can artificially synthesize antimatter in laboratory but only get very little used for scientific research, and the energy needed for synthesized antimatter is far exceeding the energy of annihilation, can not be universal applied for humans ([1], [2]).

2. **Stable.** The stable antimatter includes free antimatter and antimatter stars. The former is sloppy, freely floating without a fixed position in space. Thus, it is also difficult to collect a good supply of antimatter in this case. However, antiproton, antineutron or their combination star may be a good resource for getting plenty of antimatter in universe, extracted for application.

Problem 2. Antimatter Extracting. There are 2 preliminaries for extracting antimatter from an antimatter star. One is to determine its accurate position in space. Another is developed such a spaceship that can arrive at the antimatter star with mining tools. Notice that such a spaceship can not landed on and we can not excavate antimatter from such an antimatter star likewise mining in the earth. Otherwise, the repulsion of residual strong interaction within antiprotons and antineutrons will push it away from the star, i.e., a maybe extracting is the spaceship close to the antimatter star as possible and mines antimatter like scooping water in a pond by a spoon, on which there is a layer pushing away matter and antimatter on surface.

Problem 3. Antimatter Retaining. Clearly, it is difficult to retain antimatter in a container made by normal matter because antimatter will annihilates with the normal matter. Generally, the researchers construct an electromagnetic filed between antimatter and normal matter to separate them for retaining antimatter in laboratory, i.e., Penning trap. However, it only exists in a very short times in this way. For example, the antiproton only exists in less than 1 second in 2010, and 16 minutes in 2016 at CERN ([1]). There are no possible for applying antimatter to humans in such a retaining way.

Notice that an antiproton will annihilates and produces repulsive energy if it collides with a proton. We can construct a closed container filled with uncompressed hydrogens for retaining a mount of antiproton if its wall is strong enough to resist the repulsive energy produced in the annihilation of surface antiprotons with protons in all H's, where, it is assumed that the number of hydrogen is equal to that of antiprotons on the surface of extracted antiprotons.

Similarly, we can construct such a closed container for retaining antineutron if its wall material is stable without neutrons in theory. However, it is more difficult for retaining antineutron because of the β-Decay, i.e.,

$$n \to p + e^- + \overline{\nu}_e.$$

5 Further Discussions

There are a few topics related with antimatter further discussed following which are all important for understanding our universe.

Unmatter. By definition, unmatter is neither matter nor antimatter but something in between such as those of atoms of unmatter formed either by electrons, protons, and antineutrons, or by antielectrons, antiprotons and neutrons discussed in [19],[20]. However, there are no stable unmatter if the repulsion assumption on anigluon is true because there are no matters when antimatter appeared after the Big Bang, and as the matter

turned up, the repulsion forced antimatters to decompose into positrons, antiproton, antineutron, antihydrogen, blocked their combination naturally, and if they collided with their counterpart matter, they will annihilated into energy. Even if they combined on condition they are unstable and break down into elementary antiparticles and normal matter in a very short time. Whence, unmatter can be only found by artificially synthesized in high energy laboratory.

Gravitation. As it is well known by Newton, there exists universal gravitation $F = G\frac{m_1 m_2}{r^2}$ in 2 normal particles with masses m_1, m_2 respectively, where r is the distance of the 2 particles and G the constant of gravity, and Einstein understood it by space curvature ([7]). But, *what is it about antiparticles*? *Is it also attractive*? As we discussed, if the behavior of antigluons is repulsive, the residual strong interaction within hadrons is repulsive, and the gravitation between 2 antiparticles should be contrary to the attractive, i.e., the repulsive $F = -G\frac{m_1 m_2}{r^2}$ for 2 antiparticles with masses m_1, m_2 in distance r. We then have the behaviors of gravitation in particles and antiparticles following:

(1) **Attractive** in 2 normal particles;

(2) **Repulsive** in 2 antiparticles;

(3) **Equilibrium** in an antiparticle and its normal particle with an equilibrium distance in space.

Obviously, such gravitational behaviors can be also characterized by properties of space curvature.

Dark Energy. Clearly, the dark energy exists only in a repulsive behavior for the observed accelerating universe, without substantial evidence ([15]). *Where does it comes from*? And *what is its acting mechanism*? Why we can not hold on the dark energy is because we always understand the universe by its normal matter with an assumption that antimatter is only a mirror and follows the same rules of matter, only a partial view and results in the asymmetry of matter and antimatter. However, if we stand on a whole view, we can conclude that the dark energy naturally originates from antimatter's, i.e., antiproton's and antineutron's repulsion.

Conclusively, the Big Bang produced the equality of particles and antiparticles but different forming mechanisms, i.e., attractive and repulsive with the 4 known fundamental forces, respectively on matter and antimatter, which formed the universe, observable or unobservable by humans today.

Submitted on October 5, 2019

References

1. Andresen G.B. Confinement of antihydrogen for 1000 seconds. *Nature Phys.* 2011, v. 8, 558–564.
2. Close F. Antimatter. Oxford University Press Inc., New York, 2009.
3. Fraser G. Antimatter: the Ultimate Mirror. Cambridge University Press, 2000.
4. Ma T. View Physics by Mathematics – Elementary Particles and Unified Field Theory. Science Press, Beijing, 2014, (in Chinese).
5. Mao L. Combinatorial speculation and combinatorial conjecture for mathematics, *International J. Math. Combin.*, 2007, v. 1(1), 1–19.
6. Mao L. Combinatorial fields-an introduction, *International J. Mathematical Combinatorics*, 2009, v. 1(3), 1–22.
7. Mao L. Combinatorial Geometry with Applications to Field Theory. The Education Publisher Inc., USA, 2011.
8. Mao L. Mathematics on non-mathematics - A combinatorial contribution, *International J. Math. Combin.*, 2014, v. 3, 1–34.
9. Mao L. Extended Banach $\overrightarrow{G}$-flow spaces on differential equations with applications. *Electronic J. Mathematical Analysis and Applications*, 2015, v. 3(2), 59–91.
10. Mao L. A review on natural reality with physical equation. *Progress in Physics*, 2015, v. 11, 276–282.
11. Mao L. Mathematics with natural reality – Action flows, *Bull. Cal. Math. Soc.*, 2015, v. 107(6), 443–474.
12. Mao L. Complex system with flows and synchronization. *Bull. Cal. Math. Soc.*, 2017, v. 109(6), 461–484.
13. Mao L. Harmonic flow's dynamics on animals in microscopic level with balance recovery. *International J. Math. Combin.*, 2019, v. 1, 1–44.
14. Mao L. Science's dilemma – A review on science with applications, *Progress in Physics*, 2019, v. 15, 78–85.
15. Mazure A. and Vincent le Brun V. Matter, Dark Matter, and Anti-Matter. Springer-Verlag New York Inc., 2011.
16. Peacock O.A. Cosmological Physics. Cambridge University Press, 1999.
17. Phillips T.J. Antimatter may matter, *Nature*, 2016, v. 529, 294–295.
18. Ho-Kim Q, Yem P.X. Elementary Particles and Their Interactions. Springer-Verlag Berlin Heidelberg, 1998.
19. Smarandache F. A new form of matter – unmatter, composed of particles and anti-particles. *Progess in Physics*, 2005, v. 1, 9–11.
20. Smarandache F., Rabounski D. Unmatter entities inside nuclei, predicted by the Brightsen nucleon cluster model. *Progress in Physics*, 2006, v. 1, 14–18.

Unified Two Dimensional Spacetime for the River Model of Gravity and Cosmology

Alexander Kritov
E-mail: alex@kritov.ru

Within the proposed assumptions, including the existence of the discrete (minimally uncertain) volume of space, the possibility of mapping of Euclidean 3D to 1D space in the spherically symmetric case is considered. In introduced unified pseudo-Minkowski 2D spacetime (t,η) the river velocity for the Schwarzschild metric represents the uniform acceleration. The Rindler coordinate transforms in 2D spacetime lead to the Schwarzschild-de Sitter metric in static 4D coordinates and result in the scale factor that coincides with the one for cosmological expansion for the Universe with dark energy. The FLRW metric with such scale factor has the conformal form in unified 2D spacetime, and the varying Hubble parameter can be expressed with conformal time via the simple expression. The dynamic and continuity of the uniformly accelerated Rindler flow in unified 2D spacetime are reviewed.

The river model of gravity and the analog gravity is an alternative to the General Relativity (GR) approach to gravitation. The purpose of this article is to exhibit the analogy between the radial river velocity in three spatial dimensions with the motion along one spatial dimension. In the beginning, the three new physical parameters are to be introduced: the mass-radius, the discrete volume of space, and the new spatial coordinate η that is mapped to three spatial dimensions which allows introducing unified two-dimensional space-time (t, η). Note: Only the case of spherical symmetry is reviewed.

1 The river model of gravity and the equivalence principle

The river model of gravity [5] and the analog gravity [2] is the approach to gravity where the equivalence principle (EP) holds. But it is interpreted in such a way that instead of equivalence of gravity to the acceleration, it aligns gravity with non-uniform velocity $v(r)$ denoted as the river velocity. In the analog gravity models, the velocity $v(r)$ is considered to be a movement of some physical medium in flat background spacetime. The flow of the medium is considered to be stationary and irrotational. The use of non-uniform $v(r)$ instead of the acceleration provides the intuitively obvious connection to the metric in static coordinates

$$ds^2 = -c^2\left(1-\frac{v^2}{c^2}\right)dt'^2 + \left(1-\frac{v^2}{c^2}\right)^{-1}dr^2 + r^2 d\Omega^2 \quad (1)$$

where $d\Omega^2 = \sin^2\theta d\phi^2 + d\theta^2$ and coordinate time is denoted as t'. Contrary to that, attempts to embed the acceleration from the EP to a similar form of the metric are still highly disputable.

It was demonstrated in [8] using the coordinate transforms that the static metric (1) in the comoving reference frame has the following *equivalent* form

$$ds^2 = -c^2 d\tau^2 + a(\tau)^2\left(dR^2 + R^2 d\Omega^2\right) \quad (2)$$

which is the Robertson-Walker (FLRW) metric for the spatially flat case ($k = 0$) and $a(\tau)$ is the scale factor related to the river velocity as $v = R\dot{a}$, and v is the proper velocity of the comoving frame. Such equivalency of the static metric (1) to (2) is known for the de Sitter metric only (for example [16]), and the river velocity is associated with the Hubble flow. But the conformity between an arbitrary static metric and the comoving metric (2) in general case is missing or avoided in the literature. Recently, however, Mitra [10] proposed the clarifying view on this problem, which supports the presented approach.

2 The prerequisites of the model

Three postulates of the model are

1. The fundamental significance of the Hubble constant H_0*. The term "varying Hubble constant" can be misleading and is not applied to the approach. The constant is the fundamental value that does not vary with time. Instead it is proposed to use the varying parameter $\mathcal{H}(\tau) = \dot{a}/a$. The significance of it is distinguished from the Hubble constant. Further, the Hubble constant H_0 is denoted as H for shortness.

2. The incompressibility of the fluid and its constant density. It was given in [7], based on the conformal factor issue in the analog gravity and on the continuity equation. The significance of the moving fluid and moving space is the same in the presented approach which allows having aether overtones in the interpretation of such models.

3. The outward direction of the fluid from the center of mass. Czerniawski [4] pointed out that the Gullstrand-Painlevé metric can be written with negative and positive v equivalently. The same is given in [7, 8] for the analog gravity based on the fact that the river velocity comes to the static metric as squared value. If the river velocity depends on central mass then it hardly can be modeled by ingoing flow as the flow at a

*As an example, Dirac's large number coincidence can indirectly support this point or as it was conjectured in [9] $H_0 = m_e c^2/(2^{128}\hbar)$.

distance r somehow should "know" the value of mass located at the point $r = 0$, which intuitively would contradict to the sense of the short-range action of the hydrodynamics.

3 Mass-radius r_m and mass-volume V_m

Let m be a point mass of an elementary particle in the center of a sphere with radius r. Let's designate the certain radius r_m of the spherical volume V_m such as

$$m = \rho_0 \left(\frac{4}{3} \pi r_m^3 \right) \qquad \rho_0 = k\rho_c \tag{3}$$

denoting them respectively as mass-radius and the mass-volume. The value of the fluid density ρ_0 is expressed via the critical density ρ_c and k is some coefficient of order of unity and its estimates are given later. Then it can be also noted that

$$r_m = \left(\frac{3}{4\pi} \frac{m}{\rho_0} \right)^{1/3} = \left(\frac{2Gm}{kH^2} \right)^{1/3} . \tag{4}$$

As an example, for the river velocity in case of the Schwarzschild gravity [3, 5]

$$v(r) = \sqrt{\frac{2Gm}{r}} \tag{5}$$

the equation motion of a fluid (directed outwards as postulated) can be simplified as

$$r(t) = \left(\frac{3}{2} \sqrt{2Gm}\, t \right)^{2/3} = k^{1/3} r_m \left(\frac{3}{2} Ht \right)^{2/3} . \tag{6}$$

In such case the space is expanding in outwards direction and its spherical volume within the radius r denoted further as V increases with time as

$$V(t) = V_m k \left(\frac{3}{2} Ht \right)^2 \tag{7}$$

near the mass m. The definition of comoving distance R is $r = Ra$. Then one can note that particularly the scale factor can be represented as

$$r(t) = r_m k^{1/3} a(t) \qquad a(t) = \left[\frac{V(t)}{kV_m} \right]^{1/3} . \tag{8}$$

Importantly, the scale factor defined in such does not depend on the value of point mass. The reviewed case yields

$$a(t) = \left(\frac{3}{2} Ht \right)^{2/3} . \tag{9}$$

The expression describes the scale factor near the point mass m, for example, near the elementary particle that implies the spatial flow with river velocity (5) corresponding to the Schwarzschild space-time geometry. Further, it will be referred as the scale factor if one may still assume that it just coincidences with the cosmological scale factor.

4 The discrete volume of space V_0

The second parameter that has to be introduces is the minimal measurable volume of space V_0, the constant such as

$$V_0 = \frac{m_0}{\rho_0} \tag{10}$$

where m_0 is minimal mass quanta that is defined as

$$m_0 = \frac{\hbar}{c^2} \beta H \tag{11}$$

based on the uncertainty relation and where β is some coefficient of order of unity, which is determined later*. The existence of such volume implies the uncertainty to measure simultaneously three spatial coordinates as

$$\Delta x \, \Delta y \, \Delta y \geq V_0 . \tag{12}$$

The existence of a discrete value for the volume of space can be conjectured as its fundamental property. As the Heisenberg uncertainty principle governs the linear 1D coordinate measurement, the minimal 2D area that corresponds to one bit of the information is the Planck area, then V_0 represents 3D the volume of space with minimal entropy or unit of information that can be measured. The substitution of the value for ρ_0 into (10) leads to

$$V_0 = \left(\frac{2\beta}{3k} \frac{c}{H} \right) S_{Pl} \tag{13}$$

where S_{Pl} is the Planck area. In order to evaluate the volume V_0 as sphere the large number relations from [9, the expressions (1) and (2.3)] can be applied to obtain exactly

$$V_0 = \frac{4\pi}{3} \left(\frac{\beta}{k} \right) r_e \lambda_e \lambda_p \tag{14}$$

where λ_p and λ_e are the de Broglie wavelength of proton and electron and r_e is the classical electron radius†. Notably, the expression shows that V_0 can be expressed via the properties of fundamental particles and λ_p with the dimensionless coefficients, which are determined later.

The minimal volume V_0 can also signify one bit of information as in terms of the total entropy of the Universe within the Hubble volume as substitution leads to

$$I = \frac{V_H}{V_0} = \left(\frac{k}{2\beta} \right) \frac{S_H}{S_{Pl}} \tag{15}$$

where S_H is the area of the Hubble horizon, and the second equality represents the Holographic principle, which should have some the numerical factor here as the identity on the left-hand side represents the entropy of pure space only (without matter and energy). The expression to be used further for V_m via V_0 obviously can be obtained as

$$V_m = V_0 \frac{m}{m_0} = \frac{V_0}{\lambda_m} \frac{c}{\beta H} \tag{16}$$

where λ_m is the de Broglie wavelength of the mass m.

*So V_0 can be simply treated as the mass-volume of m_0.

†with factor of $3/10$, as per cited work.

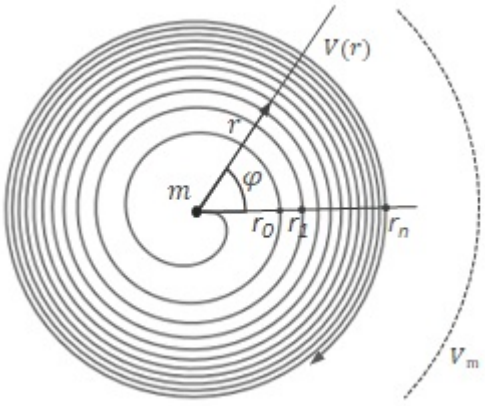

Fig. 1: The mapping of the spherical volume $V(r)$ to unified coordinate where $\eta = \phi\lambda_m/4\pi$ is represented by the angle ϕ. The spiral is given by the polar equation $r = a\phi^{1/3}$. Every turnover cycle corresponds to $dV = V_0$ and to the line segment with length λ_m in η coordinate.*

5 The unified coordinate η

The existence of discrete volumes leads to the proposition that 3D manifold may represent a countable set. Therefore all such V_0's within some spherical volume $V(r)$ can be mapped to fixed-line segments of one-dimensional coordinate. However, as V_0 is the quantity but is not an actual shape; therefore, such mapping is not uniquely defined. The new spatial-like coordinate η can be introduced† as following

$$\vec{\eta} = \lambda_m \frac{V(r)}{V_0} \vec{e_\eta} . \tag{17}$$

Such representation provides the mapping of the linear uncertainty relation for λ_m to the uncertainty for 3D volume V_0. The appearance of λ_m in the definition of η is motivated by its presence in (14), implying its fundamental significance as one of V_0's dimension. The coordinate can be understood as constituted of numbers of discrete deltas with the length of λ_m. Each of these deltas corresponds to *next in raw* V_0 within the spherical volume of $V(r)$.

The coordinate transformation likely represents the non-conformal mapping as it all angular information (ϕ,θ) of coordinates in 3D is lost as uses radial distance only. On another hand, the spherical shell with the volume $V_0 = 4\pi r^2 dr$ already does not have angular information due to the uncertainty of V_0. In such a way, the transformation is conformal. The definition can be also written in terms of differentials as

$$d\eta = dV \frac{\lambda_m}{V_0} . \tag{18}$$

*The spiral shows resemblance to the Theodorus spiral but constructed with the cubic roots instead of the square roots as $r_n = r_0[n^{1/3} - (n-1)^{1/3}]$.

†It can also be associated with the mass of space in spherical volume with postulated uniform density.

The ratio dV/V_0 corresponds to the natural number n (which is the number of spiral cycles as depicted in Fig. 1). In case if $V(r)$ as is not constant or there is a non-zero flux of the fluid, then it corresponds to the velocity

$$u = \frac{\partial\eta}{\partial t} = \frac{\lambda_m}{V_0}\left(\frac{\partial V}{\partial t}\right) . \tag{19}$$

The equation provides the direct correspondence between fluid flow in three-dimensional space and the velocity along the unified coordinate η. Then for the spherically symmetric case, the radial river velocity can be obtained as

$$v = \frac{V_0}{\lambda_m}\frac{u}{4\pi r^2} . \tag{20}$$

The meaning of the expression is evident with the help of Fig. 1, where the velocity u is angular velocity along the spiral line, and v is its projection to the radial direction. Substitution of (16) leads to

$$v = V_m \frac{\beta H}{c}\frac{u}{4\pi r^2} . \tag{21}$$

Also, the substitution of (16) into (17) provides the spherical volume expressed via η as

$$V = \eta\, V_m \frac{\beta H}{c} . \tag{22}$$

Noting the special point on η coordinate

$$\eta_m = \frac{c}{\beta H} \tag{23}$$

that corresponds to mass-radius r_m in 4D spacetime.

6 The motion along η in non-relativistic approximation

With the use of introduced coordinate, the space flow (7) can be represented as an equation of motion along η. The equation (19) for the Schwarzschild case above (7) (differentiating it with respect to time) gives

$$u = \frac{\lambda_m}{V_0}\left(V_m k \frac{9}{2} H^2 t\right) . \tag{24}$$

Applying (16)

$$u = \left(\frac{9k}{2\beta} Hc\right) t \tag{25}$$

which is the accelerated motion along coordinate η with constant acceleration‡

$$\alpha = \frac{9k}{2\beta} Hc . \tag{26}$$

Those, the Schwarzschild gravity with the river velocity (5) and for the scale factor $a(t)$ as in (9) represent *non-relativistic approximation* of motion with the constant acceleration (26) along coordinate η when $u \ll c$ or at near field of the point mass.

‡In the author's previous work [7] it was assumed that $k = 1$ and $\beta = \frac{3}{2}$ leading to $\alpha = 3Hc$ and (16) corresponds to the volume conversion relation.

7 The relativistic motion along η

It has to be considered now that unified coordinate η belongs to two dimensional Minkowski spacetime with the invariant line element

$$ds^2 = -c^2dt^2 + d\eta^2 \ . \tag{27}$$

The relativistic motion with the constant proper acceleration corresponds to the Rindler or also known as Kottler-Møller coordinates transforms [12, 13]

$$t = \frac{c}{\alpha}\sinh\left(\frac{\alpha}{c}\tau\right) \tag{28}$$

where τ is proper time and t is coordinate time and α is given by (26). The two-velocity is

$$u^i = c\left(\cosh\left(\frac{\alpha}{c}\tau\right), \sinh\left(\frac{\alpha}{c}\tau\right)\right) \tag{29}$$

where $i = 0, 1$. And the equation of motion along the coordinate is

$$\eta = \eta_0\cosh\left(\frac{\alpha}{c}\tau\right) - \eta_0 \tag{30}$$

where the initial conditions are set in such way that $\eta = 0$ at $t = 0$ (because of $V(0) = 0$ as (22)) and the Rindler horizon distance is

$$\eta_0 = \frac{c^2}{\alpha} = \left(\frac{2\beta}{9k}\right)\frac{c}{H}\,. \tag{31}$$

The significance of such distance is the fact that the moving object can not receive any information from the point of its origin anymore. Therefore, the dependency of gravitation from central mass should vanish*. The substitution of the equation of motion via η (30) to expression for spherical volume (22) leads to

$$V(\tau) = V_m\frac{\beta Hc}{\alpha}\left[\cosh\left(\frac{\alpha}{c}\tau\right) - 1\right]. \tag{32}$$

Expressing the hyperbolic cosine via half of argument of hyperbolic sine and using (8) the scale factor is

$$a(\tau) = \left(\frac{2\beta Hc}{k\alpha}\right)^{1/3}\left[\sinh\left(\frac{\alpha}{2c}\tau\right)\right]^{2/3} \tag{33}$$

where expression for α can be easily substituted from (26). The substitution of the proper velocity u^1 from (29) into (21), expressing the hyperbolic sine by the hyperbolic cosine from (32) with the use of $kr_m^3H^2 = 2Gm$ (4) lead to the solution for the radial river velocity for spherically symmetric gravitational field of point mass

$$v(r) = \left(\left[\frac{2\beta}{3k}\frac{\alpha}{3Hc}\right]\frac{2Gm}{r} + \left[\frac{\alpha}{3Hc}\right]^2H^2r^2\right)^{1/2} \tag{34}$$

which is the river velocity for the Schwarzschild-de Sitter (SdS) metric with the additional repulsive Λ-term.

*Starting from this distance the de Sitter model has to be valid, see Section 9.

The scale factor (33) coincidences with the one used in the standard cosmology for the current "dark energy dominated" epoch where it has the following form (see for example [15])

$$a(\tau) = \left(\frac{\Omega_m}{\Omega_\Lambda}\right)^{1/3}\left[\sinh\left(\sqrt{\Omega_\Lambda}\frac{3}{2}H\tau\right)\right]^{2/3} \ . \tag{35}$$

Matching the Ω's parameters with obtained result (33) leads to

$$\Omega_m = \left[\frac{2\beta}{3k}\frac{\alpha}{3Hc}\right] \qquad \Omega_\Lambda = \left[\frac{\alpha}{3Hc}\right]^2 . \tag{36}$$

Comparing this with two factors multiplying respectively the first and the second term in the expression (34) one can see that they are surprisingly *identical*.

The presented approach, however, attaches the different significance to these coefficients. The first one implies how the Newtonian gravity deviates from its usual law by simply multiplying the Newtonian potential. It should be set to unity, therefore, which is the condition explicitly equivalent to setting up the value of the acceleration α to (26). Then setting the first parameter to unity and the substitution of the value for α from (26)

$$v(r) = \left(\frac{2Gm}{r} + \left[\frac{3k}{2\beta}\right]^2H^2r^2\right)^{1/2} \ . \tag{37}$$

The second factor signifies how repulsive Λ-term differs from (H^2r^2), and it also consequently adds the pre-factor for H in the de Sitter metric and multiplies the cosmological horizon c/H with the same value (see also (13)).

Further, in the frame of this model, the second parameter is set to unity which equivalently implies the following

$$\frac{3k}{2\beta} = 1 \qquad \alpha = 3Hc \tag{38}$$

and the pre-factor in the expression for the scale factor (33) becomes unity. In such case, the Rindler horizon (23) as the radial distance from the center of mass

$$r_R = r_m\left(\frac{\beta}{3}\right)^{1/3} \tag{39}$$

and the distance where the SdS river velocity (37) as function of r approaches its minimum†

$$r(v_{min}) = r_m\left(\frac{k}{2}\right)^{1/3} \tag{40}$$

are both coincidences. The possible case can be considered if one also equates the Rindler horizon distance η_0 (23) with η_m (31) then it would lead to $\beta = 3$ and $k = 2$ then the both expressions above would have no prefactors.

†Equating the derivative to zero and using $kr_m^3H^2 = 2Gm$ as per (4). Another two extreme points of $v(r)$ where it approaches c are given in [6].

The substantial fact that the Rindler transforms in unified 2D spacetime of the form (28) results in the switch from the Schwarzschild river velocity to the SdS gravity with the repulsive Λ-term in 4D spacetime, by taking into account the relativistic consideration for the uniform acceleration along η. Importantly the obtained river velocity for the SdS metric corresponds to the proper velocity of u^1 in unified spacetime and rationale for it is given in Section 10.

8 The FLRW metric in 2D and the conformal form

As it was done for 4D in Section 2 the scale factor a' for 2D spacetime can be introduced in the same way as

$$\eta = k\,\eta_m\,a'(\tau)\,. \tag{41}$$

Using (30), (31) and (23) with determined coefficients (38) results in

$$a'(\tau) = \sinh^2\left(\frac{3}{2}\,H\tau\right) \tag{42}$$

that corresponds to the following 2D metric

$$ds^2 = -c^2d\tau^2 + \left[\sinh\left(\frac{3}{2}\,H\tau\right)\right]^4 dz^2 \tag{43}$$

where z is the comoving distance, $u^1 = z\,\dot{a}'$ and τ is the proper time in the comoving frame*. Such form is the mapping of the Robertson Walker (FLRW) metric with the scale factor (33) to 2D spacetime. The metric is written for the fluid while it moves in pseudo-Minkowski spacetime (27). Contrary to the FLRW metric with the scale factor (33), (35) this metric has the conformal form. The conformal time τ' such as $d\tau = d\tau' a'(\tau)$ is given by the transform

$$\tau' = \int \frac{d\tau}{a'(\tau)} = -\frac{2}{3H\tanh\left(\frac{3}{2}\,H\tau\right)} \tag{44}$$

where the integration constant can be set to zero. Notably, conformal time has reversed direction opposite to τ

$$\tau' \in \left(-\infty, -\frac{2}{3H}\right). \tag{45}$$

The metric (43) takes the following form

$$ds^2 = \sinh^4\left(\frac{3}{2}\,H\tau\right)\left(-c^2d\tau'^2 + dz^2\right). \tag{46}$$

Or using (44)

$$ds^2 = \left[1 - \left(\frac{3}{2}\,H\tau'\right)^2\right]^{-2}\left(-c^2d\tau'^2 + dz^2\right) \tag{47}$$

providing the conformal form of the FLRW metric in unified two dimensional spacetime.

On another hand, in four-dimensional spacetime, there is the parameter $\mathcal{H}$†

$$\mathcal{H}(\tau) = \frac{\dot{a}}{a} = \frac{v}{r} = \frac{\dot{V}}{4\pi r^3}\,. \tag{48}$$

Using (32) for $V(\tau)$ with the hyperbolic sine of half argument leads to

$$\mathcal{H}(\tau) = \frac{H}{\tanh\left(\frac{3}{2}\,H\tau\right)} \tag{49}$$

where the parameter belongs to the following interval

$$\mathcal{H}(\tau) \in (+\infty, H)\,. \tag{50}$$

Then the parameter can be written in terms of conformal time τ' as given by (44)

$$\mathcal{H}(\tau) = -\frac{3}{2}\,H^2\tau'\,. \tag{51}$$

This expression connects the "varying Hubble constant" with conformal time in unified 2D spacetime. The range of $\mathcal{H}(\tau)$ is from $+\infty$ to H and $\mathcal{H}(\tau)$ is the infinitely approaching value of H, as shown.

Interestingly that the metric (43) represents the embedding class two geometry, implying that the minimal number of dimensions of flat spacetime where it can be embedded is four. The reason why at least two additional dimensions are required is that the derivative $\dot{a}(\tau)$ has zero at $\tau = 0$, see [1, the Theorem 2.2].

9 The note on $3Hc$ and the number of spatial dimensions, the de Sitter metric

The appearance of the factor 3 in the value of the uniform acceleration (38) is closely related to the number of spatial dimensions. It can be demonstrated by the example of the de Sitter metric. Expressing the hyperbolic sine from the equation of motion (30) and substituting into the expression for proper velocity u^1 leads to

$$u(\eta) = c\,\frac{\eta}{\eta_0}\left(1 + \frac{2\eta_0}{\eta}\right)^{1/2}. \tag{52}$$

For far away distances when $\eta \gg \eta_0$ the second term in the equation can be neglected and using the value for η_0 from (31) it reduces to $u(\tau) = 3H\eta(\tau)$ with the solution

$$\eta(\tau) = a_1\exp(3H\tau) \tag{53}$$

where a_1 can be set to the Rindler horizon distance η_0 as per (39). Then it becomes

$$V = \left(\frac{\beta}{3}\right)V_m\exp(3H\tau)\,. \tag{54}$$

*The metric clearly differs from the known form in comoving Rindler frame $ds^2 = -c^2\left(1 + \alpha^2x^2\right)d\tau^2 + dx^2$ as the later uses different coordinate x that is defined locally in the observer's frame.

†Though the definition is the same as "varying Hubble constant" in the standard cosmology, their meanings have to be distinguished.

Using (8) and taking the cubic root result in

$$a(\tau) = \left(\frac{\beta}{3k}\right)^{1/3} \exp(H\tau) \tag{55}$$

which is the de Sitter metric where the factor 3 in the argument of the exponent disappears because of the cubic root. Interestingly pre-factor can not be unity in such way (the same can be shown by approximating (33)).

10 Coordinate time in 2D and in 4D spacetimes

Time is an arbitrary coordinate in gravitational theories including the GR [11] as it is not considered as absolute time. The model uses the proper time of the moving space τ that comes to the metric (2). The radial river velocity of the fluid / space v is the fluid's proper velocity in pseudo flat 4D Minkowski spacetime [3, 8] and v is the projection of proper velocity u_1 in 2D (t, η) as shown. However, the projection of coordinate velocity u_c in 2D (t, η) does not correspond to coordinate velocity of the fluid v_c in 4D because the Lorenz invariance in 2D cannot be applied to the Lorenz invariance is 4D. Therefore coordinate time in (t, η) is not synchronized with coordinate time in 4D (t', r, θ, ϕ). Such disagreement in coordinate times can be seen from the fact that time t in (t, η) implies how an observer residing at rest in $\eta = 0$ (so $r = 0$) measures its time. However, the coordinate time in 4D t' (that comes to the metric (1)) is time measured by static observer residing far away from the gravity $r = \infty$ (so $\eta = \infty$).

Whereas proper time τ of the comoving fluid in 2D is the same as proper time in 4D and such proper time invariance may imply invariance of the energy for coordinate transform from 2D to 4D but the topic requires further analysis. Coordinate time t' in four dimensional space time can be obtained from τ using the transform for the Gullstrand-Painlevé metric [3, 8]

$$d\tau = dt' - \frac{v}{c^2}\left(1 - \frac{v^2}{c^2}\right)^{-1} dr \tag{56}$$

where τ is also proper time in 2D. As v represents proper velocity $(dr/d\tau)$ then dividing both sides by $d\tau$ it takes following form

$$dt' = \frac{d\tau}{1 - \frac{v^2}{c^2}} \tag{57}$$

Then the transform from proper time to coordinate time in 4D is given by respective integral using $v(\tau)$.

11 The dynamic of the Rindler flow along η

One dimensional flow with constant acceleration and velocity u provides certain simplification of the case study on the one hand. The analogue of one dimensional density for example becomes $\rho_\eta = m_0/\lambda_m$. However, some of the parameters like pressure can not be defined. The constant two-force acting on a fluid element is

$$F^i = m_0\,\alpha\left(\sinh\left(\frac{\alpha}{c}\tau\right), \cosh\left(\frac{\alpha}{c}\tau\right)\right) \tag{58}$$

where $i = 0, 1$ and $\alpha = 3Hc$ as per (38). Using definition for m_0 (25) the norm of the constant force is

$$|F| = \frac{9k}{2c}\,\hbar H^2\,. \tag{59}$$

It is easy to see that work done by such force at distance from 0 to the Rindler horizon given by (31) is exactly

$$|F|\,\eta_0 = m_0\,c^2 \tag{60}$$

and does not depend on values of β and k. This expresses the significance of the Rindler horizon distance in the frame of the model. The relativistic energy density for such fluid is $e = \rho_\eta c^2\gamma = \rho_\eta u^0 c$. The integration yields the total energy within the line segment $(0, \eta)$ as

$$\begin{aligned} E &= \int_0^\eta e\,d\eta = \rho_\eta c \int_{\tau=0}^{\tau(\eta)} u^0 u^1 d\tau = \frac{m_0 c^4}{2\alpha\lambda_m}\cosh^2\left(\frac{\alpha}{c}\tau\right)\Big|_0^{\tau(\eta)} \\ &= \frac{m_0 c^4}{2\alpha\lambda_m}\left(\cosh^2\left(\frac{\alpha}{c}\tau\right) - 1\right) \end{aligned} \tag{61}$$

where in the last identity the value is taken at $\tau = 0$. Notable that the expression in brackets coincidences with $(u^1)^2$. Setting the hyperbolic cosine to 2 at distance η_0 as per (31) the total energy of the fluid from 0 to the Rindler horizon distance becomes

$$E(\eta_0) = \left(\frac{\beta}{2}\right)mc^2 \tag{62}$$

where $\alpha = 3Hc$ (38), (16) to express m and (31) were used. The energy invariance between 2D and 4D can be proposed based of the invariance for proper time τ between two spacetimes but it requires further analysis.

12 The continuity of the Rindler flow

The fluid flow with the relativistic uniform acceleration along η has many notable properties. As an example with the source placed at point $\eta = 0$ in case of incompressible fluid its strength is

$$\sigma = \frac{\partial m}{\partial t} = m_0\,\frac{\partial u}{\partial t} = 0\,. \tag{63}$$

However further along the coordinate such sink-source term is non-zero. It is easy to see using the equation of motion (30) for two points with initial distance λ_m (where we fix the initial line segment at $dt = \lambda_m/c$) then the distance between them increases with time as*

$$d\eta = \lambda_m \sinh\left(\frac{\alpha}{c}\tau\right). \tag{64}$$

In comoving frame of reference one can use proper velocity u^1 for the continuity equation. The divergence of proper velocity can be obtained as

$$\mathrm{div}(u^1) = \frac{\partial u^1}{\partial \eta} = \frac{\partial u^1}{\partial t}\,\frac{\partial t}{\partial \eta} = \frac{\alpha}{u_c} = \frac{\alpha}{c\tanh\left(\frac{\alpha}{c}\tau\right)}\,. \tag{65}$$

*Then the substitution of α from (38), using (17) leads to the element of the fluid growth in 3D as $V(\tau) = V_0 \sinh(3H\tau)$ which is exactly the same relation as suggested in [7] for the fluid parcel growth.

Lemma. The divergence of the proper velocity in 2D equals to divergence of the radial river velocity in 4D

$$\mathrm{div}(u^1) = \mathrm{div}(v)\,. \tag{66}$$

Proof. The radial velocity is irrotational as stated then

$$\mathrm{div}(v) = \frac{1}{r^2}\frac{\partial}{\partial r}\left(r^2 v\right) = \frac{2v}{r} + \frac{\partial v}{\partial r}\,. \tag{67}$$

Expressing v with u as given in (21)

$$\mathrm{div}(v) = \frac{V_m \beta H}{c}\frac{\partial u}{\partial r}\frac{1}{4\pi r^2} \tag{68}$$

where two identical terms dropped. As

$$\frac{\partial u}{\partial r} = \frac{\partial u}{\partial \eta}\frac{\partial \eta}{\partial r} = \frac{\partial u}{\partial \eta}\frac{c}{V_m \beta H}\,4\pi r^2 \tag{69}$$

where (22) was used the substitution into (68) proves the lemma.

Combining (65), (66) and (49), using the value for α (26) and the trigonometric identities the divergence of the river velocity becomes

$$\mathrm{div}(v) = \frac{3\dot{a}}{2a}\left[1 + \left(\frac{a}{\dot{a}}H\right)^2\right]. \tag{70}$$

The equation provides the correspondence of the parameter $\mathcal{H}(\tau) = \dot{a}/a$ to the sink-source strength of fluid with constant density.

13 The limitations of the model

The first limitation of the model is that it does not provide any feasible solution for the Kerr-Newman neither for the Reissner–Nordström metrics. In the presented model, the rotation of the in 3D can not be distinguished in η coordinate because of the uncertainty of the volume V_0 represented as the spherical shell, as depicted in Fig. 1. Though it does not create any issue for the model because the Kerr-Newman river velocity does not have any dependency on angular coordinates (ϕ, θ) but only on radial coordinate as shown in [5]

$$v(r) = \left[\frac{2Gmr - Q^2}{r^2 + A^2}\right]^{1/2} \tag{71}$$

where A is the angular momentum per unit mass of a rotating mass, and Q is its charge. The model has difficulties in obtaining the analytic expressions in the same way for such velocity. There are two arguments to support the model, particularly is that the Kerr-Newman metric is a pure theoretical consequence of the GR and is not anyhow verified experimentally. The second argument is that the model is not unique in the sense that the coordinate η can be introduced differently but in the same manner for example

$$\gamma d\eta = dV\,\frac{\lambda_m}{V_0} \tag{72}$$

where γ is u^0 in the unified 2D spacetime. In such case spatial 3D coordinates (dV at right hand side) have "mixed" projection to both η and t (contrary to reviewed case where $\eta \to dV$ directly). Introduced in such way the river velocity for the SdS metric would be simply

$$v_p = v_c\gamma = \left(\frac{r_m^3 H^2}{r}\right)^{1/2}\left(1 + \frac{r^3}{r_m^3}\right)^{1/2} \tag{73}$$

where $kr_m^3 H^2 = 2Gm$. So the coordinate velocity is the Schwarzschild river velocity. Such alternative definition of η aligns coordinate time t in 2D and t' in 4D. The case for the mixed projection can be elaborated in future work.

14 Free fall velocity and symmetries

In the frame of the presented approach, the acceleration α along η has a positive value. Its projection to 4D results in positive radial velocity v in an outward direction (that in the Schwarzschild case corresponds to the negative deceleration in outward direction). The free-fall velocity v_{ff} is connected to the river velocity as $v_{ff} = -v$. The changing of sign in the acceleration α corresponds to the transform of the river velocity to free-fall velocity as $\alpha \to -\alpha \quad v \to v_{ff}$ Alternatively, the transform of the river velocity to free-fall velocity can be given via the change of sign of proper time τ because time reversal changes a sign of u and therefore it changes a sign of the radial river velocity v as per (20) $\tau \to -\tau \quad v \to v_{ff}$. However, such time reversal does not change a sign of the acceleration α. If one would extend the direction of η coordinate to the negative values (understanding that it would correspond to negative volume or negative ρ_0) then mirroring the coordinate η (to opposite direction) means the equivalently the change of sign of the acceleration as per the equation of motion (30) $\eta \to -\eta \quad \alpha \to -\alpha$.

15 Conclusions

The proposed analogy of unified two-dimensional spacetime brought a few convenient advantages to study the cosmological metrics and gravitation via the simplification. From the perspective of unified 2D spacetime the Schwarzschild gravity can be viewed as a non-relativistic approximation of flow with the constant acceleration. Then the relativistic considerations of such movement in unified 2D spacetime lead to the appearance of the repulsive Λ-term corresponding to the SdS metric. And this is far from being analogy as the case is only possible if the unified 2D spacetime is considered as *physical* spacetime. It can be interpreted as the "internal" spacetime of the moving fluid of the analog gravity and the River model.

As shown, the FLRW metric in unified 2D spacetime has the conformal form. The conformal time is connected to the parameter $\mathcal{H}(\tau)$ that is usually associated with the "varying Hubble constant". The parameter $\mathcal{H}$ varies from the infinity in the past to the Hubble constant, which will be approaching infinite time (49). Therefore the model has no place for the

cosmological Big Crunch. The cosmological Big Bang is also absent. The model suggests that the Big Bang is going on continuously, equivalently signifying the emission of the fluid from the center of the point mass of every elementary particle where it is represented by the Rindler coordinate singularity at $\eta = 0$, $\tau = 0$. The Universe can be static as the equivalence of the metrics (1) and (2) is stressed.

The parallel of the model with the Conformal Quantum Mechanic that utilizes a 1D coordinate is yet to be analyzed. Possible outlook to the quantum properties of the Rindler fluid with constant force (59) (the linear potential) in unified 2D coordinates can be interesting. Embedding the electric charge to the metric in the frame of the model (where some of the parameters are to become imaginary) can be challenging.

Mathematical topics such as the topological coordinate transformation of 4D to 2D manifold and conformal mapping with the discrete maps in application to the presented model require further attention.

The exploration of additional coordinates is a strong trend since the foundation of Special Relativity. However, the opposite direction in the unification of known dimensions may also be surprisingly advantageous. The introduced unified 2D spacetime (t,η) via certain simplification offers a new perspective to look at gravitation and cosmology.

The presented intuitive approach reveals the significant parallel between gravity and motion in two-dimensional spacetime. As always, the analogy may be evidence of a hidden pattern in Nature; therefore, more thorough research and formal analysis are required.

Received on October 7, 2019

References

1. Akbar M. M. Embedding FLRW Geometries in Pseudo-Euclidian and Anti-de Sitter Spaces. arXiv: gr-qc/1702.00987v2.
2. Barcelo C., Liberati S., Visser M. Analogue Gravity. arXiv: gr-qc/0505065v3, 2011.
3. Czerniawski J. The possibility of a simple derivation of the Schwarzschild metric. arXiv: gr-qc/0611104.
4. Czerniawski J. What is wrong with Schwarzschild's coordinates? arXiv: gr-qc/0201037.
5. Hamilton A. J. S., Lisle J. P. The river model of black holes. *American Journal of Physics* 2008, v. 76, 519–532. arXiv: gr-qc/0411060.
6. Kritov A. Radiuses of Schwarzschild-de Sitter/AdS Black Holes. DOI: 10.13140/RG.2.2.14507.90406/2.
7. Kritov A. On the Fluid Model of the Spherically Symmetric Gravitational Field. *Progress in Physics*, 2019, v. 15 (2), 101–105.
8. Kritov A. From the FLRW to the Gravitational Dynamics. *Progress in Physics*, 2019, v. 15 (3), 145–147.
9. Kritov A. A new Large Number Numerical Coincidence. *Progress in Physics*, 2013, v. 2, 25–28.
10. Mitra A. Interpretational conflicts between the static and non-static forms of the de Sitter metric. *Scientific Reports*, 2012, v. 2, article 923.
11. Mitra A. Why the Big Bang Model Cannot Describe the Observed Universe Having Pressure and Radiation. *Journal of Modern Physics*, 2011, v. 2, 1436–1442
12. Møller C. The Theory of Relativity. Oxford Clarendon Press, 1955, p. 75.
13. Muñoz G., Jones P. The equivalence principle, uniformly accelerated reference frames, and the uniform gravitational field. arXiv: gr-qc /1003.3022v1.
14. Robertson H. P. On Relativistic Cosmology. *Phylosophy Magazin*, 1928, v. 5, 835–848.
15. Sazhin M. V., Sazhina O. S., Chadayammuri U. The Scale Factor in the Universe with Dark Energy. arXiv: astro-ph.CO, 1109.2258v1.
16. Tolman R. C. Relativity Thermodynamics and Cosmology. Oxford At the Clarenton Press, 1969, section 142.

A Simple Proof of the Second Law of Thermodynamics

G. G. Nyambuya

National University of Science and Technology, Faculty of Applied Sciences – Department of Applied Physics,
Fundamental Theoretical and Astrophysics Group, P. O. Box 939, Ascot, Bulawayo, Republic of Zimbabwe.
E-mail: physicist.ggn@gmail.com

By expressing the Boltzmann statistical weight function (W) in terms of the Boltzmann thermodynamic probabilities p_r, i.e. $\mathcal{W} = \mathcal{W}(p_1, p_2, \ldots, p_{r-1}, p_r, p_{r+1}, \ldots, p_m)$, and thereafter evoking the here set-forth Thermodynamic Probability Evolution Hypothesis – namely that, at the very least, a microstate can only evolve from a state of low thermodynamic probability to one of a higher thermodynamic probability, we demonstrate a simple and veritable proof of the Second Law of Thermodynamics (SLT), namely that the entropy of an isolated thermodynamic system always increases. Effectively and resultantly, this proof requires or points to the idea that the SLT holds not only statistically for an isolated system as currently understood, but must hold exactly for each of the microstates making up the system, hence, the restriction that the SLT holds only for an isolated thermodynamic system, may have to fall by the wayside.

The Law that entropy always increases – holds – I think, the supreme position among the Laws of Nature. If someone points out to you that your pet theory of the Universe is in disagreement with Maxwell's equations, then – so much the worse for Maxwell's equations. If it is found to be contradicted by observation[s], well – these experimentalists do bungle [up] things sometimes. But if your [pet] theory is found to be against the Second Law of Thermodynamics, I can give you no hope; there is nothing for it but to collapse in [the] deepest humiliation ... Sir Arthur Stanley Eddington (1882–1944), adapted from [1, pp. 37-38].

1 Introduction

The paramount *Second Law of Thermodynamics* (SLT) is one of the deepest, most profound and single-most important laws of physics. This seemingly sacrosanct law is born out of the solid and veritable soils of experimental philosophy. Be that as it may, this law has no corresponding fundamental theoretical justification except from the great Austrian theoretical physicist and philosopher – Ludwig Eduard Boltzmann (1844-1906)'s first (significant – albeit, failed) attempt at a proof via his all-famous and important *H-theorem* [2]. Boltzmann's attempt [2] was swiftly rejected (by Zermelo [3] and Leoschmidt [4]) as a complete proof and this is due to the assumptions made therein – i.e. critical assumptions which were rendered contrary to physical and natural reality as we know it, hence, to this day – despite the many spirited attempts at a proof, there is no accepted fundamental theoretical proof of the SLT; thus, it remains an open challenge to find a proof of the SLT. Herein, by way of writing down Boltzmann's *statistical weight function W*, as a function of the respective thermodynamic probabilities (p_r) of all the different microstates making up the given isolated thermodynamic system – i.e.:

$$\mathcal{W} = \mathcal{W}(p_1, p_2, \ldots p_{r-1}, p_r, p_{r+1}, \ldots p_{m-1}, p_m)\,, \qquad (1)$$

we humbly make an attempt at a proof that may shade some light on the very foundations and meaning of the SLT.

2 The four manifestations of entropy

Entropy manifests itself in four different forms. The first form is via Clausius' entropy, second is via Boltzmann's entropy, third is via Gibb's entropy and lastly is via the information theoretic entropy through Shannon's entropy. The main thrust of the present section is to try and link these four manifestations of entropy so that a proof of just one of them is sufficient proof for the rest of the entropies. Herein, we prove for the case of Boltzmann's entropy.

2.1 Clausius entropy

The great German physicist and mathematician – Rudolf Julius Emanuel Clausius (1822-1888), is – by and large – generally regarded as one of the central figures and founders of the science of *thermodynamics*. In his most important paper [5] entitled "*On the Moving Force of Heat*", Clausius first stated the basic ideas of the SLT and later, he introduced the concept of entropy (Clausius [6]). Further, in 1870, Clausius introduced the *Virial Theorem* which applies to heat [7]. Clausius' most famous statement of the SLT was published in both the German [8] and the English language [9]:

> Heat can never pass from a colder to a warmer body without some other change, connected therewith, occurring at the same time.

Further, in this famous paper [5], Clausius showed that there was a contradiction between Carnot's principle and the concept of conservation of energy and realising this, he restated

the two laws of thermodynamics to overcome this contradiction. For a system initially at temperature T_i and final temperature T_f and in-between these two temperature changes a net heat đQ takes place, for such a system, Clausius defined the entropy change, as:

$$\mathrm{d}\mathcal{S}_{\mathrm{C}} = \int_{T_i}^{T_f} \frac{đQ}{T}\,. \tag{2}$$

For an isolated thermodynamics system, the entropy always increases [6], and this is stated in the famous Clausius Law as:

$$\mathrm{d}\mathcal{S}_{\mathrm{C}} = \oint \frac{đQ}{T} \geq 0\,. \tag{3}$$

The landmark 1865 paper [6] in which he introduced the concept of entropy ends with the following summary of the *First* and *Second Laws of Thermodynamics*:

> The energy of the Universe is constant.
> The entropy of the Universe tends to a maximum.

2.2 Boltzmann entropy

Boltzmann's goal in his work [10] was to explain the behaviour of *macroscopic systems* in terms of the most fundamental *dynamical laws* governing their *microscopic constituents*. For example, consider clear and clean water in a container. In this container pour a drop of say potassium permanganate. If left to itself, the potassium permanganate will gradually spread in the water until the water is color blue i.e. the potassium permanganate is evenly spread throughout the water. Why does the water and potassium permanganate mixture prefer to be in the equilibrium macrostate where the potassium permanganate is evenly spread? Why?

To the mundane, the answer is that this is the way things are and to expect anything different is nothing short of asking for a miracle. The pedestrian mind will insatiably absorb this as an effect and consequence of the natural order of the world – not to Boltzmann. According to Boltzmann, this requires an answer that penetrates deep into the microscopic nature of reality at its most elementary and most fundamental level. That is, this has something to do with the evolution of the entropy of the system.

Boltzmann (1877) published his statistical interpretation of the SLT in response to objections from Loschmidt who had said that the *H-theorem* singled out the direction in time in which his H-function decreases, whereas the underlying mechanics was the same whether time flowed forward or backward. It is this paper that Boltzmann published his famous equation – where accordingly, at any give time – the Boltzmann entropy $\mathcal{S}_{\mathrm{B}}$ of this system is given by:

$$\mathcal{S}_{\mathrm{B}} = k_B \ln \mathcal{W}, \tag{4}$$

where k_{B} is the Boltzmann constant. Later, the reluctant German physicist [11], Max Karl Ernst Ludwig Planck (1858-1947), based the derivation of his black body radiation formula [12–14] on (4). Boltzmann's Eq. (4) has been successful in describing systems with minimal-most interactions in *Maxwell-Boltzmann*, *Fermi-Dirac* and *Bose-Einstein* statistics. For later instructive purposes, in the subsequent sections, we shall write down the corresponding thermodynamic weights ($\mathcal{W}$).

2.2.1 Maxwell-Boltzmann statistics

Maxwell–Boltzmann statistics (hereafter MB-statistics) describe the average distribution of non-interacting material particles over various energy states (microstates) in thermal equilibrium, and this kind of statistics is applicable in conditions where the temperature is high enough or where the particle density is low enough to render quantum effects negligible.

Suppose we have a gas of $\mathcal{N}$ identical point particles in a box of volume V. By "gas", we here-and-after mean that the particles are non-interacting with one another, or more realistically, the effects of the interactions are negligibly small. Suppose we know the single particle states in this gas. In MB-statistics, what we would like to know is what are the possible macrostates of the system as a whole. That is, how many ways are there of arranging the microstates? If n_r is the number of particles occupying the energy state ϵ_r, then, an appeal to statistics will tell us that the multiplicity W of different ways of arranging such a system is:

$$\mathcal{W}_{\mathrm{MB}} = \prod_{r=1}^{m} \frac{\mathcal{N}!}{n_r!}\,. \tag{5}$$

It was pointed out by Gibbs, that the above expression for $\mathcal{W}$ does not yield an *extensive entropy*, and as such – it must be faulty somehow. This problem is known as the *Gibbs paradox*. The problem is that the particles considered by the above equation are not indistinguishable. In other words, for two particles (A and B) in two energy sublevels the population represented by [A,B] is considered distinct from the population [B,A] while for indistinguishable particles, they are not.

2.2.2 Bose-Einstein statistics

If we carry out the same argument presented above in the MB-statistics – albeit, this time for indistinguishable particles, we are led to the Bose-Einstein (BE) multiplicity expression $\mathcal{W}_{\mathrm{BE}}$ i.e.:

$$\mathcal{W}_{\mathrm{BE}} = \prod_{r=1}^{m} \frac{(n_r + \mathrm{g}_r - 1)!}{n_r!(\mathrm{g}_r - 1)!}\,. \tag{6}$$

The MB-distribution follows from this BE-distribution for temperatures well above absolute zero, implying that $\mathrm{g}_r \lggg 1$. The MB-distribution also requires low density, implying that $\mathrm{g}_r \lggg n_r$. The BE-theory of was developed in 1924-5 by the Indian theoretical physicist Satyendra Nath Bose (1894-1974) and in full collaboration with Bose [15], the idea

was later adopted and extended by the great Albert Einstein (1879-1955). Due to Dirac [16, 17], particles that follow the BE-theory are called *bosons*.

2.2.3 Fermi-Dirac statistics

First derived in 1926 by the great Italian physicist – Enrico Fermi (1901-1954) [18, 19] and later in the same year by the finest and greatest English theoretical physicist of the modern age, Paul Adrian Maurice Dirac (1902-1984) [20], Fermi-Dirac statistics (here-and-after FD-statistics) describe a distribution of particles over energy states in systems consisting of many identical particles that obey the *Pauli Exclusion Principle*, where according no two particle can occupy the same quantum state and this has a considerable effect on the properties of the system. Further, FD-statistics apply to identical particles with half-integer spin (fermions) in a system in thermodynamic equilibrium. Additionally, the particles in this system are assumed to have negligible mutual interaction (gas) and this allows the many-particle system to be described in terms of single-particle energy states.

As is the case in the derivation of $\mathcal{W}_{\mathrm{BE}}$: suppose we have a number of energy levels, labelled by index i with each level having energy ϵ_r and containing a total of n_r particles. Further, suppose each level contains g_r (degeneracy) distinct sub-levels, all of which have the same energy, and which are distinguishable. The Pauli exclusion principle allows that only one fermion can occupy any such sub-level. The number w_r of ways of distributing n_r indistinguishable particles among the g_r sub-levels of an energy level, with a maximum of one particle per sub-level, is given by the binomial coefficient, using its combinatorial interpretation:

$$w_r = \frac{\mathrm{g}_r!}{n_r!(\mathrm{g}_r - n_r)!}\,. \tag{7}$$

The number of ways that a set of occupation numbers n_r can be realized is the product of the ways that each individual energy level can be populated, i.e.:

$$\mathcal{W}_{\mathrm{FD}} = \prod_{r=1}^{m} \frac{\mathrm{g}_r!}{n_r!(\mathrm{g}_r - n_r)!}\,. \tag{8}$$

2.3 Gibbs entropy

The great theoretician – Josiah Willard Gibbs (1839-1903), after whom the Gibbs entropy is named, was an American mathematician, chemist and physicist who made important and fundamental theoretical contributions to mathematics, chemistry and physics. Gibbs argued that for a thermodynamic system with W macrostates, if P_r is the thermodynamic probability of occurrence of the i^{th} macrostate, then the entropy $\mathcal{S}_{\mathrm{G}}$ of this system measured over all the macrostate $r = 1, 2, \ldots, m-1$, $\mathcal{W}$ is defined [21, 22]:

$$\mathcal{S}_{\mathrm{G}} = -k_B \sum_{r=1}^{\mathcal{W}} P_r \ln P_r\,, \tag{9}$$

where P_r is the probability of occurrence of the r^{th} macrostate. This definition, like Boltzmann's entropy, is a fundamental postulate whose ultimate justification is its ability to explain experimental facts, especially for systems of interacting particles.

The work of Gibbs on the applications of thermodynamics was instrumental in transforming physical chemistry into a rigorous inductive science. In *Statistical Mechanics* (a term coined by Gibbs himself), he combined the work of James Clerk Maxwell and Ludwig Boltzmann on the kinetic theory of gases, thus explaining the macroscopic laws of thermodynamics as a consequence of the underlying fundamental statistical properties of ensembles of the possible states of a physical system composed of many particles.

Gibbs' approach is very useful in the study of "equilibrium" statistical mechanics and solid state physics [22], whereas Boltzmann's approach is very useful in the study of gas-like systems such as electrons, photons, etc. However, Gibbs' approach in the treatment of nonequilibrium systems presents contentious problems [22, 23].

The American – Wayman Crow Distinguished Professor of Physics at Washington University in St. Louis – Edwin Thompson Jaynes (1922-1998), demonstrated [24] in 1965 that the Gibbs entropy is equal to the classical "*heat engine*" entropy of Clausius ($\mathrm{d}\mathcal{S} = \int_{T_i}^{T_f} \mathrm{d}Q/T$). Therefore, the Gibbs entropy is the same as the Clausius entropy, i.e.:

$$\mathcal{S}_{\mathrm{G}} = \mathcal{S}_{\mathrm{C}}\,, \tag{10}$$

hence, a proof that $\mathrm{d}\mathcal{S}_{\mathrm{G}} \geq 0$ is as well a proof that $\mathrm{d}\mathcal{S}_{\mathrm{C}} \geq 0$. Later in the paper, we will prove that $\mathrm{d}\mathcal{S}_{\mathrm{G}} \geq 0$, thus, accordingly, this proof is a proof of the Clausius entropy as well.

2.4 Shannon entropy

The concept of entropy in *Information Theory* describes how much information there is in a signal or event. The *Entropy Information Theory* was advanced by the American mathematician, electrical engineer, and cryptographer – Claude Elwood Shannon (1916 – 2001) in his now famous 1948 paper [25, 26] entitled "*A Mathematical Theory of Communication*". The Shannon entropy is a carefully constructed function of a set of probabilities that satisfies a number of constraints. These constraints are chosen such that entropy measures the uncertainty associated with a probability distribution.

An intuitive understanding of information entropy relates to the amount of uncertainty about an event associated with a given probability distribution. As an example, consider a box

containing many coloured balls. If the balls are all of different colours and no colour predominates, then our uncertainty about the colour of a randomly drawn ball is maximal. On the other hand, if the box contains more red balls than any other colour, then there is slightly less uncertainty about the result: the ball drawn from the box has more chances of being red (if we were forced to place a bet, we would bet on a red ball). Telling someone the colour of every new drawn ball provides them with more information in the first case than it does in the second case, because there is more uncertainty about what might happen in the first case than there is in the second. Intuitively, if we know the number of balls remaining, and they are all of one color, then there is no uncertainty about what the next ball drawn will be, and therefore there is no information content from drawing the ball. As a result, the entropy of the "signal" (the sequence of balls drawn, as calculated from the probability distribution) is higher in the first case than in the second.

Shannon, in fact, defined entropy as a measure of the average information content associated with a random outcome. Shannon's definition of information entropy makes this intuitive distinction mathematically precise. His definition satisfies these desiderata:

1. The measure should be continuous – i.e. changing the value of one of the probabilities by a very small amount should only change the entropy by a small amount.
2. If all the outcomes (ball colours in the example above) are equally likely, then entropy should be maximal. In this case, the entropy increases with the number of outcomes.
3. If the outcome is a certainty, then the entropy should be zero.
4. The amount of entropy should be the same independently of how the process is regarded as being divided into parts.

In his paper [25, 26], Shannon makes the claim that the only function satisfying the above requirement will be of the form:

$$\mathcal{S}_s = -k_s \sum_{r=1}^{m} p_r \log_2 p_r \tag{11}$$

where k_s is the Shannon constant. If the Shannon constant were to be set such that: $k_s = k_{\mathrm{B}} \ln 2$, then, the Shannon entropy will equal the Gibbs entropy, i.e.:

$$\mathcal{S}_s \equiv \mathcal{S}_{\mathrm{G}}. \tag{12}$$

Now, having discussed the four different manifestations of entropy, we shall proceed to describe our thermodynamic system.

3 Description of thermodynamic system

Key to our proof here is the clarity in the definition of what we here term the:

1. *Occupational Frequency of a Thermodynamic Microstate (OFTM).*
2. *Thermodynamic Probability (TP).*

As depicted in Table 1, we envisage a thermodynamic system to constitute discrete, finite and countable cells (microstates). These cells can each be numbered 1, 2, 3, ..., $r-1$, r, $r+1$, ..., $m-2$, $m-1$, m and in these cells we are to fit a total of $\mathcal{N}$ particles. The number of particles in each of these cells at a given material time is $n_1, n_2, n_3, \ldots, n_{r-1}, n_r, n_{r+1}, \ldots, \ldots, n_{m-2}, n_{m-1}, n_m$, respectively.

Now, the OFTM, f_r, of each of these microstates is such that:

$$f_r = \frac{n_r}{\mathcal{N}}, \tag{13}$$

where f_r is the total fraction of particles in the r^{th} cell at a given material time. We must note that:

$$\sum_{r=1}^{m} f_r = 1. \tag{14}$$

Now, to define the thermodynamic probability p_r, we need to introduce some new idea. This is the idea of the *potential holding capacity* of a given microstate. That is, take say the r^{th} microstate. This microstate has n_r particles occupying it, whereas the maximum possible number of particles that can occupy this microstate is q_r. What this means is that the microstate is not completely filled, but partially so. The tendency is to fill this microstate rather that empty it. The most probable state is that when this microstate is completely filled and the most unlikely is – likewise, when this microstate is empty.

Under such a setting, it follows that the ratio:

$$p_r = \frac{n_r}{q_r}, \tag{15}$$

must give the probability that the r^{th} microstate is occupied and f_r is simply the fraction of the number of particles occupying this microstate at a given material time relative to the total number of particles making up the entire system. Clearly:

$$0 \leq n_r \leq q_r, \tag{16}$$

hence:

$$0 \leq p_r \leq 1, \tag{17}$$

thus:

$$\left[\sum_{r=1}^{m} 0 \leq \sum_{r=1}^{m} p_r \leq \sum_{r=1}^{m} 1\right] \longrightarrow \left[0 \leq \sum_{r=1}^{m} p_r \leq m\right]. \tag{18}$$

Writing (18) in a more succinct manner, we will have:

$$0 \leq \frac{1}{m}\left(\sum_{r=1}^{m} p_r\right) \leq 1. \tag{19}$$

Now, having defined the occupational frequency of a thermodynamic microstate (f_r) and the thermodynamic probability (p_r), we shall proceed to lay bare the assumption or working hypothesis that will lead us to our desired proof of the SLT.

Table 1: **Arrangement of Particles in the Different Cells**

Parameter	**Cells**											
Cell Number	1	2	3	...	...	$r-1$	r	$r+1$	...	...	$m-2$	$m-1$	m
n_r	n_1	n_2	n_3	...	...	n_{r-1}	n_r	n_{r+1}	...	...	n_{m-2}	n_{m-1}	n_m
f_r	$\frac{n_1}{\mathcal{N}}$	$\frac{n_2}{\mathcal{N}}$	$\frac{n_3}{\mathcal{N}}$	...	...	$\frac{n_{r-1}}{\mathcal{N}}$	$\frac{n_r}{\mathcal{N}}$	$\frac{n_{r+1}}{\mathcal{N}}$	...	...	$\frac{n_{m-2}}{\mathcal{N}}$	$\frac{n_{m-1}}{\mathcal{N}}$	$\frac{n_m}{\mathcal{N}}$
q_r	q_1	q_2	q_3	...	...	q_{r-1}	q_r	q_{r+1}	...	...	q_{m-2}	q_{m-1}	q_m
p_r	$\frac{n_1}{q_1}$	$\frac{n_2}{q_2}$	$\frac{n_3}{q_3}$	...	...	$\frac{n_{j-1}}{q_{j-1}}$	$\frac{n_j}{q_j}$	$\frac{n_{j+1}}{q_{j+1}}$	...	...	$\frac{n_{m-2}}{q_{m-2}}$	$\frac{n_{m-1}}{q_{m-1}}$	$\frac{n_m}{q_m}$

4 Hypothesis (assumption)

We shall put forward our working hypothesis which we shall coin the name – *Thermodynamic Probability Evolution Hypothesis* (*TPE-hypothesis*), and this hypothesis states that:

> Thermodynamic probability changes are always positive, i.e. $\mathrm{d}p_r \geq 0$. That is to say, at time t_i, if the r^{th} state has energy $\epsilon_r(t_i)$, and if this energy state were to change to its next state $\epsilon_r(t_j)$, at a later time t_j $(i > j)$, then the accompanying thermodynamic probability changes $\mathrm{d}p_r$, from the state $\epsilon_r(t_i)$, to the state $\epsilon_r(t_j)$, are always such that: $\mathrm{d}p_r \geq 0$.

Given the above hypothesis (assumption), we shall now proceed to our most simple proof of the SLT from a Boltzmann entropy standpoint. But before that, we shall argue in the next section that a proof that the Boltzmann entropy always increases is sufficient proof that all the other three forms of entropy are bound by the same law, hence, a proof that the Boltzmann entropy always increases is a general proof of the SLT.

5 Boltzmann and Gibbs entropies

Our proof of the SLT to be presented in the next section makes use of the Boltzmann entropy. If we wanted a general proof that entropy always increases, this would mean we must prove the SLT for the four different manifestations of entropy. But, we do not need to do this because the Clausius and Shannon entropies are – one way or the other – equivalent to the Gibbs entropy, the meaning of which is that we would only need to prove for the two cases of the Gibbs and Boltzmann entropy. Again, because the Gibbs and Boltzmann entropy can be linked, it is sufficient to prove only for one of the two cases and in this paper, we prove for the case of the Boltzmann entropy.

To that end – i.e. in order to demonstrate this link between the Gibbs and Boltzmann entropy, we know that in the event that the probability of occurrence of all the $\mathcal{W}$ macrostate, the Gibbs entropy reduces to the Boltzmann entropy. To see this, we know that in this event where all the $\mathcal{W}$ macrostates are equally likely, we will have $P_r = 1/\mathcal{W}$, so that:

$$\mathcal{S}_{\mathrm{G}} = -k_B \sum_{r=1}^{\mathcal{W}} \left(\frac{1}{\mathcal{W}}\right) \ln\left(\frac{1}{\mathcal{W}}\right) = k_{\mathrm{B}} \ln \mathcal{W} = \mathcal{S}_{\mathrm{B}} \,. \tag{20}$$

In all other cases:

$$\mathcal{S}_{\mathrm{B}} < \mathcal{S}_{\mathrm{G}} \,, \tag{21}$$

hence, in general, we have that:

$$[\mathcal{S}_{\mathrm{B}} \leq \mathcal{S}_{\mathrm{G}}] \;\Rightarrow\; [\text{if } (\mathrm{d}\mathcal{S}_{\mathrm{B}} \geq 0), \quad \text{then}, \quad (\mathrm{d}\mathcal{S}_{\mathrm{G}} \geq 0)] \,, \tag{22}$$

hence, a proof that: $\mathrm{d}\mathcal{S}_{\mathrm{B}} \geq 0$, is also a proof that: $\mathrm{d}\mathcal{S}_{\mathrm{G}} \geq 0$. Consequently and according to the foregoing, a proof that: $\mathrm{d}\mathcal{S}_{\mathrm{B}} \geq 0$, is indeed a general proof of the SLT for all the four different manifestations of entropy.

6 Proof

As a starting point, we shall as has been done in (1), assume that the Boltzmann statistical weight function $\mathcal{W}$, of an arbitrary thermodynamic system is a function of the thermodynamic probabilities (p_r). With this assumption safely in place, we note that if we are to have:

$$\mathcal{W} = \mathcal{W}_0 \exp\left(\sum_{r=1}^{m} p_r - \sum_{r=1}^{m} p_r \ln p_r\right) , \tag{23}$$

where $\mathcal{W}_0$ is a constant for the given isolated thermodynamic system in question, then, we can very easily proffer a proof of the SLT on the basis of the TPE-hypothesis, because, from the Boltzmann Eq. (4), it follows from (1) that:

$$\mathcal{S}_{\mathrm{B}} = k_B \ln \mathcal{W}_0 + k_B \sum_{r=1}^{m} p_r - k_B \sum_{r=1}^{m} p_r \ln p_r \,, \tag{24}$$

hence, taking a differential of (24), one obtains that:

$$\mathrm{d}\mathcal{S}_{\mathrm{B}} = -k_B \sum_{r=1}^{m} \mathrm{d}p_r \ln p_r \,. \tag{25}$$

Now, since $0 < p_r \leq 1$, it follows from this – that $\ln p_r \leq 0$, and from the TPE-hypothesis where one is given that $\mathrm{d}p_r > 0$, it further follows that $\mathrm{d}p_r \ln p_r \leq 0$, hence:

$$\sum_{r=1}^{m} \mathrm{d}p_r \ln p_r \leq 0\,,$$

thus, inserting all these conditions into (25), we will have that:

$$\mathrm{d}\mathcal{S}_{\mathrm{B}} \geq 0\,, \tag{26}$$

hence result. Clearly, the SLT follows directly from a simple definition of W in terms of the thermodynamic probabilities of all the different microstates and as well as from the TPE-hypothesis.

7 General discussion

On the basis of the seemingly self-evident and reasonable *Thermodynamic Probability Evolution Hypothesis* here put forward, we have just "proved" (demonstrated) the SLT. If anything, the "proof" appears to us (and perhaps to the reader as well), to not only be very simple, but quite straight forward. Be that as it may – given the amount of effort that has gone into seeking a proof of the SLT, one can not help but wonder if this proof is really correct – are we not missing something here? How does it come about that such a very simple pedestrian proof has escaped the reach of those that have vigorously sought it? We do not know! All we can say is that, what we have before our eyes appears very strongly to be not only a veritable proof but a perdurable proof as well. We leave it up to the esteemed reader to be the judge on the validity or lack thereof the proof.

In addition, we do not know whether to call this a proof or a demonstration. The reason for this self-doubt is that, for a proof, the basis on which it stands must be firm – yet, in what we have presented, the basis is a mere hypothesis which we only evoked after we noted after a meticulous examination that if one were to express $\mathcal{S}_{\mathrm{B}}$, as function of p_r, i.e. $\mathcal{S}_{\mathrm{B}} = \mathcal{S}_{\mathrm{B}}(p_1, p_2, \ldots, p_r, \ldots p_m)$; the experimental result, $d\mathcal{S}_{\mathrm{B}} \geq 0$ can be deduced from a number-theoretic viewpoint provided that $dp_r > 0$. Realising this, we evoked this as our working hypothesis wherefrom the proof flowed smoothly. In this way, it would not appear – but strongly so that, what we have is a reverse engineered proof. In this way, it, ultimately, would mean that the SLT directly implies the TPE-hypothesis. Even if this were the case, it is still a great leap forward in our understanding of the SLT as this would mean the source of this law is the manner in which the thermodynamic probabilities evolve from one value-state to the next.

That is to say, the SLT holds because the dynamic thermodynamic probabilities $p_r(t)$, of the different microstates only change to attain at least higher values than their previous, that is, the given energy state only evolves (i.e. changes its state) to allow at least a greater thermodynamic probability. Thus, whether one decides that this is not a genuine proof because it has worked backwards from a experimental result ($\mathrm{d}\mathcal{S} \geq 0$) in which process the TPE-hypothesis is implied, one thing is pristine clear:

> It must be acknowledged that at the very least, the present demonstration (proof) has surely peered deeper into the nature of the SLT to unearth the TPE-hypothesis as a driver of this fundamental, paramount and sacrosanct law of Nature.

Hence, this paper may very well be a great – if not a giant leap forward, in humankind's endeavour to understand the mysterious and arcane foundations of the Second Law of Thermodynamics.

Entropy is (and has always been) one of those physics concepts that are difficult to define, let alone understand. Through his entropy function [Eq. (4)], Boltzmann defined it as a measure of the multiplicity of a thermodynamic system. Of the three definitions i.e. Boltzmann, Gibbs and Clausius entropy), the Clausius energy has been and is – the most difficult to define and understand. According to what we have presented herein, one can safely define entropy as:

> a measure of the probability of evolution of a thermodynamic system.

With entropy having been given this definition, it becomes much easier to understand the SLT as a simple statement about the dynamical evolution of the thermodynamic probability of the system.

Received on October 13, 2019

References

1. Eddington A. S. The Nature of the Physical World. Cambridge University Press, Cambridge and Bentley House, London Agents for Canada and India: Macmillan, 1^{st} edition, 1928.
2. Boltzmann L. E. Weitere Studien über das Wörmegleichgewicht unter Gasmolekülen. *Sitzungsberichte Akad. Wiss. (Vienna)*, 1872, v. 66 (Part II), 275–370.
3. Zermelo E. Ueber einen Satz der Dynamik und die mechanische Wärmetheorie. *Ann. der Phys.*, 1896, v. 293 (3), 485–494.
4. Loschmidt J. *Sitzungsber. Kais. Akad. Wiss. Wien, Math. Naturwiss. Classe*, 1876, v. 73, 128–142.
5. Clausius R. J. E. Ueber die bewegende Kraft der Wärme und die Gesetze, welche sich daraus für die Wärmelehre selbst ableiten lassen. *Ann. der Phys.*, 1850, v. 155 (4), 500–524.
6. Clausius R. J. E. Ueber verschiedene für die Anwendung bequeme Formen der Hauptgleichungen der mechanischen Wärmetheorie. *Ann. der Phys.*, 1865, v. 201 (7), 353–400.
7. Clausius R. J. E. On a Mechanical Theorem Applicable to Heat. *Phil. Mag. Ser. 4*, 1870, v. 40, 122–127.
8. Clausius R. J. E. Ueber eine veränderte Form des zweiten Hauptsatzes der mechanischen Wärmetheorie. *Ann. der Phys.*, 1854, v. 169 (12), 481–506.
9. Clausius R. J. E. On a Mechanical Theorem Applicable to Heat. *Phil. Mag. Ser. 4*, 1856, v. 12 (77), 81–98, .

10. Boltzmann L. E. Uber die Eigenschaften Monocyklischer und Anderer Damit Verwandter Systeme. *Crelles Journal*, 1874, v. 98, 68–94. (Also in Boltzmann L. *Wissenschaftliche Abhandlungen*, 1909, v. 3, 122–152; Hasenöhrl F. (Ed.). Leipzig. Reissued New York: Chelsea, 1969).
11. Kragh H. Max Planck: The Reluctant Revolutionary. *Physics World*, 2000, v. 13 (12), 31–36.
12. Planck M. K. E. L. Ueber das Gesetz der Energieverteilung im Normal Spectrum. *Ann. der Phys.*, 1901, v. 309 (3), 553–563.
13. Planck M. K. E. L. Entropie und Temperatur Strahlender Wärme. *Ann. der Phys.*, , 1900, v. 306 (4), 719–737.
14. Planck M. K. E. L. Ueber Irreversible Strahlungsvorgänge. *Ann. der Phys.*, 1900, v. 306 (1), 69–122.
15. Bose S. N. Plancks Gesetz und Lichtquantenhypothese. *Zeitschrift für Physik*, 1924, v. 26 (1), 178–181.
16. Miller S. Strung Together: The Cultural Currency of String Theory as a Scientific Imaginary. Univ. of Michigan Press, 2013.
17. Farmelo G. The Strangest Man: The Hidden Life of Paul Dirac, Quantum Genius. Faber & Faber, 2009.
18. Fermi E. On the Quantization of the Monoatomic Ideal Gas. *Rend. Lince*, 1926, v. 3, 145.
19. Fermi E. Zur Quantelung des Idealen Einatomigen Gases. *Zeitschrift für Physik*, 1926, v. 36 (11), 902–912.
20. Dirac P. A. M. On the Theory of Quantum Mechanics. *Proceedings of the Royal Society of London A: Mathematical, Physical and Engineering Sciences*, 1926, v. 112 (762), 661–677.
21. Riek R. A Derivation of a Microscopic Entropy and Time Irreversibility From the Discreteness of Time. *Entropy*, 2014, v. 16 (6), 3149–3172.
22. Lavis D. A. Boltzmann, Gibbs, and the Concept of Equilibrium. *Phil. Sci.*, 2008, v. 75 (5), 682–696.
23. Bishop R. C. Nonequilibrium statistical mechanics brussels–austin style. *Studies in History and Philosophy of Science Part B: Studies in History and Philosophy of Modern Physics*, 2004, v. 35 (1), 1–30.
24. Jaynes E. T. Gibbs vs Boltzmann entropies. *Am. J. Phys.*, 1965, v. 33 (5), 391–398.
25. Shannon C. E. A Mathematical Theory of Communication. *The Bell System Technical Journal*, 1948, v. 27 (3), 379–423.
26. Shannon C. E. A Mathematical Theory of Communication. *The Bell System Technical Journal*, 1948, v. 27 (4), 623–656.

Liouville's Theorem as a Subtle Statement of the First Law of Thermodynamics

G. G. Nyambuya

National University of Science and Technology, Faculty of Applied Sciences – Department of Applied Physics, Fundamental Theoretical and Astrophysics Group, P. O. Box 939, Ascot, Bulawayo, Republic of Zimbabwe.
E-mail: physicist.ggn@gmail.com

Just like the rest of the Laws of Thermodynamics, the First Law of Thermodynamics (FLT) is an empirical law firmly anchored on the unshakeable fertile soils of verifiable experimental philosophy. Be that as it may, this law (FLT) does not have a fundamental theoretical basis on which it is founded or rests upon. In the present paper, we demonstrate that Liouville's Theorem (in physics) can be cast or can be seen as an expression of the FLT. In this way, one can thus envisage Liouville's Theorem as a fundamental theoretical basis for the FLT.

A theory is the more impressive the greater the simplicity of its premises [are], the more different kinds of things it relates, and the more extended is its area of applicability ... Classical Thermodynamics ... is the only physical theory of universal content concerning which I am convinced that within the framework of the applicability of its basic concepts, it will never be overthrown ... Albert Einstein (1879-1955). Adapted from [1, p. 227].

1 Introduction

The *First Law of Thermodynamics* (FLT) is a version of the *General Empirical Law of Conservation of Energy* (GELCE) applicable to thermodynamic systems. The GELCE states that the total energy of an isolated system is a constant of time; energy can only be transformed from one form to another, but can never be created nor destroyed. The FLT is often stated as follows:

$$đQ = đU + đW\,, \tag{1}$$

where $đQ$, $đU$ and $đW$ are the change in the heat content of a thermodynamic system that accompanies a change in the internal energy $đU$ of the system, for an amount of work $đW$ performed on the system. Simple stated: the heat content of a thermodynamic system $đQ$, equals the change in the internal energy $đU$, plus the amount of work $đW$ done by the system on its surroundings. The FLT is an empirical law founded and strongly anchored on the fertile soils of experimental philosophy. There is no theoretical furnishment of this law. This paper makes an endeavour to proffer a theoretical justification of this law on the basis of Liouville's theorem [2], i.e. we demonstrate that Liouville's theorem can be viewed or can be seen as a statement of the FLT.

2 Liouville's theorem

In physics, Liouville's theorem [2], named after the great French mathematician Joseph Liouville (1809-1882), is a key theorem in classical statistical thermodynamics and in Hamiltonian mechanics*. The theorem asserts that the probability density function ϱ, is a time-constant along the trajectories describing the system – in other words, the *density of states* in an ensemble of many identical states with different initial conditions is constant along every trajectory in phase space. This time-independent density of states is in statistical mechanics known as the classical "*a priori probability*" where an "a priori probability" is a probability that is derived purely from deductive reasoning.

The probability density function (or phase space distribution function) ϱ is assumed to depend on position ($\vec{r} = \vec{r}(t)$) and momentum ($\vec{p} = \vec{p}(t)$), i.e. $\varrho = \varrho(\vec{r}, \vec{p})$, and this probability density function is constant along the trajectories of the system – i.e. the density of states of the *system points* in the vicinity of a given system point traversing through phase space remains constant through the passage of time. Liouville's theorem succinctly summarizes this through the equation:

$$\frac{d\varrho}{dt} = \frac{\partial\varrho}{\partial t} + \sum_{j=1}^{N} \dot{\vec{r}}_j \cdot \frac{\partial\varrho}{\partial\vec{r}_j} + \sum_{j=1}^{N} \dot{\vec{p}}_j \cdot \frac{\partial\varrho}{\partial\vec{p}_j} = 0\,. \tag{2}$$

Writing $\dot{\vec{r}}_j = \vec{v}_j$ and $\dot{\vec{p}}_j = \vec{F}_j$, the above can be written as:

$$\underbrace{-\frac{\partial\varrho}{\partial t}}_{\textbf{Term (I)}} = \underbrace{\sum_{j=1}^{N} \vec{v}_j \cdot \frac{\partial\varrho}{\partial\vec{r}_j}}_{\textbf{Term (II)}} + \underbrace{\sum_{j=1}^{N} \vec{F}_j \cdot \frac{\partial\varrho}{\partial\vec{p}_j}}_{\textbf{Term (III)}}\,, \tag{3}$$

where $\vec{v}_j$ and $\vec{F}_j$, are the velocity and resultant force acting on the j^{th} particle respectively. The task of the present paper is to identify Terms (I), (II) and (III) of (3) with $đQ$, $đU$ and $đW$, appearing in (1), respectively. In order for us to achieve this, it will require us to justly define – in an explicit manner – the

*There is also in complex analysis, Liouville's theorem, named after the same Joseph Liouville, and this theorem states that every bounded *entire function* (i.e., *integral function*) must be constant.

probability density function ϱ, thereby resulting in Liouville's theorem being nothing more (albeit – very insightful) than a statement of the FLT. Before we can do this, we need to set up in the next section, a theory that can explain or describe the evolution of thermodynamic fluctuations.

3 Theory of thermodynamic fluctuations

In our theory of thermodynamic fluctuations, we begin in Section 3.1 by defining what these fluctuations really are and having done that, we proceed in Section 3.2 to define the phase space on which the evolution of these thermodynamic fluctuations is defined.

3.1 Definition of thermodynamic fluctuations

That fluctuations are an intrinsic and inherent part and parcel of physical and natural reality is – indeed – common knowledge. Every observable (say, O) is – one way or the other – associated with some kind of random fluctuation (here-and-after denoted, δO). These fluctuations that we are talking about are different from the fluctuations in the measurement induced by random statistical human error. These are fluctuations that will manifest even when the impossible feat of reducing the intrinsic and inherent random statistical human error to zero.

In deeper terms, these fluctuations are no ordinary fluctuations encountered in statistics, but are intrinsic and inherent *Statistical Random Thermodynamic Fluctuations* (SRTF), they can not be eliminated even in the most idea of situations. These thermodynamic fluctuations are the quantum mechanical fluctuations that Niels Henrik David Bohr (1885-1962) and his followers in Copenhagen, Denmark envisaged (or dreamt of) in their historic, spirited and concerted effort to finding a meaningful, perdurable and lasting interpretation of Schrödinger's seemingly arcane quantum mechanical wavefunction Ψ.

About these thermodynamic fluctuations, we must hasten and categorically state that while there exists theories that attempt to explain the evolution of thermodynamic systems (in Γ-space), there does not exist similar attempts to describe the evolution of these SRTFs though some structured space as phase space. The present section makes an endeavour at such a feat.

3.2 Definition of the $\delta\Gamma$-space

Now, we shall promulgate three postulates that form the basis of our theory of thermodynamic fluctuations. In the first postulate, we shall set up an arena where these fluctuations are defined. In the second postulate, we shall propose a governing equation that describes the evolution of these fluctuations on the space on which they are defined, and lastly, in the third postulate, we set up some rules that define how changes in these fluctuations relate to changes in their corresponding canonical variables.

1. **Postulate (I):** Just as there exists the six-dimensional Γ-space ($\Gamma = \Gamma(x, y, z; p_x, p_y, p_z)$) on which the trajectory of a thermodynamic system can be traced via their evolution through this space as dictated to and governed by Liouville's theorem, there exists a corresponding six-dimensional space (which for our purposes, we shall call $\delta\Gamma$-space) on which the trajectory of the statistical random thermodynamic fluctuations $(\delta x, \delta y, \delta z; \delta p_x, \delta p_y, \delta p_z)$ can be traced.
2. **Postulate (II):** The dynamic and spatial evolution of these random statistical thermodynamic fluctuations $(\delta x, \delta y, \delta z; \delta p_x, \delta p_y, \delta p_z)$ on $\delta\Gamma$-space is governed by Liouville's equation $d(\delta\varrho)/d(\delta t) = 0$, i.e.:
$$\frac{\partial(\delta\varrho)}{\partial(\delta t)} + \sum_{j=1}^{N} \delta\vec{v}_j \cdot \frac{\partial(\delta\varrho)}{\partial\left(\delta\vec{r}_j\right)} + \sum_{j=1}^{N} \delta\dot{\vec{p}}_j \cdot \frac{\partial(\delta\varrho)}{\partial\left(\delta\vec{p}_j\right)} = 0 . \qquad (4)$$
3. **Postulate (III):** The partial differential elements of the canonical four-position $(\partial x, \partial y, \partial z, \partial t)$ and that of the canonical four-momentum $(\partial p_x, \partial p_y, \partial p_z, \partial E)$ are equal to the corresponding partial differential elements of the statistical random thermodynamic fluctuations $(\partial(\delta x), \partial(\delta y), \partial(\delta z), \partial(\delta t))$ for the four-position and $(\partial(\delta p_x), \partial\left(\delta p_y\right), \partial(\delta p_z), \partial(\delta E))$ for the four-momentum – i.e. written explicitly:
$$\begin{aligned} \partial t &= \partial(\delta t) \\ \partial x &= \partial(\delta x) \\ \partial y &= \partial(\delta y) \\ \partial z &= \partial(\delta z) \\ \partial E &= \partial(\delta E) \\ \partial p_x &= \partial(\delta p_x) \\ \partial p_y &= \partial\left(\delta p_y\right) \\ \partial p_z &= \partial(\delta p_z) . \end{aligned} \qquad (5)$$

With these three postulates (rules), we will go on to show that the Liouville Eq. (4) yields the FLT.

4 Derivation – First Law of Thermodynamics

With the theory governing the SRTFs having been set up in the previous section, we realise that if we are to set $\delta\varrho$ so that it is defined:
$$\delta\varrho = \exp\left(\frac{\delta\mathcal{S}_{\mathrm{TD}}}{\hbar}\right) , \qquad (6)$$
where $\hbar$ is Planck's normalized constant and:
$$\delta\mathcal{S}_{\mathrm{TD}} = \sum_{j=1}^{N} \left(\delta\vec{p}_j \cdot \delta\vec{r}_j - \delta E_j\, \delta t_j\right) , \qquad (7)$$
is the thermodynamic phase (or thermodynamic action) defined on $\delta\Gamma$-space, then one can very easily demonstrate that Liouville's theorem as defined in (4), is actually a subtle statement of the FLT. This thermodynamic phase has been defined along the lines of the space of a particle in the Hamilton–Jacobi theory (e.g. [3, pp. 490-491]) of particles where the energy E and momentum $\vec{p}$ of a partial are related to the particle's phase S (or action) via the equation $E = -\partial S/\partial t$ and $\vec{p} = \vec{\nabla} S$. These Hamilton–Jacobi definitions of E and $\vec{p}$

are the defining equations in the de Broglie-Bohm Pilot Wave Theory [4–7] of Quantum Mechanics (QM).

Now, with the idea in mind that $\delta\mathcal{S}_{\mathrm{TD}}$ is the thermodynamic phase (action) similar to a particle's phase (action) in the Hamilton–Jacobi theory, it is clear from the explicit definition of $\delta\mathcal{S}_{\mathrm{TD}}$ given in (7), that:

$$-\frac{\partial\left(\delta\varrho\right)}{\partial\left(\delta t\right)}=\sum_{j=1}^{N}\delta E_j=\delta E\,, \tag{8}$$

$$\frac{\partial\left(\delta\varrho\right)}{\partial\left(\delta\vec{r}_j\right)}=\delta\vec{p}_j\,, \tag{9}$$

$$\frac{\partial\left(\delta\varrho\right)}{\partial\left(\delta\vec{p}_j\right)}=\delta\vec{r}_j\,. \tag{10}$$

From these equations – i.e. (8), (9) and (10), it follows that*:

$$\sum_{j=1}^{N}\delta\vec{v}_j\cdot\frac{\partial\varrho}{\partial(\delta\vec{r}_j)}=\sum_{j=1}^{N}\vec{v}_j\cdot\frac{\partial\varrho}{\partial(\delta\vec{r}_j)}=\sum_{j=1}^{N}\vec{v}_j\cdot\delta\vec{p}_j\,. \tag{11}$$

At this point before we can proceed, we must ask the question: *What does the term $\vec{v}_j\cdot\delta\vec{p}_j$ represent?* For a clue, let us consider the classical expression for the kinetic energy of particle $K_j=p_j^2/2m$. Clearly $dK_j=p\,dp/m=v_j\,dp_j=\vec{v}_j\cdot d\vec{p}_j$. Therefore, the expression $\vec{v}_j\cdot\delta\vec{p}_j$ represents that thermodynamic induced fluctuations in the kinetic energy of the j^{th} particle constituting the thermodynamic system under consideration. These thermodynamic induced fluctuations in the kinetic energy $\vec{v}_j\cdot\delta\vec{p}_j$ constitute what we normally call or refer to as the internal energy δU of a thermodynamic system, hence:

$$\delta U=\sum_{j=1}^{N}\delta\vec{v}_j\cdot\frac{\partial\varrho}{\partial\vec{r}_j}=\sum_{j=1}^{N}\delta U_j\,. \tag{12}$$

Further, we have:

$$\sum_{j=1}^{N}\delta\vec{F}_j\cdot\frac{\partial\varrho}{\partial(\delta\vec{p}_j)}=\sum_{j=1}^{N}\delta\vec{F}_j\cdot\delta\vec{r}_j=\sum_{j=1}^{N}\vec{F}_j\cdot\delta\vec{r}_j\,. \tag{13}$$

Clearly, the expression† $\vec{F}_j\cdot\delta\vec{r}_j$, needs no explanation as it represents the work δW_j done on the j^{th} particle by the random thermodynamic fluctuations of position and forces, i.e.:

$$\delta W=\sum_{j=1}^{N}\delta\vec{F}_j\cdot\frac{\partial\varrho}{\partial\vec{p}_j}=\sum_{j=1}^{N}\delta W_j\,. \tag{14}$$

From all this, it follows that:

$$\delta E=\delta U+\delta W\,. \tag{15}$$

*The "δ" in $\delta\vec{v}_j$ in (11) is removed via the definitions given in (5).

†The "δ" in $\delta\vec{F}_j$ is removed via the definitions given in (5).

What (15) is telling us that while the fluctuations are random, they are correlated.

Now, for a system that moves from an initial state (i) to a final state (f), where the changes in the thermodynamic fluctuations ($\delta E,\delta U,\delta W$) are to be defined:

$$\begin{aligned}đQ &= \delta E_f - \delta E_i\\ đU &= \delta U_f - \delta U_i\\ đW &= \delta W_f - \delta W_i\,,\end{aligned} \tag{16}$$

where $đQ$, $đU$ and $đW$, are to have the same meaning as they have in (1), it follows from this that we will have the FLT, the meaning of which is that Liouville's theorem (4) is, in this way, a subtle expression of the FLT.

5 Discussion

As far as we can tell, the FLT is taken as an inviolable experimental fact. There has not been – at least in our survey of the literature, a similar attempt as that presented here where a fundamental theoretical basis is made to furnish the foundations of this law, hence, this work is without precedent insofar as its nature and goal is concerned. We believe the attempt presented herein is important for our deeper insight and understanding of the *Science of Thermodynamics*. The follow-up work (briefly discussed in Section 7) that we will present soon will attest to this.

For example, one may ask: *What drives thermodynamics, it is the direct changes in the canonical values of the internal energy U and the work W, or there – perhaps – is something else different from this?* If what we have presented is to be believed, then the answer is that thermodynamics is driven by the changes in the associated SRTFs in the canonical values of the internal energy U and the work W, that is to say, by $đ(\delta U)=\delta U_f-\delta U_i$ and $đ(\delta W)=\delta W_f-\delta W_i$. In a nutshell, it is the SRTFs that drive thermodynamics, and not the changes dU and dW.

6 Conclusion

Assuming the acceeptability of what has herein been presented, we hereby set the following as our conclusion:

1. From a fundamental theoretical standpoint, the First Law of Thermodynamics may very well be an expression to the effect that the Thermodynamic Evolution Probability Density Function $\delta\varrho$ is – in accordance with Liouville's theorem – an explicit time-constant along the phase-space trajectory for any thermodynamic system.
2. Liouville's Theorem can be viewed as (or may very well be) an expression of the First Law of Thermodynamics.

7 Follow-up work

In order for the effectiveness in its mission to deliver the core message it seeks to deliver, it is always prudent to keep a paper focused on the point on which it seeks to deliver – of which, the present has been to demonstrate that Liouville's

theorem can be shown to be a casting of the FLT. As always happens, there will always be follow-ups. At present, we have three immediate follow-up papers that we hope will be published in the present journal. These follow-up papers give further credence to the ideas that we have herein crafted and used to demonstrate that Liouville's theorem can be envisaged as a casting of the FLT.

1. In the first follow-up paper, we demonstrate that if $\delta\varrho$ is assumed to be a thermodynamic probability measure, then one can derive – with relative ease – Heisenberg (1927)'s quantum mechanical uncertainty principle [8].
2. In the second paper, which is a follow-up on our recent work presented in [9] on "A Simple Proof of the Second Law of Thermodynamics (SLT)", we demonstrate that – if $\delta\varrho$ is assumed to be the thermodynamic probability that derives entropy changes in thermodynamic systems, then for a Universe with a unidirectional forward arrow of time, the SLT directs that energy and time fluctuations $(\delta E, \delta t)$ are what derives thermodynamics.
3. Lastly, in the third paper, within the framework of the de Broglie-Bohm Pilot Wave Theory [4–7] of QM, commonly referred to as *Bohmian Mechanics* (BM), we set the square-root of the Schrödinger [10–12] quantum mechanical probability amplitude $\Psi^*\Psi = |\Psi|^2$ so that it equals $\delta\varrho$, i.e. $\delta\varrho = |\Psi|$, in which event, we demonstrate that all the criticism that has been levelled against BM – since its inception in 1952 – can easily be overcome. The importance of this is that it allows for a realistic interpretation of QM. This is good for the philosophy of QM.

We believe that all the above mentioned future works give *seminality* to the ideas here set forth.

Received on October 19, 2019

References

1. Holton G. and Elkana Y. Albert Einstein, Historical and Cultural Perspectives. Princeton University Press, Princeton, NJ, 2016. (ISBN 978-0-691-64026-6).
2. Liouville J. Sur la Théorie de la Variation des Constantes Arbitraires. *Journ. de Math.*, 1838, v. 3, 342–349.
3. Goldstein H. Classical Mechanics, 2nd edition. Addison-Wesley, Reading, MA, 1980. (ISBN: 978-0-201-02918-5).
4. de Broglie L. XXXV. A Tentative Theory of Light Quanta. *The London, Edinburgh, and Dublin Philosophical Magazine and Journal of Science*, 1924, v. 47 (278), 446–458.
5. Bohm D. J. A Suggested Interpretation of the Quantum Theory in Terms of "Hidden" Variables. I. *Phys. Rev.*, 1952, v. 85, 166–179.
6. Bohm D. J. A Suggested Interpretation of the Quantum Theory in Terms of "Hidden" Variables. II. *Phys. Rev.*, 1952, v. 85, 180–193.
7. Bohm D. J. Proof That Probability Density Approaches $|\psi|^2$ in Causal Interpretation of the Quantum Theory. *Phys. Rev.*, 1953, v. 89, 458–466.
8. Heisenberg W. K. Ueber den anschaulichen Inhalt der Quantentheoretischen Kinematik and Mechanik. *Zeitschrift für Physik*, 1927, v. 43 (3), 172–198. English Translation: Wheeler J. A. and Zurek W. H, eds. Quantum Theory and Measurement. Princeton University Press, Princeton, NJ, 1983, pp. 62–84.
9. Nyambuya G. G. A Simple Proof of the Second Law of Thermodynamics. *Progress in Physics*, 2019, v. 15 (3), 171–177.
10. Schrödinger E. An Undulatory Theory of the Mechanics of Atoms and Molecules. *Phys. Rev.*, 1926, v. 28, 1049–1070.
11. Schrödinger E. Quantisierung als Eigenwertproblem. *Annalen der Physik*, 1926, v. 384 (4), 361–376.
12. Schrödinger E. Quantisierung als Eigenwertproblem. *Annalen der Physik*, 1926, v. 385 (13), 437–490.

Resolution of the Smarandache Quantum Paradoxes

Robert Neil Boyd

Consulting physicist for Princeton Biotechnology Corporation, Dept. Information Physics Research, USA
E-mail: rnboydphd@comcast.net

In this paper we study the four Quantum Smarandache Paradoxes and try to explain and solve them.

1 Introduction

The **Quantum Smarandache Paradoxes** [1, 2, 3, 4, 5, 6] are enounced as follows:

- 1) Sorites Paradox (associated with Eubulides of Miletus (fourth century B.C.): Our visible world is composed of a totality of invisible particles.
- a) An invisible particle does not form a visible object, nor do two invisible particles, three invisible particles, etc. However, at some point, the collection of invisible particles becomes large enough to form a visible object, but there is apparently no definite point where this occurs.
- b) A similar paradox is developed in an opposite direction. It is always possible to remove a particle from an object in such a way that what is left is still a visible object. However, repeating and repeating this process, at some point, the visible object is decomposed so that the left part becomes invisible, but there is no definite point where this occurs. Generally, between <A> and <Non-A> there is no clear distinction, no exact frontier. Where does <A> really end and <Non-A> begin? One extends Zadeh's "fuzzy set" term to the "neutrosophic set" concept.
- 2) Uncertainty Paradox: Large matter, which is under the 'determinist principle', is formed by a totality of elementary particles, which are under Heisenberg's 'indeterminacy principle'.
- 3) Unstable Paradox: Stable matter is formed by unstable elementary particles.
- 4) Short Time Living Paradox: Long time living matter is formed by very short time living elementary particles.

2 Resolution of Smarandache Quantum Paradoxes

[R. N. Boyd]: I think some of the paradoxes may be resolved by a view that matter is infinitely subdivisible. See below:

[Paradox 1a]:
Sorites Paradox (associated with Eubulides of Miletus (fourth century B.C.): Our visible world is composed of a totality of invisible particles.
a) An invisible particle does not form a visible object, nor do two invisible particles, three invisible particles, etc. However, at some point, the collection of invisible particles becomes large enough to form a visible object, but there is apparently no definite point where this occurs.

[R. N. Boyd]: The statement was true in the 4th century BC, but it is not true now. We can now measure the masses of a vast array of elemental particles. And we now know that there are such ratios as "moles" in chemistry telling us how many atoms are involved in the situation. So today we can make such determinations. There are fabrication processes in the manufacture of integrated circuits that are capable of actually arranging very precisely, each atom in the fabrication. One example of these techniques is the use of epitaxal deposition, which is a one atom thick deposition of material. Screening and masking techniques allow atom-by-atom structuring to occur. These circuits can be small enough so that Cooper pairing is impossible and quantum phase-slips occur in the energized circuit. However, the problem has now shifted into the domains which are smaller than our present ability to perceive with our instrumentations. Typically colliders are used to attempt to make measurements of the elemental particles, and recent data seems to be pointing strongly to a realm of particles even smaller than quarks, which may indeed comprise quarks, if such creatures exist in the first place. (What we are calling quarks may be something else entirely, perhaps organizations of yet smaller particles.) I hold that there is a vast array of entities smaller than the Planck length, and have developed methods for imaging such entities.

I designed 6 methods for imaging SubQuantum particles (smaller than the Planck length). Valentini of Italy wrote a paper describing yet another way to accomplish SQ imaging. The easiest and cheapest to make SQ microscope of my design was publicized, and then tested for proof of principle by Dr. Bernd Binder of Germany. After a 2 years long effort, he verified proof of the principle of operation. The year after that, the design verified by Binder, was constructed at a university in Serbia. One of the Serbian professors sent me an email to inform me that the SQ microscope of my design has imaged entities as small as $10{\times}10^{-95}$ cm. The infinitely small is an unattainable goal in terms of technological approaches, but we know the infinitely small is there, by inferences.

It turns out, based on Kolmogorov's 5/3 law developed from studies of turbulence, that the smallest vortex resulting

from turbulence is an entity which lives at $10{\times}10^{-58}$ m, which we call a Kolmogorov Vortex. This is the smallest particle that is still influenced by gravitation. Entities smaller than this are the primary cause of gravitation.

Further on, there is a quantum coherence factor involved in palpable matter which has the quantum field communicating with all the parts of the automobile, for example, with further quantum communication occurring internal to the parts which make up the automobile. What we really need to be studying here is the coherence of objects, in the quantum field sense. What is the lower limit of quantum coherence? Is there a lower limit?

[Paradox 1b]:
b) A similar paradox is developed in an opposite direction. It is always possible to remove a particle from an object in such a way that what is left is still a visible object. However, repeating and repeating this process, at some point, the visible object is decomposed so that the left part becomes invisible, but there is no definite point where this occurs.

[R. N. Boyd]: There is, these days. But there may be a lower limit, which can be studied by quantum coherence of objects.

[Paradox 1b (continued)]:
Generally, between and there is no clear distinction, no exact frontier. Where does really end and begin? One extends Zadeh's "fuzzy set" term to the "neutrosophic set" concept.

[R. N. Boyd]: The boundary conditions are always very interesting. Those conditions which are both A and NOT A, yet neither A nor NOT A. Korzibski referred to these conditions as "NULL A". I call them boundary layers. They are a study in themselves, because boundary layers comprise a third state, and arise often.

[Paradox 2]:
2) Uncertainty Paradox: Large matter, which is under the 'determinist principle', is formed by a totality of elementary particles, which are under Heisenberg's 'indeterminacy principle'.

[R. N. Boyd]: Uncertainty does not apply to monochromatic coherent photons, nor indeed to any photonic system, by logical extension. See:
http://worlds-within-worlds.org/refutationofheisenberg.php

Indeterminacy only applies where there are elements of chance involved, most particularly involving systems of particles, which are quite susceptible to Zitterbewegung, while photons remain largely unaffected by it.

Hans Dehmelt of Germany was awarded the Nobel Prize in physics for keeping an electron pinned to one spot, so that its momentum and location could be known at the same time, for up to 3 months. Heisenburg uncertainty failed in those circumstances. This experiment is considered by many as evidence that the uncertainty principle fails, except under very limited circumstances.

It is easier to deal with this paradox when we consider that the uncertainty principle has failed, under many circumstance. A deterministic version of QM was developed based on experiential information factors, which imply an Intelligent Universe.

[Paradox 3]:
3) Unstable Paradox: Stable matter is formed by unstable elementary particles.

[R. N. Boyd]: The life time of the proton is calculated (not observed with instrumentation) to be on the order of $10{\times}10^{32}$ years. But this ignores plasma/aether factors, and more importantly, gamma ray dissociations of atoms, which cause protons to vanish back into the aether from whence they originated. Gamma ray dissociation of atoms also causes SQ particles (vortex lines, Bhutatmas) propagating with an infinite velocity, which are the cause of gravitation and are the cause of the development of new electrons, positrons, protons, neutrons, and atoms due to aether/plasma events on the surfaces of stars. Instrumented measurements have discovered that every atomic element is found streaming out from the sun in the "solar wind". SAFIRE has instrumented physical evidence that hydrogen and many other elements are created in plasma double layers (charge separation layers) verified by SEM (scanning electron microscopy) and optical correlation spectroscopy. The creation and dis-creation of elementary particles and atoms is a continuous cycle which occurs at all times in the infinite volume universe. The life span of a proton is much smaller than the calculated standard. The actual life span of the proton is determined by the number of gamma ray dissociation events passing through the given volume, per unit time. [Gustave Le Bon "Evolution of Matter" 1906]

[Paradox 4]:
4) Short Time Living Paradox: Long time living matter is formed by very short time living elementary particles. Consciousness and Experiencing informations are involved in all these processes. This information is the organization force which is responsible for many phenomena. The universe is constructed from Space, Time, matter, energy, and Experiencing. Consciousness is not limited to human beings. In fact, it has been demonstrated that all observables have some manner of consciousness, however rudimentary. Consciousness is a holographic energetic having soliton-like [coherent] properties. The best descriptions of the energetics of Consciousness arise from the works of V. Poponin (DNA Phantom Effect) and from a recent paper which shows that the radiation pattern of a symplectic E/M antenna is directly altered by the attention, intention, and emotional condition of the operators

of the transmission facility. This direct influence of the symplectic E/M also causes a divergence in the quantum field, and thus we have evidence that there is a direct relation between the quantum field and Consciousness. Let us never forget that there is a vast array of types of Consciousness, all of which will have some effect on the quantum field.

Also see the works of Andrej Detela. For example: http://www.zynet.co.uk/imprint/Tucson/4.htm#Physical.

Eventually holographic Artificial Intelligence such as HNeT (a variety of quantum computer), combined with Sub-Quantum Physics and Consciousness Physics will be able to map non-physical and dis-incarnate entities, as well as all the energetics of the commonly known life-forms. Eventually, communications will be established through this approach, with non-biological forms of Consciousness, such as rocks and stars.

Submitted on October 5, 2019

References

1. Editors, Quantum Smarandache Paradoxes, *Nature*, 2001, v. 413, no. 6854.
2. Smarandache F. Invisible Paradox, in "Neutrosophy. I Neutrosophic Probability, Set, and Logic", ProQuest & Information, Ann Arbor, MI, USA, 22–23, (1998).
3. Smarandache F. Sorites Paradoxes, in "Definitions, Solved and Unsolved Problems, Conjectures, and Theorems in Number Theory and Geometry", Xiquan Publ. House, Phoenix, 69-70, 2000.
4. Smarandache F. Quantum Quasi-Paradoxes and Quantum Sorites Paradoxes. *Progress in Physics*, 2005, v. 1, 7–8.
5. Smarandache F. Quantum Quasi-Paradoxes and Quantum Sorites Paradoxes. *Octogon*, 2005, v. 13, no. 1A, 232–235.
6. Smarandache F. Quantum Quasi-Paradoxes and Quantum Sorites Paradoxes [revisited]. *Infinite Energy*, 2006, v. 11, no. 66, 40–41.
7. Boyd R.N. Resolution of Smarandache Paradoxes, http://worlds-within-worlds.org/resolutionofsmarandache.php
8. Weisstein E.W. Smarandache Paradox. In: CRC Concise Encyclopedia of Mathematics, CRC Press, Boca Raton, Florida, p. 1661, (1998); http://mathworld.wolfram.com/SmarandacheParadox.html.

Generation of Baryons from Electromagnetic Instabilities of the Vacuum

Osvaldo F. Schilling

Departamento de Física, Universidade Federal de Santa Catarina, Campus, Trindade, 88040-900, Florianópolis, SC. Brazil.
E-mail: osvaldo.neto@ufsc.br

Baryons are generated from perturbations of magnetodynamic origin built upon a background sea of excitations at about 3.7 GeV adopting the proton state as a "substrate", as proposed by Barut. To simulate perturbations from such a state a sum over the energy spectrum of excitations is necessary. A Zeta-function regularization procedure previously adopted for the Casimir Effect is applied to eliminate divergences when the sum upon the energy spectrum states is carried out. States of negative energy compared to the background state are obtained and represent the baryons. The periodic behavior of the baryon masses with confined magnetic flux is reproduced with no further forms of energies required besides the magnetodynamic terms. This treatment implicitly supports the concept that quarks and leptons might be treated on similar theoretical grounds.

1 Introduction

In recent work [1] we have shown that through the imposition of gauge invariance conditions to the wavefunctions of a particle (represented in energy terms by a closed loop of current and performing zitterbewegung motion), it is possible to relate rest energy to magnetic energy for the baryons. Gauge covariance was imposed by making the magnetic flux linked through the region covered by the particle "orbit" quantized in units n of $\phi_0 = hc/e$, the flux quantum. We therefore *adopted* integer values of n (allowing also for half-integer values; which case depends upon the actual boundary conditions) in the analysis for the baryons, guided also by the criterion that n should be proportional to the magnetic moment (in n.m. units) in the classical limit of flux generated by self-fields.

Such model is essentially based upon heuristic arguments, and in particular the assumption that zitterbewegung currents flow inside complex particles like the baryons is the extension of a similar proposal made for the electron. The model predicts an inverse dependence of mass with the fine structure constant α, in agreement with experimental data analysis reported in the literature [1]. The model produces a reasonable agreement between the calculated magnetic (plus kinetic) energies and the rest energies, revealing also a clear dependence of rest mass upon the square root of the spin angular momentum, of the form predicted and observed in the literature. However, a noticeable scattering of data around the theoretical line still remained. The meaning of such scattering was not addressed in the previous work.

To better understand if such deviations might have a physical meaning rather than indicating possible limitations of the model, we decided that the data should be analyzed again in a slightly different way, by avoiding any previous assumption about the values of n. The number of flux quanta is now objectively determined through the model, from the product of the known values of mass and magnetic moment (through the same Eq. (3) of [1]; see below). The relation of mass with such "model-adapted" values of n, calculated from the available data, become the object of this new analysis.

To make the model expressions applicable to a sizeable number of particles, it is necessary to eliminate the effects on the rest energies of kinetic energy contributions specifically attributable to the "excess" spin angular momenta of decuplet particles (spin-3/2 particles) as compared to the spin-1/2 octet particles, which were evident in our previous paper [1]. Therefore, for the range of mass values covered by the decuplet particles, the elimination of such excess kinetic energy shall be made by subtracting from the masses of the decuplet particles the average difference between the actual masses of decuplet and octet particles, 244 Mev/c^2. The resulting "*transformed masses*" m_t of the decuplet thus have the same average as the masses of the octet particles, as shown in the Tables below.

This should eventually make all baryons fit the mass-energy expression derived for spin-1/2 in [1]. As expected, the new values of n are not substantially different from the ones adopted previously (see [1] for details in the Tables there). In this way, the margin of arbitrariness in the choice of n inherent to the previous criterion is eliminated and the determination of this parameter for each baryon becomes an objective for the model. From the new analysis, it should therefore be possible to better evaluate the internal consistency of the model itself, including the evaluation on whether the proposed interpretation of n as a true number (integer or not) of magnetic flux quanta is physically meaningful, as well as analysing how appropriate is the utilization of closed currents as a means of representing complex particles.

As shown in the following sections, the approach proved valuable. As far as results are concerned new important features have arisen from the analysis. By plotting against n both the octet baryon masses and the transformed rest masses m_t of the decuplet baryons, we obtain the novel result that a simple periodic function, with n in the argument, is capable of fitting the points. That is, the rest energy (given by magnetodynamic

Table 1: Data for the baryon octet (moments μ from [11]). According to Eq. (4) in gaussian units: $n = 1.16 \times 10^{47}\,\mu m$. The plot of m/m_{p} (m_{p} the proton mass) against n are shown in Fig. 2.

	abs μ (n.m.)	μ (erg/G)$\times 10^{23}$	m (Mev/c^2)	m(g)$\times 10^{24}$	n from Eq. (4)
p	2.79	1.41	939	1.67	2.73
n	1.91	0.965	939	1.67	1.9
$\sum^+$	2.46	1.24	1189	2.12	3
$\sum^0$	0.82 (theor.)	0.414	1192	2.12	1
$\sum^-$	1.16	0.586	1197	2.12	1.5
Ξ^0	1.25	0.631	1314	2.34	1.7
Ξ^-	0.65	0.328	1321	2.34	0.9
Λ	0.61	0.308	1116	1.98	0.7

terms) is periodic on magnetic flux.

Such result seems quite revealing since it has actually been repeatedly associated in the literature with the effect of confined flux upon the magnetic energies due to currents, flowing around multiply-connected paths, which is exactly what this research proposes to demonstrate happens inside particles. The Aharonov-Bohm effect of interfering electron beams surrounding a solenoid, as well as superconducting currents in rings [2, 3], charge density waves in dielectric structures [4], and even currents around normal metallic rings [5] (all surrounding confined magnetic flux) have been reported to display such periodic dependence of energy and current on magnetic flux.

Starting from a Lagrangian suitable to fermion fields [6], we obtain an energy spectrum for the possible current carrying states around the closed path confining magnetic flux. In order to simulate self-field perturbations involving pair creation/annihilation from vacuum, a sum over the states in the energy spectrum is necessary. An Epstein-Riemann zeta function regularization procedure previously adopted for the Casimir Effect is applied to eliminate divergences when the sum upon the energy spectrum states is carried out [7], and the periodic behavior of the baryon masses with magnetic flux is reproduced with no further forms of energies required besides the magnetodynamic terms.

It is a basic assumption of the model adopted in this treatment [1] that currents generate magnetic moments, which give rise to self-magnetic fields and flux within particles. An "anomalous" magnetodynamic energy is generated, which we identify with the additional rest energy of the "dressed" particles. It appears that the resulting trapped magnetic flux modulates the currents obtained from wavefunctions running around the closed path, through the imposition of a phase factor, and such phases vary from one baryon to another. The magnetic energy depends on such modulation, and thus also the mass along the baryon family. All these results are considered in detail in Section 2. A review of previous results of the model is also added for the sake of completeness of exposition.

2 Theory

2.1 Phenomenological determination of the parameter n

Isolated current-loops containing a single quantum of flux of value $\phi_0/2 = hc/2e$ are well known from type-II superconductivity. The formation of superconductor current loops is a many-body effect, though. In a series of papers we have investigated if there might exist single-particle systems confining flux in a similar manner [1]. It is essential that such proposal be quantitatively supported by experimental data. Let's consider the actual case of particles of the baryon octet. All the eight particles have well-established rest masses and magnetic moments. E. J. Post [8] considered how to write an energy-mass relation in a tentative model for the electron. Post showed that the magnetic moment for the electron could be obtained up to the first-order correction (from QED) with the equation:

$$mc^2 = \frac{\phi}{c}\, i + eV\,. \tag{1}$$

Here the left side is the rest energy of the electron, which from the right side is considered as fully describable by electromagnetic quantities. The first term on the right side is the energy of an equivalent current ring of value i linking an amount of flux ϕ, that should occur in a number n of flux quanta ϕ_0. In spite of the adopted parameters from electromagnetic theory, such term contains similar amounts of magnetic and kinetic energy contributions of moving charges, as discussed by London [9], and thus the kinetic effects are already included. The second (electrostatic energy) term is much smaller than the first (it will be neglected hereafter) and accounts for the radiation-reaction correction for the magnetic moment which is proportional to the fine structure constant α [8]. Post associates the current with the magnetic moment μ and the size R of the ring with the equation:

$$\mu = \frac{\pi R^2 i}{c}\,. \tag{2}$$

One then inserts (2) into (1) (without the electrostatic small term) and thus eliminates the current. The parameter R

Table 2: Data for the baryon decuplet (moments μ from ref. [11]). The average difference between the decuplet and octet particle masses is discounted as discussed in the text and the resulting mass is put in columns 4 and 5. According to Eq. (4) in gaussian units: $n = 1.16 \times 10^{47}\,\mu m$. The plot of m_t/m_p against n are shown in Fig. 2.

	abs μ (n.m.)	μ (erg/G)$\times 10^{23}$	$m_t = m - 244$ (Mev/c^2)	m_t(g)	n from (4)
Δ^{++}	4.52	2.28	986	1.75	4.64
Δ^{+}, Δ^{-}	2.81, 2.81	1.42	990	1.75	2.9, 2.9
$\sum^{+}$	3.09	1.56	1135	2.02	3.65
$\sum^{0}$	0.27	0.136	1136	2.02	0.32
$\sum^{-}$	2.54	1.28	1138	2.02	3
Ξ^{0}	0.55	0.28	1281	2.28	0.73
Ξ^{-}	2.25	1.14	1283	2.28	3
Ω^{-}	2.02	1.02	1428	2.54	3

has been calculated/measured for the nucleons only, but it remains part of the final expression for all baryons obtained after the combination of (1) and (2). We may conveniently eliminate R from this treatment by adopting for all baryons an expression which is valid for the leptons (assuming in that case $R = \lambda$, the Compton wavelength), and for the proton [1] (from experimental evidence), namely:

$$\mu = \frac{1}{2}\, e\, R\,. \tag{3}$$

In the present case we are interested in assessing a sufficiently large group of particles in order that the proposed association between mass and confined flux can be properly investigated, and the baryons form such a group.

The model by Post was devised to fit a single fundamental particle, the electron, and there was actually no discussion about the application to other particles. We are now able to justify (see Section 2.2) the proposal that the collective motion of constituents inside baryons can also be described in terms of currents, so that a similar model should apply.

The combination of equations (1) to (3) with $\phi = n\,(hc/e)$ can therefore be cast in the form (inserting $\alpha = e^2/\hbar c$):

$$n = \frac{2c^2\alpha}{e^3}\,\mu\, m\,. \tag{4}$$

Tables 1 and 2 bring the mass and magnetic moments data for all baryons of the octet and decuplet, alongside the values for n from (4). It should be noticed that according to the present treatment the proton corresponds to $n \approx 3$ (see Table 1). In a semiclassical treatment Barut [10] considered baryons and mesons as resulting from stabilized configurations of constituents linked together by dipolar magnetic forces. A quantum number is introduced and the rearrangement of parameters makes Barut's final formulas for mass quite similar to the ones obtained in [1]. In particular Barut obtains $n = 3$ for the proton, by associating one unit of angular momentum for each of three unit-charged constituents.

2.2 Heuristic model based upon field-theoretic concept

Eq. (4) stresses the fact that in this work, n is the parameter to be determined from the data available for mass and moment (note that it is the same as Eq. (3) of [1] written in another form). In addition, (4) can be rewritten in a useful form by isolating in it the expression for the nuclear magneton (n.m.), $e\hbar/2m_pc$, yielding $n = (m/m_p)\,\mu$ (n.m.). Here m_p is the proton mass and the magnetic moment is given in n.m. units.

All the parameters on the right side of (4) are known for the eight baryons of the octet, and are listed in Table 1 (data from [11]). Fig. 1 shows the plot of the calculated n against the magnetic moment for each particle, which mirrors the dependence of mass on magnetic properties for each octet baryon. Note the presence of a diagonal line. There is a tendency to form Shapiro-like steps at integer numbers of flux quanta, but the approach to the steps has an undulating shape rather than being sharply defined (note: such "Shapiro" steps for superconducting rings characterize the penetration of flux inside the ring in units of flux quanta).

The existence of a diagonal *baseline*, $n = \mu$ (n.m.) experimentally characterizes the presence of a *minimum* amount of mass in all baryons. From (4), it becomes clear that the proton mass would be this minimum mass. Barut in the 1970s proposed that the other baryons might be considered perturbations built upon a proton "fundamental state", thus providing a minimum amount of mass.

The undulations in the figure lie above the diagonal line since it characterizes a stable, fundamental-like state.

In fact the undulations can be thought as a consequence of the confinement of magnetic flux inside a multiply connected path described by each particle charge motion. Gauge covariance of a Lagrangian which describes such particle ends up imposing such periodic dependence on the magnetic properties of the particles. Similar problems have extensively been dealt with by condensed matter physics groups [2–6].

Let's consider a fermion field confined to a circular path of length L, enclosing an amount of self-induced magnetic flux ϕ in a potential A. We need to show that such a system

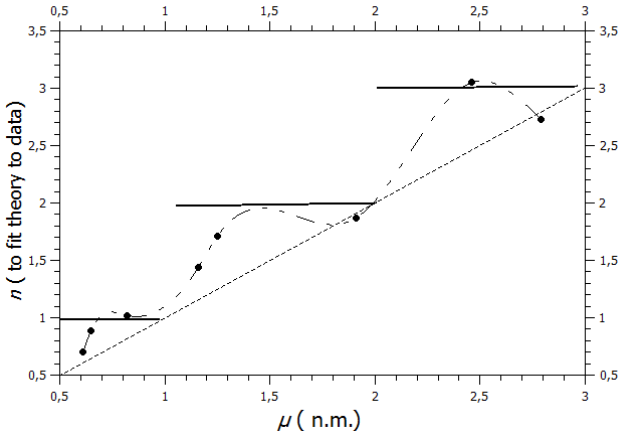

Fig. 1: Plot of n against the magnetic moment for the octet following Eq. (4) and Table 1. The diagonal line is the classical prediction of one flux quantum per nuclear magneton (n.m.). Nucleons are on the line. Horizontal (Shapiro-like) steps at integer values of n are shown. The data display undulations, and a tendency to reach for the steps (traced line as guide).

corresponds to a state detached from a higher state associated with a sea of excitations in equilibrium, and therefore might be used to represent a "quasiparticle". The relativistic Lagrangian for such a fermion can be modelled through the dressing of a proton of mass $m_{\rm p}$ in view of the presence of magnetodynamic terms [6]:

$$\mathcal{L} = \bar{\psi}\left\{i\alpha_\mu\left(\hbar\partial_\mu - i\,\frac{e}{c}\,A_\mu\right) - \alpha_4 m_{\rm p} c\right\}\psi\,, \qquad (5)$$

where the α_μ are Dirac matrices. This Lagrangian can readily be transformed into a Hamiltonian form. For A a constant around the ring path, the spectrum of possible energies for a confined fermion are obtained as:

$$\epsilon_{\rm k} = c\left\{\left(p_{\rm k} - \frac{eA}{c}\right)^2 + m_{\rm p}^2 c^2\right\}^{1/2} \qquad (6)$$

which comes straight from the orthonormalized definition of the Dirac matrices and diagonalization of the Hamiltonian. If one takes the Bohr-Sommerfeld quantization conditions, the momentum $p_{\rm k}$ (for integer k) is quantized in discrete values $2\pi\hbar k/L$. We start from this assumption but the true boundary conditions to close the wave loop might impose corrections to this rule in the form of a phase factor (see below). The potential A can be replaced by ϕ/L. Such charge motion is affected by vacuum polarization and the effects on the kinetic energy are accounted for in a way similar to that used in the analysis of the Casimir Effect, by summing over all possible integer values of k in (6) [6,7]. This summation diverges. According to the theory of functions of a complex variable the removal of such divergences requires that the analytic continuation of the terms be taken, which reveals the diverging parts which are thus considered as contributions from the infinite vacuum reservoir. A successful technique for this purpose begins with the rewriting of (6) in terms of Epstein-Riemann Zeta functions $Z(s)$ [7], including the summation over k from minus to plus infinity integers, and making a regularization (Reg) transformation. Here $M(\phi)$ is the flux-dependent dressed mass of a baryon, and $s \to -1$:

$$Mc^2 = U_0 + \mathrm{Reg}\sum_k c\left\{\left(p_{\rm k} - \frac{e\phi}{Lc}\right)^2\right\}^{-s/2} \qquad (7)$$

where we have allowed for the existence of a finite energy U_0 to represent an hypothetical state from which the individual baryons would condense, since they would correspond to lower energy states. Such particles should be characterized as states of energy Mc^2 lower than U_0. It is convenient to define from L a parameter with units of mass $m_0 = 2\pi\hbar/cL$, which will be used to define a scale in the fit to the data. We notice that m_0 is related to the parameter L in the same way field-theories regard mass as created from broken symmetries of fields, establishing a range for an otherwise boundless field distribution (e.g. as happens at the establishment of a superconductor state with the London wavelength related to an electromagnetic field "mass" by a similar expression). For convenience, we define the ratios $m' = m_{\rm p}/m_0$ and $u_0 = U_0/m_{\rm p}c^2$. For comparison with the data analysis in our previous work [1], we must introduce also the number of flux quanta n (integer or not) associated to ϕ, such that $n = \phi/\phi_0$. In terms of these parameters one may write (7) in the form:

$$\frac{M(n)}{m_{\rm p}} = u_0 + \frac{1}{m'}\,\mathrm{Reg}\sum_k\left\{(k-n)^2 + m'^2\right\}^{-s/2}\,. \qquad (8)$$

In the analysis of data, the experimental values of $M/m_{\rm p}$ for baryons will be plotted against n. The sum on the right side of (8) is a particular case of an Epstein Zeta function $Z(s)$, and becomes a Riemann Zeta function, since the summation is over one parameter k only. The summation diverges but it can be analytically continued over the entire complex plane, since the Epstein Zeta function displays the so-called reflection property. It has been shown that after the application of reflection the resulting sum is already regularized, with the divergences eliminated. The reflection formula is [7]:

$$\pi^{\frac{-s}{2}}\,\Gamma\left(\frac{s}{2}\right)Z(s) = \pi^{\frac{s-1}{2}}\,\Gamma\left(\frac{1-s}{2}\right)Z(1-s)\,. \qquad (9)$$

This replaces the diverging $Z(s)$ straight away by the regularized $Z(1-s)$, which converges (since $\Gamma(-1/2) = -2\sqrt{\pi}$, we see that the regularized sums are negative, like in the Casimir Effect solution).

For the sake of clarity we describe now the regularization of (8) below as (10), step by step (note that $s \to -1$, and the "reflected" exponent $-(1-s)/2$ replaces $-s/2$ of (8)).

In the first passage from the left, the entire summation argument is replaced by the Mellin integral which results into it. This creates a convenient exponential function to be integrated later. In the second passage, the Poisson summation formula is used, in which the summed exponential function is replaced by its Fourier Transform (note that the same notation k is used for the index to be summed in the Fourier transformed quantity). The objective is to replace the $k^2 t$ in the initial exponential by k^2/t. In this way, when the integration over t is carried out a modified Bessel function K is obtained. In the final line the $k = 0$ term in the sum is separately worked out and appears as the first term between brackets. The remaining summation in k therefore does not include 0 ("/0" as shown). The influence of the parameter n is, as we wanted to prove, to introduce a periodicity depending on the amount of flux confined by the current ring, and the regularized energy is therefore periodic in n. Therefore, $Z(1-s)$ is given as:

$$\sum_k \left\{(k-n)^2 + m'^2\right\}^{-(1-s)/2} =$$

$$= \frac{2}{\Gamma\left(\frac{1-s}{2}\right)} \int_0^\infty t^{\frac{1-s}{2}-1} \left(\sum_k e^{-(k-n)^2 t - m'^2 t} \right) \mathrm{d}t =$$

$$= \frac{2\sqrt{\pi}}{\Gamma\left(\frac{1-s}{2}\right)} \int_0^\infty t^{\frac{-s}{2}-1} \left(\sum_k e^{-2\pi i k n} \, e^{-\frac{\pi^2 k^2}{t} - m'^2 t} \right) \mathrm{d}t =$$

$$= \frac{2\sqrt{\pi}}{\Gamma\left(\frac{1-s}{2}\right)} \left(\frac{\Gamma\left(-\frac{s}{2}\right)}{m'^{-s}} + 2\pi^{\frac{-s}{2}} \sum_{k/0} \left(\frac{k}{m'}\right)^{\frac{-s}{2}} K_{\frac{s}{2}}(2\pi m' k) \, e^{-2\pi i k n} \right) \quad (10)$$

for $s \to -1$. From (9), the "Reg" summation in (8) becomes

$$\frac{\pi^{\frac{2s-1}{2}} Z(1-s)}{\Gamma\left(\frac{s}{2}\right) \Gamma\left(\frac{1-s}{2}\right)},$$

and the exponential produces a cosine term.

Since $\Gamma(-1/2) = -2\sqrt{\pi}$ we see that the regularized sum is negative, corresponding to energies lower than U_0. In the fitting to the data, we will admit that both m' and u_0 are adjustable parameters.

Fig. 2 shows the data for all baryons in Tables 1 and 2, and the plot of (8) regularized by (10), for $u_0 = 3.96$ and $m' = 0.347$ (corresponding to $m_0 = 2.88\, m_p$ and $U_0 = 3710$ MeV). The energy 3710 MeV would represent the sea of excitations from which the baryons would evolve.

Greulich [12] made a phenomenological analysis correlating the masses of all mesons and baryons with lifetimes greater than 10^{-24} s, to the electron mass and the constant α, obtaining that $m/m_e = N/2\alpha$. Such expression is consistent with our previous analysis in [1], as well as with the new results in the present work. Fig. 3 is a reproduction of Fig. 1 in his paper. We have added a traced line at 3710 MeV/c^2, which shows that such energy is in the correct range for a "parent" state from which all those particles below might evolve by symmetry breaking. There is no correction for spin in the masses of this plot and the points above the line belong to particles containing combinations of charmed, strange, and bottom quarks, which might not fit in the specific calculation considered in this paper.

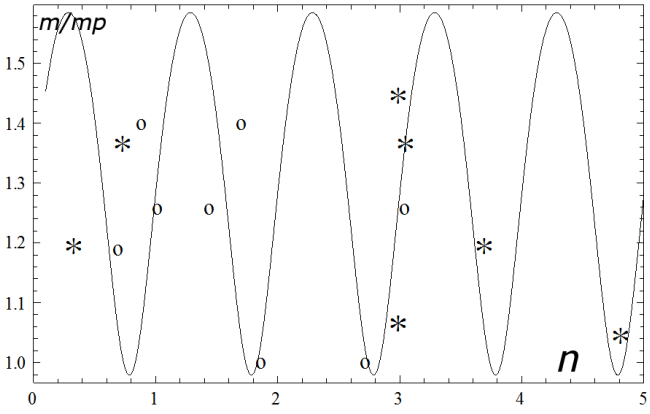

Fig. 2: Comparison of baryon masses calculated from Eq. (8) as a function of confined flux n, with data from Tables 1 and 2 for octet (open circles) and decuplet particles (m_t used, stars). The phenomenological Eq. (4) provides values for n as a function of mass and moment, and the relation between these quantities (data points) agrees quite well with the field-theoretical calculations (curve) of mass as function of n from Eq. (8). Nucleons are on the basis of the figure.

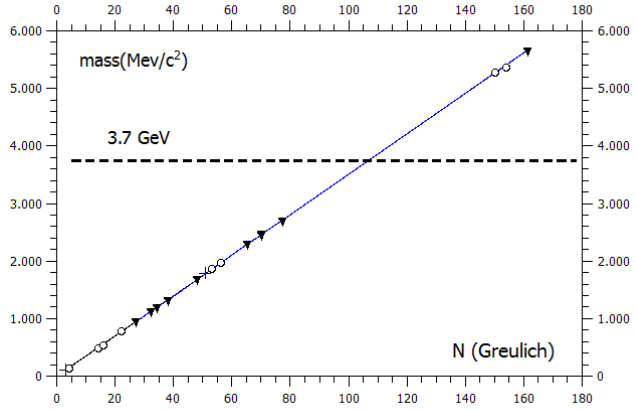

Fig. 3: This plot shows all baryons and mesons with lifetimes greater than 10^{-24} s [12] (see text for details). The traced line indicates the calculated 3710 Mev/c^2, which is in the expected range of energy for a parent-state for the particles below it.

3 Analysis and conclusions

The present paper provides a theoretical background for the phenomenological analysis of [1]. Such previous analysis has

been improved through the redefinition of the parameter n in terms of the experimental data on mass and magnetic moments for baryons. The basic idea has been the modeling of such particles by means of confined currents. The present work has shown that this is theoretically sensible. Closed currents are associated with confined magnetic flux. Since the represented particle is immersed in a sea of excitations, the energy spectrum of closed currents is summed up over all possible values of a Bohr-Sommerfeld kinetic quantum number, leaving the previously defined magnetic n as the parameter to dictate the mass differences among the baryons, in view of the fulfillment of gauge-covariance conditions. A regularization procedure is necessary since the original sums diverge. The model regards particles as the result of a type of condensation from a sea of excitations of top energy U_0, which is the accepted picture in field theories of the origin of mass (however no phase-transitions or broken symmetries are explicitly introduced in the present treatment). The lowest energy particles are the nucleons in this picture. The magnetic flux introduces a modulation of rest energy which is quite well reproduced and the parameter m' is defined with such a magnitude to cover all baryons up to the Ω^- particle. No other kinds of forces are necessary for such theoretical treatment to reproduce data, neither is necessary a detailed knowledge about inner constituents of baryons. As discussed in a previous paper [13], the good results obtained here support early treatments in which quarks and leptons are treated on the same theoretical framework. Such framework should essentially be based on quantum electrodynamics.

Received on November 8, 2019

References

1. Schilling O. F. A unified phenomenological description for the magnetodynamic origin of mass for leptons and for the complete baryon octet and decuplet. *Annales de la Fondation Louis de Broglie*, 2018, v. 43-1, 1.
2. Byers N. and Yang C. N. Theoretical considerations concerning quantized magnetic flux in superconducting cylinders. *Phys. Rev. Lett.*, 1961, v. 7, 46.
3. Parks R. D. Quantized magnetic flux in superconductors. *Science*, 1964, v. 146, 1429.
4. Kulik I. O., Roshavskii A. S., and Bogachek E. N./, Magnetic flux quantization in dielectrics. *J. Exp. Theor. Phys. Letters*, 1988, v. 47, 303.
5. Kulik I. O. Spontaneous and persistent currents in mesoscopic Aharonov-Bohm loops: static properties and coherent dynamic behavior in crossed electric and magnetic fields. *J. Exp. Theor. Phys.*, 2005, v. 101, 999 and references therein.
6. Bogachek E. N., Krive I. V., and Roshavskii A. S. Aharonov-Bohm oscillations in relativistic Fermi and Bose systems. *Theor. Math. Phys.*, 1990, v. 83, 419.
7. Lin R.-H. and Zhai X.-H. Equivalence of zeta function technique and Abel-Plana formula in regularizing the Casimir energy of hyperrectangular cavities. *Mod. Phys. Lett. A*, 2014, v. 29, 1450181.
8. Post E. J. Linking and enclosing magnetic flux. *Phys. Lett.*, 1986, v. 119A, 47.
9. London F. Superfluids, vol. I. Wiley, New York, 1950.
10. Barut A. O. Quantization of collective regular structures of particles. *Appl. Phys. (Lasers and Optics)*, 1995, v. B69, 123.
11. Simonov Y. A., Tjon J. A. and Weda J. Baryon magnetic moments in the effective quark lagrangian approach. *Phys.Rev. D*, 2002, v. 65, 094013.
12. Greulich K. O. Calculation of the masses of all elementary particles with an accuracy of approximately 1%. *J. Mod. Phys.*, 2010, v. 1, 300.
13. Schilling O. F. Heuristic methods for the calculation of mass for particles. viXra: quant/1807.0476 (http://vixra.org/abs/1807.0476).

Nuclear Fusion with Coulomb Barrier Lowered by Scalar Field

T. X. Zhang[1] and M. Y. Ye[2]

[1]Department of Physics, Chemistry, and Mathematics, Alabama A & M University, Normal, Alabama 35762, USA. E-mail: tianxi.zhang@aamu.edu
[2]School of Physical Science, University of Science and Technology of China, Hefei, Anhui 230088, China. E-mail: yemy@ustc.edu.cn

The multi-hundred keV electrostatic Coulomb barrier among light elemental positively charged nuclei is the critical issue for realizing the thermonuclear fusion in laboratories. Instead of conventionally energizing nuclei to the needed energy, we, in this paper, develop a new plasma fusion mechanism, in which the Coulomb barrier among light elemental positively charged nuclei is lowered by a scalar field. Through polarizing the free space, the scalar field that couples gravitation and electromagnetism in a five-dimensional (5D) gravity or that associates with Bose-Einstein condensates in the 4D particle physics increases the electric permittivity of the vacuum, so that reduces the Coulomb barrier and enhances the quantum tunneling probability and thus increases the plasma fusion reaction rate. With a significant reduction of the Coulomb barrier and enhancement of tunneling probability by a strong scalar field, nuclear fusion can occur in a plasma at a low and even room temperatures. This implies that the conventional fusion devices such as the National Ignition Facility and many other well-developed or under developing fusion tokamaks, when a strong scalar field is appropriately established, can achieve their goals and reach the energy breakevens only using low-techs.

1 Introdction

The development of human modern society is inseparable from energy. Since the fossil fuels are nearing exhaustion and renewable energy sources cannot be sufficient, the best choice to thoroughly solve the future energy problems must be the nuclear fusion power. The most critical issue in nuclear fusion is the extremely high Coulomb barrier between positively charged nuclei, usually over hundreds of keV or billions of Kelvins [1]. From the quantum tunneling effect, which is derived from Heisenberg's uncertainty principle and the particle-wave duality, nuclei with kinetic energy of around ten keV or hundred million Kelvins, which is about some tens times lower than the actual barrier, are energetic enough to penetrate the barrier and fuse one another with sufficient probabilities. There are in general three possible ways for nuclei to overcome the Coulomb barrier between them and hence achieve the thermonuclear fusion: (i) heating both species of nuclei (or the entire plasma including electrons) to the needed temperature, (ii) heating only the minor species of nuclei to the needed temperature, and (iii) lowing the Coulomb barrier to the needed level. Figure 1 sketches a schematic of the three approaches for nuclei to overcome their Coulomb barrier that blocks them from fusion. A combination of two or all of the three approaches will certainly work more efficiently.

Since the middle of the last century, fusion scientists have been focusing on the approach (i), i.e. study of how to efficiently heat the entire plasma for nuclei to have such high energies and how to effectively control and confine such extremely heated entire plasma. The major types of heating processes that have been applied so far include the Joule heating by driving electric currents, the injection heating by injecting energized neutral beams, and the radio frequency (rf) heating by resonating nuclei or electrons with antenna-generated radio-frequency waves. The magnetic and inertial confinements are two major types of confinements. Although having made great progresses in the development of various kinds of fusion devices or tokamaks, human beings are still not so sure how many difficulties to be overcome and how far need to go on the way of seeking this ultimate source of energy from the nuclear fusion [2].

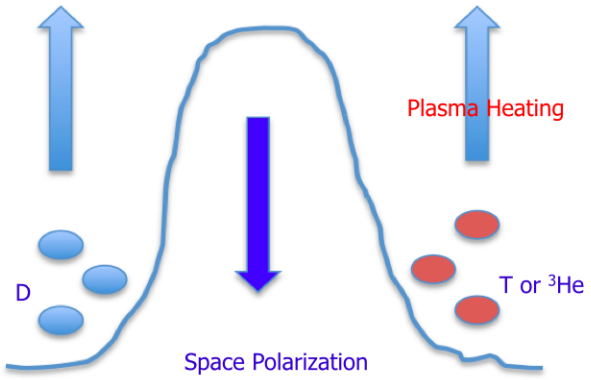

Fig. 1: A schematic of three ways for nuclei to overcome the Coulomb barrier. The first is the conventional approach that energizes both species of nuclei or the entire plasma including electrons to the needed energy for fusion. The second is the authors' recently developed approach that energizes the minor species of nuclei such as ^{3}He and T ions to the needed energy for fusion. And the third is the approach of this paper that lowers the Coulomb barrier to the needed level for fusion.

Recently, the authors innovatively proposed and further quantitatively developed the approach (ii), i.e. a new mechanism for plasma fusion at ten million Kelvins (MK) with extremely heated ^{3}He or tritium (T) ions [3–6]. This newly developed mechanism involves a two-stage heating process when an electric current is driven through a multi-ion plasma. The electric current first ohmically (or in the Joule heating process) heat the entire multi-ion plasma up to the order of 10 MK (or some keV), at which the electric resistivity in the plasma becomes too low for the electric current to be significantly dissipated further and the temperature of the entire plasma saturates at this level. When the electric current is continuously driven up to a critical point, the current-driven electrostatic H or D-cyclotron waves with frequency around twice as big as the ^{3}He or T-cyclotron frequency are excited, which can further heat ^{3}He or T ions via the second harmonic resonance to 100 MK and higher, at which the nuclear fusion between the extremely hot ^{3}He or T ions and the relative cold D ions (i.e. the D-^{3}He or D-T fusion) can occur. This new mechanism for plasma fusion at 10 MK with extremely heated ^{3}He or T ions can also greatly reduce the difficulty in controlling and confining of the plasma fusion.

In this study, we attempt to develop the approach (iii), i.e. to explore and find another new way towards this ultimate goal of using nuclear fusion energy through building an effective fusion reactor. Instead of only energizing the nuclei to the needed temperature, we lower the Coulomb barrier to the needed level. Towards this direction, there have been some analytical efforts done up-to-date by others for enhancing the quantum tunneling probability such as by catalyzing muons or antiprotons [7], driving cusps [8], spreading wave packets [9], forming coherent correlated states [10], screening with Bose-Einstein condensations [11], and so on. Rather than to catalyze the fusion, we will in this paper consider a scalar field to polarize the space or vacuum, in other words, to enhance the dielectric constant of the space or vacuum and hence reduce the electric potential energy or Coulomb barrier among nuclei. We will first calculate the effect of scalar field on the tunneling probability and the number of nuclei that can overcome the Coulomb barrier for fusion. We will then calculate the scalar field effect on the nuclear reaction rate of fusion. We will further investigate the physics and mechanism for a possible approach that generates a strong scalar field in labs to significantly lower the barrier and greatly enhance the quantum tunneling probability for nuclear fusion.

2 Lowering of the Coulomb Barrier by Scalar Field

Early studies have shown that the scalar field of a five-dimensional (5D) gravity can not only shallow the gravitational potential well by flattening the spacetime [12], or in other words, varying or decreasing the gravitational constant [13], but also lower the electric potential energy or Coulomb barrier among nuclei by polarizing the free space or vacuum [14, 15], or in other words, varying or increasing the dielectric constant [16]. From the exact field solution of 5D gravity [12, 17, 18], we can obtain the relative dielectric permittivity in the free space or vacuum polarized by a scalar field Φ as

$$\epsilon_r \equiv \frac{\epsilon}{\epsilon_0} = \frac{E_c}{E} = \Phi^3 \exp\left(\frac{\lambda - \nu}{2}\right), \tag{1}$$

where e^λ and e^ν are the $rr-$ and $tt-$ components of the 4D spacetime metric. This result implies that the electric potential energy or Coulomb barrier between nuclei is explicitly reduced by a factor of Φ^3. For a weak gravitational system such as in labs, because $e^\lambda \sim 1$, $e^\nu \sim 1$, we have $\epsilon_r = \Phi^3$. For a strong gravitational system such as nearby neutron stars or black boles, because $e^\nu \propto \Phi^{-2}$, we have $\epsilon_r \propto \Phi^4$. In quantum electrodynamics (QED) of particle physics, the vacuum polarization was calculated in accordance with the scalar Φ^3 theory [19]. The effect of scalar field vacuum polarization on homogeneous spaces with an invariant metric was obtained in [20].

The scalar field in the 5D gravity is a force field that associates with the mass and charge of a body and couples the gravitational and electromagnetic fields of the body. The scalar field associated with matter and charge in labs is negligible small, which may be able to be detected by the Laser Interferometer Gravitational-Wave Observatory (LIGO) that detected gravitational waves [21, 22]. For massive, compact, and, especially, high electrically charged objects such as neutron stars and black holes, we can have an extremely large scalar field. Although being one of the biggest unsolved mysteries in physics, the scalar field has been widely utilized to model and explain many physical phenomena such as Higgs particles, Bose-Einstein condensates, dark matter, dark energy, cosmic inflation, and so on.

Creatively, Wesson recently proposed a possible connection between the scalar field of 5D gravity and the Higgs scalar field of 4D particle physics [23]. The Higgs scalar field is an energy field that all particles in the universe interact with, and gain their masses through this interaction or Yukawa coupling [24, 25]. In the middle of 2013, CERN discovered the carrier of the Higgs scalar field, i.e. the Higgs boson, and thus confirmed the existence of the Higgs scalar field. On the other hand, according to the Ginzburg-Landau model of the Bose-Einstein condensates, the Higgs mechanism describes the superconductivity of vacuum. Therefore, the scalar field of the 5D gravity can be considered as a type of Higgs scalar field of 4D particle physics. The latter can be considered as a type of Ginzburg-Landau scalar field of Bose-Einstein condensates [26–28]. Then, that the scalar field of the 5D gravity can shield the gravitational field (or flatten the spacetime) and polarize the space or vacuum must imply that the Ginzburg-Landau scalar field of superconductors and superfluids in the state of Bose-Einstein condensates may also shield the gravitational field (or flatten the spacetime) and polarize the space or vacuum.

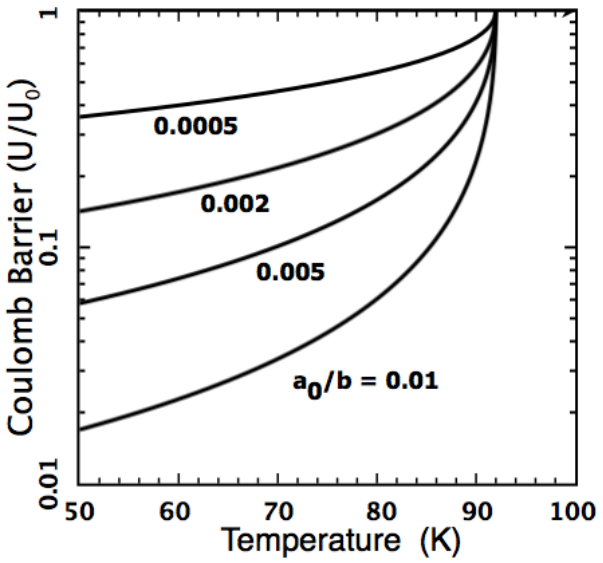

Fig. 2: The Coulomb barrier between two charges in the vacuum polarized by the Ginzburg-Landau scalar field of the Bose-Einstein condensate associated with the type II superconductor or superfluid, normalized by the barrier without the polarization, is plotted as a function of the temperature of the superconductor in the cases of different ratios of the two phenomenological constants a_0 and b.

In 1992, Podkletnov and Nieminen experimentally showed that a rotating disk of the type-II ceramic superconductor could shield Earth's gravity on a sample by a factor of $\sim 2-3\%$ [29]. If the disk is static, the shielding effect reduces $\sim 0.4\%$ [30]. Recently, we have explained these measurements as the gravitational field shielding by the Ginzburg-Landau scalar field of Bose-Einstein condensates associated with the type II ceramic superconductor disk [31], according to the 5D fully covariant gravity [12, 16, 18]. In the quantum field theory or quantum electrodynamics, many phenomena occurred or observed must be explained or described by relying on the physics of scalar field, for instances, the scalar field for cosmic inflation [32], the scalar field for dark matter or dark energy, and so on.

In the vacuum that is polarized by a Ginzburg-Landau scalar field of Bose-Einstein condensate associated with superconductor and superfluid, Φ_{GL}, the Coulomb barrier can be given by

$$U = \frac{U_0}{(1+\Phi_{GL})^3} \tag{2}$$

where

$$\Phi_{GL} = \sqrt{-\frac{a_0}{b}(T-T_c)} \tag{3}$$

with a_0 and b the two phenomenological constants, T and T_c the temperature and transition temperature of the condensate. For a quantitative study, we plot in Figure 2 the ratio of the Coulomb barrier in the vacuum that is polarized by the Ginzburg-Landau scalar field of Bose-Einstein condensates associated with a type II superconductor to that without polarization as a function of the temperature of the superconductor. In this plot, we have chosen the values $T_c = 92$ K and $a_0/b = 10^{-8}, 10^{-7}, 10^{-6}$ K^{-1} as done in [31, 33]. The vacuum polarization by a high magnetic field was measured by the Polarization of the Vacuum with Laser (PVLAS) using a superconducting dipole magnet of more than 8 Teslas magnetic field [34]. By a scalar field, a direct measurement of the vacuum polarization has not yet been conducted.

3 Penetrating of the Coulomb Barrier with Scalar Field

According to Gamow's tunneling probability [35] and Maxwell-Boltzmann's distribution function, one can find the relative number density of nuclei with energy from E to $E + dE$ in the plasma with temperature of T per unit energy that can penetrate the Coulomb barrier to be given by

$$\frac{dN}{dE} = \frac{2\pi}{(\pi kT)^{3/2}}\sqrt{E}\exp\left(-\frac{E}{kT}-\sqrt{\frac{E_g}{E}}\right), \tag{4}$$

where E_g is the Gamow energy determined by

$$E_g = 2m_r c^2(\pi\alpha Z_a Z_b)^2. \tag{5}$$

Here k is the Boltzmann constant, m_r is the reduced mass of nuclei, c is the light speed, Z_a and Z_b are the ionization states of nuclei, and $\alpha = e^2/(2\epsilon_0 hc)$ is the fine-structure constant. Considering the vacuum to be polarized by a scalar field (i.e. $\Phi > 1$), we modify the fine-structure constant by replacing ϵ_0 as $\epsilon = \Phi^3\epsilon_0$. It is seen that the scalar field can significantly reduce the Gamow energy and thus greatly increases the tunneling probability.

To see in more details for the increase of the tunneling probability, we plot in Figure 3 the Gamow peak in a D-T plasma first in the case of no scalar field (i.e. $\Phi = 1$). The plasma temperature has been chosen to be 10^7, 5×10^7, and 10^8 K, respectively. The result indicates, in a D-T plasma with density 2×10^{19} m^{-3} at 10^8 K, there are about two thousandth of total amount of nuclei to be able to tunnel through the barrier and participate in the fusion. Since the ion collision frequency in a fully ionized plasma can be estimated as $\nu_i = 4.8\times10^{-8} Z_i\sqrt{m_p/m_i}\ln\Lambda T_i^{-3/2} \sim 5$ Hz, for 10% of nuclei to react, the plasma must hold this temperature over 10 seconds. If the temperature is 5×10^7 or 10^7 K, then only around a few percent of or one in million nuclei can react within 10 seconds. Here we have used $\ln\Lambda = 6.8$ for ions.

With a scalar field, the tunneling probability will be significantly enhanced. Figure 4 plots the Gamow peak in a D-T plasma in the case of four different values of the scalar field (corresponding to the four lines in each panel, $\Phi = 1, 2, 10, 100$) and two different plasma temperatures of $T = 10^8$ K for the top panel and 10^7 K for the bottom panel. It is

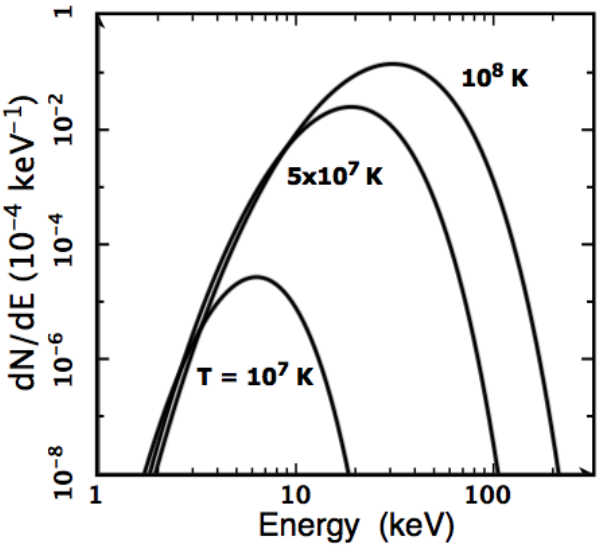

Fig. 3: The Gamow peak without a scalar field in a ^{2}H-^{3}H plasma with different temperatures or, in other words, the energy spectra of nuclei that are able to penetrate the Coulomb barrier for fusion. The relative number density of nuclei per unit energy with energy in the range from E to $E + dE$ is plotted as a function of the energy with temperature to be $T = 10^8, 5 \times 10^7, 10^7$ K, respectively. The maximum is usually called the Gamow peak [35].

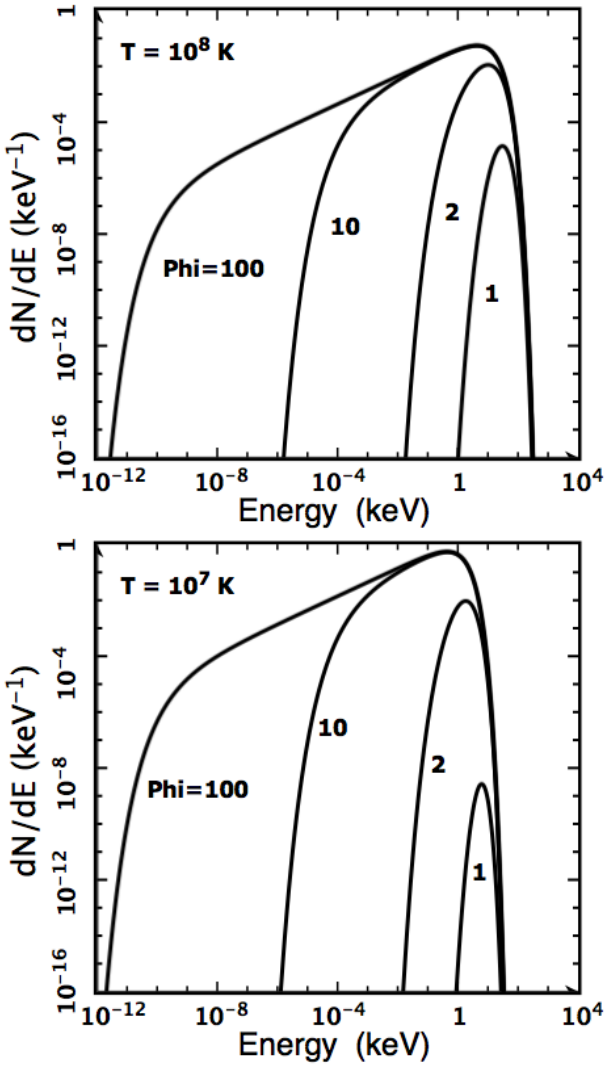

Fig. 4: The Gamow peak with a scalar field in a D-T plasma with different temperatures. This plots the energy spectra of nuclei that are able to penetrate the Coulomb barrier for fusion, i.e. the relative number density of nuclei per unit energy with energy in the range from E to $E + dE$ as a function of the energy with the scalar field $\Phi = 1, 2, 10, 100$ and temperatures to be $T = 10^8$ K for the top panel and 10^7 K for the bottom panel.

seen that when $\Phi > 2$ the number of nuclei that can tunnel through the barrier is enhanced by a factor of 1000 or greater at $T = 10^8$ K. At $T = 10^7$ K, the factor of enhancement can be 10^7 or greater. In addition, there are large amount of nuclei with extremely low energy can also tunnel through the barrier for fusion.

To see more details on the fusion of low energy nuclei, we plots the Gamow peak in Figure 5 for the D-T plasma with temperature equal to 10^6 K and 300K, respectively. In a 10^6 K plasma, the fusion can occur and be readily completed in seconds if $\Phi > 2$. At the room temperature, the nuclear fusion are also possible when $\Phi > 6$.

4 Fusion Rate

The fusion rate between two (i^{th} and j^{th}) species of ions, whose charge or ionization states are Z_i and Z_j, respectively, can be usually represented as [36–38]

$$R_{ij} = \frac{N_i N_j}{1 + \delta_{ij}} < \sigma v > \tag{6}$$

where N_i and N_j are the number densities of the two species of ions, δ_{ij} is the Kronecker symbol, which is equal to the unity if the two species of ions are identical, otherwise, it is zero, v is the relative velocity, and σ is the cross section, determined by

$$< \sigma v >= \frac{6.4 \times 10^{-18}}{A_r Z_1 Z_2} \Phi^3 S \xi^2 \exp(-3\xi) \quad \text{cm}^3/\text{s}, \tag{7}$$

with ξ to be defined as

$$\xi = 6.27 \Phi^{-2} (Z_i Z_j)^{2/3} A_r^{1/3} T^{-1/3}. \tag{8}$$

Here we have considered the effect of space polarization on both the Coulomb barrier and the Gamow factor, simply by replacing $Z_i Z_j$ into $Z_i Z_j / \epsilon_r$ with $\epsilon_r = \Phi^3$ due to the space

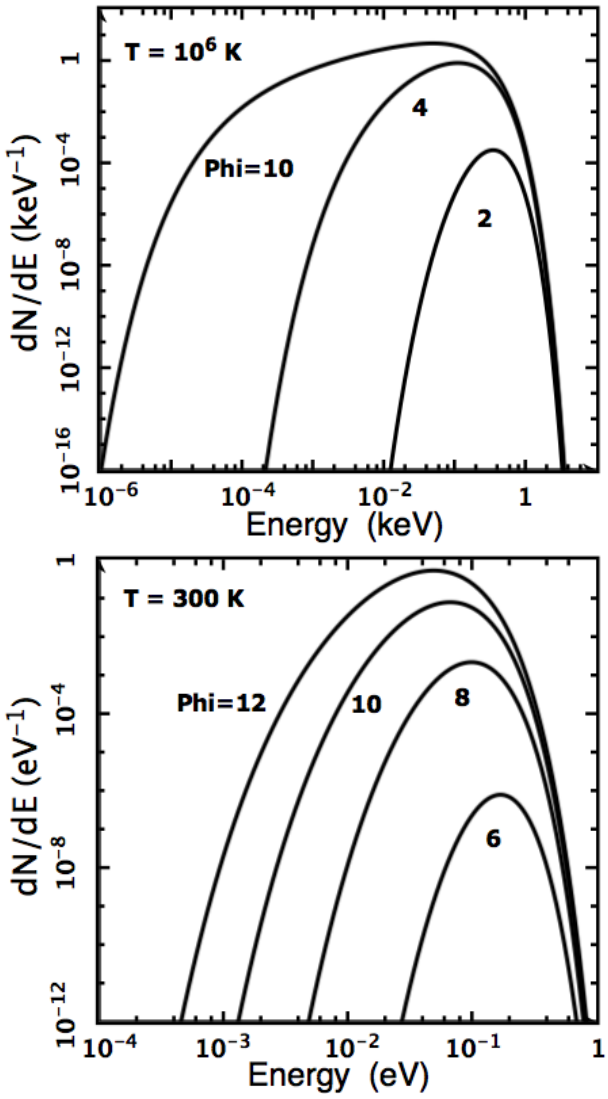

Fig. 5: The Gamow peak with a scalar field in a D-T plasma with different temperatures. This plots the energy spectra of nuclei that are able to penetrate the Coulomb barrier for fusion, i.e. the relative number density of nuclei per unit energy with energy in the range from E to $E + dE$ as a function of the energy with the scalar field $\Phi = 2, 4, 10$ and temperatures to be $T = 10^6$ K for the top panel. For the bottom panel, the scalar field is chosen to $\Phi = 6, 8, 10, 12$ and the temperature is chosen to be $T = 300$ K.

polarization by the scalar field Φ. In equations (7) and (8), the parameter S is the cross section factor, A_r is the reduced mass number, and T is the plasma temperature in keV. For the D-T fusion, we have $Z_i = Z_j = 1$, $A_r = 1.2$, and $S = 1.2 \times 10^4$ keV b.

To see how the scalar field to affect or enhance plasma fusion via the space polarization, we plot in Figure 6 the reaction rate of fusion as a function of the plasma temperature

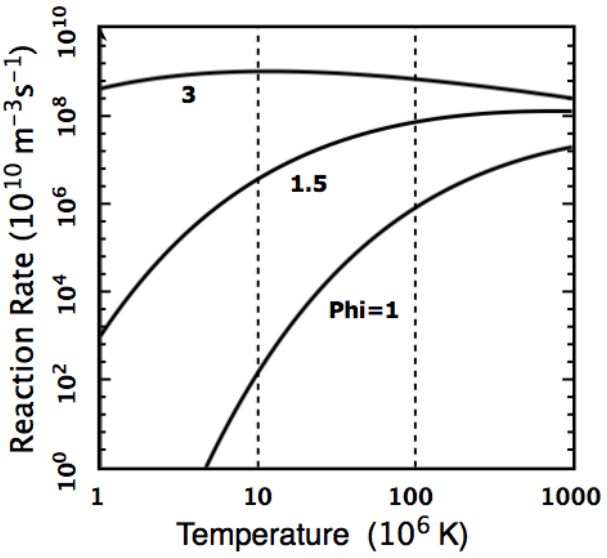

Fig. 6: The reaction rate of D-T fusion. The number of fusion reactions occurred in an unit volume (or m^3) of D-T plasma in one second is plotted as a function of the plasma temperature. Here the number densities of D and T nuclei are both chosen to 10^{19} m^{-3}, and the scalar field is chosen to 1, 1.5, and 3, respectively.

in the cases of the scalar field to be equal to $\Phi = 1, 1.5, 3$, respectively. It should be noted that the effect of scalar field comes from the difference of the scalar field from the unity or, in other words, there is no scalar field effect if $\Phi = 1$. The number densities of D and T nuclei are chosen to be $n_D = n_T = 10^{13}$ cm^{-3}. It is seen from the plot that the scalar field can significantly enhance the reaction rate of fusion. Without the effect of scalar field (i.e. $\Phi = 1$), the reaction rate of D-T fusion is about one thousandth m^{-3} s^{-1} (i.e. per cubic meters and per seconds) at temperature of about 10^8 K. With the effect of scalar field (i.e., $\Phi > 1$), the rate can be increased by 100 times to 10 percent m^{-3} s^{-1} when $\Phi = 1.5$ and by 1000 times to 100 percent m^{-3} s^{-1} when $\Phi = 3$.

5 Conclusion

We have developed a new mechanism for plasma fusion with the Coulomb barrier to be lowered by a scalar field. The result obtained from this study indicates, by polarizing the free space, a scalar field in associated with Bose-Einstein condensates can increase the electric permittivity of the vacuum and hence reduce the Coulomb barrier and enhance the tunneling probability. With a strong scalar field, nuclear fusion can occur in a plasma at a low and even room temperatures. Therefore, by appropriately generated a strong scalar field to polarize the space, we can make the conventional fusion devices to readily achieve their goals and reach the breakevens only using low-techs.

Acknowledgements

The authors thank reviewers for their scientific comments and editors for their great editions that significantly improve the manuscript qualities.

Submitted on November 18, 2019

References

1. Miyamoto K. Plasma Physics for Nuclear Fusion. Revised Edition, Cambridge, Masseschussetts, MIT Press, 1989.
2. Jassby D.L. Fusion reactors: Not what they are cracked up to be. *Bulletin of the Atomic Scientists of Chicago*, April 19, 2017.
3. Zhang T.X. Two-stage heating mechanism for plasma fusion at 10 MK, *Proceedings of IEEE 25th Symposium on Gusion Engineering (SOFE*, 2013, 978-1-4799-0171-5/13.
4. Zhang, T.X.,Ye M.Y. Plasma fusion at 10 MK with extremely heated ^{3}He ions. *IEEE Transactions on Plasma Science*, 2014, v. 42, 1430–1437.
5. Zhang T.X., Ye M.Y. Plasma fusion at ten million Kelvins with extremely heated tritium. *Physics of Plasmas*, 2017, Submitted.
6. Zhang T.X., Ye M.Y. Plasma fusion of deuterons at kiloelectron-volts with extremely heated tritons. *IEEE Trasaction on Plasma Science*, 2019, in reviewing.
7. Perkins L.J., Orth, C.D., Tabak, M. On the utility of antiprotons as drivers for inertial confinement fusion. *UCRL-ID-TR-200850*, 2003.
8. Ivlev B. Low-energy fusion caused by an interference. *Physical Review C*, 2013, v. 87, id. 034619.
9. Dodonov A.V. and Dodonov V.V. Tunneling of slow quantum packets through the high Coulomb barrier. *Physics Letters A*, 2014, v. 378, 1071–1073.
10. Vysotskii V.I. and Vysotskyy M.V. Formation of correlated states and tunneling for a low energy and controlled pulsed action on particles. *Journal of Experimental and Theoretical Physics*, 2017, v. 125, 195–209.
11. Premuda F. Coulomb barrier total screening by Bose-Einstein condensed deuterium in palladium blisters and reaction chains in high-density hysteresis. *Fusion Technology*, 1998, v. 33, 350–366.
12. Zhang T.X. Gravitational Field Shielding and Supernova Explosions. *The Astrophysical Journal Letters*, 2010, v. 725, L117–L121.
13. Dirac P.A.M. The electron wave equation in De-Sitter space. *Annasl of Mathematics*, 1935, v. 36, 657–669.
14. Nodvik J.S. Suppression of singularities by the g55 field with mass and classical vacuum polarization in classical Kaluza-Klein theory. *Physical Review Letters*, 1985, v. 55, L2519–L2522.
15. Dragilev V.M. Vacuum polarization of a scalar field in anisotropic multidimensional cosmology. *Theoretical Mathematics in Physics*, 1990, v. 84 887–893.
16. Zhang T.X. The 5D Fully-Covariant Theory of Gravitation and Its Physical Applications. *Galaxies*, 2015, v. 3, 18–51.
17. Chodos A., Detweiler S. Spherically-Symmetric Solutions in Five-Dimensional General Relativity. *General Relativity and Gravitation*, 1982, v. 14, 879–890.
18. Zhang T.X. Electric redshift and quasars. *Astrophysical Journal Letters*, 2006, v. 636, L61–L64.
19. Schwartz M. 2012 Quantum Field Theory and the Standard Model (Cambridge Univ. Press).
20. Breev A.I. Scalar field vacuum polarization on homogeneous spaces with an invariant metric. *Theoreticl and Mathematical Physics*, 2014, v. 178, 59–75.
21. Zhang T.X. Testing 5D Gravity with LIGO for Space Polarization by Scalar Field. *Progress in Physics*, 2017, v. 13, 180–186.
22. Abbort B.P. *et al.* Observation of Gravitational Waves from a Binary Black Hole Merger. *Physical Review Letters*, 2016, v. 116. 061102.
23. Wesson P.S. The Scalar Field of 5D Gravity and the Higgs Field of 4D Particle Physics: A Possible Connection. *arXiv: 1003.2476*, 2010.
24. Higgs P.W. Broken Symmetries and the Masses of Gauge Bosons. *Physical Review Letters*, 1964, v. 13, L508–L509.
25. Yukawa H. On the Interaction of Elementary Particles. *Proceedings of Physics and Mathematics Society of Japan*, 1935, v. 17, 48–57.
26. Ginzburg V.l., Landau L.D. On the theory of superconductivity. *Zh. Eksp. Teor. Fiz.*, 1950, v. 20, 1064–1082.
27. Castellanos E., Escamilla-Rivera C., Macias A., and Nunez D. Scalar field as a Bose-Einstein condensate? *Gen. Relat. Quant. Cosmol.*, 2014, DOI: 10.1088/1475-7516/2014/11/034.
28. Das S. Bose-Einstein condensation as an alternative to inflation, *Intern. J. of Mod. Phys.*, 2015, v. D24, 1544001.
29. Podkletnov E., Nieminen R.A. Possibility of gravitational force shielding by bulk $YBa_2Cu_3Q_{7-x}$. *Physica C*, 1992, v. 203, 441–444.
30. Li N., Noever D., Robertson T., Koczer R., Brantley W. Static test for a gravitational force coupled to type II YBCO superconductor. *Physica C*, 1997, v. 281, 260–267.
31. Zhang B.J., Zhang T.X., Guggilla P., Dohkanian M. Gravitational field shielding by scalar field and type II superconductors, *Progress in Physics*, 2013, v. 9, 69–75.
32. Guth A. Inflationary universe: A possible solution to the horizon and flatness problems. *Physical Review D*, 1981, v. 23, 347–356.
33. Zhang B.J., Zhang T.X. Vacuum polarization by scalar field of Bose-Einstein condensates and experimental design with laser interferences. *Progress in Physics*, 2017, v. 13, 210–214.
34. Bakalov D. *et al.* The measurement of vacuum polarization: The PVLAS experiment, *in Hyperfine Interactions*, 1998, v. 114, 103–113.
35. Gamow G. Quantum theory of the atomic nucleus. *Z. Phys.*, 1928, v. 51, 204.
36. Bahcall J.N.,, Ulrich R.K. Solar models, neutrino experiments, and helioseismology. *Review of Modern Physics*, 1988, v. 60, 297–372 .
37. Bahcall J.N. *et al.* Standard solar models and the uncertainties in predicted capture rates of solar neutrinos. Review of Modern Physics, 1982, v. 54, 767–799.
38. Ichimaru S. Nuclear fusion in dense plasma. *Review of Modern Physics*, 1993, v. 65, 255–299.

LETTERS TO PROGRESS IN PHYSICS

Instability of Protons Beyond 3 GeV Kinetic Energies Explains the Flux Profiles Observed in Cosmic Rays

Osvaldo F. Schilling

Departamento de Física, Universidade Federal de Santa Catarina, 88040-900, Florianópolis, SC. Brazil.
E-mail: osvaldo.neto@ufsc.br

We analyze available data for the flux of cosmic rays protons, and find evidence for instability of these particles as their kinetic energy increases beyond about 3 GeV. This is expected from our recent model [1] which proposes the existence of a parent state at 3.7 GeV, from which protons of about 1 GeV mass (as well as the other baryons) would condense in the form of flux-confining vortices. Therefore, this energy difference imposes that beyond 2.7 GeV kinetic energies such vortex states would become unstable compared to the parent, in agreement with the observation that highly energetic protons are rare in cosmic rays. The observation of protons of higher energies is attributed to cohesion provided, e.g. by strong forces, between proton constituents not considered in the vortex model.

We have recently developed a field-theoretical model for baryons in which such particles are modelled as vortices confining magnetic flux, which would "condense" from a parent state at 3.7 GeV, under the effect of electromagnetic instabilities of such a state [1,2]. This model has been shown to reproduce the relation of the masses of baryons with their magnetic moments (through an amount of confined magnetic flux) in a consistent, quantitative way. We here concentrate on the case of protons. Since the particles are assumed to be the result of the creation of states stabilized from a higher energy level, it should be expected that the number of protons will markedly decrease in cosmic rays for excessive kinetic energies. This is what we propose and actually verify in this Letter.

In Fig. 1, we show data for the number flux of protons plotted as $E\,(dN/dE)$ against kinetic energy E in GeV, for cosmic rays below 10 GeV kinetic energy, taken from the upper left corner of figure 1.1 of [3]. Below about 2 GeV kinetic energy there is an approximate plateau. From 2 GeV on, a marked decrease in the flux of protons is observed. The interpretation is that the number N of detected protons is reaching saturation above 2 GeV. To quantify such saturation, we have obtained the actual functional relations in the original double-log plot, to calculate the number N of particles in units of $(\mathrm{m}^2\ \mathrm{sr\ s})^{-1}$ for several energy intervals. Assuming from Fig. 2 below that the plateau in $E\,(dN/dE)$ would begin at about 0.1 GeV and goes up to 3 GeV, we obtain N=6800 by integration in this interval. Beyond 3 GeV the ordinate decays as $E^{-3/2}$. Therefore, one obtains by integration N=1100 between 3 and 10 GeV, and at last a very small N=204 between 10 and 100 GeV. That is, well over 80% of the protons in cosmic rays have energies below about 3 GeV, and the numbers beyond 10 GeV are negligible in absolute terms in spite of the great interest on them from the high-energy physics standpoint.

According to our model in [1], protons accelerated beyond 2.7 GeV kinetic energy (which comes from the difference between the parent level at 3.7 GeV and the proton rest mass of about 1 GeV, i.e. the "energy advantage") should become unstable since they lose the energy advantage acquired by settling in the lower energy vortex state. A related effect breaks Cooper pairs in superconductors if the energy associated with current becomes greater than the pairing interaction provided by phonon-intermediated coupling. Fig. 2 shows a plot of the estimated (from collected data) energy distribution for the interstellar flux of protons [3], which peaks exactly at 2.7 GeV. In view of the gigantic values of E beyond the peak one realizes the minute amount of very energetic particles to the right of the peak. That is, once more one concludes that protons are essentially unstable above 2.7 GeV kinetic energy.

In conclusion, this Letter analyzes data collected for the flow of protons in cosmic rays in the light of a recently proposed model in which protons are modelled as vortices in an energy state 2.7 GeV below a parent state from which they would have condensed [1]. We have indeed found evidence for a critical kinetic energy of 2.7 GeV in both the number distribution of protons and in their energy distribution. Although it is clear that 2.7 GeV represents a critical value for the energies of protons in cosmic rays, a very small ("tail") population of particles is detected at high energies. The expected question is: why do these particles still exist? In spite of providing a picture on how baryons condense from instabilities of the vacuum, the vortex model does not go as far as considering the internal structure of the baryons. The survival of some particles to high energies is certainly related to internal short-range strong forces between constituents, not considered in the model. The good results of the vortex model of [1] however suggest that the existence of the proton constituents cannot be neglected when dynamic effects take place at scales shorter than L/π with L the size of the current loop in [1], which is on the order of 10^{-16} m. It must be pointed out

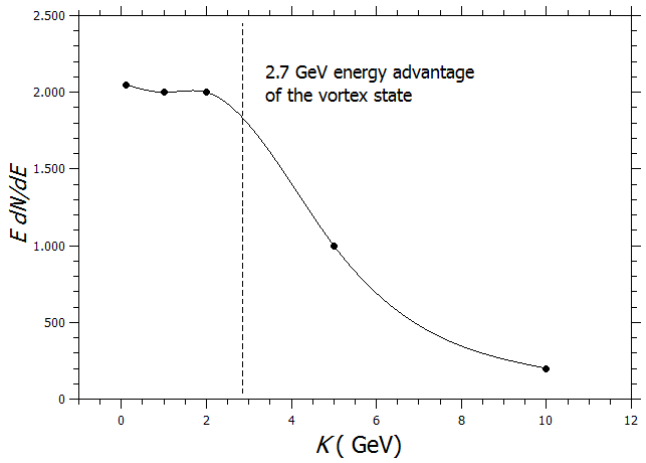

Fig. 1: Reproduction of the upper left part of the double-log plots in figure 1.1 of [3] (linearized scales are adopted here). The number flux of protons in 10^3 m^{-2} (sr. s)$^{-1}$ units is plotted against the protons kinetic energy in GeV. The vertical line is placed at the value of K that corresponds to total loss of the vortex energy advantage compared to the vacuum parent state (see [1]). Fast saturation in the detected N of protons is manifest in the drop of dN/dE as the energy increases. Integration shows that beyond 80% of N concentrates below 3 GeV energies. The solid line is a guide.

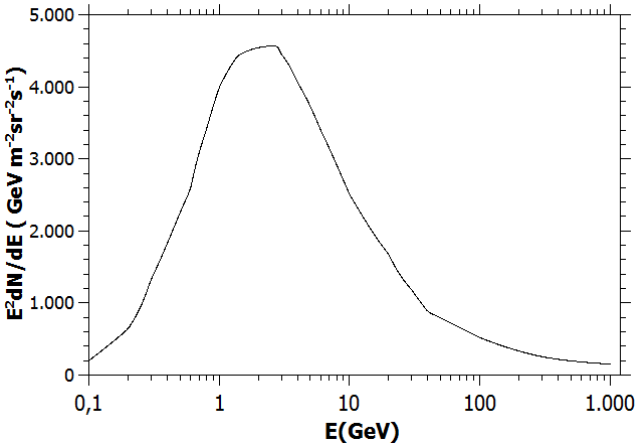

Fig. 2: Estimated energy flux distribution of interstellar protons in cosmic rays, which peaks at exactly K=2.7 GeV [3].

that [3] also displays data for the flux of electrons in cosmic rays in its Fig. 2.1. In this case there are few points in the plot but they peak at the expected range of about 3 GeV, and decay faster than the protons at higher energies. The electron is represented as the very first cross symbol to the left in figure 3 of our paper [1]. If the model applies also to leptons [2], the most energetic electrons might theoretically reach 3.7 GeV kinetic energies (although this requires acceleration to speeds quite close to the light speed). The fact that the electrons data peaks at lower energies and drops faster would be consistent with a greater instability of its structure as compared to the proton. Further investigations on this subject are clearly needed, mainly on the lower range of cosmic rays energies.

Received on December 6, 2019

References

1. Schilling O. F. Generation of Baryons from Electromagnetic Instabilities of the Vacuum. *Progress in Physics*, 2019, v. 15 (3), 185–190.
2. Schilling O. F. A unified phenomenological description for the magnetodynamic origin of mass for leptons and for the complete baryon octet and decuplet. *Annales de la Fondation Louis de Broglie*, 2018, v. 43-1, 1.
3. Gaisser T. K., Engel R. and Resconi E. Cosmic Rays and Particle Physics. Cambridge Universiy Press, Cambridge, 2016.

Progress in Physics is an American scientific journal on advanced studies in physics, registered with the Library of Congress (DC, USA): ISSN 1555-5534 (print version) and ISSN 1555-5615 (online version). The journal is peer reviewed and listed in the abstracting and indexing coverage of: Mathematical Reviews of the AMS (USA), DOAJ of Lund University (Sweden), Scientific Commons of the University of St.Gallen (Switzerland), Open-J-Gate (India), Referential Journal of VINITI (Russia), etc. Progress in Physics is an open-access journal published and distributed in accordance with the Budapest Open Initiative: this means that the electronic copies of both full-size version of the journal and the individual papers published therein will always be accessed for reading, download, and copying for any user free of charge.
The journal is issued quarterly (four volumes per year).

Electronic version of this journal: http://www.ptep-online.com

Postal address:
Department of Mathematics and Science, University of New Mexico,
705 Gurley Avenue, Gallup, NM 87301, USA